ANNALS

XVI LATIN AMERICAN CONGRESS ON ORGANIC GEOCHEMISTRY

ARACAJU 2023

ORGANIZATION:

ANNALS

XVI LATIN AMERICAN CONGRESS ON ORGANIC GEOCHEMISTRY

Editors:

Alexandre Andrade Ferreira
Alberto Wisniewski Junior
Boniek Gontijo Vaz
Marcelo Corrêa Bernardes
Georgiana Feitosa da Cruz

ISBN nº 978-65-00-75016-4

ARACAJU - SE
2023

ORGANIZATION:

SPONSORS:

GOLD

SILVER

GRAPHITE

SUPPORT:

ORGANIZING COMMITTEE

ORGANIZING COMMITTEE ALAGO 2023

Boniek Gontijo Vaz (President of Organizing Committee - UFG, Brazil)
Alberto Wisniewski Junior (Vice-President of Organizing Committee- UFS, Brazil)
Débora de Almeida Azevedo (UFRJ, Brazil)
Georgiana Feitosa da Cruz (UENF, Brazil)
Jandyson Machado Santos (UFRPE, Brazil)
Laercio Lopes Martins (UFC/UENF Brazil)
Mário Duncan Rangel (UFG, Brazil)
Rut Amelia Díaz Ramos (UFF, Brazil)
Vinícius Barreto Pereira (UFRJ, Brazil)

CIENTIFIC COMMITTEE ALAGO 2023

Alexandre Andrade Ferreira (Petrobras, Brazil)
Ana Luiza Albuquerque (UFF, Brazil)
Carin von Muhlen (UERJ, Brazil)
Celeste Yara dos Santos Siqueira (UFRJ, Brazil)
Darlly Érika S. dos Reis (UFRJ, Brazil)
Elena Stashenko (UIS, Colombia))
Eliane Soares de Souza (UENF, Brazil)
Eugênio Vaz dos Santos Neto (UFF/GEO, Brazil)
Georgiana Feitosa da Cruz (UENF, Brazil)
Luiz Antonio F. Trindade (UFRJ, Brazil)
Liliana Lopez (UCV, Venezuela)
Marcelo Corrêa Bernardes (UFF, Brazil)
Marcelo da Rosa Alexandre (UFS, Brazil)
Sidney Gonçalo de Lima (UFPI, Brazil)

SUMMARY

XVI LATIN AMERICAN CONGRESS ON ORGANIC GEOCHEMISTRY

ARACAJU 2023

ORGANIZATION:

ABSTRACTS

XVI LATIN AMERICAN CONGRESS ON ORGANIC GEOCHEMISTRY

ARACAJU 2023

ORGANIZATION:

ALA
PETROLEUM SYSTEMS

INTEGRATED GEOCHEMICAL EXPLORATION IN THE NORTH SECTOR OF OFFSHORE ARGENTINA BASIN

ALEJANDRO GÓMEZ DACAL[a*], OFELIA SILIO[a], FERMÍN PALMA[b], SEBASTIÁN PRÍNCIPI[b], FABIÁN BREA[b], NÉSTOR BOLATTI[a]

[a]**YPF S.A.,** [b]**YPF Tecnología S.A.**

*correspondence: alejandro.dacal@ypf.com

Introduction

Surface geochemical analyses are a valuable resource for exploring frontier areas that lack well data, including offshore basins. This is because source rocks and reservoirs release liquid and gaseous hydrocarbons from the subsurface to the marine seabed. Various geochemical techniques have been developed over the years for offshore prospecting to identify hydrocarbon anomalies in core samples taken from the ocean floor sediments.

The Pampa Azul Project is an interdisciplinary initiative of the Argentine government to study the Argentine sea. In this framework, YPF and CONICET signed an agreement to study the Continental Margin by the execution of oceanographic research cruises onboard the R/V Austral Vessel. This work describes the seafloor geochemistry results obtained from the samples taken in the northern offshore Argentina Basin during the YTEC-GTGM 4 cruise in 2019.

In the present contribution, we identified migrated hydrocarbons through the integrated analysis of the organic, inorganic, chromatographic and isotope data. Furthermore, we analyzed the origin, distribution, maturity, and secondary processes which affected the hydrocarbon accumulations. Finally, we estimated which geochemical proxies are related to the presence of seeps and which are associated with the sedimentary dynamic.

Experimental

Thirty-three gravity core samples of three different areas were collected: north, central and south. These were analyzed by organic geochemistry, gas chromatography (occluded/adsorbed gas), stable isotopes and energy-dispersive X-Ray fluorescence (ED-XRF) to identify the presence of seeps and differentiate them from the sedimentary dynamic features.

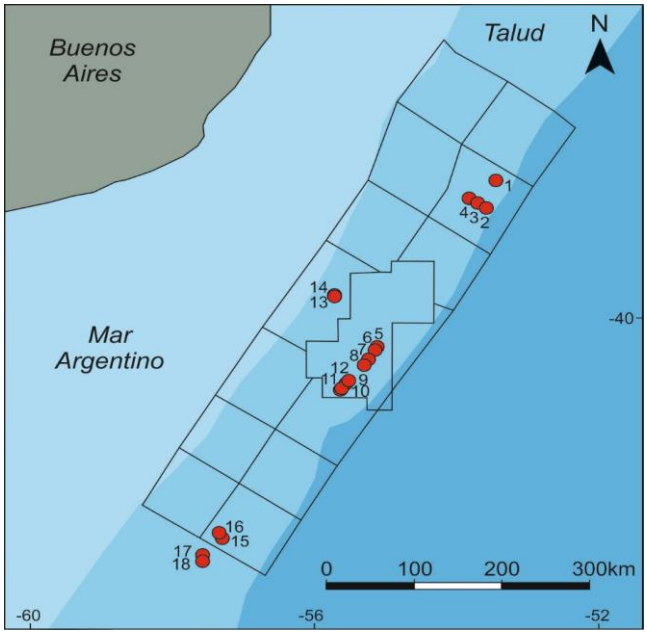

Figure 1. Location of the thirty-three samples in the three study areas collected during the YTEC-GTGM 4 cruise onboard the R/VAustral in the Argentine Continental Margin.

Results and Discussion

The results obtained show that the region with the highest concentrations of total organic carbon (TOC) is situated in the northern area. Conversely, the most mature organic matter are located in the southern area. According to the parameters proposed by Peters [1], the outcomes obtained through organic geochemistry are categorized as poor to moderate, and do not show anomalies related to seeps. Additionally, the areas with the higher accumulation of TOC coincide with the areas with higher S1 and S2 values. These pieces of evidence lead us to conclude that the TOC accumulations are likely linked to the current sedimentary dynamics

The southern region contains the most significant accumulations of occluded/adsorbed gases, which contrasts with the area with the highest TOC values. By examining molecular relation diagrams [2], [3] and isotope relation diagrams [4], [5], it was determined that the origin of occluded/adsorbed gases is thermogenic and related to oil.

Based on the stable isotope analysis and using the parameters proposed by Whiticar [6], the maturity of the hydrocarbons was calculated, and the equivalent vitrinite reflectance values are in the oil window. Additionally, no secondary or mixing processes were identified in the deeper samples analyzed using stable isotopes.

The ED-XRF findings indicate that the northern region has higher values of redox-sensitive proxies, coincident with the area with the best TOC values. In contrast, the southern area has higher carbonate productivity proxies, which corresponds with the area with the most mature organic matter and the highest accumulations of occluded/adsorbed gases.

To estimate the migration distance, GASTAR diagrams and principal component analysis (PCA) models proposed by Prinzhofer [6] were utilized. Although a more substantial number of samples would be required to establish more robust conclusions, potential directions of increasing migration distance of gases were identified. In the central and northern areas, the direction of increasing migration distance is towards the southwest, while in the southern area, it is towards the north.

Conclusions

The main conclusions of this contribution are:

- No evidence of a connection with seeps was observed through organic geochemistry results
- TOC accumulations would be related with the sedimentary dynamic.
- The most significant seafloor expressions of occluded/adsorbed gases were found in the southern area
- The origin of occluded/adsorbed gas accumulations is thermogenic and associated with oil.
- The maturity of hydrocarbons, as calculated using stable isotopes, is within the oil window.
- No secondary or mixing processes were identified in the deeper samples.
- The highest values of redox-sensitive proxies are located in the northern area, which corresponded to the area with the best TOC values.
- The higher carbonate productivity proxies are in the southern area, coincident with the most mature organic matter and the highest values of gas.
- In the central and northern areas, the direction of increasing migration distance is towards the southwest, while in the southern area, it is towards the north.

Acknowledgements

The authors would like to thank all the staff of Instituto de Geociencias Básicas, Aplicadas y Ambientales de Buenos Aires (IGEBA); YPF Tecnología (Y-TEC); DTP Laboratorios; Instituto de Geocronología y Geología Isotópica (INGEIS); and Exploración Offshore de YPF, which collaborated in obtaining and analyzing the samples. Thank you also to Dr. Alejandro Tassone and the Grupo de Trabajo de Geología Marina (GTGM), the Consejo Nacional de Investigaciones Científicas y Técnicas (CONICET), and the captain, officers, and crew of the r/v Austral.

References

[1] Peters, K.E.; Walters, C.C.; Moldowan, J.M., 2005. The Biomarker Guide, Volume 1. Biomarkers and Isotopes in the Environment and Human History.

[2] Jones, V.T.; Drozd, R.J., 1983. Predictions of oil or gas potential by near-surface geochemistry. AAPG Bulletin **67**, 932–952.

[3] Haworth, J.H.; Sellens, M.; Whittaker, A., 1985. Interpretation of hydrocarbon shows using light (C1-C5) hydrocarbon gases from mud-log data. AAPG bulletin **69 (8)**, 1305-1310.

[4] Schoell, M., 1983. Genetic characterization of natural gases. AAPG bulletin **67**, 2225-2238.

[5] Milkov, A.V.; Etiope, G., 2018. Revised genetic diagrams for natural gases based on a global dataset of >20,000 samples. Organic Geochemstry **125**,109-120.

[6] Whiticar, M.J. 1994. Correlation of natural gases with their sources. In: Magoon, L.B., Dow W.G. (Eds.), The Petroleum System from Source to Trap, Memoir, AAPG, Tulsa **60**, 261-283.

XVI LATIN AMERICAN CONGRESS ON ORGANIC GEOCHEMISTRY
9 - 11 AUGUST, 2023
ARACAJU, SERGIPE, BRAZIL

GEOCHEMICAL CHARACTERIZATION OF STRATIGRAPHIC WELL 2-ANP-6-MT, PARECIS BASIN: IMPLICATIONS ON THE EVALUATION OF OIL SYSTEMS

ISMAEL RAMOS PEREIRA[a], ANTÔNIO FERNANDO DE SOUZA QUEIROZ[a], OLÍVIA MARIA CORDEIRO DE OLIVEIRA[a], KARINA SANTOS GARCIA[a], JOSÉ ROBERTO CERQUEIRA[a], SARAH ADRIANA ROCHA SOARES[a], RAMSES CAPILLA[b], CLEVERSON JOSÉ FERREIRA DE OLIVEIRA[b]

[a] **IGEO/UFBA - INSTITUTE OF GEOCIENCES OF THE FEDERAL UNIVERSITY OF BAHIA / [b]CENPES/PETROBRAS**

ismaelpereira@ufba.br

Introduction

The 2-ANP-6-MT stratigraphic well (4450m deep) was drilled by Petrobras/ANP between 2015 and 2016 in the Parecis Basin, aiming to investigate the existence of elements inherent to an oil system, and with the purpose of supporting exploratory processes in the basin. The cores obtained in this well were sampled to carry out geochemical analyzes and verify the potential for the generation of hydrocarbons from the rocks. However, the only analysis performed, due to the characteristics and volume of the samples, was the Rock-Eval pyrolysis to verify the amount of organic matter and the real potential for oil generation.

Materials and methods

Initially, the 169 (one hundred and sixty-nine) rock samples from the cores were visually evaluated to observe their lithologies and possible impurities. After that, this material was fragmented and, soon after, pulverized (size of 80 Mesh) using the planetary ball mill Retsch GmbH (model PM 400). These samples were duly prepared for the Rock-Eval Pyrolysis analysis, where approximately 100 mg of each one was heated from 300 to 600 °C, with an increment of 25 °C/min, in a nitrogen atmosphere. For this analysis, a Rock Eval-6 pyrolyzer was used, where the following parameters were obtained: total organic carbon (TOC); free hydrocarbons contained in the rock (S_1); the hydrocarbon generating potential (S_2); the CO_2 released by the organic matter during the analysis (S_3); the temperature at which the maximum generation of hydrocarbons occurred during pyrolysis (Tmax); the hydrogen index (HI); and the oxygen index (OI).

From the observation of the rock samples and the description of the provided core, it was noted that most of the samples are not shale, but rather sandstone, siltstone, mudstone, various carbonates, and anhydrite, with evidence of metamorphism. Therefore, they should not have a considerable content of organic matter. Taking this characteristic into account and due to the small volume available for each sample, the TOC was not obtained through the elemental analyzer, but during the pyrolyization process in Rock-Eval.

Results and discussions

TOC contents ranged from 0.02 to 0.38%. S_1 values were between 0.01 and 0.1. The hydrocarbon generating potential (S_2) showed values between 0.04 and 0.46. S3 values were between 0.01 and 2.26. The hydrogen and oxygen indices (HI and IO) varied between 13 and 800 and 4 and 1850, respectively. Tmax presented values within an interval of 314 and 529 ºC. The TOC and S_2 contents indicate that all analyzed samples have a poor potential for hydrocarbon generation [1] [2] (Figure 1). The high values of HI do not agree with the very low values of TOC and S_2, since these parameters have a close and interdependent relationship, being highly correlated.

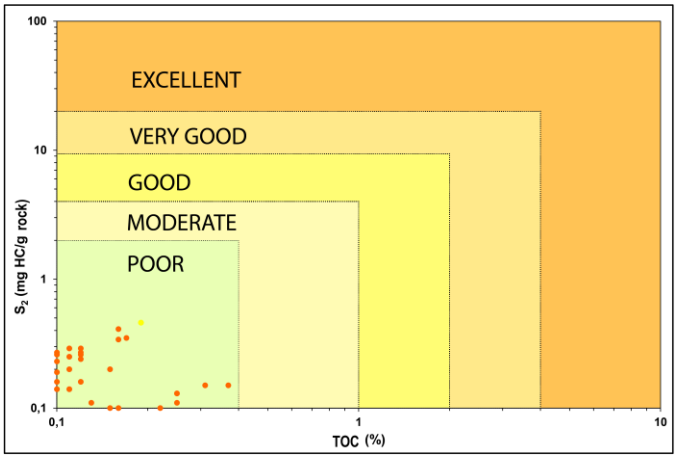

Figure 1. Classification of potential for hydrocarbon generation of samples from well 2-ANP-6-MT, Parecis Basin. Source: Adapted from [2].

The HI and OI values plotted on the Van Krevelen diagram (Figure 2) indicate high results for both indices in a large set of samples, which makes the indication of the possible types of kerogens present in the analyzed samples inconsistent.

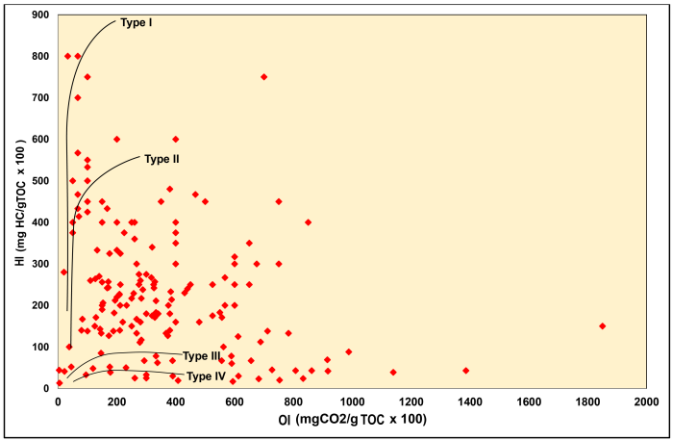

Figure 2. HI and OI values of the analyzed samples, plotted in a Van Krevelen diagram. Source: Adapted from [3].

The relationship shown in the Tmax versus HI diagram (Figure 3) indicates that most of the analyzed samples are mature or senile for the generation of hydrocarbons, which would be an indication of the generation of liquid oil and gas. However, as these temperatures are related to very low values of S_2, the values of Tmax do not have interpretative reliability.

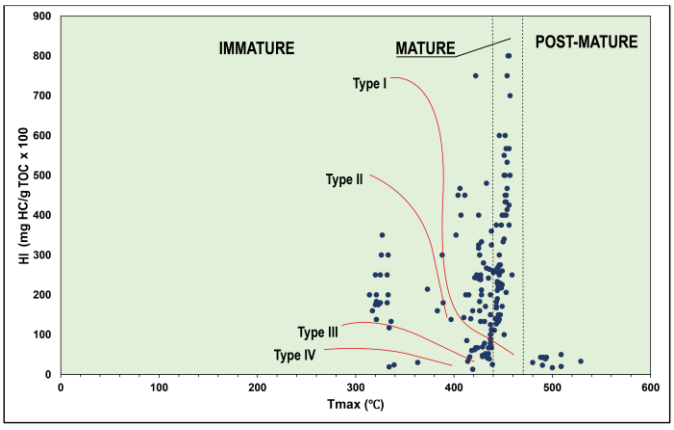

Figure 3. Graph of the Hydrogen Index (HI) versus Tmax for the analyzed samples from well 2-ANP-6-MT, Parecis Basin. Source: Adapted from [4].

These inconsistencies may be related to the effect of the high thermal maturation to which the rocks were submitted. It is likely that the TOC and S_2 contents were originally low due to lithology and are residual since the rocks are metamorphosed. This also affected the other parameters, such as HI, OI and Tmax, so that the results of the analyzed samples did not allow the evaluation of the true potential for the generation of hydrocarbons in the basin.

Conclusions

The studied samples do not have characteristics of potentially hydrocarbon-generating rocks, since the indicative parameters did not show relatively considerable results, and this may be a result of the high thermal maturity to which the organic matter was subjected.

Acknowledgements

The authors are grateful for the ongoing R&D project “Geochemical Characterization of Stratigraphic Well 2-ANP-6-MT, Parecis Basin: Implications for the Assessment of Petroleum Systems”, sponsored by Petrobras under the ANP R&D application as “Investment Commitment” with Research and Development”; and to the National Council for Scientific and Technological Development (CNPq), for the Ismael Ramos scholarship.

References

[1] Tissot, B.P.; Welte, D.H. 1984. **Petroleum formation and occurrence:** a new approach to oil and gas exploration. 2nd Edition. Berlin: Springer Verlag.

[2] Peters, K.E.; Cassa, M.R.1994. Applied source rock geochemistry. *In*: **THE PETROLEUM SYSTEM-FROM SOURCE TO TRAP**. TULSA, OKLA. USA: American Association of Petroleum Geologists Memoir, 60, 93-117.

[3] Espitalié, J.; Deroo, G.; Marquis, F. 1986. La pyrolise Rock-Eval et ses applications. **Revue de l’Institute Français du Pétrole**, 40, 563-579.

[4] Mukhopadhyay, P.K.; Wade, J.A.; Kruge, M.A. 1995. Organic Facies and Maturation of Jurassic/Cretaceous Rocks, and Possible Oil-Source Correlation Based on Pyrolysis of Asphaltenes, Scotian Basin, Canada. **Organic Geochemistry**., 22, 85-104.

XVI LATIN AMERICAN CONGRESS ON ORGANIC GEOCHEMISTRY
9 - 11 AUGUST, 2023
ARACAJU, SERGIPE, BRAZIL

HABITAT OF THE GASEOUS HYDROCARBONS IN THE AUSTRAL BASIN, CONTINENTAL SECTOR (ARGENTINA).

DAMIÁN VILLALBA[a] / HÉCTOR J. VILLAR[a] / DAMIÁN M. JAIT[b] / MARTÍN F. CEVALLOS[b]

[a]GEOLAB SUR S.A. / [b]CGC S.A.

damian.villalba@geolabsur.com

Introduction

Given the limited chemical components in a gas system, the research of a gas accumulation depends on the distribution of the light hydrocarbons and their isotopic composition. Despite that, the analytical results contain rich geochemical data in terms of the petroleum system. This study is aimed to understand the gas reservoirs behavior: the source, the thermal maturity and the migration pattern. Palermo Aike Inferior Fm. (PAI) is the main source rock in the basin, characterized by a moderate-good quality organic content described as a marine Type II to II/III kerogen.

Experimental

The project is based on twenty-seven reservoir gas samples, with compositional analyses of hydrocarbons for C_1-C_5. Twelve samples gathered isotopic $\delta^{13}C$ value from C_1 to C_5 and for δ^2H in CH_4 and the other fifteen samples, $\delta^{13}C$ for C_1-C_3. Composition was acquired in a Shimadzu 2014 Gas Chromatograph, equipped with both thermal conductivity (TCD) and flame ionization (FID) detectors. Carbon isotope and deuterium composition were online acquired with GC-C-IRMS systems.

A previous geochemical basin model for the Austral Basin, continental sector, was performed (GeoLab Sur – CGC) on the basis of a multi-1D of forty-seven modeled wells combined with several structural grids into a pseudo-3D model. The outcomes for source rock evolution, thermal maturity distribution and geological timing are the platform for the petroleum system discussions in this article.

Results and Discussion

Composition: in general, all of the samples show very low atmospheric air (N_2 < 2.7%) and methane is the most abundant component varying between 73 and 95%. The resulting fluid characterization typified eighteen samples as wet gas (probably associated to light oils or condensates) and nine samples as very wet gas (probably associated to medium gravity oils; Haworth et al., 1985).

Isotopes ratio: $\delta^{13}C$ in methane ranged from -53 to -33‰ indicating a wide range of origin and of thermal maturity stage; this variability is indicating mixing of thermogenic and biogenic gases. However, in higher carbon number the $\delta^{13}C$ variety is smaller: -31 to -26‰ in C_2, -28 to -24‰ in C3, pointing to reduced genetic sources.

According to Lorant parameters, all of the samples are from primary kerogen, meaning mainly thermogenic origin from the source rock; C_2/C_3 ratio from 0.8 to 3.3 and $\delta^{13}C$ C_3-C_2 from 0 to 3. The Bernard ratio $C_1/(C_2+C_3)$ vs. $\delta^{13}C$ in methane is indicating mainly thermogenic origin, possible kerogen mixing and biogenic mixing tendency.

The isotopic variation of δD in CH_4 resulted in a range from -230 to -152‰ which, compared with $\delta^{13}C$ methane, also denotes variation in the genesis of gases from thermogenic to biogenic mixture (Whiticar, 1999), as well as a different thermal maturity range. (Schoell, 1983).

During the analysis of $\delta^{13}C$ variations between C_1 to C_5 in twelve samples and the variation between C_1 to C_3 in fifteen samples, the distribution of the inverse of the carbon number as proposed by Chung et al. (1988; Fig. 1), perceives the differences and similarities between the samples. First, two groups of samples outstand of apparently equivalent source rock but of greater and lesser thermal maturity. Second, the projection towards the high molecular weight indicates a range of original isotopic imprinting of -23 to -29‰, consistent with the value measured in a core sample with bulk kerogen of $\delta^{13}C$ of -27.5‰. Third, the biogenic admixture component is ~9% in LP.a-2 and ~47% in EaAF-05, for the less mature group; while for the other group of greater maturity, it is scarce to null. Fourth, in the case of AA-02 there is a negative deviation in methane, a possible indicator of mixing with a dry gas of greater thermal maturity.

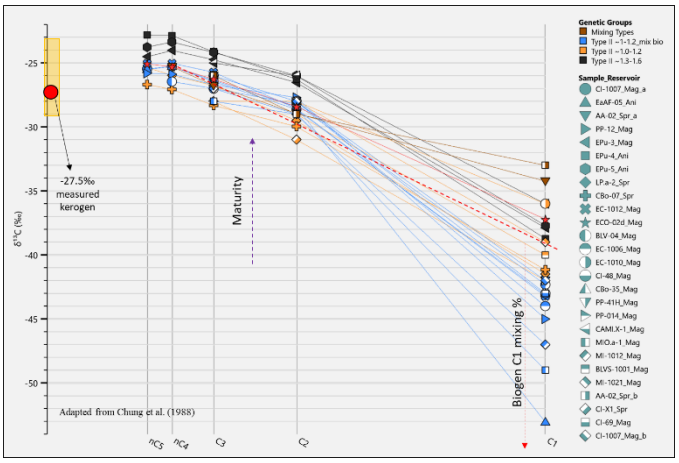

Figure 1. Natural gas plot (Chung et al., 1988).

The specific analysis of the $\delta^{13}C$ relationships between C_1, C_2 and C_3 according to Berner & Faber (1996), adjusted for the measured kerogen value of -27.5‰, shows a first group of ~1-1.2% maturity with high methane variability, a second group of greater maturity (~1.3-1.6%) and a third one that is suggested as a possible mixture with imported methane of greater maturity (Fig. 3). The ethane-propane co-genetic relationship correlates with a type II kerogen, where the groups are subdivided by thermal maturity apart from the methane influence.

Altogether, during the above analyzes three groups of samples are formed. Two of them with type II kerogen of greater and less maturity and a third with a possible mixture of kerogens. With this comes the analysis of the oil system and gas distribution in the basin (Fig.2).

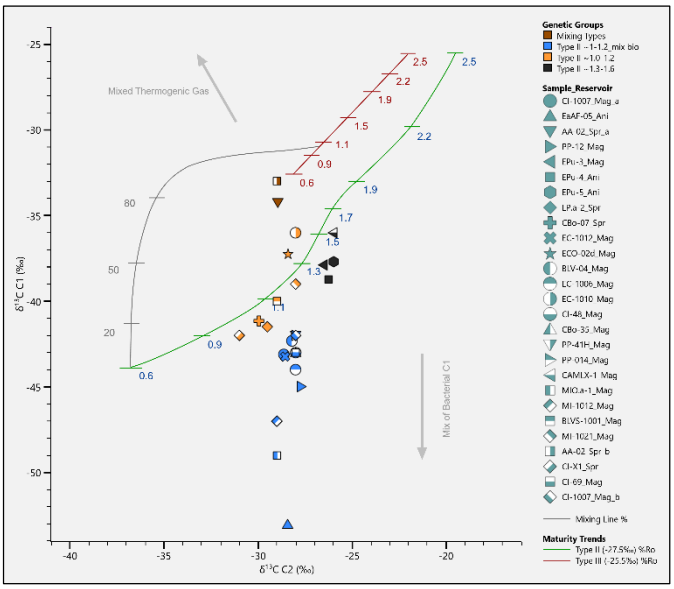

Figure 2. $\delta^{13}C$-C_2 vs $\delta^{13}C$-C_1 diagram. Type II set to -27.5‰ (adapted from Berner & Faber, 1996).

Conclusions

The distribution of the gases shows a particular relationship with the basin modeling and, together with the isotopic genetic analysis, the relationship with the petroleum system can be established and genetic groups proposed: Gas of type II origin, possibly PAI of moderate maturity (1.0 -1.2%); type II equivalent to the previous one but with marked input of methane of biogenic origin; type II of advanced maturity (~1.3-1.6%); type II mix with high maturity dry methane input. The regional preferential carrier of the basin is Springhill Fm. that is capable to connect the areas of greatest thermal maturity, in the direction of the basin depocenter (Fig. 3).

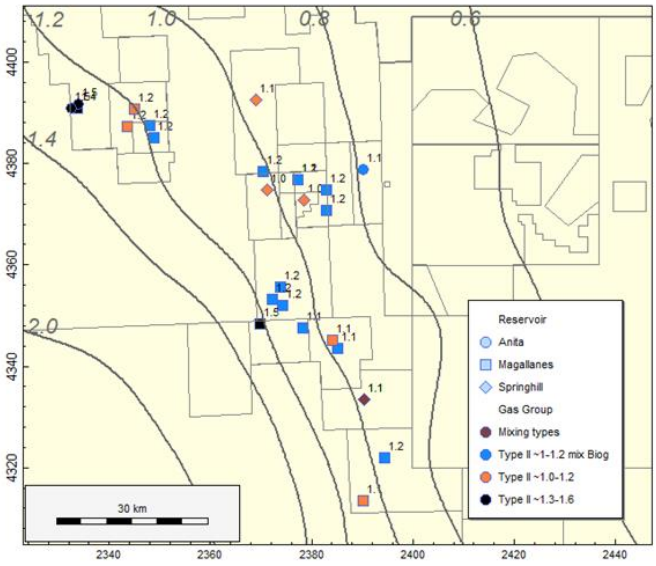

Figure 3. Map of the area. Black curves: modeled top PAI maturity.

Acknowledgements

The authors thank Compañía General de Combustibles S.A. (CGC) for allowing the data publication and support.

References

Berner, U. & Faber, E., 1996. Empirical carbon isotope/maturity relationships for gases from algal kerogens and terrigenous organic matter, based on dry, open-system pyrolysis, Organic Geochemistry **24**(10), 947–955.

Chung, H.M.; Gormly, J.R.; Squires, R.M., 1988. Origin of gaseous hydrocarbons in subsurface environments: Theoretical considerations of carbon isotope distribution, Chemical Geology **71**(1–3), 97–104.

Schoell, M., 1983. Genetic Characterization of Natural Gases, AAPG Bulletin **67** No. 12, 2225-2238.

Whiticar, M.J., 1999. Carbon and hydrogen isotope systematics of bacterial formation and oxidation of methane, Chemical Geology **161**(1), 291–314.

XVI LATIN AMERICAN CONGRESS ON ORGANIC GEOCHEMISTRY
9 - 11 AUGUST, 2023
ARACAJU, SERGIPE, BRAZIL

Deduction of Unconventional Formations Depositional Settings from Total Organic Carbon Determination Together with Pyrolysis measurements of Hydrocarbons Generation Potential and Residual Carbon

Albert Maende

Wildcat Technologies, LLC

albertmaende@wildcattechnologies.com

Introduction

Currently, detailed sedimentological descriptions of cores, outcrops or drilled cuttings samples supplemented with seismic data are required to be done before deduction of their applicable depositional setting can be determined. These detailed sedimentological descriptions require very specialized expertise as well as considerable time and in a number of instances, are not reproducible from one expert to another. Seismic data is often hard to come by and also requires certain processing techniques that at times are not easily reproducible.

This study seeks to provide an alternative methodology that can be used to deduce depositional settings of unconventional formations in a reproducible, quick and numbers based system that is not subject to the level of expertise or thinking process of the person who is doing the deduction. In this study, a total of fifteen unconventional formations have been analyzed for their total organic carbon (TOC) together with their pyrolysis measurements of hydrocarbons generation potential and residual carbon. These formations are; Cisco Canyon, Clear Fork, Cline, Jet Rock, Lias Shale, Low Wolfcamp, Woodford Outcrop, Middle Wolfcamp, Mowry Shale, Woodford Shale, Upper Spraberry Lime, San Andres, Skull Creek, Strawn and Upper Avalon. For each of the TOC and pyrolysis analyses of these fifteen unconventional formations, two graphic plots were done; these plots are that of residual carbon (S4CO2) versus hydrocarbons generation potential (S2) and the one of residual carbon normalized to TOC versus hydrocarbons generation potential normalized to TOC (Hydrogen Index). These pair of graphic plots for each of these fifteen unconventional formations were then interpreted to occur in five groups, each of which is representative of a unique depositional setting.

Experimental

Core, drill cuttings and outcrop samples were ground to 60 mesh size using a mortar and pestle and then an accurately weighed quantity of about 70 mg of each sample was analyzed on the HAWK Pyrolysis, TOC, and Carbonate Carbon instrument in two cycles; the first of which comprised of a pyrolysis run using helium as the carrier gas for a ramp rate of 25°C per minute initiated at an oven temperature of 100 °C and ran through to 650 °C whereby measurements of thermally vaporizable hydrocarbons (S1) as well as the hydrocarbons generated from the breakdown of kerogen (S2) were measured. In addition during this pyrolysis run, both carbon dioxide and carbon monoxide that were generated from organic matter, were measured as S3CO2 and S3CO respectively. On completion of the pyrolysis run, CO_2 free air was used as the carrier gas for the oxidation cycle for each of the samples whereby using a ramp rate of 25°C per minute, the samples were analyzed in an oven that was heated from 300 °C to 750 °C, with the measured residual carbon being recorded as S4CO2 and S4CO. Detection of the generated hydrocarbons during the pyrolysis run was done by using an FID (Flame Ionization Detector), while InfraRed (IR) detectors; IRCO and IRCO2, were used to measure the generated CO and CO_2 respectively. Total Organic Carbon (TOC) was summed up from all the organic carbon that was measured in both the pyrolysis and oxidation cycles.

Results and Discussion

Measurements of TOC, residual carbon (S4CO2), and hydrocarbons generated from the breakdown of kerogen (S2), were determined for fifteen unconventional formations, namely; Cisco Canyon, Clear Fork, Cline, Jet Rock, Lias Shale, Low Wolfcamp, Woodford Outcrop, Middle Wolfcamp, Mowry Shale, Woodford Shale, Upper Spraberry Lime, San Andres, Skull Creek, Strawn and Upper Avalon. Graphic plots of residual carbon (S4CO2) versus hydrocarbons generation potential (S2) and residual carbon normalized to TOC versus hydrocarbons generation potential normalized to TOC (Hydrogen Index), were then constructed for each of these fifteen unconventional formations and appeared as shown in the graphics below (Fig. 1).

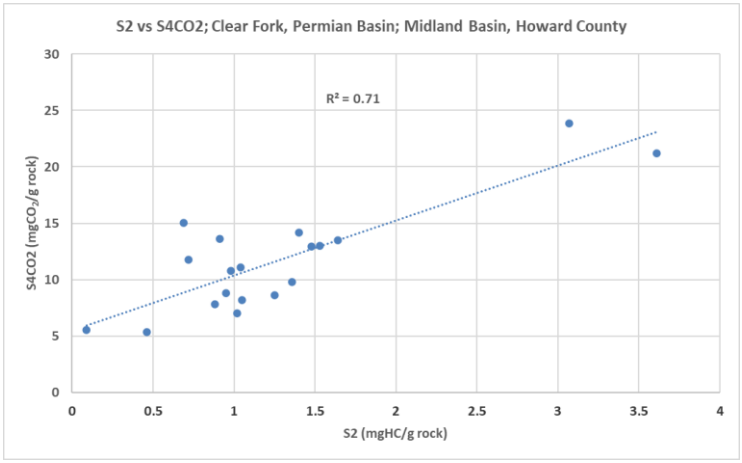

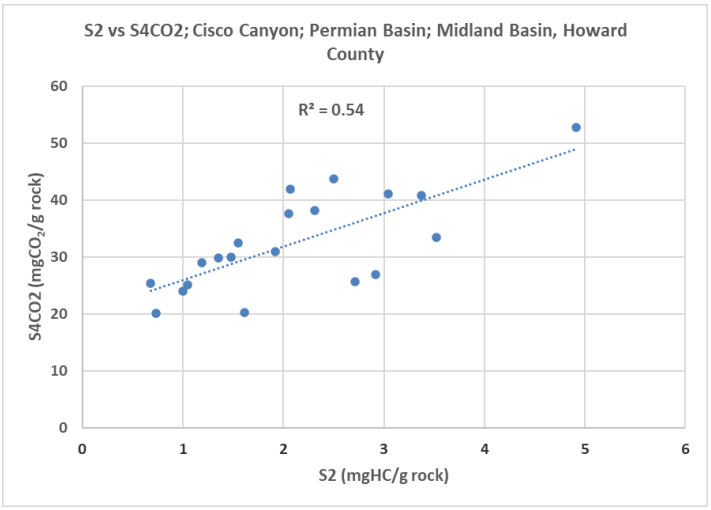

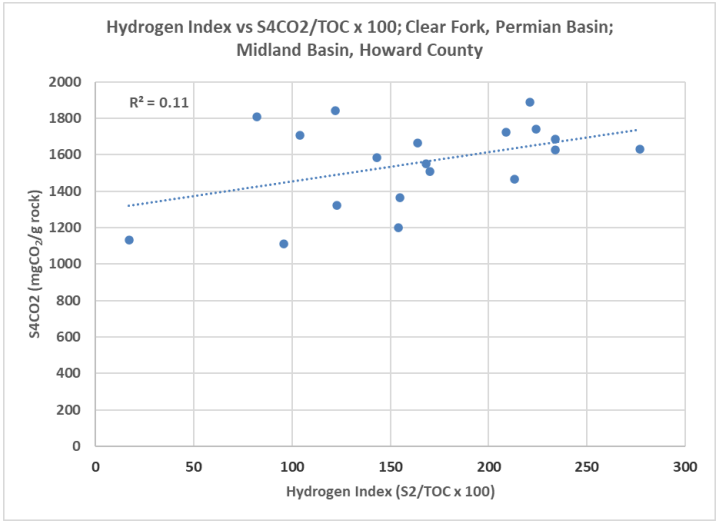

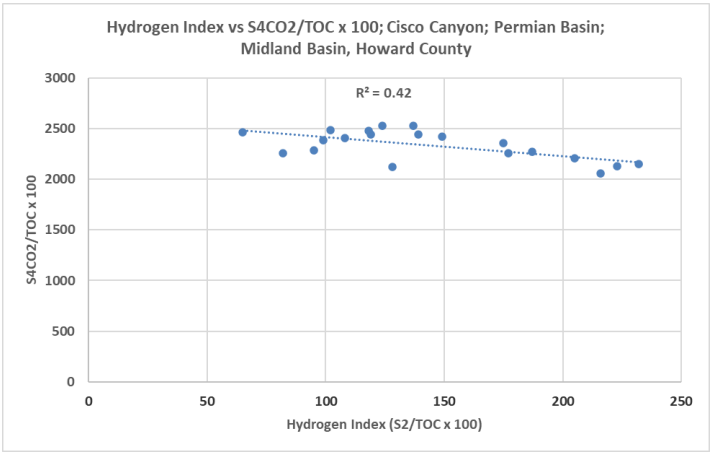

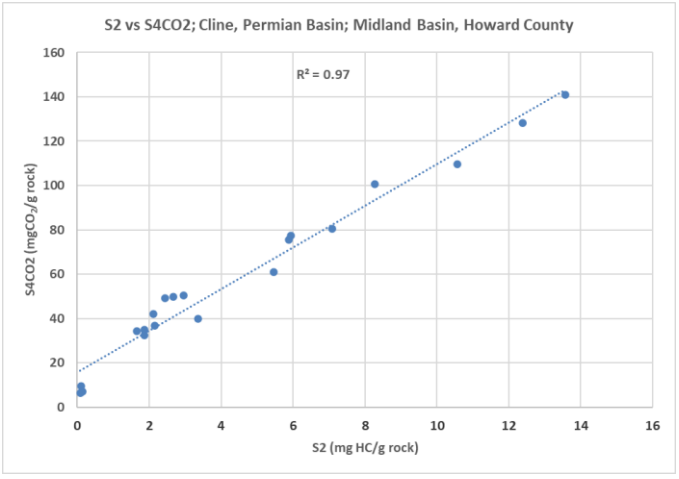

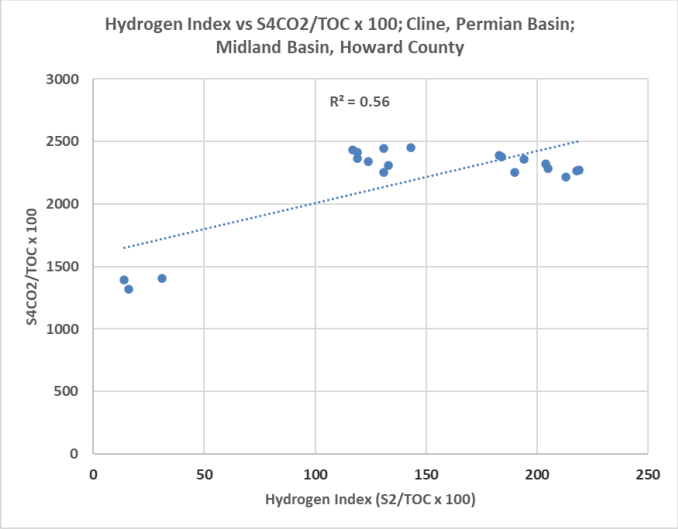
Hydrogen Index vs S4CO2/TOC x 100; Cline, Permian Basin; Midland Basin, Howard County
R² = 0.56
S4CO2/TOC x 100
Hydrogen Index (S2/TOC x 100)

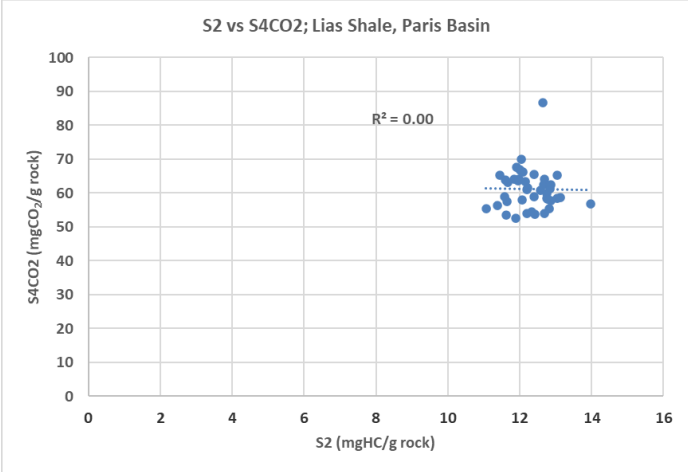
S2 vs S4CO2; Lias Shale, Paris Basin
R² = 0.00
S4CO2 (mgCO2/g rock)
S2 (mgHC/g rock)

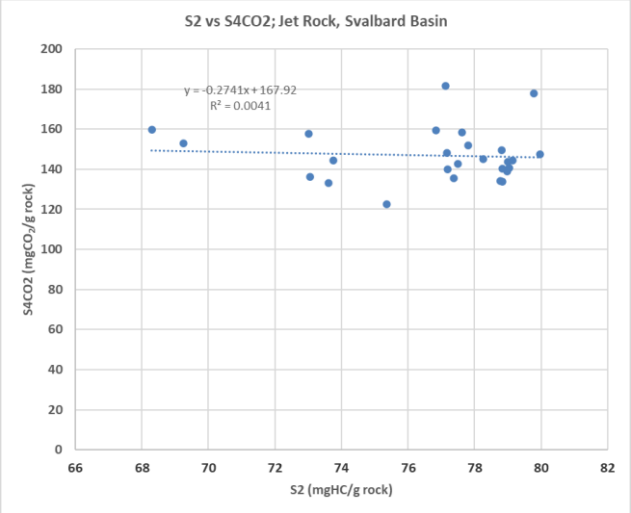
S2 vs S4CO2; Jet Rock, Svalbard Basin
y = -0.2741x + 167.92
R² = 0.0041
S4CO2 (mgCO2/g rock)
S2 (mgHC/g rock)

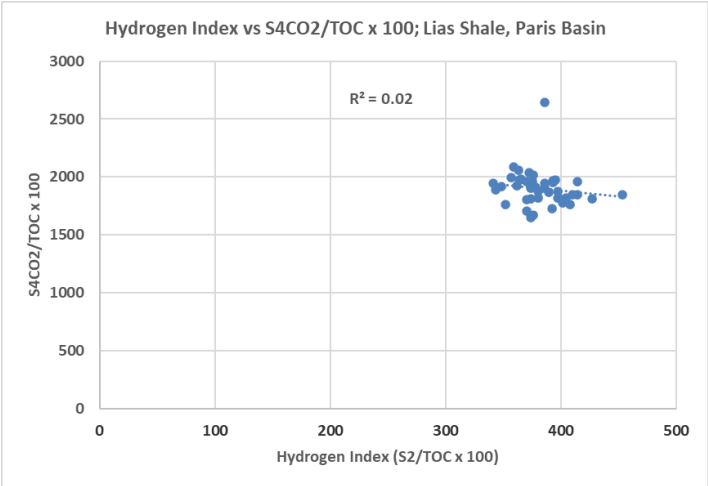
Hydrogen Index vs S4CO2/TOC x 100; Lias Shale, Paris Basin
R² = 0.02
S4CO2/TOC x 100
Hydrogen Index (S2/TOC x 100)

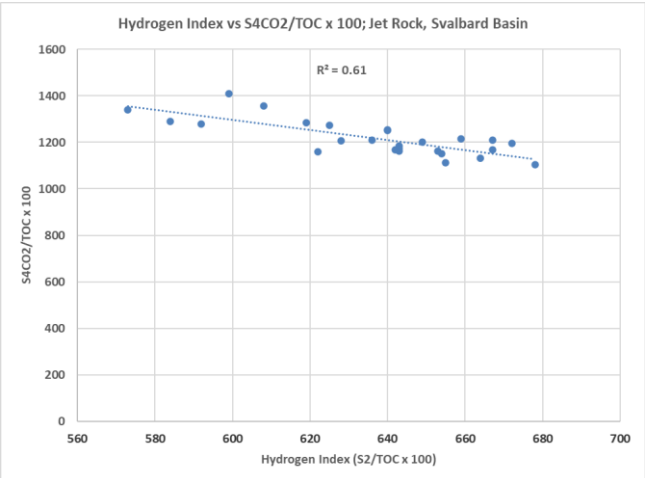
Hydrogen Index vs S4CO2/TOC x 100; Jet Rock, Svalbard Basin
R² = 0.61
S4CO2/TOC x 100
Hydrogen Index (S2/TOC x 100)

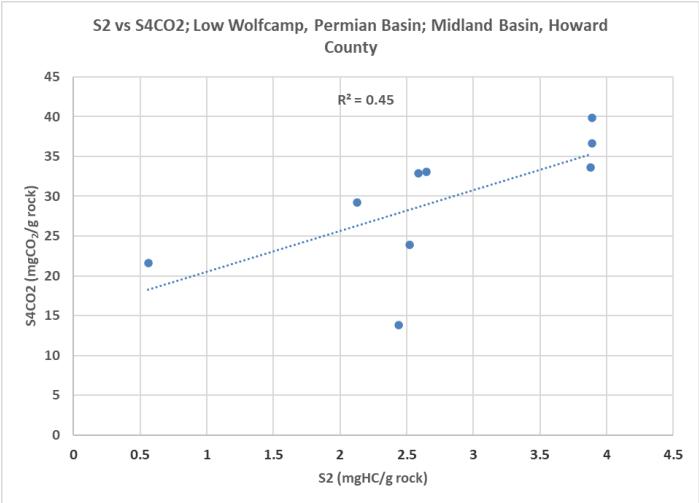
S2 vs S4CO2; Low Wolfcamp, Permian Basin; Midland Basin, Howard County
R² = 0.45
S4CO2 (mgCO2/g rock)
S2 (mgHC/g rock)

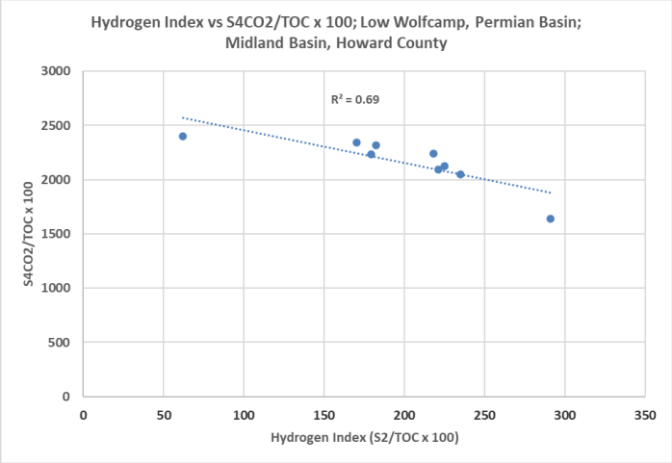
Hydrogen Index vs S4CO2/TOC x 100; Low Wolfcamp, Permian Basin; Midland Basin, Howard County
R² = 0.69
S4CO2/TOC x 100
Hydrogen Index (S2/TOC x 100)

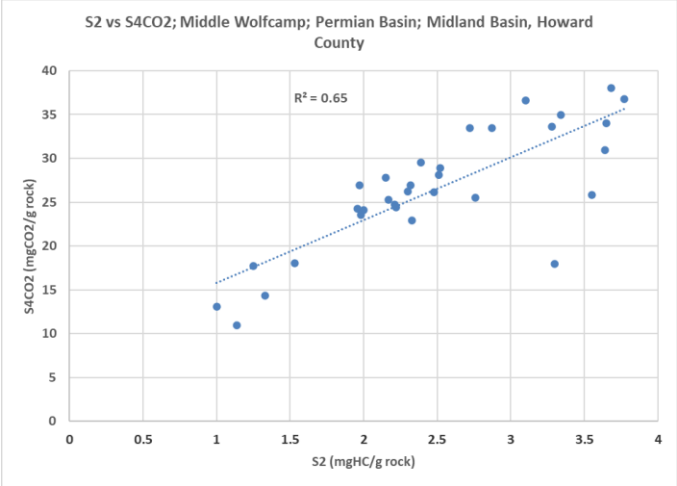
S2 vs S4CO2; Middle Wolfcamp; Permian Basin; Midland Basin, Howard County
R² = 0.65
S4CO2 (mgCO2/g rock)
S2 (mgHC/g rock)

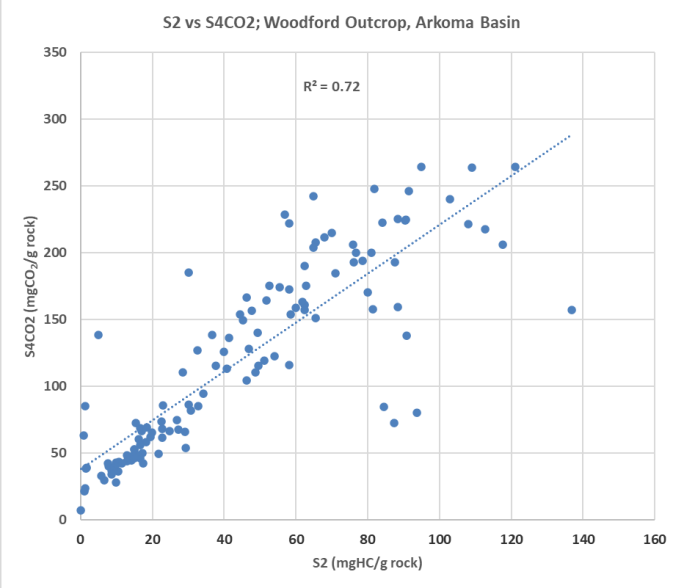
S2 vs S4CO2; Woodford Outcrop, Arkoma Basin
R² = 0.72
S4CO2 (mgCO2/g rock)
S2 (mgHC/g rock)

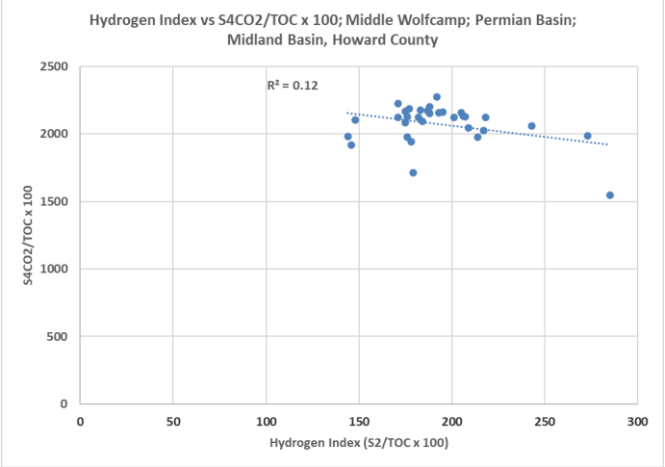
Hydrogen Index vs S4CO2/TOC x 100; Middle Wolfcamp; Permian Basin; Midland Basin, Howard County
R² = 0.12
S4CO2/TOC x 100
Hydrogen Index (S2/TOC x 100)

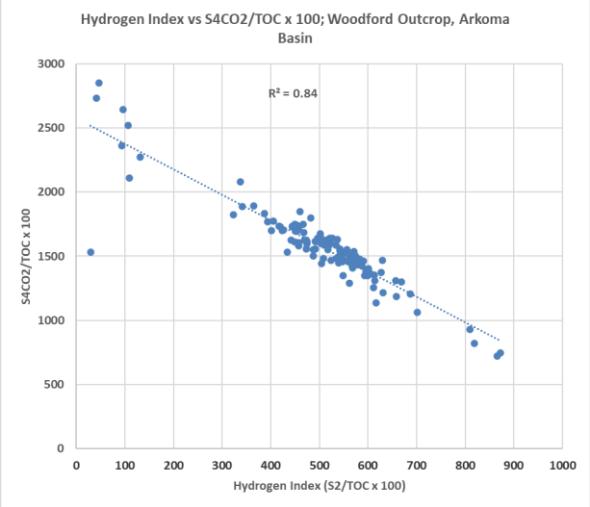
Hydrogen Index vs S4CO2/TOC x 100; Woodford Outcrop, Arkoma Basin
R² = 0.84
S4CO2/TOC x 100
Hydrogen Index (S2/TOC x 100)

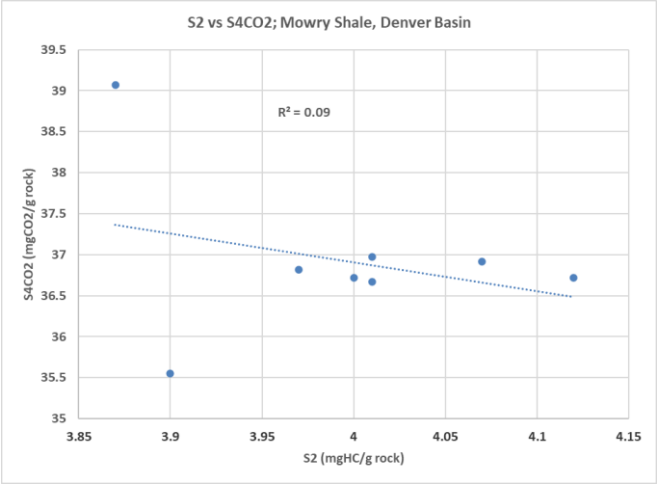
S2 vs S4CO2; Mowry Shale, Denver Basin
R² = 0.09
S4CO2 (mgCO2/g rock)
S2 (mgHC/g rock)

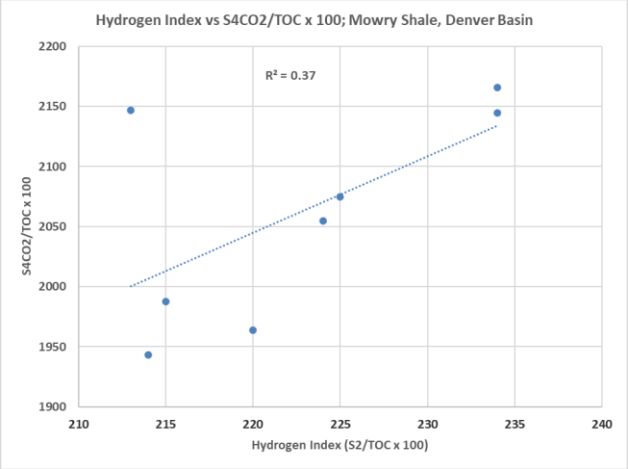
Hydrogen Index vs S4CO2/TOC x 100; Mowry Shale, Denver Basin
R² = 0.37
S4CO2/TOC x 100
Hydrogen Index (S2/TOC x 100)

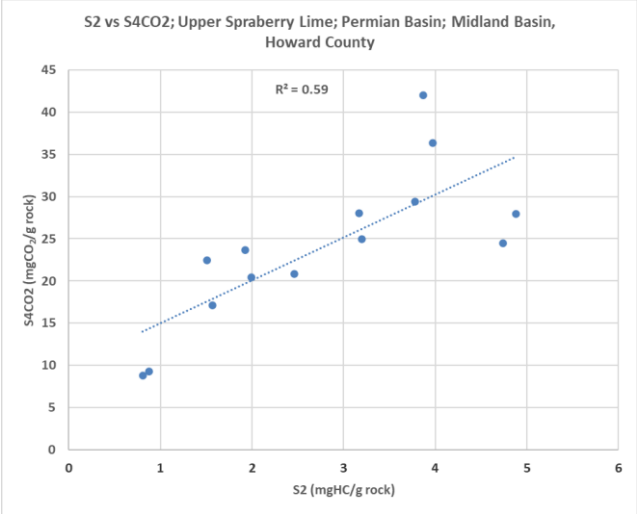
S2 vs S4CO2; Upper Spraberry Lime; Permian Basin; Midland Basin, Howard County
R² = 0.59
S4CO2 (mgCO2/g rock)
S2 (mgHC/g rock)

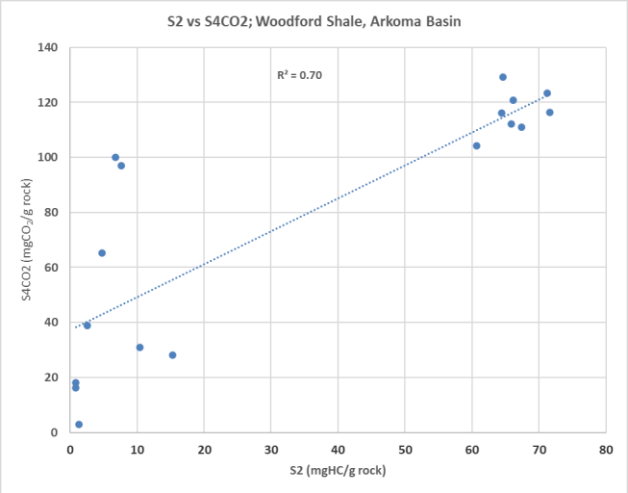
S2 vs S4CO2; Woodford Shale, Arkoma Basin
R² = 0.70
S4CO2 (mgCO2/g rock)
S2 (mgHC/g rock)

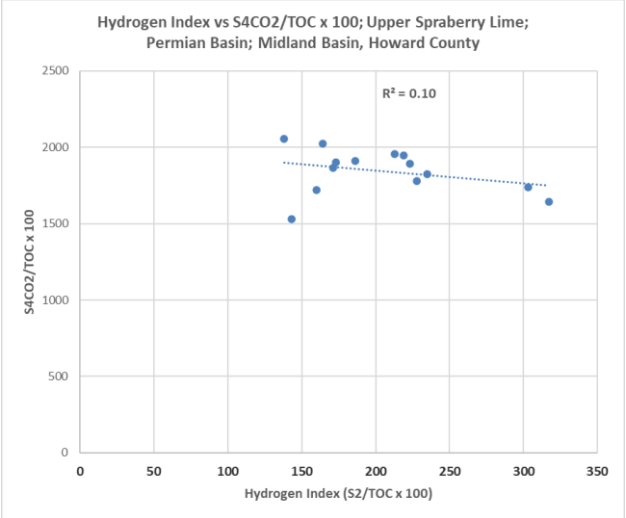
Hydrogen Index vs S4CO2/TOC x 100; Upper Spraberry Lime; Permian Basin; Midland Basin, Howard County
R² = 0.10
S4CO2/TOC x 100
Hydrogen Index (S2/TOC x 100)

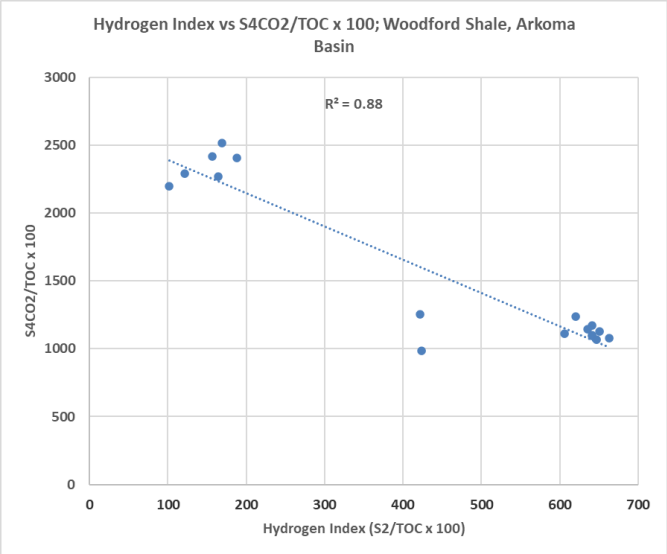
Hydrogen Index vs S4CO2/TOC x 100; Woodford Shale, Arkoma Basin
R² = 0.88
S4CO2/TOC x 100
Hydrogen Index (S2/TOC x 100)

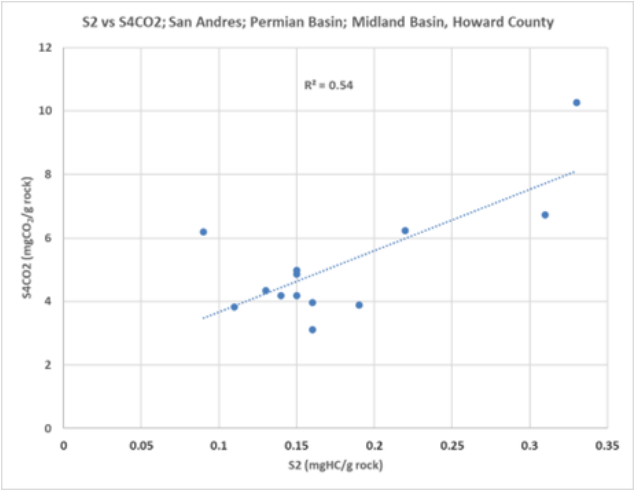
S2 vs S4CO2; San Andres; Permian Basin; Midland Basin, Howard County
R² = 0.54
S4CO2 (mgCO2/g rock)
S2 (mgHC/g rock)

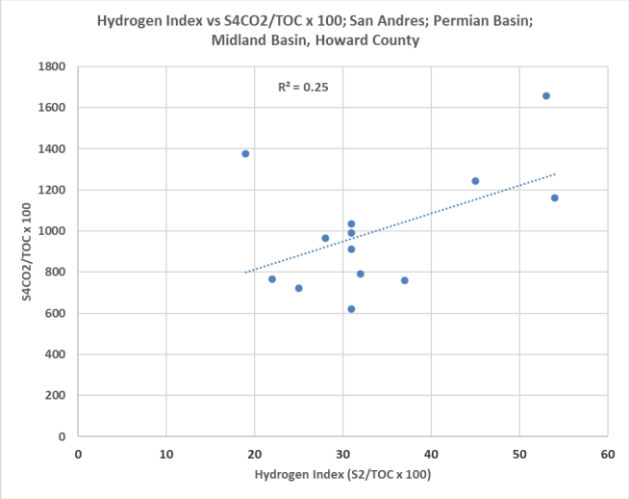
Hydrogen Index vs S4CO2/TOC x 100; San Andres; Permian Basin; Midland Basin, Howard County
R² = 0.25
S4CO2/TOC x 100
Hydrogen Index (S2/TOC x 100)

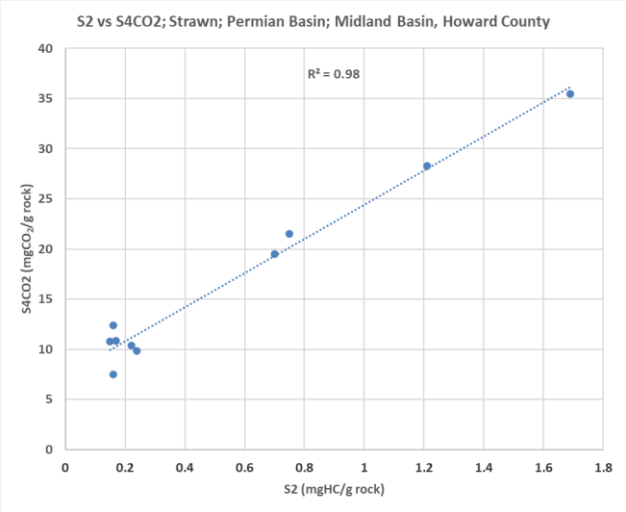
S2 vs S4CO2; Strawn; Permian Basin; Midland Basin, Howard County
R² = 0.98
S4CO2 (mgCO2/g rock)
S2 (mgHC/g rock)

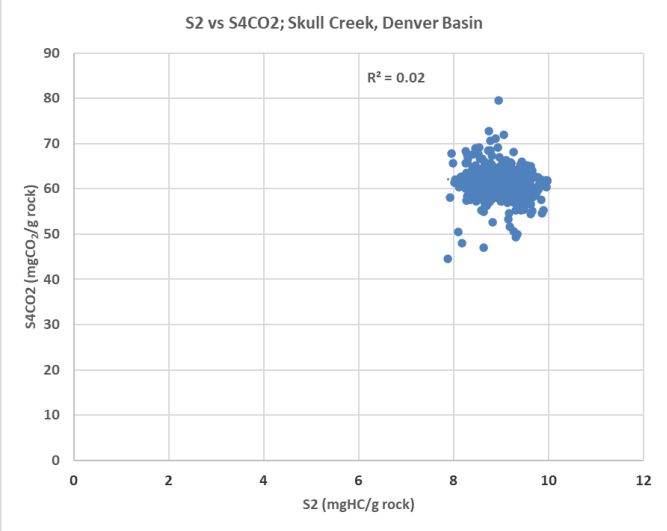
S2 vs S4CO2; Skull Creek, Denver Basin
R² = 0.02
S4CO2 (mgCO2/g rock)
S2 (mgHC/g rock)

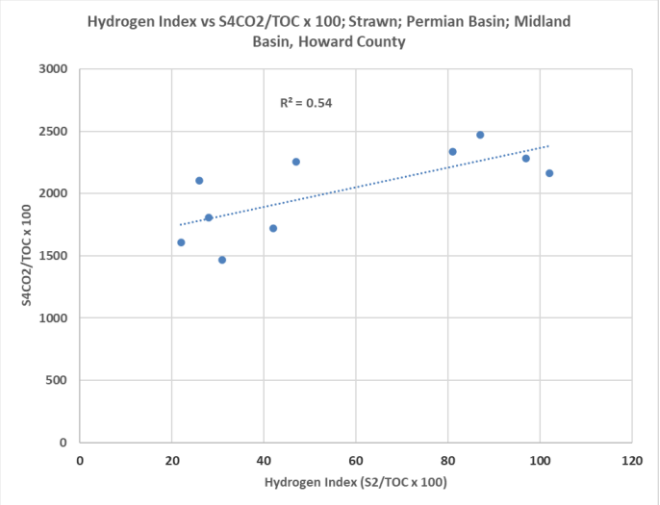
Hydrogen Index vs S4CO2/TOC x 100; Strawn; Permian Basin; Midland Basin, Howard County
R² = 0.54
S4CO2/TOC x 100
Hydrogen Index (S2/TOC x 100)

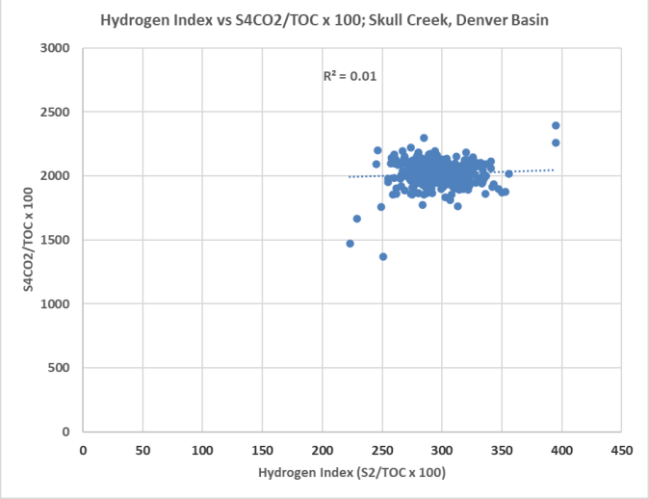
Hydrogen Index vs S4CO2/TOC x 100; Skull Creek, Denver Basin
R² = 0.01
S4CO2/TOC x 100
Hydrogen Index (S2/TOC x 100)

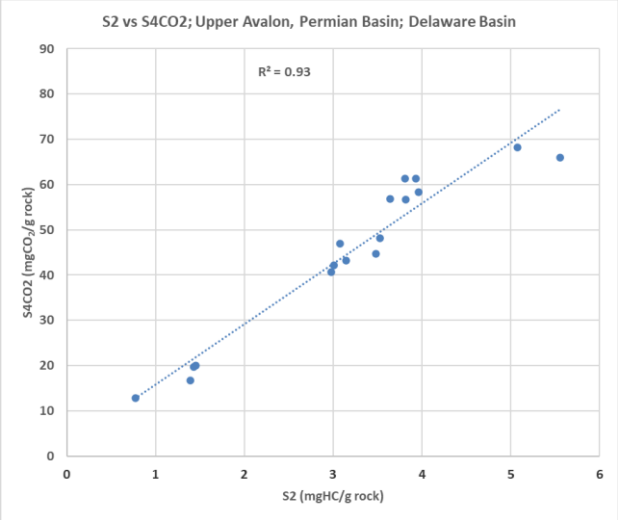

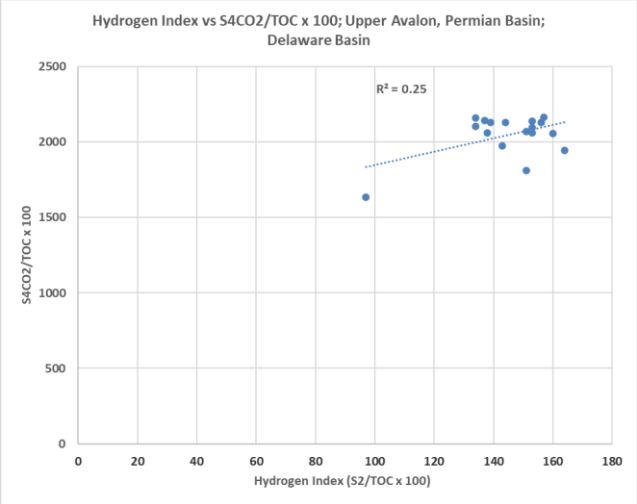

Figure 1.

Graphic plots of residual carbon (S4CO2) versus hydrocarbons generation potential (S2) and residual carbon normalized to TOC versus hydrocarbons generation potential normalized to TOC (Hydrogen Index), for fifteen unconventional formations.

The graphical plots that are depicted in Figure 1 are interpreted as being grouped into the five groups that are shown in table one below.

Formation	Basin	R^2 for S2 vs S4CO2 (i)	R^2 for HI vs S4CO2/10 x 100 (ii)	Formation Group
Cisco Canyon	Permian; Midland	0.54	0.41	B
Clear Fork	Permian; Midland	0.71	0.2	B
Cline	Permian; Midland	0.97	0.56	A
Jet Rock	Svalbard	0	0.61	C
Lias Shale	Paris	0	0.02	E
Low Wolfcamp	Permian; Midland	0.45	0.69	A
Woodford Outcrop	Arkoma	0.72	0.84	A
Middle Wolfcamp	Permian; Midland	0.65	0.12	B
Mowry Shale	Denver	0.09	0.37	D
Woodford Shale	Arkoma	0.7	0.87	A
Upper Spraberry Lime	Permian; Midland	0.6	0.1	B
San Andres	Permian; Midland	0.54	0.25	B
Skull Creek	Denver	0.02	0.01	E
Strawn	Permian; Midland	0.98	0.54	A
Upper Avalon	Permian; Midland	0.93	0.25	B

Note: R^2 is correlation coefficient

A) R^2 > or = 0.5 for (i) and (ii)
B) only (i) has R^2 > or = 0.5
C) only (ii) has R^2 > or = 0.5
D) only (ii) has R^2 > or = 0.3
E) R^2 < or = 0.05 for (i) and (ii)

Table 1.

The assigned five groups for the fifteen unconventional formations that were analyzed in this study.

The assignment of the five groups was based on the respective R^2 values for the two graphic plots that were generated for each of the fifteen unconventional formations. These are the graphic plots of residual carbon (S4CO2) versus hydrocarbons generation potential (S2) and residual carbon normalized to TOC versus hydrocarbons generation potential normalized to TOC (Hydrogen Index).

The depositional units that have been deduced for each of these fifteen unconventional formations are hereby categorized into five formation groups based on their respective R^2, as shown in Table 2 below.

Formation	Formation Group	Depositional Setting
Cisco Canyon	B	Foreland basin's shelf, reef, incised-valley, deltaic and slope (Ambrose and Hentz, 2019)
Clear Fork	B	Foreland basin's shelf sub-tidal, slope and basin carbonates (mudstones/wackestones), shales/mudstones plus turbidites (Molnar, 2015) and (Atchley *et. al*., 1999)
Cline	A	Foreland basin; an epicratonic foreland basin. Restricted seaway basin; sediment input to the basin comprised a combination of calcareous mudrocks and fine-grained siliciclastics (Peng *et. al.*, 2020).
Jet Rock	C	Distal shallow shelf and deep shelf major marine transgression; Svalbard Island rare outcrop of continental shelf in Norway, most of the continental shelf in Norway is presently deeply buried (Vajda and Wigforss-Lange, 2009)
Lias Shale	E	Intracratonic basin; restricted marine shale infill overlain by carbonate platform and underlain by sandstones and mudstones (Chatelier and Urban, 2010)
Low Wolfcamp	A	Foreland Basin's slope and basinal turbidites; siliceous and carbonate with the carbonate being detrital limestone sourced from a carbonate platform. Basinal siliceous mudstone (Richards *et. al*, 2023)
Woodford Outcrop	A	Failed Rift arm and platform; Deep marine basin overlying unconformity on top of a carbonate platform that was subject to erosional incision prior to Woodford Shale deposition; major transgression (McCullough and Slatt, 2015)
Middle Wolfcamp	B	Foreland Basin's slope and basinal turbidites; siliceous and carbonate with the carbonate being detrital limestone sourced from a carbonate platform. Basinal siliceous mudstone (Richards *et. al*, 2023)
Mowry Shale	D	Intracratonic basin; detrital silciclastic input from cordilleran mountain range into restricted seaway, prograding delta, & quiet basin infill. Biogenic infill; fish scales and radiolarian tests. Volcanic input ((French *et. al*., 2022)
Woodford Shale	A	Failed Rift arm and platform; Deep marine basin overlying unconformity on top of a carbonate platform that was subject to erosional incision prior to Woodford Shale deposition; major transgression (McCullough and Slatt, 2015)
Upper Spraberry Lime	B	Foreland Basin's slope and basinal plus turbidites (Atchley *et. al*., 1999)
San Andres	B	Foreland Basin's carbonate platform (Atchley *et. al*., 1999)
Skull Creek	E	Intracratonic basin; silciclastic slope and basinal infill in restricted seaway (siliceous siltstones and mudstones), marine; bioclastic input basin infill (mudstones and siltstones) (Sullivan *et. al.*, 2023)
Strawn	A	Foreland basin's deltaic silisiclatics interfingering with carbonate platform carbonates. Also has platform to ramp carbonates, basinal carbonates and marine shale; fluvial delta and tidally influenced estuarine embayment, with fluvial delta depositing in estuary while tidal deltas inbetween the estuary and open sea, on a mixed carbonate-siliciclastic shelf. (Roberts *et. al.*, 2021)
Upper Avalon	B	Foreland basin's slope and basinal turbidite siliciclastic and calcareous deposits (Hurd *et. al*., 2018)

Table 2.

Deduced depositional units for the fifteen unconventional formations categorized into five formation groups

The fifteen unconventional formations that were analyzed for this study have been categorized into five depositional units, namely; A, B, C, D and E as described in Table 2. A comprises of Foreland Basin's restricted seaway, slope and basinal turbidites, together with failed rift arm and platform. B comprises

of Foreland Basin's shelf subtidal together with slope and basinal turbidites. C consists of a shallow shelf and deep shelf marine transgression. Both D and E comprise of intracratonic basins.

Conclusions

This study seeks to provide an alternative methodology that can be used to deduce depositional settings of unconventional formations in a reproducible, quick and numbers based system that is not subject to the level of expertise or thinking process of the person who is doing the deduction.

In this study, a total of fifteen unconventional formations have been analyzed for their total organic carbon (TOC) together with their pyrolysis measurements of hydrocarbons generation potential and residual carbon. These formations are; Cisco Canyon, Clear Fork, Cline, Jet Rock, Lias Shale, Low Wolfcamp, Woodford Outcrop, Middle Wolfcamp, Mowry Shale, Woodford Shale, Upper Spraberry Lime, San Andres, Skull Creek, Strawn and Upper Avalon. For each of the TOC and pyrolysis analyses of these fifteen unconventional formations, two graphic plots were done; these plots are that of residual carbon (S4CO2) versus hydrocarbons generation potential (S2) and the one of residual carbon normalized to TOC versus hydrocarbons generation potential normalized to TOC (Hydrogen Index). These pair of graphic plots for each of these fifteen unconventional formations were then interpreted to occur in five groups, each of which is representative of a unique depositional setting.

The assignment of the five groups was based on the respective R^2 values for the two graphic plots that were generated for each of the fifteen unconventional formations. These are the graphic plots of residual carbon (S4CO2) versus hydrocarbons generation potential (S2) and residual carbon normalized to TOC versus hydrocarbons generation potential normalized to TOC (Hydrogen Index).

The fifteen unconventional formations that were analyzed for this study were then categorized into five depositional units, namely; A, B, C, D and E. Whereby, A comprises of Foreland Basin's restricted seaway, slope and basinal turbidites, together with failed rift arm and platform. B comprises of Foreland Basin's shelf subtidal together with slope and basinal turbidites. C consists of a shallow shelf and deep shelf marine transgression, while both D and E comprise of intracratonic basins.

Acknowledgements

I am thankful to Wildcat Technologies, LLC for financing this study.

References

Ambrose, W.; Hentz, T. F., 2019. Outcrop to Subsurface Linkages, Canyon and Cisco Groups, Eastern Shelf of the Permian Basin. AAPG Bulletin, v. 104, No. 7 (July 2020), pp. 1593-1624.

Atchley, S. C.; Kozar, M. G.; Yose, L. A., 1999. A Predictive Model for Reservoir Distribution in the Permian (Leonardian) Clear Fork and Glorieta Formations, Robertson Field Area, West Texas. AAPG Bulletin, v. 83, No. 7 (July 1999), pp. 1031-1056.

Chatellier, J-Y.; Urban, M., 2010. Williston Basin and Paris Basin, Same Hydrodynamics, Same Potential for Unconventional Resources?. AAPG Search and Discovery Article # 10291 (2010) Posted December 31, 2010.

French, K. L.; Birdwell, J. E.; Lillis, P. G., 2022. Geochemistry of the Cretaceous Mowry Shale in the Wind River Basin, Wyoming. GSA Bulletin; published online 11 November 2022. https://doi.org/10.1130/B36382.1

Hurd, G. S.; Kerans, C.; Frost, E. L.; Simo, J. A.; Janson, X., 2018. Sediment gravity-flow deposits and three-dimensional stratigraphic architectures of the linked Cutoff, upper Bone Spring, and upper Avalon system, Delaware Basin. AAPG Bulletin, v. 102, No. 9 (September 2018), pp. 1703-1737.

McCullough, B. J.; Slatt, R. M., 2015. Paleotopographic Control on the Variability of Woodford Shale strata Across the Southern Cherokee Platform Area of Central Oklahoma: a Mechanism for Increased Preservation-Potential of Organic Content. AAPG Search and Discovery Article # 51125 (2015) Posted August 18, 2015.

Molnar, P. S., 2015. Characterizing and Exploiting the "Clear Fork Shale" near the Midland Basin Margin in Eastern Andrews County, Texas. AAPG Search and Discovery Article # 110211 (2015) Posted August 31, 2015.

Peng, J.; Milliken, K. L.; Fu, Q.; Janson, X.; Hamlin, H. S., 2020. Grain Assemblages and diagenesis in organic-rich mudrocks, Upper Pennsylvanian Cline shale (Wolfcamp D), Midland Basin, Texas. AAPG Bulletin, v. 104, No. 7 (July 2020), pp. 1593-1624.

Richards, H. B.; Wehner, M.; Pope, M. C.; Donovan, A. D., 2023. An integrated chemostratigraphic and sequence stratigraphic analysis of extended (>1000 ft) lower Permian Wolfcamp cores, Reagan County, southern Midland Basin. AAPG Bulletin, v. 107, No. 5 (May 2023), pp. 823-847.

Roberts, A. K.; Ambrose, W. A.; Flaig, P. P.; Steel, R. J.; Olariu, C., 2022. Controls on facies variability and distribution during the Pennsylvanian glacial period from the lower Strawn Group, Fort Worth basin, Texas. AAPG Bulletin, v. 106, No. 8 (August 2022), pp. 1679-1702.

Sullivan, P. M.; Sonnenberg, S. A.; Hankins, B. T.; Hagadorn, J. W., 2023. Sedimentological and geochemical insights into the opening of the Cretaceous interior seaway: The Lower Cretaceous Skull Creek Formation, Colorado. AAPG Bulletin, v. 107, No. 5 (May 2023), pp. 761-784.

Vajda, V.; Wigforss-Lange, J., 2009. Onshore Jurassic Scandinavia and related areas, GFF, 131:1-2, 5-23, DOI: 10.1080/11035900902975309.
https://doi.org/10.1080/11035890902975309

XVI LATIN AMERICAN CONGRESS ON ORGANIC GEOCHEMISTRY
9 - 11 AUGUST, 2023
ARACAJU, SERGIPE, BRAZIL

Estimativa da maturação térmica equivalente das frações líquida e gasosa expulsas da rocha geradora e avaliação do processo cumulativo x instantâneo de preenchimento dos reservatórios do Campo de Mero e PAD de Libra Central

CAROLINE MARCHON CAETANO[1*]

[1]PETROBRAS

*carolcaetano@petrobras.com.br

Introdução

O Bloco de Libra está localizado na região Nordeste da Bacia de Santos, com uma área de 1.547 Km^2. Esse bloco é subdividido em setores: Noroeste, Central e Sudeste. O compartimento Noroeste, atualmente corresponde ao Campo de Mero, enquanto o Central e o Sudeste continuam em fase de Plano de Avaliação de Descobertas (PAD) (Rancan et al., 2018).

Para o Campo de Mero e o PAD de Libra Central foram estimadas as maturações térmicas, expressas pela reflectância da vitrinita equivalente (VReq). A partir dos fluidos coletados nos reservatórios, podemos inferir a VReq e obter os estágios de evolução térmica, que a rocha geradora foi submetida, durante a geração e expulsão dos hidrocarbonetos. Esses dados são utilizados como *input* para a calibração térmica nas simulações numéricas de modelagem de sistemas petrolíferos. E são essenciais, principalmente, em áreas exploratórias, onde não há informações de análises laboratoriais das seções geradoras.

A aplicação desse método também pode ser utilizada para o entendimento dos processos de migração e preenchimento de rochas reservatório. Por meio da verificação dos parâmetros de maturação de óleo e gás, é possível averiguar se a acumulação é composta por um fluido gerado em uma faixa de maturação térmica restrita, correspondendo ao aporte de uma carga instantânea, ou se as acumulações correspondem ao processo cumulativo, produto de vários pulsos, com diferentes níveis de maturação.

Métodos

Para a investigação da fração líquida do petróleo, a análise da maturação térmica equivalente foi realizada empregando-se os métodos descritos nas bibliografias indicadas: para os biomarcadores saturados e aromáticos (Peters et al., 2005), hidrocarbonetos poliaromáticos (HPAs) (Radke e Welte, 1983), diamantóides (Chen et al., 1996) e a análise da fração C_7 expressa pela razão do heptano versus isoheptano (Isaksen, 2004).

Na fração gasosa do petróleo, empregou-se o programa GOR-Isotopes 2.0 (GeoIsoChem), para cálculo das inversões da reflectância da vitrinita equivalente (VReq) e da temperatura equivalente (T°Ceq) do C_1, C_2, e C_3, aplicando uma taxa de aquecimento de 2°C/Ma.

Contexto Geológico

Os setores Noroeste, Central e Sudeste do Bloco de Libra são individualizados por compartimentos estruturais e atravessados por duas feições lineares maiores em nível de embasamento: a Zona de Transferência de Libra (ZTL, de direção NW-SE) e o Lineamento de Curitiba (LC, de direção WSW-ESE).

Os principais reservatórios são carbonáticos, com altos valores de permeabilidade. As rochas geradoras possuem um bom potencial gerador e são ricas em matéria orgânica amorfa. Rochas ígneas, do Cretáceo, intercaladas aos reservatórios, também foram constatadas.

Essas ígneas tiveram o seu magmatismo condicionado pela tectônica, que ocorre predominantemente na seção do pré-sal no Campo de Mero, nas seções do pré e intra-sal no PAD de Libra Central e nas seções do pré, intra e pós-sal no compartimento Sudeste. Os dados de poços sugerem que esta suíte ígnea está encaixada, em sua maior parte, nas rochas da Formação Itapema (Rancan et al., 2018).

Resultados e Discussões

A Tabela 1 sintetiza todas as informações sobre as estimativas de maturação térmica, com base nos fluidos estudados. Além de apresentar os dados das propriedades globais dos fluidos (ºAPI e RGO).

Examinando a Tabela 1 e a Figura 1 percebe-se que embora, o PAD de Libra Central seja portador de gás

condensado com RGO de 3000 m3/m3 (838 m3/m3, sem CO2), a fração pesada do petróleo registrou um grau de maturação térmica similar ao black oil do Campo de Mero (RGO de 232 m3/m3, sem CO2).

Campos	°API	RGO (m^3/m^3)	Estágio de geração de óleo	Req (óleo)Min - %	Req (óleo)Max - %	Req ($gásC_1$) - %	Req ($gásC_2$) - %	Req ($gásC_3$) - %
PAD de Libra	37	2797-3102 (838)*	Início de geração de óleo a geração de condensado/ gás úmido	0,56	1,65	4,8	1,8 (189 °C)	1,83 (190 °C)
Mero	27,5-28	400-460 (232)*	Início de geração de óleo a geração de condensado/ gás úmido	0,55	1,76	3,68 (255 °C)	1,97 (196 °C)	2,1 (202 °C)

* RGO sem CO_2

Tabela 1. Dados de maturidade térmica calculados de acordo com valores de VReq e T°Ceq estimada nos petróleos investigados. Fonte: Banco de dados da Petrobras.

Os indicadores de maturidade, investigados nos óleos de Mero e condensado do PAD de Libra Central, no que se refere aos biomarcadores saturados, apontam valores de até 0,8% de VReq. Na fração leve, os valores de VReq alcançam níveis de maturação maiores: os HPAs em Mero VReq de 0,87% e no PAD Libra Central VReq de 0,88%; os dados da fração C_7, indicam valores máximos de VReq de 1,12% para o PAD de Libra Central e 1,06% para Mero; Já as VReq referentes aos diamantóides, apresentam uma evolução térmica muito maior, com VReq chegando a 1,65% no PAD de Libra Central, e 1,57% em Mero, sugerindo a entrada posterior da fração leve, em relação a fração mais pesada, no processo cumulativo.

O gráfico da Figura 1, correlaciona os valores de composição isotópica dos gases C_2, C_1 e C_3 com a VReq. Neste gráfico nota-se que o deslocamento da assinatura isotópica do metano, acima da curva de laboratório (construída, a partir da cinética da geradora Jiquiá), sugere a focalização de metano muito mais evoluído que o etano e o propano. Destaca-se que, no PAD de Libra Central, apesar do metano está ainda mais evoluído do que os gases metanos encontrados em Mero, os gases úmidos do PAD de Libra Central possuem o mesmo grau de evolução térmica que os de Mero. Indicando gases úmidos cogenéticos, que receberam um aporte de metanos mais pesados. Em Mero e no PAD de Libra Central, esses aportes acontecem em escalas diferentes, sendo no PAD de Libra Central mais intenso.

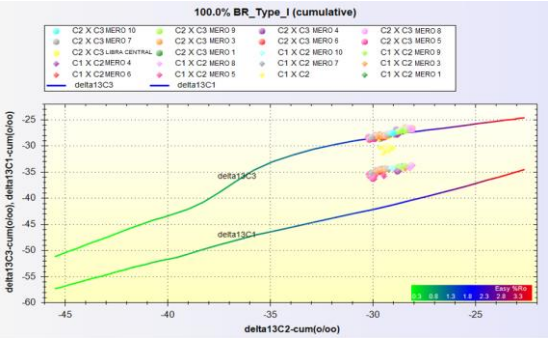

Figura 1. Relação entre δC_2 x δC_1 e δC_3 e a VReq, calculada no programa GOR-isotopes 2.0 para gases associados do Campo de Mero e PAD de Libra Central. Os poços do Campo de Mero estão codificados.

Confirmando o processo cumulativo de suprimento das cargas, a fração gasosa registra grau de maturação térmica ainda bem mais elevado. Em Mero, constata-se valores de VReq de C_2 e C_3: VReq ~2% -200 °C e o C_1 VReq de 3,68 – 255 °C. No PAD de Libra Central, a VReq atinge C_2 e C_3: Roeq ~1,8% -190 °C e o metano alcança VReq de 4,8%, assinalando janela de gás seco.

Conclusões

Examinando as frações líquida e gasosa, pode-se concluir que, a rocha geradora foi submetida a um amplo intervalo de estágios de geração dos fluidos, registrando um processo cumulativo do início da geração do óleo até a geração de gás seco, revelando um complexo sistema de preenchimentos nas acumulações estudadas, com saltos no estágio de maturação térmica entre os registros da fração líquida e o da fração de condensado e gases. Importante ressaltar, que o gás metano apresenta assinatura ainda muito mais evoluída em relação aos gases úmidos amostrados.

Para esses valores anomalamente altos de maturação térmica, com VReq de 3,7% e 4,8%, que foram calculadas a partir da composição isotópica ($\delta^{13}C_1$) do Campo de Mero e para o PAD de Libra Central, interpreta-se duas hipóteses: 1) gases derivados da maturação instantânea, devido a geração *flash*, por rochas ígneas intrusivas nas rochas geradoras encaixantes; ou 2) gases de origem mantélica, relacionados ao aporte de CO_2 que alcançaram os reservatórios do pré-sal.

Agradecimentos

Os autores gostariam de agradecer à Petrobras pela liberação do trabalho e dos dados, especialmente às gerências da EXP/TPGG/TDGEO, EXP/AEXP/PEX1, EXP/PEN/AB e LIBRA/RESEE.

Referências

Dahl, J. E. et al., 1999. Diamondoid hydrocarbons as indicators of natural oil cracking. Nature, v. 399, n. 6731, p. 54.

Isaksen, Gary H. 2004.Central North Sea hydrocarbon systems: Generation, migration, entrapment, and thermal degradation of oil and gas. AAPG bulletin, v. 88, n. 11, p. 1545-1572

Peters, Kenneth E. et al., 2005. The biomarker guide. Cambridge university press, (Vol. 2).

Radke, M. 1983.The methylphenanthrene index (MPI): a maturity parameter based on aromatic hydrocarbons. Advances Organic Geochemistry p. 504-512.

Rancan, C. C. et al., 2018. ASPECTOS GEOLÓGICOS DO CAMPO DE MERO, BACIA DE SANTOS.

Rancan, C. C., et al., 2018. ROCHAS ÍGNEAS DO BLOCO DE LIBRA, BACIA DE SANTOS.

XVI LATIN AMERICAN CONGRESS ON ORGANIC GEOCHEMISTRY
9 - 11 AUGUST, 2023
ARACAJU, SERGIPE, BRAZIL

The importance of using local kinetics on modelling Petroleum Systems: Parnaiba Basin Atypical Petroleum System case study.

Lopes, H. A [1]**; Mio, E.** [1,2]

[1]**ENEVA SA;** [2] UFPR

henrique.lopes@eneva.com.br; eduado.demio@eneva.com.br

Introduction

The Parnaiba Basin is a cratonic basin of 600.000km^2 filled by a 3.5km sedimentary succession. The Devonian Shales of the Pimenteiras Formation are the main source rock interval and comprises four source rock intervals named A, B, C and D, A being the older and D the younger. All four intervals have not reached petroleum generation temperatures through overburden, but by the heat input from igneous intrusions. Therefore, all proven Parnaíba Basin' petroleum systems (PS) are atypical PS (Miranda *et al*. 2018). Thermal maturity varies and depends on the temperature of emplacement, thickness of igneous intrusions and how far they are from the four main source rock intervals within the Pimenteiras Formation. All these parameters will be referred as Source Rock (SR) – Sills Setting. The Atypical PSs are very sensitive to temperature on a local scale as the igneous intrusion-source rock interval may vary vertically and laterally.

Kinetics analysis allows explorationists to know the effects of changing pressure and temperature on the petroleum type that is generated from a given source rock. This kind of data is almost unique for each basin but may also vary geographically on the same source rock interval within a basin (Dolson *et al* 2014). The lack of publications on the Brazilian Paleozoic basins have forced PS modelers to use analogues of similar ages from different basins. Considering the sensibility of the atypical petroleum system, the new data acquired on two out of the four main source rock intervals increases the understanding on rate, conversion, type, and timing of the petroleum generation of the Atypical PS of the Parnaíba Basin. On consequence, PS modelling is more accurate and calibrated to the gas and gas/condensate fields on the basin and will be more precise for prospects evaluation.

Experimental

A screening workflow was performed on fourty one samples to select twelve samples for Bulk Kinetics Analysis and then two Compositional Phase Kinetics. Cutting samples were collected from two different wells from the four different Pimenteiras Formation source rock intervals for petroleum generation characteristics at the GeoS4 Lab. Firstly, based on TOC and Pyrolysis analysis, twenty-one samples were selected for organic petrographic analysis for thermal maturity levels estimation. Then, twelve samples were selected for Bulk Kinetics Analysis and two were selected for Compositional Phase Kinetics Analysis. Phase kinetics analysis were performed combining an open- and closed-systems.

Results and Discussion

The Pimenteiras Formation samples are organic lean to rich with TOC contents varying from 0.4 to 4%. Based-on Rock-Eval results, kerogens can be classified as Type III, with a few Type II-III. Regarding the organofacies classification of Horsfield (1989), the kerogens of the four source rock intervals plot along a trend typical of dominantly marine type II kerogen that indicates potential for paraffinic-naphthenic-aromatic (PNA) low wax petroleum generation. The samples are classified as aquatic to terrestrial on the phenol abundance diagram (Larter, 1984) and aromatic to aromatic-aliphatic intermediate on the kerogen type diagram (Eglinton *et al*. 1990). Thermal extract yields are low for all samples and consist mainly of a complex hydrocarbon mixture and no real presence of an unresolved complex mixture suggesting that biodegradation is not an issue. The maceral assemblage of the Pimenteiras Formation is homogeneous containing assemblages of alginate, vitrinite, zooclasts, amorphous, organic matter and bituminite. The mostly homogeneous composition yields a narrow activation energy distribution, >70% of the bulk reaction. Consequently, all samples show a steep increase in TR with increasing temperature and generate petroleum

(10-90% TR) over a narrow temperature interval (20-40ºC). The geologic onset (10% TR), T_{peak}, and end (90% TR) temperatures for petroleum generation are within the ranges 122-140°C, 137-154°C, and 142-170°C, respectively, indicating high thermal stabilities (Figure 1).

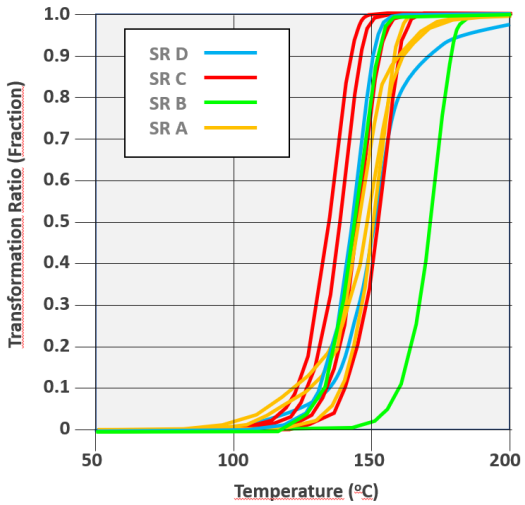

Figure 1. Transformation ratio curve.

The new kinetics data were used as input to PS models in two different scenarios: all source rocks with SR A kinetics (Figure 2B); and SR A & B with SR A Kinetics and SR C & D with SR C kinetics (Figure 2C). These two scenarios were compared with the previously used analogous kinetics scenario (Figure 2A) on a given gas field to see the impact of acquiring kinetics on multiple source rock levels. The main difference from the analogous kinetics model to the scenario with Parnaiba Basin kinetics was the gas column height calibration. The last was more accurate to the gas field column. Comparing the two scenarios using new kinetics data, the main improvement was on the fluid composition. When both kinetics analysis results were used, the fluid composition was better calibrated with the fluid composition of the gas field which is condensate rich.

Conclusions

The acquisition of kinetics data on the basin of interest is essential for PS modeling calibration. However, it has even more important role on atypical petroleum systems as the thermal variability is more heterogeneous and thermal dependent. The homogeneous composition, thermal resistant and narrow activation energy distribution of the Devonian shales of the Pimenteiras Formation has proved that the hydrocarbon can only be generated within a high temperature window (137-154°C) that only specific SR-Sill setting may provide.

In conclusion, the new acquired kinetics data were used to calibrate gas fields PS modelling and must be more accurate on pre-drilling evaluation of a prospect.

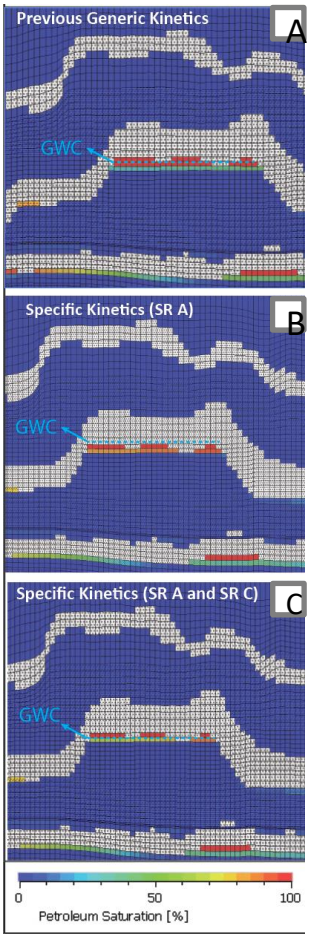

Figure 2. Petroleum Saturation of different PS model Scenarios of a given Gas Field

Acknowledgements

The authors thank Eneva SA for allowing to publish and the Brian Horsfield and Nicolaj Mahlstedt for performing the analysis at the GeoS4 Lab.

References

Dolson, J., et al. 2014. The discovery of the Barmer Basin, Rajasthan, India, and its petroleum geology. AAPG Bulletin v.99, no 3, pp. 433-465.

Eglinton, T.I., S et al.., 1990. Rapid estimation of the organic sulphur content of kerogens, coals and asphaltenes by pyrolysis-gas chromatography. Fuel 69, 1394-1404.

Horsfield, B., 1989. Practical criteria for classifying kerogens: Some observations from pyrolysis-gas chromatography. Geochimica et Cosmochimica Acta 53, 891-901.

Larter, S.R., 1984. Application of Analytical Pyrolysis Techniques to Kerogen Characterisation and Fossil FuelExploration/Exploitation, in: Voorhees, K. (Ed.), Analytical pyrolysis, methods and applications. Butterworth,London, pp. 212-275.

Miranda, F. S. et al. 2018. Atypical igneous-sedimentary petroleum systems of the Parnaíba Basin, Brazil: seismic, well Logs and cores. Geological Society, London, Special Publications, v. 472, n. 1, p. 341-360.

XVI LATIN AMERICAN CONGRESS ON ORGANIC GEOCHEMISTRY
9 - 11 AUGUST, 2023
ARACAJU, SERGIPE, BRAZIL

Occurrence of Immature Condensate in Biogenic Gas from Colombian Caribbean and its geological implications

André Luiz Durante Spigolon[a], Jarbas Vicente Poley Guzzo[a], Igor Viegas A. F. de Souza

[a] Division of Geochemistry, Petrobras Research and Development Center (CENPES), Av. Horácio Macedo, 950, Cidade Universitária, 21.941-915 Rio de Janeiro, RJ, Brazil

andrespigolon@petrobras.com.br

guzzo@petrobras.com.br

igorviegas@petrobras.com.br

Introduction

Offshore Colombia has been reported in the literature as having great potential for biogenic gas generation, mainly due to the large thickness and low thermal gradient of the sedimentary section (Katz and Williams, 2003).

Petroleum exploration in the Colombian Caribean relative to the Tayrona Block, located at Guarija Basin (Figure 1), has been taking place since 2004 with the drilling of 4 wells and the occurrence of two gas discoveries. The results of the molar and isotopic composition of these gases found in sandstone reservoirs suggest a biogenic origin with a predominance of isotopically light methane (dry gas; Spigolon et al., 2023). In the same way, the gas discoveries corresponding to Chuchupa and Ballena fields in the 70 decade have also been interpreted to have a biogenic origin (Rangel et al., 2003).

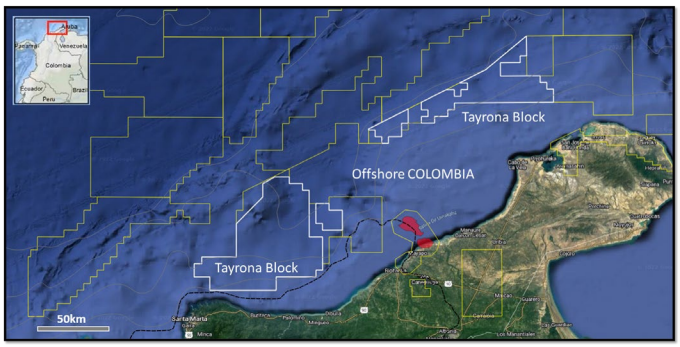

Figure 1 – Location map of the studied area in the Colombian Caribbean, Guajira Basin. Red area corresponds to Chuchupa and Ballena gas fields.

Associated with dry gas, small amounts of a liquid colorless to slightly yellowish occur (condensate), which were sampled for geochemical characterization in order to determine its origin and thermal evolution degree, for the better understanding of the Colombian petroleum systems in the offshore areas.

Material and Methods

Small amounts of condensate were extracted from the gas cylinders (PVT bottles) by cryogenic distillation for geochemical analysis.

The samples were submitted to a Gas Chromatography (GC) analysis to the identification of the main hydrocarbons ranging from 8 to 40 atoms of carbon (n-alkanes and some isoprenoids), through the chromatography in gaseous phase coupled to a Flame Ionization Detector (FID). A detailed characterization of the light compounds (C_{15-}) was done by GC-Carburane technique.

For biomarkers determinations, aliquots of the condensates were fractionated using a medium pressure liquid chromatography (MPLC) technique to provide saturated hydrocarbon fraction that was analyzed by a Gas chromatography-mass spectrometry (GC-MS) for hopanes and steranes compounds.

Results and Discussions

The geochemical analyses of GC, GC-Carburane and GC-MS indicate thermally immature and aromatic-naphthenic character for these condensates (Figures 2, 3 and 4). This interpretation is based on the following geochemical indicators: low abundance of n-paraffins, High concentration of aromatics (toluene> n-C8), Aromaticity = 6.16 (very high), Paraffinicity = 0.28 (very low), Isoheptane index = 0.42 (very low), Heptane index = 10.4 (very low), Pristane / n-C17 > 2,High proportions of moretanes, Homohopanes R> S and C29 steranes 20S / (20S + 20R) < 0.1.

In some samples, the high contamination by drilling fluid severely impacted the C_{15-} light compounds characterization given by GC-Carburane.

The richness of aromatic and naphthenic components between the light compounds (C_{15-}) and a high ratio of pristane/phytane (> 4) suggest an origin of the liquid fraction from a terrestrially derived organic matter (Type III kerogen (Figure 2 and 3), as documented by Connan and Cassou (1980).

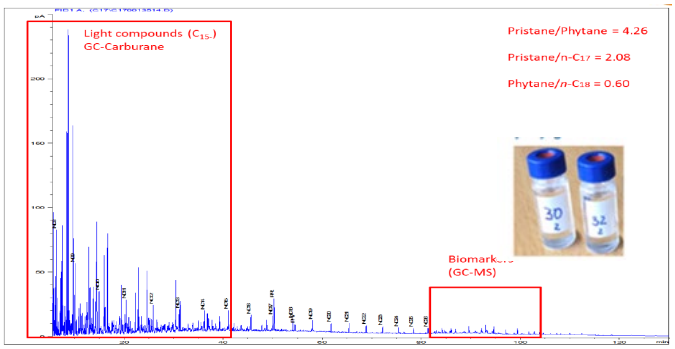

Figure 2. Gas chromatogram displaying the distribution of hydrocarbons in the condensates. The red rectangles represent the range of specific components analyzed by GC-Carburane and GC-MS.

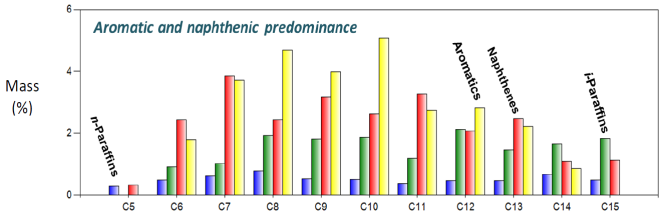

Figure 3. Results of light compounds (C_{15-}) based on GC-Carburane analysis.

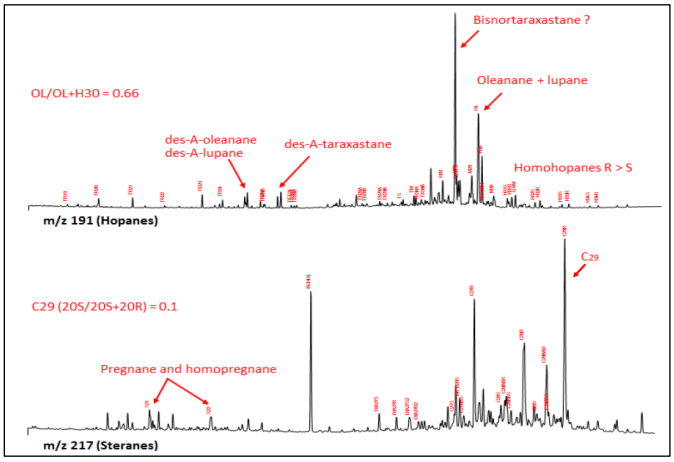

Figure 4. Biomarker composition of hopanes and steranes in the condensates.

The distribution of biomarkers in terms of hopanes and steranes confirms the thermal immaturity of the liquid fraction based on the predominance of thermally less stable compounds (or immature isomerization) like ββ and βα hopanes and ααα*R* steranes, and its origin from Type III organic matter (land-derived debris), as indicated by the presence of oleanane, des-A-oleanane, lupane, des-A-lupane and probably taraxastane and bicadinanes (Figure 4; e.g., Clayton, 1993).

This composition is compatible with immature rock extracts of the Cenozoic sedimentary section in the Offshore Colombia.

Immature condensates were initially described by Connan and Cassou (1980). These authors suggested that in almost cases, immature condensates are source controlled and are produced under mild thermal conditions from terrestrially derived organic matter. It is important mentioning that these condensates are associated with dry biogenic gas, as in the case this case.

Conclusions

The very low amount of condensate obtained from the gas cylinders presents an origin related to a terrestrially derived organic matter (Type III kerogen) based on the richness of aromatic and naphthenic components, high ratio of pristane/phytane (> 4) and the presence of oleanane, des-A-oleanane, lupane, des-A-lupane. The very low heptane and Isoheptane indices and the predominance of biological configuration of steranes (ααα20R) indicate a thermally immature condensate.

The recognition of petroleum-derived compounds (e.g. condensate) associated with biogenic gas is not something common in petroleum geochemistry that is documented in textbooks.

In terms of geological implications, the genesis of the liquid fraction (condensate) is compatible with the low thermal condition that the pelitic rocks were submitted, suggesting an in-situ formation. The gas captures the hydrocarbons produced by the host rock containing type III organic matter interbedded to the sandstone reservoirs.

Acknowledgments

The authors would like to thank Petrobras for the authorization to publish this work.

References

Clayton, J.L., 1993. Composition of crude oils generated from coals and coaly organic matter in shales. In: Law, B.E., Rice, D.D. (Eds.), Hydrocarbons from coal. AAPG Studies in Geology 38, 185–201.

Connan, J.; Cassou, A.M., 1980. Properties of gases and petroleum liquids derived from terrestrial kerogen at various maturatian levels. Geochemica et Cosmochimica Acta 44, 1-23.

Katz, B., Williams, K., 2003. Biogenic gas potential offshore Guajira peninsula, Colombia. In: C. Bartolini, R. T. Buffler, and J. Blickwede, (Eds.), The Circum-Gulf of Mexico and the Caribbean: Hydrocarbon habitats, basin formation, and plate tectonics. AAPG Memoir 79, 961–968.

Rangel, A., Kats, B., Ramirez, A., Santos Neto, E.V., 2003. Alternative interpretations as to the origin of the hydrocarbons of the Guajira Basin, Colombia. Marine and Petroleum Geology 20, 129-139.

Spigolon, A.L.D., Guzzo, J.V.P., Souza, I.V.A.F., Ferreira, A.A., Nakatsubo, C.K.V., 2023. New gas frontier of biogenic origin in the Colombian Caribbean. First EAGE Conference on Deepwater Equatorial Margin, Extended abstracts, Rio de Janeiro, Brazil.

ALB

SOURCE ROCK, OIL AND GAS CHARACTERIZATION

XVI LATIN AMERICAN CONGRESS ON ORGANIC GEOCHEMISTRY
9 - 11 AUGUST, 2023
ARACAJU, SERGIPE, BRAZIL

Paleoenvironment assessment of Irati Formation based on the semi-quantification of S-markers Fourier Transform Ion Cyclotron Resonance Mass Spectrometry

Lua Morena Leoncio de Oliveira[a]*, Antonio Fernando Queiroz[ab], Karina S. Garcia[ab], Olivia M.C de Oliveira[ab] , José Roberto Cerqueira[ac] ,Maria Elisabete Machado[ab], Thomas B.P. Oldenburg[d]

[a] Universidade Federal da Bahia, Instituto de Geociências, Programa de Pós-Graduação em Petróleo e Meio Ambiente, 40170-115, Salvador, BA, Brazil
[b]Rua Adhemar de Barros, s/n°, Instituto de Geociências, UFBA, Sala 303-A - Ondina, Salvador - BA, 40170-110
[c]Darcy Ribeiro North Fluminense State University (UENF), Macaé, RJ, 27930-000, Brazil
[d] PRG, Department of Geoscience, University of Calgary, Calgary, Alberta T2N 1N4, Canada
correspondência: lmleoncio@hotmail.com

Introduction

Organic sulfur compounds (S-markers) like benzothiophene (BT), dibenzothiophene (DBT) and benzonaphtothiophene (BNT) have been studied for years because they can provide essential information about thermal maturity, paleoenvironment, biodegradation and oil migration (Oliveira et al., 2023). S-markers have been employed especially because of their thermodynamic stability (Han et al., 2020). In recent years, Fourier Transform Ion Cyclotron Resonance Mass Spectrometry (FTICR-MS) has been used for the evaluation of heterocompounds from nitrogen, sulfur and oxygen (NSO) since it has high mass resolving power. Although FTICR-MS is a powerful analytical technique that allows the unequivocal analysis of tens of thousands compounds in a single analysis, qualitative assessment of the sulfur class was little used in the interpretation of the paleoenvironment. Paraná Basin is one of the most important Brazilian sedimentary basins. However, no published study has employed S-markers to assess the depositional paleoenvironment of Irati Formation, neither by GC-MS nor FTICR-MS. In the literature, little is reported about the quantification of the compounds from the analysis by FTICR-MS, most of the published articles reported results only in qualitative form. Therefore, the aim of the present study was to semi-quantify S-markers by FTICR-MS in APPI positive ion mode to assess the paleoenvironment of the Irati Formation, in the Paraná basin.

Experimental

Sixteen samples representing a profile of the Amaral Machado outcrop (base 4), middle (9) and top (3) from source rocks samples (bitumen) were analyzed without fractionation using an ultrahigh resolution 12 Tesla Bruker SolariX FTICR-MS. Samples were diluted to a final concentration of 50 mg mL^{-1} in toluene. 2.5 mg L^{-1} of dibenzothiophene- d_8 ($C_{12}D_8S$) was added to the samples and 0.028 mg L^{-1} of reserpine ($C_{33}H_{40}N_2O_9$) to ensure mass accuracy and assess internal calibration efficiency. APPI used a krypton lamp at 10.6 eV. The samples were introduced into the mass spectrometer using a syringe pump set to deliver 240 µl/h. The resolving power at 400 Da was > 500,000 (M/ΔMfwhm) and the mass accuracy was typically < 200 ppb (Oldenburg et al., 2014). The CaPa software (Aphorist Inc.) was employed for recalibration and peak assignments and the output data were visualized using the Ragnarök software (Aphorist Inc.). The specific information to ionization conditions are found in Oldenburg et al. (2014).

Results and Discussion

The DBT-d8 internal standard was applied in the semiquantification of sulfur compounds and the results found show that both the concentration and intensity have the same pattern in the S1 profile graphs, being perfectly possible to transform through the pattern, without changing the interpretation of the data. The bituminous extract analyzed is immature (Martins et al., 2020) As these are immature samples, the DBE variation occurs mainly due to the difference in paleoenvironment. In the samples from the base (AMA 1 and 5) the environment is hypersaline (Martins et al. (2021). In paleoenvironments typically poor in oxygen, sulfate reduction occurs and the supply of sulfide leads to an extensive incorporation of thiophene compounds into organic matter. Towards the top of the outcrop (AMA 27, 29 and 30) (Fig. 1a) there are the presence of terrestrial organic matter and a paleoenvironment rich in oxygen are the lowest concentrations of sulfur (Hughes et al., 1995). In the marine paleoenvironment samples, the most intense DBE group is 6 (likely benzothiophenes) and 7 ($C_{27\text{-}30}$ likely sulfurized steroidal structures) and 9 (likely dibenzothiophenes). On the other hand, in terrestrial samples (towards the top of the outcrop) the most intense DBE group is 9, 10 which could be naphthenodibenzothiophenes, acenaphthenothiophenes, or benzothiophenes with a phenyl group as a substituent (Hegazi et al., 2012), and 11. From the base to the middle of the outcrop a strong presence of C_{40} (Fig. 1b) species was observed in samples that have a strong contribution from marine and hypersaline paleoenvironment. A possible formation mechanism of these $C_{40}S_1$ compounds could be the intramolecular sulfurization of carotenoid molecules. Carotenoids contain numerous conjugated carbon-carbon double bonds that are readily to be

sulfurized or hydrogenated during early diagenesis (Zhang & Li, 2023).

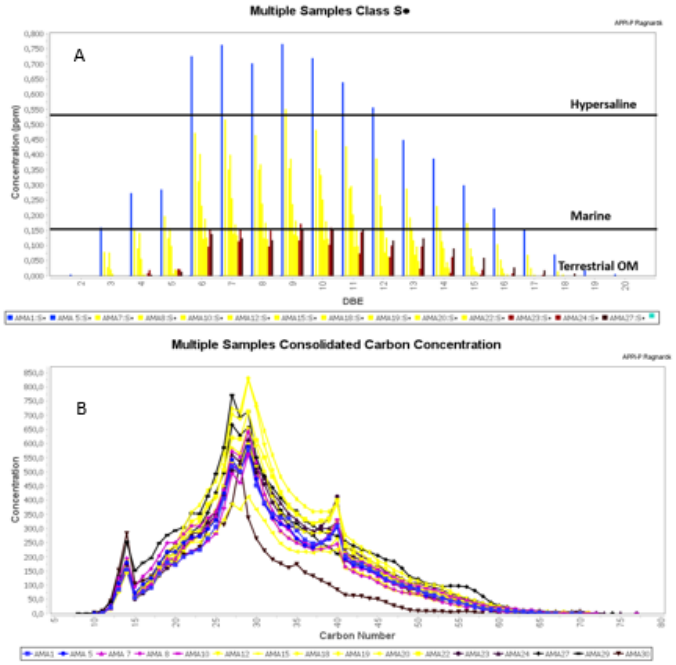

Figure 1. - Concentration of double bond equivalents (DBE) compound groups within S compound class (radical ions) analyzed in the APPI–P ion mode (a) and overall carbon number concentration of the samples (b).

In the Radar plot (Fig. 2), samples from the base of the outcrop (AMA 1, 5, 7 and 8) show a strong affinity with S/C ratio representing a hypersaline/marine environment. N/C is well represented in samples from the middle of the outcrop (from AMA 12 to AMA 24), which is likely due to great algae input (Baxby et al., 1994). Meanwhile, O/C has more affinity with the terrestrial organic matter samples, with high abundance of carboxylic acid groups (AMA 27, AMA 29 and AMA 30).

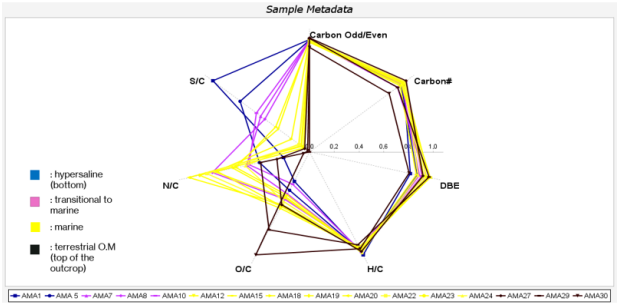

Figure 2. Radar plot showing the averaged compositional parameters derived from FTICR-MS data, including heteroatom (nitrogen, sulfur, and oxygen) to carbon ratios, carbon number and double-bond equivalent

Conclusions

The semiquantification results using the FTIRCMS are suitable for evaluating the paleoenvironment of the samples. At the base of the outcrop, a hypersaline paleoenvironment is evidenced. In paleoenvironments typically poor in oxygen, sulfate reduction occurs and hence the supply of sulfide, which leads to an extensive incorporation of thiophenic sulfur into OM. Towards the top of the outcrop the paleoenvironment is transformed with a greater presence of terrestrial OM and a paleoenvironment rich in oxygen and the lowest concentrations of sulfur due to freshwater input.

Acknowledgements

The authors gratefully acknowledge the support from Shell Brasil through the “Project Petroleum Systems Research in Brazilian Sedimentary Basins” Areas at Instituto de Geociências da Universidade Federal da Bahia (UFBA) - GEOQPETROL - PS” - ANP 20720-9 project and the strategic importance of the support given by ANP through the R&D levy regulation. We also thank CNPq/DAI (Brazilian research council) for fellowships, and PRG group at the University of Calgary for the use of the equipment and guidance given. Aphorist Inc. is thanked for providing the peak assignment software CaPA and the visualization software Ragnarök.

References

Baxby, M., Patience, R.L., & Bartle, K.D. The origin and diagenesis of sedimentary organix nitrogen. Journal of Petroleum Geology, v.17(2), p.211–230, 1994.

Han, J., Guo, X., Dong, T., He, S., Wang, Y., Wang, X., Hua, Y., Zhao, W., & Chen, J. Oil origin and secondary migration pathway in the Bonan sag, Bohai Bay Basin, China. Marine and Petroleum Geology, v.122, p.104702, 2020.

Hegazi, A.; Fathalla, E. M., Panda, S. K., Schrader, W.; Andersson, J. T. High-molecular weight sulfur-containing aromatics refractory to weathering as determined by Fourier transform ion cyclotron resonance mass spectrometry. Chemosphere, v.89(3), p.205–212, 2012.

Hughes, W.B.; Holba, A.G.; Dzou, L.I.P. The ratios of dibenzothiophene to phenanthrene and pristane to phytane as indicators of depositional environment and lithology of petroleum source rocks. Geochimica et Cosmochimica Acta, v.59(17), p.3581–3598. 1995.

Martins, C.M.S.; Cerqueira, J.R.; Ribeiro, H.J.P.S.; Garcia, K.S.; da Silva, N. N.; Queiroz, A.F.S. Evaluation of thermal effects of intrusive rocks on the kerogen present in the black shales of Irati Formation (Permian), Paraná Basin, Brazil. Journal of South American Earth Sciences, v.100, p. 102559, 2020.

Oldenburg, T.B.P.; Brown, M.; Bennett, B.; Larter, S.R. The impact of thermal maturity level on the composition of crude oils, assessed using ultra-high resolution mass spectrometry. Organic Geochemistry, v.75, p.151–168, 2014.

Oliveira, L.M.L.; Nery, D.; Lopes, K.F.A.; Santiago, C.; Mara, G.; Elisabete, M. Polycyclic aromatic sulfur heterocycles used as molecular markers in crude oils and source rocks. Organic Geochemistry, v.178, p.104571, 2023.

Shi, Q.; Hou, D.; Chung, K.H.; Xu, C.; Zhao, S.; Zhang, Y. (2010). Characterization of heteroatom compounds in a crude oil and its saturates, aromatics, resins, and asphaltenes (SARA) and non-basic nitrogen fractions analyzed by negative-ion electrospray ionization fourier transform ion cyclotron resonance mass spectrome. Energy and Fuels, v.24(4), p. 2545–2553, 2010.Zhang, H.; Li, S. GC–MS and ESI FT-ICR MS characterization on two type crude oils from the Dongying depression. Fuel, v.333, p.126408, 2023.

Changes on molecular structure during artificial maturation of kerogen from the Neuquen Basin, Argentina

JORGE DONADELLI*, GERARDO MARTINEZ DELFA, SMAL CLARA

YPF Tecnología S.A., Avenida del Petróleo s/n (entre 129 y 143), (1923) Berisso, Buenos Aires, Argentina

*correspondence: jorge.a.adonadelli@ypftecnologia.com

Introduction

Buried organic matter responsible for hydrocarbon generation (kerogen) suffer several changes in its molecular structure after being exposed to reservoir temperature. These changes can be accelerated by exposing kerogen to higher temperatures in an inert atmosphere, allowing hydrocarbons generation and molecular alterations in just a few hours. These process, normally referred as artificial maturation, is highly useful for studding the changes suffer by organic matter during thermal exposition, isolated from other phenomena, such as differences in ambient depositions and/or conservation conditions. Moreover, it can be used to estimate the hydrocarbon potential of shales during in-situ and ex-situ retorting [1].

Vaca Muerta formation is the main source rock of the Neuquen Basin, Argentina, and one of the biggest shales proved reservoirs of the world [2]. In this work, kerogen from this formation was artificial matured and studied by ^{13}C-NMR spectroscopy to observe its molecular changes.

Experimental

Kerogen was isolated from immature Argentinian shale outcrops coming from the Neuquen basin by subsequent treatment with HCl, HF and dichloromethane (DCM). A portion of 400 mg of kerogen were sealed in a glass pirex tube filled with argon. These tubes where exposed 2 hours to temperatures ranging from 380-420°C to simulate maturation process. Fluids generated during maturation were extracted with DCM. Obtained kerogen was dried until constant mass and studied by ^{13}C-NMR with cross-polarization magic angle spinning with total sideband spinning suppression (CPMAS/TOSS). To obtain quantitative results, the variable contact time (VCT) approach was used.

Results and Discussion

^{13}C-NMR spectra could be classified in three zones:

- The aliphatic band, between 0-92 ppm, that includes methyl, aliphatic alcohols and ethers, methylene, methine and quaternary carbons. All this groups decrease during maturation, particularly methylene groups.
- The aromatic band, between 92-162 ppm, that includes aromatic carbons included protonated, bridgehead, aromatic branched and phenols. An increase of the proportion of these carbons is observed during maturation, particularly of the bridgehead carbons.
- The oxygenated band, between 162-260 ppm, including carbonyls and carboxyl groups.

To simultaneously analyze the contributions of these groups, structural parameters are normally calculated. One of the main parameters that characterize the molecular structure of kerogen it's the content of aromatic structure (%Aromaticity). During maturation, kerogen increases its aromatic content forming a graphitic-like structure. In a previous work [3], we have found that the %aromaticity estimated by ^{13}C-NMR have a linear relationship with %Ro estimated by bitumen reflectance (%RoE) according to the following formula:

%Aromaticity= 62 (±7) * %RoE – 13 (±8)

Figure 1 shows the obtained spectra along with the %aromaticity (%Ar) and the estimated %Ro (%RoE, according to the previous formula, of the original kerogen extracted (KerOr), and for kerogens exposed to 380 °C (Ker380), 400 °C (Ker400) and 420 °C (Ker420).,

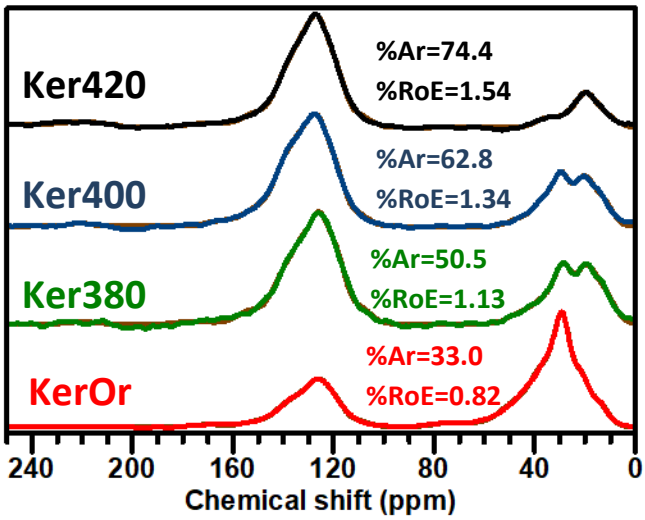

Figure 1. ^{13}C-NMR spectra of kerogens

Apart from %aromaticity, there are other two key parameters obtained from ^{13}C-NMR spectra that describes general kerogen molecular structure: the average aliphatic chain length (Cn´), and the average aromatic cluster size (C). The last parameter is directly related to the average size of aromatic fused rings on each cluster [4].

A direct decrease of Cn´ is observed during artificial maturation (Figure 2), from a value of 5.5 in KerOr to 1.0 in Ker420, indicating that every aliphatic chain remaining is in the form methyl and single carbon bridges. For the case of C, an increase with maturation is observed, increasing from a value of 12.8 in KerOr (equivalent to island of 2-3 fused aromatic rings) to 16.3 in Ker420 (compatible con islands of 4 fused rings or higher). These values are in range of previously reported results of natural samples of equivalent maturity coming from Vaca Muerta formation [3].

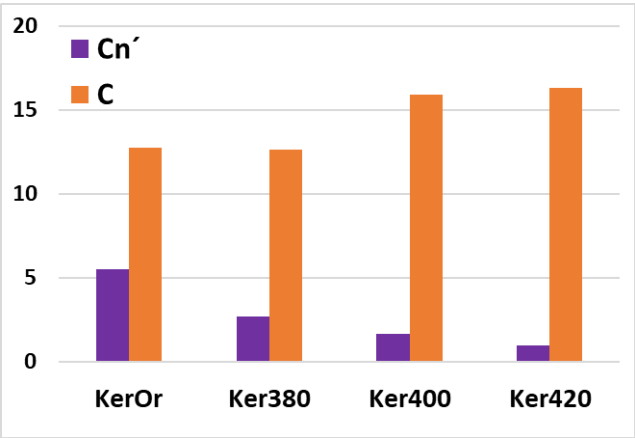

Figure 2. Structural parameters obtained from ^{13}C-NMR spectra.

Conclusions

We have obtained artificial maturated samples trough exposing extracted kerogen to temperatures ranging from 380 to 420 °C and obtained kerogen with ^{13}C-NMR structural parameters (%aromaticity, average chain length and average aromatic cluster size) equivalents to Vaca Muerta organic matter from wells coming from different production stages of maturity (from late oil to dry gas).

Acknowledgements

The authors thank CONICET (Argentinian research council) and YPF-Tecnologia for financial support.

References

[1] Xie, X., Li, M., Xu, J., Snowdon, L.R., Volkman, J.K., 2019. Geochemical characterization and artificial thermal maturation of kerogen density fractions from the Eocene Huadian oil shale, NE China. Organic Geochemistry 103947.

[2] Stinco, L., Barredo, S., 2017. Unconventional shale and tight reservoirs of Argentina.Opportunities and challenges. In: 22nd World Petroleum Congress Proceedings. World Petroleum Council, Istambul, pp. 1–39.

[3] Donadelli, J.A., Canneva, A., Garro Linck, Y., Martinez Delfa, G., Erra, G., Velasco, M.I., Franzoni, M.B., Silletta, E. V., Acosta, R.H., Calvo, A., 2021. Molecular changes in the organic geochemistry of the Vaca Muerta Shale Formation as a consequence of natural maturation. Organic Geochemistry 157.

[4] Kelemen, S.R., Afeworki, M., Gorbaty, M.L., Sansone, M., Kwiatek, P.J., Walters, C.C., Freund, H., Siskin, M., Bence, A.E., Curry, D.J., Solum, M., Pugmire, R.J., Vandenbroucke, M., Leblond, M., Behar, F., 2007. Direct characterization of kerogen by X-ray and solid-state 13C nuclear magnetic resonance methods. Energy & Fuels 21, 1548–1561.

XVI LATIN AMERICAN CONGRESS ON ORGANIC GEOCHEMISTRY
9 - 11 AUGUST, 2023
ARACAJU, SERGIPE, BRAZIL

Evolution of biomarkers in extracts of artificially matured kerogen from the Neuquen Basin, Argentina

JUAN BOTTO, SANTIAGO ORDUNA, JORGE DONADELLI*, GERARDO MARTINEZ DELFA

YPF Tecnología S.A., Avenida del Petróleo s/n (entre 129 y 143), (1923) Berisso, Buenos Aires, Argentina

*correspondence: jorge.a.adonadelli@ypftecnologia.com

Introduction

The transformations of buried kerogen responsible to produce hydrocarbons involve processes that take several million years under natural conditions. However, it can be accelerated by exposing the extracted organic matter to high temperatures for a few hours. This procedure makes it possible to study the characteristics of the hydrocarbons generated from an outcrop sample. In addition, it allows to generate oil from immature samples by retorting. Biomarkers are molecules derived from biogenic precursors whose structure is relatively stable and have not undergone major modifications after their incorporation into organic matter. Some of these biomarkers undergo small changes when exposed to thermal stress, such as cracking, aromatization and isomerization, so they can be used as witness molecules for the degree of kerogen maturation [1].

In this work, extracts of artificially matured kerogen from the Vaca Muerta formation located in the Neuquén basin, Argentina, were studied to follow the evolution of several biomarkers. This procedure allows a simple approximation for source rock/produced oil laboratory correlations.

Experimental

Kerogens were isolated from immature Argentinian shale outcrops coming from the Neuquen basin by subsequent treatment with HCl, HF and dichloromethane (DCM). Portions of 400 mg of kerogen were sealed in a glass pirex tube filled with argon. These tubes where exposed 2 hours to temperatures ranging from 360-440°C to simulate maturation process. Fluids generated during maturation were extracted with DCM, filtered, and dried. Obtained extracts were redissolved with 3 ml of DCM Saturated and aromatic fraction of the extracts were obtained by open column chromatography using silica gel as stationary phase and hexane and dichloromethane as mobile phase, respectively. D-pregnane was used as internal standard for the saturated fraction and o-terphenyl for aromatics. Biomarker analysis was performed with an Agilent 7890B GC coupled to an Agilent 7000C triple quadrupole mass spectrometer. A volume of 0.2 ul of each fraction was injected, using a 50 m DB-1 capillary column and Helium as carrier gas at a flow rate of 1 ml/min. The injector was used in splitless mode at a temperature of 320°C. Detection of saturated and aromatic biomarker was done by multiple reaction monitoring (MRM) and single ion monitoring (SIM), respectively.

Results and Discussion

Three extracts corresponding to kerogens exposed to 380 °C (Ex380), 400 °C (Ex400) and 420 °C (Ex420) were obtained. The degree of maturation reached by each corresponding kerogen was estimated from the aromatic carbon content determined by ^{13}C-NMR [2], obtaining an estimated vitrinite reflectance of 1.13%, 1.34% and 1.54% respectively. Table 1 summarizes the values obtained for the main maturity indices of the biomarkers studied. The range of applicability of each parameter is also listed.

Table 1. Results of biomarkers indexes of each extract.

Index/Sample	Ex380	Ex400	Ex420	Range
20S/(20S+20R) C_{29}Steranes	0.55	0.55	0.56	%Ro<0.8
22S/(22R+22S) C_{32}Hopanes	0.59	0.60	0.60	%Ro<0.5
ββ/(ββ+αα) C_{29}Steranes	0.54	0.53	0.56	%Ro<0.9
Diaster/aa Ster (C27)	1.96	2.09	2.88	%Ro<1.5
Tricyclic terpanes/Hopanes	0.09	0.15	0.17	%Ro<1.5
Ts/(Ts+Tm) Trisnorhopanes	0.63	0.62	0.68	%Ro<1.5

Of the six indices studied, the first three have a range of change below the maturity of the samples (1.13-1.54 %Ro), and therefore should have reached the equilibrium value for the three extracts. For example, the isomerization of C-20 in the C29,5α,14α,17α(H)-steranes during thermal stress reaches equilibrium at a value of 0.52-0.55 [1], in line with obtained results.

A similar case occurs with the isomerization of C-22 in C_{32} hopanes where ratios in the range 0.57–0.62 indicate that the main phase of oil generation has been reached or exceeded. The isomerization at C-14 and C-17 in the regular steranes C-29 20S and 20R should reach an equilibrium value of 0.67-0.71 in samples of %Ro>0.9 [1]. The extracts have values below these (0.54-0.56), despite it was expected to have reached the equilibrium according to ^{13}C-NMR results of kerogen.

Diasterans are more stable than steranes to thermal stress, and the ratio between the two increases with kerogen maturity, particularly in post-mature stages, as observed in the case of the extracts where the ratio increases from 1.98 in Ex380, to 2.88 in Ex420. Tricyclic terpanes (TT) are more resistant to thermal maturation than hopanes (H), so the TT/H ratio increases with maturity, going from 0.09 to 1.17 in the extracts.

Finally, the C-27 17α-trisnorhopane (Tm) is less stable to thermal stress than C27 18α-trisnorhopane II (Ts), and therefore Tm/(Ts+Tm) ratio should increase with maturity. In the extracts, a small increase from 0.62-0.63 to 0.68 is observed. It is important to take into account that tricyclic terpanes could co-elute with Tm, thus affecting the values obtained.

Conclusions

Six maturity biomarkers were evaluated in three extracts obtained by artificial maturation of kerogen from the Vaca Muerta formation. The value of the indexes obtained are in agreement with the ^{13}C-NMR results indicating a highly matured kerogen, with the exception of C-29 steranes.
The evaluation of biomarker parameters for extracts produced by immature kerogen thermal treatment in the laboratory is a simple approach to study source rock/oil relationships without the interference of other parameters (such as difference in organic matter composition or the oil conservation). Additionally, it can be used in formations where underground source rock samples are not available.

Acknowledgements

The authors thank CONICET (Argentinian research council) and YPF-Tecnologia for financial support.

References

[1] Peters, K.E., Walters, C.C., & Moldowan, J.M., 2007. The biomarker guide: Volume 2, Biomarkers and isotopes in petroleum systems and earth history. Cambridge University Press.

[2] Donadelli, J.A., Canneva, A., Garro Linck, Y., Martinez Delfa, G., Erra, G., Velasco, M.I., Franzoni, M.B., Silletta, E. V., Acosta, R.H., Calvo, A., 2021. Molecular changes in the organic geochemistry of the Vaca Muerta Shale Formation as a consequence of natural maturation. Organic Geochemistry 157.

XVI LATIN AMERICAN CONGRESS ON ORGANIC GEOCHEMISTRY
9 - 11 AUGUST, 2023
ARACAJU, SERGIPE, BRAZIL

Simple approach to sediment washing for drill cuttings description of Pre-salt rocks

Daniela França[1], Fabia Emanuela R. Bobco[2], Wagner Moreira Lupinacci[1,2], Antônio Fernando Menezes Freire[1,2]

[1]Universidade Federal Fluminense, Instituto de Geociências, Campus Praia Vermelha, Niterói, Rio de Janeiro, 24210-346, Brazil

[2]National Institute of Science and Technology of Petroleum Geophysics (INCT-GP/CNPQ), Niterói, Rio de Janeiro, 24210-346, Brazil

e-mail: danielafranca@id.uff.br

Introduction

Since the discovery of giant oil fields in the Pre-salt reservoirs, many efforts have been directed mainly toward understanding the genesis and late processes that control the properties of these rocks. One of the main methods employed, mainly in correlation with well-logs during and after drilling, is the macroscopic description of drill cuttings. Rock fragments are generated during the well drilling process, and these cuttings are brought to the surface by the drilling fluid flowing through the drill bit (Santos *et al*., 2018). The fluids can be aqueous-based or non-aqueous-based, and the choice of the components will depend on the geological characteristics, it is possible to carry out the lithological identification using the macroscopic and microscopic description. Techniques such as X-Ray Fluorescence (XRF) and X-Ray Diffraction (XRD) can also be used, which help in the geochemical and mineralogical characterization of the rocks, respectively. However, the adherence of the drilling fluid to the fragment surface often becomes a challenge in analyzing the fragments. The choice of products that guarantee effective, quick, and low-cost cleaning, with preservation and minimal contamination of the rocks, and that still allow for proper disposal of waste is essential before starting the analysis. The present study proposes the use of the organic solvent n-hexane in the washing of evaporitic and carbonate drill cuttings from the Brazilian Salt and Pre-salt intervals. Initially, this solvent proved effective in decontamination, aiming to describe the macroscopic characteristics of the sediments.

Experimental

Five drill cuttings were tested, corresponding to depths 5364m; 5379m; 5433m; 5466m, and 5796m, from well 1-BRSA-1363-RJS. The fluid used during the drilling of the samples has a non-aqueous composition based on Olefinic with Calcium Chloride Brine (Olecore), density of 11.3 (lb/gal), and viscosity of 161.0 (s). This study proposes a simple approach to drill cuttings washing. For this, 3.0 g of each sample was added to a beaker and washed with three portions of 10 mL of n-hexane with manual stirring. The washed fragments were dried at room temperature. In order to perform a comparison, the same samples were cleaned with water and detergent. The macroscopic description of the fragments was carried out using a stereomicroscope ZEISS Stemi 508 Stereo with front lens Apo 2.0x and FWD 35 mm. They were also photographed using a Zeiss Axioncam ERc 5s camera.

Results and Discussion

Aspects observed before and after treatment of the samples with water and detergent and with n-hexane are illustrated and described below. Figure 1 shows images obtained from the samples: 5364m (A, B, and C) corresponding to evaporitic rocks (sulfates) from the Salt interval, and 5466m (D, E, and F) referring to carbonates from the Pre-Salt interval. In Figure 1A, dirty sulfate crystals with orange-colored drilling fluid can be seen, interfering with the separation of the crystals and mainly with the color. Since sulfates are soluble minerals, washing with water and detergent was not recommended for the description (Fig. 1B). The sediments immediately disintegrated after being washed with n-hexane (Fig. 1C), allowing one to see the crystals' habit and primary color, predominantly hyaline. After the macroscopic description, the XRD analysis would confirm the composition of the sulfates (gypsum and/or anhydrite). Figure 1D exhibits the larger carbonate fragments as disaggregated, although numerous smaller sediments adhere to them, some of which were mixed with the fluid during drilling. The fluid adhered to the carbonate samples results in a light color similar to the original rock. This material generates a rounded appearance, obliterating the structures and colors of the rocks. The washing with water and detergent improved the identification of color and some structures, however it is still possible to observe the drilling material glued to the fragments (Fig. 1E). When observing the n-hexane washed samples (Fig. 1F), the color of the carbonates is described as light cream, and the structures are

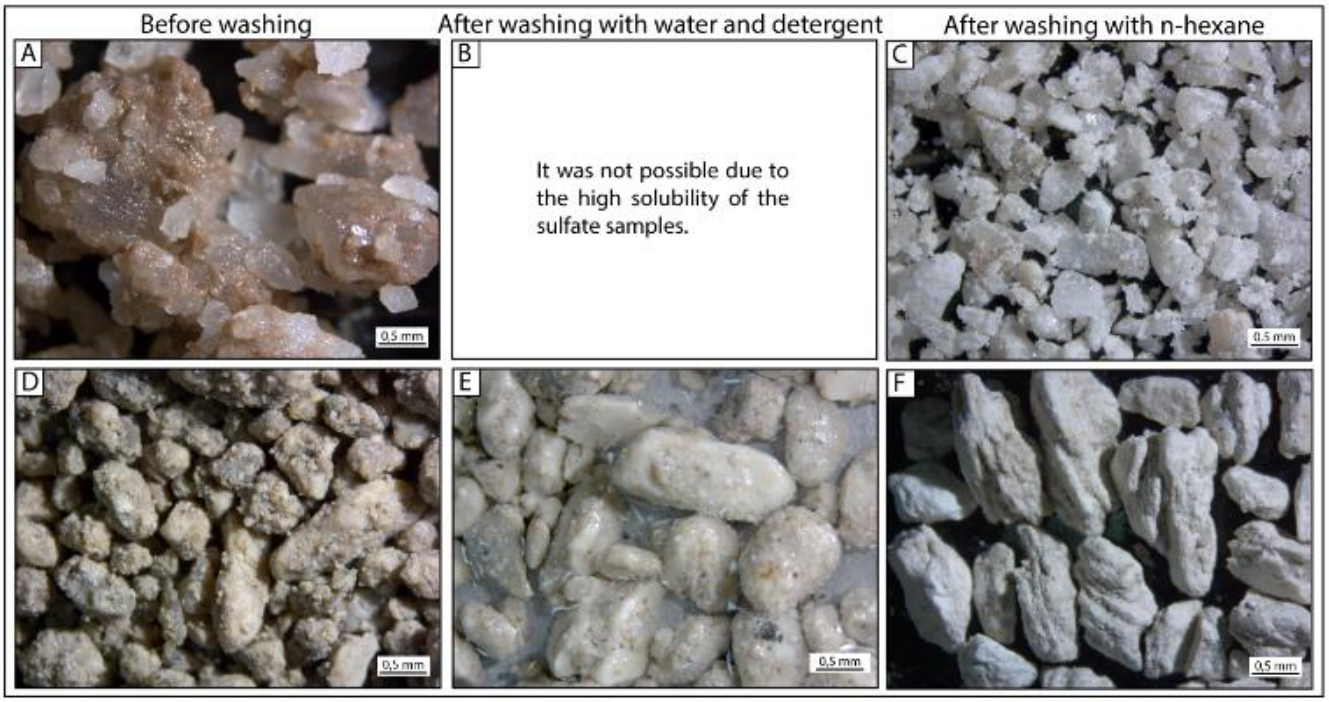

Figure 1. Sample images of drill cuttings before and after washing processes. Sample 5364m: A) Aspect of the sulfate fragments with drilling fluid before washing, B) Due to the high solubility of sulfates, the samples were dissolved, and C) Disaggregated crystals with the original color and habit after cleaning. Sample 5466m: D) Fluid material aggregated to rock fragments, with no visible structure before washing, E) Partially cleaned fragments, but still with fluid material obliterating the features, and F) Structure, color, and porosity of carbonate rocks of the pre-salt highlighted after cleaning.

recognizable. Elongated features possibly associated with shrubs are observed. Shrubs comprise crystalline aggregates of fascicular calcite (Herlinger et al., 2017), characteristic of pre-salt rocks. Furthermore, the permo-porous aspects of these reservoirs could be evaluated and are shown in figure 1F. The porosity of these rocks, which reaches around 16% (Herlinger et al., 2017), was qualitatively classified as good in the drill cuttings, visually standing out after the washing process. Behind the evaporation of n-hexane, the carbonate fragments can be washed, normally with water, helping in the macroscopic description.

Conclusions

The results of this study demonstrated that a simple approach using the organic solvent n-hexane is effective in cleaning drill cuttings of carbonates and evaporites, especially for rocks from the Brazilian Pre-salt. After the treatment, essential aspects in characterizing these rocks were visually highlighted, such as color, structures, and porosity. Cleaning with water and detergent can also be used, but it does not work for soluble rocks, and drilling fluid residues may remain after the process. The washing with n-hexane increased the reliability of the macroscopic description of drill cuttings, highlighting the relevance of this method in studies involving rock data. One question for future studies is the influence of n-hexane in organic geochemistry analysis such as TOC and Pyrolysis Rock-Eval, and also for biomarkers identification, since its geochemical signature is easily recognized in difractograms.

Acknowledgements

The authors thank to the Universidade Federal Fluminense (UFF) and Instituto Nacional de Ciência e Tecnologia de Geofísica do Petróleo (INCT-GP/CNPq) for supporting this research.

References

Herlinger Jr, R., Zambonato, E. E., & De Ros, L. F. (2017). Influence of diagenesis on the quality of Lower Cretaceous pre-salt lacustrine carbonate reservoirs from northern Campos Basin, offshore Brazil. Journal of Sedimentary Research, 87(12), 1285-1313.

Santos, J. M., Petri, I. J., Mota, A. C. S., dos Santos Morais, A., & Ataíde, C. H. (2018). Optimization of the batch decontamination process of drill cuttings by microwave heating. Journal of Petroleum Science and Engineering, 163, 349-358.

SYNCHRONOUS FLUORESCENCE SPECTROSCOPY: APPLICATION FOR IDENTIFYING LIQUID HYDROCARBONS ANOMALIES IN SURFACE GEOCHEMICAL STUDIES

ELÍAS KASSABJI [a*]

[a]**SENIOR PETROLEUM GEOCHEMIST AT FUGRO INC, USA**

e.kassabji@fugro.com

Introduction

Fluorescence analysis in shallow core sediments is a useful tool for detecting aromatic hydrocarbons, such as polycyclic aromatic hydrocarbons (PAHs). Fluorescence intensity and color can be used to infer the presence and composition of hydrocarbons, respectively. While single wavelength UV lamps are commonly used for rapid oil assessment in the field, synchronous fluorescence spectroscopy (SFS) offers a more objective, sensitive, and consistent method for qualitative characterization of oil-range hydrocarbons. SFS can differentiate liquid hydrocarbons and identify thermogenic anomalies. The study aims to evaluate the effectiveness of SFS in detecting and characterizing hydrocarbons in shallow core sediments by comparing results obtained from different oil and extract samples.

Experimental

Oil samples with different characteristics, surface sediment extracts, and perylene were analyzed using a Perkin Elmer fluorescence spectrometer LS-55, with data processed using BL Studio software. To prepare the samples, a small amount of sample was placed in a cuvette and filled with optima grade *n*-hexane, then homogenized. Synchronous mode was used with a $\Delta\lambda$ of 40 nm, based on previous research (Lloyd, 1971 and Patra & Mishra, 2002).

Results and Discussion

The results obtained from the spectra analysis of the oil and surface samples are presented in Figures 1 and 2. The spectra clearly indicate that the fluorescence intensity of light oil is highest over 260 nm, while the maximum intensity for medium oil is observed in the 270-360 nm range. This is consistent with previous studies that suggest that petroleum products contain a complex mixture of aromatic hydrocarbons that fluoresce in proportion to the number of aromatic rings present.

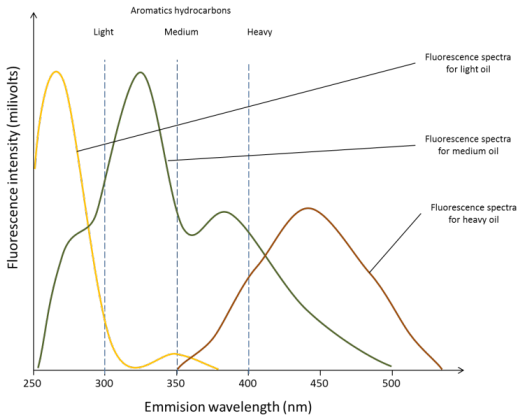

Figure 1. Synchronous fluorescence spectra for oil samples in *n*-hexane.

The spectral fingerprints of lighter and medium oils were observed to have peaks mainly in an intermediate wavelength region (260-400 nm), while heavy and biodegraded oils showed maximum fluorescence in the emission wavelength region (410-550 nm). A distinct group of samples was also observed, corresponding to non-thermogenic or 'background' samples that were dominated by recent organic matter. The predominant peaks of this group matched those of the perylene spectra.

Monoaromatic compounds, such as benzene, toluene, and xylene, emit fluorescence between 250-290 nm, while two aromatic ring compounds, such as naphthalene, show a peak at 310-330 nm, and three and four aromatic ring compounds, such as phenanthrenes and pyrene, emit fluorescence between 345-355 nm.

Perylene and other compounds with more than 5 aromatic rings, emits fluorescence above 400 nm (Pharr et al., 1992; Abbas et al., 2006) (see Figure 3).

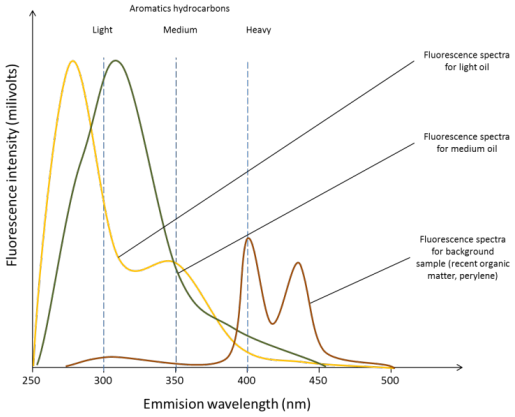

Figure 2. Synchronous fluorescence spectra for extract surface samples in *n*-hexane.

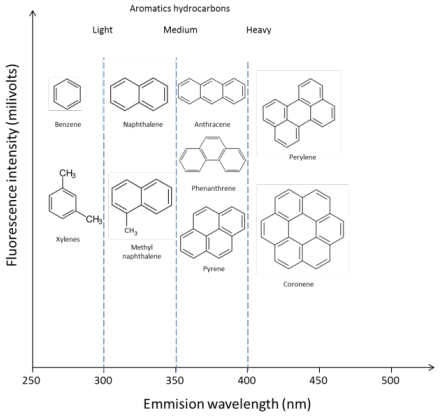

Figure 3. Fluorescence responses of oil compounds.

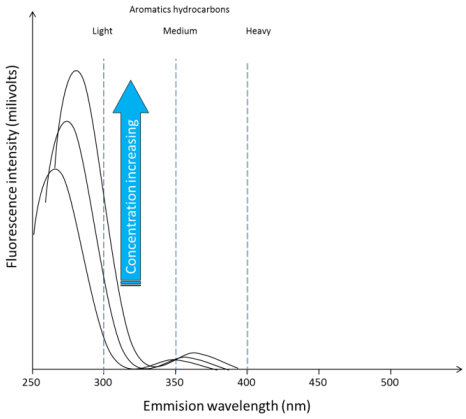

Figure 4. Fluorescence responses for light hydrocarbons at different concentrations.

Furthermore, the fluorescence intensity was noted to change according to the concentration of the oil/extracts, although the change differed for lighter/medium oils and heavy/biodegraded oils. For the first group, the fluorescence intensity increased with increasing concentration (see Figure 4), while for the heavy/biodegraded oils, the fluorescence intensity decreased with increasing concentration (see Figure 5). Quenchers, such as asphaltenes, are responsible for the decrease in fluorescence intensity of the latter group.

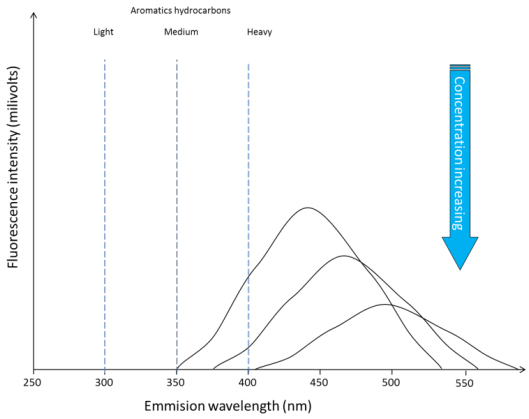

Figure 5. Fluorescence responses for heavy hydrocarbons at different concentrations.

Conclusions

This study demonstrates the potential of synchronous fluorescence spectroscopy to differentiate and characterize different types of oils based on their synchronous spectra at a fixed wavelength-interval. This method can serve as a useful tool to identify and investigate oil anomalies in surface sediment samples and can complement other exploration techniques for oil detection.

Acknowledgements

The author thanks FUGRO for financial support to present this study at this conference.

References

Abbas, O.; Rebufa, C.; Dupuya, N.; Permanyer, A. & Kister, J., 2006. Assessing petroleum oils biodegradation by chemometric analysis of spectroscopic data. Talanta, Vol. 75, No. 4, pp. 857–871, ISSN 0039-9140.

Lloyd, J. B. F., 1971. Synchronyzed excitation of fluorescence emission spectra, Nature (London) Phys. Sci., 231, 64-65.

Patra, D.; Mishra, A. K., 2002. Total synchronous fluorescence scan spectra of petroleum products, Anal. Bioanal. Chem., Vol. 373, Is. 4-5, 304-309.

Pharr, D.Y.; McKenzie, J.K.; Hickman, A.B., 1992. Fingerprinting petroleum contamination using synchronous scanning fluorescence spectroscopy. Groundwater, Vol. 30, No. 4, pp. 484–489, ISSN 1745-6584.

XVI LATIN AMERICAN CONGRESS ON ORGANIC GEOCHEMISTRY
9 - 11 AUGUST, 2023
ARACAJU, SERGIPE, BRAZIL

THE POSTGLACIAL HYDROCARBON SOURCE ROCK OF THE PARNAÍBA BASIN

AILTON S. BRITO[a*], JOELSON L. SOARES[b], IARA S. DE ALCANTARA SILVA[a], SIDNEY G. DE LIMA[a]

[a] **Laboratório de Geoquímica Orgânica, Centro de Ciências da Natureza, Universidade Federal do Piauí**
[b] **Programa de Pós-Graduação em Geologia e Geoquímica, Instituto de Geociências, Universidade Federal do Pará**

asbrito@ufpa.br, sidney@ufpi.edu.br

Introduction

Organic geochemistry is a powerful tool extensively applied in the petroleum industry, as are organic geochemical biomarkers in correlating oil-oil and oil-source rock to determine the origin of organic matter and provide insight into the paleoenvironment. Thus, a postglacial scenario's molecular composition and depositional conditions in a different geological time can be evaluated. The Parnaíba Basin (Figure 1) records two Paleozoic glaciations that are followed by the deposition of gray to black shale. In the last decades, three possible source rocks have been considered for this basin. Although some studies have been carried out, their precise characterization and actual hydrocarbon production are still controversial. Two source rock units are the postglacial transgressive shale deposits of the Tianguá (Lower Silurian) and Longá formations (Devonian-Carboniferous). The former overlies a 200 m thick sequence that is in conformity with the Ipu Formation, and the latter overlies the diamictites of the Cabeças Formation, composing a 220 m thick package (Vaz et al. 2007). Despite the geologic time span, both units have similar lithofacies, preserved organic matter (~ 1 wt% TOC (Rodrigues, 1995)), and, based on sedimentology, similar depositional conditions. What about the microbial and plankton life in the glacial aftermath, are these also similar in both Silurian and Devono-Carboniferous seas? To better characterize the source rocks of the Parnaíba Basin, this study uses biomarkers to assess organic matter composition, unraveling similarities and changes in those postglacial settings.

Experimental

Total organic carbon (TOC), Rock-Eval pyrolysis, and classical biomolecular marker data from four samples from two outcrops in the southwestern and northeastern Parnaíba Basin were used for this study (Figure 1). Biomarker analyzses were performed in the Laboratório de Geoquímica Orgânica of the Universidade Federal do Piauí (UFPI), using an internal standard to extract the saturated fractions, and gas chromatography-mass spectrometry analyses (GC-MS) were performed using a Shimadzu GCMS-QP2010 SE chromatograph. The study used new and previous data from Brito et al. (2020) and Silva et al. (2023).

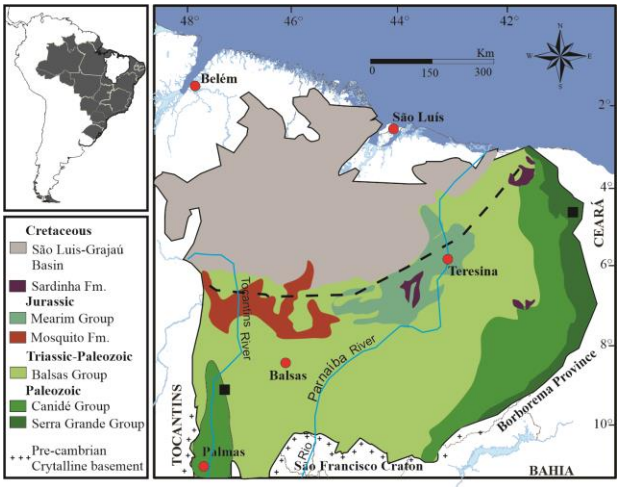

Figure 1. The Parnaíba Basin location and simplified geologic map. The black squares in the map mark the sampling location.

Results and Discussion

Both the Tianguá and Longá shales have a total organic carbon content of about 1 %, consistent with the pioneering work of Rodrigues (1995). The molecular fossils studied here are well preserved due to the thermally immature shales of both units, enhancing their application in paleoenvironmental interpretation (Brito et al., 2021). The very low thermal evolution of the samples is indicated by the maximum pyrolysis temperature (T_{max}), carbon preference index (CPI), C_{31}, C_{32} (22S/22S + 22R) hopanes, and 18α(H),22,29,30-trisnorneohopane (Ts)/ (Tm) 17α(H),22,29,30-trisnorhopane (Figure 2).

The organic extract from the Silurian shale exhibits a striking unimodal distribution of *n*-alkanes (*n*-C_{14} to *n*-C_{37})

with *n*-C_{16} to *n*-C_{18} predominating, and the pristane (Pr)/ phytane (Ph) ratio < 1 (Figure 3), indicating a marine algae contribution, preserved in an anoxic environment. The marine algae source is supported by the predominance of C_{29} and C_{27} steranes (table 1). Nevertheless, tricyclic/17α-hopanes such as C_{23}Tric/C_{30} hopane indicate bacteria as a significant organic source.

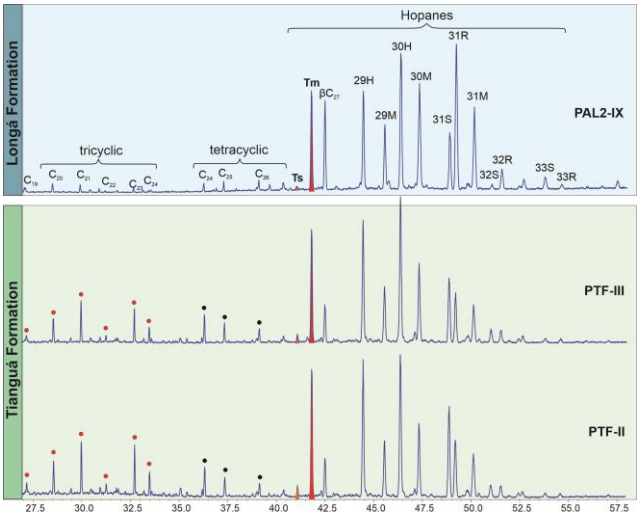

Figure 2. GC-MS ion chromatograms (m/z 191) of tricyclics, tetracyclic, and hopanes from the Silurian Tianguá Formation and Devono-Carboniferous Longá Formation.

On the other hand, the Devono-Carboniferous organic extract exhibits a bimodal distribution of *n*-alkanes (also *n*-C_{14} to *n*-C_{37}) with a Pr/Ph ratio > 2, suggesting a mixed marine and terrestrial origin in an oxic environment. The mixed source is confirmed by the sterane distribution and ternary plots of the C_{27}-, C_{28}- and C_{29}-steranes (see Brito et al., 2020). The low molecular weight n-alkanes, terrigenous/aquatic ratio (TAR), Pr/nC_{17}, and Ph/nC_{18} (table 1) also indicate a high land plant contribution.

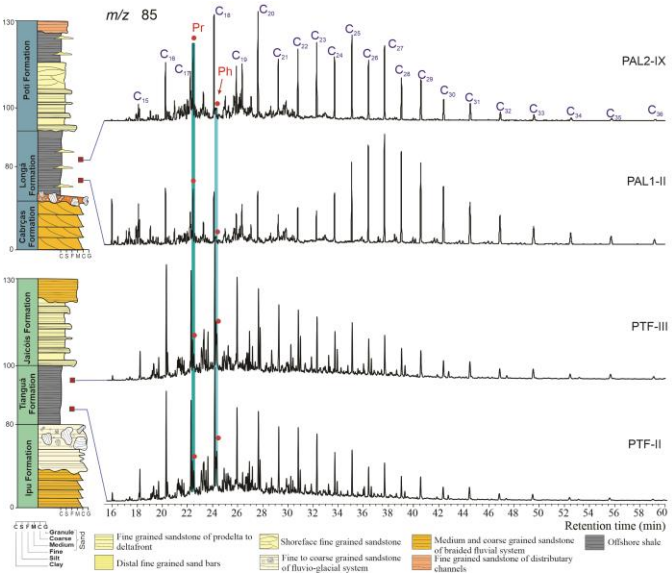

Figure 3. GC-MS Ion chromatograms (m/z 85) showing the distribution of *n*-alkanes and the respective position of the samples in the sedimentary logs of the Tianguá and Longá formations.

Conclusions

The two postglacial marine shales of the Parnaíba Basin have different organic source origins. While in the aftermath of the Silurian glaciation, algae flourish, overcoming cyanobacterial production, algae production in the deglaciation scenario of the Devono-Carboniferous was constantly suppressed by the high terrigenous input, which also renews the free oxygen of the water. Despite the good quality of the Silurian organic matter, both units have been shown unsuitable as petroleum sources due to the low amount of preserved organic carbon.

Table 1. Geochemical molecular parameters of the Tianguá and Longá shales. Parameters calculation are after Peter et al (2005).

Parameters	PAL1-II	PAL2-IX	PFT-II	PFT-III
TAR	0.42	1.14	0.39	0.45
CPI	1.00	1.43	0.70	1.47
Pr/Ph	3.23	2.79	0.82	0.37
Pr/*n*-C_{17}	1.16	1.25	0.66	0.64
Ph/*n*-C_{18}	0.37	0.27	0.44	0.58
Ts/Tm	0.94	1.11	0.07	0.05
H_{31} (22S/22S+22R)	0.15	0.28	0.59	0.58
H_{32} (22S/22S+22R)	0.22	0.20	0.50	0.52
C_{27} 20S/(20S+20R)	0.29	0.16	0.53	0.36
C_{29} 20S/(20S+20R)	0.20	0.16	0.54	0.36
hopane/sterane	11.03	7.89	9,80	9,98

References

Brito, A.S., 2021. Preservação de geopolímeros no registro estratigráfico e suas implicações paleoambientais, in: de Lima, S. G. (Eds.) Fósseis moleculares e aplicações em geoquímica orgânica, pp: 180-193.

Brito, A.S.; Soares, J.L.: de Lima, S.G.; Nogueira, A.C.R.; Romero, G.R.; Sousa, E.S., 2020. Postglacial transgressive shales of Upper Devonian–Lower Carboniferous boundary of the Parnaíba Basin. Journal of South American Earth Sciences, **101**, 102621.

Peters, K. E., Peters, K. E., Walters, C. C., & Moldowan, J. M. 2005. The biomarker guide (Vol. 2). Cambridge university press.

Rodrigues, R. 1995. A Geoquímica Orgânica da Bacia do Parnaíba. (Doctoral dissertation, Programa de Pós-graduação em Geociências, Universidade Federal do Rio Grande do Sul, 225p.

Silva, I. S. D. A.; Chaves, M. R. D. B.; Brito, A. S.; Nogueira, A. C.; Lima, S. G., 2023. Fósseis moleculares da matéria orgânica siluriana da Formação Tianguá (Bacia do Parnaíba), nordeste do Brasil: implicações paleoambientais e maturação térmica. Química Nova, **46**, 02-12.

Vaz, P.T., Rezende, N.G.A.M., Wanderley Filho, J.R., Travassos, W.S., 2007. Bacia do Parnaíba. Boletim de Geociencias da PETROBRAS, 15(2), 253-263.

VACA MUERTA SHALE GEOCHEMICAL PATTERNS REVISITED, NEUQUEN BASIN, ARGENTINA

MARTIN E. FASOLA[a*], HECTOR J. VILLAR[b], IGNACIO E. BRISSON[a]

[a]**YPF S.A.,** [b]**GeoLab Sur S.A.**

*martin.fasola@ypf.com

Introduction

The Vaca Muerta (Late Jurassic - Early Cretaceous) shales bears a high-quality, oil-prone kerogen deposited under mostly generalized anoxic, marine conditions, and constitutes a world-class source rock with outstanding geochemical features for the generation of liquid and gas hydrocarbons throughout the Neuquén Basin [4]. The unit has been for long time identified as the main source for most of the hydrocarbon pools found in conventional reservoirs of the basin but in the last twelve years has acquired a significant role as an unconventional shale resource system for both oil and gas [2, 3].

This paper aims to review the present knowledge of the Vaca Muerta shale as resource system for oil and gas in the entire Neuquén Basin. Source rock distribution, hydrocarbon generating quality and thermal maturity trends are shown in updated maps based on TOC, programmed pyrolysis parameters and vitrinite reflectance data of several tens of thousands of cuttings and core samples from nearly 900 wells that penetrated the Vaca Muerta Formation, in addition to tens of outcrop sections, highlighting the core areas for gas, gas-condensate and oil. The associated liquid and gas patterns are supported on abundant bulk and molecular data that show individual trends for each particular area of the basin.

Experimental

The evaluation of an extended database that comprises several tens of thousands samples, including cuttings, cores, sidewall cores and outcrops of the Vaca Muerta Formation from wells and sections along the entire basin allowed formulating solid patterns regarding organic-richness, hydrocarbon source quality and distribution of free hydrocarbons in six reference areas of the basin, defined either based on the impact of the sedimentary rock on generated hydrocarbons and/or on significant thermal maturity differences. More than 300 Vaca Muerta oils and organic extracts, and nearly 500 mud and production gas samples completed the dataset in order to understand the key features of the fluids occurring in the prospectable plays for shale oil and shale gas. Collected and evaluated analytical data included: TOC (total organic carbon), programmed pyrolysis, visual kerogen analyses, bulk chemical composition of fluids, GC (gas chromatography) and GCMS (gas chromatography-mass spectrometry for biomarker fingerprints), stable carbon isotopes, bulk and compositional kinetics, XRF (X-Ray Fluorescence).

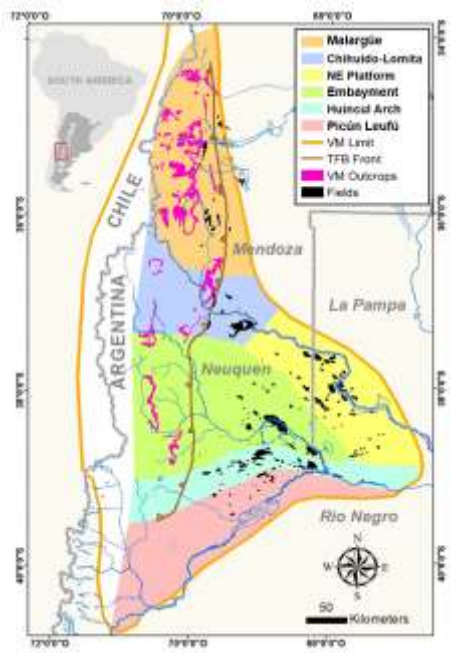

Figure 1. Neuquén Basin. Vaca Muerta index map. Colored areas (Malargüe, Chihuido-Lomita, Northeastern Platform, Embayment, Huincul Arch and Picún Leufú) are used for geochemical description and characterization. VM: Vaca Muerta Formation; TFB: thrust fold belt. Modified from Brisson [4].

Results and Discussion

The integration and interpretation of rock geochemistry data, involving organic content and hydrocarbon yield, kerogen microscopy, and organic matter depositional environment and the petroleum geochemistry data, focusing on the patterns of liquid and gas fluids produced from Vaca Muerta. Following, the main geochemical patterns are described for main areas of the basin. The presented data highlights the Embayment as the main generation pool, regarding organic richness, maturity and thickness, being the most attractive area for non-conventional developments. This area is favorable to produce mid to light oil with low sulfur content in addition to gas-condensate to the west. The Chihuido-Lomita and Huincul Arch areas close to the Embayment, with similar source rock characteristics but overall lower thermal maturity, can also host significant liquid and gas accumulation within the source rock. In the Northeast fringe of Chihuido-Lomita and Embayment areas in transition to the NE Platform, Vaca Muerta itself becomes thinner and display lower TOC, bears mid to low maturity and hosts mid to heavy, mostly sulfur-rich, oils. This area is characterized by limited gas potential. The Malargüe area shows comparable minor thickness, lower than average TOC content, overall mid-maturity and limited quality (mid to heavy), predominantly sulfur-rich, oils. Most of the prospectable shale source rock is within the thrust fold belt area and could be locally affected by Tertiary intrusions. The Picún Leufú area is the one with less data available, related to minor conventional production history. This is related to low source rock potential due to thin organic rich interval and low to mid maturity, which restricts the productivity of the generation pod and the shale prospectivity.

Conclusions

Compilation and analysis of a huge geochemical data base was critical for delineating main properties trends of organic richness, hydrocarbon potential and thermal maturity of Vaca Muerta Formation in six regions of the Neuquén Basin, namely: Malargüe, Chihuido-Lomita, Embayment, NE Platform, Huincul Arch and Picún Leufú.

Vaca Muerta shale is a world class source rock with excellent organic content (average original TOC~ 5.5% for the total unit, with individual values around 30%) and quality (highly prolific, oil-prone, amorphous marine kerogen, with an original HI of 680 mgHC/gTOC). No significant change in kerogen type is detected by pyrolysis and microscopy across the basin. Both organically rich thickness and thermal maturity increase basinward defining the most attractive generation pools to the West. This trend makes critical the accurate measurement of thermal maturity for the prediction of the most likely producible hydrocarbon types. Such maturity assessment is difficult due to the nature of the Vaca Muerta kerogen (lack of or equivocal vitrinite particles), therefore a multi-approach with different techniques (pyrolysis Tmax, GC and GCMS data of extracts and oils, and gas isotopes) proved to be of great help in defining the variations of thermal maturities in the core areas for black-oil, light-oil and gas-condensate.

Presented data shows that Vaca Muerta source rock exceeds all the geochemical cut off standard values for a shale play. Its vast geographical extension, thickness, richness, kerogen quality, broad thermal maturity range, and hydrocarbon production compliance, position Vaca Muerta as a world top shale resource system (Table 1).

Parameters	SHALE PLAYS						
	Barnett	Haynesville	Marcellus	Eagle Ford	Woodford	Fayetteville	Vaca Muerta
Basin	Fort Worth	Salt	Appalachian	Eagle Ford	Arkoma	Arkoma	Neuquén
Age(Ma)	Mississippian	Late Jurassic	Devonian	Cretaceous	Devonian	Mississippian	Late Jurassic-Early Cretaceous
Prospectable Area (km2)	13.000	23.000	250.000	5.000	28.900	23.000	30.000
Depth to top (km)	2,0 - 2,6	3,2 - 4,2	1,2 - 2,6	1,2-3	1,8 - 3,4	0,3 - 2,1	2,0 - 3,5
Porosity (%)	4,0 - 5,0	8,0 - 9,0	10,0 - 11,0	jun-14	3,0 - 9,0	2,0 - 8,0	4,0 - 12,0
Thickness (m)	60 - 90	60 - 90	30 - 120	20 - 150	90 - 300	30 - 210	200 - 800
Kerogen Type	II	III	II - III	II-III	II	II - III	(I)/II - III/S
Maturity (%Ro)	0,5 - 1,3	0,94 - 2,82	0,5 - 2,0	0,8-1,6	0,5 - 3,0	1,0 - 3,0	0,8 - 2
TOC present-day (%)	3,0 - 12	0,5-4	2,0-13	2-8,5	0,6 - 1,0	4,0 - 9,8	1,8-14,9
TOC original (%)	5,92	7,79	8,2	4,24	9,33	5,74	6,8
Gas Type	Thermogenic	Thermogenic	Thermogenic	Thermogenic	Thermogenic	Thermogenic	Thermogenic
Adsorbed gas(%)	35	25	45	25	60	50-70	30
Free gas (%)	40	75	55	75	40	30-50	70
HI original	434	722	507	411	503	404	680
S2 original (mg/g)	25,65	55,51	40,33	17,42	46,91	23,18	46,24
Ethane isotopic reversal	Yes	Yes	Yes	Yes	Usually		Occasional

Table 1. Geochemical parameters in main U.S.A. Shale Plays and their comparison with Vaca Muerta Shale.

Acknowledgements

The authors thank YPF S. A. for the authorization to publish this paper.

References

[1] Legarreta L., C.E. Cruz, G. Vergani, G. A. Laffitte, and H.J. Villar, 2004. Petroleum Mass-Balance of the Neuquén Basin, Argentina: A Comparative Assessment of the Productive Districts and Non-Productive Trends., Search and Discovery Article #10080, 2004 AAPG International Conference & Exhibition, Oct. 24-27, 2004, Cancún, México.

[2] Minisini, D., Fantín, M., Lanusse Noguera, I. and Leanza, H. eds., 2020. Integrated geology of unconventionals: The case of the Vaca Muerta Play, Argentina: AAPG Memoir 121.

[3] González Tomassini, F., Hryb, D., Sagasti, G., Massaferro, J. L. and Smith, L. 2016. Why do we have to care about detailed reservoir characterization? We will break it all. Do we?. URTeC #2460837, p. 1-10.

[4] Brisson, I. E., Fasola M. E. y Villar H.J., 2020, Organic geochemical patterns of the Vaca Muerta Formation, in D. Minisini, M. Fantín, I. Lanusse Noguera y H. Leanza, eds., Integrated geology of unconventionals: The case of the Vaca Muerta Play, Argentina: AAPG Memoir 121, p. 297–328.

FT-ICR-MS Characterization of NSO Compounds in Crude Oil and its Geochemical Implications

Jorge Armando Orrego-Ruiz, Silvia A. Pedraza-Rodríguez, Jael Y. Pacheco-Mendoza, Fernando A. Rojas-Ruiz, Miguel F. Jimenez-Jácome, Claudia J. Orejuela-Parra and María del Rosario Sánchez-Fuentes

Instituto Colombiano del Petróleo-Ecopetrol SA

jorge.orrego@ecopetrol.com.co and miguel.jimenezja@ecopetrol.com.co

Introduction

The characterization by ultra-high resolution mass spectrometry of crude oils from the major Colombian basins have been compiled in the Petroleomics Laboratory from Ecopetrol, during the last 7 years. The information obtained allowed us to propose diagrams to differentiate Colombian oils according to depositional environment, thermal maturity and biodegradation, using compositional parameters obtained by ESI(-) and APPI(+), especially in biodegraded or high maturity oils, where the conventional chromatographic analysis do not have the resolution. With this information it is possible to identify genetic and post-genetic similarities and differences in test samples.

Experimental

Fifty-four Colombian crude oils from different basins were selected due to their differences in thermal maturity, depositional environment, and biodegradation. All samples were characterized by FTMS in APPI (+) and ESI (-) modes, following the procedure published by Orrego-Ruiz et al [1].

Results and Discussion

For depositional environment, the ratio of relative abundances of the O1 and S1 classes detected by APPI can be used. A high O/S ratio can imply oxic conditions and vice versa. Likewise, the DBE4/DBE5 ratio of the O1 class can also be used as an indicator of the environment in non-biodegraded samples. These parameters allowed the classification by their oxidation conditions [1]. **Figure 1** is a tri-plot used to represent tri-variate data [2] that includes the parameters mentioned above, DBE 4/5 class O, O APPI+ (relative abundance of O class detected by APPI(+)), and sulfur compounds (relative abundance of sulfur classes detected by APPI(+)).

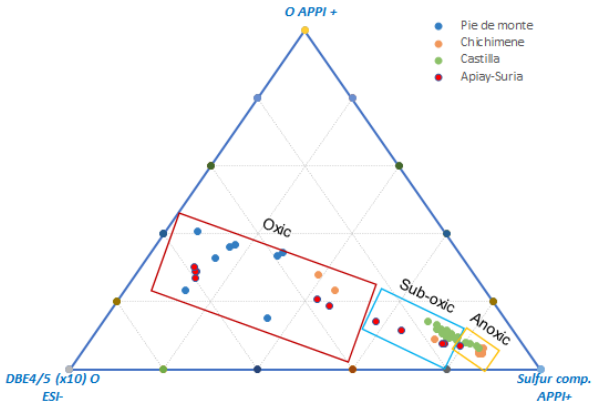

Figure 1. Tri-plot representing depositional environment for all samples.

To assess thermal maturity, three parameters were proposed. The crude oils that (i) concentrated more aromatic compounds of the O2 class, (ii) presented a lower contribution of benzo and dibenzothiophene derivatives (low aromatic sulfur), and (iii) had a low concentration of pyridine and benzopyridine derivatives (low aromatic nitrogen) turned out to be the most mature [3-6]. **Figure 2** was built with the parameters the sum of the relative abundance of compounds with DBE 8-12 for the class N1, detected by APPI+; the sum of the relative abundance of compounds with DBE 12+ for the class O2, detected by ESI-; and the sum of the relative abundance of compounds with DBE 1-9 for the class S1, detected by APPI+.

Finally, due to the importance of post-accumulation processes in heavy crudes, the work was completed using oxygenated classes O1 and O2 detected by (-) ESI. Through the ratio of the relative abundances of the O1 and O2 classes, it is possible to distinguish the effect of these factors on the oils analyzed. That is, in samples where the incorporated oxygen comes from the environment (surrounding oxygen) or from the matter that gave rise to the crude, the O1/O2 ratio would have high values. On the contrary, for biodegraded oils, said ratio

would tend to zero. In accordance with what was observed by [7], in highly biodegraded crudes, the relative abundance of O1 compounds with DBE 4 present minimal or null values. On the other hand, O1 species with DBE > 4 tend to persist in more degraded oils, so that species with DBE 5 to 7 are, in general, more abundant in highly biodegraded samples [8]. This allows us to introduce parameters to evaluate biodegradation considering as a reference the relationship between the relative abundances of the DBE 5 and DBE 7 compounds. In this study, there was a wide set of crudes from null to severe biodegradation, verified by the relative abundance of DBE 4 in the O1 class. **Figure 3** is a tri-plot built with the abundances of compounds DBE 5 and 7 of class O detected by ESI- and the ratio between the relative abundances of classes O and O2, detected by ESI-.

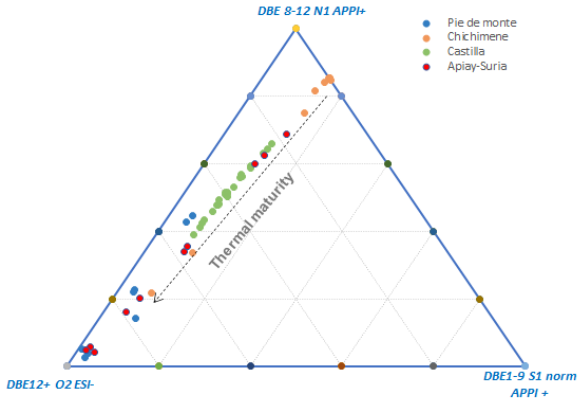

Figure 2. Tri-plot representing thermal maturity for all samples.

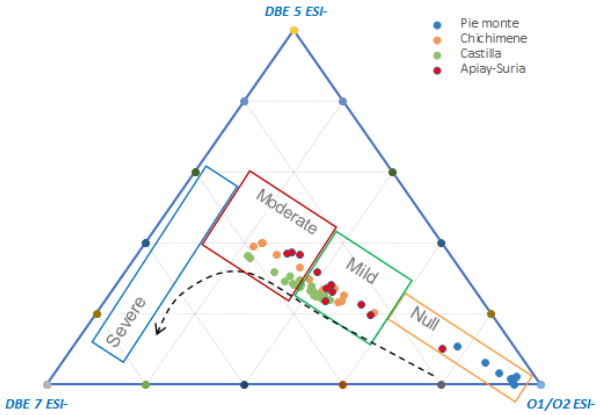

Figure 3. Tri-plot representing biodegradation for all samples.

Conclusions

Three crude oil classification diagrams were presented according to the depositional environment of the organic matter that gave rise to the crude oil, thermal maturity, and biodegradation. The parameters used in the diagrams were obtained from FTMS in ESI- and APPI+ modes. Although the classification boundaries in each case must be better defined from conventional geochemical parameters, all the diagrams allow to capture large differences between the samples. With this, we intend that the characterization of NSO compounds in crude oil be used routinely in geochemical studies.

Acknowledgements

The authors thank Ecopetrol for allowing the publication of this work and for the financial support it provided to carry out this research. We also thank the geologist Mario Guzmán for reviewing the work.

References

1. Jorge A. Orrego-Ruiz, Robert E. Marquez, and Fernando A. Rojas-Ruiz. New Insights on Organic Geochemistry Characterization of the Putumayo Basin Using Negative Ion Electrospray Ionization Fourier Transform Ion Cyclotron Resonance Mass Spectrometry. Energy & Fuels 2020 34 (5), 5281
2. Graham, D.J. and Midgley, N.G. (2000), Graphical representation of particle shape using triangular diagrams: an Excel spreadsheet method. Earth Surf. Process. Landforms, 25: 1473-1477
3. Thomas B.P. Oldenburg, Melisa Brown, Barry Bennett, Stephen R. Larter, The impact of thermal maturity level on the composition of crude oils, assessed using ultra-high resolution mass spectrometry, Organic Geochemistry, Volume 75, 2014, Pages 151-168.
4. Gang Yan, Yaohui Xu, Yan Liu, Wenxiang He, Xiangchun Chang, Penghai Tang, The evolution of acids and neutral nitrogen-containing compounds during pyrolysis experiments on immature mudstone, Marine and Petroleum Geology, Volume 115, 2020, 104292.
5. Ygor dos Santos Rocha, Rosana Cardoso Lopes Pereira, João G. Mendonça Filho. Negative electrospray Fourier transform ion cyclotron resonance mass spectrometry determination of the effects on the distribution of acids and nitrogen-containing compounds in the simulated thermal evolution of a Type-I source rock. Organic Geochemistry 115 (2018) 32–45.
6. Hong Ji, Sumei Li, Paul Greenwood, Hongan Zhang, Xionqi Pang, Tianwu Xu, Nannan He, Quan Shi, Geochemical characteristics and significance of heteroatom compounds in lacustrine oils of the Dongpu Depression (Bohai Bay Basin, China) by negative-ion Fourier transform ion cyclotron resonance mass spectrometry, Marine and Petroleum Geology, Volume 97, 2018, Pages 568-591
7. Sunghwan Kim, Lateefah A. Stanford, Ryan P. Rodgers, Alan G. Marshall, Clifford C. Walters, Kuangnan Qian, Lloyd M. Wenger, Paul Mankiewicz. Microbial alteration of the acidic and neutral polar NSO compounds revealed by Fourier transform ion cyclotron resonance mass spectrometry. Organic Geochemistry 36 (2005) 1117–1134
8. Laercio L. Martins, Marcos A. Pudenzi, Georgiana F. da Cruz, Heliara D. L. Nascimento and Marcos N. Eberlin. Assessing Biodegradation of Brazilian Crude Oils via Characteristic Profiles of O1 and O2 Compound Classes: Petroleomics by Negative-Ion Mode Electrospray Ionization Fourier Transform Ion Cyclotron Resonance Mass Spectrometry. Energy Fuels 2017, 31, 7, 6649–6657

XVI LATIN AMERICAN CONGRESS ON ORGANIC GEOCHEMISTRY
9 - 11 AUGUST, 2023
ARACAJU, SERGIPE, BRAZIL

Correlação de fácies, análise de porosidade e permeabilidade do Pré-Sal da Bacia de Santos e implicações na qualidade de reservatórios

Filipe Constantino dos Santos [a]*, Alessandro Batezelli (orientador) [b]**

[a] Bolsista no Programa de Recursos Humanos na ANP, Graduação em Geologia, Instituto de Geociências, Universidade Estadual de Campinas

[b] Análise de Bacias e Geologia do Petróleo, Coord. do Prog. de Pós-grad. em Geociências, Inst. de Geociências, Universidade Estadual de Campinas

*correspondência: f167579@dac.unicamp.br; **correspondência: batezeli@unicamp.br

Introdução

A Bacia de Santos está localizada na margem leste brasileira, ao sul da Bacia de Campos e ao norte da Bacia de Pelotas, possui uma área de aproximadamente 350 mil km², que subentende os litorais desde Florianópolis-SC até Cabo Frio-RJ avançando cerca de 600 km em direção ao Oceano Atlântico (Figura 1). Com reservas petrolíferas da ordem de 100 bilhões de barris [1], a Bacia de Santos é uma das mais importantes províncias de óleo e gás natural do país.

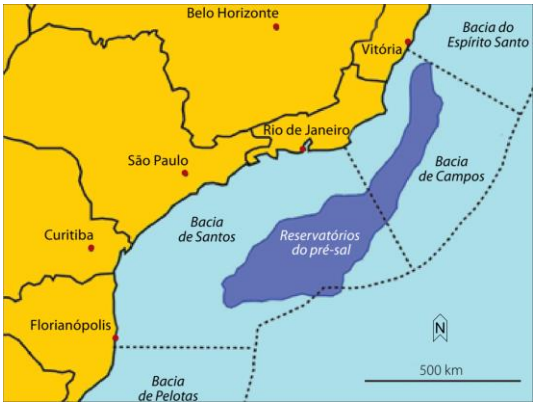

Figura 1: Mapa regional da Bacia de Santos e bacias adjacentes. Em detalhe, distribuição das rochas-reservatório do Pré-Sal. Modificado de [2].

O entendimento dos carbonatos da Formação Barra Velha (FBV) é um grande desafio para os geocientistas, devido à sua configuração deposicional e história diagenéticas complexas, em que as características de textura e composição dos litotipos diferem de qualquer outra rocha-reservatório análoga já descrita [3].

Para compreender os padrões de qualidade dos reservatórios de hidrocarbonetos do Pré-Sal, este trabalho de Iniciação Científica (IC) busca fazer a correlação de fácies com o ordenamento da porosidade e permeabilidade das rochas carbonáticas da FBV por meio da petrografia de amostras provenientes do Campo de Tupi. Nesse sentido, o objetivo é elaborar um modelo 3D de fácies e distribuição da porosidade e permeabilidade para os reservatórios carbonáticos do Pré-Sal na Bacia de Santos, de modo que se possa inferir as porções com as melhores condições de armazenamento de óleo e/ou gás.

Metodologia

O autor fará descrições quantitativas e qualitativas de amostras de rochas em lâminas delgadas e de dados de poços (testemunhos, raios-gama, resistividade etc.) provenientes do campo de Tupi na Bacia de Santos, obtidos do Banco de Dados de Exploração e Produção (BDEP/ANP) sob o regime de disponibilização de dados públicos da ANP.

Com o uso de microscópios petrográficos de luz transmitida (MPLT), a descrição de fácies sedimentares das amostras usará a classificação proposta por Gomes et al. (2020) [4], que se baseia na proporção entre as características texturais e mineralógicas dos principais componentes que atualmente caracterizam os sedimentos lacustres do Pré-Sal: *mud* (argilominerais magnesianos sem alumínio), *spherulites* (esferulitos associados a lamitos calcíticos e dolomíticos) e *shrubs* (lâminas fibrosas arbustiformes que se formaram in situ a partir do substrato) (Figura 2). As fácies serão agrupadas de acordo com as associações genéticas e do gradiente de variação das mesmas. As descrições contemplarão aspectos de coloração, textura, cimentação, arredondamento e tamanho dos grãos, matriz e mineralogia. Os minerais serão analisados por meio dos perfis geofísicos e/ou dos dados de microscópio eletrônico de varredura (MEV) e difração de raios-X (DRX) disponível na base de dados do Prof. Alessandro Batezelli. Essas análises serão feitas nos laboratórios do Instituto de Geociências da Universidade Estadual de Campinas (IG-UNICAMP).

A porosidade das lâminas delgadas será quantificada em imagens digitais com o uso do *software* JMicroVision® 1.2.7, o qual utiliza das tonalidades dos pixels para quantificar a porosidade do campo analisado. A permeabilidade será medida com o permeâmetro portátil

TinyPerm® II, fornecido pelo Centro de Estudos de Energia e Petróleo (CEPETRO).

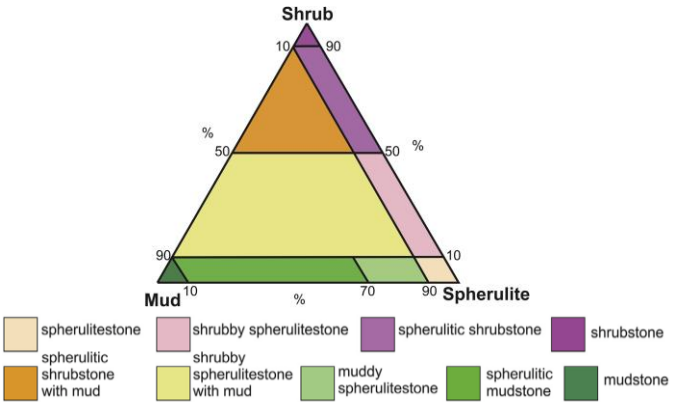

Figura 2: Diagrama ternário mostrando a classificação de fácies para sedimentos gerados in situ na FBV. Fonte: [4].

Resultados e discussão

Até o início deste segundo trimestre de 2023, esta pesquisa tem finalizado sua fase inicial, em que as seguintes etapas já foram concluídas: 1) Levantamento bibliográfico; 2) Desenvolvimento do tema; 3) Solicitação de amostras e dados técnicos de poços junto ao BDEP/ANP.

Seguindo nosso cronograma de trabalho, até o fim do terceiro trimestre de 2023, continuaremos o desenvolvimento da pesquisa passando pelas etapas de 4) Avaliação e estudo do material obtido; 5) Descrições das amostras.

Portanto, semelhantemente ao trabalho de Rebelo et al. (2022) [3], que através da descrição e interpretação de fácies (Figura 3) inferiram a qualidade dos reservatórios de óleo e gás natural da FBV, no momento do evento da ALAGO 2023 estaremos com aproximadamente metade da pesquisa finalizada, aptos a apresentar as primeiras descrições e relações litoestratigráficas dos reservatórios petrolíferos da Bacia de Santos.

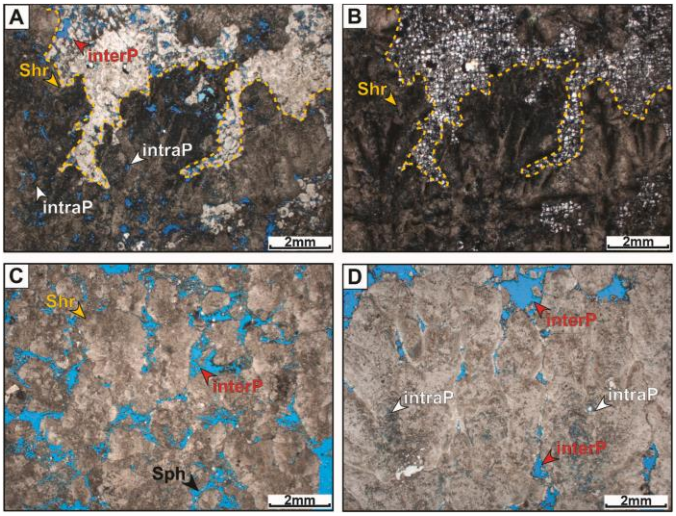

Figura 3: Fácies *Spherulitic Shrubstone* (foto A e abaixo da linha tracejada na foto B), *Shrubby spherulitestone* com spherulites (foto C) e *Shrubstone* (foto D) descritas em lâminas delgadas. As fotos foram tiradas no MPLT com nicóis descruzados, exceto a foto B, em nicol cruzado. intraP: porosidade intra-*shrub*; interP: porosidade intragranular; Shr: *Spherulitic Shrubstone*; Sph: *Shrubby spherulitestone* com *spherulites*. Fonte: [3].

Conclusões

As rochas-reservatório de petróleo da Bacia de Santos correspondem à FBV, que são sequências deposicionais aptianas compostas principalmente por fácies carbonáticas de *mud*, *spherulites* e *shrubs* abaixo das camadas de evaporitos albianos da Formação Ariri. Os depósitos carbonáticos lacustres do Pré-Sal possuem uma configuração complexa de fácies, difíceis de serem interpretadas devido à sobreposição das mesmas e da própria heterogeneidade intrínseca às rochas carbonáticas, causada por processos diagenéticos com silicificação e dolomitização [4].

Dessa forma, a descrição de fácies e sua relação com a porosidade e permeabilidade permitirá o entendimento do comportamento petrofísico dos reservatórios do Pré-Sal, tanto para o desenvolvimento do conhecimento acadêmico, quanto para a otimização da exploração e produção de hidrocarbonetos na margem leste brasileira.

Reconhecimentos

Agradeço ao Prof. Dr. Alessandro Batezelli pela orientação no IC; ao Programa de Recursos Humanos da Agência Nacional do Petróleo, Gás Natural e Biocombustíveis (PRH-ANP) pelo suporte financeiro; ao IG-UNICAMP pela estrutura acadêmica e laboratorial sem o qual nada disso seria possível.

Referências

[1] Souza, L. & Sgarbi, G., 2016. *Bacia de Santos: de promissora a principal bacia produtora de hidrocarbonetos do Brasil.* Porto Alegre, Brasil, XLVIII Congresso Brasileiro de Geologia.

[2] Riccomini, C., Sant'anna, L. G. & Tassinari, C. C. G., 2012. Pré-sal: geologia e exploração. *Revista USP,* Volume 95, pp. 33-42.

[3] Rebelo, T. B., Batezelli, A., Mattos, N. & Leite, E., 2022. Flow units in complex carbonate reservoirs: A study case of the Brazilian pre-salt. *Marine and Petroleum Geology*, Volume Volume 140.

[4] Gomes, J. et al., 2020. Facies classification and patterns of lacustrine carbonate deposition of the Barra Velha Formation, Santos Basin, Brazilian Pre-salt. *Marine and Petroleum Geology, Volume 113. 104176.*

POSSIBLE MARINE INFLUENCE ON BATATEIRA BEDS, BARBALHA FORMATION – ARARIPE BASIN

ARTUR LEAL DE CARVALHO BARROS[a]; ANDRÉ LUIZ DURANTE SPIGOLON[b]; SIDNEY GONÇALO DE LIMA[a]

[a]Laboratório de Geoquímica Orgânica - Universidade Federal do Piauí -Teresina-PI
[b]PETROBRAS, CENPES, Seção de Geoquímica Orgânica, Brasil, Rio de Janeiro-RJ

arturbarros@ufpi.edu.br, sidney@ufpi.edu.br

Introduction

The Batateira Beds, Barbalha Formation, represent the record of the implantation of the first lacustrine system characterized by anoxic conditions in the Araripe Basin (Assine, 2007). Characterized by the presence of bituminous shales with a high Total Organic Carbon (TOC) content (Spigolon et al., 2015), the Batateira Beds were deposited in a fluvial-lacustrine environment with possible proximity to the sea and are essential for the Araripe Basin because they are a stratigraphic landmark and for present lithological characteristics easily differentiated from other basin intervals (Assine, 2007). The objective of this work is to carry out an analysis of neutral biomarkers and investigate a possible marine influence on Batateira Beds.

Experimental

A rock sample collected in the city of Barbalha (CE) was subjected to the extraction of organic matter by soxhlet using a mixture of dichloromethane/methanol (12%) as extracting solvent for 24 hours. Then, the extract was concentrated and fractionated by liquid column chromatography, using silica gel impregnated with silver nitrate (10%) as the stationary phase and eluted with n-hexane, n-hexane/ethyl acetate (8%), and ethyl acetate/methanol (5%) to obtain the saturated, aromatic, and polar fractions, respectively (Moura et al., 2015).

The saturated fraction was analyzed by GC-MS and GC-MS/MS, and the identification of 24-*n*-propyl-cholestane was carried out through the co-injection of a standard synthesized by the UNICAMP as showed by da S. Sousa et al., 2019.

Results and Discussion

The total ion chromatogram (TIC) (**Figure 1**) shows a low abundance of *n*-alkanes, with 5α-14α-17α-Methyl Cholestane and hop-13(18)-ene being the most intense signals in the chromatogram. However, it is still possible to identify a signal whose mass spectrum is equivalent to a structure of derivative of β-carotene, β-carotediene, as presented by Barros et al., 2021.

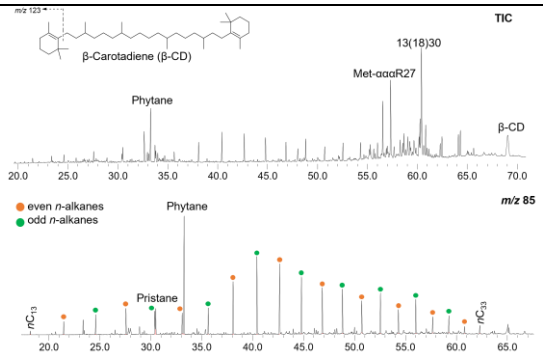

Figure 1. TIC of the SC-01 sample and identification of *n*-alkanes performed by monitoring the *m/z* 85 ion.

The monitored ion chromatogram *m/z* 85 shows a unimodal distribution of n-alkanes ranging from *n*-C_{13} *n*-C_{35}, with a maximum at *n*-C_{21} with a greater predominance of *n*-alkanes with higher molecular weight, as can be seen as observed in **Figure 1**. The predominance of linear hydrocarbons with greater mass and the greater abundance of odd-chain n-alkanes suggests a contribution related to algae typical of lake environments (Peters et al., 2005). The Pristane/Phytane ratio (Pr/Ph) presented a value equal to 0.20, suggesting an anoxic reducing depositional environment during the process of deposition of organic matter (Peters et al., 2005).

Through monitoring the *m/z* 191 ion (**Figure 2.**), it was possible to identify 17α(H)22,29,30-trisnorhopane (Tm) and 17β(H)22,29,30-trisnorhopane (βTm) indicating a low thermal evolution of the sample, given that βTm is considered the precursor of Tm due to its biological configuration at C-17 (Peters, K. E.;Walters, C. C.; Moldowan, 2005; Barros et al., 2021)). The low maturation of the sample can also be sustained by the absence of 18α(H) 22,29,30-trisnorneohopane (Ts) and by presenting a distribution of hopanes whose signals essentially present the biological configuration. Identification of gammaceran allowed the calculation of the gammaceran index (GI), which showed a value of 60.54. The high GI, associated with the low Pr/Ph ratio and the identification of β-carotediene (**Figure 1**), suggests reducing conditions in the paleoenvironment,

accompanied by a stratified water column, probably due to salinity. These conditions favored the high preservation of organic matter (Peters et al., 2005).

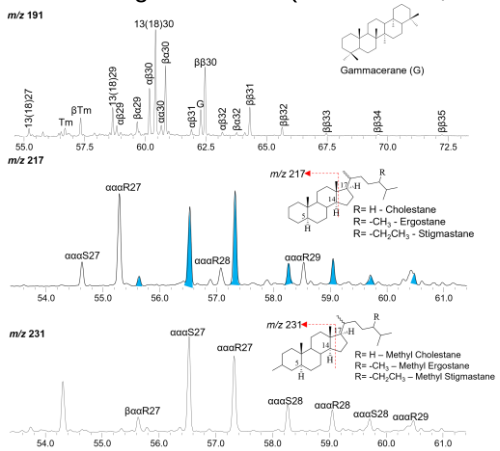

Figure 2. The distribution of pentacyclic terpanes, steranes and methyl steranes was identified by monitoring the *m/z* 191, *m/z* 217 and *m/z* 231 ions, respectively. (The blue signals correspond to the methylesterane crosstalk in the *m/z* 217 ion monitoring).

The distribution of steranes, monitored by the *m/z* 217 ion (**Figure 2**), reveals a predominance of C_{27} and C_{28} over C_{29}, suggesting organic matter derived from algae and/or plankton (Peters et al., 2005). It is possible to observe a distribution of methyl steranes in monitoring the m/z 217 ion and *m/z* 231 (C_{27} – C_{29}, **Figure 2**). These compounds do not have a common precursor and therefore do not have a well-defined biosynthetic origin but are of great geological importance due to their unusual substitution pattern.

As a result of the great relative abundance of methyl steranes, co-elution of some compounds was observed, and therefore, analyzes were carried out in GC-MS/MS. Through co-injection of the 24-*n*-propyl-cholestane standard (**Figure 3**), it was possible to identify this biomarker in the Batateira Beds sample, as these compounds are usually found in low concentrations in geological samples.

24-*n*-propyl-cholestane is a biomarker associated with organic matter of marine origin due to its precursor being 24-*n*-propyl cholesterol biosynthesized by seaweed Chrysophytes of the order Sarcinochrysidales (Moldowan et al., 1990). Thus, the unprecedented identification of 24-*n*-propyl-cholestane (**Figure 3**) suggests a contribution of marine organic matter to the Batateira Beds sample, since this compound is mainly associated with seaweed. In addition, the proximity to the sea, already discussed in the literature, and the high concentrations of C_{27} sterane corroborate a possible marine influence in the Araripe Basin earlier than reported.

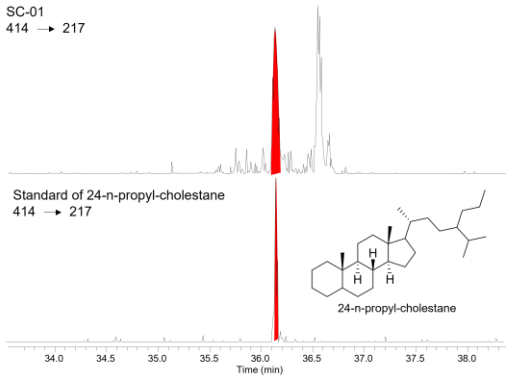

Figure 3. Co-injection of standards: GC-MS/MS ion chromatograms for C_{30} steranes *m/z* 414 – 217.

Conclusions

The distribution of n-alkanes, steranes, pentacyclic terpenes, and the presence of gammacerane and β-carotediene, suggest a low level of thermal evolution, as well as an anoxic depositional environment with saline conditions and a stratified water column, which favored the preservation of organic matter.

The identification of 24-*n*-propyl-cholestane through standard co-injection and a predominance of C_{27} sterane suggests a possible influence of marine organic matter in the Batateira Beds.

Acknowledgements

The authors thank CNPq (Brazilian research council) for fellowships; Petrobras S/A and PPGQ – UFPI for financial support.

References

Assine, M.L., 2007. Bacia do Araripe. Boletim de Geociencias da Petrobras 15, 371–389.

Barros, A.L. de C., Silva, A.F., Sousa Junior, G.R., Spigolon, A.L.D., Lima, S.G., 2021. ANÁLISE DE HIDROCARBONETOS SATURADOS E CAROTENOIDES AROMÁTICOS EM AMOSTRA DE FOLHELHO DAS CAMADAS BATATEIRA, BACIA DO ARARIPE, in: Fósseis Moleculares e Aplicações Em Geoquímica Orgânica. pp. 27–41.

da S. Sousa, E., Júnior, G.R.S., Silva, A.F., de A. M. Reis, F., de Sousa, A.A.C., Cioccari, G.M., Capilla, R., de Souza, I.V.A.F., Imamura, P.M., Rodrigues, R., Lopes, J.A.D., de Lima, S.G., 2019. Biomarkers in Cretaceous sedimentary rocks from the Codó Formation - Parnaíba Basin: Paleoenvironmental assessment. Journal of South American Earth Sciences 92, 265–281.

Moldowan, J.M., Fago, F.J., Lee, C.Y., Jacobson, S.R., Watt, D.S., Slougui, N., Jeganathan, A., Young, D.C., 1990. Sedimentary 24-n-Propylcholestanes , Molecular Fossils Diagnostic of Marine Algae. Science 247, 309–312.

Peters, K. E.;Walters, C. C.; Moldowan, J.M., 2005. The Biomarker Guide, Cambridge University Press.

Peters, K.E., Walters, C.C., Moldowan, J.M., 2005. The Biomarker Guide, 2nd ed, Cambridge University Press. Cambridge. doi:10.1017/cbo9781107326040

Spigolon, A.L.D., Lewan, M.D., de Barros Penteado, H.L., Coutinho, L.F.C., Mendonça Filho, J.G., 2015. Evaluation of the petroleum composition and quality with increasing thermal maturity as simulated by hydrous pyrolysis: A case study using a Brazilian source rock with Type I kerogen. Organic Geochemistry 83–84, 27–53.

XVI LATIN AMERICAN CONGRESS ON ORGANIC GEOCHEMISTRY
9 - 11 AUGUST, 2023
ARACAJU, SERGIPE, BRAZIL

IGNEOUS INTRUSIONS INFLUENCE IN SERRA ALTA FORMATION SHALES (PARÁNÁ BASIN)

LORENA T.G. DE ALMEIDA[a], AILTON DA S. BRITO[a], SIDNEY G. DE LIMA[a*]

[a]**Programa de Pós-Graduação em Química, Universidade Federal do Piauí, Teresina-PI, Brazil**

e-mail: sidney@ufpi.edu.br

Introduction

The Paraná Basin is in the central-eastern part of the South American continent, covering about 1,700,000 km² (MILANI et al., 2007). The Serra Alta Formation (FSA) is part of the Upper Permian section of the Paraná Basin and is characterized by dark gray shales and is considered one of the least studied lithostratigraphic units mainly due to its low potential for hydrocarbons (ROHN, 2001). The FSA rocks hosts diabase dikes and sills, and the thermal effect caused by these geological conditions can lead to the maturation of organic matter and the generation of hydrocarbons. Therefore, this work aims to evaluate the effect of igneous intrusions on the maturation of organic matter in Serra Alta Formation rocks using neutral biomarkers.

Experimental

The pulverized rocks were subjected to extraction in a Soxhlet-type system using a mixture of dichloromethane: methanol 12% (v/v) for 36 h to obtain the organic extract. The organic extracts obtained were fractionated by column chromatography using silica as the stationary phase. The eluent system employed were: hexane; hexane: 12% ethyl acetate and ethyl acetate: 5% methanol.

The analysis of the saturated fraction by GC-MS was carried out on a gas chromatograph model GCMS-QP2010 SE (Shimadzu) following the following analysis conditions: injector 290 °C, initial oven temperature of 60 °C for 1 minute, with rate heating of 4 °C min^{-1} until the final temperature of 315 °C, maintained for 15 min. For component chromatography, helium was used as carrier gas with a flow rate of 1.0 mL/min and a DB-5MS IU column (30 m x 0.25 mm x 0.25 µm). The interface and ion source temperatures were 320 °C and 230 °C, respectively. The mass analyzer used was of the quadrupole type operating by electron impact (70 eV) and the fragments detected in the range of 57 to 600 Da in full scan mode.

Results and Discussion

The analyzed samples come from a borehole drilled in the city of Papanduva-SC, which have diabase sills in the upper portion of the deposits that acted as catalysts for the formation of hydrocarbons due to thermal stress.

The chromatographic profile of *n*-alkanes (*m/z* 85, **Figure 1**) for bitumens from rocks of the FSA ranged from nC_{14}-C_{40}, with a predominance of nC_{25}-nC_{27}, except for sample A60 which showed a higher relative abundance of nC_{19}-$_nC_{21}$.

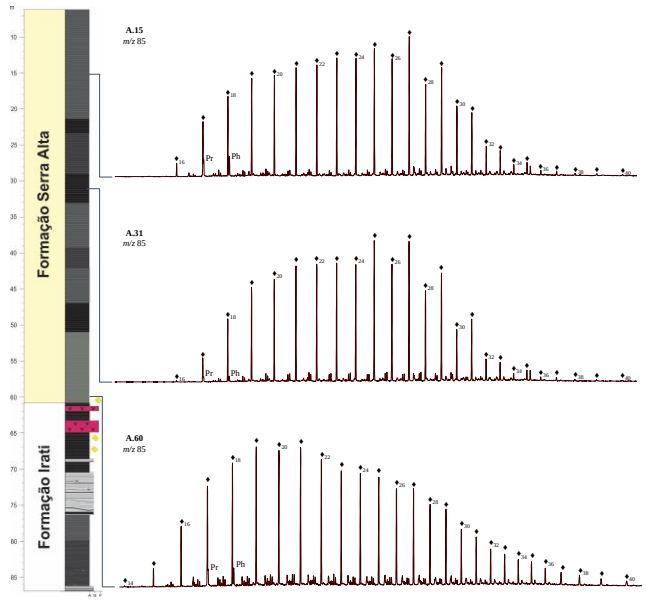

Figure 1. Distribution of chromatographic profiles (*m/z* 85) of Serra Alta Formation samples along the stratigraphic column.

CPI and OEP are parameters calculated from the relative abundance of odd versus even *n*-alkanes and are often used to estimate the thermal evolution and source of organic matter in oils and rock extracts. CPI and OEP values ranged from 1.07 to 1.41 and 1.04 to 1.35, respectively, indicating odd/even preference characteristic of a greater contribution of terrestrial organic matter during its deposition.

Maturation parameters were calculated using hopanes (**Figure 2**) and steranes (**Figure 3**) which show better thermodynamic stability and resistance to biodegradation. The Ts/Tm and Ts/(Ts+Tm) ratios showed values between 0.04-0.19 and 0.04-0.16, suggesting immature samples. The interpretation of these parameters consists in the fact that 18α(H)-trisneohopane (Ts) is more resistant to thermal degradation than 17α(H)-trisnorhopane (Tm), therefore, it is expected that the values of the Ts/Tm ratio increase with increasing maturation until an equilibrium in the 0.45 range (PETERS et al., 2005).

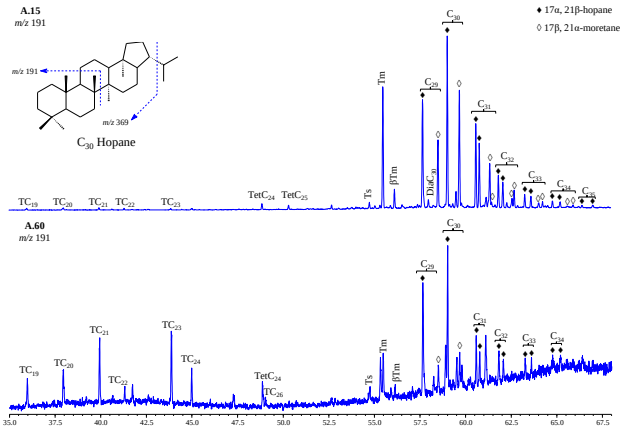

Figure 2. Distribution of tricyclic, tetracyclic and pentacyclic terpanes (*m/z* 191) in samples from the Serra Alta Formation.

The stability of hopanes and moretanes increases according to the sequence ββ <βα <αβ, with αβ being the most stable. Ratios based on homohopanes HC_{31} and HC_{35} S/(S+R) can reach values of 0.50-0.54 at the beginning of the oil generation window and the balance settles in the range of 0.57-0, 62. The studied samples showed values of 0.58 for HC_{31} and 0.43 and 0.52 for HC_{35}, and it was not possible to calculate the last ratio for sample A60. The C_{27} ααα S/(S+R) and C_{29} ααα S/(S+R) ratios ranged from 0.38 to 0.43 and 0.06 to 0.24, respectively, corroborating this interpretation, since these parameters did not reach the equilibrium window (PETERS et al., 2005).

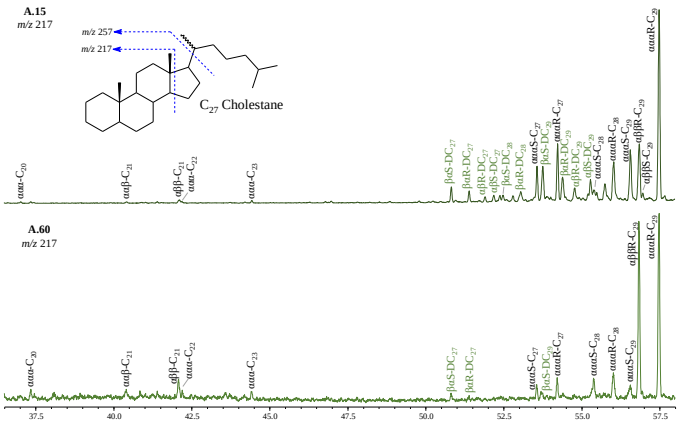

Figure 3. Chromatographic profile showing the distribution of steranes (*m/z* 217) in samples from the Serra Alta Formation.

Although the analyzed samples were predominantly immature, alterations were observed in the chromatographic profiles and in the parameters calculated based on biomarkers for the A60 sample, which is in direct contact with the igneous intrusive. Thermal stress caused a greater relative abundance of light *n*-alkanes in the C_{13}-C_{18} range and tricyclic terpanes (C_{19} to C_{24}) when compared to the other samples, in addition to a significant decrease in the relative concentration of C_{27} 17β(H)-22,29,30-trisnorhopane. This compound is characteristic of immature rocks and as thermal maturation increases its relative concentration decreases because it is more thermally unstable when compared to Tm.

The 5α,14α,17α configuration steranes showed discrete changes in their stereochemistry, with the C_{27} ααα S/(S+R) ratio being higher, while the C_{29} ααα S/(S+R) ratio is lower for the A60 sample when compared to the other samples that were not exposed to contact with the igneous intrusive. The decrease in C_{29} ααα S/(S+R) and the increase in the C_{29} αββS/(αββ+ααα) ratio may be an indication that under thermal stress the direct conversion from the less stable configuration to the more stable one (5α,14β,17β 22R) appears to be more thermodynamically favorable, and this is demonstrated by the increase in its relative abundance in the monitored ion chromatogram (*m/z* 217).

Conclusions

The sample from the Serra Alta Formation in contact with the igneous intrusive showed significantly different characteristics when compared to those from immature zones. The greater relative abundance of low *n*-alkanes and tricyclic (C_{19} to C_{24}), as well as the decrease in the relative concentration of β-Tm, increase in the values of the maturation parameters based on hopanes and C_{27} ααα S/(S+R) steranes indicate that thermal stress was enough to cause changes in organic matter at the molecular level.

Acknowledgements

The authors thank CNPq (Brazilian research council) for fellowships; ANP (Brazilian Petroleum Agency), Petrobras S/A and PPGQ – UFPI for financial support.

References

Milani, E. et al. 2007. Bacia do Paraná. Boletim de Geociencias-Petrobras**15**, 265–287.

Peters, K. E.; Walters, C. C.; Moldowan, J. M. 2004. The Biomarker Guide: Volume 2: Biomarkers and Isotopes in Petroleum Systems and Earth History. 2. ed. Cambridge: Cambridge University Press.

Rohn, R. 2001. A estratigrafia da Formação Teresina (Permiano, Bacia do Paraná) de acordo com furos de sondagem entre Anhembi (SP) e Ortigueira (PR). Correlação de Seqüências Paleozóicas Sul-Americanas**20**, 209–218.

XVI LATIN AMERICAN CONGRESS ON ORGANIC GEOCHEMISTRY
9 - 11 AUGUST, 2023
ARACAJU, SERGIPE, BRAZIL

APPLICATION OF PCA IN DETERMINING THE CONTROLS AND INDICATORS OF HYDROCARBON GENERATION

ALEK ANDRÉ COSTA DE SOUSA [a]* / AILTON SILVA BRITO [a] / ALEXANDRE ARAÚJO DE SOUZA [a] / AGOSTINHO MUSSA [b] / EDYMILAÍS DA SILVA SOUSA [a] / WOLFGANG KALKREUTH [b] / SIDNEY GONÇALO DE LIMA [a]

[a]Laboratório de Geoquímica Orgânica, Centro de Ciências da Natureza, Universidade Federal do Piauí, Teresina, PI, Brazil
[b]Laboratório de carvão e rochas regadoras de petróleo, Instituto de Geociências, Universidade Federal do Rio Grande do Sul, Porto Alegre, RS, Brazil

alekdesousa@ufpi.edu.br, sidney@ufpi.edu.br

Introduction

Principal Component Analysis (PCA), an important chemometric statistical approach, allows to group of samples with similar geological characteristics and the correlations of geological parameters directly related to hydrocarbon generation processes. Therefore, PCA also offers great potential to reveal the controlloing factors for the evolution of the different oil and gas production processes if appropriate parameters are used in the analysis. Therefore, this study aimed to evaluate organic geochemical data through PCA in samples from the Codó (Early Cretaceous) and Pimenteiras Formations (Devonian) to identify factors considered as controls and/or indicators of hydrocarbon generation characteristics in the Parnaíba Basin.

Experimental

A set of 26 samples were used, 11 samples from the Codó Formation (Sousa et al. (2019) and 15 from the Pimenteiras Formation (Mussa et al. (2021). Total organic carbon (TOC), free volatile hydrocarbons (S1), oil generation potential (S2), amount of CO_2 released (S3), maximum temperature (T_{max}), hydrogen index (HI), oxygen index (OI), production index (PI) sulfur content (S, %) and the ratio between total organic carbon and sulfur content (TOC/S) were used as variables. Using the correlation matrix, the PCA was performed with OriginPro 2023 software. The missing values were filled with the average values of the respective column of the same geological unit. The procedure of Sousa et al. (2022) was used to extract and analyze the acidic biomarkers in a sample of each formation.

Results and Discussion

PC1, PC2, and PC3 cumulatively explain 86 % of the data variance. Figure 1 shows the biplot graph of loadings and Scores. A brief analysis of the loadings reveals that the first principal component (PC1) is positively related to the PI, TOC, followed by oil S2 and S1 and to some extent with S3. PC2 is positively related to T_{max}, negatively related to S, and positively related to TOC/S. PC3, not shown, was calculated and is positively related to the HI and negatively to the OI.

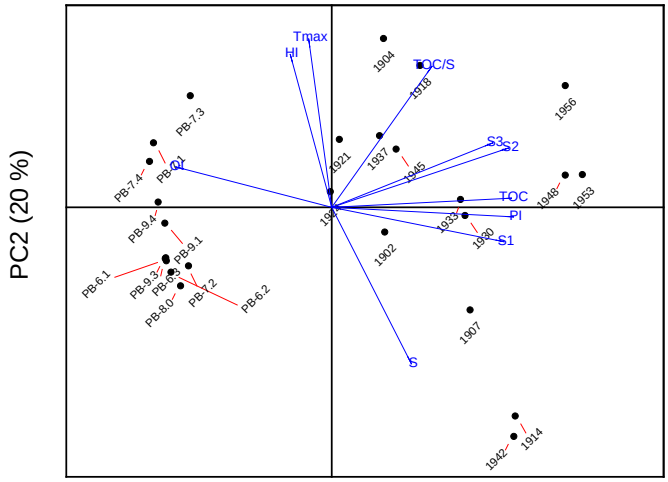

Figure 1. Biplot graph of the first two main components (PC1 vs PC2) performed with geochemical data of samples from the Codó and Pimenteiras Formations.

The PC2 loadings (Figure 1) shows that there is a negative relationship between T_{max} and sulfur content (S, %). Organically bound sulfur reduces the stability of kerogen due to the low C–S bond energy (Orr, 1985) or the sulfur radicals that allow faster thermal decomposition of the C–C bonds at lower thermal stress (Lewan, 1998). Thus, the higher the bound organic sulfur content, the greater the thermal instability of kerogen and the lower the T_{max} measured in Rock-Eval pyrolysis. These observations by PCA suggest that sulfur contributes to the low T_{max} values in the Pimenteiras Formation. Therefore, the T_{max} values measured for the Pimenteiras Formation should be somewhat higher, suggesting that the organic matter is in a stage of

greater thermal evolution than expected through T_{max} analysis.

Although the Pimenteiras Formation does not have high levels of sulfur, the PCA indicates that this factor may exert considerable influence on kerogen's thermal stability, probably being potentiated by low diagenetic evolution. Thus, the low-temperature values as a response to the burial together with the concentration of sulfur, may have been the main controllers of the maturation of the OM of this formation. Similar behavior between bound organic sulfur content and T_{max} is observed for the Codó Formation samples. However, the Codó Formation has less OM preserved, a main condition for hydrocarbon generation. The evaluation of the thermal maturation of OM based on the T_{max} values recorded does not strongly differentiate these two formations because, was previously discussed the T_{max} recorded is being controlled by the sulfur content. Therefore, it is necessary to use other information that indicates the actual condition of thermal maturation.

Hopanoic carboxylic acids are considered as precursors of hopane biomarkers. This suggests that the higher the concentration of hopanoic acids, the lower the thermal maturation of the organic matter. The concentration of carboxylic acids in the Codó Formation is about 2522 ppm, while in the Pimenteiras Formation it is only about 1400 ppm. This difference in the concentration of the acids is shown normalized in Figure 2. Comparing the trend of the OI vector in the PCA biplot (Figure 1) with the concentration of acids between these two formations, the OI index seems to be related to some extent to the abundance of carboxylic acid compounds in the organic extracts of the two formations. This trend appears to be better indicator of the state of thermal maturation of organic matter than the T_{max} recorded during Rock-Eval pyrolysis because the recorded T_{max} is controlled by the sulfur content. This information indicates that the organic matter of the Pimenteiras Formation has a higher thermal maturity than the organic matter from the Codó Formation. Thus, although the organic matter from the Codó Formation has been preserved under favorable conditions for generation compared to the Pimenteiras Formation, it does not achieve the same good conditions for hydrocarbon generation as the Pimenteiras formation (high maturation, TOC, S2, PI). Moreover, from the PCA scores (Figure 1), the total concentration of carboxylic acids can be used to predict the trend of the OI index and vice versa.

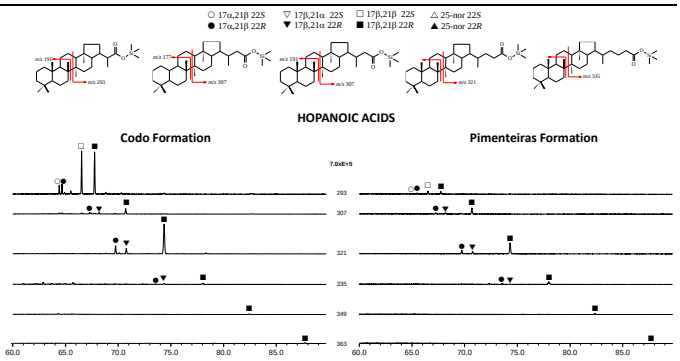

Figure 2. Hopanoic carboxylic acids present in the Codó and Pimenteiras Formations.

Conclusions

From the PCA-based biplot, it can be concluded that paleoenvironmental conditions influence the systematic differences in T_{max} of the two formations. Furthermore, the correlated information provided by PCA biplot allows for rapid assessments of how hydrocarbon generation characteristics are controlled by paleoenvironmental factors and how precursors can be used to reveal these characteristics.

Acknowledgements

The authors thank Conselho Nacional de Desenvolvimento Científico e Tecnológico (CNPq), Petróleo Brasileiro S.A. (PETROBRAS), Coordenação de Aperfeiçoamento de Pessoal de Nível Superior (CAPES), and Universidade Federal do Piauí (UFPI) for financial support.

References

Lewan, M.D., 1998. Sulphur-radical control on petroleum formation rates. Nature 391, 164–166.

Mussa, A., Kalkreuth, W., Mizusaki, A.M.P., Bicca, M.M., Bojesen-Koefoed, J.A., 2021. Geochemical characterization of the organic matter in the Devonian Pimenteiras Formation, Parnaiba Basin, Brazil – Implications for depositional environment and the potential of hydrocarbon generation. Journal of Petroleum Science and Engineering 201. doi:10.1016/j.petrol.2021.108461

Orr, W.L., 1985. Kerogen/asphaltene/sulfur relationships in sulfur-rich Monterey oils. Advances in Organic Geochemistry 10, 499–516.

Sousa, A.A.C. de, Sousa, E. da S., Sousa Junior, G.R. de, Carbonezi, C.A., Spigolon, A.L.D., Brito, A.S., de Lima, S.G., 2022. An alternative method for the separation and analysis of acidic biomarkers from crude oil samples. Journal of South American Earth Sciences 120, 104054.

Sousa, E. da S., Sousa Júnior, G.R., Silva, A.F., Reis, F. de A.M., Sousa, A.A.C., Cioccari, G.M., Capilla, R., de Souza, I.V.A.F., Imamura, P.M., Rodrigues, R., Lopes, J.A.D., de Lima, S.G., 2019. Biomarkers in Cretaceous sedimentary rocks from the Codó Formation - Parnaíba Basin: Paleoenvironmental assessment. Journal of South American Earth Sciences 92, 265–281.

XVI LATIN AMERICAN CONGRESS ON ORGANIC GEOCHEMISTRY
9 - 11 AUGUST, 2023
ARACAJU, SERGIPE, BRAZIL

IDENTIFICATION AND CHARACTERIZATION OF SOURCE ROCK INTERVALS ON THE PRE-SALT APTIAN DEPOSITS OF SANTOS BASIN

RAFAELA L. LENZ [ab*]; JAQUES S. SCHMIDT [a]; TAÍS F. SILVA [b]; ARGOS B. S. SCHRANK [ab]; THISIANE C. DOS SANTOS [a]; ELIAS CEMBRANI [a]; SABRINA D. ALTENHOFEN [a]; FELIPE DALLA VECCHIA [a]; ROSALIA BARILI [a]; ANDERSON J. MARASCHIN [a]

[a] **INSTITUTE OF PETROLEUM AND NATURAL RESOURCES;** [b] **FEDERAL UNIVERSITY OF RIO GRANDE DO SUL**

*rafaela.lenz@pucrs.br

Introduction

The Santos Basin Pre-Salt deposits represents approximately 75% of the Brazil hydrocarbon production (ANP, 2021). The Aptian Pre-Salt deposits consist mainly of carbonate sequences from the Barra Velha Formation (BVF), deposited in a lacustrine environment (Rebelo *et al*., 2023). The carbonate rocks from the BVF are subdivided in to *in situ* and redeposited facies. The *in situ* rocks are composed by three main components: silicatic Mg-clay matrix (Mud), calcite spherulites and calcite shrubs; forming mud-rich (mudstone), mud and spherulite-rich (muddy spherulstone), mud and shrub-rich (muddy shrubstone) facies, among others (De Ros & Oliveira, in prep). The redeposited rocks are composed by intraclast of the same composition. The BVF is the main reservoir rock in the Santos Basin, being generally understood that the Formation is charged with hydrocarbons (HCs) generated in the underlying Piçarras and Itapema Formations (Zou *et al*., 2022). However, the BVF also comprises HC generating intervals (intercalated with reservoir intervals) that have not been extensively investigated yet, and its better understanding could lead to significant economic impacts on the Santos Basin petroleum exploration. Therefore, the aim of this study is to identify source rocks intervals within the BVF, characterizing the HC generation potential, the type of organic matter, and the characteristic of the most favorable facies for HC generation.

Experimental

The study was carried out using core samples from three wells located in distinct oil fields and varying depths. Each sample was analyzed through Rock-Eval pyrolysis and transmitted-light petrography. The Rock-Eval pyrolysis was performed in the samples with the free HCs (S1 peak) extracted, because they can interfere in the S2 peak, increasing it, and, as the studied samples can be charged with migrated HCs from the underlying source rocks, this could lead to errors in the analysis.

Results and Discussion

The following results consider only the well A, as data from the wells B and C is currently being acquired. The Well A was separated into five different intervals, according to S2 peak values and facies (Fig. 1).

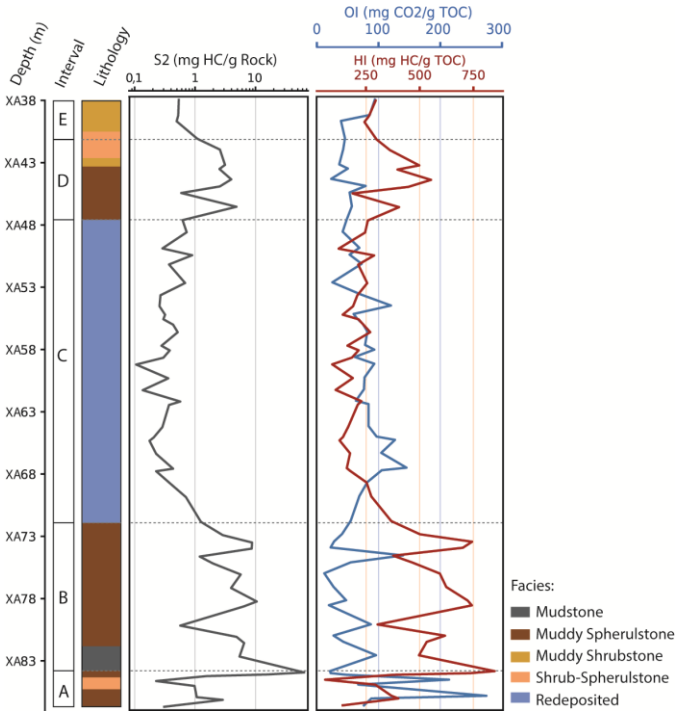

Figure 1. Well A: intervals, facies, S2 peak values, Hydrogen Index (HI) and Oxygen Index (OI).

The HCs generation potential was evaluated by the values of the S2 peak, according to Peters and Cassa (1994). The *in situ* rocks show, in general, higher values (avg. 3.26 mg HC/g rock; fair) than the redeposited rocks

(avg. 0.37 mg HC/g rock; poor) (Fig. 2 A), possibly because the more energetic redeposition processes favor the degradation of organic matter. In the well A, the interval C is characterized by redeposited facies, with constantly poor HCs generation potential (Fig. 1). Among the *in situ* facies there is a positive correlation with the volume of laminated Mg-clay matrix and the HC generation potential, confirmed by linear regression analysis (slope coefficient of 0.1757) (Fig. 2 B). So that, the mudstones showed the highest HCs generation potential (avg. 34.09 mg HC/g rock, excellent), followed by the muddy spherulstones (avg. 3.64 mg HC/g rock, fair).

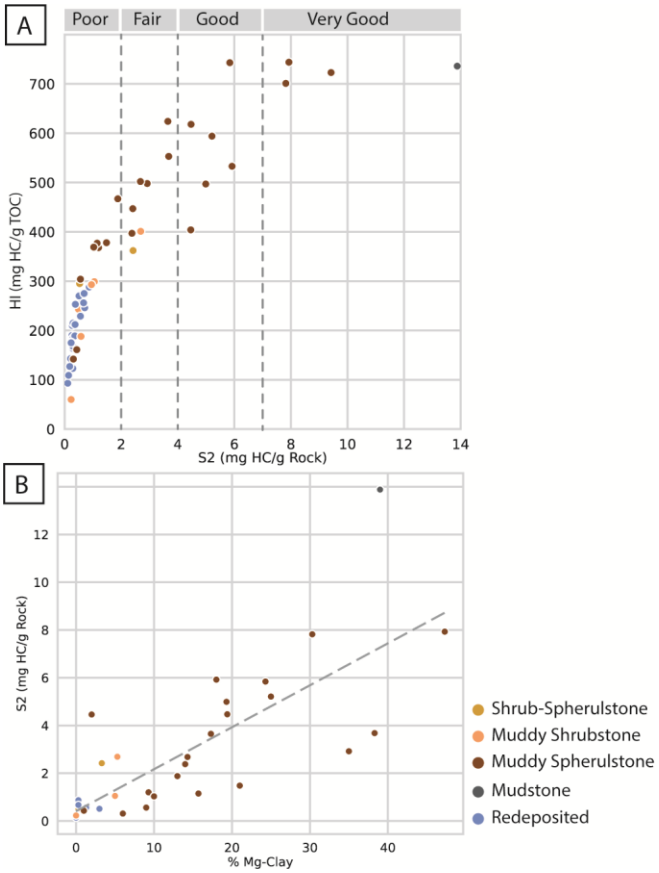

Figure 2. (A) Hydrogen Index (HI) versus S2 values, with the evaluation of the HC generation potential (Peters and Cassa, 1994); (B) Positive correlation between S2 values (HC generation potential) and Mg-clay matrix volume.

Nonetheless, some muddy spherulstones and muddy shrubstones samples have poor HC generation potential, this samples usually have a pale-colored Mg-clay matrix, in contrast with the dark-brown Mg-clay matrix found in samples with good HCs generation potential. This leads to the possibility that the organic matter occurs associated with the Mg-clay matrix, darkening its color. In the well A, the intervals A and E have mostly pale matrix and poor HC generation potential (Fig. 1), whereas the intervals B and D have mostly dark-brown matrix and average fair to good HC generation potential.

The samples with good to very good HC generation potential presented high values of Hydrogen Index (HI) (avg. 649.27 mg HC/g TOC) and low values of Oxygen Index (OI) (avg. 34.64 mg CO_2/g TOC). These indexes were used to evaluate the organic matter type, as a result 55% of these samples presented organic matter type I (oil-prone) and 45% type II (oil and gas-prone). Moreover, the T_{max} values varied between 431 and 458°C, considered within the oil generation window, indicating that these samples have already started the generation process.

Conclusions

Therefore, the source rocks intervals in the BVF are composed by *in situ* facies that contains significant amount of dark-brown Mg-clay matrix, mainly mudstones, muddy spherulstones and muddy shrubstones facies. These source rocks contain organic matter type I and II, oil and gas prone. In well A, the interval B (Fig. 1) can be considered a source rock interval, with an average good HC generation potential.

Acknowledgements

The authors thank Equinor ASA, for financial support, and ANP (Brazilian Petroleum Agency), for providing the samples.

References

ANP – Agência Nacional do Petróleo, Gás Natural e Biocombustíveis, 2021. Boletim da Produção de Óleo e Gás Natural. ANP, março, 2021. https://www.gov.br/anp/pt-br/centrais-de-conteudo/publicacoes/boletins-anp/bmp/2021/2021-03-boletim-pdf.pdf

De Ros, L.F.; Oliveira, D.M. An operational classification system for the South Atlantic Pre-Salt rocks. In prep.

Peters, K. E.; Cassa M.R., 1994. Applied source rock geochemistry. In: Magoon LB, Dow WG, editors. The Petroleum System—From Source to Trap. 60th ed. USA: American Association of Petroleum Geologists, 93–120.

Rebelo, T. B.; Batezelli, A.; Mattos, N. H.; Leite, E. P., 2023. Sedimentary processes and paleoenvironment reconstruction of the Barra Velha formation, Santos Basin, Brazilian pre-salt. Marine and Petroleum Geology 150, 106141.

Zou, G.; Wang, H.; Fan, G.; Zhang, J.; Zhang, Y.; Wang, C.; Yang, L.; Ding, L.; Pang, X.; Zuo, Y., 2022. Geochemical Characteristics and Distribution of the Subsalt Source Rocks in the Santos Basin, Brazil. ACS Omega 7(29), 25715–25725.

DIRECT ANALYSIS OF ADAMANTANES AND DIAMANTANES IN APPI (+) FT-ICR MS APPLING IN THERMAL EVOLUTION STUDIES

DANIELLE M. M. FRANCO[a], TAYNARA. R. COVAS[a], ROSANA C.L. PEREIRA[a], MÁRIO D. RANGEL[a], ROSINEIDE C. SIMAS[a,b],YGOR S. ROCHA[c], JOELMA P. LOPES[c], IGOR V.A.F. SOUZA[c], BONIEK G. VAZ[a]

[a]Federal University of Goiás, Brazil,[b]Mackenzie Presbyterian University, Brazil, [c]CENPES, Brazil.

daniellemitze@ufg.br

Introduction

Diamondoids are cage-like, ultra-stable, saturated ringed hydrocarbons. Isomerization ratios of these compounds have been widely used as markers to assess organic matter issues and the thermal maturity of oils and source rocks.[1] However, predicting maturation levels, especially at over-mature stages, is still challenging. [2]
Traditionally, diamondoids determination is performed by gas chromatography-mass spectrometry (GC-MS). However, as crude oil is a complex mixture, a preparative group separation step is mandatory to avoid matrix interference, which becomes time-consuming and laborious. [3] As diamondoids bring much information about crude oil, a direct screening method for analyzing them is welcome and a challenge. Here we introduce the development of one feasible and straightforward approach to analyze diamondoids directly from crude oil for thermal maturity assessment.

Experimental

In this study, 9 Brazilian crude oil samples (numbered 1 to 9) were used. The °API of the samples ranged from 30 to 50. In this way, samples with very high thermal evolution, as condensates, were included. A set of nine expelled oil (named A to G) from hydropyrolysis (HP) experiments of Type II-kerogen (temperature ranging from 300 to 365°C) was used for validation. APPI in positive-ion mode MS analyses were carried out in an FT-ICR MS 7T SolariX 2xR (Bruker Daltonics - Bremen, Germany. The samples in a concentration of 0.5 mg/mL in solutions of toluene/methanol (1:1 v/v) were directly injected using a syringe pump with a flow rate of 600 µL.h-1. 8MW data sets were acquired through magnitude mode within the mass range of *m/z* 107-2000, with 300 scans. For MS/MS experiments, a 2 Da of window isolation (m/z 187-189 for diamantane) and energy of 8 eV were used. For data processing and visualization, software Composer 64 v. 1.5.3 (Sierra Analytica - Modesto, CA, USA Thanus (LaCEM, UFG – Goiânia, GO, Brazil).

Results and Discussion

Figure 1 presents the #C distribution of DBE 5 class HC of 9 oil samples (Figure 1a) and 9 HP samples (Figure 1b). Higher relative abundances in the range of C14-C16 range were observed. An attempt to identify these species suggested C0-C2-diamantanes (C14H20). The MSMS experiment was done, results presented in Figure 2, confirm the diamantane structure.
A potential approach for evaluation thermal evolution of oils based on naphthalene and diamantane index using APPI (+) FT-ICR MS is shown in Figure 3, where the naphthalene index is represented by the sum of intensities of C10-13 DBE 7 class HC divided by the summed of intensities for all carbons range and the diamantane index by C14 intensity divided by the sum of intensities of C14 and C15 for DBE 5 class HC.
A tendency of increase in the indexes is observed with the increasing °API of some samples (Figure 3a). The HP samples results (Figure 3b) were consistent with the simulated thermal maturation process and validated this approach. For oil samples, the whole procedure was successfully done considering adamantane.

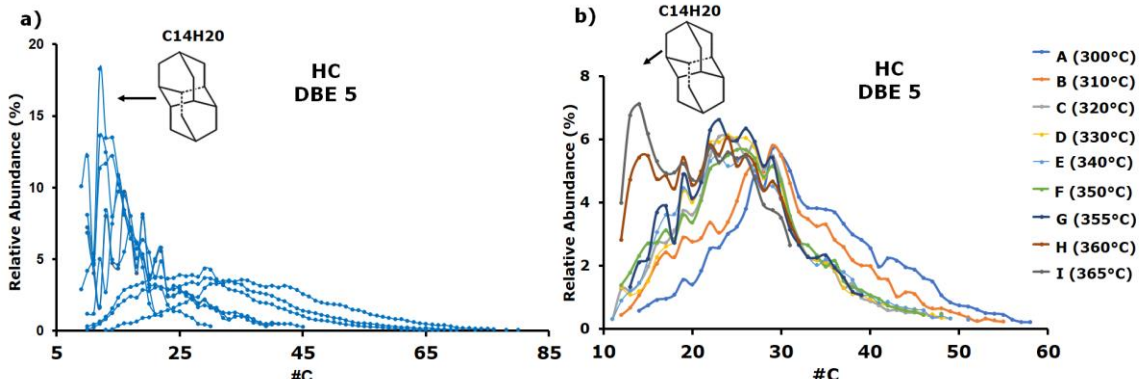

Figure 1: #C distribution of class HC of DBE 5 detected in APPI (+) 7T FT-ICR MS. A) 9 samples of the same basin and B) 9 samples of HP experimental.

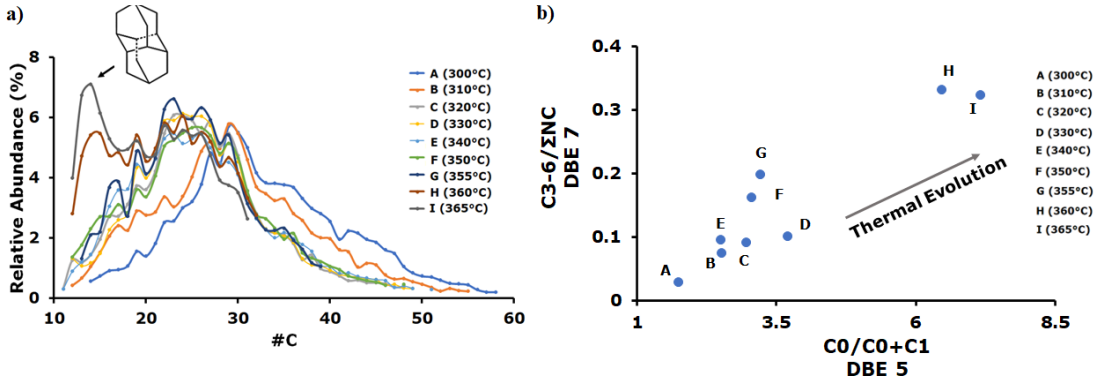

Figure 2: Plotting to naphthalene C10-13/sum of intensities for all carbons of DBE 7 by the diamantane C14 divided by the sum of intensities of C14+C15 of 9 samples of oil by the same basin detected in APPI (+) 7T FT-ICR MS.

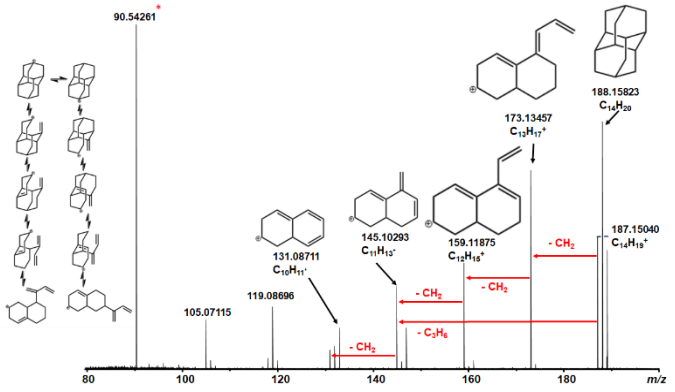

Figure 3: Fragmentation spectra of diamantane compound analyzed in APCI (+) FT-ICR MS (m/z 187-189), 8 eV collision energy.

Conclusions

This study demonstrates high potential applications by directly analyzing diamondoids by APPI (+) FT-ICR MS for thermal evolution studies of oil samples, including condensates.

Acknowledgements

The authors thank CENPES Petrobras S/A for financial support.

References

1. Peng, Y., et al., Diamondoids and thiadiamondoids Generated from Hydrothermal Pyrolysis of Crude Oil and TSR Experiments. Scientific reports, 2021.

2. Noah, M., et al., Precise maturity assessment over a broad dynamic range using polycyclic and heterocyclic aromatic compounds. Organic Geochemistry, 2020. **148**.

3. Mei, M., et al., Improved method for simultaneous determination of saturated and aromatic biomarkers, organosulfur compounds and diamondoids in crude oils by GC–MS/MS. Organic Geochemistry, 2018. **116**: p. 35-50.

XVI LATIN AMERICAN CONGRESS ON ORGANIC GEOCHEMISTRY
9 - 11 AUGUST, 2023
ARACAJU, SERGIPE, BRAZIL

USE OF THE NITROGEN MARKERS FOR PALEODEPOSITIONAL EVALUATION OF THE CANDEIAS (RECÔNCAVO BASIN) AND BARREIRINHA (AMAZONAS BASIN) FORMATION

AMARAL, D.N. [a] **/** MIRANDA, F.L.C. [a] / QUEIROZ, A.F. [a] / GARCIA, K.S [a] / MACHADO, M.E. [a,b,c] / FERREIRA, S.L.C. [a,b]

[a] **Universidade Federal da Bahia, Instituto de Geociências, Programa de Pós-Graduação em Geoquímica: Petróleo e Meio Ambiente, 40170-115, Salvador, BA, Brazil** /
[b] Universidade Federal da Bahia, Instituto de Química, 40170-115, Salvador, BA, Brazil
[c] Universidade Federal da Bahia, Centro Interdisciplinar de Energia e Ambiente - CIENAM, 40170-115 Salvador, BA, Brazil

e-mails: d.nery9@gmail.com, maria.elisabete@ufba.br

Introduction

In the Recôncavo Basin, located in the State of Bahia, the petroleum systems are recognized by having in common the source rock, represented by the Candeias Formation, deposited during the Cretaceous (Berriasian). In this basin, occur of black shales, rich in organic matter with average of total organic carbon (TOC) of 4% and Type I kerogen [1]. The Amazonas Basin, on the other hand, is located mostly in the States of Amazonas and Pará and has the Barreirinha Formation as the source rock of its petroleum systems. This geological formation bears dark gray to black shales, deposited in an anoxic marine environment, associated with the preservation of a large volume of organic matter in the Devonian (Frasnian), generating TOC with of around 3% and type II kerogen [2].

Nitrogen compounds such as indoles, carbazoles and benzocarbazoles and their alkylated analogues, has been employed as markers (N-markers) to evaluate depositional facies, thermal maturity and biodegradation [3]. The determination of the N-markers in general is by GC-MS. However, recently the GC-MS/MS an advanced technique, has been proven adequate instrumentation with high selectivity and sensibility [4].

The aim of this study was to use the GC-MS/MS to determine the N-markers in samples from the Candeias and Barreirinha Formations for geochemical interpretation regarding the type of organic matter, depositional conditions and thermal maturation.

Experimental

Samples from two basins were collected in different periods in the vertical direction in the outcrops. In the Recôncavo Basin, the collection of samples from the Candeias Formation took place on the outskirts of the city of Santo Amaro, Bahia, named from bottom to top as 5B1 to 5B10, with a total of 10 samples. In the Amazon Basin, samples from the Barreirinha Formation were collected at different sites in the municipality of Rurópolis (PA), and the outcrops were named IT02, IT06, totalizing 17 points. In the laboratory, the rock samples were pulverized and underwent accelerated solvent extraction to obtain the organic extract. Afterward, the extracts were fractionated via SARA method.

Fractions containing aromatic compounds and NSO were analyzed in a GC-MS/MS system equipped with a 7890B gas chromatograph with split/splitless injector and a 7000C triple quadrupole mass detector, both from Agilent (Santa Clara, CA, USA).

For the identification and quantification of N-markers, a 100 ppb mix solution containing twenty-one standards was prepared, with 9-phenylcarbazole and cabazole-d_8 used as internal standards.

Results and Discussion

In general, the highest concentrations of carbazoles (CA), methylcarbazole (C1CA) and dimethylcarbazoles (C2CA) were obtained in extracts from the Amazon Basin, while extracts from the Recôncavo Basin had lower concentrations of C0-C2 carbazoles. These results are in accordance with [5] that found low concentrations of nitrogenous compounds in non-marine source rock extracts.

The ternary diagram containing the isomeric distribution of methylcarbazoles (Figure 1) allowed us to verify the higher concentrations of 1-methylcarbazole and 2-methylcarbazole when compared with 4-methylcarbazole. [6] observed that alginite-rich samples (maceral from algae, whether lake or marine) exhibit higher proportions of 1-methylcarbazole and 2-methylcarbazole and low concentrations of 4-methylcarbazole. Therefore, even if they have different origins, all samples under study represent strata with algalic input.

Therefore, even if they have different origins, all samples under study represent strata with algalic input.

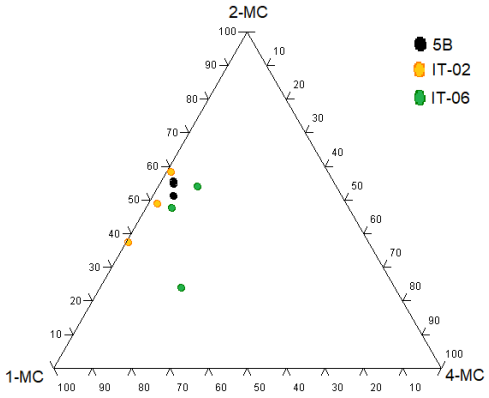

Figure 1. Ternary diagram containing the isomeric distribution of methylcarbazoles for samples from the Candeias Formations (samples 5B, Recôncavo Basin) and Barreirinha (IT samples, Amazonas Basin)

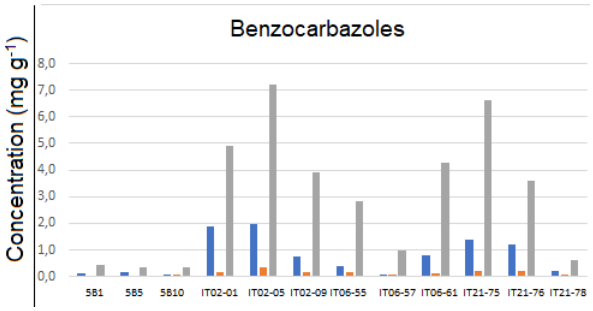

Figure 2. Concentrations of benzocarbazole isomers for samples from the Candeias Formations (samples 5B, Recôncavo Basin) and Barreirinha (IT samples, Amazonas Basin)

By the benzocarbazole concentration data, the differences between the values are accentuated between the samples from the Recôncavo Basins (lower concentrations) and the Amazon (higher concentrations) (Figure 2). This difference in concentrations may be linked to different oxygenation conditions in depositional environments [7]. Furthermore, ratios using benzocarbazoles suggest that the samples are thermally immature. This interpretation is in accordance with saturated biomarker data by [1] and [2].

Conclusions

The analysis of the N-markers by GC-MS/MS allowed interpreting that samples from Candeias Formation, Recôncavo Basin are those with the lowest concentrations of carbazoles (CA) methylcarbazole (C1CA) and dimethylcarbazoles (C2CA). On other hand, the analysis of isolated nitrogenous compounds or diagnostic ratios indicates input predominantly from algae, compatible with M.O. type I, well preserved, deposited predominantly under anoxic conditions.

The samples from Barreirinha Formation, Amazon Basin where those with the highest concentrations of carbazoles (CA), methylcarbazole (C1CA) and dimethylcarbazole (C2CA), while the analysis of isolated nitrogenous compounds or diagnostic ratios indicates input from marine constituents, predominantly algae, compatible with M.O. type II, mostly deposited under oxidizing conditions.

The variability of the concentrations of N-markers and also geochemical properties of organic matter, reflect different environments and conditions during the deposition of sediments from the Candeias and Barreirinha Formations. Therefore, the use of GC-MS/MS for identification of N-markers was efficient for the characterization of depositional environments, organic matter input, conditions of the depositional environment and thermal maturation from organic extracts of source rocks.

Acknowledgements

The authors gratefully acknowledge the support from Shell Brasil through the “Project Petroleum Systems Research in Brazilian Sedimentary Basins” Areas at Instituto de Geociências da Universidade Federal da Bahia (UFBA) - GEOQPETROL - PS” - ANP 20720-9 project and the strategic importance of the support given by ANP through the R&D levy regulation.

References

[1] Amaral, D.N. et al., 2020. Paleoenvironmental characterization of a Lower Cretaceous section of the Recôncavo Basin, Bahia, Brazil. Brazilian Journal of Geology, v. 50, n. **3**, p. 1-11.

[2] Góes, V.C.M. et al., 2022. Hydrocarbon source potential and paleodepositional environment of the (Devonian) Barreirinha formation on the south edge of the Amazonas basin border, Brazil. Journal of South American Earth Sciences **115**.

[3] Dias, L.C, Bahia, P.V.B., Amaral, D.N., Machado, M.E., 2020. "Nitrogen Compounds as Molecular Markers: An Overview of Analytical Methodologies for Its Determination in Crude Oils and Source Rock Extracts." Microchemical Journal 157.

[4] Dias, L.C, Bahia, P.V.B., Amaral, D.N., Machado, M.E., 2021. "Nitrogen Compounds as Molecular Markers: An Overview of Analytical Methodologies for Its Determination in Crude Oils and Source Rock Extracts." Microchemical Journal 157.

[5] Zhang, C., Zhang, Y., Zhang, M., Zhao, H., Cai, C., 2008. Carbazole distributions in rocks from non-marine depositional environments. Org. Geochem. **39**, 868–878.

[6] Clegg, H., Wilkes, H., Horsfield, B., 1997. Carbazole distributions in carbonate and clastic source rocks. Geochim. Cosmochim. Acta **61**, 5335–5345.

[7] Bakr, M. M. Y.; Wilkes, H., 2002. The influence of facies and depositional environment on the occurrence and distribution of carbazoles and benzocarbazoles in crude oils: a case study from the Gulf of Suez, Egypt. Org. Geochem. **33**, 561–580.

XVI LATIN AMERICAN CONGRESS ON ORGANIC GEOCHEMISTRY
9 - 11 AUGUST, 2023
ARACAJU, SERGIPE, BRAZIL

OPTIMIZATION OF A GC-MS/MS METHOD FOR QUANTIFICATION OF NITROGEN MARKERS IN CRUDE OIL SAMPLES FROM DIFFERENT SEDIMENTARY ENVIRONMENTS

MIRANDA, F.L.C [a] **/** AMARAL, D.N [a]/ GARCIA, K.S [a]/ QUEIROZ, A.F [a]/ MACHADO, M.E [a, b, c]

[a] **Universidade Federal da Bahia, Instituto de Geociências, Programa de Pós-Graduação em Geoquímica: Petróleo e Meio Ambiente, 40170-115, Salvador, BA, Brazil** /
[b] Universidade Federal da Bahia, Instituto de Química, 40170-115, Salvador, BA, Brazil/
[C] Universidade Federal da Bahia, Centro Interdisciplinar de Energia e Ambiente - CIENAM, 40170-115 Salvador, BA, Brazil

e-mail: cimaflavia@gmail.com, maria.elisabete@ufba.br

Introduction

In petroleum, nitrogen compounds range from 0.1% to 2.0% and can be found as basic and neutral compounds [1]. In organic geochemistry, the distributions of these compounds in source rocks and crude oils can be used as markers (N-markers) because they present large and systematic variations due to the fractionation effects associated with the migration process [2]. Studies show that N-markers distribution can also be influenced by depositional facies, thermal maturity and biodegradation [1].

In a previous study [3] developed for the first time, a GC-MS/MS method for the quantification of thirteen N-markers. However, the authors analyzed crude oils without fractionation steps, which makes the identification of compounds more laborious due to the complexity of these samples. In this sense, fractionation methods such as the classical SARA method allowed elimination interferences before instrumental determination by gas chromatography. The gas chromatography coupled to triple quadrupole mass spectrometry (GC-MS/MS) is adequate to trace analysis due to low detection limits, possibility of structural information, and greater selectivity.

In the present study, a GC-MS/MS method was optimized based on [3] for the determination and quantification of twenty-one N-markers in crude oils from different sedimentary environments. The MS/MS was operated in multiple reaction monitoring (MRM) mode after the selective choice of precursor ion and product ion as well as collision energy and time windows. The samples were fractionated prior to GC-MS/MS analysis.

Experimental

GC-MS/MS optimization

To optimization of the GC-MS/MS method, a mix solution with 21 standards of the N-markers from carbazole, indole and quinoline classes was prepared at a concentration of 100 µg L^{-1}. All standards were purchased from Chiron AS (Trondheim, Norway) with purity greater than 99%. First, the instrument was operated in SCAN mode to obtain retention time and mass spectrum from each compound. After, analysis in SIM mode was employed for a comparative study of sensibility. Finally, the mass spectrometer was operated as MS/MS in PIS mode to define the optimum energies in the collision cell and in MRM mode for the transitions.

Quantification

The quantification was performed by the method of internal standards (IS) using 9-phenylcarbazole and carbazole-d_8 area. These two IS were added for a ratio of 0.02 g of sample to 2 mL of solvent (Toluene P.A) the final concentration of 10 µg L^{-1}.

Application of the optimized method in real samples

Three oil samples from the Recôncavo Basin (Brazil), Campos Basin (Brazil) and Valle Superior del Magdalena (Colombia) were selected to evaluate the applicability of the proposed method. First, these samples were fractionated by SARA method in order to obtain the aromatic (ARO) and NSO fractions. Since there are studies that report the inefficiency of the SARA fractionation for selective isolation of N-markers in the ARO fraction [4], these two fractions were eluted together. The SARA method, 30 mL of a 4:1 mixture of n-hexane: dichloromethane was used to separate the aromatic hydrocarbons. Finally, 30 mL of a 4:1 mixture of dichloromethane: methanol was added to elute the NSO compounds, in the same flask as the ARO fraction. All samples were concentrated in a rotary evaporator (Model R-210 Labortechnik, AG Switzerland) and transferred to 2 mL vials, previously weighed and identified. The IS were added in this step.

In GC (Agilent, model 7000D), automatic injection of 1µL of sample fraction occurs with the injector maintained at 300 ºC. The gas carried was helium 99.999% (White Martins, RJ, Brazil) purity. The instrumental conditions of separation are described in [4].

Results and Discussion

GC-MS/MS optimization

The scan analysis with the mix of the 21 N-markers allowed optimize the GC conditions for optimum separation and identification by the mass spectrum of each individual target compound. By the mass spectrum, the parent ions could be selected considering the best fragment (ions with the highest abundance), ions with higher m/z ratios, and no interference with the matrix.

Then, the product ion scan (PIS) mode allowed determine the product ion by fragmentation of the precursor perform test at various collision energies (5, 10, 20, 30, 40, 50 and 60 eV). Based on these tests, the collision energy that generated the highest intensities for the product ions was selected for a new analysis in MRM mode. In Figure 1, an example of optimized transitions of the N-markers in the MRM mode is shown.

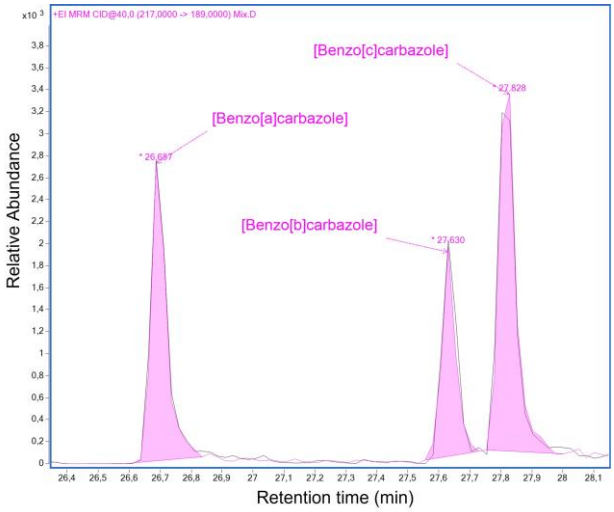

Figure 1. MRM chromatogram showing the transitions optimized (217-189) for Benzo[a]carbazole, Benzo[b]carbazole and Benzo[c]carbazole standards (concentration of 100 µg L^{-1}).

Application of the method for crude oil samples

The optimized method was adequate to quantify all N-markers in three samples from the Recôncavo Basin (Brazil), Campos Basin (Brazil) and Valle Superior del Magdalena (Colombia), the concentration ranged from 0.4 µg L^{-1} to 30 µg L^{-1} (carbazole). The chromatographic resolution of the peaks perfectly demonstrated the applicability of GC-MS/MS in the determination of N-markers in oil samples. In Figure 2 it is possible to observe the peak of carbazole in three samples, where the different concentrations may indicate different sedimentary environments.

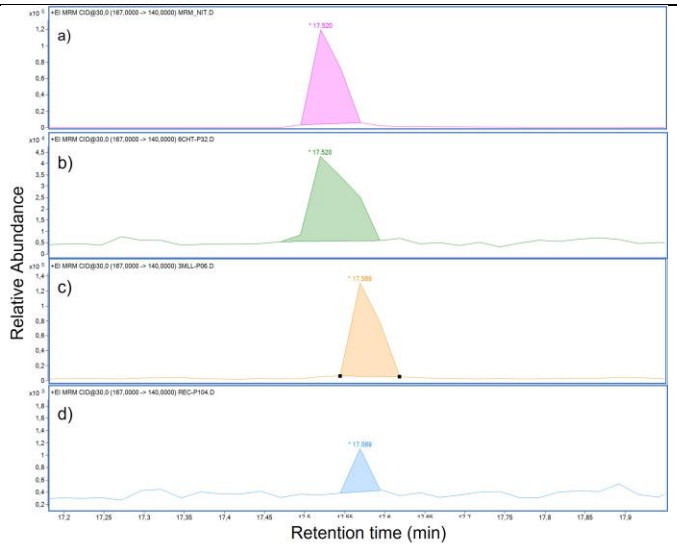

Figure 2. Chromatogram in MRM mode (transition 167-140) for carbazole in: a) standard b) Valle Superior del Magdalena (Colombia), c) Campos Basin (Brazil), d) Recôncavo Basin (Brazil).

Conclusions

The GC-MS/MS optimized method proved to be efficient, sensitive and selective for quantification of target N-markers from complex samples of oil. The application in samples indicates that the analytical methodology was adequate and may use in the future to assess the depositional environment.

Acknowledgements

The authors gratefully acknowledge the support from Shell Brasil through the project “Research in Petroleum Systems of Brazilian Sedimentary Basins - Federal University of Bahia (UFBA) – GEOQPETROL-PS” - ANP 20075-8 and the strategic support given by ANP through the R&D levy regulation.

References

[1] Dias, L.C; Bahia, P.V.B; Amaral, D.N; Machado, ME.; 2020. Nitrogen compounds as molecular markers: An overview of analytical methodologies for its determination in crude oils and source rock extracts. Microchem J, 157:105039.

[2] Li, M., Larter, S.R., Stoddart, D., Bjorøy, M.; 1995. Fractionation of pyrrolic nitrogen compounds in petroleum during migration: derivation of migration-related geochemical parameters. Geological Society, London, Special Publications, 86(1):103–23.

[3] Dias, L.C, Bahia, P.V.B., Amaral, D.N., Machado, M.E., 2021. "Nitrogen Compounds as Molecular Markers: An Overview of Analytical Methodologies for Its Determination in Crude Oils and Source Rock Extracts." Microchemical Journal 157.

[4] Radke, M., Willsch, H., Welte, D. H.; 1980. Preparative hydrocarbon group type determination by automated medium pressure liquid chromatography. Anal. Chem., 52: 406–411.

XVI LATIN AMERICAN CONGRESS ON ORGANIC GEOCHEMISTRY
9 - 11 AUGUST, 2023
ARACAJU, SERGIPE, BRAZIL

A COMPARISON OF TOTAL ORGANIC CARBON CONTENT ACROSS THE OCEANIC ANOXIC EVENT 1b (OAE1b, KILIAN LEVEL) IN THE SOUTH ATLANTIC

MAURO D. R. BRUNO[a*], FERNANDA LUFT-SOUZA[a], BERNARDO VÁZQUEZ-GARCÍA[a], EDNA DE J. F. TUNGO[a], VICTÓRIA H. SANDER[a], MARCOS A. B. S. FILHO[a], HENRIQUE P. KERN[a], ALESSANDRA SANTOS[a], LILIAN M. LEANDRO[a], GERSON FAUTH[a]

[a] **INSTITUTO TECNOLÓGICO DE PALEOCEANOGRAFIA E MUDANÇAS CLIMÁTICAS (Itt Oceaneon), UNISINOS UNIVERSITY, BRAZIL**

*Correspondence: dbruno@unisinos.br

Introduction

The Oceanic Anoxic Events (OAEs) represent episodes related to significant perturbations in the global carbon cycle, normally, associated with multiple organic-rich black shale horizons, deposited simultaneously in different regions of the North Atlantic and Tethys Sea during the Cretaceous Period [1,2,3]. These black shales have been associated with significant hydrocarbon source rocks, consisting essentially of a high concentration of algal marine organic matter [4].

The Early Cretaceous sedimentary sequences of the South Atlantic Ocean are known to be a world-class petroleum province, particularly the Sergipe-Alagoas (Brazil) and Kwanza (Angola) basins (Figure 1). In this context, records of OAEs in the South Atlantic Ocean have been recognized in recent years [5,6,7], representing a new exploratory frontier.

In Brazil, the early Albian deposits of the Sergipe-Alagoas Basin contain some of the most important petroleum systems in the region, where shales associated with the OAE1b (Kilian Level) have recently been found in the Riachuelo Formation [7]. In the Parnaíba and São Luís basins (Brazil), the early Albian OAE1b event was recorded in the Codó Formation shales [5]. This event was also recorded in the Kwanza Basin, where black shales interbedded with calcareous sediments were observed in horizons possibly related to the Binga Formation [6].

The Kilian Level (OAE1b) marks the Aptian–Albian boundary and is characterized by a negative excursion of the ^{13}C isotope, associated with the first occurrence (FO) of *Microhedbergella renilaevis* (planktic foraminifera) and the FO of the calcareous nannofossil *Prediscosphaera columnata.* These geochemical and paleontological data have been used to identify the base of the Albian in the Global Stratotype, Vocontian Basin from France [2,8]. The studies that identified the OAE1b in the South Atlantic included the negative excursion and paleontological information used globally to define the Kilian Level. However, a comparison between the Total Organic Carbon (TOC) content in the Vocontian Basin and the South Atlantic sites (Sergipe-Alagoas, Parnaíba, São Luís, and Kwanza basins) has not yet been carried out. Therefore, in this study, we present a review of the paleoceanographic conditions that influenced the TOC concentrations recorded for OAE1b in the South Atlantic Ocean.

TOC of Studied Sites

During the global event OAE1b (Kilian Level), depositional conditions in the Parnaíba and São Luis basins were characterized by restricted marine paleoenvironments, showing significative TOC values up to 15% in the São Luís Basin and 10% in the Parnaíba Basin [5].

In the Kwanza Basin, a maximum of 8.91% TOC was deposited in open marine conditions during the OAE1b [6]. In the Sergipe-Alagoas Basin, the OAE1b was recorded in a sedimentary section deposited in a shallow marine paleoenvironment with ~1.5% of TOC [7].

Discussion

The highest TOC values recorded for the OAE1b in the South Atlantic Ocean were in the São Luís (TOC reaching up to 15%) and Parnaíba (TOC reaching up to 10%) basins. The restricted marine paleoenvironments characterized by these sedimentary sections indicate low oxygen waters and a significant contribution of marine organisms, terrestrial plants, and microbial communities to the composition of organic matter deposits [5].

For the open marine conditions registered in the Kwanza Basin (TOC up to 8.91%) during OAE1b, organic matter is essentially composed of marine algal communities. The paleoenvironments were characterized by extreme paleoceanographic conditions such as dysoxia/anoxia, hydrothermal activity, and high salinity which did not allow favorable conditions for the evolution of marine biota [6].

Figure 1. Paleogeographic reconstruction at ~113 Ma (modified from http://www.odsn.de) shows the location of the Kwanza Basin, (KB), Parnaíba Basin (PB), São Luís Basin (SL), Sergipe-Alagoas Basin (SA), Vocontian Basin (VB), Poggio le Guaine (PLG), and Santa Rosa Canyon (SRC).

The OAE1b in the Sergipe-Alagoas Basin was recorded in a sedimentary section deposited in shallow marine paleoenvironment (TOC up to ~1.5%), characterized by low oxygenated bottom water [7]. Similar conditions were observed for OAE 1b in the North Atlantic and Tethys Sea sections, characterized by increased TOC content at the PLG - Italy (TOC >2%; [3]), Santa Rosa Canyon - USA (TOC ~1.5%; [1]), and Vocontian Basin - France (TOC >6%; [2].

Conclusions

A high content of organic matter (high TOC) was registered in several sedimentary sections deposited during the early Albian around the world, related to the OAE1b. We explored paleoceanographic conditions associated with the deposition of TOC content during the OAE1b in the South Atlantic Ocean to perform a comparative analysis between restricted marine, shallow marine, and open marine environments.

Restricted marine conditions (Parnaíba and São Luís basins) exhibit organic matter content associated with marine algae, microbial communities, and terrestrial plants, showing the highest TOC values in the South Atlantic. On the other hand, marine environments to which essentially algal communities contribute, show TOC values very similar to those measured in marine sections of the North Atlantic and Tethys. In future studies, we intend to analyze the preservation conditions of TOC in post-depositional processes.

Acknowledgments

The authors were grateful to CNPq (Brazilian Research Council) for grant 405679/2022-0; M.D.R.Bruno and E.J.F.Tungo are CAPES (Coordenação de Aperfeiçoamento de Pessoal de Nível Superior) fellows.

References

1. Bralower, T.J., Cobabe, E., Clement, B., Sliter, W.v., Osburn, C.L., Longoria, J., 1999. The record of global change in mid-Cretaceous (Barremian-Albian) sections from the Sierra Madre, Northeastern Mexico. J. Foraminifer. Res. 29, 418-437.
2. Herrle, J.O., Kößler, P., Friedrich, O., Erlenkeuser, H., Hemleben, C., 2004. High- resolution carbon isotope records of the Aptian to Lower Albian from SE France and the Mazagan Plateau (DSDP Site 545): a stratigraphic tool for paleoceanographic and paleobiologic reconstruction. Earth Planet. Sci. Lett. 218, 149-161.
3. Coccioni, R., Sabatino, N., Frontalini, F., Gardin, S., Sideri, M., Sprovieri, M., 2014. The neglected history of Oceanic Anoxic Event 1b: insights, new data from the Poggio le Guaine section (Umbria-Marche Basin). Stratigraphy 11, 245-282.
4. Tissot, B., Demaison, G., Masson, P., Delteil, J.R., Combaz, A., 1980. Paleoenvironmentand petroleum potential of middle Cretaceous black shales in Atlantic basins.AAPG Bulletin 64 (12), 2051-2063.
5. Bastos, L.P.H., Pereira, E., Cavalcante, D. da C., Alferes, C.L.F., Menezes, C.J., Rodrigues, R., 2020. Expression of Early Cretaceous global anoxic events in Northeastern Brazilian basins. Cretac. Res. 110.
6. Bruno, M.D.R., Fauth, G., Watkins, D.K., Savian, J.F., 2020. Albian–Cenomanian calcareous nannofossils from DSDP Site 364 (Kwanza Basin, Angola): biostratigraphic and paleoceanographic implications for the South Atlantic. Cretac. Res. 109.
7. Fauth, G., Krahl, G., Kochhann, K. G. D., Bom, M. H. H., Baecker-Fauth, S., Bruno, M. D. R., ... & de Oliveira Lima, F. H. (2022). Astronomical calibration of the latest Aptian to middle Albian in the South Atlantic Ocean. Palaeogeography, Palaeoclimatology, Palaeoecology, 602.
8. Kennedy, J.W., Gale, A.S., Huber, B.T., Petrizzo, M.R., Bown, P.R., Jenkyns, H.C., 2017. The global boundary stratotype section and point (GSSP) for the base of the Albian stage, of the Cretaceous, the col de Pr´e-guittard section, arnayon, drˆome, France. Episodes 40, 177-188.

XVI LATIN AMERICAN CONGRESS ON ORGANIC GEOCHEMISTRY
9 - 11 AUGUST, 2023
ARACAJU, SERGIPE, BRAZIL

Analysis of vanadyl porphyrins and sulfur containing vanadyl porphyrins in several asphaltenes by APPI and LDI

Matthias Witt*[1], Estrella Rogel [2]

[1] **Bruker Daltonics GmbH & Co. KG, MRMS Solutions, Fahrenheitstrasse 4, 28359 Bremen, Germany**

[2] **Chevron Energy Technology Company, 100 Chevron Way, Richmond, California 94802, United States**

Matthias.Witt@bruker.com

Introduction

Metallo porphyrins are present in crude oil and enriched in asphaltenes. The most common forms are vanadyl porphyrins which are used as biomarkers for the oil. Therefore, the different forms of these petro-porphyrins are of high interest [1-3]. These metallo porphyrins can be purified via chromatographic methods. However, due to the quite high abundance of these petro-porphyrins in the asphaltene, these compounds can be directly detected in the asphaltene fractions by ultra-high resolution mass spectrometry. Beside the vanadyl porphyrins also sulfur containing vanadyl porphyrins could be detected directly from the asphaltene without any separation step.

Experimental

Data acquisition:
- scimaX MRMS with 7 T superconducting magnet and new dynamically harmonized analyzer cell and quadrupolar detection
- mass range m/z 151 – 3000
- ionization: APPI and LDI in positive ion mode
- resolving power of 1,100,000 at m/z 400 using absorption mode processing
- 300 single scans were added for the final mass spectrum for APPI and LDI
- APPI: 100 ppm in 90% toluene/10% MeOH
- LDI: 1% in DCM
  1 ul spotted on stainless steel target
  100-400 laser shots per scan with LP of 10%

Molecular formula assignment:
- PetroOrg 18.3 (Florida State University)
- Max. molecular formula: $C_cH_hN_4O_3S_3V$
- H/C ratio: $0.2 \leq H/C \leq 2.3$
- Electron configuration: odd and even
- Mass tolerance: 0.5 ppm

Results and Discussion

Several asphaltene samples containing different amounts of vanadium (630 - 5000 ppm) and sulfur (3.8 – 8.8%) were analyzed by Atmospheric pressure photo ionization (APPI) as well as laser desorption ionization (LDI) using a scimaX MRMS instrument (Bruker Daltonics GmbH & Co. KG, Bremen, Germany). In this study we focused especially on the detection of vanadyl porphyrins and sulfur-containing vanadyl porphyrins which could be directly detected in the sample without any further purifications step.

The vanadyl porphyrins were detected as radical cations $[M^{+\cdot}]$ as well as protonated molecules $[M+H]^+$ with a relative abundance varying between 0.3 and 9% using APPI as well as LDI. A detailed analysis of the vanadyl porphyrins was performed by plotting the DBE vs. carbon number detected as radical cations using APPI and LDI (Fig. 1).

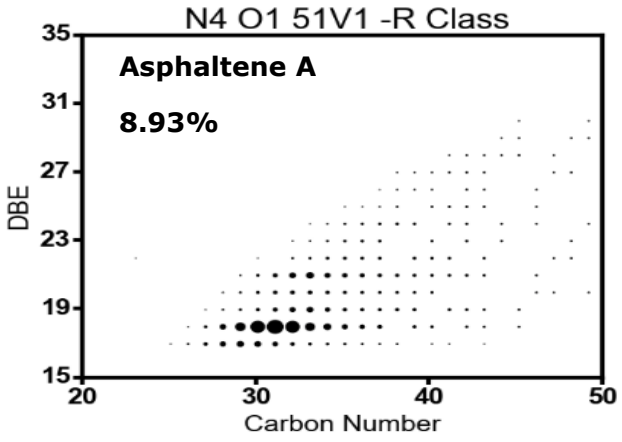

Figure 1. DBE vs. C atom number plot of vanadyl porphyrins of sample A detected by APPI.

The distribution of the detected vanadyl porphyrins (C number and DBE) was similar for all asphaltenes when using the same ionization method. However, the distribution was different for APPI and LDI. Using LDI, vanadyl porphyrins with higher DBE compared to APPI were detected as shown in Figure 2. The relative abundances of the different forms of the vanadyl porphyrins such as Etio, DPEP, Di-DPEP, Rhodo-Etio, Rhodo-DPEP and porphyrins with higher DBE are shown in figure 2 for both ionization methods. The relative abundances were slightly different for the samples when using APPI with the main difference in Etio and DPEP porphyrins. In LDI the difference between different types of vanadyl porphyrins were more pronounced.

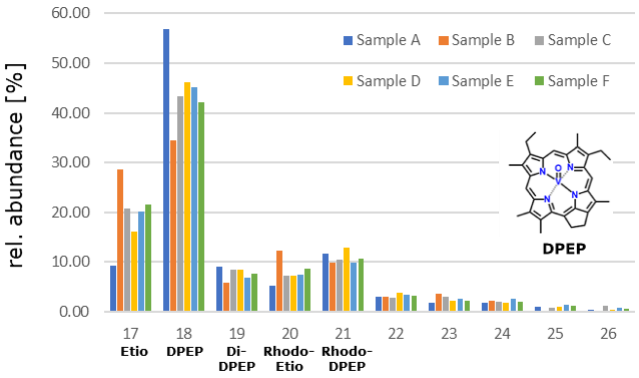

Figure 2. Plot of relative abundance of different vanadyl porphyrin types (numbers in DBE) in asphaltene samples detected by APPI.

Additionally, a good correlation was observed for APPI between rel. abundance of vanadyl porphyrins and amount of vanadium in the asphaltene with a correlation factor R^2 between 0.97 and 0.99

Conclusions

Vanadyl porphyrins could be directly detected in asphaltenes by MRMS using APPI and LDI. Sulfur-containing vanadyl porphyrins could also be detected in asphaltenes by APPI. Main difference between asphaltenes was observed for vanadyl porphyrin species Etio and DPEP. A good correlation was observed between rel. abundance of vanadyl porphyrins and amount of vanadium in asphaltene for APPI.

References

[1] X. Zhao; Y. Liu; C. Xu; Y. Yan; Y. Zhang; Q. Zhang; S. Zhao; K. Chung; M. R. Gray; Q. Shi, Energy & Fuels, 27 (2013), 2874.
[2] A. M. McKenna; J. M. Rurcell; R. P. Rogers; A. G. Marshall, Energy & Fuels, 23 (2009), 2122.
[3] K. Qian ; A. S. Mennito; K. E. Edwards ; D. T. Ferrughelli, Rapid Commun. Mass Spectrom., 22 (2008), 2153.

XVI LATIN AMERICAN CONGRESS ON ORGANIC GEOCHEMISTRY
9 - 11 AUGUST, 2023
ARACAJU, SERGIPE, BRAZIL

Effect of precipitation time on deposit characteristics upon crude oil blending

Matthias Witt*[1], Marta Lezcano,[2] Estrella Rogel [2]

[1] **Bruker Daltonics GmbH & Co. KG, MRMS Solutions, Fahrenheitstrasse 4, 28359 Bremen, Germany**

[2] **Chevron Energy Technology Company, 100 Chevron Way, Richmond, California 94802, United States**

Matthias.Witt@bruker.com

Introduction

In this study, we evaluate the characteristics of precipitated material recovered from the blend of two crude oils. The deposit was recovered by filtration and its characteristics were analyzed as function of time. In general, the deposits are enriched in asphaltenes and waxes in comparison to the parent crude oils. They also contain a significant amount of maltenes. Studies about the effect of asphaltenes on waxes have indicated that asphaltene concentration,[1] degree of dispersion,[2,3] and chemical composition is determining wax behavior in crude oils.[4-6]

Experimental

Asphaltene concentrations and asphaltene solubility profiles were determined using on-column filtration techniques and an ELSD**.** Asphaltene solubility profile, the mobile phase is changed gradually from pure n-heptane to 90/10 dichloromethane (DCM)/methanol and then to 100% methanol using an ELSD. Elemental Analysis was performed with a Carlo Erba model 1108 analyzer.

Wax content was determined with the Differential Scanning Calorimeter TA Q20, with controlled cooling capability (RCS40). Samples and reference empty containers were heated to 100 °C and then cooling down at a cooling rate of 2 °C/min in an inert atmosphere.

HTGC: Hewlett Packard/Agilent 6890 with a 7673 autosampler, Flame Ionization Detector (FID) and a J&W Scientific DB-1HT 30m x 0.320mm ID x 10 µm film thickness column.

MRMS: scimaX 7T (Bruker Daltonics GmbH & Co. KG, Bremen, Germany) equipped a Apollo II Dual ESI/MALDI ion source. Samples were analyzed by APCI in positive ion mode (mass range *m/z* 129 – 2000).

Results and Discussion

The results indicate that amount and composition of the deposit changes as the deposit ages. The deposit becomes more hydrogen deficient showing an increase in asphaltene content at longer times (Figure 1).

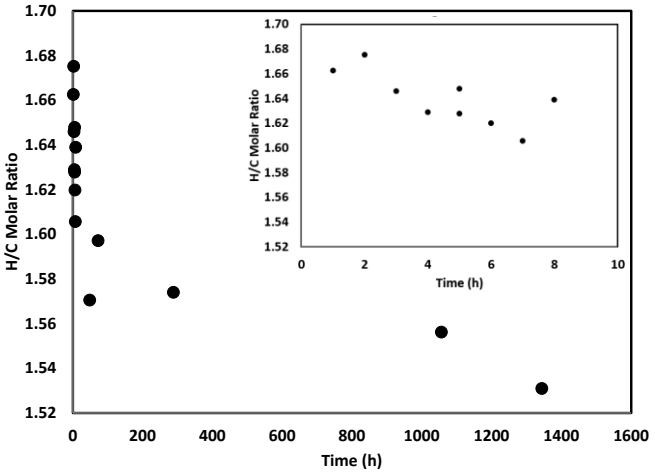

Figure 1. H/C molar ratio of the deposits as a function of time.

Waxes also show variations in their composition that are reflected in higher wax appearance temperatures. Comparison with precipitation behavior induced by n-heptane shows similar, but less pronounced tendencies. Magnetic Resonance Mass Spectrometry (MRMS) of the deposits (APCI) shows subtle changes in molecular distributions (Fig. 2). Analysis of these changes indicate an enrichment in heteroatom-containing species as the deposit ages (Fig. 3). The main goal of this study is to shed light on the changes that occur in sludges at the bottom of tanks produced by the blend of crude oils.

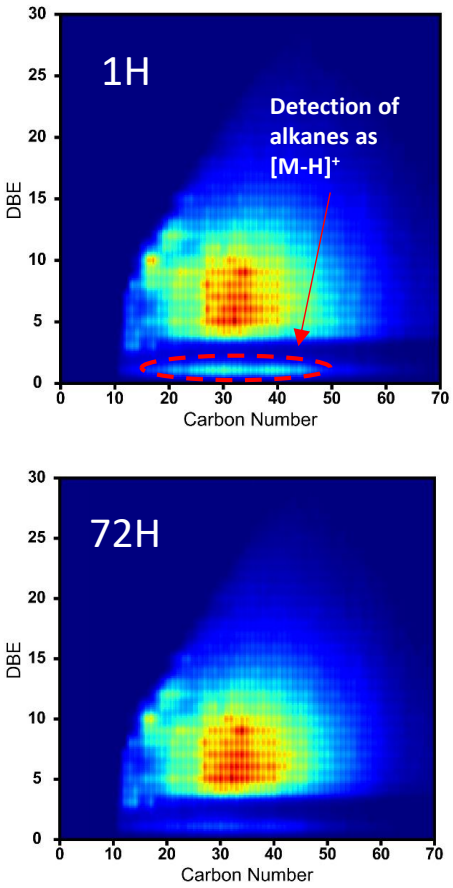

Figure 2. DBE as a function of Carbon number obtained for deposits at different times.

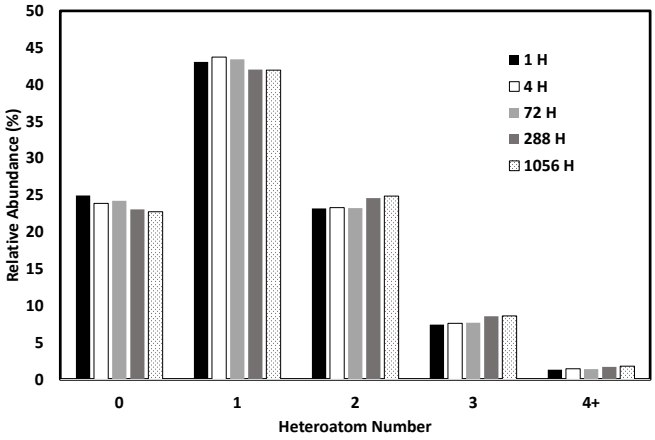

Figure 3. MRMS relative abundance of species containing different heteroatom content as a function of deposit age.

Conclusions

There are clear changes in the composition of deposits because of aging. As the deposit ages, it becomes more aromatic containing more asphaltenes, but also the amount of long waxes increases. These two characteristics indicate that the older the deposit, the more difficult is their removal as it is composed of the less soluble components in hydrocarbons. Deposit formation was the instability of the blend towards asphaltene precipitation. Deposits were enriched in asphaltenes and waxes in comparison to the parent crude oils. MRMS revealed that the deposit becomes enriched in species containing more than 2 heteroatoms as it ages.

This study provides additional experimental evidence that the precipitation of asphaltenes is a complex process that involves not only aggregation but also reorganization of the aggregates. The presence of waxes added an extra layer of complexity to these systems and more studies are required to fully understand the interactions between asphaltenes and waxes and how these interactions affect the formation and temporal evolution of deposits.

Acknowledgments

The authors are grateful to CTC for providing funding and for allowing the publication of this work.

References

[1] Venkatesan, R.; Östlund J. A.; Chawla, H.; Wattana, P.; Nydén, M.; Fogler, H. S. The effect of asphaltenes on the gelation of waxy oils. Energy Fuels 2003, 17, 1630-1640.
[2] Kriz, P.; Andersen, S. I.; Alcazar-Vara L. A.; Garcia-Martinez, J. A.; Buenrostro-Gonzalez, E. Effect of asphaltenes on equilibrium and rheological properties of waxy model systems. Fuel. 2012, 93, 200-212.
[3] Kriz, P.; Andersen, S. I. Effect of asphaltenes on crude oil wax crystallization. Energy Fuels. 2005, 19, 948-953.
[4] Molina, V. D.; Ariza León, E.; Chaves-Guerrero, A. Understanding the effect of chemical structure of asphaltenes on wax crystallization of crude oils from Colorado oil field. Energy Fuels. 2017, 31, 8997-9005.
[5] Ruwoldt, J.; Subramanian, S.; Simon, S.; Oschmann, H.; Sjöblom, J. Asphaltene fractionation based on adsorption onto calcium carbonate: Part 3. Effect of asphaltenes on wax crystallization. Colloids and Surfaces A: Physicochemical and Engineering Aspects. 2018, 554, 129-141.
[6] Pahlavan, F.; Mousavi, M.; Hung, A.; Fini, E. H. Investigating molecular interactions and surface morphology of wax-doped asphaltenes. Physical Chemistry Chemical Physics. 2016, 18, 8840-8854..

CARACTERIZAÇÃO PALEOCEANOGRÁFICA DO EVENTO ANÓXICO OCEÂNICO 1d (OAE1d) NA BACIA SERGIPE-ALAGOS E SUA ASSOCIAÇÃO COM AS ROCHAS GERADORAS DE HIDROCARBONETOS

BERNARDO VÁZQUEZ-GARCÍA[a*], MAURO DANIEL RODRIGUES BRUNO [a- *], FERNANDA LUFT-SOUZA[a], HENRIQUE PARISI KERN[a], JORGE VILLEGAS-MARTIN[a], ANTÔNIO ROSALES GONÇALVES OLIVEIRA[a], CAROLINA CORRÊA DA CUNHA[a], ANA MARIA SCHERER THIESEN LUCCA[a], ALESSANDRA SANTOS[a], GERSON FAUTH[a]

[a] **INSTITUTO TECNOLÓGICO DE PALEOCEANOGRAFIA E MUDANÇAS CLIMÁTICAS (ITT OCEANEON), UNISINOS UNIVERSITY, BRAZIL**

*Correspondence: bernardovg32@gmail.com

Introdução

As seções sedimentares do Eocretáceo da Bacia Sergipe-Alagoas contêm importantes rochas geradoras, e os níveis contendo folhelhos relacionados ao Eventos Anóxicos Oceânicos (OAEs) identificados nas formações Muribeca (OAE1a) e Riachuelo (OAE1b) do intervalo Aptiano–Albiano (e.g., Tedeschi et al., 2020) consistem em um tema relevante para o entendimento das condições paleoambientais relacionadas a formação de rochas geradoras de hidrocarbonetos nesta bacia. De modo complementar, a identificação e caracterização dos OAE nesta bacia podem permitir o melhor entendimento das condições paleoceanográficas do Oceano Atlântico Sul.

Este estudo tem como objetivo a identificação e caracterização do OAE 1d no testemunho UFRJ-2-LRJ-1-SE perfurado na Bacia Sergipe-Alagoas, e sua correlação com as camadas ricas em matéria orgânica depositadas durante o Albiano superior na bacia. A partir destes resultados será possível determinar se os níveis estudados, relacionados ao OAE1d, possuem potencial como rochas geradoras de hidrocarbonetos para a Bacia Sergipe-Alagoas.

Materiais e Métodos

O material estudado provém do testemunho UFRJ-2-LRJ-1-SE (10°50'49"S; 37°10'2.34"W) perfurado no município de Laranjeiras, estado de Sergipe, Brasil (Figura 1). Os dados litológicos, micropaleontológicos e geoquímicos deste testemunho foram compilados de trabalhos anteriormente publicados (Valle et al., 2019a, b; Silva Jr. et al., 2020, 2023; Vázquez-García et al., 2022). Estes dados foram correlacionados com os resultados publicados em Koutsoukos et al., (1991a,b) para os poços 1-CA-1-SE (10°54'30"S; 37°07'45"W); 1-CN-1-SE (10°49'45"S; 37°06'45"W); 1-CAU-3-SE (10°55'14.581"S; 37°6'11.272"W).

Resultados e Discussão

Os dados litoestratigráficos, bioestratigráficos e geoquímicos do testemunho UFRJ-2LRJ-1-SE indicam deposição durante o Albiano superior, correspondendo a Formação Riachuelo. O intervalo de estudo apresenta um predomínio de querogênio tipo III, com uma amostra detectada com querogênio misto, tipo II e III (Valle et al., 2019b).

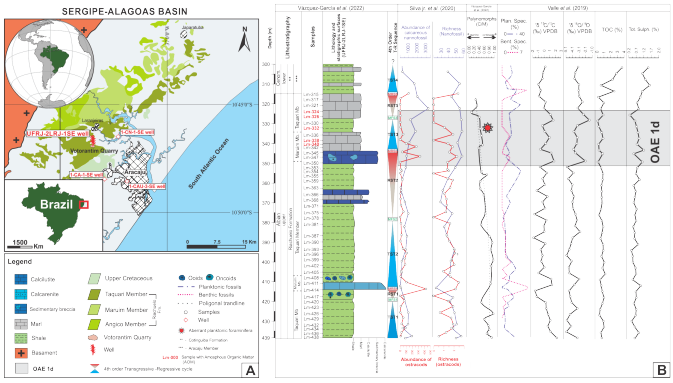

Figure 1. Área de estudo (A) e dados bioestratigráficos, estratigráficos e geoquímicos do testemunho UFRJ-2-LRJ-1-SE (B) (modificado de Vázquez-García et al., 2022)

O OAE1d está registrado em de um intervalo estratigráfico com espessura aproximada de até 30 m, que consiste em uma intercalação entre carbonatos e sedimentos finos. Este evento é caracterizado por uma excursão positiva do ^{13}C, assim diminuição na abundância de foraminíferos planctônicos, aumento na abundância de calcíferas, equinodermos e ostracodes (Figura 1). Estas características também são observadas

em diversas seções sedimentares globais (Leckie et al., 2002). Também, foi observada uma relação direta com a assembleias de nanofósseis calcários descritas para o testemunho por Silva Jr. et al. (2020). Além disso, a presencia de Matéria Orgânica Amorfa (AOM) em cinco amostras e a dominância de foraminíferos planctônicos do gênero *Clavihedbergella*? sp. com testas deformadas em uma amostra, são o resultado do estresse ambiental como consequência das baixas quantidades de oxigênio dissolvido na água (Figura 1).

Os estudos realizados por Koutsoukos et al. (1991a, b) na Bacia Sergipe-Alagoas identificam diferentes eventos disóxicos-anóxicos na sucessão Aptiano–Albiano. A sequência está caracterizada pela ocorrência de matéria orgânica com valores que oscilam entre 2 e 12% de Carbono Orgânico Total (TOC). Os dados de pirólise Rock-Eval indicam uma predominância de querogênio tipo II/I, os dados de refletância da vitrinita < 0,6%Ro e T-max a 440ºC indicando MO imatura.

Considerando as características litoestratigráficas e geoquímicas reconhecidas no testemunho UFRJ-2LRJ-1-SE, e os dados publicados anteriormente para os estrados depositados durante o Albiano Superior na Bacia Sergipe-Alagoas, é possivel correlacionar as seções e verificar que os niveis de rochas geradoras correspondem ao OAE1d.

Na atualidade o avanço das tecnologias de exploração, prospecção e produção de hidrocarbonetos permite a promoção de novas abordagens para o entendimento dos processos geológicos relacionados aos sistemas petrolíferos das bacias sedimentares.

Conclusões

A identificação e caracterização estratigráfica e de distribuição geográfica dos OAEs do Cretáceo em seções sedimentares na Bacia Sergipe-Alagoas resultam em uma nova fronteira exploratória em relação aos hidrocarbonetos não convencionais.

Para o Albiano Superior da Formação Riachuelo se registra o OAE1d no testemunho UFRJ-2-LRJ-1-SE. A composição da biota bentônica sugere águas de fundo disóxicas/anóxicas ao longo do evento e a biota planctônica apresenta condições de alta produtividade primária. Condições similares aos registros do OAE1d a nível global.

O contexto geológico associado aos critérios bioestratigráficos, litoestratigráficos e geoquímicos levam a considerar que o intervalo Aptiano superior–Albiano apresenta um grande potencial na acumulação de rochas geradores de hidrocarbonetos não convencionais (*gas shale* e *oil shale*). Neste sentido, considera-se que estudos posteriores permitirão a melhor descrição e entendimento destas novas fronteiras para os sistemas petrolíferos da Bacia Sergipe-Alagoas.

Agradecimentos

Os autores agradem ao CNPq (Conselho Nacional de Desenvolvimento Científico e Tecnológico) pelo projeto 405679/2022-0.

Referências

Koutsoukos, E. A., Mello, M. R., & de Azambuja Filho, N. C. (1991a). Micropalaeontological and geochemical evidence of mid-Cretaceous dysoxic-anoxic palaeoenvironments in the Sergipe Basin, northeastern Brazil. Geological Society, London, Special Publications, 58(1), 427-447.

Koutsoukos, E. A., Mello, M. R., de Azambuja Filho, N. C., Hart, M. B., & Maxwell, J. R. (1991b). The upper Aptian–Albian succession of the Sergipe Basin, Brazil: an integrated paleoenvironmental assessment. AAPG bulletin, 75(3), 479-498.

Leckie, R.M., Bralower, T.J., Cashman, R., 2002. Oceanic anoxic events and plankton evolution: Biotic response to tectonic forcing during the mid-Cretaceous. Paleoceanography 17 (3).

Silva Jr., R., Erba, E., de Moraes Rios-Netto, A., Silva, S. C., Alves, T. D., Motta, A. L. G.; Valle, B.; Borghi, L.; Abbots-Queiroz, F. 2023. Oceanic anoxic event 2 in Sergipe-Alagoas Basin, Brazil: New paleoecological insights from calcareous nannofossils assemblages. Marine Micropaleontology, 178, 102197.

Silva Jr., R., de Moraes Rios-Netto, A., Silva, S.C., Valle, B., Borghi, L., AbbotsQueiroz, F., 2020. Middle Cretaceous calcareous nannofossils from the cored well UFRJ-2-LRJ-01-SE, Sergipe-Alagoas Basin, Brazil: new biostratigraphy and paleobiogeographic inferences. Cretac. Res. 106, 104245

Tedeschi, L. R.; Jenkyns, H. C.; Robinson, S. A.; Lana, C. C., Menezes Santos, M. R. F.; Tognoli, F. M. 2019. Aptian carbon-isotope record from the Sergipe-Alagoas Basin: New insights into oceanic anoxic event 1a and the timing of seawater entry into the South Atlantic. Newsletters on Stratigraphy.

Valle, B.; Dal'Bó, P. F.; Mendes, M.; Favoreto, J.; Rigueti, A. L. Borghi, L.; Mendoça, J. O. L.; Silva Jr, R. 2019a. The expression of the oceanic anoxic event 2 (OAE2) in the northeast of Brazil (Sergipe-Alagoas Basin). Palaeogeography, Palaeoclimatology, Palaeoecology**529**, 12-23.

Valle, B.; Dal'Bó, P. F.; Mendes, M.; Favoreto, J.;Rigueti, A. L.; Borghi, L.; Silva, R. 2019b. Stratigraphic evolution of a Brazilian carbonate platform during the Cretaceous: the late Albian–early Turonian of the Sergipe–Alagoas Basin. Facies**65**, 1-17.

Vázquez-García, B., Kern, H. P., dos Santos Filho, M. A. B., Fauth, G., de Araujo Carvalho, M., Borghi, L., & Netto, A. D. M. R. (2022). Albian/Cenomanian boundary in the Sergipe-Alagoas Basin: Sea-level changes and paleoecology based on ostracods. Marine Micropaleontology**177**, 102172.

XVI LATIN AMERICAN CONGRESS ON ORGANIC GEOCHEMISTRY
9 - 11 AUGUST, 2023
ARACAJU, SERGIPE, BRAZIL

Changes in kerogen composition of the Vaca Muerta Fm., Argentina, across a thermal gradient affected by igneous intrusions

Juan A. Pineda [a*], Juan Spacapan [b*], Marcos Comerio [a*], Ignacio Jausoro [a*], Ignacio Brisson[b*]

[a]**Y-TEC–CONICET. Av. Del Petróleo s/n (entre 129 y 143), Berisso, Argentina**

[b] **YPF S.A., Macacha Güemes 515 (C1106BKK), C.A.B.A., Buenos Aires, Argentina**

Presenting author email: juan.a.pineda@ypftecnologia.com

Introduction

The Vaca Muerta Formation (Late Jurassic–Early Cretaceous), considered a world-wide unconventional shale, constitutes the most prolific source rock of the Neuquén Basin, Argentina (Brisson et al., 2020). Recent studies have shown that organic matter has an impact on organic porosity development and thus exert a main control on oil and gas storage capacity. The evolution of organic porosity has been analyzed across the east–west regional maturation gradient of the basin (Spacapan et al., 2021). However, this evolution in local areas of the basin where igneous intrusions enhanced source rock maturation is not reported in the literature.
Igneous intrusions can lead to an atypical maturation process on organic-rich shales, which can result in positive or negative effects on hydrocarbon generation and accumulation as was determined in Los Cavaos region (Mendoza, Argentina) of the Neuquén Basin (Spacapan et al., 2020). The objective of the present contribution is to reconstruct the changes on the kerogen composition across the thermal effects induced by horizontal intrusions (sills) and the development of organic pores in the Vaca Muerta Formation (VMF).

Methods

The present study focuses on the VMF in the north of the Neuquén Basin (Fig 1.), where based on subsurface data, horizontal igneous intrusions (sills) enhanced source rock maturation and act as oil reservoirs of the basin (Spacapan et al., 2020). At Y-TEC laboratories, cutting and core samples from nearby Well A and Well B, the latter affected by sill intrusions (maximum of 12 m in thickness), were analyzed for organic petrography (%Ro), Rock-Eval programmed pyrolysis, raman spectroscopy, and scanning electron microscope (SEM).

Results and Discussion

Three zones are recognized in the Well B (Fig 2,3) that describes the thermal evolution of kerogen of the VMF altered by igneous intrusions.

Unaltered zone: Pyrolysis parameters shows average values of TOC (3.11 wt%), S2 (14.09 mgHC/rock), HI (441.17 mgHC/gTOC), and Tmax 438℃. Mean 0.7 %Ro indicates the early oil window stage. Kerogen is type I/II, dominated by liptinite macerals including discrete alginite bodies, lamellar and filamentous lamalginite, liptodetrinite and bituminite. Solid bitumen (SB) occurs as void or fracture filling and in minor proportion. Organic porosity is scarce or absent. This is in agreement with the observed data of the unaltered Well A.

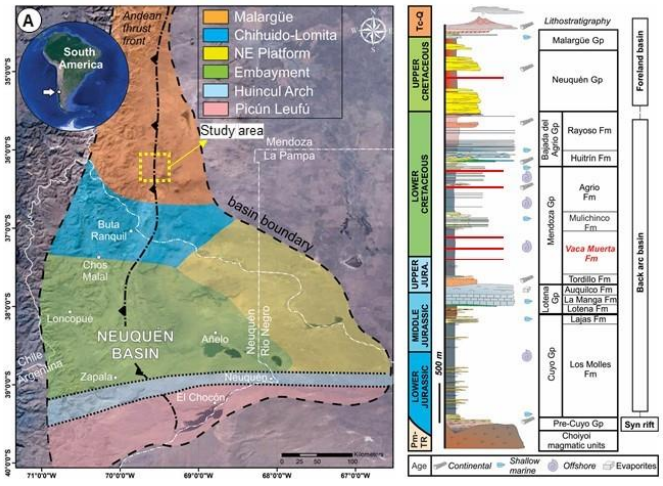

Figure 1. A, Neuquén Basin, Argentina, Vaca Muerta Formation map. B, Simplified stratigraphic chart for the Neuquén Basin; red rectangle=igneous intrusions.

Outer aureole: organic geochemical parameters show a gradual decrease compared with the non-disturbed zone and the unaltered Well A (TOC, avg. 3.15 wt%; S2, avg. 3.66 mgHC/rock; HI, avg. 135.84 mgHC/gTOC;). The reflectance of vitrinite increases towards the inner aureole with avg. of %Ro 0.92 indicating a shift towards a late oil window. A decrease in proportion and loss of

fluorescence of liptinite macerals is observed, which is evidenced by a strong decrease of HI values. Fluorescent bitumen is common around the carbonate grains. Organic porosity documented through SEM images appears in the secondary organic products (solid bitumen).

Inner aureole: organic geochemical data show important anomalies in TOC (avg. 2.74 wt%), S2 (avg. 2.51 mgHC/rock), and HI (avg. 125.75 mgHC/gTOC) parameters. Maturity reached the dry gas window to a post-mature stage with an abrupt change of %Ro >3.4. Evidence of highly thermal alteration of OM are expressed by the absence of liptinite macerals, development of devolatilization vacuoles in vitrinite/inertinite, and coke textures and the presence of pyrolytic carbon. Solid bitumen is the most abundant organic component, occurring disseminated in the mineral matrix with granular texture and more porous which was evidenced by SEM studies.

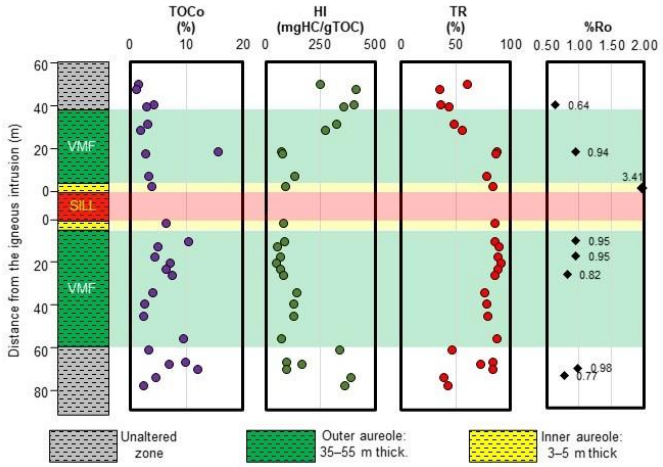

Figure 2. Organic geochemistry and vitrinite reflectance (%Ro) profiles of Vaca Muerta Fm. in Well B. The decrease of HI and increase of TR allowed to define the thermal aureole of avg. 45 m in thickness.

Conclusions

The thermal effect of igneous intrusions induced a local maturation of the source rock (Vaca Muerta Fm.) resulting in the alteration of geochemical parameters, variation in kerogen composition and development of organic porosity. The transformation of the kerogen (type I/II) to solid bitumen with increasing organic porosity towards the contact with the sill is observed. The formation of organic pores related to secondary organic products is related to the thermal shock that disturbed the normal thermal gradient in this part of the basin.

Our results show that the VMF could be an attractive unconventional exploration target in areas affected by igneous intrusions, particularly where this unit is immature to early mature. The thermal effect of the intrusions not only increases the hydrocarbon generation rate but also contributes to the development of kerogen porosity, which would increase storage capacity and retention efficiency of hydrocarbons. Future studies should incorporate the geomechanical characterization of the altered zones in order to evaluate these potential unconventional targets through geonavigation of horizontal wells.

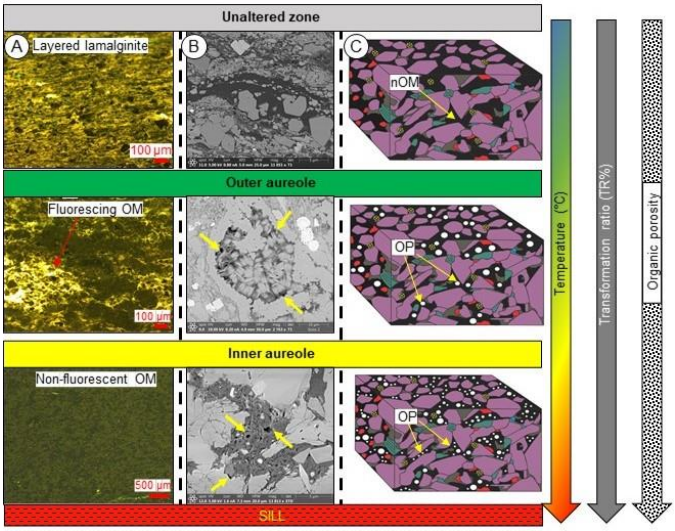

Figure 3. A, organic petrography: changes of organic matter (OM) composition under ultraviolet fluorescence light. B, SEM: organic porosity characterization; yellow arrow indicates organic pore C, interpretation of organic pores development related to distance from igneous intrusion. Nonporous organic matter (nOP) characterizes the unaltered zone. Appearance of organic pores (OP) in outer aureole. Abundant organic porosity, mostly in the secondary OM, are observed in inner aureole.

Acknowledgements

We would like to thank YPF for the permission and samples, and Y-TEC (YPF-Tecnología) for the laboratory equipment and financial support. We also thank Dr. Remigio Ruiz for his support with the Raman spectroscopy at Y-TEC.

References

Brisson, I. E., Fasola, M. E., and Villar, H. J., 2020. Organic Geochemical Patterns of the Vaca Muerta Formation. Memoir 121: Integrated Geology of Unconventionals: The Case of the Vaca Muerta Play, Argentina, Pages 297-328.

Spacapan, J. B., D'Odorico, A., Palma, O., Galland, O., Vera, E. R., Ruiz, R., ... & Manceda, R., 2020). Igneous petroleum systems in the Malargüe fold and thrust belt, Río Grande Valley area, Neuquén Basin, Argentina. Marine and Petroleum Geology, 111, 309-331.

Spacapan, J.B., Comerio, M., Brisson, I., Rocha, E., Cipollone, M., Hidalgo, J. C., 2021. Integrated source rock evaluation along the maturation gradient. Application to the Vaca Muerta Formation, Neuquén Basin of Argentina. Basin Research 33, 3183-3211.

XVI LATIN AMERICAN CONGRESS ON ORGANIC GEOCHEMISTRY
9 - 11 AUGUST, 2023
ARACAJU, SERGIPE, BRAZIL

EVALUATION OF THE PRESENCE OF ORGANIC MATTER IN ROCKS OF TREMEMBÉ FM., TAUBATÉ BASIN, BY REFLECTANCE SPECTROSCOPY

TAINÁ THOMASSIM GUIMARÃES [a*], JOICE CAGLIARI [a,b], DANIEL CAPELLA ZANOTTA [a], LUIZA CARINE FERREIRA DA SILVA [a], HENRIQUE BAVARESCO [a], ANDRÉ LUIZ DURANTE SPIGOLON [c], LUIZ GONZAGA JUNIOR [a], MAURÍCIO ROBERTO VERONEZ [a*]

[a] **Vizlab | X-Reality and Geoinformatics Lab, Graduate Program in Applied Computing – UNISINOS (Av. Unisinos, 950, Cristo Rei, São Leopoldo/RS, Brazil).** [a] **Graduate Program of Geology – UNISINOS (Av. Unisinos, 950, Cristo Rei, São Leopoldo/RS, Brazil).** [c] **Division of Geochemistry, Petrobras Research and Development Center – CENPES (Av. Horácio Macedo, 950, Cidade Universitária, Rio de Janeiro/RJ, Brazil).**

tainat@edu.unisinos.br; veronez@unisinos.br

Introduction

Laboratory analyzes to determine geochemical parameters involve approaches that require cost, time, skilled labor and generally are destructive [1,2]. An attractive alternative for inference of some parameters is the use of hyperspectral remote sensing, through methods that return to reflectance spectroscopy.

Reflectance is the fraction of the light intensity from a source that reaches the target and is reflected [3] and is generally presented in percentage values in the form of a curve over the various radiation lengths. Reflectance spectroscopy is widely exploited to collect compositional information about rocks in a fast, non-destructive, and replicable way. [4] highlight that these inferences are possible because processes that occur on a molecular scale in the rock cause light absorption at specific wavelengths, generating absorption features.

For these data to be used in the characterization of source rocks, it is necessary to know the spectral behavior of the different minerals and compounds that constitute these rocks. Regarding clay minerals, the most common absorption feature related to the hydroxyl ion is centered at 1400nm, but in some cases it may also be present at 2200nm [3]. The curves of carbonate minerals such as calcite and dolomite have their strongest absorption bands located approximately at 2300 and 2500nm [3]. In addition to the influence of minerals on the spectral signature of rocks, it is extremely important to know the signature of the organic fraction. [2] point out that bituminous shale spectra exhibit distinct absorption bands at 1400, 1700, 1900 and 2300nm, being: 1400 and 1900nm mainly due to the presence of clay minerals and water; the 2300nm band is the result of the combination of kerogen and carbonate minerals; and the 1700nm band is caused exclusively by kerogen, with no interference from any of the main minerals. [1] also point out that the 1700 and 2300nm bands are related to organic matter.

In this sense, the present work aims to analyze the spectral signature of potentially generating rocks from the Taubaté Basin in order to understand differences in terms of their organic composition, especially related to the amount of organic matter expressed by the Total Organic Carbon (TOC, %).

Experimental

For this study, were collected samples of oil-generating potential rocks of the Tremembé Formation, Taubaté Basin (SP/Brazil). These rocks were deposited in a lake paleoenvironment, analogous to the pre-salt source rocks. In the Santa Fé mine were collected 20 samples from five key horizons of the outcrop for geochemical and spectral characterization. Another 76 samples were collected from the drill core carried out near the area.

Analyzes for TOC quantification were performed using a Leco SC-144DR carbon analyzer. For the hyperspectral data acquisition, was used the spectroradiometer Spectral Evolution, model SR-3500, which scans the spectral range from 350 to 2500 nm, containing 1018 bands. The methodology adopted was the spectral measurement of absolute reflectance using a contact probe. These collected spectral data were submitted to the continuum removal (CR) process [3], which aimed to normalize the spectra and highlight their absorption features, allowing a better comparison between different spectral curves and their absorption bands.

Results and Discussion

The TOC results obtained for the outcrop samples ranged from 0.3 to 4.3%, while the core samples ranged from 0.3 to 22.8%.

The reflectance data generated a spectral library of over 250 spectral data in curve format. These curves, after CR, were compared to each other to analyze the absorption features present, their possible meanings, and respective depths. Figure 1 presents the mean of these signatures extracted from the drill core, related to their TOC content range.

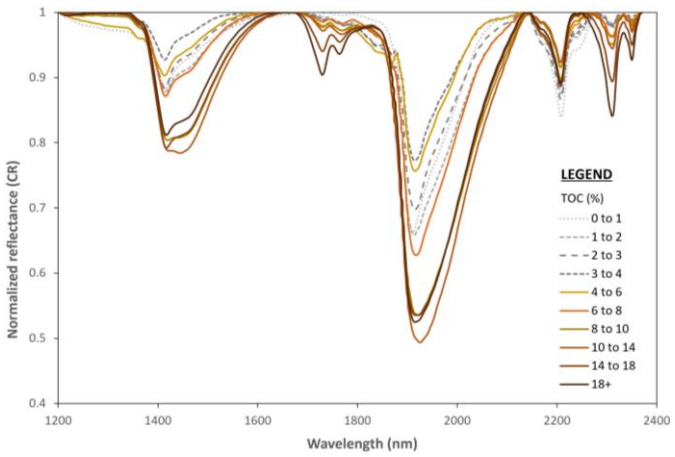

Figure 1.

Reflectance after CR process of cores TOC content ranges.

It is possible to note that all curves have spectral features at wavelengths 1400, 1900 and 2200nm, which are associated with the presence of clay minerals and water in the rock. In addition, features at 1700 and 2300nm stand out, being present in samples with high TOC value. These features tend to decrease with the reduction of TOC concentration, until they become absent in spectral signatures of samples with low values (below 1%).

The relationship between TOC data and the depth of the absorption feature located at 1700nm can be observed in Figure 2, where a high linear correlation between the data can be seen ($R^2 = 0.75$, p-value < 0.05). Furthermore, this correlation can be perceived when analyzing the profile of the two variables plotted according to the depth of one of the cores (Figure 2b).

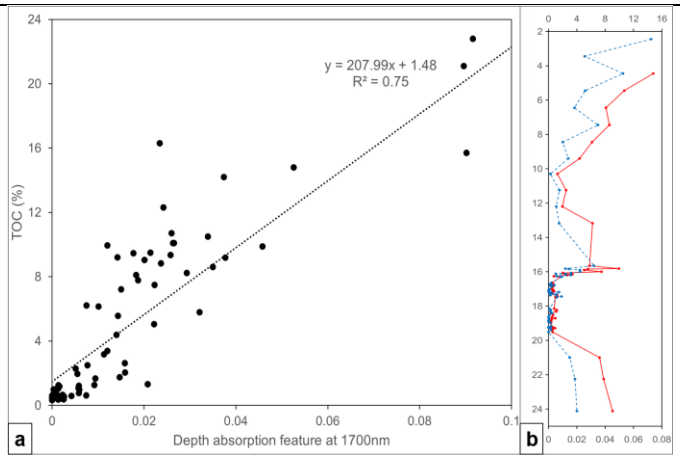

Figure 2.

(a) Correlation between TOC content and feature depth at 1700nm. (b) Profiles of TOC (red line, upper axis) and 1700nm band depth (blue dashed line, lower axis), plotted according to core depth.

Conclusions

Obtaining qualitative or quantitative information about the organic matter present in sedimentary rocks from a fast and non-destructive method such as reflectance spectroscopy, can facilitate and complement the process of geochemical characterization of these rocks. Although it does not replace the need to carry out detailed and accurate laboratory geochemical analyzes, this indirect data acquisition tool (i.e., spectra) could be used for preliminary or prompt characterization, as well as for screening samples of interest. Moreover, if these hyperspectral data come from images, these parameters can still be estimated spatially in samples or outcrops.

Acknowledgements

The authors thank ANP (Brazilian Petroleum Agency), Petrobras S/A and PGQu – UFRJ for financial support and authorization to publish this work.

References

[1] Speta, M., Rivard, B., Feng, J., Lipsett, M., Gingras, M., 2015. Hyperspectral imaging for the determination of bitumen content in Athabasca oil sands core samples. AAPG Bulletin 99, 1245–1259.

[2] Mehmani, Y., Burnham, A. K., Berg, M. D. V., Tchelepi, H. A., 2017. Quantification of organic content in shales via near-infrared imaging: Green River Formation. Fuel 208, 337–352.

[3] Clark, R. N., 1999. Spectroscopy of rocks and minerals, and principles of spectroscopy. Manual of remote sensing 3, 3–58.

[4] Burns, D. A., Ciurczak, E. W., 2007. Handbook of near-infrared analysis. CRC press.

THERMAL ANALYSIS OF SOURCE ROCKS BEFORE AND AFTER HYDROUS PYROLYSIS

FELIPE J. S. BISPO[a], JULIA CANELLA[a], TATIANA S. L. MARAVILHA[a], ANDRÉ LUIZ DURANTE SPIGOLON[b], RONALD W. P. ORTIZ[a], VINICIUS KARTNALLER[a], VINICIUS OTTONIO O. GONÇALVES [a*], JOÃO CAJAIBA[a]

[a]NQTR-IQ-UFRJ – NÚCLEO DE DESENVOLVIMENTO DE PROCESSOS E ANÁLISES QUIMICAS EM TEMPO REAL, INSTITUTO DE QUÍMICA, UNIVERSIDADE FEDERAL DO RIO DE JANEIRO, [b]Division of Geochemistry, Petrobras Research and Development Center (CENPES), Av. Horácio Macedo, 950, Cidade Universitária, 21.941-915 Rio de Janeiro, RJ, Brazil

*cajaiba@iq.ufrj.br, viniciusottonio@iq.ufrj.br

Introduction

Thermal analysis is widely utilized for the study of source rocks, providing crucial information such as maturity degree, kerogen and bitumen characteristics, sedimentary rock thermal history, and biomarker identification (Zhang et al., 2019; Ganeeva et al., 2022). The literature reports several studies that have employed complementary or alternative techniques to Rock-Eval pyrolysis, the fundamental method for assessing the oil-generating potential of oil-source rocks. Among these techniques, thermogravimetric analysis (TGA), differential thermal analysis (DTA), and differential scanning calorimetry (DSC) have been extensively used. In air atmosphere, thermal analysis records the course of oxidation reactions and assesses differences in both the organic matter and mineral composition of the rocks (Labus and Matyasik, 2019; Ganeeva et al., 2022). Furthermore, thermal analysis offers additional information to supplement results obtained through other methods such as pyrolysis gas chromatography mass spectrometry (Py-GC-MS), which is essential for biomarker identification in oil exploration (Labus and Matyasik, 2019; Zhang et al., 2019).

This work presents thermal analysis to evaluate the effects of hydrous pyrolysis (HP) on source rocks, which is an artificial maturation technique that better simulates oil and gas generation and expulsion (Spigolon et al., 2015). By utilizing thermal analysis, it becomes possible to obtain results and enhance the understanding of the phenomena that occur during the HP of source rocks.

Experimental

This work examines samples of source rocks from the Araripe basin, located in northeastern Brazil. This onshore basin consists primarily of late Jurassic and early Cretaceous sediments. 150 mg of the rocks were subjected to hydrous pyrolysis, where oil and gas generation and expulsion occurs. The HP was performed in a 1 L high-pressure vessel by adding 400 ml of water and maintaining the temperature at 320°C for 72 hours. Further details about the HP process can be found elsewhere (Spigolon et al., 2015). Subsequently, the rocks were dried at room temperature until a constant weight was achieved.

For the thermal analysis, 10 mg samples of the rocks before and after HP were analyzed using a Shimadzu DTG-60 simultaneous DTA/TG apparatus (Kyoto, Japan). the analysis conditions included a temperature range from 30°C to 550°C, a heating rate of 10ºC min^{-1} and a synthetic air flow of 100 ml min^{-1}.

Results and Discussion

Figure 1 shows the thermal analysis results (DTA, TGA, and DTG) of the fresh source rocks. The sample exhibits three distinct events of mass loss.

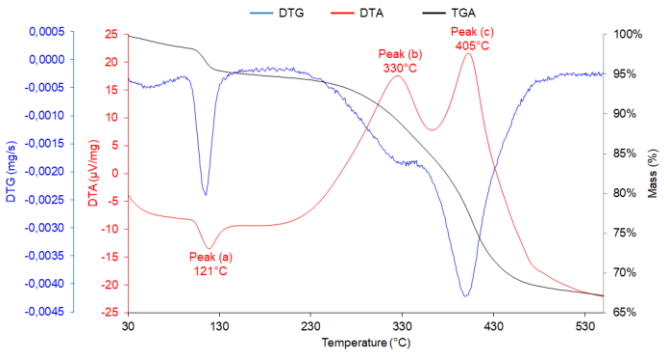

Figure 1. Thermal Analysis of Source Rocks Prior to Hydrous Pyrolysis.

The first event, denoted as peak (a), is an endothermic peak occurring at 121°C and is associated with matrix dehydration (Labus and Matyasik, 2019). The second event takes place between 230°C and

approximately 360°C, during which a significant mass loss is observed, corresponding to the release of free hydrocarbons or bitumen from the rocks. This event is accompanied by a maximum exothermic peak at 330°C denoted as peak (b), which is attributed to oxidation. The third event is characterized by a substantial increase in the mass loss rate, indicating kerogen degradation, with a maximum exothermic peak occurring at 405°C, denoted as peak (c).

Figure 2 shows the thermal analysis (DTA, TGA, and DTG) of the source rocks after being submitted to HP. In contrast to the thermal analysis results of the fresh source rocks, the DTG/DTA profiles of the samples after HP do not exhibit the peak observed at lower temperatures (peak a), indicating changes in the rock matrix. This observation may be attributed to the loss of inorganic matrix due to the submersion of the rocks in water and subsequent heating during the HP process.

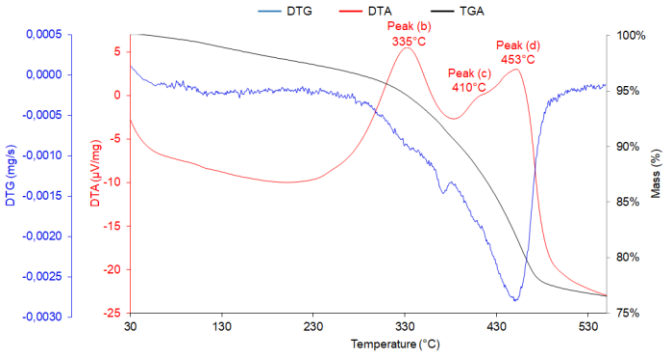

Figure 2. Thermal Analysis of Source Rocks after Hydrous Pyrolysis.

The release of bitumen from the rocks after HP showed a similar behavior to that observed for the fresh source rocks, with an event occurring between 230 ºC and approximately 380 ºC, with a maximum exothermic peak at 335 ºC (peak b) due to oxidation. However, the intensity of this peak was greater than that observed for the fresh rocks, which suggests a higher bitumen content in the rocks after HP. The HP was performed at 320 °C, a temperature known to yield the maximum bitumen due to kerogen decomposition at lower temperatures (260-320 °C), and marks the beginning of the oil generation stage, which reaches a maximum of expelled oil yield at 360 °C (Spigolon et al., 2015; Birdwell et al., 2018). Additionally, Figure 2 indicates an event with a DTA peak at 410 °C (peak c) of lower intensity, confirming the conversion of kerogen into bitumen in the rocks after HP. Therefore, these thermal events (peak b and c) suggest that HP had a significant effect on the bitumen yield of the rocks.

Figure 2 illustrates another important finding, which is a new thermal event at 453°C (peak d). As mentioned earlier, the majority of the kerogen in the rocks decomposes into bitumen at temperatures below 320°C. However, with increasing temperature and time during HP, the remaining kerogen becomes more mature and harder to decompose. Hence, this thermal event indicates the higher temperature required to decompose the remaining kerogen, and it may provide insight into the amount of kerogen present in the rocks after HP.

Conclusions

This work demonstrates the suitability of thermal analysis as an alternative technique for studying the effects of hydrous pyrolysis on source rocks. It focuses specifically on the impact of hydrous pyrolysis temperature on the yields of bitumen and kerogen. This finding is particularly noteworthy because thermal analysis requires less sample material and a shorter time compared to other methods, such as extraction with organic solvents. Overall, these results offer valuable insights into the effects of hydrous pyrolysis on source rocks and highlight the potential benefits of thermal analysis for the continuity of the work.

Acknowledgements

The authors thank Petrobras S/A, ANP (Brazilian Petroleum Agency), and PGQu–UFRJ for financial support.

References

Birdwell, J.E., Lewan, M.D., Bake, K.D., Bolin, T.B., Craddock, P.R., Forsythe, J.C., Pomerantz, A.E., 2018. Evolution of sulfur speciation in bitumen through hydrous pyrolysis induced thermal maturation of Jordanian Ghareb Formation oil shale. Fuel, 219, 214–222.

Ganeeva, Y., Barskaya, E., Okhotnikova, E., Yusupova, T., Morozov, V., Khayuzkin, A., Fazylzyanova, G., 2022. Simultaneous thermal analysis method for studying the oil source rocks. Arab. J. Geosci., 15, 1–10.

Labus, M., Matyasik, I., 2019. Application of different thermal analysis techniques for the evaluation of petroleum source rocks. J. Therm. Anal. Calorim., 136, 1185–1194.

Spigolon, A.L.D., Lewan, M.D., de Barros Penteado, H.L., Coutinho, L.F.C., Mendonça Filho, J.G., 2015. Evaluation of the petroleum composition and quality with increasing thermal maturity as simulated by hydrous pyrolysis: A case study using a Brazilian source rock with Type I kerogen. Org. Geochem., 83–84, 27–53.

Zhang, T., Wang, Z., Wang, Y., Wei, Z., Li, X., Hou, X., Sun, Z., Wang, G., Qian, Y., 2019. The characteristics of free/bound biomarkers released from source rock shown by stepwise Py-GC-MS and thermogravimetric analysis (TGA/DTG). J. Pet. Sci. Eng., 179, 526–538.

XVI LATIN AMERICAN CONGRESS ON ORGANIC GEOCHEMISTRY
9 - 11 AUGUST, 2023
ARACAJU, SERGIPE, BRAZIL

Py-GCMS as a tool to directly assess heptane Thompson's index for maturity evaluation of rock samples

Sandra B. Jorge[a], Regina Binotto[b], Daniel Silva Dubois[b], Andre Luiz Durante Spigolon[b]; Tatiana Simões Loureiro Maravilha[a], Ronald W. Pacheco Ortiz[a], Vinicius Kartnaller[a], João Cajaiba[a], Vinicius Ottonio O. Gonçalves[a]*

[a]NQTR-IQ-UFRJ – NÚCLEO DE DESENVOLVIMENTO DE PROCESSOS E ANÁLISES QUIMICAS EM TEMPO REAL, INSTITUTO DE QUÍMICA, UNIVERSIDADE FEDERAL DO RIO DE JANEIRO, [b]Division of Geochemistry, Petrobras Research and Development Center (CENPES), Av. Horácio Macedo, 950, Cidade Universitária, 21.941-915 Rio de Janeiro, RJ, Brazil

e-mail: viniciusottonio@iq.ufrj.br

Introduction

Light hydrocarbons are useful components for assessing geochemical information, particularly in estimating catagenetic degree of sediments and oils (Mango, 1997). In the late 1980s, Thompson (Thompson, 1983) proposed the heptane (H) index for correlating oil and source rock extracts. In his words, these parameters assess the level of paraffinicity, distinguishing the oils and rock extracts in different categories based on the type: normal, mature, supermature and biodegraded.

Thompson's index refers to the ratios of normal-paraffins-to-naphthenes, H index. Lower values of H indicate a biodegraded state, while higher values indicate a supermature state(Thompson, 1983). This parameter is widely used for both oil and source rocks. Furthermore, it is known that these H values are related to the kerogen type of its source rock, which may be used to distinguish the parent source rocks of a crude oil, particularly in the case of mixed oils.

While this parameter is useful, its evaluation for oils needs to be approached with caution as their history is a complex process due to migration from the source rock to the reservoir (or reservoirs, in the case of secondary reservoirs). However, sediments extracts undergo a simpler history process of progressive heating at the burial rate.

It is worth noting that the compounds of interest for the H index are light hydrocarbons, which are found in low amounts in source rocks and can be easily released from the media when manipulating either oil or rock. Therefore, direct analysis of these compounds without solid-liquid or liquid-liquid extraction is advantageous for obtaining reliable Thompson's indexes. In addition, the quantity of these rock samples may be limited, hence decreasing the amount per analysis is also advantageous.

In the present study, we propose to use Py-GCMS (Pyrolysis–Gas Chromatography–Mass Spectrometry) for obtaining Thompson's index by directly introducing rocks into a closed-system furnace kept at a constant temperature. In this method, the hydrocarbons will be thermally released from the rock under helium flow and carried directly to the GCMS analysis, eliminating the need for solid-liquid extraction or any further treatment.

Experimental

To thermally release free hydrocarbons from solid samples, a Pyrolizer PY-3030D (Frontier Lab, Japan) was, which consisted of a stainless-steel sample cup and a closed-system furnace kept at a constant temperature, both under helium flow. To start the analysis, the sample was dropped into the furnace, promoting the thermal release of the free hydrocarbons. The Pyrolizer was coupled with a gas chromatograph with a quadrupole mass spectrometer (GC–MS QP-2010, Shimadzu, Japan) which was equipped with an HP-PONA chromatographic column (50 m x 0.20 mm x 0.5 µm) and operated with helium as the carrier gas.

50 mg of the sample was weighed in a sample cup and positioned inside the pyrolizer compartment. Prior to the analysis, the temperature of the furnace was set at 300 °C and then the sample fell into this furnace. The injector temperature was at 300 °C with split mode using 1:10 ratio. The GC oven temperature started at 30 °C and held for 5 minutes, increased to 320 °C at a 15 °C min^{-1} and then held for 10 minutes. The He flow rate in the column was 1.05 mL min^{-1}. The MS detector worked with an ion source temperature of 250 °C, an interface temperature of 310 °C and with measurements within the range of 35 to 500 m/z.

Labeled samples were provided by Petrobras S.A. For each sample, the heptane index was calculated as follows:

H index = 100 x n-C7 / (sum of cyclohexane and methylcyclohexane) (Isaksen, 2004)

Results and Discussion

Based on the S1 values presented in Table 1, it was expected that the amount of free hydrocarbons in the samples would be low. As a result, it was anticipated that the light hydrocarbons of interest might only be present in trace amounts. Figure 1 shows the chromatogram for the sample with the highest total organic carbon (220117362), which confirms the low abundance of free hydrocarbons compared to those with higher molecular weight.

Table 1. Samples information

Sample	Depth (m)	TOC (wt.%)	S1 (mg/g rock)	S2 (mg/g rock)	H index
220117362	4461	22.2	0.32	126.87	15.5
220117443	4463	13.4	0.45	74.88	17.3
220117286	4459	13.0	0.13	69.46	15.9
220117527	4467	6.61	0.09	36.7	17.6

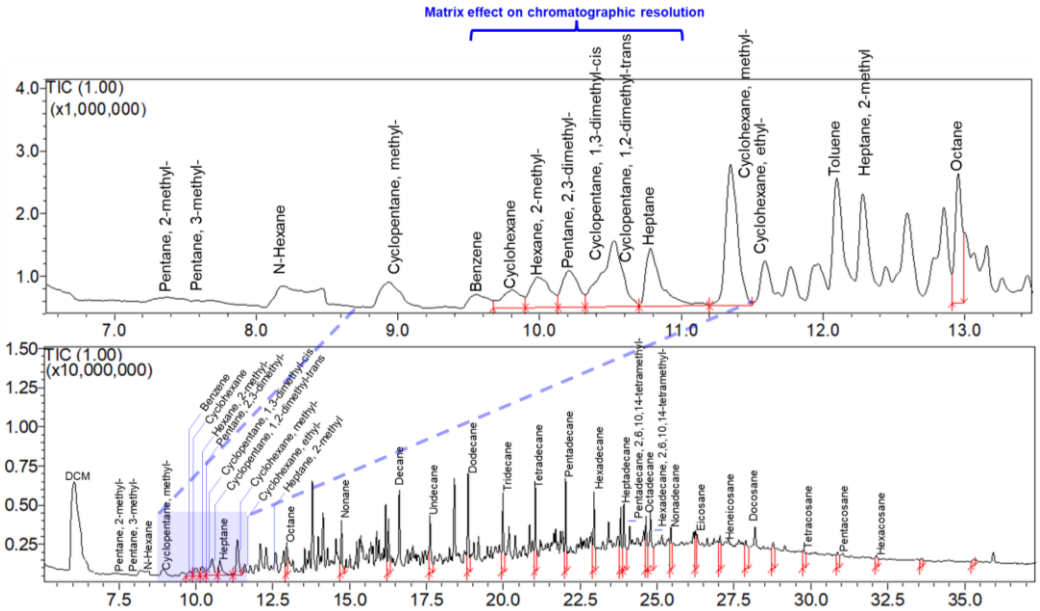

Figure 1. Chromatograms of Sample 220117362, showing (a) a zoomed-in view of the compounds of interest for the H index, and (b) the full chromatogram.

In Figure 1, a strong matrix effect can be observed in the chromatographic separation of the compounds, resulting in the enlargement of the peaks, which was observed for all rock samples. In contrast, liquid hydrocarbon samples injected using the pyrolizer system with the same chromatographic method did not show this behavior. This loss of resolution may be attributed to the nature of the sample, i.e., hydrocarbons are inside the rock's pores, the inorganic matrix may play a role and the rock particles are piled inside the sample cup. Nevertheless, despite the enlarged peaks, separation was still achieved for n-heptane compared to its isomers, enabling the estimation of the H index. All samples were analyzed in at least three replicates, and the results were consistent, with the same profile and proportions between the observed compounds. This indicates that despite alterations in chromatography resolution, factors such as thermal/diffusion or rock matrix did not affect the reproducibility of the results.

The H index was calculated for each replicate and each sample, and the results are presented in Table 1, along with their TOC and Rockeval analysis. The H index ranged from 15.5 to 18.1 (+- 0.3) across the samples (Thompson, 1983; Isaksen, 2004), which classifies them between normal and early mature.

Conclusions

The proposed Py-GCMS method was shown to be a reliable and advantageous technique for the assessment of rock maturity based on the Thompson's H index. This method offers the advantage of handling rock samples directly for the analysis, thereby reducing the number of experimental steps required, such as extraction, which could lead to errors due to the volatilization of the hydrocarbons of interest.

Acknowledgements

The authors thank CNPq and CAPES for fellowships; ANP (Brazilian Petroleum Agency), Petrobras S/A, FAPERJ and PGQu – UFRJ for financial support.

References

Isaksen, G.H., 2004. Central North Sea hydrocarbon systems: Generation, migration, entrapment, and thermal degradation of oil and gas. AAPG Bulletin 88, 1545–1572.

Mango, F.D., 1997. The light hydrocarbons in petroleum: a critical review. Organic Geochemistry 26, 417–440.

Thompson, K.F.M., 1983. Classification and thermal history of petroleum based on light hydrocarbons. Geochimica et Cosmochimica Acta 47, 303–316.

XVI LATIN AMERICAN CONGRESS ON ORGANIC GEOCHEMISTRY
9 - 11 AUGUST, 2023
ARACAJU, SERGIPE, BRAZIL

PHYSICAL SIMULATIONS OF PETROLEUM CHANGES RELATED TO INTERACTION WITH CO_2 and CH_4

[a]JOELMA PIMENTEL LOPES, [a]ALEXANDRE JAIME MELLO VIEIRA, [b]HENRIQUE LUIZ DE BARROS PENTEADO

[a]PETROBRAS Research Center, Av Horácio Macedo ,950, Cidade Universitária, 21941-915, Rio de janeiro, RJ, Brazil
[b]PETROBRAS EDISEN, Av. Henrique Valadares, 28 - Centro, 20231-030, Rio de Janeiro - RJ, Brazil

Joelma.lopes@petrobras.com.br

Introduction

The use of carbon dioxide as an oil recovery agent in petroleum reservoirs has been extensively researched for many years. Both laboratory and field studies have established that CO2 can be an efficient oil-displacing agent. However, in this study the objective is to evaluate the compositional changes of oil due to interaction with a pure CO2 stream, to understand the alterations of the PVT and geochemical properties, thus providing guidelines for the exploration and production processes.

Different accumulations in Brazilian marginal basins have CO2 contents varying between 0 to 80 mol %. Where the CO2 values reach their maximum, two distinct fluids were observed at the reservoir: a rich gas condensate at the top, and a heavy oil at the bottom.

Experiments were carried out to investigate several intensities of interaction between CO2, CH4 and live oil, under reservoir pressure and temperature conditions, without forced mixing.

Experimental

Physical simulations were performed in three types of PVT apparatus: The first one is a Visual cell, one traditional PVT equipment that was used at first trying to understand the mechanism of the CO2 and Oil interaction even though the volume is only 80 cm3. The second one is a Blind cell, that consists of two PVT bottles, with T and P control. Where the internal volume reaches 700 (seven hundred) and allows us to have a higher oil column and to evaluate the possibility of some gravitational segregation. These two experiments occur as a closed system while the third one is related to an open system. After each phase separation, the gas phase is recovered and the residual oil is washed again for more gas. In this case, we were interested to evaluate the differences in the results when the CO2 or Methane are injected. The cells' volume reaches more than 1 liter and allows us to have samples from each step.
The volumes of live oil and gas initially introduced into the cell must allow the reproduction of the proportions of oil and de gas, in the studied under area (reservoir conditions at 60°C and 9000 psig).

Results and Discussion

The objectives of the first experiment were to visualize the CO2 and the oil interaction; mimic the composition of real reservoirs with high CO2 content and evaluate the results of CO2-Oil interaction related to bulk properties, Light HC and biomarker ratio.

Immediately upon the contact of CO_2 with live oil, interactions by diffusion and convection occur due to the difference in density and the extraction capacity of the compounds of the oilphase by CO_2, giving rise to three phases at the end of the experiments. The CO_2 and petroleum mixture was left to rest for a period of 48 hours (visual cell) after which samples from the upper gas and the lower liquid phases were recovered for further analyses.

The results of the condensate recovered from the gas phase, that was produced after the injection of the CO2 were compared with the original and the residual oil. The first one shows that the API gravity increase for the condensate and decrease for the residual oil, while the methane isotopic composition remains constant around 26. On the other hand, we can observe a good correlation with the API gravity between light and heavy compounds.

The maturity-related biomarkers show only small differences and did not affect the interpretation of the indication of the thermal evolution of the fluid.

The most affected biomarker ratios by the phase separation occur when the differences among the

compounds are too high like Dia/C27, Tric/ hop, Tri x esterane. In addition, the most common ratio to evaluate the biodegradation intensity didn't change.

The products resulting from the simulations show important changes in the values of the API and gas-oil ratio when compared to those observed in the original oil, confirming the phase and composition changes due to its interaction with CO2.

The second experiment was carried out to evaluate the CO2 and the oil interaction related to the possibility of phase segregation; Test different ways to introduce the CO2 at the cell, clarify the filling history of the reservoir and mimic the composition of real reservoirs with high CO2 content.

In this simulation, CO2 was injected into the blind cell in different ways: (1) injection of oil and then CO2 from the top; (2) injection of CO2 and then oil from the bottom of the PVT cell. (3) the injection of oil and then CO2 from the bottom of the cell. After seven days, the volume of 50 cm3 each time was collected to discrete the oil column.

The correlation between GOR and API shows different behavior of the fluid. When CO2 is placed stratigraphically in the upper part of the cell: occur the presence of a homogeneous column of the gas phase. On the contrary, when CO2 is introduced below a previously placed oil column, a vertical compositional gradation along the gas and liquid phase column is observed.

A contradictory result was observed looking at the concentration of CO2, which increases from the top to the bottom. We believe this occurs due to this T and P condition the CO2 behaves as a supercritical fluid, denser than the oil (Lopes et al. 2018).

The third experiment at the contact cell aims to evaluate the oil interaction with the injection of CO2 or CH4 and mimic the cumulative evaporative fractionation (leakage). In this experiment, the excess gas injected was recovered from the system, and in each step the gas cap and the residual oil were sampled. In this case, before sampling, the fluid was mixed to force an equilibrium.

When the gas injected is the CO2 the extraction is more severe with only 4 contacts, while the CH4 is more selective, and we could reach 8 contacts. In addition, the differences in the API gravity are higher with the CO2 than with the CH4.

The biomarker ratios increase the differences as the number of contacts increases among the residual oils and condensates (Figure 1).

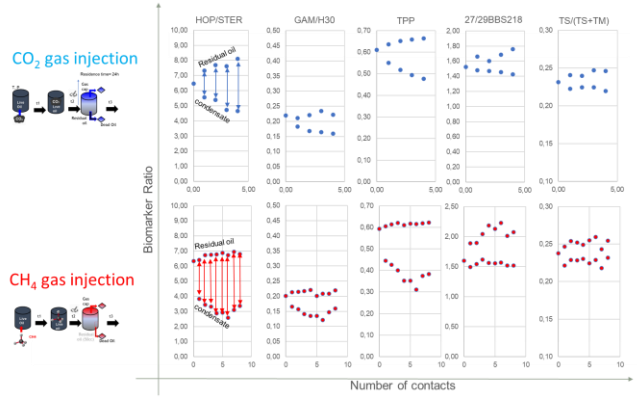

Fig 1. The biomarker ratios increase the differences as the number of contacts increases among the residual oils and condensates

Conclusions

The experimental values are similar to those found in the fluids recovered from the studied area, suggesting a fluid change in this field due to the effect of its interaction with CO2.

It is important to be cautious when evaluating parameters from oils recovered from reservoirs with phase separation or tertiary migration.

It has been experimentally demonstrated that the mixing sequence during reservoir filling (CO2 at the top-oil below or oil at the top-CO2 below) significantly alters not only the distribution of the components but also the composition of the phases.

Based on the comparison of experimental and field data, it is possible to suggest the relative timing of the oil or CO2 filling in the reservoirs. This knowledge provides guidelines for the understanding of the filling history, and contributes to the improvement of the characterization of the petroleum system operating in the area, thus allowing the optimization of the exploration and exploitation strategies.

Acknowledgements

The authors thank The Federal University of Rio de Janeiro collaboration to conduct some of the experiments. and to PETROBRAS for the permission to publish this work.

References

Lopes J.P., Vieira A.J.M., Rocha Y.S., Penteado H.L.B., 2018, Physical Simulations of Petroleum Changes Related to Interaction with CO2 - Comparison of Different Mixture Scenarios In: Proceedings of the XV ALAGO Congress, Salvador, 4-7 November

XVI LATIN AMERICAN CONGRESS ON ORGANIC GEOCHEMISTRY
9 - 11 AUGUST, 2023
ARACAJU, SERGIPE, BRAZIL

GEOCHEMICAL CHARACTERIZATION IN SHALES OF THE INTERCEMENT QUARRY (MORRO DO CHAVES FORMATION, SERGIPE-ALAGOAS BASIN)

RAMSÉS CAPILLA[a], HANNA CAROLINA LINS DE PAIVA[b], VALÉRIA GALLO[b]

[a] **CENPES/PETROBRAS/** [b] **LABORATÓRIO DE SISTEMÁTICA E BIOGEOGRAFIA (LabSisBio-UERJ)**

capilla@petrobras.com.br, hanna.clp@gmail.com, gallo@uerj.br

Introduction

The Morro do Chaves Formation (MCF) is composed by coquina beds and shales interbedded. In addition, the most remarkable outcrop of MCF is known as InterCement quarry (formerly Atol quarry), placed in São Miguel dos Campos county, AL.

The main objective of this abstract is to evaluating the geochemical characteristics from organic content and extracts, as well as to comprehend the development of the InterCement quarry depositional system. Thus, fourteen mining front samples was collected by researchers from the Laboratory of Systematics and Biogeography at the State University of Rio de Janeiro (LabSisBio-UERJ). Posteriorly, these samples were analyzed by the Fluid Technology Management and Petrobras Research and Development Center (CENPES) laboratories.

Material and Methods

The samples were submitted to analytical techniques in Organic Geochemistry, such as Total Organic Carbon (TOC) and Rock-Eval Pyrolysis; extraction and separation of fractions by Medium Pressure Liquid Chromatography (MLMP), Gas Chromatography (GC) and Gas Chromatography Coupled to Mass Spectrometry (GC-MS).

Results and Discussion

The list of shale samples collected at the mining fronts of the InterCement quarry can be observed in table I.

The most representative results from TOC and Pyrolysis analyzes were only observed in F01, F04-D, F05, F07-B and F08 (TOC ≥ 1%). On the other hand, 65% of the samples (F02, F03, F04-C, F04-B, F04-A, F06, F07-D, F07-C and F07-A) showed a TOC content lower than 1%, which were not used to other geochemical analyzes.

Table I
Samples for the geochemical characterization of extracts from shales (mining front of the InterCement quarry) of the Morro do Chaves Formation.

Sample	Identification
1	F01
2	F02
3	F03
4	F04-D Topo
5	F04-C
6	F04-B
7	F04-A Base
8	F05
9	F06
10	F07-D Topo
11	F07-C
12	F07-B
13	F07-A Base
14	F08

Geochemical Caracterizaion of the Extracts

The values of the main biomarkers and the isotopic ratio are observed in Table II.

Table II
Biomarker data and isotopic composition obtained from five samples from the Morro do Chaves Formation.

Amostra	HOP/STER	TRIC/HOP	H28/H30	H29/H30	GAM/H30	HSS/H34	Z1/Z3TR	Z6/Z5TR	NORNEO/H29	TS/(TS+TM)	20S/(20S+20R)St	aaR/(aaR+aaa)	%27aaBBR&S	%28aaBBR&S	%29aaBBR&S	TPP	TET24/H30	H29/C29TS	δ13C
F01	2,50	0,64	0,11	0,42	0,54	1,02	1,65	2,81	0,20	0,15	0,11	0,21	27,61	19,51	52,89	0,89	0,02	4,94	-28,94
F04-D Topo	9,63	0,12	0,02	0,71	0,31	0,59	1,32	2,18	0,15	0,15	0,15	0,25	36,54	18,43	45,02	0,83	0,02	6,63	-27,48
F05	5,72	0,16	0,02	0,28	0,41	0,84	1,77	2,87	0,27	0,18	0,11	0,21	28,83	22,30	48,87	0,91	0,01	3,74	-30,59
F07-B	3,79	0,35	0,05	0,68	0,64	0,57	1,12	1,79	0,15	0,16	0,12	0,21	34,07	21,57	44,36	0,96	0,05	6,65	-27,64
F08	2,33	0,02	0,09	0,43	0,69	0,90	1,40	2,60	0,25	0,15	0,12	0,20	30,37	21,52	48,12	0,96	0,03	3,97	-26,67

Both biomarkers and isotopic composition may reflect the system in which the organic matter was deposited (Peters et al., 2005).The geochemical signatures of InterCement quarry extracts suggest a deposition in transitional

conditions. It is also supported by the Hopane/Sterane ratio and the proportions of steranes C_{27}, C_{28} and C_{29} (Figure 1).

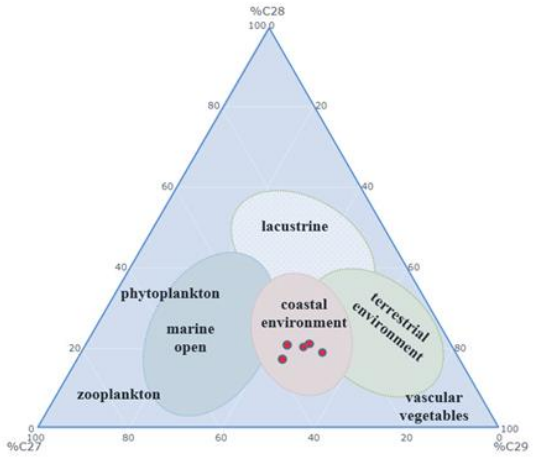

Figure 1. Ternary diagram of the relationships between C_{27}, C_{28} and C_{29}. sterane proportions (InterCement Quarry, AL), (modified of Huang and Meinschein, 1979).

In addition, the Gam/H_{30}, 26/25Tri and $H_{35}/_{34}$ ratios (Table II), suggest the presence of restricted carbonate paleoenvironments with high salinity and associated anoxia. The H_{29}/H_{30} and H_{35}/H_{34} ratios are important in the interpretations between carbonate and siliciclastic contribution in the system, as well as the water stratification.

The variations of oxy-reductive conditions also can be observed from the Pri/Phi ratio. Values less than 1.0 suggest a predominantly reducing paleoenvironment, while values greater than 1.0 suggest more oxic conditions. (Didyk et al., 1978 apud Killops & Killops, 2005). Therefore, the samples F01, F05, F07-B and F08 represent a probable reductor paleoenvironment (Pri/Phi ratio ≤ 1.0), while F04-D (Pri/Phi ratio = 3.0) is a possible indicative of oxic scenario (figures 2 and 3).

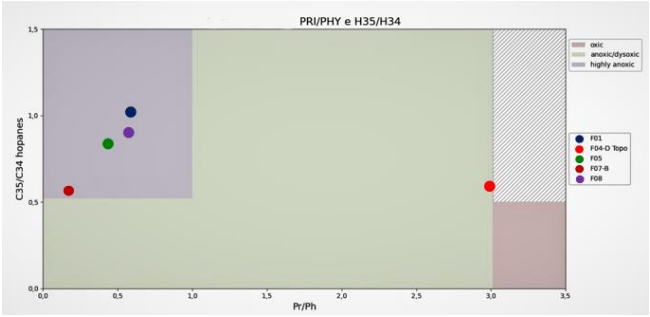

Figure 2. The relationship between the Pr/Ph and H_{35}/H_{34} ratios, as well as the redox conditions.

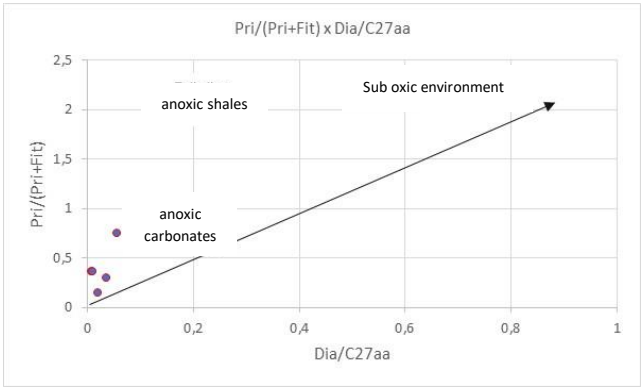

Figure 3. Correlation between the ratios Pr/(Pr+Fit) and Dia/C27αα) controlled by the depositional environment (adapted from Peters et al. 2005)

Conclusions

According to these results, the shales of the InterCement quarry are indicative of a transitional environment. Although the analyzed data reflect a strong continental influence, they also may be indicative of lagoonal ecosystems.

Also, the geochemical characterization showed variable redox conditions along the facies, as well as events of water stratification, with high salinity and anoxia.

Acknowledgments

The authors are grateful for the V. G. Productivity Grant (308071/2022-0), as well as for the PROCIÊNCIA (FAPERJ). Special thanks to the management laboratories of Fluid Technology (PDIEP/TF/CENPES) and Geochemistry (PDIEP/GEOQ/CENPES) for the geochemical analyses. H.C.L.P. thanks for her PhD. affiliation (PPGEE-UERJ) and was financed by the Coordenação de Aperfeiçoamento de Pessoal de Nível Superior – Brasil (CAPES) – Finance Code 001".

References

Huang W. Y. & Meinschein W. G. (1979). Sterols as ecological indicators. Geochim. Cosmochim. Acta, 43, 739–45.

Killops, S. & Killops, V. (2005). Introduction to Organic Geochemistry. Ed. Blackwell Publishing, 393 p.

Peters, K. E.; Walters, C.C. & Moldowan, J.M. The Biomarker Guide. 2nd ed., 2v., University Express, Cambridge, 1155p. 2005.

XVI LATIN AMERICAN CONGRESS ON ORGANIC GEOCHEMISTRY
9 - 11 AUGUST, 2023
ARACAJU, SERGIPE, BRAZIL

Paleodepositional interpretation of an interval in the Tremembé Formation, Taubaté Basin

NELSON FERREIRA DOS SANTOS JUNIOR*, RAMSES CAPILLA*, ANDRE LUIZ DURANTE SPIGOLON*

[a] **CENPES/PETROBRAS**

*nelsonferreira@petrobras.com.br, *capilla@gmail.com, andrespigolon@petrobras.com.br

Introduction

The Tremembé Formation (Oligocene, Taubaté Basin) is an example of a lacustrine system that presents significant facies variations, very common in lacustrine source rocks, related to climatic, biological, and tectonic factors [1].

The paleodepositional context of this formation is related to environmental changes that occurred in the Paleogene, between 65 and 23 million years ago. At the Paleocene-Eocene Boundary, there was a large and sudden increase in temperature on Earth, probably related to the collision of India with Asia [2]. In the Eocene-Oligocene Boundary, there was an abrupt drop in temperature, which culminated in the formation of the Arctic polar ice cap and in the global climate change from a hot and humid climate to a cold and dry one. At the end of the Oligocene, the planet experienced a new warming, causing the melting of the Antarctic ice cap [3].

Thus, the present work proposes a paleodepositional model of the Tremembé Formation using analytical data of organic geochemistry (Total Organic Carbon, Rock-Eval Pyrolysis, saturated biomarkers and stable carbon d13C isotopes) obtained from shale samples and their organic extracts.

Fifteen samples were collected from a mining front of the mining company Sociedade Extrativa Santa Fé, Tremembé, SP, and these samples were analyzed in the laboratories of the Fluid Technology Management and by the Geochemistry Management of the Leopoldo Américo Miguez de Mello Research and Development (Cenpes).

Materials and Methods

The methodology was the standard one, following the analyzes of Total Organic Carbon (TOC), Rock-Eval Pyrolysis, extraction and separation of fractions by Soxhlet and Medium Pressure Liquid Chromatography (CLMP), Gas Chromatography (GC), Gas Chromatography Coupled to Mass Spectrometry (GC-MS) and Isotopic Ratio Mass Spectrometry (IRMS).

For the interpretation of geochemical data, organic facies were delimited according to Jones (1987), in addition to ternary sat/aro/NSO diagrams, Van Krevelen diagram, geochemical profiles and analysis of chromatograms and fragmentograms ions *m/z* 85, 191 and 217.

Results and Discussions

The TOC results of the 15 samples are shown in Table I.

The Total Organic Carbon of the samples ranged from 0.99 to 24.8%, with the highest levels associated with shales. Such values suggest paleoenvironmental conditions favorable to the great productivity of organic matter and anoxic conditions that favored its preservation and accumulation.

Table I - List of samples from the mining front of Sociedade Extrativa Santa Fé selected for organic geochemical analyses.

Sample	Depth (m)	Lithology	TOC (%)
SF-01	2.9	Papyraceous shale	24.8
SF-02	3.4	Fossiliferous dark gray shale	10.87
SF-03	3.9	Fossiliferous dark gray shale	9.92
SF-04	4.4	Fossiliferous dark gray shale	7.36
SF-05	4.9	Fossiliferous dark gray shale	0.99
SF-10	5.2	Massive greenish mudstone	1.32
SF-10A	5.25	Massive greenish mudstone	1.04
SF-06	5.4	Fossiliferous dark gray shale	14.19
SF-07	5.9	Fossiliferous dark gray shale	13.57
SF-08	6.4	Massive greenish mudstone	2.15
SF-09	6.6	Massive greenish mudstone	2.07
SF-11	6.9	Light gray clayey siltstone	2.37
SF-12	7.6	Papyraceous shale	16.35
SF-13	8.3	Fossiliferous dark gray shale	10.67
SF-14	8.8	Papyraceous shale	7.53

The Rock-Eval pyrolysis data were immature, with Maximum Temperature (T_{max}) between 363 and 439°C [4]. The Hydrogen Index (HI) between 130.77 and 764.96 mg HC/g of TOC and the Oxygen Index (IO) ranging from 7.14 to 96.58 mg CO_2/g of TOC, indicating predominance of type kerogen I (HI > 600 mg HC/g TOC) and secondarily type III (HI 50 – 200 mg HC/g TOC) [4].

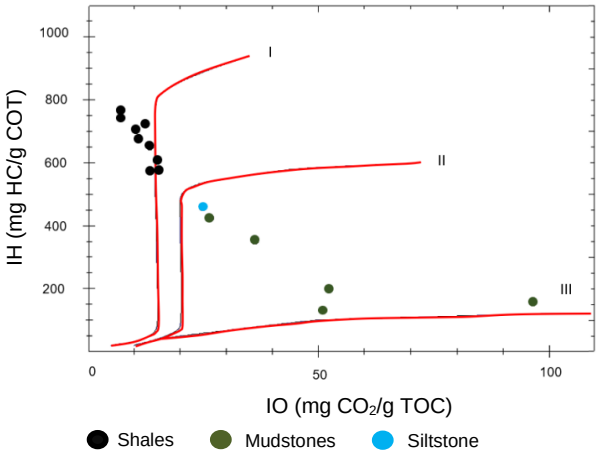

Figure 1. Van Krevelen diagram of the 15 samples under study.

Four organic facies were distinguished in the sedimentary succession under study: AB (IH 650 – 850 mg HC/g TOC), B (400 – 650 mg HC/g TOC), BC (250 – 400 mg HC/g TOC) and C (125 – 250 mg HC/g TOC). Thus, the distribution of organic matter varies from amorphous organic matter (MOA) with little terrestrial contribution to predominantly terrestrial and oxidized organic matter, being under the influence and alternation of dry and humid climate.

The distribution of fractions of organic extracts shows a significant preponderance of aromatic compounds and NSO to the detriment of saturated ones, corroborating the thermal immaturity.

The saturated biomarkers show alternation in the predominance of organic matter in the section, sometimes with high concentrations of C_{28} sterane, sometimes with high concentrations of C_{29}, indicating a greater contribution of algalic and terrestrial organic matter, respectively [5].

Conclusions

The analytical results with abrupt and alternating variations reflect the cyclic paleodepositional changes of the Tremembé paleolake, in a context of dry and humid climate, which directly influenced the production, accumulation, preservation and type of organic matter. The data suggest anoxic-disoxic background redox conditions, with stratification of the water column.

Acknowledgements

Special thanks from the authors to the management laboratories of Fluid Technology (CENPES/PDIEP/GEOQ/TF) and Geochemistry (CENPES/PDIEP/GEOQ), for carrying out the analyses.

References

[1] TEXTURAL AND COMPOSITIONAL VARIABILITY ACROSS LITORAL SEGMENTS OF LAKE TANGANIKA: THE EFFECT OF ASYMMETRIC BASIN STRUCTURE ON SEDIMENTATION IN LARGE RIFT LAKES. Soreghan, M. J & Cohen, A. S., 1996. American Association of Petroleum Geologists Bulletin, v. 80, n. 3, p. 382-409.

[2] MUDANÇAS AMBIENTAIS E DESDOBRAMENTOS EVOLUTIVOS DURANTE O PALEÓGENO. MONOGRAFIA (TRABALHO FINAL DE CURSO). Chimetto, E. N., 2008. Universidade Estadual Paulista "Júlio de Mesquita Filho", Rio Claro, SP.

[3] PALEOBOTANY AND EVOLUTION OF PLANTS. Stewart, W. N.; Rothwell, G. M., 1993. Cambridge University Press, 521 p.

[4] APPLIED SOURCE ROCK GEOCHEMISTRY. Peters, K. E. & Cassa, M. R., 1994. Mobil Exploration and Producing Technical Center, Dallas, Texas, USA, pp: 93-115.

[5] BIOMARKERS FOR GEOLOGISTS: A PRACTICAL GUIDE TO THE APPLICATION OF STERANES AND TRITERPANES IN PETROLEUM GEOLOGY. Waples, D. W., Machihara, T., 1991. AAPG Methods in Exploration Series, v. 9, pp. 1-76.

XVI LATIN AMERICAN CONGRESS ON ORGANIC GEOCHEMISTRY
9 - 11 AUGUST, 2023
ARACAJU, SERGIPE, BRAZIL

Source rock modelling for the Sergipe Basin using Achilles.BR 1D

ABREU, P.V. [a*], **VENANCIO, I.M.**[a], **SANTOS, T.P.**[b], **CARREIRA, V.R.**[c], **MOREIRA, M.A.**[c], **SPIGOLON, A.L.D.**[d], **SOUZA, I.V.A.F.**[d], **ALBUQUERQUE, A.L.S.**[c]

[a]PROGRAMA PÓS-GRADUAÇÃO EM GEOCIÊNCIAS (GEOQUÍMICA), UNIVERSIDADE FEDERAL FLUMINENSE, NITERÓI, BRASIL

[b]ESCOLA DE ARTES, CIÊNCIAS E HUMANIDADES, UNIVERSIDADE DE SÃO PAULO, SÃO PAULO, BRASIL

[c]PROGRAMA DE PÓS-GRADUAÇÃO DINÂMICA DOS OCEANOS E DA TERRA, UNIVERSIDADE FEDERAL FLUMINENSE, NITERÓI, BRASIL

[d]DIVISION OF GEOCHEMISTRY, PETROBRAS RESEARCH AND DEVELOPMENT CENTER (CENPES), RIO DE JANEIRO, BRAZIL

*correspondence: pvabreu7@gmail.com

Introduction

The growing demand for oil and gas has driven exploration to drill in deep and ultra-deep waters [1], which present multiple challenges. One of these challenges is predicting the potential of the source rock, which is an important element for modeling the petroleum system, providing a better estimate of exploratory risk [2]. In this context, total organic carbon (TOC) is a quantitatively important and widely used component in source rock modelling [3].

With regard to source rock modelling, new approaches have been used to simulate organic carbon content and quality. In this context, the Geochemistry Management (CENPES/PDIEP/GEOQ) in partnership with the Federal Fluminense University (UFF) developed a program called Achilles.BR bringing significant gains in the 1D predictive models of source rock quality when compared to the softwares available in the market. With Achilles.BR 1D it is possible to simulate, over a sequence of logical steps, scenarios of accumulation and preservation of organic carbon and to estimate the quality of organic carbon prior to advanced diagenetic processes, generating fundamental information about the potential of source rocks.

In this sense, with the objective of testing the program in a known source rock interval of the Brazilian continental margin, this work aims to present the 1D modeling results carried out by Achilles.BR in the Upper Middle Cretaceous marine source section of the Sergipe Basin in its deep-water portion.

Experimental

In the total organic carbon simulation stage, the equations from [4] were chosen for wells SES-1, SES-2 and SES-3 and the *Definition Equation* [5] for well SES-4 to estimate the marine organic carbon. The equation of [4] does not require input of paleobathymetric information and performs relatively well on the Brazilian margin [6]. Paleoproductivity scenarios were experimented, until an optimal value of a maximum of 400 gC/m²/year was found to be sufficient to reproduce the previously measured TOC values. In the case of terrestrial organic carbon estimates, the low terrestrial carbon input regime was chosen. Furthermore, anoxic conditions were established, with a maximum preservation factor of 10%, during anoxic events (e.g. OAE2) present in the wells. For the estimates of HI, OI, the default values of the mixture model implemented in Achilles.BR 1D were used, and the classification of organic facies was performed in fuzzy logic.

In the maturation simulation stage, equations from the studies of [7] and [8] were selected to estimate the original parameters (e.g. TOC_0, HI_0). Transformation ratios were estimated based on Ro data from the wells, and using the relationships established in the work of [9].

Results and Discussion

The tests carried out with the previously mentioned wells in the Sergipe basin show that the results obtained in the total organic carbon simulation stage are in agreement with the TOC values measured in the wells, with the highest simulated percentages coinciding satisfactorily with the highest measured values. Maturation simulation indicates that, prior to advanced diagenetic processes, values of up to ~16% TOC existed in the depositional environment. In general, these values coincide with organic facies AB, B or BC, which may indicate type I, II or III kerogens. These results are corroborated by the

results of palynofacies present for some of these wells, which also indicate type I, II or III kerogens.

Thus, the data obtained through 1D modeling proved to be very promising for predicting the quality of the source rock, and can be considered a very useful tool for assessing exploratory risk (Figure 1).

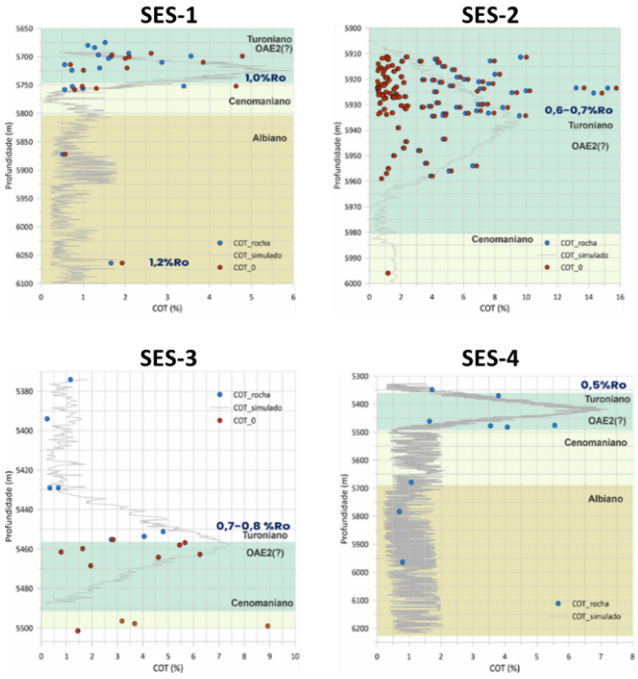

Figure 1. Modelling results using the Achilles.BR 1D program for deep waters of the Sergipe Basin wells and their comparison with total organic carbon data measured in the Albo-Turonian interval.

Conclusions

The simulations for the Sergipe Basin wells showed good results, where it was possible to simulate the increases in TOC values of the wells through the establishment of anoxic conditions. In some wells, the simulated TOC values slightly under or overestimated the measured TOC values, which indicates that productivity and/or preservation could be adjusted somewhat for further simulations in these wells. The Achilles.BR 1D simulations provided important information about the paleoenvironment for the deep water's region of the Sergipe Basin. The data indicate that the organic matter contents can be estimated considering that the productivity in the region reached maximum values of approximately 400 gC/m^2/year and a carbon preservation of at most 10%.

Acknowledgements

The authors thank ANP (Brazilian Petroleum Agency), Petrobras S/A, UFF and Project PR4 for financial support.

References

[1] Kelessidis, V.C., 2009. Challenges for very deep oil and gas drilling - will there ever be a depth limit. In: 3rd AMIREG International Conference. Assessing the Footprint of Resource Utilization and Hazardous Waste Management, 2009.

[2] Tissot, B. P., Welte, D. H., 1984. Petroleum Formation and Occurrence. Springer Berlin Heidelberg. https://doi.org/10.1007/978-3-642-87813-8

[3] Calvert, S.E., 1987. Oceanographic controls on the accumula-tion of organic matter in marine sediments. Geol. Soc. London, Spec. Publ. 26, 137–151. https://doi.org/10.1144/GSL.SP.1987.026.01.08.

[4] Müller, P.J., Suess, E., 1979. Productivity, sedimentation rate, and sedimentary organic matter in the oceans—I. Organic carbon preservation. Deep Sea Research Part A. Oceanographic Research Papers 26, 1347–1362. https://doi.org/10.1016/0198-0149(79)90003-7

[5] Tyson, R.V., 2005. The "productivity versus preservation" controversy: cause, flaws, and resolution in: deposition of Organic-Carbon-Rich Sediments: Models. SEPM (Society for Sedimentary Geology) 82, 17–33. https://doi.org/10.2110/pec.05.82.0017.

[6] Venancio, I.M., Belem, A.L., Santos, T.P., Lessa, D.O., Leonardo, N.F., Bione, F.R.A., Díaz, R., Moreira, M., Bernardes, M.C., Souza, I.V.A.F., Coutinho, L.F.C., Albuquerque, A.L.S., 2022. Temporal and spatial differences between predicted and measured organic carbon in South Atlantic sediments: Constraints to organic facies modelling. Marine and Petroleum Geology 138, 105524. https://doi.org/10.1016/j.marpetgeo.2022.105524

[7] Dahl, B., Bojesen-Koefoed, J., Holm, A., Justwan, H., Rasmussen, E., & Thomsen, E., 2004. A new approach to interpreting Rock-Eval S2 and TOC data for kerogen quality assessment. Organic Geochemistry, 35(11–12), 1461–1477. https://doi.org/10.1016/j.orggeochem.2004.07.003

[8] Justwan, H., & Dahl, B. (2005). Quantitative hydrocarbon potential mapping and organofacies study in the Greater Balder Area, Norwegian North Sea. Geological Society, London, Petroleum Geology Conference Series, 6(1), 1317–1329. https://doi.org/10.1144/0061317

[9] Waples, D. W., & Marzi, R. W. (1998). The universality of the relationship between vitrinite reflectance and transformation ratio. Organic Geochemistry, 28(6), 383–388. https://doi.org/10.1016/S0146-6380(97)00122-8

Unveiling the Composition of Crude Oil: A Comprehensive Study Using Ultra-High Mass Spectrometry and Multiple Ionization Sources

João V. A. Oliveira[a], Deborah V. A. Aguiar[a], Iris M. S. Júnior[b], Alexandre de O. Gomes[b], Luiz A. N. Mendes[b], Gesiane S. Lima[a], Boniek G. Vaz[a]

[a]Chemistry Institute, Federal University of Goiás, Goiânia, Goiás, Brazil

[b]CENPES, PETROBRAS, Rio de Janeiro, RJ, 21941-915, Brazil

oliveiraataide@discente.ufg.br

Introduction

Crude oil is a complex mixture composed mostly of hydrocarbons (HC) but also includes heteroatom-containing compounds, such as nitrogen (N), oxygen (O), sulfur (S) and some metals in different proportions (Cho et al., 2015). In this way, the characterization of compounds in crude oils is of utmost importance for their pricing and destination. However, most current refinery models are based on general information about the oil, such as API density, total acid number (TAN), and others.

In this context, analytical techniques, such as ultra-high-resolution mass spectrometry, have been widely applied in developing methods for the comprehensive characterization of petroleum. This field, currently known as petroleomics, aims to provide a comprehensive understanding of the complex chemical composition of crude oil (Marshall and Rodgers, 2008). Nevertheless, the absence of a universal ionization technique capable of simultaneously ionizing all compounds present in crude oils is evident.

Therefore, to achieve a comprehensive characterization, different ionization sources must be used, governed by distinct ionization mechanisms. In this regard, this study aimed to analyze a light crude oil sample applying different atmospheric pressure ionization (ESI, APCI, and APPI) sources to access an extensive composition of the crude oil.

Experimental

A light crude oil sample with API density 35.9 and TAN 0.11 mg KOH.g^{-1}, was supplied by Petrobras. The MS analysis was performed using an FT-ICR MS 7 T SolariX 2xR (Bruker Daltonics) coupled to electrospray ionization (ESI), atmospheric pressure chemical ionization (APCI), and atmospheric pressure photoionization (APPI) sources. Initially, a stock solution was prepared by dissolving 2 mg of oil in 2 mL of toluene; for ESI(-) analysis, 500 µL of the stock solution was collected and transferred to a vial containing methanol doped with 2.5% ammonium hydroxide, resulting in a final concentration of 0.5 mg.mL^{-1} methanol:toluene (1:1, v/v). Similarly, for ESI(+) analysis, 500 µL of the stock solution was collected and transferred to a vial containing methanol doped with 1% formic acid, yielding a final concentration of 0.5 mg.mL^{-1} methanol:toluene (1:1, v/v). For APPI(+) and APCI(+) analyses, both solutions were prepared by diluting 500 µL of the stock solution in methanol to achieve a final concentration of 0.5 mg.mL^{-1} methanol:toluene (1:1, v/v). The spectral data were recalibrated using DataAnalysis 5.0 SR1 (Version 5.0, Bruker Daltonik GmbH) software and compositional assignment using Composer software (version 1.5.3 Sierra Analytics, USA).

Results and Discussion

Assessing the heteroatom content in crude oil is indispensable for petroleum evaluation and geochemical studies (Angolini et al., 2017). However, due to the distinct ionization mechanisms governing each ionization source, the compound response to each ionization source varies. In this context, **Figure 1** illustrates the compound class distribution in the crude oil analyzed using different ionization sources.

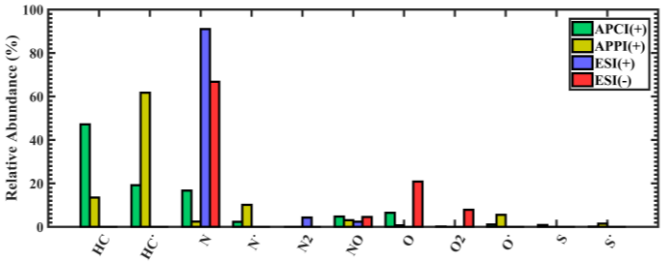

Figure 1. Class distribution obtained from different ionization sources by FT-ICR MS.

The ESI ionization source preferentially ionizes compounds of higher polarity, owing to its mechanism facilitating the generation of highly charged ions in the gas phase. Therefore, compound classes containing heteroatoms, specifically polar compounds, are observed in positive and negative ionization modes.

From ESI(+) analysis, it was possible to access diverse compositional information about the compounds found in the oil. Notably, the N class predominates with an abundance exceeding 80% in this ionization mode. This class encompasses compounds derived from pyridine, exhibiting varying degrees of aromaticity and alkylation. In addition, the N, O, and O2 classes emerged as the most prominent relative abundance for ESI(-). These classes comprised carbazoles and their benzo homologs, phenolic compounds, and carboxylic acids.

In contrast, a more significant number of low-polarity or nonpolar compounds, such as those belonging to the S class and hydrocarbon (HC) classes, were accessed by the APPI(+) and APCI(+) analyses. Among the mechanisms governing these sources, charge exchange leading to the formation of $[M^{+\bullet}]$ ions and protonation resulting in the formation of $[M+H]^+$ ions are the most common mechanisms for APPI(+) and APCI(+) sources, respectively. Moreover, APPI(+) for a light crude oil sample becomes attractive, as it allows accessing both the nonpolar composition and, to a lesser extent, the polar composition of the oil.

Figure 2 shows the number of molecular formulas assigned for the analysis of each API sources by composer processing. Applying different API sources contributes to obtaining the chemical profile of the crude oil sample. These API sources are complementary, i.e., they provide different information about the compounds in a sample (Cho et al., 2015). The APCI(+) source facilitated the assignment of a greater number of unique formulas, implying its broader coverage of compounds compared to other sources. Furthermore, the cumulative number of formulas assigned by all ionization sources indicates that their combined utilization provides a more comprehensive understanding of the analyzed crude oil sample.

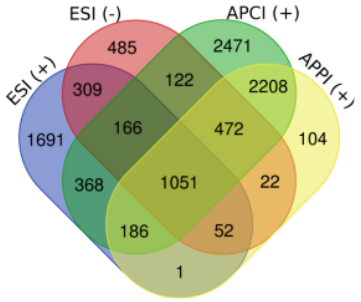

Figure 2. Venn diagram constructed based on the number of molecular formulas assigned to each source at atmospheric pressure.

Conclusions

These findings highlight the significance of employing diverse ionization sources in order to obtain a comprehensive chemical profile of the light crude oil sample. The synergistic utilization of ESI, APCI, and APPI sources enables the detection and characterization of a wide range of molecules in a complementary fashion, thereby facilitating a thorough comprehension of the molecular composition within the sample.

Acknowledgments

The authors thank Petrobras S/A, CNPq, and CAPES for financial support.

References

Angolini, C.F.F., Pudenzi, M.A., Batezelli, A., Eberlin, M.N., 2017. Comprehensive Petroleomics: Multiple Mass Spectrometry Strategies for Crude Oil Characterization. Encyclopedia of Analytical Chemistry, Major Reference Works.

Cho, Y., Ahmed, A., Islam, A., Kim, S., 2015. Developments in FT-ICR MS instrumentation, ionization techniques, and data interpretation methods for petroleomics. Mass Spectrometry Reviews 34, 248–263.

Marshall, A.G., Rodgers, R.P., 2008. Petroleomics: Chemistry of the underworld. Proceedings of the National Academy of Sciences 105, 18090–18095.

Geochemical Characterization of Crude Oil Mixtures in a Brazilian Basin by FTICR-MS Analysis

YURI A. ROCHA[a]*; LEONARDO M. FERREIRA[a]; DANIELLE M. M. FRANCO[a]; ROSANA C.L. PEREIRA[a]; MÁRIO D. RANGEL[a]; ROSINEIDE C. SIMAS[a]; YGOR S. ROCHA[b]; JOELMA P. LOPES[b]; IGOR V.A.F. SOUZA[b]; BONIEK G. VAZ[a]

[a] Laboratório de Cromatografia e Espectrometria de Massas, Institute of Chemistry, Universidade Federal de Goiás, Goiânia, Brazil, 74690-900.
[b] CENPES, PETROBRAS, Rio de Janeiro, RJ, 21941-915, Brazil.

*yuriarrates@hotmail.com

Introduction

Throughout the extension of the Brazilian territory, several types of petroleum-generating rocks are found, resulting in petroleum with distinct chemical characteristics due to their origins. These differences arise due to the physicochemical conditions of the paleoenvironments where the organic matter was deposited, such as lacustrine and marine origins [1].

It is common in the daily work of geochemists to come across mixtures of oils from different origins in order to infer a characterization. Such mixtures may have a predominance of lacustrine or marine origin oils. By characterizing the mixture and identifying its predominant origin, it's easier to understanding the geological history of the region and the environmental conditions in which the oil was generated and migrated. Based on this information, it is possible to optimize the exploration of the area, identify new exploration targets, and maximize the potential for oil extraction.

The Fourier-Transform Ion Cyclotron Resonance Mass Spectrometry has revolution the characterization of crude oil samples, enabling a molecular-level analysis of their polar composition. With its ultra-high resolution and accuracy, FTICR-MS is perfectly suited for analyzing complex mixtures, allowing the assignment of detected masses to chemical formulas [2].

The study examined oil samples from a brazilian sedimentary basin, located in costal margin. They were analyzed using FTICR-MS with atmospheric pressure photon ionization as the ionization source, Atmospheric Pressure Photoionization (APPI). The objective of this study is characterize mixtures of crude oils from distincts origins using the APPI POS (+) FT-ICR MS technique, to perform the analyses.

Experimental

Thirty-seven samples were prepared by mixing two distinct endmembers oils - one of lacustrine origin and the other of marine origin - from the same sedimentary basin. The samples were prepared in varying proportions, ranging from 0% to 100%.

Each mixture contained a total of 100mg of oil, which was dissolved in 10 mL of toluene, and diluted to the final concentration of 0.5 $mg.mL^{-1}$ (50:50, methanol: toluene). All generated samples were analyzed using FT-ICR (7T SolariX 2xR Bruker Daltonics - Bremen. Germany) with APPI as the ionization source in positive mode.

For oil samples, 300 scans were acquired to obtain spectra with excellent signal-to-noise values. The samples were injected using a syringe pump with a flow rate of 500 $\mu L.h^{-1}$. It is important to note that the raw spectra obtained by FT-ICR were internally recalibrated using the DataAnalysis 5.0 SR1 software (Version 5.0 Build 203.2.3586 64-bit Copyright © 2017 Bruker Daltonik GmbH). Next, molecular formulas were assigned to the recalibrated spectra using the Composer software (Version 1.5.3 16 Sierra Analytics. USA). Finally, output spreadsheets, called Detail Reports were generated. These spreadsheets were imported into Thanus software, that software was applied to generate figures that characterize samples to provide better graphical visualization of the data.

Results and Discussion

It is important to note that sample 31 was excluded from data analysis and model construction as it was an outlier, due to the significant deviation in its class distribution. Possible reasons for this anomaly may be attributed to operational errors during the experimental procedure or faults in spectrum acquisition.

Through analysis of 36 samples, the Thanus software produced a graph that characterizes the samples, as in the Figure 1. The graph shows that the relative abundance of hydrocarbons compounds

increases as the marine oil content increases in the mixtures.

On the other hand, the opposite occurs in the N, NO, and S class, as the relative abundance in these class decreases when the marine oil content in the mixtures increases. Regarding the O class, it can be inferred that it is not a good parameter to characterize the mixtures, as there is no standard behavior in the relative abundance when the content of one of the end members is increased.

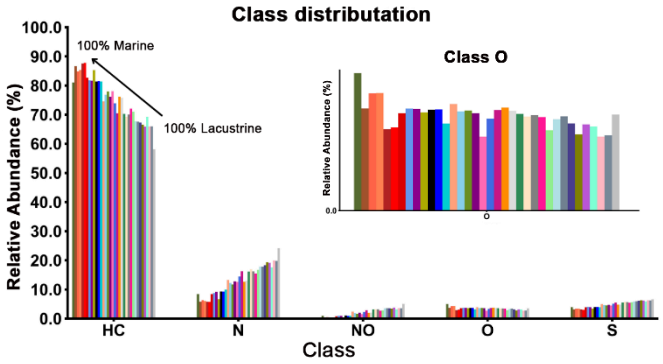

Figure 1. Relative abundance of determinate class in oil mixtures. The endmembers, from left to right, are respectively 100% marine and 100% lacustrine. With O class highlighted.

The results are based on the classification of kerogens that generate oils according to specific organic matter [3]. Thus, Type I kerogen is mainly derived from algal material deposited in lacustrine origin. This type of kerogen predominantly produces paraffinic oils, characterized by a high initial H/C ratio and a low initial atomic O/C ratio. On the other hand, Type II kerogen is mainly derived from organic matter originating from higher plants (leaf cuticles, spores, and pollen) deposited under reducing conditions in marine origin. This type of kerogen predominantly produces naphthenic oils, characterized by a moderately high H/C atomic ratio and a moderate O/C ratio in its initial state.

It is observed that samples of marine origin exhibit a higher relative abundance of the HC class, while the opposite happens to lacustrine origin, since APPI source results in the ionization of more aromatic compounds. This means that this source does not effectively access more saturated compounds and therefore the H/C ratio cannot be evaluated by this source. It is observed that through the ternary diagram, in Figure 2, using the three most discriminant classes of environments, HC, N, and S, it is possible to satisfactorily describe the mixtures of analyzed samples and their end members. This enables a better differentiation and separation of these samples based on the proportions of the three classes.

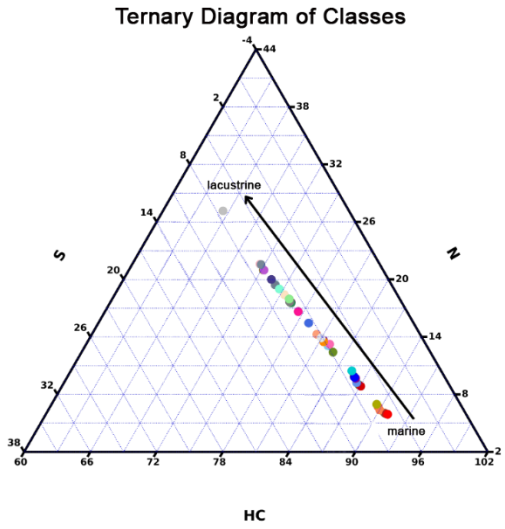

Figure 2. Ternary diagram with the most abundant classes (S, N, and HC) when analyzing samples via FT-ICR MS. Samples with a higher content of marine oil are predominantly located in the lower part, while those with a higher content of lacustrine oil are located in the upper part.

Conclusions

With the analysis of the 36 samples and data processing, it was possible to characterize the mixtures of crude oils highlighting their main characteristics, and assigning classes in a way samples were directed towards corresponded endmembers. In this sense, the study demonstrated significant potential in characterizing oil mixtures from two different origins.

Acknowledgements

The authors thank CNPq (Brazilian research council) for fellowships, Petrobras S/A and LaCEM – UFG.

References

[1] Cavalcante, J. et.al. 2018. Correlações Geoquímicas entre Amostras de Petróleo da Bacia Potiguar e Definição de suas Possíveis Rochas Geradoras. Quim. Nova, 41, 1.

[2] Rocha, Y. et.al. 2018. Geochemical Characterization of Lacustrine and Marine Oils from Off-Shore Brazilian Sedimentary Basins Using Negative-Ion Electrospray Fourier Transform Ion Cyclotron Resonance Mass Spectrometry. Organic Geochemistry, 124, 29-45.

[3] Tissot, B., Durand, B., Espitalie, J. and Combaz, A. 1974. Influence of Nature and Diagenesis of Organic Matter in Formation of Petroleum. AAPG Bulletin, 58, 499-506.

POTENTIAL OF THE SOURCE ROCKS OF THE DEEP-WATER POTIGUAR BASIN: A NEW EXPLORATION FRONTIER IN EQUATORIAL BRAZIL

NARELLE MAIA DE ALMEIDA[a*] / **ANA CLARA BRAGA DE SOUZA**[b*] / **ALINA DE OLIVEIRA CUNHA**[a]

[a] **FEDERAL UNIVERSITY OF CEARÁ (UFC),** [b] **FEDERAL UNIVERSITY OF MARANHÃO (UFMA)**

narelle@ufc.br; acb.souza@ufma.br

Introduction

Source rocks are essential elements for the development of a petroleum system [1]. These rocks have organic matter in adequate quantity and quality and are able to produce oil and/or gas when subjected to a process of thermal evolution [2]. Geochemical studies are valuable in comprehending the conditions involved in hydrocarbon generation, expulsion, and migration. They also facilitate a more accurate assessment of the hydrocarbon habitat, thereby reducing exploration risks [3].

Discoveries of hydrocarbons on the African Equatorial Margin have drawn the attention of the oil industry to transform margins. The giant Jubilee field and the TEN fields, located offshore Ghana, have a considerable production of more than 100,000 barrels of oil equivalent per day (boe /d) [4, 5].

As well as in the African Equatorial Margin, there were also important more recent discoveries in the extreme west of the South American Equatorial Margin. In Guianas and Suriname, several discoveries were disclosed. For example, on the Stabroek Block including Payara, Liza Deep (2017), and Maka and Sapakara fields (2020) [6]. In the Brazilian Equatorial Margin (MEB), we had some discoveries in the deep-water regions: The Pecém well drilled in Ceará Basin (2012) and the Pitu well (2013) in Potiguar Basin [7].

The Brazilian Equatorial Margin is considered a new exploratory frontier for the oil industry [8, 9, 10]. However, due to the scarcity of geochemical studies in the Potiguar Basin, it is not known about the real petroleum potential of the source rocks of the deep water of this basin, nor the degree of maturation of the organic matter.

Therefore, this work aims to characterize the source rocks of the deep-water Potiguar Basin, concerning the type, quantity, quality, and degree of the thermal evolution of the organic matter, and, for such purposes, organic geochemical methods were used.

Material and Methods

The Brazilian Agency for Petroleum, Natural Gas, and Biofuels (ANP) provided the geochemical dataset from five exploratory wells of the deep-water Potiguar Basin (Figure 1). The dataset includes the analysis of total organic carbon (TOC) and Rock-Eval pyrolysis indexes (free hydrocarbons–S1, hydrocarbon generative potential–S2, hydrogen index–HI, oxygen index–OI, the temperature at the maximum of the S2 peak–Tmax).

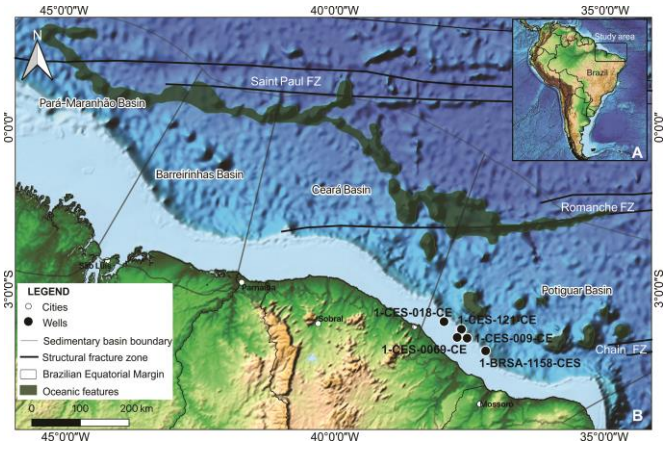

Figure 1. A) Location of the Brazilian Equatorial Margin in South America. B) Location of the five wells in the Potiguar Basin.

Results and Discussion

TOC % values for the Potiguar Basin rocks are ranging from 0.27 to 9.53 (Figure 2). The TOC% of the rift tectonic phase ranges from good to excellent, with values greater than 1% and less than 5%. In the post-rift phase, the samples can be classified as excellent hydrocarbon

generators and the drift phase presents a poor to intermediate potential with some samples reaching from good to excellent, above 3%.

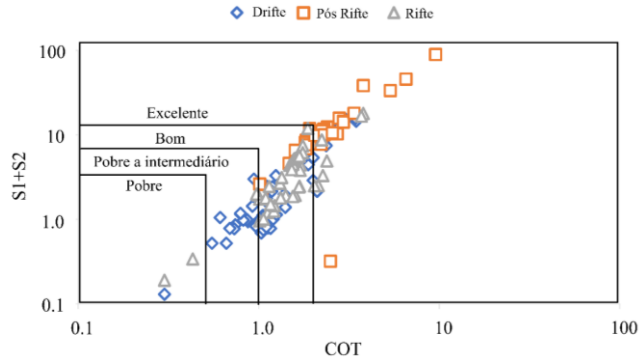

Figure 2. TOC % versus S1+S2 showing the potential of a generation of source rocks of deep-water Potiguar Basin.

Figure 3 presents the type of kerogen and the thermal maturation. The rift phase samples concentrated predominantly in the type II and III zone (generation of oil and gas). The post-rift phase samples are concentrated in the type II zone, being prone to oil. And the data corresponding to the drift phase also are located in the types II, II, and III zones.

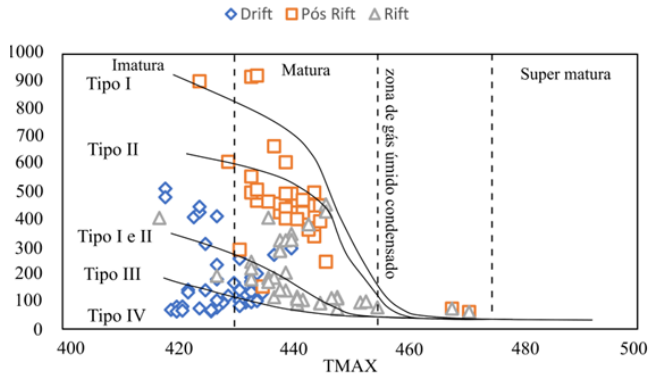

Figure 3. The relation between the HI and the Tmax values shows the type and the thermal maturity of the organic matter.

For thermal maturation (Figure 3), we can affirm that the rift and post-rift phases samples are considered mature, and the drift phase is immature, having a maximum temperature below that proposed by Peters (1986) [11, 12]. The Potiguar Basin, compared to the neighboring Ceará Basin, also demonstrates significant potential for hydrocarbon generation associated with rift and post-rift sequences in the deep-water domain. [7, 9, 13].

Conclusions

This study evaluated the potential of source rocks from the deep-water Potiguar Basin, characterizing them in terms of total organic carbon content, type of kerogen, maturity of organic matter, and tectonic phase. The results show that the rift and post-rift phases present good to excellent generation potential and mature within the oil window.

Acknowledgments

The authors thank ANP (Brazilian Agency for Petroleum, Natural Gas, and Biofuels), Schlumberger, and PPGG – UFC.

References

[1] Magoon L. B.; Dow, W. G. (1994). The petroleum system – From source to trap: AAPG Memoir 60.
[2] Hunt, J. M. (1973). Organic geochemistry of the marine environment. Advances in organic geochemistry, 593-605.
[3] Welte, D. H., & Tissot, P. (1984). Petroleum formation and occurrence. Springer-Verlag.
[4] Dailly, P., Henderson, T., Kanschat, K., Lowry, P., & Sills, S. (2017). The jubilee field, Ghana: Opening the late Cretaceous play in the West African transform margin.
[5] Tullow Oil, P. L. C. (2014). Tullow Oil PLC 2013 Annual Report & Accounts. London: Tullow Oil.
[6] Cedeño, A., Ohm, S., Escalona, A., Narain, E., de Jager, J. (2021). Source rocks in the Guyana Basin: Insights from the geochemical investigation of 15 heavy oils from onshore Suriname.
[7] ANP, (2018). BACIA POTIGUAR. 15a Rodada de Licitação da Agência Nacional do Petróleo, Gás Natural e Biocombustíveis. Superintendência de Definição de Blocos.
[8] Maia de Almeida, N; Alves, TM; Nepomuceno Filho, F.; Sá Freire, GM; Souza, ACB; Normando, MN; Oliveira, KML; Barbosa, THS. (2020a). Tectono-sedimentary evolution and petroleum systems of Mundaú Sub-Basin: a new deep-water exploration frontier in equatorial Brazil. AAPG Bulletin.
[9] Maia de Almeida, N., Alves, T.M., Nepomuceno Filho, F., Freire, G.S.S., Souza, A.C.B., Leopoldino Oliveira, K.M., Normando, M.N., Barbosa, T.H.S., (2020b). A tridimensional (3D) structural model for an oil-producing basin of the Brazilian Equatorial margin. Mar. Petrol. Geol.
[10] Leopoldino Oliveira, K.M., Bedle, H., Branco, R.M.G.C., de Souza, A.C.B., Nepomuceno Filho, F., Normando, M.N., de Almeida, N.M., da Silva Barbosa, T.H., (2020). Seismic stratigraphic patterns and characterization of deepwater reservoirs of the Mundaú sub-basin, Brazilian Equatorial Margin. Mar. Petrol. Geol.
[11] Peters, K. E. (1986). Guidelines for evaluating petroleum source rock using programmed pyrolysis. AAPG bulletin.
[12] Espitalié, J., Laporte, J. L., Madec, M., Marquis, F., Leplat, P., Paulet, J., & Boutefeu, A. (1977). Rapid method for source rock characterization, and determination of their petroleum potential and degree of evolution. Rev. Inst. Fr. Pet.
[13] Souza, A. C. B., do Nascimento Jr, D. R., Nepomuceno Filho, F., Batezelli, A., dos Santos, F. H., Oliveira, K. M. L., & de Almeida, N. M. (2021). Sequence stratigraphy and organic geochemistry: An integrated approach to understand the anoxic events and paleoenvironmental evolution of the Ceará basin, Brazilian Equatorial margin. Mar. Petrol. Geol.

EXPLORING THE PERFORMANCE OF APPI (+) AND ESI (−) ION SOURCES IN FT-ICR MS ANALYSIS FOR DISCRIMINATING LACUSTRINE AND MARINE OILS

LIDYA C SILVA[a*], JUSSARA V ROQUE[a*], JOÃO VICTOR A OLIVEIRA[a], DANIELLE M M FRANCO[a], TAYNARA R COVAS[a], GESIANE S LIMA [a], BONIEK G VAZ [a]

[a]**LABORATORY OF CHROMATOGRAPHY AND MASS SPECTROMETRY, INSTITUTE OF CHEMISTRY, FEDERAL UNIVERSITY OF GOIÁS, GOIÂNIA, GO, BRAZIL**

lidya_cardozo@ufg.br

Introduction

The paleodepositional environment understanding is crucial for the oil industry as it directly affects the origin and quality of oil reservoirs (Webb et al., 2015). Geochemical analysis, particularly using mass spectrometry (MS), provides valuable insights into the composition of oil samples and their associated source rocks (Cornford, 2005). Advancements in MS technology, such as the development of the Fourier transform ion cyclotron resonance (FT-ICR) mass analyzer, combined with the electrospray ionization (ESI) and atmospheric pressure photoionization (APPI), have expanded the capabilities of geochemical characterizations (Cooper et al., 2022).

This study aimed to explore the use of different ionization sources (ESI and APPI) in FTI-CR MS analyses of lacustrine and marine oils. The samples were subjected to multivariate analysis to assess the performance of the sources in distinguishing between the samples and to examine differences among oils from various geological basins. Additionally, the stability of asphaltenes in each oil was investigated to explore potential correlations with the depositional environment.

Experimental

Ten oils from five different Brazilian basins were used in this study (Table 1). The samples were submitted to chemical characterization through FT-ICR MS, using ESI (−) and APPI (+). In addition, the oil's instability, concerning their tendencies to precipitate asphaltenes was evaluated by the optical analyzer TurbiscanLab®.

The molecular formula assignments were performed using Composer 1.0.6 software. These data were imported to Matlab R2020a software (Mathworks Inc) to perform data analysis. Then, an exploratory data analysis was carried out using principal component analysis (PCA) with the aim of visualizing difference between lacustrine and marine oils. samples in multidimensional space. PCA was carried out on the normalized and autoscaled data set.

Table 1. Description of the oil samples from the Brazilian basins.

Basin	Oil	Class	Maturation	Biodegradation
A	1	Marine	High	No
	2	Lacustrine	Moderate	
	3			
B	4	Marine		
	5			
C	6	Marine		
	7	Lacustrine		
	8			
D	9	Marine		
E	10	Lacustrine		

Results and Discussion

Chemometric analysis of data obtained by ESI (−) e APPI (+) reveals the separation of lacustrine and marine oils from the Brazilian basins. Distinction among the lacustrine and marine samples was better accessed when using APPI (+) for the oils analysis. Figure 1A depicts the optimal separation using PCA for the marine samples with minimal dispersion on both, PC1 and PC2, scores, which accounted for 57,48% of the variance. The lacustrine samples were similarly discriminated, except for sample 10. However, this result is highly positive, as sample 10 comes from an onshore field (Base E). Thus, APPI (+) has proven effectivity not only in discriminating lacustrine from marine samples but also in discriminating samples from onshore fields from the offshore ones.

This can be attributed to a greater number of classes accessed by APPI (+). Additionally, there is a noticeable better differentiation between lacustrine and marine samples in all the accessed classes (Figure 1B). As seen, marine samples exhibited lower relative abundances of compounds from the N and S classes, while showing

higher abundances of hydrocarbons. Furthermore, lacustrine samples from offshore fields showed differentiation from the terrestrial lacustrine sample due to lower levels of oxygenated compounds, while displaying higher levels of sulfur compounds.

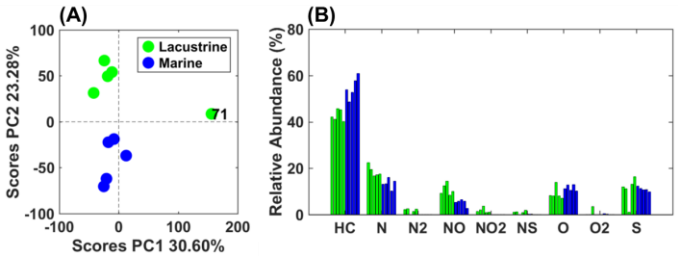

Figure 1. (A) PCA scores and **(B)** class distribution plots for the lacustrine and marine samples analyzed by APPI (+) FT-ICR MS.

Further insights into the separation of samples based on the different basins were obtained through PCA analyses conducted separately for lacustrine and marine samples. This approach allowed for a more detailed understanding of the distinct patterns and variations within each basin. Regarding the lacustrine samples, better results were also obtained when APPI (+) was used. Figure 2A shows the optimal separation of lacustrine samples from different basins. The better clustering of samples 3 and 2 is consistent with class distribution data (Figure 2B), which reveal similarities in the abundances (%) of compounds detected in these two oils. Finally, the terrestrial lacustrine sample was differentiated due to lower abundances of compounds from the N and S classes, contrasting with higher abundances of oxygenated compounds. Similarly, the differentiation of marine oils from different basins was more effective when using APPI.

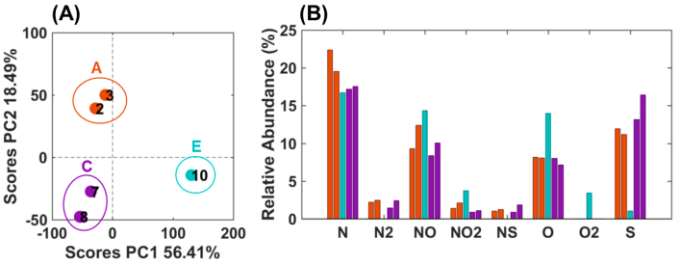

Figure 2. (A) PCA scores and **(B)** class distribution plots for the lacustrine samples analyzed by APPI (+) FT-ICR MS.

Finally, correlations between the instability of the asphaltenes from the oils were studied. For this analysis, negative ion-ESI showed a better performance, as 47.15% of its variables presented correlations with the instability data higher then 0.8. In contrast, only 19.45 % of the variables detected by APPI (+) showed correlations with the instability data.

Conclusions

The chemometric results indicate that APPI (+) is the preferred ion source for distinguishing lacustrine from marine oils and separating samples according to their basins. However, ESI (-) is more suitable for studying operational risks due to its ability to detect a larger number of variables correlated with oil instability. The choice between APPI (+) and ESI (-) depends on the specific objectives of the study, with APPI (+) providing better differentiation between oils according to their source rock, and ESI (-) offering a more comprehensive understanding of variables related to oil instability and associated operational risks.

Acknowledgements

The authors thank CAPES and Petrobras S/A for financial support.

References

Cooper, W. T., Chanton, J. C., D'Andrilli, J., Hodgkins, S. B., Podgorski, D. C., Stenson, A. C., Tfaily, M. M., & Wilson, R. M. (2022). A History of Molecular Level Analysis of Natural Organic Matter by FTICR Mass Spectrometry and The Paradigm Shift in Organic Geochemistry. *Mass Spectrometry Reviews*, *41*(2), 215–239. https://doi.org/10.1002/MAS.21663

Cornford, C. (2005). PETROLEUM GEOLOGY | The Petroleum System. *Encyclopedia of Geology*, 268–294. https://doi.org/10.1016/B0-12-369396-9/00247-1

Webb, N. D., Seyler, B., & Grube, J. P. (2015). Geologic reservoir characterization of Carboniferous fluvio-tidal deposits of the Illinois Basin, USA. *Developments in Sedimentology*, *68*, 395–443. https://doi.org/10.1016/B978-0-444-63529-7.00013-4

Exploring Polar Compounds Variations in Crude Oils from Pre-Salt and Post-Salt Reservoirs through ESI FT-ICR MS.

Gesiane da Silva Lima[a], Deborah V. A. de Aguiar[a], Rodolfo R. da Silva[a], Iris Medeiros Júnior[b], Alexandre de O. Gomes[b], Luiz A. N. Mendes[b], Boniek G. Vaz[a]

[a] Chemistry Institute, Federal University of Goiás, Goiania, Gois, 74690-900, Brazil

[b] CENPES, PETROBRAS, Rio de Janeiro, RJ, 21941-915, Brazil.

E-mail: lima.gesiane12@gmail.com

Introduction

The chemical composition and properties of crude oils depend on their compounds and the environmental and/or reservoir conditions where they are found (Nascimento et al., 2018). Nitrogen, oxygen, and sulfur (NOS) compounds comprise a minor fraction of crude oil and its polar components. However, these compounds can have significant impacts, leading to issues such as corrosion, emulsion formation, deposition on processing units, catalyst poisoning, and pore blockage, all of which pose critical challenges for the petroleum industry (Häger et al., 2005; Coutinho et al., 2018). Moreover, heteroatomic compounds serve as valuable geochemical indicators. They can be used to differentiate sources and track compositional changes during biodegradation, migration, and thermal maturity evolution (Smith et al., 2007). These compounds offer insights into the origin and transformation of crude oil, providing important information for understanding its geochemical behavior and predicting its behavior in various environments.

Over the last few decades, ultra-high-resolution mass spectrometry (UHRMS) has been a powerful technique for analyzing complex mixtures. Fourier Transform Ion Cyclotron Resonance Mass Spectrometry (FT-ICR MS) combined with electrospray ionization (ESI) has also provided extensive molecular-level information relating to polar compounds from crude oil samples (Zhao et al., 2019). The resolution and accuracy of FT-ICR MS are exceptional for analyzing complex heteroatom compounds. In this regard, this study aims to elucidate the comprehensive individual molecular characterization of five Brazilian pre-salt crude oils by comparing their chemical composition with four post-salt crude oils analyzed by ESI (-) FT-ICR MS. Based on the ESI (-) FT-ICR MS data. This study also aims to understand better the differences in pre- and post-salt crude oil composition in terms of oxygen- and nitrogen-containing compounds.

Experimental

Sample preparation

Nine crude oils (five from pre-salt and four from post-salt reservoirs) were used in this study. For sample preparation, 2 mg of crude oil was dissolved in toluene, then diluted in toluene: methanol (1:1, *v/v*) and doped with ammonium hydroxide.

ESI (-) FT-ICR MS analysis

The MS analysis was performed using an FT-ICR MS 7 T SolariX 2xR (Bruker Daltonics). The general ESI (-) conditions were as follows: spray voltage of 3.8 kV; tube lens voltage of −150 V. The mass range was set from *m/z* 100 to 2000, with 200 micro scans. The calibrated mass spectra were processed using Composer software (version 1.5.3, Sierra Analytics).

Results and Discussion

Polar compounds were classified by the type and number of heteroatoms: N, N2, NO, NO2, O, and O2. The N class was the most prominent for all crude oils analyzed. However, the relative abundance for the N class was more intense for the pre-salt crude oils (**Fig. 1**). Subtle differences can be noted between the pre-and post-salt crude oil samples. Similar abundances were found for the N, N2, and NO classes for samples **01, 02, 03,** and **04** (pre-salt crude oil samples). Furthermore, the relative abundances of these classes, combined with information on the relative abundances of the O and O2 classes, were essential to differentiate post-salts from pre-salt crude oil samples. The O2 classes were mainly identified in crude oils **05** and **09** (both characterized as heavy oil). The high abundance of the O2 class detected mainly in post-salt crude oil **09** may suggest a biodegradation process, as the oxygenated class distribution for the post-salt crude oils indicates that these oils demonstrate different biodegradation levels. There was no substantial difference in the distribution of nitrogen compounds in pre- and post-salt crude oil samples, suggesting that this criterion is not the most critical factor in distinguishing these reservoirs.

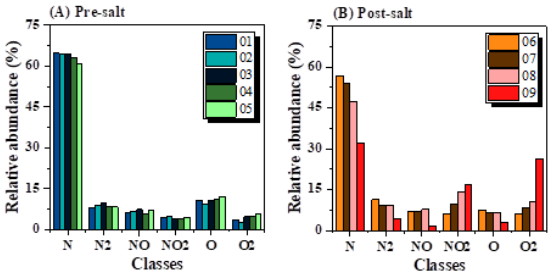

Fig. 1. Relative abundances of heteroatomic compound classes for pre- and post-salt crude oil samples analyzed by ESI (-) FT-ICR MS.

Differences were observed in the relative abundance of the NO class among pre- and post-salt crude oils: for NO-containing compounds, the distributions were similar for pre-salt crude oil samples, and the crude oil samples **06, 07,** and **08** from post-salt reservoirs also presented a similar distribution; however, the oil sample **09** showed a decrease in its intensity for NO-containing compounds. The decrease in the relative abundance of the NO-containing compounds and an increase in NO2 relative abundance may suggest that this crude oil is biodegraded. The O2 and O-containing compounds analysis have been widely applied to investigate the biodegradation level of crude oil samples from different reservoirs(Field and Basin, 2019). **Fig. 1** also illustrates an increase in O2 class and a decrease in the O class for post-salt crude oils, which was not observed for pre-salt crude oils. The O classes are more affected by biodegradation processes. Biodegradation is the primary process that leads to high concentrations of carboxylic acid compounds in crude oils. The ternary diagram (**Fig. 2A**) predicted acidity levels between pre- and post-salt crude oil samples. The crude oil **01** (pre-salt) showed the lowest acidity expressed by TAN, and compositionally, it is constituted by a high content of linear acids (DBE 1), O2 class. On the other hand, the increase in naphthenic content (DBE 2-4) pointed to high acidity oils as observed in crude oil **09** (post-salt). Besides, it was possible to group the crude oils concerning their reservoirs by employing O2-containing compounds with DBEs 1, 3, and 5 (**Fig. 2B**).

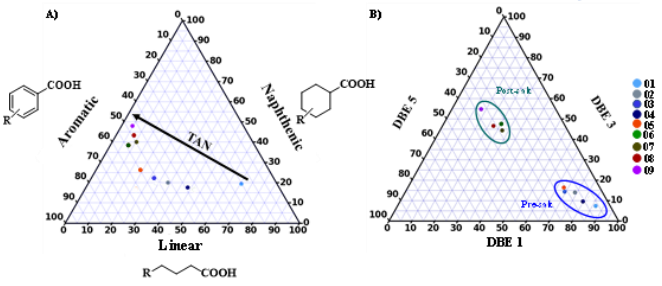

Fig. 2. (A) Ternary diagram of relative ion abundances of the linear, naphthenic, and aromatic O2 compounds and (B) ternary diagram of relative abundance of O2 compounds with DBE 1, 3, and 5 for pre- and post-salt crude oils detected by ESI (-) FT-ICR MS.

Fatty acids and isoprenoid acids (DBE 1) were identified predominantly in pre-salt crude oil samples. Compounds with DBE 1 and carbon numbers of 16 and 18 have been commonly described in non-biodegraded oils.

Conclusions

Negative-ion ESI FT-ICR MS analysis was conducted to understand better the chemical composition of polar compounds in crude oils from pre- and post-salt reservoirs. Based on their heteroatomic distribution, N-containing compounds are the major class in all crude oil samples. Subtle differences were observed between the crude oil samples, allowing the differentiating of pre- and post-salt reservoirs. ESI (-) FT-ICR MS analysis showed that the N2- and NO-containing compounds are the most susceptible to biodegradation processes.

Acknowledgments

The authors acknowledge financial support from Petróleo Brasileiro SA-Petrobras, CNPQ, and CAPES.

References

Coutinho, D.M., França, D., Vanini, G., André, L., Mendes, N., Gomes, A.O., Pereira, V.B., Ávila, B.M.F., Azevedo, D.A., 2018. Rapid hydrocarbon group-type semi-quanti fi cation in crude oils by comprehensive two-dimensional gas chromatography. Fuel 220, 379–388.

Field, M., Basin, S., 2019. Geochemical assessment of oils from the Mero Field, Santos Basin, Brazil. Organic Geochemistry. doi:10.1016/j.orggeochem.2019.01.011

Häger, M., Ese, M., Sjöblom, J., 2005. Emulsion Inversion in an Oil-Surfactant-Water System Based on Model Naphthenic Acids under Alkaline Conditions. Journal of Dispersion Science and Technology 26, 673–682.

Nascimento, M.H.C., Oliveira, B.P., Rainha, K.P., Castro, E.V.R., Silva, S.R.C., Filgueiras, P.R., 2018. Determination of fl ash point and Reid vapor pressure in petroleum from HTGC and DHA associated with chemometrics. Fuel 234, 643–649.

Smith, D.F., Schaub, T.M., Rahimi, P., Teclemariam, A., Rodgers, R.P., Marshall, A.G., 2007. Self-Association of Organic Acids in Petroleum and Canadian Bitumen Characterized by Low- and High-Resolution Mass Spectrometry. Energy & Fuels 21, 1309–1316.

Zhao, S., Pu, W., Varfolomeev, M.A., Yuan, C., Qin, S., Wang, L., Emelianov, D.A., Khachatrian, A.A., 2019. Thermal behavior and kinetics of heavy crude oil during combustion by high pressure differential scanning calorimetry and accelerating rate calorimetry. Journal of Petroleum Science and Engineering 181, 106225.

XVI LATIN AMERICAN CONGRESS ON ORGANIC GEOCHEMISTRY
9 - 11 AUGUST, 2023
ARACAJU, SERGIPE, BRAZIL

THE WOODFORD SHALE AND DISTINCTIVE OILS IN THE CHEROKEE PLATFORM, OKLAHOMA.

DAMIÁN VILLALBA[a] / R. PAUL PHILP[b]

[a]GEOLAB SUR S.A. / [b]UNIVERSITY OF OKLAHOMA

damian.villalba@geolabsur.com

Introduction

The Arkoma Basin and the Cherokee Platform are famous thanks to the highly prolific late Devonian – early Mississippian source rock, the Woodford Shale. It has provided conventional hydrocarbon production for more than a century and it has become distinguished as an unconventional resource. The classic organic rich-marine platform has also recently shown highly vertical variability based on lithology, sequence stratigraphy, and geochemical analyses associated with sea level fluctuations. Moreover, besides the superlative Woodford sourcing, the oils of the area are known to show certain extra input, suspected hydrocarbon mixtures (Li et al., 2017).

Experimental

For this study, twelve core samples were collected from Upper to Middle Woodford in the Ray 1-13 well (4585-4729 ft). They were screened to determine total organic carbon content (TOC), thermal maturity, and kerogen quality. Crushed rocks were extracted, fractionated, and subjected to gas chromatography (GC), gas chromatography-mass spectrometry (GCMS) and gas chromatography-mass spectrometry-mass spectrometry (GCMSMS) analyses. In addition, fifteen oil samples were collected from the area; they were deasphaltened and then fractionated into saturates, aromatics and polar components. The saturate and aromatics were analyzed by GC, GCMS and GCMSMS.

Results and Discussion

Core Extracts: The core samples showed a rich organic content, with a maximum TOC of 13% and an average of 9%, with hydrogen index (HI) values from 473 to 563 mg HC/g TOC and very low oxygen index (OI < 10 mg CO_2/g TOC) plotting between Type I and Type II that describes an oil prone marine kerogen. The thermal maturity was evaluated following different methods from pyrolysis and various biomarkers that cover the immature to early mature stage, and also, the vitrinite reflectance measured 0.59 VRo% at 4701 ft.

The extracts GC data points out marine plankton input and redox variability, from suboxic to reducing environment. The steranes present a high abundance of diasteranes and the presence of C_{30} st., meaning a marine siliciclastic depositional environment. The tricyclic terpanes also suggest marine and shale lithology, while the homohopanes indicate suboxic and H_{29}/H_{30} also to non-carbonate. Gammacerane is present, indicating high salinity. DBT/Phen and Pr/Ph also show marine-shale with tendency to anoxic and sulfate-rich waters. The presence of carotenoids (paleorenieratane, isorenieratane, and renierapurpurane) are indicators for photic zone of anoxia (PZA) throughout the water column (Connock et al., 2018). The total aryl isoprenoids is indicating a PZA in the Upper Woodford (Fig. 1).

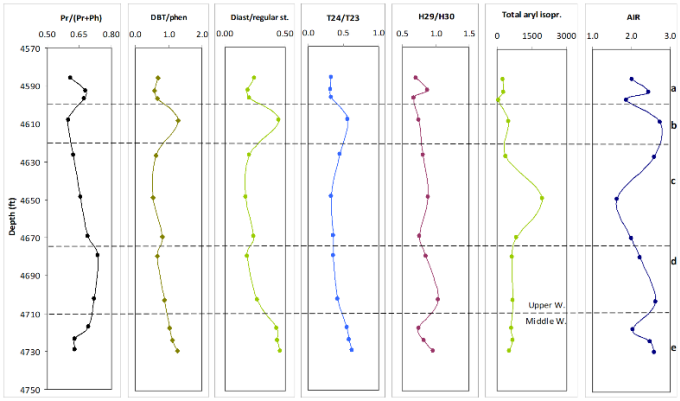

Figure 1. Source rock depth log based on GC and GCMS data showing the vertical variations.

Ray 1-13 Oil: The oil is produced from within the Woodford section. The GC chromatogram showed it was depleted in higher carbon number *n*-alkanes, indicative of biodegradation process but with a peculiar abundance of C_4 to C_9 range. The Pr-Ph ratio is indicative of slight to moderate biodegradation and so, this preserved light end could be indicative of a more mature fluid. The C_{29}ααS/αα (R+S) and the C_{29}ββ/(ββ+αα) ratios indicate a higher level

of maturity than the core extracts. Phenanthrene and MPI-1 estimate a vitrinite reflectance equivalent (VRE) of 1.04%, even higher than the estimated from steranes and terpanes. Also adamantanes projected a VRE of 1.33%. Therefore, the thermal maturity the oil is reflecting a dual stage, on one side, the early window and on the other, a main to late oil window, suggesting recharging episodes with a lighter fluid, possibly a condensate type.

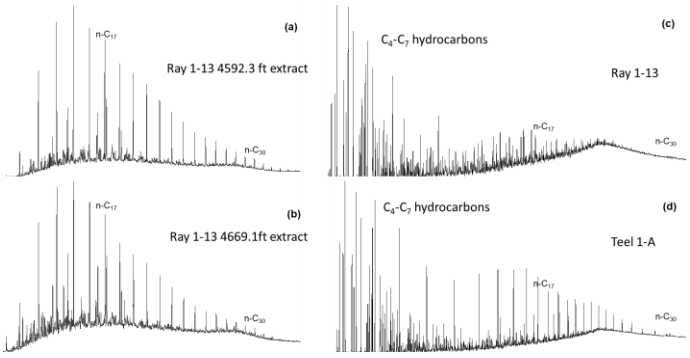

Figure 2. GC of an Upper Woodford core extract (a) and Middle Woodford (b). WOGC of the Ray1-13 oil (c) and Teel 1-A oil (d).

In terms of the depositional environment for the oil, the biomarkers showed consistency with the core extracts, where the tricyclic terpanes T22/T21 vs T24/T23 and the hopanes H31R/H30 vs T26/T25 ratios indicate, marine shale source rock, away from the lacustrine and carbonate influences. The C_{27}, C_{28}, and C_{29} steranes, plus the C_{30} presence, is also indicative of a siliciclastic marine platform. Finally, the carotenoids paleorenieratane and isorenieratane are present too, and even in higher abundance than in the extracts, in difference to the rock.

Pottawatomie oils: Fourteen additional oils from Pottawatomie County were analyzed and should be noted that all of these oils had a very similar biomarker distribution, indicating source related and derived from the Woodford Shale. WOGC showed the entire carbon range number from C_2 to C_{34}, with bimodal distributions resulting from mixing of different oil types. Two more oils showed indications of biodegradation as well as Ray 1-13. Additionally, the oils from two horizontal wells showed a more even distribution between the light hydrocarbons (C_4-C_9) and the medium-weight hydrocarbon compounds (C_{13}-C_{19}), probably as a result of a smaller contribution from the commingled condensate. The C_{40} carotenoids were present in all samples in varying abundance, too. Maturity analysis was based on the same parameters, steranes and terpanes indicate an early thermal stage whereas the MPI-1 and MAI indicate a maturity level in the main to late oil window. These data indicate mixing of a partially biodegraded oil and a more mature condensate-type, except for the horizontal wells.

Selected oil samples were analyzed by GCIRMS showing similarity of the C isotope values for all the light hydrocarbons, indicating a common source and similar level of maturity for the light condensate samples in the oils.

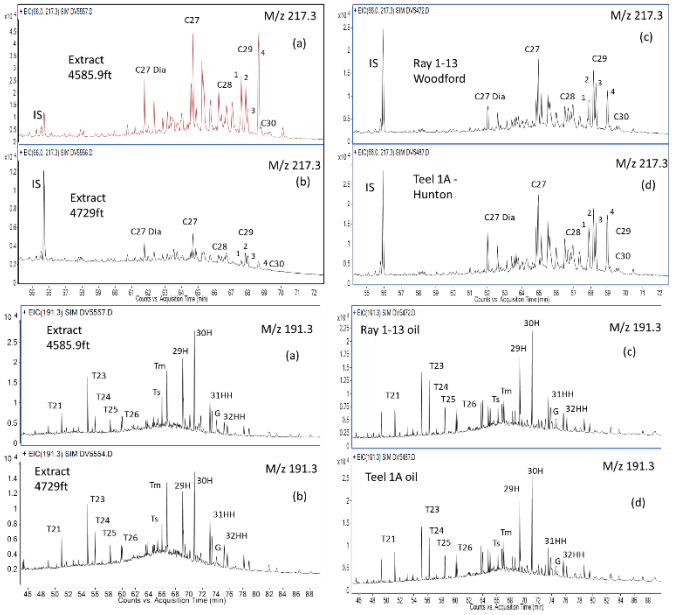

Figure 3 (M/z 217.3 and 191.3). Sterane and terpane distributions determined for the rock extracts at 4585.9 ft (a), 4729 ft (b), Ray 1-13 oil (c), Teel 1A oil (d).

Conclusions

The core showed to be a clastic marine source rock with redox fluctuations along the column, in the early oil window stage. In detail, the biomarkers expressed that certain interval of the Upper Woodford was also euxinic-anoxic with persistent PZA conditions. The Ray 1-13 oil was slight to moderately biodegraded and unusually enriched in light components; the steranes and terpanes specify early maturity while the aromatics and diamondoids, mid to late maturity meaning commingled oil from a condensate. The oil matches the rock, but in a slightly higher maturity. The oil to oil correlation shows strong similarities along WOGC and biomarkers. Almost all of the oils are believed to be mixed with a condensate. GCIRMS showed strong correlation for the light components, therefore, similar source.

Acknowledgements

The authors thank GeoLab Sur S.A. for pyrolysis and dedication time; School of Geosciences, OU for fellowships; West Star Oil for providing the samples.

References

Connock G. T.; Nguyen T. X.; Philp, R. P., 2018. The development and extent of photic-zone euxinia concomitant with Woodford Shale deposition. AAPG Bulletin **102**, 959–986.

Li, L.; R.P. Philp; Nguyen, T. X., 2017. Origin and history of the oils in the Lawton oil field, southwestern Oklahoma. AAPG Bulletin **101**, 205-232.

Unveiling the hydrocarbon generation capacity of Pelotas Basin: an integrated geochemical approach

MONIQUE A.M. RIZZI [a*], TIAGO J. GIRELLI. [a], MATHEUS F. DA CRUZ [a], HENRIQUE SERRAT [a], CLAUDIA D. TEIXEIRA [a], FARID CHEMALE JR. [a]

[a] **PROGRAMA DE PÓS-GRADUAÇÃO EM GEOLOGIA, UNIVERSIDADE DO VALE DO RIO DOS SINOS, SÃO LEOPOLDO, RIO GRANDE DO SUL, BRAZIL**

*Correspondence: moniquemr@edu.unisinos.br or mmonique.rizzi@gmail.com

Introduction

Organic geochemical characterization and evaluation of hydrocarbon generation potential are fundamental aspects of understanding the exploratory frontier basins. In the Pelotas Basin, Southernmost Brazil, a detailed analysis has been conducted with the objective of understanding the presence and viability of potential reservoirs (Figure 1), using the Total Organic Carbon (TOC) content as a primary indicator. Additionally, other parameters such as free and bound hydrocarbon indices (S1 and S2), Tmax, types of kerogen, and inorganic geochemical data are considered. Thus, the present work aims to provide a comprehensive review of the hydrocarbon generation potential, contributing to a better understanding of the geology and petroleum resources of the Pelotas Basin.

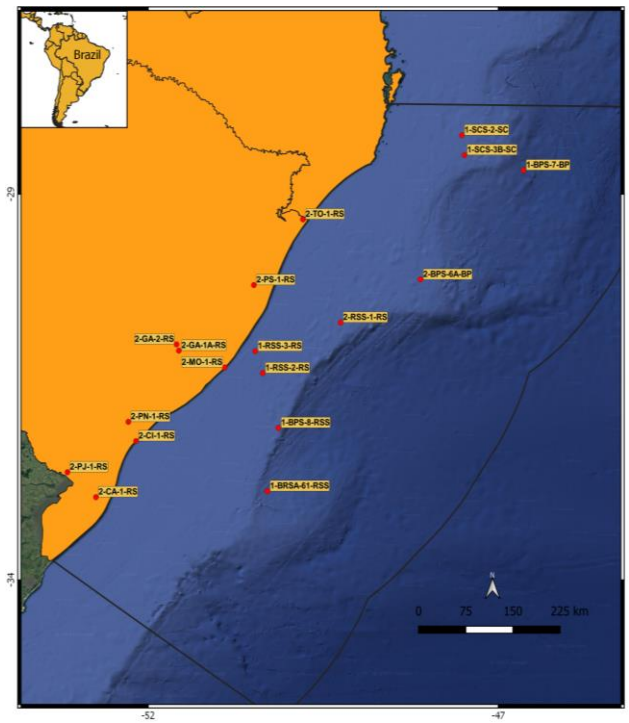

Figure 1. Location of wells analyzed in the Pelotas Basin.

Experimental

To perform this study, we analyzed samples from selected intervals of the wells in Figure 1. These intervals are: Miocence-Recent (0-23 Ma), Eocene-Oligocene (23-56 Ma), Paleocene (56-66 Ma), Turonian-KPg (66-89 Ma), Albian-Turonian (89-100 Ma), Aptian-Basement (100-115 Ma). Hydrocarbon generation potential was evaluated using organic analyses of TOC and Rock-Eval Pyrolysis and inorganic multi-elemental XRF (X-ray Fluorescence) and ICP-MS (Inductive Coupled Plasma Mass Spectrometry) techniques.

Results and Discussion

Regarding TOC > 1% as the minimum cutoff for reservoir potential, we selected wells with representative analyses in the Pelotas Basin as evaluation criteria. These wells are 1-SCS-3-SC, 1-BPS-7-BP, 2-BPS-6-BP, and 2-RSS-1-RS. However, it is noteworthy that while the presence of organic matter in a reservoir is a possible indicator of hydrocarbon generation, other factors must be evaluated, and for this purpose, we used a combination of inorganic geochemical proxies.

In the northernmost portion of the basin, well 1-SCS-3B-SC exhibits fair source rock potential for hydrocarbon generation [1] in the interval mapped as Turonian-KPg (from 3252 to 2670 meters), with a TOC content reaching 1.53% at the top of the interval. In consonance, S1 reaches up to 1.2 mg HC/g rock and S2 up to 3.17 mg HC/g rock, especially from 3100 to 2900 m. The Tmax shows average values of 430°C within this interval (immature window). Meanwhile, the HI varies from 62 to 252 mg HC/g rock, indicating as the main products are oil and gas, at this peak maturity. The OI and HI parameters indicate a good capacity for hydrocarbon production potential, with the PI reaching 0.337. Within the same well, there is a second interval of interest, with a TOC content of up to 1.65% in the period identified as the Older-Turonian, from 3900 to 3684 m. The Tmax is higher, until 437ºC - early oil window. However, this

interval has fewer analyses than the previous one, with less pronounced S1 and S2 values, HI values until 207 mg HC/g rock (indicating gas), and lower PI. Both intervals exhibit types II/III kerogen (oil and gas prone) and type III kerogen (gas prone), derived from terrestrial organic matter input, both within an immature thermal maturity window. No inorganic geochemical analyses were conducted for these intervals in the respective well.

In well 1-BPS-7-BP, there are two intervals of interest: one in the Paleocene period (4800 to 4500 m) and another in the KPg-Turonian (5645 m). The KPg-Turonian interval, despite having the highest LOI (Loss on Ignition) values in the well (indicating a high concentration of organic matter), does not have results for all the parameters analyzed in organic geochemistry, requiring further investigation. When examining inorganic geochemistry, two peaks of high paleoproductivity are observed, at ~5650 m and at the boundary with the Paleocene, at 4800 m. The first peak indicates a hot and arid climate, while the second peak suggests higher humidity, but both occurred under oxic conditions. Regarding the Paleocene interval, this one presents a good to excellent source rock potential, with S1 values from 3.18 to 5.28 mg HC/g rock, and S2 reaching 7.8 mg HC/g rock. The Tmax ranges from 377 to 430°C, indicating an immature to early oil window, with oil as the main product (444 to 489 mg HC/g rock of HI), and PI reaching 0.49. The identified kerogen type for this interval was type II (oil-prone), derived from marine input, with an immature maturity window for oil generation. In terms of inorganic geochemistry, there is a variation along the depth, generally indicating good paleoproductivity, high weathering indices (indicating high humidity), and anoxic conditions at the top of the interval, which is favorable for hydrocarbon generation.

In well 2-BPS-6-BP, high TOC contents are observed in the Paleocene (3000 to 3315 m), Turonian-Albian (4169 to 4170 m and ~4950 m), and Aptian (5289 m) intervals, reaching 3.7% in the Turonian interval. Despite having fewer analyses, the two deepest intervals are the most interesting for hydrocarbon generation in the well, with the Paleocene being less significant in terms of production capacity (PI = 0.05 to 0.2). The identified kerogen types are as follows: 1) type II/III for the Paleocene, oil/gas-prone, derived from terrestrial organic matter and immature; 2) type II for the Turonian-Albian interval, oil-prone, derived from marine organic matter, and immature to oil generation; 3) types II/III and III for the Aptian, derived from terrestrial organic matter, and immature. In terms of inorganic geochemistry, the well exhibits low paleoproductivity at the top, with the highest indices in the late Turonian-Albian interval and the Aptian. The climate is hotter and drier in the Aptian, transitioning to a colder and wetter condition as it progresses towards the Paleocene. The sedimentation rates are generally low, except for the Aptian, which also exhibits anoxic conditions. Above, the profile transitions from a suboxic to subanoxic environment towards the top.

The well 2-RSS-1-RS, located in the central sector of the basin closer to the platform edge, shows TOC values of up to 1.8% in the Paleogene, with levels > 1% at depths of 3915 m, 3702 m, and within the interval of 3405 to 3150 m. Additionally, a representative sample was obtained from the Cretaceous at a depth of 4440 m. In the Paleogene, there is a poor to fair source rock potential, with S1 < 0.5 mg HC/g rock and S2 < 2.5 to 5.53 mg HC/g rock. The Tmax values vary from 429 to 439 ºC (immature to early oil maturity window), with HI values from 105 to 359 mg HC/g rock (gas to oil as a main product at peak maturity), and low PI, reaching a value of 0.097. For this interval, kerogen types II, II-III, and III were identified, with an immature maturity window for oil generation, originating from marine and terrestrial organic matter. No inorganic geochemical proxies were analyzed for the respective well or for the same interval in a neighboring well.

Conclusions

The integration of organic and inorganic geochemical studies has allowed for a direct comprehension of the geological process evolution, from those that acted in the source areas to the evolution of the Pelotas Basin, providing a better understanding of paleoenvironments. Regarding the intervals with the highest potential for hydrocarbon generation and preservation, overall, good indices were observed for the Paleocene (wells 2-RSS-1-RS and 1-BPS-7-BP) and Cretaceous (wells 2-BPS-6-BP and 1-SCS-3-SC), along with a dominant potential for gas generation throughout the basin.

Acknowledgements

The authors thank CNPq (Brazilian National Council for Scientific and Technological Development) for fellowships (#311175/2019-8 and #408194/2021-9); ANP (Brazilian Petroleum Agency); Petrobras S/A and CNODC S/A for financial support.

References

[1] Jarrett, A. J. M.; Chen, J.; Hong, Z.; Long, I.; Pallaty, P.; Anderson, J.; McLennan, S.; Lewis, C.; Henson, P., 2018. Exploring for the Future- Source rock geochemistry of Northern Australia. Part 1: Total organic carbon (TOC) and Rock-Eval pyrolysis of samples from the South Nicholson Basin and Isa Superbasin, Queensland. Geoscience Australia, Canberra. http://dx.doi.org/10.11636/Record.2018.045

Characterization of alkene-based drilling fluids and petroleum compounds by GC×GC-TOFMS

[a]Darlly Erika Silva dos Reis*, [a]Livia Poty Manso, [a]Taís de Oliveira Reis, [a]Dayane Magalhães Coutinho, [a]Mônica Cardoso Santos, [a]Luiz Antonio Freitas Trindade, [b]Daniel Silva Dubois, [b]Joelma Pimentel Lopes , [a]Francisco Radler de Aquino Neto, [a]Celeste Yara dos Santos Siqueira, [a]Débora de Almeida Azevedo

[a]Universidade Federal do Rio de Janeiro, Instituto de Química, Ilha do Fundão, Rio de Janeiro, RJ 21941-909, Brazil

[b]Petrobras/CENPES/PDIEP/GEOQ, Cidade Universitária, Rio de Janeiro, RJ 21941-915, Brazil

*desr@iq.ufrj.br

Introduction

Drilling fluid additives have been used to perform different functions during oil well drilling, such as maintaining stability and safety conditions (Stout and Litman, 2022). If the oil/contaminant ratio is too low, properties derived from pressure-volume-temperature (PVT) evaluation, which are of great importance for understanding the flow of fluids during the production of crude oil, petrophysical analyzes, and especially the geochemical signatures in rock samples and fluids, obtained through TOC (total organic carbon), *Rock–Eval* pyrolysis and gas chromatography, can be seriously altered, making geochemical correlations between oil-source rock or oil-oil impossible (Ratnayake et al., 2018). Therefore, the motivation of this work is to identify the occurrence of contamination in oils caused by drilling mud additives, and from there, to separate the "signature" of the contaminant from the occurrence of the oil, to obtain better geochemical information of the studied samples. Its aim is to recognize the occurrence of contamination and to determine whether its extent is significant enough to change the interpretation of geochemical data.

Experimental

A pool of crude oil was analyzed using a GC-FID 6890 (Agilent Technologies Leco, Santa Clara, CA, USA) by the conventional method of whole oil analysis to verify the contamination level of the samples. Internal standards n-hexadecanes-D34 and n-tetracosane-D50 were used, helping to identify the major components of the samples. The crude oil samples were analyzed using comprehensive two-dimensional gas chromatography coupled to time-of-flight mass spectrometry system (GC×GC-TOFMS, Pegasus 4D, Leco, St. Joseph, MI, USA), using a non-polar × polar column set. Deuterated standards of different classes of hydrocarbons was used to evaluate the performance of the system. The samples were divided into contaminated and non-contaminated. Whenever possible internal standards were used for the identification step. The compounds were identified based on four characteristics: score of the National Institute of Standards and Technology (NIST version 2.0) mass spectra library, the retention times, elution order, and deuterated standards retention times.

Results and Discussion

In the evaluated samples the main component of oil-based drilling fluids observed in the GC-FID analyses are olefins compared to the sample without contamination (Figure 1A and 1B).

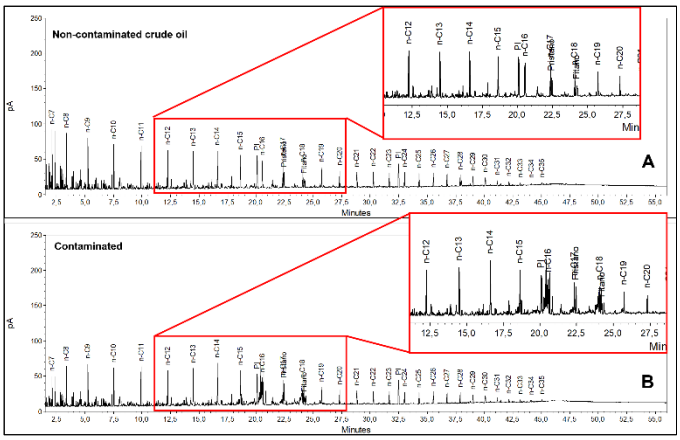

Figure 1: GC-FID whole oil chromatograms profile showing the presence of (A) Non-contaminated crude oil; (B) Contaminated crude oil, contamination between *n*-C_{12}- *n*-C_{20}.

The GC-FID showed that this mixture bears a strong chemical similarity to crude oil, these compounds elute within intervals of the same retention time (t_R) as some cycloalkanes and *iso*-alkanes, between C_{12} and C_{20} (Figure 1B). It was identified that the constituents of

drilling fluids affect the results of geochemical analyses, making it difficult to interpret oil/oil or oil/rock correlations. Therefore, to sort out the contaminants and characterize the compounds present in the samples, GC×GC-TOFMS was applied due to its greater separation power, sensitivity, and detectability. The GC×GC-TOFMS enabled greater detailing of the analytes present in the sample, through its greater selectivity of components (Figure 2). As expected, it was observed that olefins elute in a retention time in the second dimension longer than *n*-alkanes and *iso*-alkanes. It is possible to distinguish between contaminated and non-contaminated (Figure 2A and 2B)

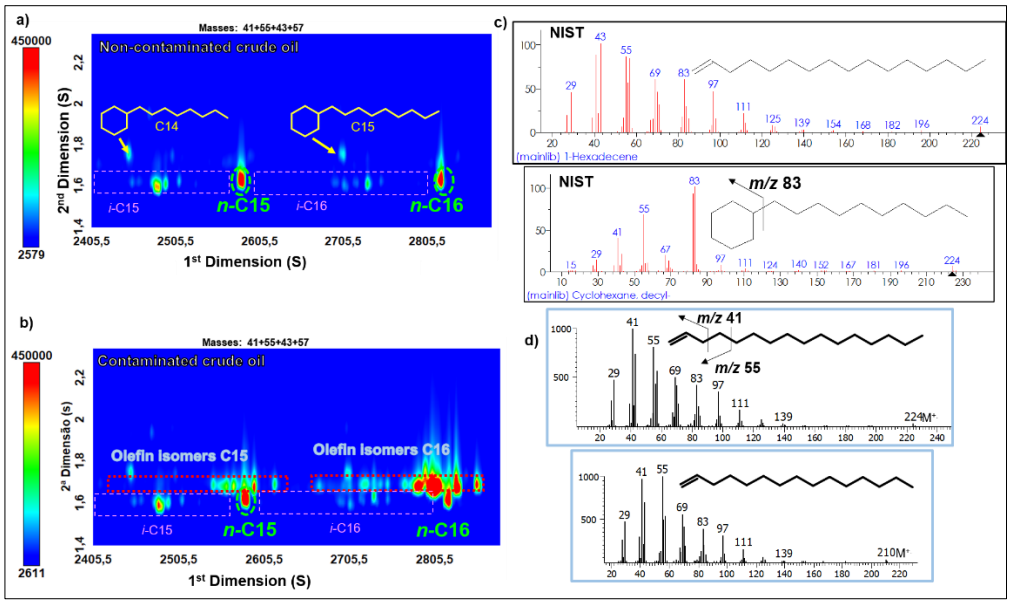

Figure 2 - Extracted Ion Chromatogram (EIC) m/z 41+55 and m/z 43+57 containing n-alkanes, iso-alkanes, cycloalkanes and olefins identified in: a) Non-contaminated crude oil, b) Contaminated crude oil; c) mass spectrum of 1-hexadecene and decyl-cyclohexane from NIST; d) mass spectrum of 1-hexadecene and 1-pentadecene by GC×GC-TOFMS.

oil and perform the separation and identification of contaminants using the GC×GC-TOFMS. For example, even if a C_{16} cycloalkane (Figure 2C) presents a mass spectrum containing the same m/z 41+55 of an olefin with C_{16} (Figure 2D), It is possible through the interaction of the components with the chromatographic column, as well as the different intensities of the m/z and the order of elution of the compounds in the structured chromatogram, the clear separation of the compounds. From these results it was observed that there are olefins from the drilling fluid of those compounds in the oil sample in the range between *n*-C_4- *n*-C_{16}.

Conclusions

It was possible to observe, using the GC × GC-TOFMS technique, a good separation between the olefins belonging to the drilling fluid and *n*-alkanes, iso-alkanes, cycloalkanes present in the oil samples in the range between C_{12} and C_{20}. This can help to understand the behavior of compounds in crude oil and provide more accurate geochemical data with more reliable geochemical interpretations and possible correlations between crude oil and its source rock.

Acknowledgements

The authors thank to PETROBRAS-UFRJ by financial code n°. 0050.0121394.22.9, CNPq, FAPERJ and Capes, financial code 001, for support.

References

Ratnayake, A.S., Sampei, Y. 2018. Organic geochemical evaluation of contamination tracers in deepwater well rock cuttings from the Mannar Basin, Sri Lanka. J Petrol Explor Prod Technol 9, 989–996.

Stout, S. A., Litman, E. R. 2022. Quantification of synthetic-based drilling mud olefins in crude oil and oiled sediment by liquid column silver nitrate and gas chromatography. Environmental Forensics, 1-13.

XVI LATIN AMERICAN CONGRESS ON ORGANIC GEOCHEMISTRY
9 - 11 AUGUST, 2023
ARACAJU, SERGIPE, BRAZIL

Hopenes in the Irati Formation - Permian of the Paraná Basin, Brazil

[a]Darlly Érika S. dos Reis; [b]Marco António Ruivo de Castro e Brito, [c]René Rodrigues
[a]Universidade Federal do Rio de Janeiro; [b]Universidade Federal Fluminense; [c]Universidade do Estado do Rio de Janeiro

*desr@iq.ufrj.br

Introduction

Hopenes are unsaturated biomarkers derived from bacteria that live in different types of environments (e.g., Talbot et al, 2008). In the Permian Irati Formation of the Paraná Basin, Brazil, the distribution of these compounds is unknown. In order to understand this distribution and relate it to paleoenvironmental variations, samples were studied from well SC-20-RS, drilled in the extreme south of the Paraná Basin, where occurs the connection of this basin with the past open ocean (Panthalassa), and well PL-13-SP, whose drilling was carried out in the northern part of the basin, in the State of São Paulo, in a paleogeographic situation markedly more inland (e.g., Faure and Cole, 1999).

Experimental

The 37 organic extracts from the well SC-20-RS and 32 extracts from the well PL-13-SP were analyzed on an Agilent 6890 gas chromatograph, coupled to an Agilent 5973 Network mass spectrometer. From each extract, was monitored the ion m/z 367, specific to Hop-17(21)-ene series. Analyzes were carried out at the Laboratory of Chemostratigraphy and Organic Geochemistry (LGQM) of the State University of Rio de Janeiro.

Results and Discussion

The organic extracts from the well SC-20-RS are characterized by the predominance of C_{30} and C_{31} hopenes compared to the C_{32} to C_{35} hopenes, while in extracts from the well PL-13-SP higher relative proportions of C_{32} to C_{35} hopenes were observed (Figure 1). Compared to samples from the well SC-20-RS, those samples from the well PL-13-SP have higher percentages of organic matter derived from bacterial attack (amorphous) (Reis et al., 2018 and unpublished data). Isotopic evidence suggests the existence of microbial mats during the deposition of the Irati Formation (Faure and Cole, 1999). In other sedimentary basins, the high relative proportions of C_{32} to C_{35} hopenes have been associated with cyanobacteria, both in oxic and anoxic environments (e.g., Talbot et al., 2008). This perhaps explains the high relative proportion of C_{32} to C_{35} hopenes in the extracts from well PL-13-SP, in samples with predominance of oxidized organic matter (chemostratigraphic units A and C; figures 1A and 1C), as well as in samples rich in organic matter with high hydrogen values (units B, D, E, G and H; figures 1B, 1D-E and 1G-H). The innermost paleogeographic situation in the area where the well PL-13-SP was drilled (e.g., Faure and Cole, 1999), possibly facilitated the proliferation of cyanobacteria.

In the marls and limestones (units D and G) of the two wells and in the bituminous shales (units E and H) in well PL-13-SP, the predominance of C_{34} hopene over C_{33} hopene is highlighted (figures 1D-E and 1G-H). These rocks were deposited in a hypersaline environment (Reis et al., 2018 and unpublished data). In hypersaline environments of other sedimentary basins, the dominance of compound C_{34} over compound C_{33} has been verified among hopanes (e.g., Fu Jiamo et al., 1986). These findings lead us to suggest that the configuration C_{34} hopene > C_{33} hopene is linked to the hypersalinity of the environment. As in the well SC-20-RS site, the hypersalinity of the environment began during the deposition of non-bituminous shales from the base of the Irati Formation (units A and C) (Reis et al., 2018), their extracts also exhibit the predominance of C_{34} hopene related to the C_{33} hopene (figures 1A and 1C).

Another striking feature in the hopenes of the shales of the first sedimentary cycle (units A-C and E) in well PL-13-SP and in the marls of Unit D in well SC-20-RS, is the configuration C_{35} hopene > C_{34} hopene (figures 1A-E), which suggests a greater contribution of cyanobacteria (Boon et al., 1983) in the composition of the organic matter of these rocks.

.

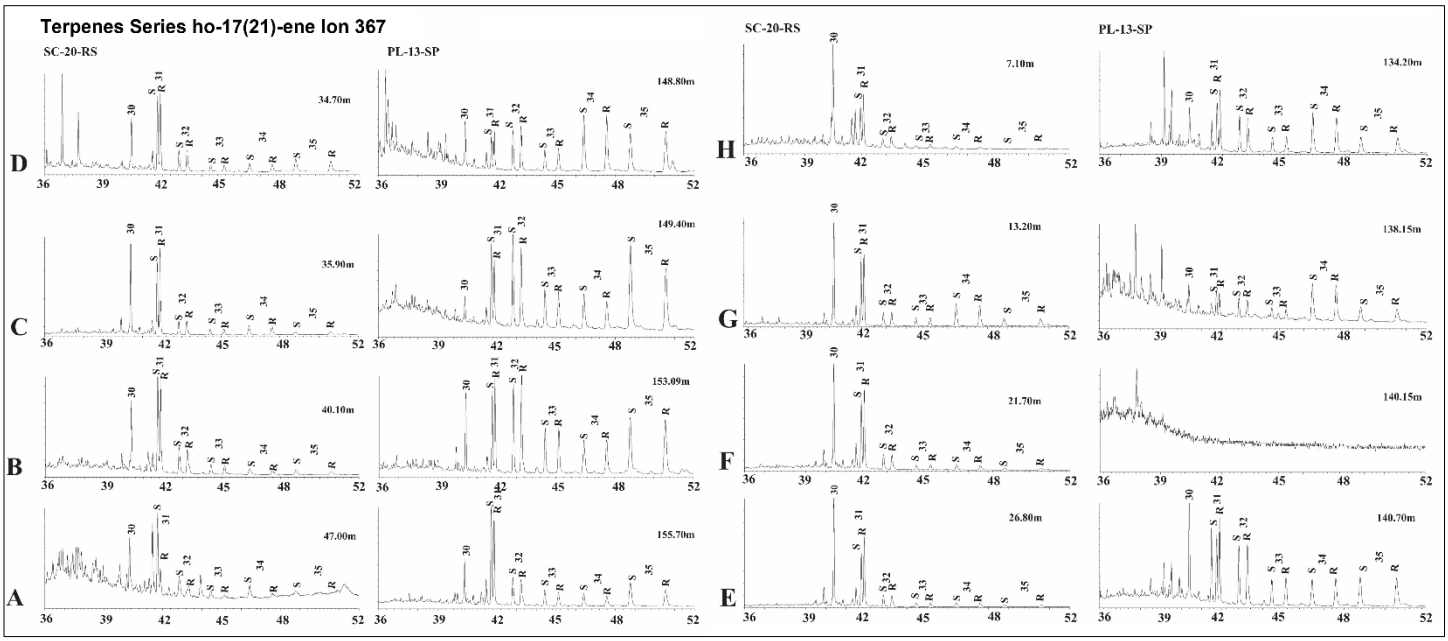

Figure 1 - Hopenes (m/z 367) in organic extracts from the Irati Formation in wells SC-20-RS and PL-13-SP. A to H = chemostratigraphic units A to H.

Conclusions

In the Irati Formation, the distribution of hopenes is controlled by variations in the composition of organic matter, with emphasis on the greater or lesser contribution of cyanobacteria, and salinity of the depositional environment. These variations are possibly linked to the different paleogeographic position of the places where the studied wells were drilled.

Acknowledgment

The “INOG” Project, for the supporting research financed by CNPq and FAPERJ, the LGQM for geochemical analyses. To CPRM for the well samples. Darlly Reis and Marco Brito also thank the PRH-17/ANP and the “Rede GASBRAS” Project, sponsored by Finep, for the scholarships.

References

Boon, J.J., Hines, H., Burlingame, A.L., Klok, J., Rijpstra, W.I.C., De Leeuw, J.W., Edmunds, K.E., Eglinton, G., 1983. Organic geochemical studies of Solar Lake laminated cyanobacterial mats. In: Bjory, M. et al. (Eds,), Advances in Organic Geochemistry, pp. 207-227.

Faure, K., Cole, D.,1999. Geochemical evidence for lacustrine microbial blooms in the vast Permian Main Karoo, Paraná, Fakiand Islands and Huab basins of southwestern Gondwana. Palaeogeography, Palaeoclimatology, Palaeoecology 152, 189-213.

Fu Jiamo, Scheng Guoying, Peng Pingan, Brassell, S.C., Eglinton, G., Jigang, J., 1986. Peculiarities of Salt Lake sediments as potencial source rocks in China. Organic Geochemistry 10, 119-126.

Reis, D. E.S., Rodrigues, R. Moldowan, J. M., Jones, C.M., Brito, M., Cavalcante, D. C., Portela, H. A., 2018. Biomarkers stratigraphy of Irati Formation (Lower Permian) in the southern portion of Paraná Basin (Brazil). Marine and Petroleum Geology 95, 110–138

Talbot. H.M., Summons, R.E., Jahnke, L.L., Cockell, C.S., Rohmer, M., Farrimond, P., 2008. Cyanobacterial bacteriohopanepolyol signatures from cultures and natural environmental settings. Organic Geochemistry 39, 232-263.

ALC

RESERVOIR GEOCHEMISTRY

XVI LATIN AMERICAN CONGRESS ON ORGANIC GEOCHEMISTRY
9 - 11 AUGUST, 2023
ARACAJU, SERGIPE, BRAZIL

Organic geochemical analysis of the basal potentially generating intervals of the Bambuí Group in the São Francisco Basin

DANIEL ANDRADE MIRANDA[a]*; CARLOS ROBERTO DE SOUZA FILHO[a]*; ÁQUILA FERREIRA MESQUITA[a]*

[a] DEPARTAMENTO DE GEOLOGIA E RECURSOS NATURAIS, INSTITUTO DE GEOCIÊNCIAS, UNIVERSIDADE ESTADUAL DE CAMPINAS - CAMPINAS, SP, BRASIL

danmir@unicamp.br

Introduction

The Proterozoic São Francisco Basin, located in central Brazil, covers an area of ~380,000 km^2 between the states of Bahia and Minas Gerais. The development of the petroleum system in this basin occurred simultaneously with post-depositional deformational processes (between ~950Ma-800Ma and 510Ma-490Ma), when the Bambuí Group rocks and underlying sequences reached burial and pressure conditions for the generation and migration of hydrocarbons (HCs) [1].

The source rocks of the petroleum system in this basin are [1]: (i) radioactive and locally carbonate marine shales from the top of the Upper Paranoá-Espinhaço Sequence, with a total organic carbon (TOC) content greater than 1%; (ii) fine siliciclastic rocks from the Macaúbas Group, with TOC up to 15.6%; (iii) mudstones and carbonate mudstones from the Sete Lagoas Formation (base of the Bambuí Group), exhibiting ~3.5% TOC. The Lagoa do Jacaré Formation also presents potential generating intervals. In general, the TOC contents identified for these rocks are potential for HCs exploration. However, the known generating sequences need further investigation regarding the current and historical stage of thermal maturation of the basin. Chemostratigraphic studies of the São Francisco basin have been coordinated in order to obtain a better understanding of the origin of the organic material present there [2].

Potential reservoirs are of the unconventional type due to low porosity and permeability of a secondary nature. Produced natural gas singly or together during formation tests carried out in multiple wells in the basin [3].

Since the basal rocks of the Bambuí Group have potential both as generators and as reservoirs and have remaining TOC values around ~3.5% [4], the identification and detailed characterization of the mineralogy, based on petrographic, geochemical and spectroscopic analyses, can provide important information to assess the potential for generation and storage of HCs in these rocks.

The objective of this work is the analysis of geochemical survey data available at the Exploration and Production Database of the National Petroleum Agency (BDEP/ANP) of the basal intervals of the Bambuí Group in the São Francisco Basin (Figure 1). It is intended to discuss the degree of maturation and origin of organic matter and evaluate the potential for generation and storage of HCs in these rocks.

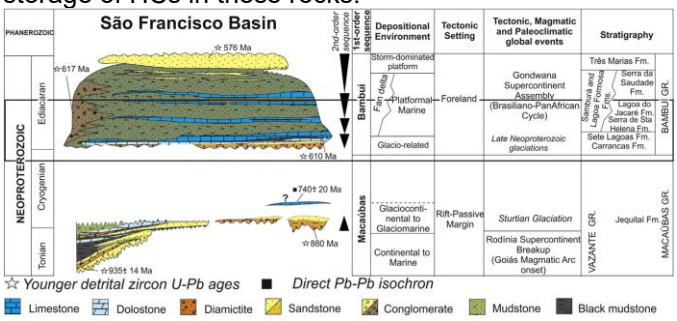

Figure 1. Stratigraphic Chart of the São Francisco Basin with emphasis on the basal portion of the Bambuí Group highlighted by the black rectangle (modified from [3]).

Experimental

All available geochemical data for wells drilled in the São Francisco Basin were requested from the ANP. A data compilation on the basal portion of the Bambuí Group was performed. In total, data were collected from 17 wells in the basin. However, few wells comprise data on the Bambuí Group. Table 1 indicates well intervals for which TOC and pyrolysis data are available.

Well	Unity	Top depth (m)	TOC (%)	S_1	S_2	S_3	T_{max} (ºC)	Calc. %Ro	HI	OI	S_2/S_3	S_1/TOC*100	PI	Insoluble Residue (Carbon)
1-PTRA-14-MG	Fm. Sete Lagoas	1871	0.40	0.28	0.40	0.39	306	*	100.00	97.50	1.03	70.00	0.41	-
	Fm. Sete Lagoas	1873	0.46	0.49	0.32	0.31	425	0.49	69.57	67.39	1.03	106.52	0.60	-
	Fm. Sete Lagoas	1916	0.29	0.41	0.32	0.27	301	*	110.34	93.10	1.19	141.38	0.56	-
	Fm. Sete Lagoas	1918	0.26	0.35	0.34	0.26	431	0.60	130.77	100.00	1.31	134.62	0.51	-
	Fm. Sete Lagoas	1920	0.37	0.21	0.32	0.30	434	0.65	86.49	81.08	1.07	56.76	0.40	-
	Fm. Sete Lagoas	2046	0.64	0.24	0.29	0.46	436	0.69	45.31	71.88	0.63	37.50	0.45	-
	Fm. Sete Lagoas	2070	0.26	0.18	0.24	0.35	438	0.72	92.31	134.62	0.69	69.23	0.43	-
1-RF-1-MG	Fm. Lagoa do Jacaré	311.85	0.54	1.47	0.53	0.26	261	*	98.15	48.15	2.04	272.22	0.74	74.00
	Fm. Lagoa do Jacaré	312.1	0.50	1.21	0.45	0.19	289	*	89.64	37.85	2.37	241.04	0.73	85.00
	Fm. Lagoa do Jacaré	315.75	0.60	2.45	1.25	0.22	289	*	207.30	36.48	5.68	406.30	0.66	84.00
	Fm. Lagoa do Jacaré	482.8	0.51	2.07	0.49	0.25	261	*	95.33	48.64	1.96	402.72	0.81	81.00
	Fm. Sete Lagoas	1634.75	0.61	1.50	0.46	0.35	418	0.36	75.53	57.47	1.31	246.31	0.77	70.00
1-RC-1-GO	Fm. Sete Lagoas	1131	0.50	0.01	0.05	0.34	416	0.33	9.94	67.59	0.15	1.99	0.17	54.00
1-BRSA-948-MG	Fm. Lagoa do Jacaré	690	0.81	0.01	0.03	0.37	335	*	3.71	45.74	0.08	1.24	0.25	42.00

Table 1. S_1 - volatile hydrocarbon content (HC), mg HC/g rock; S_2 - remaining HC generation potential, mg HC/g rock; S_3 - carbon dioxide content, mg CO_2/g rock; Calculation of vitrinite reflectance %Vro = 0.0180 x T_{max} – 7.16 (Jarvie et al., 2001) "* Negative values = not measured or invalid value for T_{max}"; HI - Hydrogen Index = S_2 x 100/TOC, mgHC/g TOC; OI - Oxygen Index = S_3 x 100/TOC, mgCO_2/g TOC; PI - Production Index = $S_1/(S_1+S_2)$.

Preliminary results

No sample has a TOC value equal to or greater than 1% (wt.%), considered as having good potential for HCs [5]. Some samples have TOC above 0.6 (wt. %), which indicates fair to good potential for HCs, but lack greater data density to reveal their real content.

Rock-Eval Pyrolysis indicates a low degree of maturation for the samples from the wells, being classified as immature following the criteria of [5] with T_{max} less than 435°C and low vitrinite reflectance calculated %Vro of 0.2-0.6. Due to the greater depth, the last three analyzes of the 1-PTRA-14-MG well can already be classified as precociously mature.

The HI x OI data in the Van Krevelen diagram and S_2 x TOC (Figure 2) point to a type II-III quality kerogen (prone to oil and gas) for well 1-RF-1-MG, type III (gas) for well 1-PTRA-14-MG and type IV (inert) for well 1-RC-1-GO and 1-BRSA-948-MG.

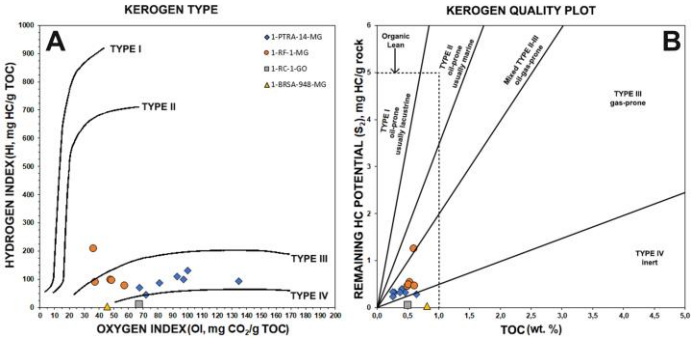

Figure 2. A) Van Krevelen diagram according to HI and OI values. B) Kerogen Quality diagram.

Conclusions

The geochemical data obtained from the BDEP/ANP, including Petra Energia S.A. wells, show a TOC value equal to or less than 1% (wt. %), although there are indications of values of up to 3.5% in the literature [4].

Pyrolysis values from wells classify kerogen as Type III, prone to gas. Although the data predominantly point to immaturity, some samples indicate precocious maturity. HI, OI and PI values for T_{max} ~435°C can be considered anomalous. However, high PI values may indicate contamination by drilling fluid or migrated oil.

Future work involves in situ analysis of drill cores, with expansion of pyrolysis data and vitrinite reflectance. In addition, XRD and elemental analysis of C, N, O and S will be used to evaluate the potential for generation and storage of HCs from these rocks. It is also intended to use reflectance spectroscopy and imaging methods for mineralogical characterization and inference of TOC levels based on predictive models calibrated by geochemical data.

Acknowledgment

The authors would like to thank the National Agency of Petroleum, Natural Gas and Biofuels (ANP) for granting a scholarship and financial support for this research through the Human Resources Program for Petroleum Exploration and Reservoir Geology (PRH 19.1). The authors also thank BDEP/ANP for the availability of data and samples and IG/UNICAMP for the physical structure, which helped to carry out this work. C.R.S.F thanks CNPq for the support (Proc. No. 309767/2022-9).

References

[1] Reis, H.L.S., 2018. Gás natural. In: Pedrosa-Soares, A.C., Voll, E., Cunha, E.C., (Eds.). Recursos Minerais de Minas Gerais. Belo Horizonte: Companhia de Desenvolvimento de Minas Gerais (CODEMGE), p. 1-39.

[2] Caetano-Filho, S., Paula-Santos, G.M., Guacaneme, C., Babinski, M., Bedoya-Rueda, C., Peloso, M., Amorim, A., Afonso, J., Kuchenbecker, M., Reis, H.L.S., Trindade, R.I.F., 2019. Sequence stratigraphy and chemostratigraphy of an Ediacaran-Cambrian foreland related carbonate ramp (Bambuí Group, Brazil). Precambrian Research, v. 331, p. 1-20.

[3] Lima, G.F.C., Ferreira, V.G., Duarte, J.C. de M., Lima, J. da S.D., Fuccio, A.F.A., 2021. Geologia e sistemas petrolíferos da Bacia do São Francisco dentro do contexto das reservas não convencionais nas regiões dos rios Indaiá e Borrachudo. Atena, 68p.

[4] Reis, H.L.S., Alkmim, F.F., 2015. Anatomy of a basin-controlled foreland fold-thrust belt curve: The Tres Marias salient, São Francisco basin, Brazil. Marine and Petroleum Geology, v. 66(4), p. 711-731.

[5] Peters, K.E., Cassa, M.R., 1994. Applied source rock geochemistry. In: Magoon, L.B., Dow, W.G., (Eds.). The Petroleum system- From source to trap, APPG Memoir 60, p. 93-117.

GEOCHEMICAL FINGERPRINTING ANALYSIS FOR ALLOCATION OF COMMINGLED OIL PRODUCTION: A CASE STUDY

CLAUDIA JULIANA OREJUELA-PARRA [a], JAEL YANINE PACHECO-MENDOZA [a], CLAUDIA JULIANA QUINTERO-AZUERO [b] , DAVID LEONARDO CANAS-JAIMES [b]

[a]ECOPETROL - ICP, [b]TIP

claudia.orejuela@ecopetrol.com.co

Introduction

From a financial point of view, it is important to know the volume of crude oil from a specific reservoir and from a regulatory perspective, it is mandatory to report the production allocation per semester in wells where there is more than one reservoir producing. For over twenty-five years gas chromatography has been used in the study of production allocation with accurate results. This geochemical analysis had replaced the traditional production logging (PLT) that requires well intervention with several advantages, it is a simple analysis, inexpensive and with a short response time (McCaffrey et al., 2012, Kaufman et al., 1990, Halpern 1995, Hwang R.J et al., 2000).

In this case study, we present the results of production allocation of four commingled wells, mixtures between formations A and B, with eight endmembers of formation A and ten endmembers of formation B; all crude oils are located in a field in the Llanos Basin. Additionally, artificial mixes were prepared to verify the quality of the production allocation calculation, applying the Chromedge Suite™ software in the data processing.

Experimental

Four samples of commingled oils were analyzed by gas chromatography with flame ionization detector (GC-FID) to obtain the distribution of n-paraffin and inter-paraffinic compounds in the range of n-C8 to n-C40 and the isoprenoids phystane and phytane.

All samples were prepared with the same concentration using CS2 as solvent. The compounds were separated using a DB-1 column (60m; 0,25mm; 0,25µm), the gas chromatographic method include an oven temperature between 35 to 320°C, heating ramp 3°C/min with He as carrier gas with a flow rate of 2 mL/min.

For the identification or the n-parafins, AccuStandar DRH-008S-R1 was used, which contains a mixture between n-octane and n-pentacosane and Open Lab CDS was employed for data processing. In the assignment of inter-paraffinic peaks and the data processing for the calculation of production allocation, the Chromedge Suite™ software was used.

Results and Discussion

The chromatographic analysis allowed to obtain the fingerprints (**Figure 1**) of crude oils and the interval of inter-paraffinic compounds used for production allocation was between n-C6 to n-C19, with approximately 100 peaks.

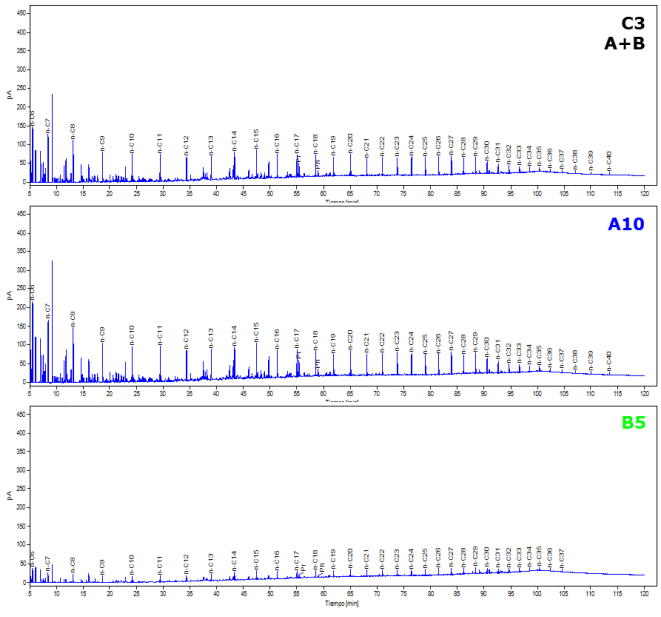

Figure 1. Fingerprints of commingled C3, endmembers A10, B5 of the formations A and B.

The data obtained from the processing with Chromedge Suite™ software was analyzed using principal components to do quality control and to identify trends, this analysis reveals that the endmembers are extremes that form a mix axis along which the commingled samples lie (**Figure 2**).

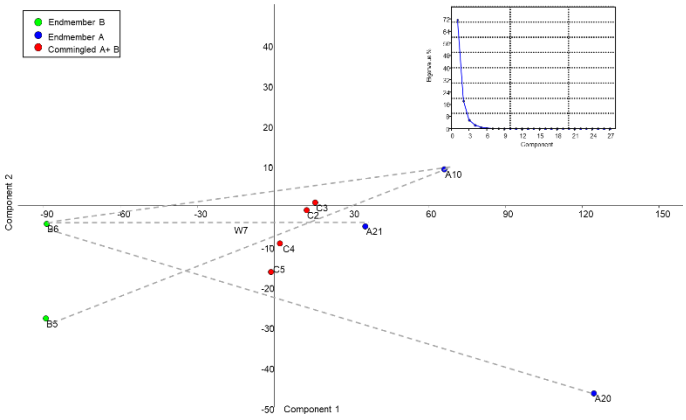

Figure 2. Principal components analysis showing variations between samples.

The samples analyzed were identified as one of two types: pure composition from a single formation (endmembers) and mixed composition between the two formations (commingled). The results are presented as a percentage of endmember contribution to the commingled, accompanied with the standard error for a given confidence interval.

Table 1 shows the production allocation results for the samples studied. The deviation associated with the calculation is greater for formation B with a maximum of 3,5%, while for formation A it is 1,9%, with a confidence interval of 80%; all values are acceptable within the criteria allowed by methodology.

Commingled	Reservoir	Endmembers			
		A	%	B	%
C2	A+B	A10	72,78	B6	27,22
C3	A+B	A10	74,21	B5	25,79
C4	A+B	A10	73,29	B6	26,71
C5	A+B	A21	65,88	B6	34,12

Table 1. Result for the production Allocation

For the artificial control samples, an allocation result was obtained with an error of less than 5% regarding the preparation ratio and a standard error of less than 3% in the expected results, within a confidence interval of 80%.

Conclusions

The determination of production allocation using gas chromatography allows to achieve good approximations to the measurement with low deviation values.

The use of the principal components is a good tool to identify the most representative endmembers for each commingled oil.

The analysis of the artificial mixture is a good practice to verify the quality of the GC runs and to validate the results of the real commingled oils

Acknowledgements

The authors thank Ecopetrol S.A for giving permission to present these results and for the financial support it provided to carry out this research. We also thank the geologist Mario Guzmán for reviewing the work.

References

1. HALPERN. H.I. 1995. Development and applications of light-hydrocarbon-based star diagrams. AAPG Bulletin 79 (6). 801–815.
2. HWANG. R.J. D.K. BASKIN AND S.C. TEERMAN. 2000. Allocation of Commingled Pipeline Oils to Field Production. Organic Geochemistry.
3. KAUFMAN. R.L. AHMED. A.S. & ELSINGER. R.J. (1990) Gas Chromatography as a Development and Production Tool for Fingerprinting Oils from Individual Reservoirs; Application in the Gulf of Mexico. in D. Schumaker and B.F. Perkins. Eds. Proceedings of the 9Th Annual Research Conference of the Society of Economic Palaeontologists and Mineralogists.
4. MCCAFFREY. M. BASKIN. D. PATTERSON. B. OHMS. D. STONE. C. REISDORF. D. 2012. Oil fingerprinting dramatically reduces production allocation costs. World Oil, march 2012, 55-59.

XVI LATIN AMERICAN CONGRESS ON ORGANIC GEOCHEMISTRY
9 - 11 AUGUST, 2023
ARACAJU, SERGIPE, BRAZIL

APPLICATION OF CHROMATOGRAPHIC ANALYSIS TO CHARACTERIZATION AND EVALUATION OF OIL PRODUCTS OF COMBUSTION TUBE EXPERIMENTS

JAEL PACHECO-MENDOZA[a], CLAUDIA OREJUELA-PARRA[a], JULIA HERRERA[a], MARTHA TRUJILLO[a], ROMEL PEREZ[a]

[a]**ECOPETROL-ICP**

jael.pacheco@ecopetrol.com.co

Introduction

High viscosity oils are a challenge for production, particularly when it is necessary to implement enhanced oil recovery (EOR) methods (either thermal or non-thermal). One of the most representative thermal EOR process is the *In situ* combustion (ISC) which injects compressed air into the reservoir and the oxygen reacts with the oil and promoting a series of reactions creating a high temperature zones which advance toward producers improving oil displacement and upgrading (Moore et al., 1995). Experimental evaluations have been conducted aiming to physically simulate the ISC process through combustion tube (CT) experiments under wet and dry conditions for a Colombian heavy oil reservoir (Cavanzo et al., 2016; Yatte et al., 2011), also a pilot on in-situ combustion has been carried out in the recent years in the Chichimene field (Manrique et al., 2002). The scope of this study was to analyze the oils product of one CT test in the absence of water, using gas and liquid chromatography and identify its effects on the oil.

Four samples product of the CT experiment (CT-3, CT-6, CT-8 and CT-10) were collected at different times along the test applied to an extra-heavy oil (Oil 1), that is considered the baseline. For this analysis, the reservoir continuity methodology was applied to identify the minimal variations in the oils identified through GC/FID chromatography.

Experimental

Oil product samples were taken between 16 and 22 hours of the experiment on the same day. Then, the conventional oil characterization workflow was applied, starting with SAR analysis that was conducted using Medium Performance Liquid Chromatography (MPLC) to obtain the saturate, aromatic and NSO fractions. GC/FID Whole Oil analysis was used to quantify the n-paraffins between n-C6 and n-C40 and isoprenoids pristane and phytane well as the interparaffinic compounds, using an Agilent 6890N gas chromatograph. Finally, GC/MS analysis for the study of aromatic in whole oil and saturate biomarkers in the saturate fraction was realized in a GC-7890A coupled to a mass spectrometer MSD-5975C, allowed us to study the variations in composition along the different stages of the experiment.

The interparaffinic compounds were identified and processed using the reservoir continuity methodology, that involves the Chromedge software, property of Stratum Reservoir, that is designed for chromatographic data analysis. According to Kornacki et al., (2017), the methodology is commonly used for reservoir continuity but, could be used in any project where subtle differences in chromatographic fingerprints are to be compared. For the application of this work, most of the interparaffinic compounds are identified in the rank of n-C7 to n-C20, to obtain a matrix of heights and ratios.

Results and Discussion

Oil 1 is a viscous fluid with a whole oil fingerprint that exhibits minor abundances of n-paraffins in the rank n-C6 to n-C12 and little to no interparaffinic compounds, low to abundances between n-C13 to n-C30 with minor interparaffinic compounds.

The oils product of the experiments exhibits an enrichment both in the n-paraffins in the n-C6 to n-C30 range, but especially in the n-C6 to n-C14 and the interparaffinic compounds in the same range but, heavier n-paraffins are prevalent through all the samples. Pristane/Phytane ratios showed an increase of 12% from the baseline to the first sample analyzed, and after that, it becomes more stable, showing light variation with the increase of temperature. The parameters that exhibited more variation were the nC17/n-C29 in 84%, due to the increase of light n-alkanes. Ratios relating the low carbon number n-paraffins to n-C14 (**Figure 1**) were used to assess the variations. No reduction of the compounds up

to C30 was observed, then, it is presumed that the increase in the lighter n-paraffins and interparaffinic compounds are a product of cracking of heavier molecules.

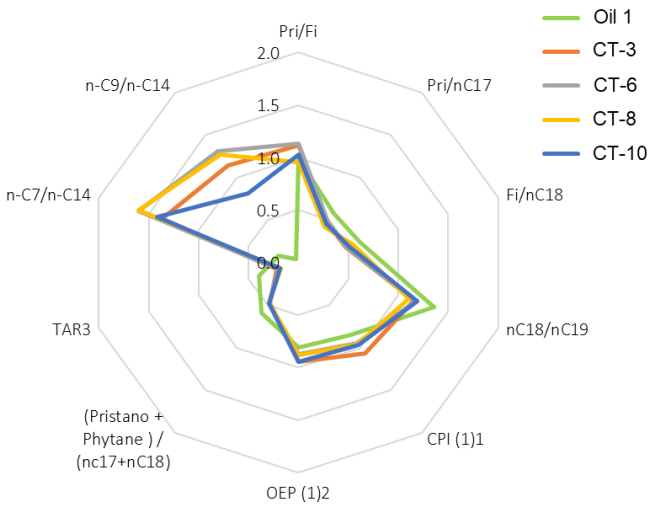

Figure 1. Whole oil parameters in star diagram showing variations between samples.

SAR analysis showed most variation in the Saturate and NSO fractions, especially from the Oil 1 to CT-3, where the saturate fraction increased in 41.1%. However, the analysis also reflected variations in the NSO fraction after CT-3. The final sample, CT-10 described an increase of the Saturate fraction from 19 to 24% and a reduction from 41 to 31% in the NSO compounds. The aromatic fraction was the most stable, between 37 and 44%, see **Figure 2**.

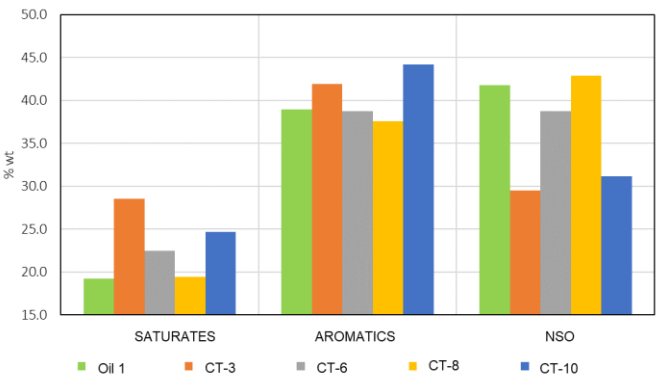

Figure 2. Comparison of whole oil parameters for baseline and the four samples from CT test.

No major variations were observed in the saturate biomarkers and in the mono and tri-aromatic biomarkers. However, in the poly-aromatic compounds such as dibenzothiophene, dimethylnaphtalene and methyl-dibenzothiophene there were some variations. For instance, the DBT/Phen increased from 0.57 to 0.81 from Oil 1 to CT-3 and the value becomes stable in the following samples, indicating an increase in DBT. Ratios such as the TDE-1 doubled its value in the samples of the experiments, indication of an increase in the 1, 2, 5 – Trimethyl Naphthalene. No direct impact was observed on the Rm calculated from aromatics, with values between 0.68 and 0.69.

Conclusions

The combustion tube experiments showed an enrichment in the lighter fraction of the oil, in the n-C6 up to n-C12, suggesting that oil upgrading could be expected in ISC field applications.

The SAR analysis showed an increase in the saturate fraction in the oil samples product of the experiment and a decrease of the NSO compounds, reinforcing the interpretation from Whole Oil analysis.

No major variations were identified in the saturate biomarkers but, in the aromatic biomarkers, some variations were observed in the poly-aromatic compounds such is the case of increase in DBT/Phen, TDE-1, MDR1 and decrease of DNR-1 and DNR-2.

Acknowledgements (ARIAL 11 BOLD)

The authors thank Ecopetrol S.A for giving permission to present these results.

References (ARIAL 11 BOLD)

CAVANZO, E., MUÑOZ, S., BOTTIA, H., NIZ, E., ORDOÑEZ, A. 2016. Combustion in situ humeda: alternativa para el recobro mejorado en colombia. Revista Fuentes Vol. 14 No. 1 pp. 5-18.

KORNACKI A., ADAMS J., McCAFFREY M. A. (2021). Reservoir Continuity and Production Allocation Workflow Using Chromedge. Latest update November 20, 2017. Stratum Reservoir.

MANRIQUE, E., TRUJILLO, M., LIZCANO, J., CARDENAS, D., VANEGAS, J., PORTILLO, F., SALAZAR, H., CAICEDO, N. 2022. Comprehensive Fluid Compositional Analysis Program to Support the Interpretation of Chichimene Field In-Situ Combustion Pilot. SPE-209390-PA.

MOORE, R. G., LAURESHEN, C. J., BELGRAVE, J., URSENBACH, M., MEHTA, S.A. 1995 In situ combustion in Canadian heavy oil reservoirs, Fuel, Volume 74, Issue 8, Pages 1169-1175.

YATTE, F., MUÑOZ, S. 2011. Una nueva mirada a la combustión in-situ: tratando de romper un viejo paradigma. Revista Fuentes, Vol. 9 No.1. pp. 41-56.

A molecular study using FT-ICR MS of oils recovered by injection alternated of water and gas.

Silva J. B. S. J.; Franco D. M. M; Roque J. V; Silva L. C; Rangel M. D; Pereira R. C. L; Simas R. C; Covas T. R. Vaz B. G.

UFG

e-mail joveiltonjunior@hotmail.com

Introduction

Petroleum recovery can be divided into primary, secondary, and tertiary. Primary recovery involves the natural expulsion of petroleum from the well using the pressure inside. Gas lifts or pumps can also be used to assist the process. Secondary recovery involves injecting water or gas (depending on the characteristics of the well) to push the petroleum toward the wellbore. Tertiary recovery can be further divided into different methods, such as viscosity reduction, fluids that reduce interfacial tension, microbiological treatment, and WAG (water alternating gas) injection to enhance the interaction between the injected fluid and the petroleum in the well.

Experimental

The samples were collected in the field by PETROBRAS and sent to UFG for analysis using FT-ICR MS 7T SolariX 2xR (Bruker Daltonics- Bremen, Germany) with ESI (-) mode. To prepare the sample, weighing 1 µg of petroleum and adding 1000 µl of toluene to create the stock solution is necessary. Then, add 500 µl of the stock solution to another container along with 500 µl of methanol. Finally, add 50 µl of NaOH (a basic solution) to the container, as shown in Figure 1.

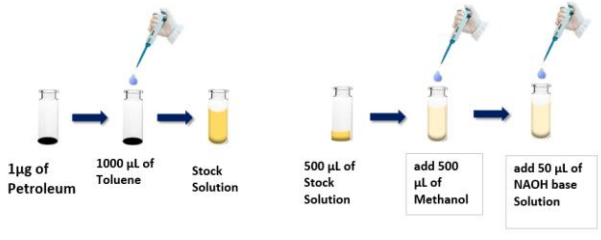

Figure1. shows the scheme for preparing the samples.

After preparing the solution, it was injected into FT-ICR, and the data was collected. The analysis was conducted three times using the same sample, with each analysis consisting of 300 scans. The final spectrum was obtained by averaging the 300 scans.

Results and Discussion

The alternating water and gas injection is an advanced petroleum recovery technique capable of increasing well production. However, to achieve increased production, it is necessary to understand the influence of this process on the well. Figure 2 shows the scheme of how the WAG was performed and the duration of each injection period.

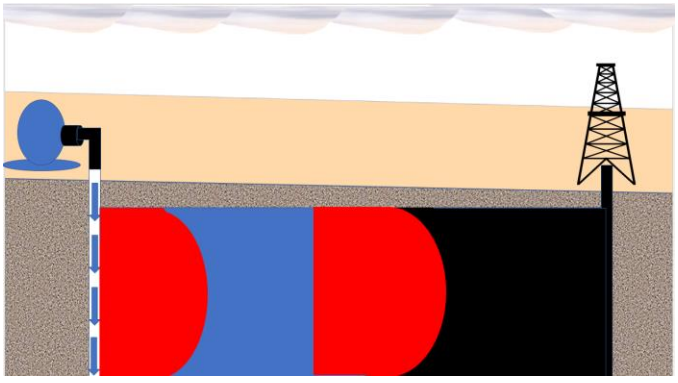

Figure 2. Scheme of alternate injection using water and gas and the date of each injection.

The samples were analyzed in the FT-ICR using ESI (-). There were three sets of samples: one set was taken before the injection of WAG, four samples were taken during the injection of water, and three samples were taken during the injection of gas.

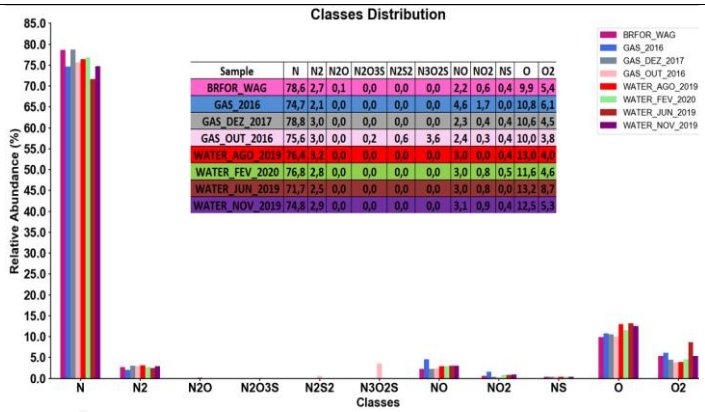

Sample	N	N2	N2O	N2O3S	N2S2	N3O2S	NO	NO2	NS	O	O2
BRFOR_WAG	78,6	2,7	0,1	0,0	0,0	0,0	2,2	0,6	0,4	9,9	5,4
GAS_2016	74,7	2,1	0,0	0,0	0,0	0,0	4,6	1,7	0,0	10,8	6,1
GAS_DEZ_2017	78,8	3,0	0,0	0,0	0,0	0,0	2,3	0,4	0,4	10,6	4,5
GAS_OUT_2016	75,6	3,0	0,0	0,2	0,6	3,6	2,4	0,3	0,4	10,0	3,8
WATER_AGO_2019	76,4	3,2	0,0	0,0	0,0	0,0	3,0	0,0	0,4	13,0	4,0
WATER_FEV_2020	76,8	2,8	0,0	0,0	0,0	0,0	3,0	0,8	0,5	11,6	4,6
WATER_JUN_2019	71,7	2,5	0,0	0,0	0,0	0,0	3,0	0,8	0,0	13,2	8,7
WATER_NOV_2019	74,8	2,9	0,0	0,0	0,0	0,0	3,1	0,9	0,4	12,5	5,3

Figure 3. Graphical distribution of classes was obtained from the well that was injected with WAG. The samples were analyzed using FT-ICR. The percentage of each class was determined before WAG injection, during gas injection, and during water injection.

Conclusions

During the WAG process, different tendencies during the injection of gas can be seen to see that larger abundance of N compound; on the other hand, when water was injected, water is possible to see a compound with more abundance of compound O.

Acknowledgements

The authors thank Petrobras S/A for financial support.

References

da Rosa, K. R. S. A.;* Bezerra, M. C. M.; Ponzio, E. A.; Rocha, A. A.,2016. Recuperação Avançada de Petróleo: Potencialidades da Injeção WAG (*Water Alternating Gas*). *Rev. Virtual Quim*. https://rvq.sbq.org.br/.

Afzali. S., Rezaei. N., & Zendehboudi. S. (2018). A comprehensive review on Enhanced Oil Recovery by Water Alternating Gas (WAG) injection. In *Fuel* (Vol. 227. pp. 218–246). Elsevier Ltd. https://doi.org/10.1016/j.fuel.2018.04.015

Asemani. M., Rabbani. A. R., & Sarafdokht. H. (2021). Implementation of an Integrated Geochemical Approach Using Polar and Nonpolar Components of Crude Oil for Reservoir- Continuity Assessment: Verification with Reservoir-Engineering Evidences. *SPE Journal*. *26*(5). 3237–3254. https://doi.org/10.2118/205388-PA

Hughey. C. A., Hendrickson. C. L., Rodgers. R. P., & Marshall. A. G. (2001). Elemental composition analysis of processed and unprocessed diesel fuel by electrospray ionization fourier transform ion cyclotron resonance mass spectrometry. *Energy and Fuels*. *15*(5). 1186–1193. https://doi.org/10.1021/EF010028B

COMPARISON BETWEEN GEOCHEMICAL RESULTS OF CARBONATE ROCKS OBTAINED FROM TOTAL WDXRF DATA AND STOICHIOMETRIC RECALCULATIONS FROM XRD-RIETVELD QUANTITATIVE PHASE ANALYSIS

Sotero, A.M.[1]; Paz, S.P.A.[1]; Lucas, C.R.S.[1,2];Aum, P.T.P.[2]; Angélica, R.S.[1]

[1] PPGG, Programa de Pós-Graduação em Geologia e Geoquímica, Instituto de Geociências, Universidade Federal do Pará, Belém, Pará.

[2] LCPetro, Laboratório de Ciência e Engenharia de Petróleo, Campus Universitário de Salinópolis, Universidade Federal do Pará, Salinópolis, Pará.

amsotero@ufpa.br; paz@ufpa.br; claudiolucas@ufpa.br; pedroaum@ufpa.br; rsangélica@gmail.com.

Introduction

Carbonate reservoirs hold more than 60% of the world's oil reserves. The geological evaluation of such formations requires accurate mineralogical and geochemical analyses due to their strong heterogeneities [1]. The conciliation of calcite and dolomite quantification by the Rietveld method (XRD) is excellent against XRF analyses (wt %), thermogravimetry and carbon elemental analysis [2]. The present study combines WDXRF analysis with XRD and Rietveld refinement for quality control in carbonate-focused characterization.

Experimental

Laboratory tests were carried out on two well-known carbonates widely used as standard rocks for laboratory petrophysical analysis: *Indiana Limestone (IL)* and *Silurian Dolomite (SD),* besides several other carbonate samples. Mineralogical and chemical (major and trace elements) measurements were respectively performed on Malvern Panalytical Diffractometer (Empyrean) and WDXRF Spectrometer (Axios Minerals). Sample preparation for XRF analysis included both *fused bead (fb - 1000ºC)* and *pressed powder (pp - 20 tons)*. Mineral analysis included: phase ID and phase quantification (Rietveld refinement) using the HSP, Highscore Plus 5.0 software. Based on known phase concentrations, the “chemistry calculator” tool of the HSP breaks down phase chemistry into simple oxides, enabling a direct comparation with the WDXRF results. The CO_2 contents are considered equivalent to LOI values of all samples. Carbon determination is thermogravimetric and not by XRF because this element is below the excitation and detection limit of the XRF.

Results and Discussion

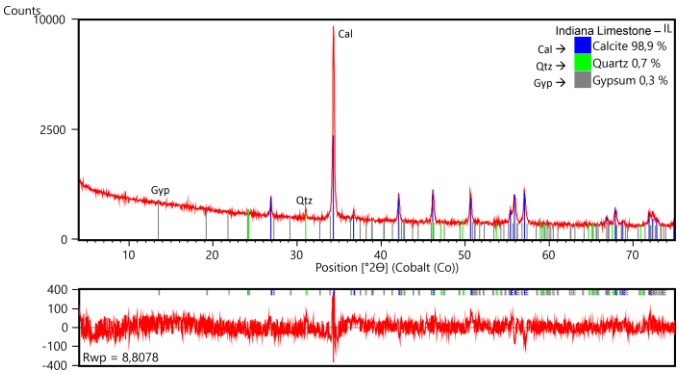

Figure 1. Phase ID and Rietveld refinement of Indiana Limestone.

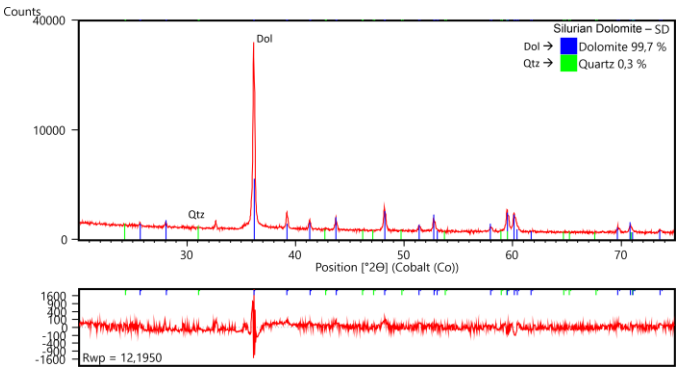

Figure 2. Phase ID and Rietveld refinement of Silurian Dolomite.

The *IL* refinement (Figure 1) showed calcite=98.9% (CaO=55.1%; CO_2=43.6%) consistent with both $XRF_{(fb)}$ (CaO=54.7%; LOI=43.5%) and $XRF_{(pp)}$ (CaO=55.3%; LOI=43.5%) (Table 1). The *SD* (Figure 2) is composed of dolomite=99.7% (CaO=30.3%; MgO=21.6%; CO_2=47.6%) that is compatible with $XRF_{(fb)}$ (CaO=29.9%; MgO=21.2%; LOI=48.4%) but incompatible with $XRF_{(pp)}$ (CaO=34.4%; MgO=16.7%; LOI=48.4%).

Table 1. Comparison between WDXRF, XRD-Rietveld and Theoretical data for Indiana Limestone.

Compound Name	$XRF_{(fb)}$ (%)	$XRF_{(pp)}$ (%)	HSP Calculator (%)	Theoretical Calcite (%)
CaO	54.7	55.3	55.1	56.03
SiO_2	0.73	0.41	0.49	-
MgO	0.55	0.40	0.40	-
SO_3	0.26	0.26	0.17	-
Al_2O_3	0.18	-	-	-
Fe_2O_3	0.13	0.12	-	-
LOI	43.5		43.6 (CO_2)	43.97 (CO_2)

Table 2. Comparison between WDXRF, XRD-Rietveld and Theoretical data for Silurian Dolomite.

Compound Name	$XRF_{(fb)}$ (%)	$XRF_{(pp)}$ (%)	HSP Calculator (%)	Theoretical Dolomite (%)
CaO	29.9	**34.4**	30.3	30.41
MgO	21.2	**16.7**	21.6	21.86
Fe_2O_3	0.29	0.21	-	-
SiO_2	0.23	0.22	-	-
LOI	48.4		47.6 (CO_2)	47.73 (CO_2)

.

The $XRF_{(fb)}$ method proved to be more efficient than $XRF_{(pp)}$ for *SD* geochemistry. This is due to the strong matrix effect between Ca and Mg witch is attenuated by $XRF_{(fb)}$ method. $XRF_{(fb)}$ allows more accuracy for quantification of CaO/MgO ratios in dolostones (Table 2). The results of $XRF_{(pp)}$ *and* $XRF_{(fb)}$ analyses of *IL* were similar. In this case there is no overestimation of CaO contents because limestones are composed essentially by calcite [$CaCO_3$] and the MgO content can be despised (Figure 3).

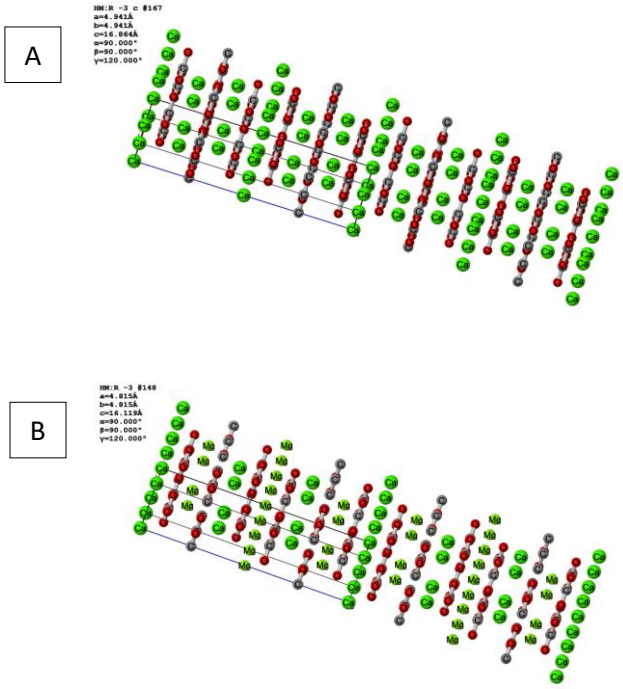

Figure 3. Theoretical chemical structure of Calcite (A) and Dolomite (B).

Conclusions

In general, this research showed that the geochemistry of carbonates requires *fused bead* as the main method of sample preparation. The efficiency of the XRF-Rietveld tool depends on the mineralogical complexity of the rock.

Acknowledgements

The authors thank UFPA (Universidade Federal do Pará) for infrastructure support (LCM and LCPETRO); CNPq (Brazilian research council) for financial support; PPGG (Programa de Pós-Graduação em Geologia e Geoquímica).

References

[1] Dunham, R. J. 1967. Classification of carbonate rocks according to depositional texture. In: Ham, W. E. (ed.) Classification of Carbonate Rocks. American Association of Petroleum Geologists, Tulsa, OK, 108–121.

[2] Dos Santos, H.N.; Neumann, R.; Ávila, C.A. Mineral Quantification with Simultaneous Refinement of Ca-Mg Carbonates Non-Stoichiometry by X-ray Diffraction, Rietveld Method. *Minerals* **2017**, *7*,164.

Assessment of crude oil basic polar components onto carbonate by ESI (+) FT-ICR MS, after modified cationic starch injection (EOR)

Luciana Gicovate[a]*, Lorraine L. G. C. de Araujo [a,b], Danielle M. M. Franco[c], Boniek G. Vaz[c], Georgiana F. da Cruz[a]

[a]State University of the North Fluminense Darcy Ribeiro; [b]Federal University of Rio de Janeiro; [c]Federal University of Goiás

*lugicovate@hotmail.com

Introduction

Modified starch has been considered a good candidate for the development of additives with the aim of oil additional fractions recovering in reservoirs, once this method relies on the adsorption of the polymer on rock walls [1]. Modified cationic starches application, conducted on a laboratory scale, for oil production improvement and its interaction with the carbonate rock focusing on the basic polar components, using above all an ultra-high-resolution mass spectrometry (FT-ICR MS), coupled to electrospray ionization in a positive-ion mode source [ESI (+)] to the recovered oil characterization, have not been previously documented. So, ESI (+) FT-ICR MS was applied to evaluate the effects of brine injection (waterflooding, [2]) and modified cationic starch on basic polar compounds of Brazilian oil.

Experimental

A displacement test was carried out in a porous medium with a high-pressure core holder (1000 psi) to simulate the injection experiments, using Original Oil (OO) (50:50 v/v, crude oil:cyclohexane). After core flooding experiments, it was obtained Oil OW (waterflooding with 3%NaCl solution) and Oil OMS (EOR injection with aqueous solution of modified cationic starch 1%). All the samples were prepared and direct injection in a final solution of toluene:methanol (0.5 mg.mL^{-1}) with 0.1% formic acid and then characterized by positive-ion ESI mode using a 7T SolariX 2xR ultra-mass spectrometer (Bruker Daltonics, Bremmen, Germany).

Results and Discussion

The compounds detected by mass spectra were organized and divided according to their heteroatom classes (NnOoSs) (Figure 1).

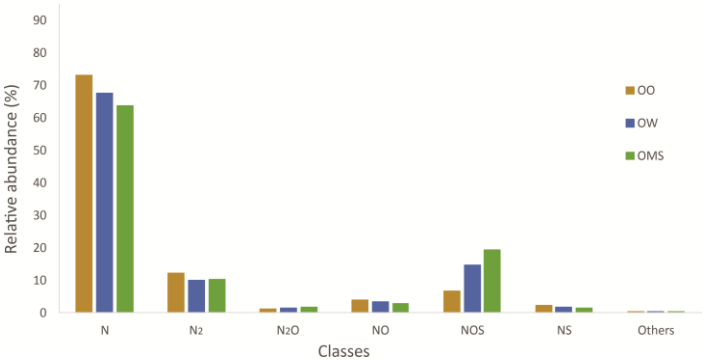

Figure 1. Heteroatom classes distribution for the oil samples.

The N species is the predominant chemical class in all oils, whose compounds can be attributed to pyridine, quinoline and acridine derivatives [3]. There is a considerable trend to N class decrease in the oils recovered, mainly in OMS, in relation to OO. However, OW and OMS (mainly) are enriched with NOS compounds, being the second most abundant class.

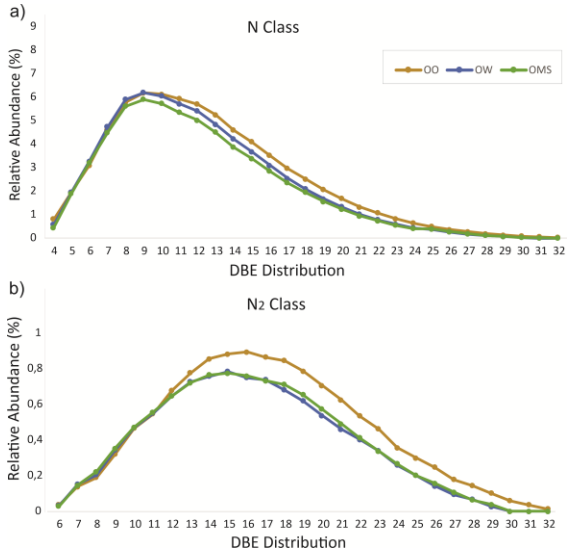

Figure 2. N and N_2 classes DBE distributions of oils samples.

Further insight of into individual heteroatom species (N, N_2) can be gleaned by examining the DBE distribution plots (Figure 2).

It is noted, in N class' DBE distribution (Figure 2a), a more accentuated decrease in the relative abundances in compounds with DBEs between 8 and 23 for OMS, in relation to OO and even to the OW. In view of this, the reductions in the relative amounts of N compounds for the OW, mainly for OMS (Figure 1), are clearly related to medium to high DBE compounds ranging from 13 to 31, showing thus a tendency to decrease the aromaticity of these oils, compared to OO (OMS being the most affected). DBE 9 was, overall, the most abundant in the oils studied. The N species with DBE values of 9, 12 and 15 determined under ESI (-) FT-ICR MS, for instance, are likely carbazoles, benzocarbazoles and dibenzocarbazoles, respectively [4]. However, these compounds can't be detected under ESI (+), due to weaker basicity. Thus, the N species with DBE values of 9, 12 and 15 detected in a positive-ion mode are most likely to have the structure of quinolines flanked with naphthenic side chains, benzoquinolines and dibenzoquinolines with alkyl or naphthenic side chains, respectively [4], [5].

In N_2 class' DBE distribution (Figure 2b), the oils profiles are similar, with OW and OMS having the lowest relative abundances of DBE values 13 to 31, also a decreasing trend in the aromaticity of these oils.

Beyond, a star diagram was plotted (Figure 3) to investigate the oils relative abundances concerning to aromaticity, according to N, N_2, and NOS classes DBEs distributions, using new ratios suggest in this work.

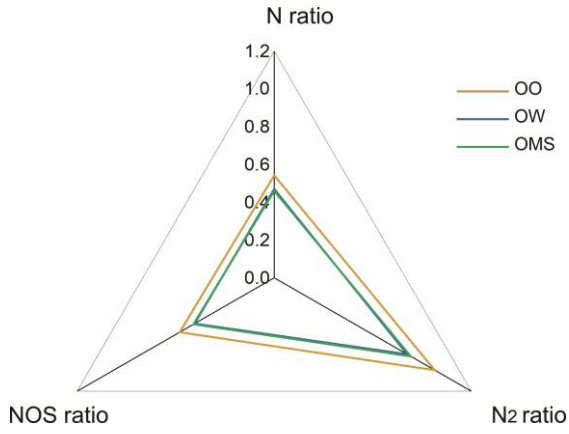

Figure 3. Star diagrams showing the DBE ratios for the N, N_2 and NOS classes in the oil samples.

The ratios were based on the sum of the relative abundance of compounds with higher DBE over the sum of the relative lot of compounds with lower DBE: DBE 14-23/DBE 4-13 for class N; DBE 17-25/DBE 8-16 for class N_2; DBE 15-22/DBE 7-14 for NOS class, once the analysis of the plots (Figure 2a and 2b) indicate changes in the medium to high values of DBE for the recovered oils. Thus, as can be seen in Figure 3, the recovered oils show a decrease of the greater DBE compounds in relation to the OO, mainly for the N_2 class, which points to the preferential loss of the most aromatic compounds during the recovery experiments with brine and modified cationic starch, possibly by solubilization in water or carbonate rock adsorption. Although the OW and OMS oils had shown a significant increase in the relative abundances of NSO class (mainly OMS) (Figure 1), this is unrelated to the higher aromaticity compounds.

Conclusions

The waterflooding and modified cationic starches injection (EOR) methods can modify the oil basic polar compounds distribution. The OMS was the most different, in general, with the lowest relative abundances of classes analyzed by different aspects. It is suggested nitrogen basic compounds and their analogs may have been carried out by the solutions injected, or mainly adsorbed by carbonate rock, once there was favorable loss of oil basic compounds with higher aromaticity. Modified cationic starch injection (EOR) was considered one of the most dominant processes for changes in petroleum chemical composition.

Acknowledgements

The authors are grateful to PETROBRAS for the crude oil donations, and for the financial support provided by PRH20-ANP and CAPES.

References

[1] Leslie, T.; Xiao, H.; Dong, M., 2005. Tailor-modified starch/cyclodextrin-based polymers for use in tertiary oil recovery. Journal of Petroleum Science and Engineering, v. 46.

[2] Sodré, L. G. P.; Martins, L. L.; De Araújo, L. L. G. C; Franco, D. M. M.; Vaz, B. G.; Romão, W.; Merzel, V. M.; Da Cruz, G. F., 2022. Implications of microbial enhanced oil recovery and waterfl ooding for geochemical interpretation of recovered oils. Annals of the Brazilian Academy of Sciences, v. 94 (Suppl. 3)

[3] Terra, L. A.; Filgueiras, P. R.; Tose, L. V.; Romão, W.; De Castro, E. V. R.; De Oliveira, L. M. S. L.; Dias, J. C. M.; Vaz, B. G.; Poppi, R. J., 2015. Laser desorption ionization FT-ICR mass spectrometry and CARSPLS for predicting basic nitrogen and aromatics contents in crude oils. Fuel, 160, 274-281.

[4] Wang, Q., Hao, F., Cao, Z., Tian, J., 2021. Heteroatom compounds in oils from the Shuntuoguole low uplift, Tarim Basin characterized by (+ESI) FT-ICR MS: Implications for ultra-deep petroleum charges and alteration. Marine and Petroleum Geology, 134, 105321.

[5] Kong, J., Wei, X., Yan, H., Li, Z., Zhao, M., Li, Y., Zong, Z., 2015. Analysis of extractable basic nitrogen compounds in Buliangou subbituminous coal by positive-ion ESI FT–ICR MS. Fuel 159, 385–391.

XVI LATIN AMERICAN CONGRESS ON ORGANIC GEOCHEMISTRY
9 - 11 AUGUST, 2023
ARACAJU, SERGIPE, BRAZIL

IDENTIFYING PRE-SALT CRUDE OILS COMPOSITIONAL VARIATIONS IN PRODUCTION MONITORING BY COMPREHENSIVE TWO DIMENSIONAL GAS CHROMATOGRAPHY

Clarisse L. Torres[a], Dayane M. Coutinho[a], Vinícius B. Pereira[a], Mônica C. Santos[a], Luiz A. F. Trindade[a], Daniel S. Dubois[b], Joelma P. Lopes[b], Gabriela Vanini[a], Francisco R. Aquino Neto[a], Débora A. Azevedo[a]

[a]Universidade Federal do Rio de Janeiro, Instituto de Química, NUGEM – LAGOA – LADETEC, Ilha do Fundão, Rio de Janeiro, RJ 21941-909, Brazil
[b]Petrobras/CENPES/PDIEP/GEOQ, Cidade Universitária, Rio de Janeiro, RJ 21941-915, Brazil

clarissetorres@iq.ufrj.br

Introduction

Typical Brazilian pre-salt crude oils from Santos Basin (ºAPI ~27) present a significant contribution of light hydrocarbons (LHs) in the range of C_5-C_{15}. Therefore, it is essential to obtain molecular composition information within this range that can be diagnostic of source, thermal maturity, and in-reservoir alteration processes (Walters et al., 2003). Because LHs are the first compounds perturbed by secondary alteration process, they are suitable for detecting slight variations in fluid compositions. Understanding how fluid varies in spatial and temporal time scales within a geological setting is especially important in reservoir geochemistry studies, where oil-oil correlation can be used to infer reservoir connectivity and aid oil recovery activities (Dekker et al., 2017).

This work is concerned with compositional variations in the low molecular weight compounds of pre-salt crude oils produced in a field located in the Santos basin, Brazil. Comprehensive two-dimensional gas chromatography coupled to time-of-flight mass spectrometry (GC×GC-TOFMS) was employed to obtain a detailed characterization of LHs from the pre-salt fluids collected from the same well, however, considering different production times and Water-Alternating-Gas (WAG) injection. Compound ratios from selected LHs were used for tracking variations in the low molecular weight distribution. This approach can be valuable for supporting the oil industry in optimizing field development.

Experimental

Eight Brazilian pre-salt crude oil samples collected from a well during a seven-year production period were selected for the present study (Table 1). Over this period, WAG injection with CO_2 was performed to increase oil recovery. The analyses of the oil samples diluted in carbon disulfide were performed on a GC×GC–TOFMS system (Pegasus 4D, Leco, St. Joseph, MI, USA) using a non-polar × polar column set (DB-5ms 30 m, 0.25 mm ID, 0.25 µm and DB-17ht 1.0 m, 0.25 mm ID, 0.15 µm). A standard oil sample was injected at different times during the batch analysis to guarantee data reliability. Data processing for the qualitative and quantitative analyses was obtained by ChromaTOF™ software version 4.51.

Table 1. Selected samples analyzed by GC×GC–TOFMS

Sample #	Sampling date
1	Dec-2012
2	Jun-2016
3	Oct-2016
4	Dec-2017
5	Jun-2019
6	Aug-2019
7	Nov-2019
8	Feb-2020

Results and Discussion

The analyzed samples are displayed in Table 1. Sample #1 reflects the initial fluid distribution, and #8 represents the last composition of the set of samples. Figure 1 shows the detailed characterization of LHs by classes in the C_4-C_8 range. Compound identification was inferred according to the elution order and mass spectrum of each analyte. The aromatic compounds clearly presented increased retention times in the second dimension due to the selected column set configuration (non-polar × polar).

The distribution of low molecular weight hydrocarbons during the seven-year production time was investigated using GC×GC-TOFMS analysis data. The tracking of chromatograms revealed distinct fingerprints among the analyzed samples. In general, aromatic and iso-alkane compounds were more susceptible to compositional variability.

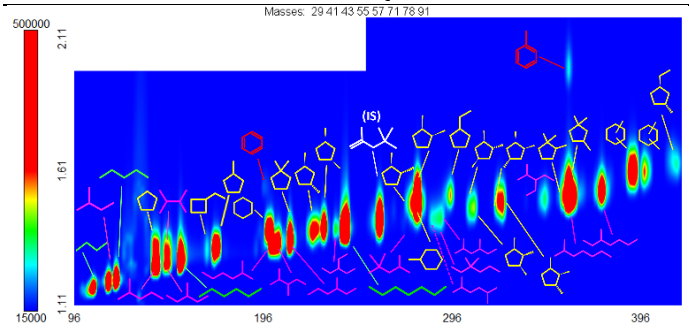

Figure 1. GC × GC-TOFMS Extracted Ion Chromatogram (EIC) with identification of C_4 to C_8 hydrocarbons based on Nist library.

Figure 2 shows an example of star plot diagrams encompassing all eight samples for a set of key substances using normalized peak ratios between individual iso-alkane and aromatic components as indices. Compounds were selected according to Dubois and Mendonça Filho (2022), where the authors described indices based on specific saturated/aromatic compounds that highlighted the heterogeneities in oil composition. If the fluid distribution among the samples is similar, the "star" shapes will display similar patterns. On the contrary, if the fluids are distinct, differences will be emphasized by the different patterns of the plots. Visualization of the star diagrams in figure 2 indicated that changes in this set of fingerprints have occurred from one sample to the next.

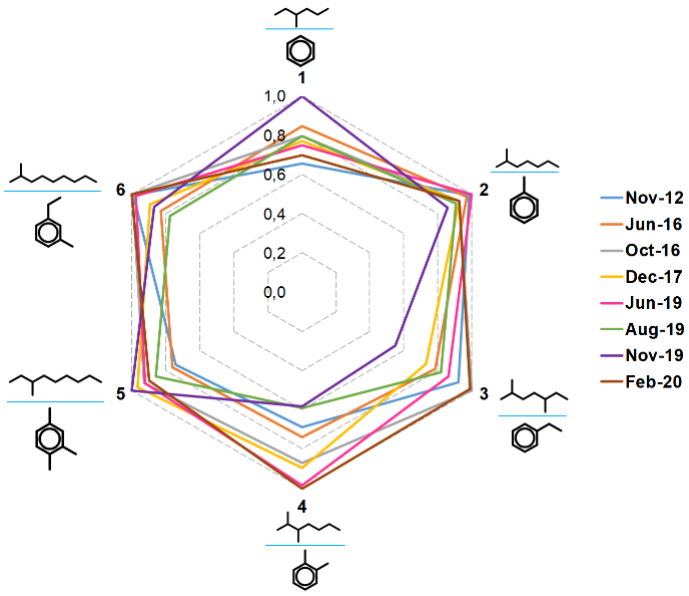

Figure 2. Star plot diagrams for samples #1 to #8 produced from a single well using normalized peak ratios between individual low molecular weight iso-alkane and aromatic components.

These results show that the WAG injection can change the produced oil composition with typical characteristic of enrichment in light components (Feng et al., 2016). The star diagrams also indicate that sample #7 (collected in Nov-2019) showed the most distinct profile among the analyzed samples. The ratios 1 (2-methylhexane / benzene), 3 (2,5-dimethylheptane / ethylbenzene), and 4 (2,3-dimethylheptane / o-xylene) were more prone to compound fractionation for this set of oils, showing that the hydrocarbon distribution has not been affected in the same manner during the production time scale. This feature may be attributed to different interactions between the hydrocarbons in the oil composition and water/CO_2 injection events.

Conclusions

The detailed analysis of the LHs by GC×GC-TOFMS revealed differences among the analyzed samples along the production time and WAG injection. The star plots using peak ratios between individual iso-alkane and aromatic components as indices illustrated these differences. As the fluid compositions change with the WAG events, these results may provide insights into the fluid movement according to the production process.

Acknowledgements

The authors thank CNPq and FAPERJ (Brazilian research councils) for fellowships; Petrobras S/A (0050.0121394.22.9), and CAPES financial code 001, for financial support.

References

Dekker, R., Tegelaar, E., Perrotta, S., Miller, S.D., Le Varlet, X., Hasler, C.A., Narhari, S.R., Rao, J.D., Neog, N., Dwindt, A.A., Al-Haidar, S., Dashti, Q., 2017. Determination of fluid connectivity in the middle marrat of the jurassic fields of north Kuwait using oil fingerprinting, in: Society of Petroleum Engineers - SPE Abu Dhabi International Petroleum Exhibition and Conference 2017. doi:10.2118/188375-ms

Dubois, D.S., Mendonça Filho, J.G., 2022. Reservoir geochemistry on compositional grading settings - a molecular approach, in: Second International Meeting for Applied Geoscience & Energy. pp. 1044–1048.

Feng, H., Haidong, H., Yanqing, W., Jianfeng, R., Liang, Z., Bo, R., Butt, H., Shaoran, R., Guoli, C., 2016. Assessment of miscibility effect for CO2 flooding EOR in a low permeability reservoir. Journal of Petroleum Science and Engineering 145, 328–335.

Walters, C.C., Isaksen, G.H., Peters, K.E., 2003. Applications of light hydrocarbon molecular and isotopic compositions in oil and gas exploration, in: Hsu, C.S. (Ed.), Analytical Advances for Hydrocarbon Research. Springer-Science+Business Media, LLC, New York. doi:10.1007/978-1-4419-9212-3

XVI LATIN AMERICAN CONGRESS ON ORGANIC GEOCHEMISTRY
9 - 11 AUGUST, 2023
ARACAJU, SERGIPE, BRAZIL

RESERVOIR COMPOSITIONAL GRADIENT UNVEILED BY ASPHALTENE CHARACTERIZATION USING FT-ICR MS

GABRIEL H. M. DUFRAYER[a], LIDYA C. SILVA, DANIELLE M. M. FRANCO[a], JOVEILTON B. S. JUNIOR, ROSANA C.L. PEREIRA[a], MÁRIO D. RANGEL[a], JOELMA P. LOPES[b], IGOR V. A. F. SOUZA[b], BONIEK G. VAZ[a]

[a]Federal University of Goiás, Brazil, [b]CENPES, Brazil

gabrielhenry@discente.ufg.br

Introduction

Reservoir geochemistry plays a vital role in understanding the composition and dynamics of hydrocarbon reservoirs. One significant fraction of petroleum, known as asphaltenes, holds valuable information about the reservoir's characteristics [1]. Asphaltenes are heavy compounds that retain properties resembling kerogen, providing insights into the reservoir's geological history and fluid behavior. The composition of petroleum can undergo substantial changes within reservoirs due to various factors, including density variations and the passage of time [2]. To unravel the complexities of reservoir gradients and their impact on petroleum composition, advanced analytical techniques are required. Fourier Transform Ion Cyclotron Resonance Mass Spectrometry (FT-ICR MS) coupled with Laser Desorption Ionization (LDI) has emerged as a powerful tool for characterizing asphaltenes and studying specific properties of reservoir samples. This technique enables the determination of molecular formulas and provides detailed molecular information that allows for the analysis of reservoir connectivity, depth-dependent variations, and spatial distribution. Using asphaltene sample characterization, we conducted a vertical reservoir gradient composition analysis on crude oil samples collected from two wells at different depths.

Experimental

Firstly, five samples of two different sets (wells) were used. In this study the asphaltenes were separated by using n-heptane (n-C7) as a precipitation solvent at a ratio of 40 mL per 1 g of crude oil. The mixture underwent ultrasonic radiation for 60 minutes and was then left to stand in the absence of light for 24 hours to induce asphaltene precipitation. The precipitated asphaltenes were collected through filtration using a Whatman glass filter, transferred to a Soxhlet apparatus, and washed with hot n-heptane until the solvent became clear (72 h), **Figure 1**. All of samples were analyzed using FT-ICR MS 7T SolariX 2xR (Bruker Daltonics- Bremen, Germany) with LDI (+) mode.

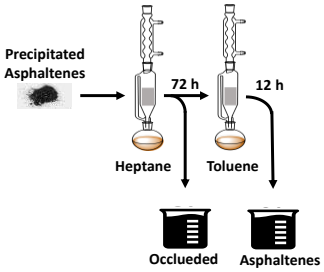

Figure 1. General scheme for the asphaltene extraction [1].

All the samples were injected three times into FT-ICR in order to ensure data reproducibility and analytical reliability. Each spectrum was acquired using 300 scans.

Results and Discussion

The comparison of the class diagram presented in Figure 2 highlights the significance of focusing on the asphaltene fraction for obtaining valuable insights and distinctions between samples. Unlike the oil fraction, which displayed relatively consistent class intensities across different samples, the asphaltene fraction exhibited more pronounced intensity variations and provided access to additional classes, including N2O. This emphasizes the importance of prioritizing the analysis of asphaltene fraction to enhance understanding and differentiation among samples.

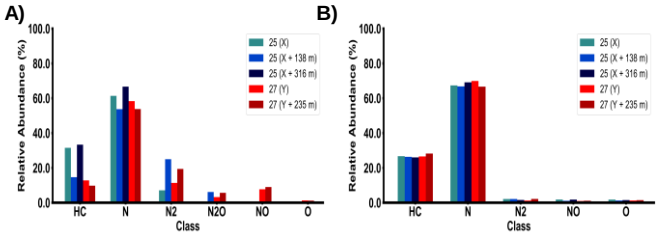

Figure 2. Graphical distribution of classes using LDI (-) FT-ICR MS. **A)** Crude Oil. **B)** Asphaltenes.

The class profile analysis of oils obtained through LDI FT-ICR MS did not reveal significant compositional differences within each well, with the N-class and HC-class being the predominant classes. However, analyzing the class profile of asphaltene samples allowed for the identification of subtle differences, particularly with increasing depth where multi-heteroatomic classes became more prominent. This suggests potential variations in the molecular composition of the reservoir fluids. To further investigate these differences, DBE vs. carbon number diagrams were constructed for the N-class. The diagrams clearly showed distinct changes in the asphaltene profile as depth increased in both wells. Notably, in well 27, the deeper oil sample originated from a different formation compared to well 25, which was not apparent from the class profile analysis alone. These findings highlight the importance of analyzing asphaltene samples in conjunction with the class profile to obtain a comprehensive reservoir characterization and a better understanding of its heterogeneity.

Examining the DBE distribution versus carbon number graph (Figure 3), it became evident that an increase in depth corresponded to higher DBE and carbon numbers, primarily due to the density effect. The graph also revealed the presence of two distinct compositional environments: one characterized by a higher concentration of compounds with elevated DBE and carbon numbers, indicating a greater content of aromatic chains, and another dominated by compounds with higher carbon numbers, suggesting the prevalence of aliphatic chains. The deeper sample exhibited a behavior influenced by differences in the depositional environment. Furthermore, the DBE vs. carbon graph of the asphaltene fraction from the deeper section of well 27 exhibited a distinct profile, confirming its origin from a different formation than the oils collected within the same well. This distinct profile serves as additional evidence of compositional variations within the reservoir and underscores the influence of different formations on the molecular characteristics of the extracted fluids.

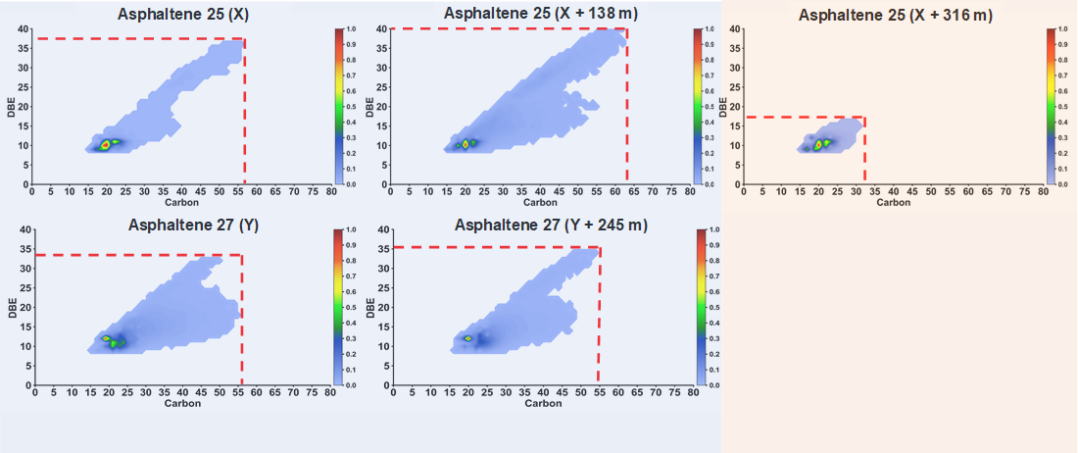

Figure 3. DBE distribution versus carbon number: asphaltene samples from lowest to highest depth in wells 25 and 27.

Conclusions

The study revealed that the composition of asphaltene samples exhibited noticeable differences as depth increased, indicating potential variations in the molecular composition of the reservoir fluids. In contrast, the class profiles of the oil samples within each well did not show significant compositional differences. This emphasizes the importance of analyzing asphaltene samples to obtain a more comprehensive understanding of reservoir composition and heterogeneity. By focusing on the asphaltene fraction, researchers can gain valuable insights and distinctions between samples that may not be evident from analyzing the oil fraction alone. These findings highlight the significance of asphaltene characterization in reservoir studies and its potential to enhance reservoir characterization and optimize hydrocarbon recovery strategies.

Acknowledgments

The authors thank CNPq (Brazilian research council) for fellowships and Petrobras S/A.

References

[1] da Silva, L. C.; Dávila, J. V.; Fleming, F. P.; Combariza, M. Y.; & Vaz, B. G., 2022. Laser desorption ionization and collision induced dissociastion as powerful tools for FT-ICR mass

[2] Lopes J. P.; Rangel M. D.; de Morais E. T.; de Aguiar H. G., 2008. Geoquímica de reservatórios. Brazilian Journal of Geology**38**, 3-18.

XVI LATIN AMERICAN CONGRESS ON ORGANIC GEOCHEMISTRY
9 - 11 AUGUST, 2023
ARACAJU, SERGIPE, BRAZIL

RESERVOIR GEOCHEMISTRY 4D: THE USE OF FINGERPRINTING AS A WAY TO MONITOR WAG EFFICIENCY

[a]JOELMA PIMENTEL LOPES, [a] IGOR VEGAS ALVES FERNANDES DE SOUZA, [a] DANIEL SILVA DUBOIS, [a] JARBAS VICENTE POLEY GUZZO, [a] ALEXANDRE JAIME MELLO VIEIRA, [a] ALEXANDRE DE ANDRADE FERREIRA, [b]MARCIA IDA DE OLIVEIRA SILVA, [b]JOSE SÉRGIO DE ARAUJO CAVALCANTE FILHO, [b]VICTOR DE SOUZA RIOS

[a]PETROBRAS Research Center, Av Horácio Macedo ,950, Cidade Universitária, 21941-915, Rio de janeiro, RJ, Brazil
[b]PETROBRAS EDISEN, Av. Henrique Valadares, 28 - Centro, 20231-030, Rio de Janeiro - RJ, Brazil

Joelma.lopes@petrobras.com.br

Introduction

Reservoir geochemistry studies the compositional variations of petroleum reservoir fluids at a variety of spatial and temporal scales, it can address kilometer-scale questions of faults acting as barriers vs. conduits, meter-scale problems of assessing the interconnectivity, or micron-scale issues concerning the impact of solid reservoir bitumen to the economic reserve analysis. The goal is to understand these variations in terms of how accumulations filled from an evolving source rock system, together with the effects of processes such as diffusive and convective mixing, gravitational and thermal segregation, biodegradation, phase changes and leakage, in support of exploration, appraisal, development and production strategies.

The enhanced oil recovery technique of using water alternating gas (WAG) injection has been implemented in the very early stages of production and there remain some questions concerning its efficiency (time, investment, recovery factor). There is a necessity to improve the knowledge regarding the miscibility process between CO_2 and oil, and the potential compositional changes during the production history.

PETROBRAS developed a methodology linked to time-lapse reservoir geochemistry application (4D Reservoir Geochemistry). In this study we used reservoir geochemistry fingerprinting as a way to monitor water alternating gas injection (WAG) efficiency in order to provide valuable information to support the field management.

Experimental

The reservoir fluid characterization was done using GC-Carburane®, a special gas chromatography configuration associated with a software that provide accurate characterization of the light fraction of crude oils and condensate samples. Carburane® software is a data processing commercial program developed by IFP Energies Nouvelles, the French Petroleum Institute, that performs the identification and automatic quantification of more than 500 compounds present in the n-C_5 to n-C_{15} fraction.

The methodology used involves three main phases:

1. Static characterization of the fluid (t0, time zero), through the evaluation of the original composition of the Field fluid (fingerprint) based on samples recovered from DST and MDT tests from different wells;

2. Dynamic assessment of oil composition based on a produced fluid sampling program to monitor WAG efficiency as well as newly sampled production fluids.

3. Definition of the methodology to monitor the efficiency of water alternating gas (WAG) injection, from the detailed composition of the oil during production, using geochemical analysis techniques.

Representative samples from the field were selected to evaluate the lateral as well as vertical variation in the composition of the fluids, including 56 samples related to 21 wells. In addition, four wells have been selected and monitored since 2016, and more intensely in 2019, due to adherence to the WAG injection phase at that time in this part of the field.

Results and Discussion

Field data used in this study were obtained through the performance report of the WAG method and the behavior of injectivity to water and gas in wells with fluid exchange in the field. The study is very detailed and includes

information from WAG exchanges carried out up to 28/Feb/2021. It considers the influence on nearby producing wells, with a consolidation of information on fluid arrivals and tracers, when available.

The duration of the cycles of each fluid has been quite variable, often being carried out as a way to reduce the impacts of operational problems and/or to minimize production losses. There are cycles lasting from 1 day to cycles lasting more than two years. In operational terms, fluid changes in the field have been successful.

In addition to monitoring the injectivity of the WAG injection well and the composition of the injected fluid, it is important to evaluate the evolution of the fluids produced in the adjacent wells.

It is expected that the Gas-Oil Ratio (GOR) and the BSW of the produced well are the main parameters that are influenced by the alternating injection of water and gas. Depending on the dynamics of the fluids in the porous medium, with a sufficiently long period of observation, it is possible to develop analogies between the reservoirs and WAG injection scenarios to characterize the porous medium and evaluate the performance of the method.

As a mean of corroborating the observations for GOR and complementing the compositions of the gas and produced water, chemical tracer injection projects were developed. Chemical tracers are substances that are foreign to nature and have a high affinity for a fluid in the reservoir. Gas chemical tracers, for example, have a high affinity for the gas phase in the reservoir. In this way, it is possible to qualitatively infer the path that fluids travel through the porous medium and confirm whether or not part of the gas produced in a given well originated from the injection gas.

Samples produced by well A in the period 2012-2020 showed compositional variation over time. It is possible to verify a positive correlation between the mass gain of light compounds and the increase in GOR (Figure 1).

Conclusions

The methodology developed in this work allowed the monitoring of the compositional variation of the fluid throughout production, using the CG-Carburane® technique. This data, integrated with field-monitored parameters such as chemical tracers, RGO, and BSW, promoted a better understanding of the effects of WAG injection.

These results can be used to evaluate the effectiveness of the enhanced recovery processes, allowing the adjustment of the fluid exchange and the production curve, with the objective of increasing the field recovery factor.

The next steps consist in performing physical and mathematical simulations to predict the compositional variation of fluids throughout production to assist in reservoir flow models.

The investment was low since only oil geochemical analyses were used. On the other hand, the potential benefits are high, as we estimate an increase of 0.2% of the recovery factor (an increment of 12-16 Million of barrels of oil equivalent being produced).

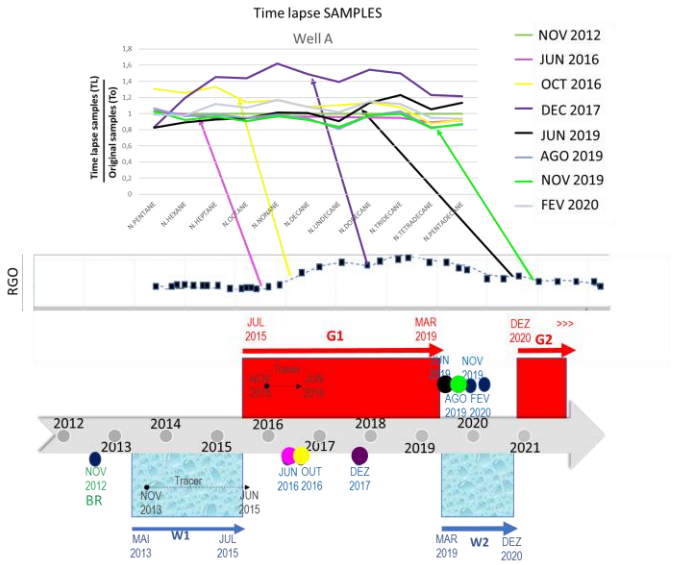

Fig.1. Samples produced by well A in the period 2012-2020 show compositional variation over time. It is possible to verify a positive correlation between the mass gain of light compounds and the increase in GOR.

Acknowledgements

The authors thank Shell collaboration during the Technical Cooperation Agreement with PETROBRAS and to PETROBRAS for the permission to publish this work.

References

Kaufman R. L., Ahmed, A. S., and Elsinger, R. J., 1990, Gas Chromatography as a development and production tool for fingerprinting oils from individual reservoirs: applications in the Gulf of Mexico: In: Proceedings of the 9th Annual Research Conference of the Society of Economic Paleontologists and Mineralogists. (D. Schumaker and B. F. Perkins, Ed.), New Orleans. 263-282.

XVI LATIN AMERICAN CONGRESS ON ORGANIC GEOCHEMISTRY
9 - 11 AUGUST, 2023
ARACAJU, SERGIPE, BRAZIL

CARACTERIZATION OF MARINE AND LACUSTRINE OILS FROM SERGIPE-ALAGOAS BASIN, BRAZIL, BY APPI(+) FT-ICR MS

Rafael Moreira Silva[a,*], Letícia Fernandes Sakai[a], Caroline Adolphsson do Nascimento[b], Danielle Mitze Muller Franco[c], Boniek Gontijo Vaz[c], Georgiana Feitosa da Cruz[a], Laercio Lopes Martins[a,d]

[a]North Fluminense State University; [b]State University of Rio de Janeiro; [c]Federal University of Goiás; [d]Federal University of Ceará

e-mail: rafaelsilva@lenep.uenf.br

Introduction

The compositional analysis of petroleum at a molecular level provides valuable information about its geochemical characteristics. High-resolution mass spectrometry (MS) techniques, such as Fourier transform ion cyclotron resonance (FT-ICR), have been expanding these analyses, allowing the detection of less volatile and more polar compounds [1]. Using Atmospheric Pressure Photoionization (APPI) it is possible to analyze high molecular weight aromatic hydrocarbon compounds, as well as sulfur, oxygen, and nitrogen species [2].

In this context, this work aims to investigate the depositional environment of the source rock of oils from the Sergipe-Alagoas Basin, Brazil, based on compounds analyzed by APPI(+) FT-ICR MS. It is also our goal to expand the applicability of the APPI(+) FT-ICR MS analysis in geochemical investigations of crude oils.

Experimental

Five crude oil samples from Sergipe-Alagoas Basin were investigated in this research, in which samples SEAL01, SEAL02, SEAL03, and SEAL05 have a marine origin, and the sample SEAL04 has a lacustrine origin [3]. After fractionation, the saturated and aromatic fractions were analyzed by gas chromatography coupled to mass spectrometry (GC-MS) to assess biomarker compounds, and by APPI(+) FT-ICR MS to assess the aromatic and polar compounds.

Results and Discussion

Based on the heteroatom and hydrocarbon class distribution of the oil samples obtained by APPI(+) FT-ICR MS (**Figure 1a**), it was possible to differentiate the marine samples (SEAL01, 02, 03, and 05) from the lacustrine sample (SEAL04), since they have sulfur classes (O_2S, OS, and S) in considerable amount, which were not detected in the lacustrine sample.

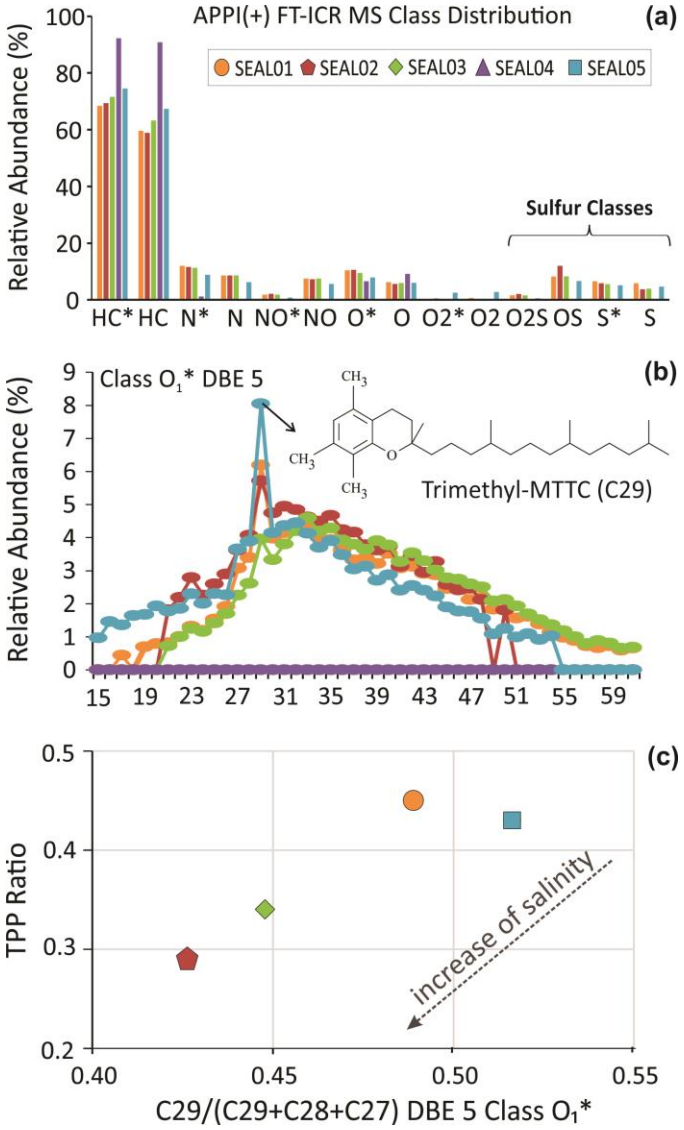

Figure 1. (a) APPI(+) FTICR-MS heteroatom and hydrocarbon class distribution of the oil samples. (b) Carbon number distribution of heteroatomic class O_1* DBE 5. (c) Graphic of TPP ratio *vs* C29/(C29+C28+C27) of Class $O_1^{\cdot}$ DBE 5. *Refer to radical ions, while the absence of it refer to protonated ions.

The marine oil samples also show a considerably higher abundance of the N*, N, NO*, and NO classes, which were barely detected in the lacustrine oil (**Figure 1a**). This means that the marine oils have a higher abundance of pyridinic nitrogen compounds (N class), which is a contrary observation of the lower abundance of pyrrolic nitrogen compounds in this type of oil.

From the analysis of the distribution of DBE (double bond equivalent) 5 of the class O_1* (**Figure 1b**), it was possible to observe a notably high abundance for the $C_{29}H_{50}O$ compounds to the marine oil samples, which are probably related to the trimethyl-MTTC (methyltrimethyltridecylchroman). However, they were not detected in the lacustrine sample, as the whole O_1* class. These results indicate that these oxygenated compounds are characteristic of marine depositional environments, being another APPI(+) feature to differentiate lacustrine and marine crude oils. In addition, the strong dominance of the $C_{29}H_{50}O$ compounds should indicate non-hypersaline environmental conditions [4], consistent with the low to medium values of the gammacerane index (0.52, 0.50, 0.52, and 0.49 for samples SEAL02, SEAL03, and SEAL05, respectively).

Based on the MTTC ratio, which is used as a proxy for paleosalinity assessment, calculated as 5,7,8-trimethyl-MTTC/total MTTCs [4], it was suggested in this work the ratio C29/(C29+C28+C27) DBE 5 class O_1*. For marine oil samples, high values were observed for the ratio C29/(C29+C28+C27) due to the markedly higher amount of C29 compounds. From the good correlation of this ratio versus the TPPs ratio (**Figure 1c**), it was possible to infer that the SEAL02 sample comes from a source rock deposited in a marine environment with higher salinity than the others, while samples SEAL03 and SEAL05 comes from a source rock deposited in lower salinity, with a possible higher influx of freshwater. The SEAL04 sample, on the other hand, presents the highest value of the TPP ratio (0.95) and non-detection of chromans, corroborating its lacustrine depositional environment.

Figure 2 shows the carbon number distribution of class S_1*. As can be observed, there is a higher intensity of C40 species in all four oil samples with marine characteristics. The prominence of these C40 compounds was also observed in the S, OS, and O_2S classes. These compounds are mostly sulfur aromatic carotenoids, originating from reactions of the carotenoids with sulfur during diagenesis since they have multiple reactive sites for sulfur incorporation [2]. Here we corroborate the presence of C40 sulfur carotenoids in marine environments and their absence in lacustrine environments, being another APPI(+) feature to differentiate lacustrine from marine crude oils.

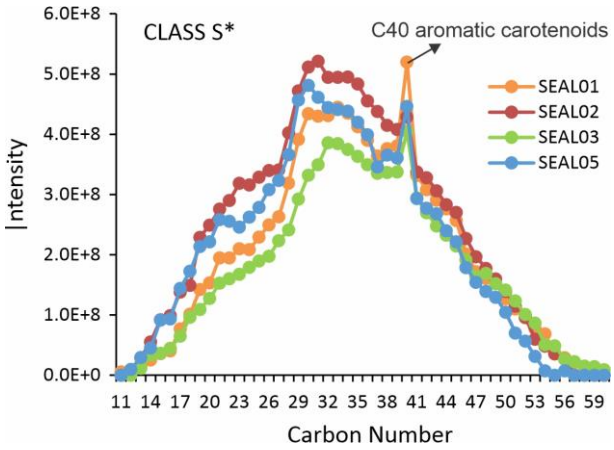

Figure 2. Carbon number distribution of heteroatomic class S_1* of the crude oil samples assessed in this study.

Conclusions

The APPI(+) FT-ICR MS analysis is a powerful tool to differentiate lacustrine and marine oils. It was useful to geochemically characterize the Sergipe-Alagoas crude oils, in which the marine oils present a higher abundance of sulfur compounds, with prominent C40 sulfur aromatic carotenoids, and also a high abundance of pyridinic and other nitrogen compounds. The marine oils also present a higher abundance of the C29 species of the DBE 5 class O_1*, which is probably related to the trimethyl-MTTC. From these results, we propose the C29/(C29+C28+C27), mirroring the chroman ratio, to assess paleosalinity, which pointed out that the marine oils are from source rocks deposited in non-hypersaline environmental conditions.

Acknowledgements

The authors thank PIBi/UENF for fellowship, FAPERJ (E-26/010.0011197/2019) for financial support, and UFG for the research partnership.

References

[1] Rodgers et al., 2005 Petroleomics: MS Returns to Its Roots. Analytical Chemistry 77, 22–27.

[2] Silva et al., 2020. Mechanistic insights into sulfur rich oil formation, relevant to geological carbon storage routes. A study using (+) APPI FTICR-MS analysis. Organic Geochemistry 17, 104067.

[3] Sakai et al., 2022. Analysis of biodegradation, thermal maturity and depositional environment of oils from the Sergipe-Alagoas Basin using petroleomics by ESI(-) FT-ICR MS. 30th International Meeting on Organic Geochemistry, Sep 2021.

[4] Schwark et al., 1990. Aromatic hydrocarbon composition of the Permian Kupferschiefer in the Lower Rhine Basin, NW Germany. Organic Geochemistry 16, 749–761.

XVI LATIN AMERICAN CONGRESS ON ORGANIC GEOCHEMISTRY
9 - 11 AUGUST, 2023
ARACAJU, SERGIPE, BRAZIL

LAESI mass spectrometry imaging as a tool to investigate a wettability alteration case in carbonate rock

Lorraine Louise G. C. de Araújo[a,b*], Gesiane da S. Lima[c], Lidya C. da Silva[c], Gabriel Franco dos Santos[c], Boniek G. Vaz[c], Regina Sandra V. Nascimento[b], Georgiana F. da Cruz[a]

[a]State University of the North Fluminense Darcy Ribeiro; [b]Federal University of Rio de Janeiro; [c]Federal University of Goiás

greco.lorraine@gmail.com

Introduction

Determining some properties such as wettability is important in reservoir evaluation. Understanding the way in which petroleum, rock and water interact and thus influence petroleum wettability, viscosity and the formation of features in reservoirs is a second application of reservoir geochemistry [1]. The technical literature demonstrates that acid and base interactions are one route in which crude oil components, specially asphaltenes and naphthenic acids, may alter the wetting properties of a rock surface. Recently, results [2] showed that CTAB is a commercial surfactant that can alter wettability and improve oil recovery from carbonate reservoirs. But still, there is a lack of direct application of mass spectrometry to characterize the distribution of these polar and non-polar crude oil components that may influence the wettability alteration studies. In this present work, laser ablation electrospray ionization mass spectrometry (LAESI) imaging has been used to investigate the class of components directly detected on the surface of a series of limestone outcrop after they passed through different treatments to promote wettability alteration.

Experimental

Wettability Alteration Tests. The wettability was evaluated by measuring the water contact angle on the limestone outcrop before (θ initial) and after (θ after) an aged process for 15 days at 333K in crude oil. In the sequence, a series of post-treatment with brine, cationic surfactant (CTAB) and three different cationic polysaccharides (HTPS 1,2,3) were conducted and had the contact angle determined (θ altered). All contact angle determinations were measured using a DSA100 Drop Shape Analyzer (Kruss Company, Germany) and measured towards a water drop at ambient pressure and 297K by sessile drop method. The left and right contact angle measurement was conducted four times and the average of measured values and the mean error bars were reported. Contact Angle values between 0° and 70° were classified as water-wet substrates, values between 70 and 105° as mixed-wet substrates and values higher than 105° indicated oil-wet substrates. The wettability alteration index (WAI) was calculated based on the Eq. 1 [3].

$$WAI = \frac{\theta_{aged} - \theta_{altered}}{\theta_{aged} - \theta_{initial}} \quad (1)$$

LAESI Analysis. The LAESI system consists of a pulsed IR optical parametric oscillator (IR Opolette, Opotek, Carslband) combined with the Omni Spray Ion Source 2D and the Thermo Scientific Q-Exactive Hybrid Quadrupole Orbitrapis and the analysis details have been described previously [4]. The rocks were mounted on the 2D moving stage, irradiated by a 3.4 µm IR laser beam at a 90° angle and ionized by a spray of charged droplets from an electrospray emitter positioned above the rock surface. The geometric parameters were optimized. A stable electrospray was obtained with MeOH (0.1% formic acid) at 2.0 µL/min and MeOH (0.1% ammonium hydroxide) at 1.5 µL/min with a spray voltage of 4.5 kV for positive and negative ion mode analyses, respectively. The maximum injection time was set to 100 ms.

Results and Discussion

Wettability Alteration Tests. The data in Table 1 summarized the average contact angles measured and the calculated WAI index. Initially, these carbonate surfaces expressed the water-wet state and the aging time in crude oil was efficient to do substrate wettability modifications from water-wet to oil-wet. According to the values of the contact angle measured after the solutions treatment process with HTPS and CTAB solutions, the carbonate surfaces went from oil-wet to a mixed-wet state.

Table 1. Contact angles results and WAI

Sample	$\theta_{initial}$	θ_{aged}	$\theta_{altered}$	WAI
HTPS 1	52.3± 1.3 (WW)	119.3±2.8 (OW)	103.6±1.4 (MW)	0.235
HTPS 2	**49.9±1.4 (WW)**	**122.4±0.9 (OW)**	**84.7±2.0 (MW)**	**0.520**
HTPS 3	59.1±0.9 (WW)	122.4±2.4 (OW)	102.0±2.6 (MW)	0.322
CTAB*	**32.6±1.4 (WW)**	**106.8±2.3 (OW)**	**82.6±2.2 (MW)**	**0.326**
Brine (3%NaCl)	52.9±2.8 (WW)	109.6±2.2 (OW)	109.5±1.5 (OW)	0.001

*CTAB concentration = 0.33% equal to 10CMC of CTAB; OW- oil wet; MW – mixed wet; WW- water wet

LAESI Analysis. LAESI positive ion mode detected and monitored the distribution of several organic compounds on the surface of carbonate rocks studied and their relative abundance distribution is shown in Figure 1.

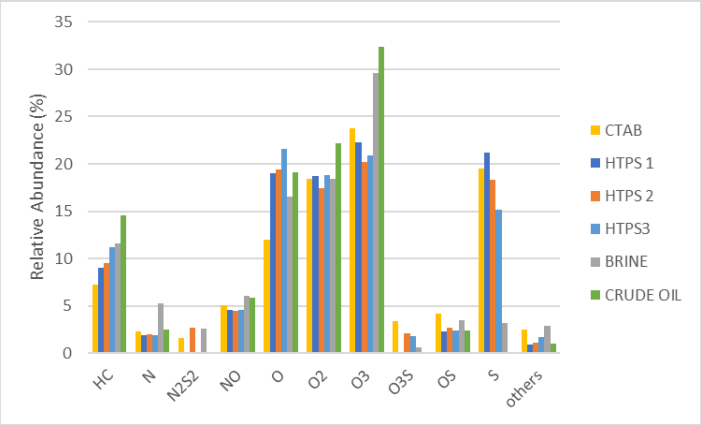

Figure 1. Heteroatom classes distribution in the rock surfaces

The treatment with brine, HTPS and CTAB solutions in the oil-wet rock surfaces caused differences in the species distribution when compared with the profile of the oil-wet surface without any treatment (crude oil sample). The brine should act more as a physical cleaning and be able to remove the weakly adsorbed compounds from the surface which reflect the lowest relative reduction of HC, NO and O3 classes and the increase in the relative abundance of N class when compared with the other treatment profiles. The more efficient cleaning promoted by the CTAB and HTPS solutions, observed previously, is corroborated by the increase of the relative abundance of suppressed ions from the crude oil sample as S, O3S and OS classes and the preferential removal of HC and O3 classes. The LAESI results were also processed and converted into heteroatom ratios (Table 2). The reduction in the O/C ratio observed mostly for the samples with HTPS and CTAB treatment indicated a reduction in polarity compounds detected on the rock´s surface. The use of these cationic chemical treatments promoted the modification of carbonate wettability through the preferential removal of polar compounds may be relationship with the formation of the ionic pair.

Table 2. Heteroatoms' ratios obtained from LAESI results.

Sample	H/C	N/C	O/C	S/C
HTPS1	1,37	0,01	0,12	0,01
HTPS2	**1,37**	**0,01**	**0,12**	**0,01**
HTPS3	1,38	0,01	0,12	0,01
CTAB	**1,37**	**0,01**	**0,13**	**0,01**
Brine	1,36	0,02	0,16	0,01
Crude oil	**1,36**	**0,01**	**0,18**	**0,00**

The results agree with previous reports of contact angle, which suggest that the HTPS could show a similar or even better result than the commercial surfactant CTAB, whereas brine appears to have a small effect on the rock surface cleaning up.

Conclusions

The LAESI results proved to be able to detect polar and non-polar compounds on carbonate rock surfaces which indicates the potential of this technique to support the investigation of wettability alteration. Therefore, this technique can be useful in studies of reservoir geochemistry together with reservoir engineering procedures.

Acknowledgements

The authors are grateful to PETROBRAS for the crude oil donations and for the financial support provided by FAPERJ and CAPES (Finance code 001).

References

[1] Larter, S. R.; Aplin, A. C. 1995. Reservoir geochemistry: methods, applications, and opportunities. Geological Society, London, Special Publications, **86**(1), 5–32.

[2] Rellegadla, S.; Jain, S.; Sangwai, J.; Lavania, M.; Gieg, B.; Rajasekar, A.; Bera, A.; Agrawal, A. 2021. Wettability Alteration of the Oil-Wet Carbonate by Viscosity-Augmented Guar Galactomannan for Enhanced Oil Recovery. ACS Appl. Polym. Mater., **3**(4), 1983–1994.

[3] Souraki,Y.; Hosseini, E.; Yaghodous, A. 2019 Wettability alteration of carbonate reservoir rock using amphoteric and cationic surfactants: Experimental investigation. Energy Sources, Part A: Recovery, Utilization, and Environmental Effects, **41**(3), 349-359.

[4] Pereira,I.; Ramalho, R.; Maciel, L.; Aguiar,D.; Trindade, Y.; da Cruz,G.; Vianna, A.; Júnior, I.; Lima, G.; Vaz, B. 2022. Directly Mapping the Spatial Distribution of Organic Compounds on Mineral Rock Surfaces by DESI and LAESI Mass Spectrometry Imaging. Analytical Chemistry **94** (40), 13691-13699.

XVI LATIN AMERICAN CONGRESS ON ORGANIC GEOCHEMISTRY
9 - 11 AUGUST, 2023
ARACAJU, SERGIPE, BRAZIL

Effect of biodegradation on crude oil mixing

BRUNO Q. ARAÚJO *, FERNANDA B. S. MAGALHÃES, BRUNO F. PAQUELI, CRISTINA M. S. SAD, PAULO R. FILGUEIRAS, EUSTAQUIO V. R. DE CASTRO

Universidade Federal do Espírito Santo, Departamento de Química, NCQP - LABPETRO, Vitória, Espírito Santo, ES, 29075-910, Brazil *

bquirinoa@gmail.com

Introduction

Numerous studies have been performed for the evaluation of the effects of biodegradation and oil mixing on biomarker profiles (LARTER et al., 2012; BENNETT et al., 2022). LÓPEZ et al. (2015) verified the distributions of *n*-alkanes, acyclic isoprenoids, the presence of prominent 25-norhopane combined with unresolved complex mixture (UCM), which are support for mixed and different biodegradation levels. In this sense, the present work evaluates the geochemical parameters and biomarkers from light and heavy crude oils and their mixtures for the understand as the biodegradation influences the blends of oils.

Experimental

Two Brazilian crude oils with ºAPI 16,8 ± 0,5 (OIL C) and 56,3 ± 0,1 (OIL F) and TAN (total acid number, mg KOH/g) of 3,35 ± 0,02 and 0,0055 ± 0,0004, respectively. The mixtures of crude oils were prepared in proportions of 100:0; 75:25; 50:50; 25:75; 0:100 (OIL C:OIL F, w/w). An aliquot of 50 mg of each sample was submitted to the fractionation into activated silica gel column to afford saturate, aromatic, and polar fractions by the elution with 10 mL of *n*-hexane, 10 mL of *n*-hexane/dichloromethane 9:1 (v/v) and 10 mL de methanol. The residual solvents were removed by reduced pressure on evaporative rotary. The saturated fractions were analyzed by gas chromatography coupled to mass spectrometry (GC-MS) using a Shimadzu QP2010 ultra equipped with VB5 capillary column (30 m, 320 µm id, 0,25 µm film ValcoBond®, Vici metronics). An aliquot (1 µL) was injected into split mode (10:1) at 300 ºC. The oven program was initial temperature of 70 ºC (2 min) and temperature ratio of 20 °C/min to 170 °C and then ratio of 3 °C/min to 300 °C (10 min). Helio was used with carrier gas at constant flow of 1.3 mL/min. The mass spectrometer with quadrupole (qMS) analyzer and electron ionization source (70 eV) operated in scan mode (50 to 600 Da) and solvent delay of 3 min. Total ion chromatogram (TIC) and mass spectra were obtained from GCMS solution/LabSolutions version 2.72 (Shimadzu). The identification of chemical compounds was performed based on elution order and mass spectral data. The geochemical rations were calculated based on peak area.

Results and Discussion

The evaluation of TIC from saturated fraction of oils C and F, and their mixtures showed the increase in the intensity of *n*-alkanes. In addition, the decrease of humps (Figure 1) and cyclic/branched compounds were observed with additional amount of OIL F.

It is important to note that trends on geochemical biomarkers were also observed with the oil mixing. The 25NH (EIC *m*/*z* 177)/H30 ratio shows values < 1 (OIL C, MIX 75C:25F and 50C:50F, w/w) and values <<1 for OIL F, which had highest intensity of *n*-alkanes (Figure 2). Moreover, a value of 25NH (EIC *m*/*z* 177)/H30 = 0.04 suggests absence of biodegradation and/or low intensity of 25NH.

The pristane (Pr/nC17) and phytane (Fi/nC18) and *n*-alkanes ratios indicated a high value for oil C, which may be associated to a low content of *n*-alkanes. On the other hand, blends with a higher contribution of OIL F showed lower values for these geochemical parameters, indicating an increase in the intensity of *n*-alkanes. This increase in the total ion chromatograms (TIC) of the 50C:50F, 25C:75F and OIL F in relation to the other samples can be observed mainly (*i*) by the increase in peak intensity (Y axis) and (*ii*) by the fact that the chromatographic peaks of *n*-alkanes are more prominent with increase in the proportion of light oil.

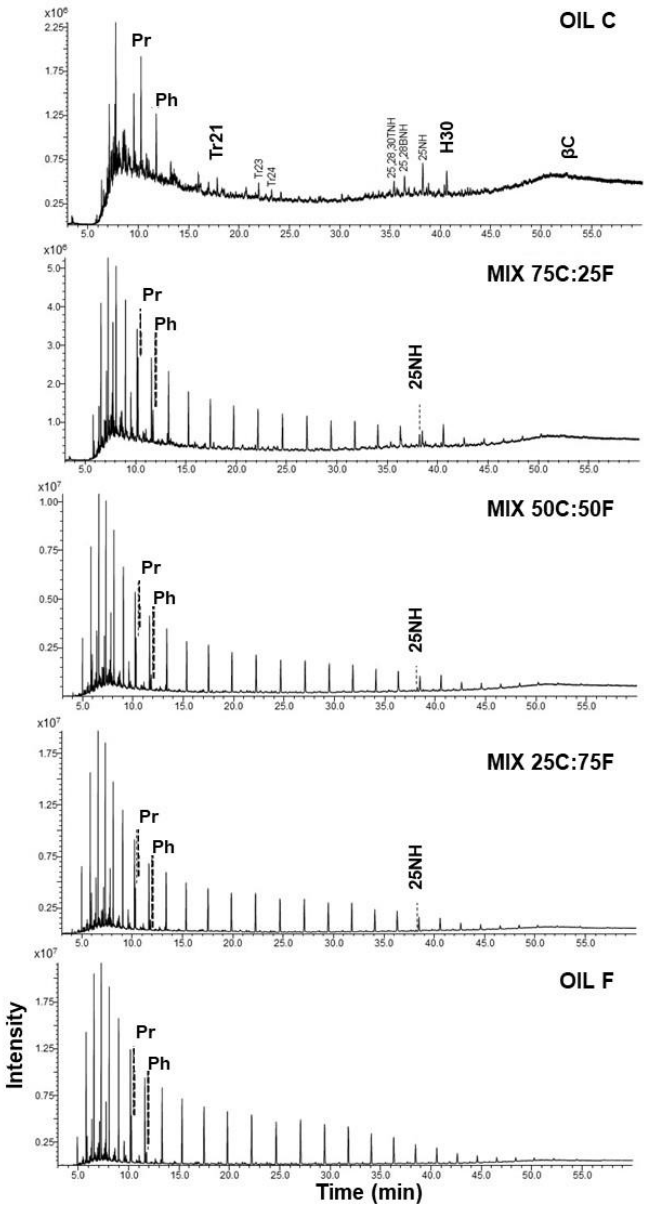

Figure 1. Total ion chromatograms of saturated fractions from crude oils C and F and their mixtures (oil C/F; 75/25; 50/50; 25/75, w/w). Pr – pristane, Ph – phytane, tricyclic terpanes – Trn (e.g., Tr21, Tr23, Tr24), hopanes (Hn), C_{30} 17α(H),21β(H)-hopane (H30), C_{29} 17α(H),21β(H)-25-norhopane (25NH). n – number of carbon atoms.

Conclusions

The hydrocarbon profiles of heavy and light crude oils and their mixtures show evidence of the effect of oil mixing and the dramatic changes in geochemical parameters. The oil mixing may be used as a general explanation for the differences in geochemical fingerprinting and the biomarker profiles from Brazilian crude oils.

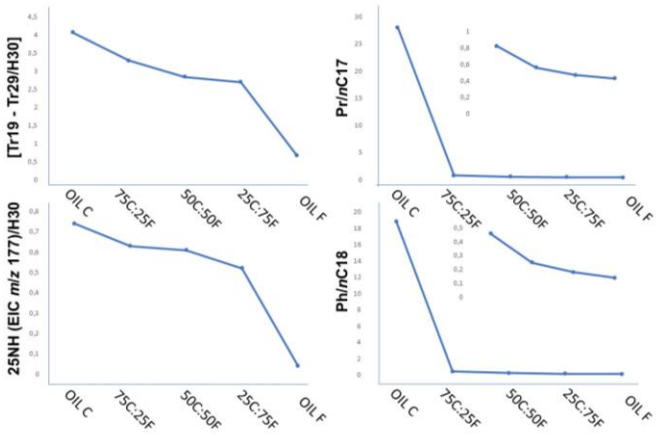

Figure 2. Trend on geochemical parameters from oil mixing: OIL C, OIL F and their mixtures.

Acknowledgements

The authors thank CNPq (Brazilian research council), CAPES and FAPES for fellowships and financial support.

References

Bennett, B.; Larter, S. R.; Taylor, P. N., 2022. Geochemical rationalisation for the variable oil quality in the Orcutt reservoir, California, USA. Organic Geochemistry **163**, 104348.

Larter, S. R.; Huang, H.; Adams, J.; Bennett, B.; Snowdown, L. R., 2012. A practical biodegradation scale for use in reservoir geochemical studies of biodegraded oils. Organic Geochemistry **45**, 66-76.

López, L.; Lo Mónaco, S.; Volkamn, J. K., 2015. Evidence for mixed and biodegraded crude oils in the Socororo field, Eastern Venezuela Basin. Organic Geochemistry **82**, 12-21

XVI LATIN AMERICAN CONGRESS ON ORGANIC GEOCHEMISTRY
9 - 11 AUGUST, 2023
ARACAJU, SERGIPE, BRAZIL

The impact of natural supercritical CO_2 on the chemical composition of in-reservoir oils

Thomas B.P. Oldenburg[1], Hossein Hosseini[1], Joelma P. Lopes[2], Ygor dos Santos Rocha[2], Igor V.A.F. de Souza[2]

[1]**University of Calgary, Canada; [2]Petrobras, Brazil**

toldenbu@ucalgary.ca

Introduction

The Santos Basin's pre-salt area is among the largest offshore petroleum systems in the South Atlantic margins and plays a vital role in Brazil's oil production. However, a major challenge in exploration and production programs is the wide range of CO_2 concentrations in the reservoirs, ranging from 0 to 96 mol%. A CO_2 distribution map reveals that the eastern part of the basin is a high-risk zone due to CO_2 levels up to 96 mol%. This research investigates the impact of CO_2 on the chemical composition of oil in the ultra-deep pre-salt reservoirs by analyzing oils from the Júpiter oilfield, one of the basin's primary CO_2-rich prospects. Isotopic analysis indicates that the source of CO_2 is mantle degassing.

Experimental

84 oils from 9 oil fields within the Santos Basin, offshore Brazilian were investigated in a larger study. The concentration of CO_2 in these oil fields varied largely. This presentation will focus on oil fields with highest CO_2 content and its impact on crude oil composition by using bulk composition, traditional GC-MS techniques and ultrahigh resolution mass spectrometry.

Results and Discussion

A compositional grading was observed in oil columns, resulting in an unusual fluid association with a dense gas and light oil on top, separated by a sharp boundary from the heavy oils in the lower parts. The light oils at the top section have the highest API gravity (34°), CO_2 concentration (77 mol%), and gas to oil ratio (>3200 m3/m3). However, these parameters gradually decrease with increasing depth in the lower heavy oil section. The compositional grading is attributed to phase segregation due to high concentrations of supercritical CO_2. The light oils had high concentrations of biomarkers, which is unusual for light oils formed through thermal cracking at high maturation levels. This suggests that the formation of the light oils in this study is due to compositional grading caused by an excess of supercritical CO_2, rather than thermal processes. Although both the light and heavy oils were confirmed to have a common source based on source-sensitive parameters, maturity indicators showed conflicting results. αββ-C29 steranes and phenanthrene-based indicators showed the highest maturation levels, while naphthalene- and dibenzothiophene-based parameters indicated the lowest maturation levels (Fig. 1-B). Molecular imbalances like this have been reported in oils from various locations worldwide (Curiale, 2002), but in this study, the imbalance is not due to migrating or trapped crude oil, but rather to supercritical CO_2 acting as a solvent and dissolving low molecular weight components, which ultimately led to the observed molecular imbalances.

The FTICR-MS analysis provided additional information about the chemical composition of the oils, which is closely linked to the amount of CO_2. The light oils are non-biodegraded and contain high levels of oxygenated components, with their concentrations directly correlated with the CO_2 content. Moreover, the intensities of the most abundant compound classes are highest at lower DBEs, indicating lower maturity levels (below the oil window). These results are consistent with the fact that supercritical CO_2 selectively dissolves low molecular weight components rather than thermogenic cracking causing the formation of these light oils. Therefore, caution must be exercised when interpreting geochemical results in discoveries with high concentrations of supercritical CO_2, as it can severely alter the molecular composition of the oils.

Conclusions

- Mantle-derived supercritical carbon dioxide (SCO_2) plays an important role in the Santos Basin.
- SCO_2 is responsible for the phase segregation that ultimately led to the unusual fluid association (e.g.,

'condensate'-like fluids on the top of heavy oils) in the oil columns and hence, changes in the chemical composition of both light and heavy oils due to its function as a solvent.

- Imbalances were observed particularly in the maturity-sensitive molecular parameters.
- Light oils are enriched in oxygenated species – unlikely in cases of thermogenic processes.
- Robust maturity indicators based on pyrrolic species indicate very low maturity (~0.50 Roe) for the light oils which must be induced by supercritical CO_2 functioning as a solvent.
- Relative abundances of N_1, O_1 and N_1O_1 classes are systematically changing with depth and CO_2 content variations, especially, the relative species abundances are found to be highest at lower DBEs as well as short alkylation degrees at highest CO_2 contents.
- This study demonstrates that higher concentrations of naturally occurring supercritical CO_2 in oil reservoirs have segregation effects and strongly impacts the molecular oil composition vertically throughout the reservoir, and hence, molecular geochemical process indicators may be compromised and to be used only with caution in those settings.

Acknowledgements

We thank the TESLA Phase II project sponsor (Petrobras) for their financial support and permission for publication. Aphorist Inc. is thanked for providing access to the FTICR–MS data analysis (CaPA) and visualization software Ragnarök.

References

Curiale, J.A., 2002. A review of the occurrences and causes of migration-contamination in crude oil. Organic Geochemistry 33, 1389–1400.

Nascimento, F.P., Pereira, V.J., Souza, R.P., Lima, R.C.A., Costa, G.M.N., Rosa, P.T. V, Forca, A.F., Vieira de Melo, S.A.B., 2021. An experimental and theoretical investigation of asphaltene precipitation in a crude oil from the Brazilian pre-salt layer under CO2 injection. Fuel 284, 118968.

Pedrosa Jr, O.A., Peres, W., Mello, M.R., Rostirolla, S.P., Carmo Jr, G., Branco, V., 2021. Challenges for reservoir management and field development in the pre-salt, Santos Basin, Brazil: Memoir 124. AAPG Special Volumes.

ALD

ISOTOPIC GEOCHEMISTRY

XVI LATIN AMERICAN CONGRESS ON ORGANIC GEOCHEMISTRY
9 - 11 AUGUST, 2023
ARACAJU, SERGIPE, BRAZIL

Comparative Analysis of Two Horizontal Wells in the Vaca Muerta Formation Using Stable Isotopes in Hydrocarbon Gases and Rock Geochemical Data

MARTÍN E. FASOLA [a*], **FEDERICO D. WEIBEL** [b]

[a]**YPF S.A.,** [b]**Instituto de Geocronología y Geología Isotópica (INGEIS), Argentina**

*correspondence**:** martin.fasola@ypf.com

*correspondence**:** fedeweibel@gmail.com

Introduction

The isotopic composition of carbon in hydrocarbon gases is capable of providing information that can be complemented with that obtained by other types of more conventional geochemical tests on rocks (%TOC, visual analysis of kerogen, pyrolysis). The characterization together of the isotopic composition with the molecular composition of a gas is capable of providing information about the origin and associated thermal maturity, as well as identifying migration or mixing processes between gases of different origin.

Experimental

This study presents a comparative analysis, taking as a starting point the results obtained in geochemical tests of total rock (pyrolysis and organic richness:%TOC) and in isotopic analyzes ($\delta^{13}C$) in geological control gases from two horizontal wells in the Vaca Formation. Muerta (shale) located in the same field within the Neuquén Basin, Argentina. The navigation of the wells was carried out on two different levels vertically separated by about 115 m. The samples analyzed for isotopic composition were 20 for well A and 20 more for well B. Also for geochemical test in rock sample were 7 samples for well A and 14 samples for well B.

Results and Discussion

The characterization of the gases from the isotopic composition ($\delta^{13}C$ - C_1 to C_4) allowed us to infer that in both wells it is a gas of thermogenic origin with thermal maturity associated with oil window [1]. The results of $\delta^{13}C$ in carbon dioxide also allow us to infer a thermogenic origin for it (-20 ‰ < $\delta^{13}C$ vs V-PDB < -18 ‰). The average isotopic composition of well A yields results of -48.9 ‰ $\delta^{13}C$ vs V-PDB for methane, -36.7 ‰ $\delta^{13}C$ vs V-PDB for ethane and -32.9 ‰ $\delta^{13}C$ vs V-PDB for propane. The average isotopic composition of well B results in -51.2 ‰ $\delta^{13}C$ vs V-PDB for methane, -37.9 ‰ $\delta^{13}C$ vs V-PDB for ethane and -33.9 ‰ $\delta^{13}C$ vs V-PDB for propane. These results allow us to affirm that these are two gases with different compositions or isotopic families. In Figure 1, the Chung's [2] plot can show these differences.

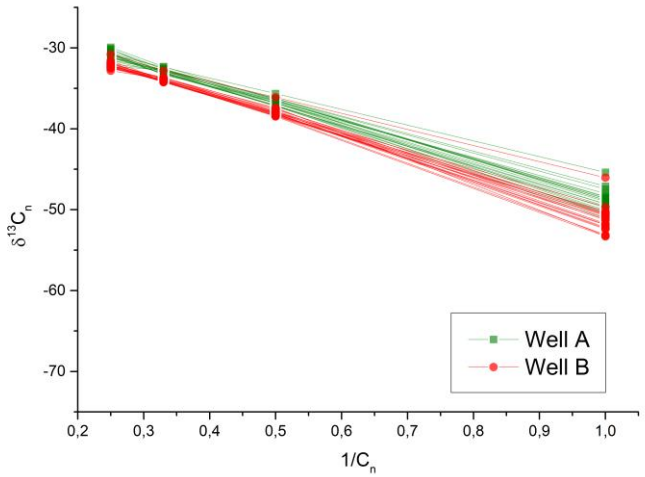

Figure 1. Chung's plot showing the differences in the two set of samples from well A and well B. Isotopic compositions suggest that maturity in A is greater than in B.

The results from geochemistry analysis for Well A (7 samples) are presented as mean ± standard deviation. This has the following results: TOC (%) = 3.7 ± 0.5; Tmax= 449.4 ± 1.4°C; HI = 128 ± 7 mg HC/g TOC and S_2= 4.7 ± 0.8 mg HC/g TOC. The results for well B (14 samples) are presented in the same way: TOC (%) = 5.0 ± 1.6; Tmax = 448.2 + 0.7°C; HI = 203 ± 15 mg HC/g TOC and S_2= 10.3 ± 3.6 mg HC/g TOC. Although the data present a certain dispersion, it can be observed that well B goes through levels with higher organic carbon content, the S_2 peak is also higher (and therefore a higher HI). so it can be inferred that it is of two levels with differences in

thermal maturity (A>B), which agrees with the vertical layout of the wells.

In addition, this geochemical differentiation is key in the identification of vertical communication or interferences between the levels or reservoirs contacted by both wells, which is key in the development of unconventional shale-type reservoirs.

Conclusions

In this work, we used two approaches to understand differences within same source rock in two different horizontal wells: a) the carbon isotopic composition for gases and b) rock geochemical analysis. The results showed that they could be complementary to highlight differences, as can be seen in Figure 2. In addition, another couple of variables can be used to illustrate differences and make predictions about the type of fluid to be produced.

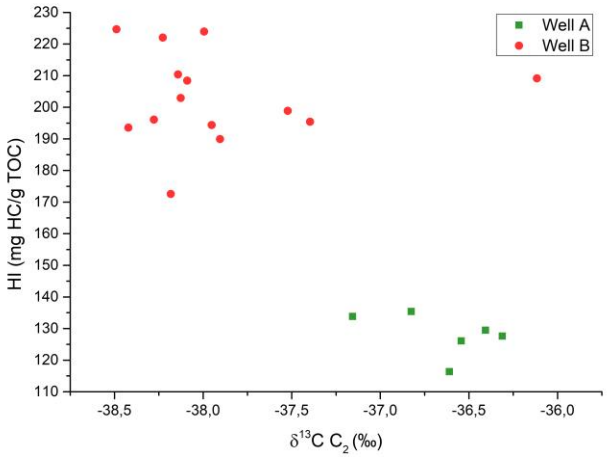

Figure 2. Two variables plot using Hydrogen Index (y-axis) and ethane carbon isotopic composition (x-axis) to illustrate same way variation to understand differences.

Acknowledgements

The authors thank YPF S. A. and INGEIS for the authorization to publish this paper

References

[1] Milkov, A. V., Etiope, G. 2018. Revised genetic diagrams for natural gases based on a global dataset of> 20,000 samples. Organic Geochemistry, 125, 109-120.

[2] Chung, H. M., Gormly, J. R., Squires, R. M. 1988. Origin of gaseous hydrocarbons in subsurface environments: theoretical considerations of carbon isotope distribution. Chemical Geology, 71(1-3), 97-104.

XVI LATIN AMERICAN CONGRESS ON ORGANIC GEOCHEMISTRY
9 - 11 AUGUST, 2023
ARACAJU, SERGIPE, BRAZIL

ELEMENTAL AND ISOTOPIC COMPOSITION OF SEDIMENTARY ORGANIC MATTER FROM PARANAGUÁ ESTUARINE SYSTEM

MARINES M. WILHELM[a,*], ANA LÚCIA LINDROTH DAUNER[c], MARCIA CARUSO BÍCEGO[d], MICHEL MICHAELOVITCH DE MAHIQUES[d], CÉSAR C. MARTINS[b,d,*]

[a] GRADUATE PROGRAM IN COASTAL AND OCEANIC SYSTEMS (PGSISCO), FEDERAL UNIVERSITY OF PARANÁ, BRAZIL.

[b] CENTER FOR SEA STUDIES, CAMPUS PONTAL DO PARANÁ, FEDERAL UNIVERSITY OF PARANÁ, BRAZIL.

[c] ECOSYSTEMS AND ENVIRONMENT RESEARCH PROGRAM, UNIVERSITY OF HELSINKI, FINLAND, BRAZIL.

[d] OCEANOGRAPHIC INSTITUTE, UNIVERSITY OF SÃO PAULO, BRAZIL.

e-mail , * wilhelm.marines@gmail.com, * ccmart@usp.br

Introduction

The organic matter (OM) present in estuarine sediments is a complex mixture, in different states of degradation, and consist of autochthonous and continental material. The allochthonous material comes from the surface runoff of drainage basins and includes agricultural, forestry and urban areas [1]. The Paranaguá Estuarine System (PES) plays an important ecological and economic role for the coastal zone of Brazil. It is home to relevant remaining areas of the Atlantic rainforest, considered a World Heritage Site by UNESCO. At the same time, PES accommodates the largest bulk port and the first place in container handling in Latin America. Thus, the understanding and the distinction of main sources of sedimentary OM becomes fundamental to evaluate the environmental quality of this important estuarine system in Brazil. The objective of this study was to study the spatial distribution of OM composition in surface sediments, using the elemental and isotopic composition of OM as geochemical tools. This study generates information that contributes to the understanding of local alterations in biogeochemical cycles, in the processes of material transfer between continent and estuary, as well as trying to elucidate general aspects of the current scenario of environmental quality in the PES.

Material and Methods

Surface sediments (0 - 3 cm) from the E-W and N-S axes in PES were collected in two sampling campaigns: the first carried out in March 2018, and the second in April 2019. The material was collected with a Van Veen-type dredger. The collected material was placed in aluminum containers, previously calcined in a furnace, and then frozen at -20 ºC. The samples were then freeze-dried, gently macerated, and stored in previously decontaminated glass vials according to the procedure described above.

In total, 82 samples of surface sediment were analysed. The total organic carbon (TOC) and total nitrogen (TN) contents and their respective isotopic ratios ($\delta^{13}C$ and $\delta^{15}N$) were determined using the elemental analyzer (EA) *Costech Elemental Combustion System*, coupled to the isotopic ratio mass spectrometry detector *Thermo Scientific Delta V Advantage Isotope Ratio MS* (IRMS). The granulometric analyzes were carried out in a granulometer *Malvern Hydro 2000,* using 2 g of sediments from each sample, and to obtain the percentages of gravel, sand, silt, and clay from each sample were obtained by the *Software Sysgram* 3.2.

Results and Discussion

The percentages of sand, silt, and clay in the samples varied between 1.0 and 100.0 % (mean= 55.1 ± 30.8); 0.0 a 77.0 % (mean = 35.2 ± 24.5) e 0.0 a 45.3 % (mean = 9.7 ± 7.9), respectively. The predominant grain size in these samples was sand, followed by silt and clay, as previously presented by Angeli *et al*. (2020). Based on granulometry and hydrodynamics, PES presents intrinsic characteristics for each bay. The upstream section, located in Antonina Bay, receives greater fluvial influence and, therefore, has a higher content of fine sediments than the other sections. In the intermediate section of PES, the fluvial influence and the marine contribution predominate, with a lower content of fine fractions. The outter section (downstream) has a greater marine influence and, consequently, there is a predominance of sand. The TOC and TN contents in the samples varied between 0.10 a 4.70 (mean = 1.60 ± 1.27) and 0.02 a 0.43 (mean = 0.15 ± 0.12). The TOC/TN ratio (or simply C/N) ranged from 5.0 to 17.9 (mean = 11.3 ± 2.8).

The values of the $\delta^{13}C$ and $\delta^{15}N$ ranged from -27.15 to -22.88 ‰ (mean = - 25.24 ± 0.93) and from 1.99 to 12.96‰ (mean = 5.15 ± 2.14), respectively. The C/N ratio values showed a spatial distribution similar to that of fine sediments. Higher values are associated with the presence of material produced by terrigenous plants, once they are rich in cellulose and poor in proteins. [2]. The predominance of OM of terrigenous origin occurred in specific locations in the upper and intermediate parts of the estuary, followed by a mixture of sources. The samples that presented OM of marine origin (algae, phyto- and zooplankton) predominated at the mouth of the PES and in sites of Laranjeiras Bay, a place of high energy and closer to the shallow platform. The highest values of TOC and TN present distribution patterns similar to that of fine sediments, being accumulated mainly on the north bank of the E-W axis of the estuary, which are low energy sites, which facilitates deposition (Fig. 1).

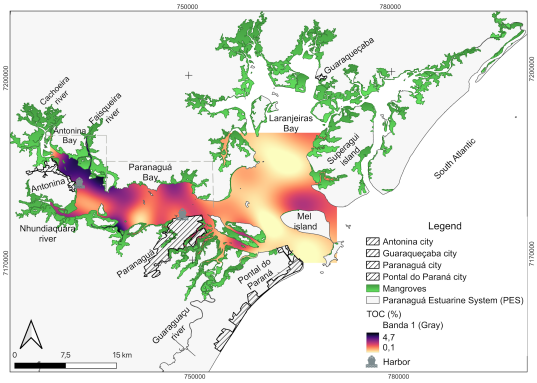

Figura 1. Total organic carbon (TOC) distribution map in the Paranaguá Estuarine System.

The spatial distribution of $\delta^{13}C$ *vs* C/N values showed that the CEP has sites with sediments rich in terrigenous OM, originating from mangrove vegetation, close to the estuary margins. However, most of the samples suggest that there is a predominance of mixture of terrigenous and marine sources, as shown by the Fig. 2. Two sites (46 and 66) had C/N ratio values lower than expected for OM from planktonic organisms. As this is a place with intense vessel traffic and constant dredging of the main access channel to the port, such events can cause disturbance of the bottom in this region, favoring the aerobic degradation of the OM and reducing the values of the C/N ratio, making with values compatible with the presence of bacteria. The $\delta^{13}C$ isotopic ratio, together with the C/N ratio, allows identifying the samples with the greatest influence on indigenous OM production, as they present an enrichment of $\delta^{13}C$. The sector of the PES that presented the greatest influence of phytoplankton was the mouth estuary and the Laranjeiras Bay, as shown by the Fig. 2.

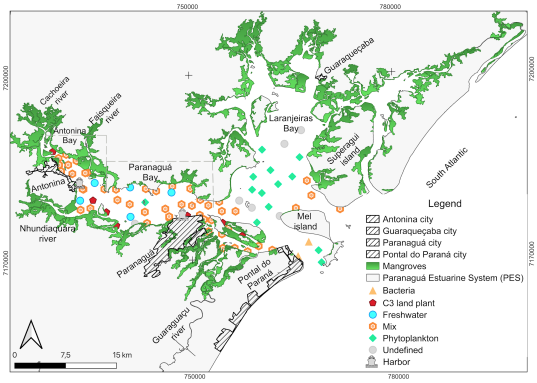

Figura 2. Spatial distribution of the main OM sources presented in the Paranaguá Estuarine Complex according to the scatter plot of $\delta^{13}C$ vs C/N.

Conclusions

PES is an environment characterized by intense anthropic activity although it is classified as a Natural Reserve by UNESCO. The results show that the main origin of the OM is the terrigenous contribution, due to the fluvial influence that, together with tidal currents, dominates the hydrodynamics of the estuary. The mouth region and Laranjeiras Bay have a strong influence of marine OM. It was also observed that the local hydrodynamics controls the deposition of OM in the Antonina Bay due to the low energy, which favors the deposition of fine sediments in this region. In Paranaguá Bay, due to the mixing zone in the intermediate portion of the estuary, there are sites of preferential accumulation of OM due to the flocculation of fine materials and the presence of the maximum turbidity zone. The next steps of this study intend to study sediment cores in this region in order to understand if the variability in OM sources over time can be associated with increasing human activity over the last few centuries.

Acknowledgements

This work was carried out with the support of Coordenação de Aperfeiçoamento de Pessoal de Nível Superior (CAPES). C.C. Martins e M.M. Mahiques thanks the CNPq (Conselho Nacional de Desenvolvimento Científico e Tecnológico) for financial support (441265/2017-0).

References

[1] Canuel, E.A., Hardison, A.K. (2016). Sources, ages, and alteration of organic matter in estuaries. Annual Review of Marine Science, 8, 409-434.

[2] Meyers, P. A. 1994. Preservation of elemental and isotopic source identification of sedimentary organic matter. Chemical geology, 114(3-4), 289-302.

ELEMENTAL AND ISOTOPIC COMPOSITION OF SEDIMENTARY ORGANIC MATTER FROM ADMIRALTY BAY (KING GEORGE ISLAND, ANTARCTICA)

VIVIANE KORRES BISCH[a,*], SATIE TANIGUCHI[b], MARCIA CARUSO BÍCEGO[b], RAFAEL ANDRÉ LOURENÇO[b], AMANDA CÂMARA DE SOUZA[b], CESAR DE CASTRO MARTINS[a,b,*]

[a] CENTRO DE ESTUDOS DO MAR, UNIVERSIDADE FEDERAL DO PARANÁ, BRASIL

[b] INSTITUTO OCEANOGRÁFICO, UNIVERSIDADE DE SÃO PAULO, BRASIL.

Correspondence: vivikorres@gmail.com, ccmart@ufpr.br

Introduction

The elemental (C, N) and the stable isotopes ($\delta^{13}C$ and $\delta^{15}N$) composition are important geochemical tools to understand the physical and biogeochemical environmental processes and even the Earth's paleoclimatic conditions (Corbett et al., 2015). The Antarctica Peninsula region is considered one of the few relatively preserved areas on Earth. The ecological and cryospheric systems of the Antarctica environment respond dynamically to the environmental changes occurring on a local and global scale. Despite of this importance, the knowledge of the sedimentary organic carbon cycle and the isotopic composition of organic matter (OM) in marine Antarctica sediments is limited (Monien et al., 2011). Therefore, this study analysed the elemental and isotopic composition of surficial sediments from different regions of Admiralty Bay, King George Island, Antarctica, in order to evaluate the main sources of OM for the region.

Experimental

Surface sediment samples (0 – 2 cm) were collected at 17 sites in the three inlets of Admiralty Bay (Martel, Mackelar, and Ezcurra Inlets – Fig. 1) using a Van Veen stainless steel bottom sampler. Sediments were frozen immediately after the sampling, freeze-dried, and homogenized before analyses. For the determination of $\delta^{15}N$ and the percentage of total nitrogen (TN), about 6 - 8 mg of dry samples were weighed, placed in tin capsules, and measured in an elemental analyser (EA) Costech coupled with an isotopic ratio mass spectrometer Thermo-Finnigan IRMS Delta V Plus. For the determination of $\delta^{13}C$ and total organic carbon (TOC), sediments were treated with 2 mL of HCl (1 mol L^{-1}) to remove inorganic carbon. After that, sediments were repeatedly washed with Milli-Q water until pH ~7 and dried before being placed in the tin capsules.

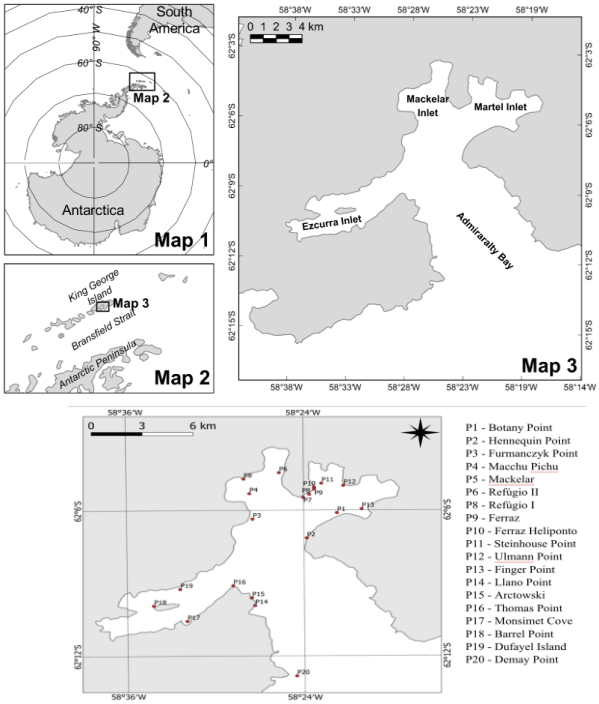

Fig. 1. Location of the study area (Map 1: Antarctica; Map 2: King George Island; Map 3: Admiralty Bay) and sampling sites.

Results and Discussion

The mean TOC in Admiralty Bay was 0.44 ± 0.29%, ranging from 0.09 (P15) to 0.99% (P11). The TN presented an average of 0.07 ± 0.05%, with the highest value of 0.18% in P10 and the lowest (0.01%) near the Peruvian Machu Picchu station (P4). The proxy TOC/TN ratio (represented as C/N) presented a mean value of 8.5 ± 3.7, varying from 2.5 (P16) to 16.0 in P1 (Fig. 2).

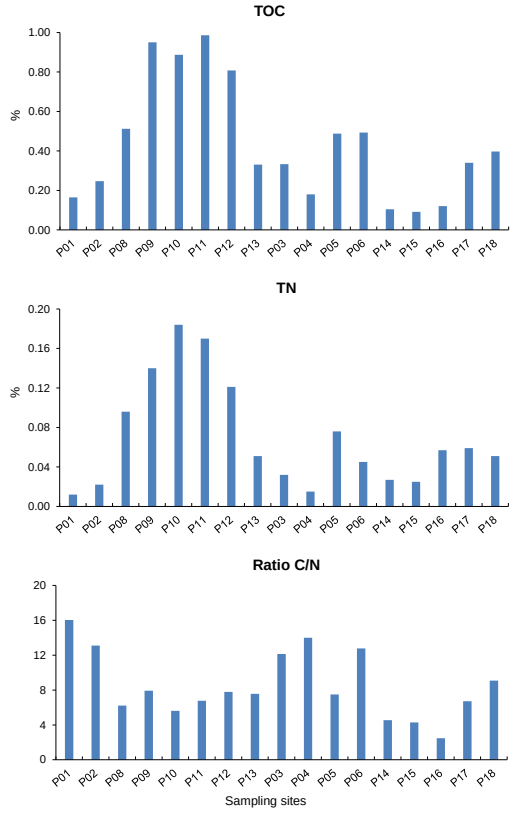

Fig. 2. Distribution of %TOC, %TN and C/N ratio to the Admiralty Bay, Antarctica surficial sediments.

For $\delta^{13}C$, the mean value was -23.05 ± 2.14‰, with the lowest value of -25.88‰ in P3 and the highest of -18.42‰ in P13. The $\delta^{15}N$ presented an average of 7.46 ± 8.65‰, with a minimum of -10.42‰ in P14 and a maximum of -22.66‰ in P1.

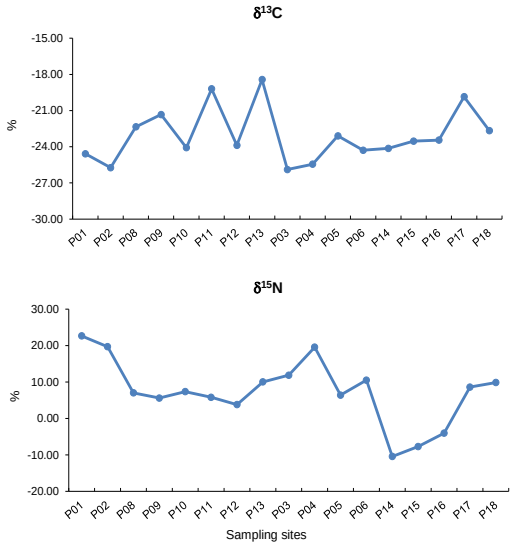

Fig. 3. Distribution of $\delta^{13}C$ and $\delta^{15}N$ to the Admiralty Bay, Antarctica surficial sediments.

The $\delta^{13}C$ results show that the OM may have its origin in Antarctic lichens, mosses, algae, planktonic grazers, and phytoplankton in the Antarctic Ocean. The C/N ratio indicates multiple sources of OM, varying locally to each inlet. The $\delta^{15}N$ values higher than 7‰ are significantly influenced by marine mammals and other organisms, except for the Ezcurra Inlet sites, which may present sediments enriched with seabird excrement (Liu et al., 2006; Muniz et al., 2018).

Conclusions

The carbon and nitrogen elemental and isotopic compositions of the sediments from Admiralty Bay indicated a variety of sources, such lichens, mosses, algae, planktonic grazers, and phytoplankton as the main contributors to the sedimentary OM of this region, and animal excrements may be also an important source.

Acknowledgements

The work was supported by the Antarctic Brazilian Program (PROANTAR) and National Council for Research and Development (CNPq, 442692/2018-8). The authors wish to thank the Brazilian Antarctic Station staff for their support during the sampling program. Finally, this work is part of the CARBMET project (The multiple faces of organic CARBon andMETals in the sub-Antarctic ecosystem) sponsored by CNPq, CAPES, and the Brazilian Ministry of Science, Technology, and Innovation (MCTI).

References

Corbett, P.A., King, C.K., Mondon, J.A., 2015. Tracking spatial distribution of human-derived wastewater from Davis Station, East Antarctica, using δ ^{15}N and δ ^{13}C stable isotopes. Marine Pollution Bulletin. 90, 41-47.

Liu, X.D., Li, H.C., Sun, L.G., Yin, X.B., Zhao, S.P., Wang, Y.H., 2006. $\delta^{13}C$ and $\delta^{15}N$ in the ornithogenic sediments from the Antarctic maritime as palaeoecological proxies during the past 2000 yr. Earth Planet. Sci. Lett. 243, 424–438.

Monien, P., Schnetger, B., Brumsack, H.R., Hass, H.C., Kuhn, G., 2011. A geochemical record of late Holocene palaeoenvironmental changes at King George Island (maritime Antarctica). Antarctic Science 23, 255-267.

Muniz, M. C., Anjos, R. M., Cardoso, R. P., Rosa, L. H., Vieira, R., Marotta, H., Macario, K., Ayres Neto, A., Felizardo, J. P., Barbosa, C. D. N., Rodrigues, L. F., Alves, E. Q. (2018). Post-caldera evolution of Deception Island (Bransfield Strait, Antarctica) over Holocene timescales. Palaeogeography, Palaeoclimatology, Palaeoecology, 501, 58-69.

XVI LATIN AMERICAN CONGRESS ON ORGANIC GEOCHEMISTRY
9 - 11 AUGUST, 2023
ARACAJU, SERGIPE, BRAZIL

STUDY OF ^{13}C MOLECULAR AND ISOTOPIC BEHAVIOR DURING IN SITU BIOREMEDIATION OF N-ALCANES PRESENT IN OIL CONTAMINATED MANGROUND SEDIMENT

NAIANA DIAS DOS SANTOS* / MARIA DO ROSÁRIO ZUCCHI* / JOSÉ ROBERTO BISPO DE SOUZA / DANÚSIA FERREIRA LIMA / ALEXANDRE BARRETO COSTA

* Correspondence: naiana.dias@ufba.br; mrzucchi@ufba.br

INTRODUCTION

The study of molecular and isotopic variations in petroleum hydrocarbons is an essential tool to observe bioremediation processes. In accidents involving oil spills these geochemical analyzes can be fundamental to estimate qualitatively and quantitatively the action of degrading agents in acting in the decontamination of environmental matrices using methods based on physicochemical biotechnological processes. This work aimed to study the molecular and isotopic compositions of carbon as a significant factor on the magnitude and direction of n-alkanes degradation in bioremediation test.

EXPERIMENTAL

The degradation test was performed in a prototype temporary immersion bioreactor, as shown in Figure 1, where it was possible to perform the combination of biostimulation and bioaugmentation processes.

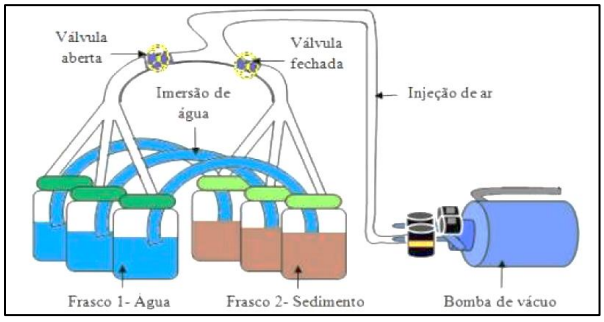

Figure 1. Schematic drawing of the temporary immersion bioreactor system.

The experiment was composed of mixed microbial consortium encapsulated with coconut fiber and oil from the Recôncavo Basin.

The evaluation of the removal efficiency of linear alkanes, as well as the carbon isotopic analysis of the samples were carried out for the times of 30, 60 and 90 days of degradative process.

The saturated fraction of the oil was extracted for qualitative and quantitative analysis of organic compounds by GC-FID and subsequent investigation of $\delta^{13}C$ by GC-IRMS. It was possible to observe, by means of the efficiency rate, the decrease in the concentration of the linear alkanes (n-C_{16} to n-C_{30}).

To observe the relationship between the residual concentrations of the n-alkanes with their isotopic ratios the Rayleigh equation (Equation 1) was used.

Equation 1. $$\frac{R_t}{R_0} = f^{(\alpha-1)}$$

Where R0 and Rt are the carbon isotope ratios at the initial time (0) and at the given time (t), f the fraction of the remaining compound and α the fractionation factor.

RESULTS AND DISCUSSION

The treatment with biostimulus and bioenhancement caused a removal percentage higher than 50% for alkanes from n-C_{15} to n-C_{30}. In this research project, the results showed a considerable variation between the isotopic values of the control oil for each established time interval. Some alkanes were found to have ^{13}C depletion when compared to the control oil.

The chromatographic profiles, figure 2, corroborated with the calculated isotopic values, demonstrating that those more recalcitrant compounds were the ones that presented lower removal efficiency, as well as lower changes in carbon isotopic ratios.

It was found that the alkanes (C_{16} to C_{27} and C_{29}), figure 3, showed ^{13}C depletion when compared to the control oil. Some long-chain alkanes (C_{27}, C_{28} and C_{30}) during treatment showed isotopic enrichment, presenting more positive values compared to the control oil. This may be

an indication that the isotopic composition may not be significantly affected by the microbial action of the mixed biostimulated consortium, but by other physical processes linked to the treatment, such as sorption, volatilization and diffusion, thus causing depletion rather than isotopic enrichment.

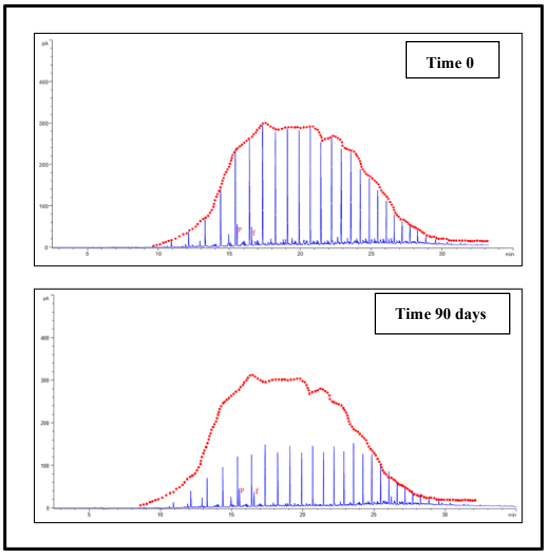

Figure 2: Chromatographic profiles of n-alkanes evaluated during treatment by biostimulation and bioaugmentation at initial and final time.

Rayleigh fractionation indicated a negative linear correlation of isotopic ratios versus molecular concentrations, with a correlation coefficient of 0.84; as well as the Pearson correlation coefficient which ranged from 0.92. The enrichment factors ranged from -0.27 to -0.05‰.

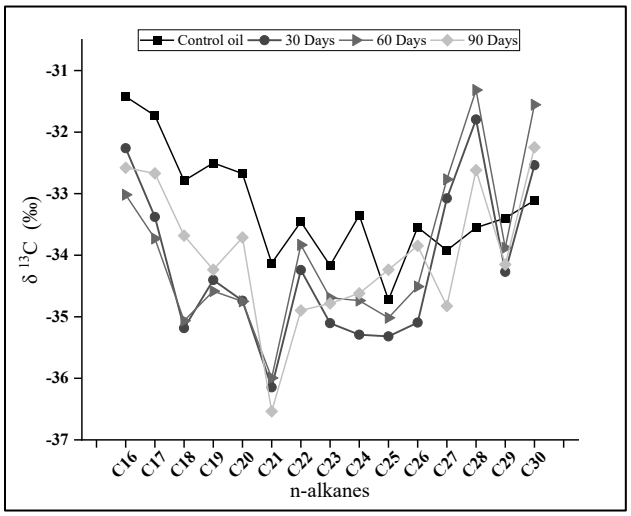

Figure 3. Distribution of $\delta^{13}C$ values of individual n-alkanes in control oil and oil after degradation with biostimulus and bioenhancement for 30, 60 and 90 days.

CONCLUSIONS

The results presented in this study indicate that carbon isotope fractionation can be used to distinguish between biochemical reactions and physical processes present in bioremediation treatments under biostimulation and bioenhancement. The relationship between concentrations and isotopic values made it possible to understand the direction and magnitude of the carbon isotope effect on partitioning linked to the degradation of organic contaminants such as petroleum hydrocarbon contamination in marine environments.

ACKNOWLEDGMENTS

To FAPESB and CAPES for the support granted for the development of this research project.

REFERENCES

ABENA, M.T.B.; SODBAATAR, N.; DAMDINSUREN, T. N.; CHOIDASH, B.; ZHONG, W. Crude oil biodegradation by newly isolated bacterial strains and their consortium under soil microcosm experiment. **Applied biochemistry and biotechnology**, v. 189, n. 4, p. 1223-1244, 2019.

AELION, C. M.; HUNKELER, D.; ARAVENA, R. (Ed.). **Environmental isotopes in biodegradation and bioremediation**. CRC Press, 2010.

AZUBUIKE, C. C.; CHIKERE, C. B.; OKPOKWASILI, G. C. Bioremediation: An eco-friendly sustainable technology for environmental management. In: **Bioremediation of Industrial Waste for Environmental Safety**. Springer, Singapore, p. 19-39, 2020.

BOLL, M.; ESTELMANN, S.; HEIDER, J. Anaerobic degradation of hydrocarbons: mechanisms of hydrocarbon activation in the absence of oxygen. **Anaerobic utilization of hydrocarbons, oils, and lipids**, p. 3-29, 2020.

CHEN, B.; YE, X.; ZHANG, B.; JING, L.; LEE, K. Marine oil spills—Preparedness and countermeasures. **World Seas: An Environmental Evaluation**, p. 407-426, 2019.

DANTAS, C. P. **Utilização de protótipo de biorreator de imersão temporária na biodegradação de petróleo em sedimento de manguezal**. Dissertação (Mestrado em Geoquímica do Petróleo e Meo Ambiente) – Instituto de Geociências- Universidade Federal da Bahia - UFBA. Salvador, 2017.

RAYLEIGH, L. L. Theoretical considerations respecting the separation of gases by diffusion and similar processes. The London, Edinburgh, and Dublin Philosophical Magazine and **Journal of Science**, v. 42, n. 259, p. 493-498, 1896.

XVI LATIN AMERICAN CONGRESS ON ORGANIC GEOCHEMISTRY
9 - 11 AUGUST, 2023
ARACAJU, SERGIPE, BRAZIL

Stable Isotope Analysis of Benzoic Acid Using Electrospray Orbitrap Mass Spectrometry

Gabriel F. dos Santos [a], Gesiane S. Lima [a], Giovanni B. Bevilaqua [a], Nerilson M. Lima [a], Rodrigo C. da Silva [b], Alexandre A. Ferreira [b], Boniek G. Vaz [a*]

[a] Chemistry Institute, Federal University of Goiás, Goiania, Gois, 74690-900, Brazil

[b] CENPES, PETROBRAS, Rio de Janeiro, RJ, 21941-915, Brazil.

E-mail: gfs.dossantos@gmail.com

Introduction

Stable isotopes have been used for decades to elucidate petroleum accumulations' geochemical aspects and support basin modeling. Specifically, the total isotopic composition from specific H, C, and S compounds has been used for paleodepositional environment studies, thermal evolution, biodegradation, oil-oil, and oil-rock correction studies (Eiler, 2007).

Conventional isotope ratio determination requires the analyte's initial conversion to a simple molecular gas such as CO_2, H_2, or N_2 for the isotope ratio measurement (Zeichner et al., 2022). Thus, the resulting isotopic ratio represents an average for a given element over the entire molecule or the sample as a whole (Eiler et al., 2017). These techniques sacrifice the study of variation at a specific molecular position and measurements of clumped information that can improve existing interpretations or enable new applications.

Developing isotopic ratio analysis using high-resolution mass spectrometers with Fourier transform, such as Orbitrap-type equipment coupled to an ESI ionization source, has significantly expanded the diversity of molecules capable of being analyzed. These advanced instruments offer exceptional accuracy and precision, enabling the resolution of numerous isobaric species in compounds containing H, C, N, O, and S.

Recently, there has been a growing emphasis on developing and evaluating the Orbitrap system for Isotopic Ratio measurements of polar compounds. Notably, studies have focused on isotopic analysis of compounds such as acetate, nitrate, phosphate, caffeine, and others. These investigations have explored the performance and capabilities of Orbitrap-based instruments for high-precision isotopic measurements. Prominent works by Neubauer et al. (2020), Hilkert et al. (2021), and Mueller et al. (2022) have contributed to advancing our understanding of isotopic analysis using Orbitrap analyzers and their application to different molecular systems. To date, no studies have explored the isotopic ratios of organic compounds in the context of petroleum geochemistry using the Orbitrap system. This study aims to fill this research gap by introducing a pioneering method for analyzing the isotopic ratios of carboxylic acids, with a focus on benzoic acid as a proof-of-concept, using ESI-Orbitrap MS. By showcasing the application of this method to organic acids, the research paves the way for future investigations into the isotopic analysis of organic acid biomarkers within the field of petroleum geochemistry.

Experimental

Chemicals

Benzoic acid analytical standard was purchased from Sigma-Aldrich, and benzoic acid isotopic reference from the International Atomic Energy Agency (IAEA).

Análise por ESI-Orbitrap MS

Mass spectrometry was analyzed using a Q-Exactive Orbitrap (Thermo Scientific, Germany) coupled to a commercial electrospray (ESI) source. Analyzes were performed in negative ionization mode. The parameters used for the analysis were: spray voltage 3.0 kV, capillary temperature 320 °C, S-lens 50, and AGC 5e5.

Results and Discussion

First, an analytical standard of benzoic acid was used to develop an ESI-Orbitrap MS method to analyze petroleum acid biomarkers. Figure 1 shows the ESI(-)-Orbitrap MS spectrum of benzoic acid, encompassing the *m/z* range of 120 to 124.

The mass spectrum exhibited the M0, M1, and M2, where M0 is the ion $C_7H_5O_2^-$, M1 is the ion $C_6{}^{13}CH_5O_2^-$, and M2 is the ion $C_7H_5O^{18}O^-$. However, due to the limitations in the resolution of the Orbitrap system, the ^2H isotopologue coeluted with ^{13}C and ^{17}O.

Based on the studies by Hilkert et al. (2021) and Mueller et al. (2022), a dual inlet system with a divert valve was constructed for stable isotope analyses. This study analyzed samples of benzoic acid obtained from Sigma Aldrich in blocks, alternating with reference samples of

benzoic acid from an international isotope exchange (IEA) reference. The analysis was conducted for 35 minutes, divided into 7 blocks of 5 minutes each, with 3 blocks dedicated to the samples and 4 blocks to the reference. The Total Ion Chromatogram (TIC) representing this analysis is depicted in Figure 2.

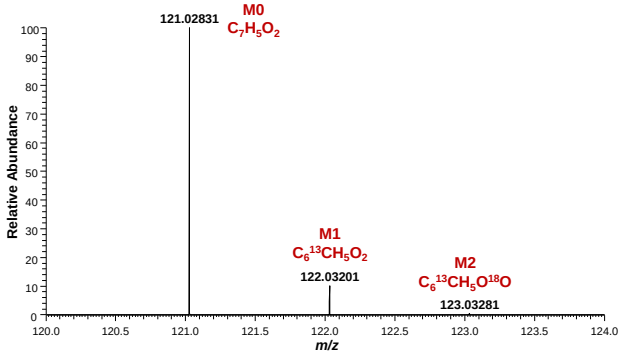

Figure 1. ESI(-) Orbitrap mass spectrum of benzoic acid where the ions M0, M1 and M2 has been observed.

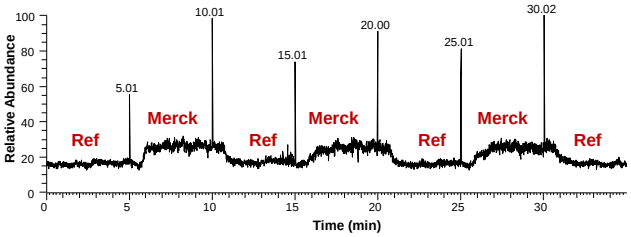

Figure 2. TIC obtained by 35 min analysis of benzoic acid using ESI(-)-Orbitrap MS.

A custom-built IsoX software module of the Thermo Fisher Scientific was used for the unsupervised extraction of ion counts from RAW files. After extraction of ion counts, the site https://isoorbi.shinyapps.io/IsoXL/ were used to calculate the isotope ratios for all blocks and samples. Table 1 shows the 13C isotope ratio for Merck and Reference benzoic acid.

Table 1. ^{13}C Isotope Ratio values for Merck and Reference benzoic acid.

Samples	Isotopologue	Ratio	SD
Merck	^{13}C	0.0841690	0.00004
Reference	^{13}C	0.0841067	0.00003

After obtaining the isotope abundance ratio for both benzoic acids, a Delta (δ) value was calculated following the equation $\delta_{sample/REF} = (R_{sample}/R_{REF} - 1) * 1000$, where sample represented the Merck benzoic acid, REF represents the reference standard by IAEA, and R is the isotope abundance ratio. Using the equation $\delta_{sample/VPDB} = \delta_{sample/REF} + \delta_{REF/VPDB} + [(\delta_{REF/VPDB} * \delta_{sample/REF}) /1000]$, present in Mueller et al. (Mueller et al., 2022), the δ value obtained can be correct to the primary standard. For the benzoic acid from Merck, the $\delta^{13}C_{sample/VPDB}$ obtained was -28.09‰, a value very similar to that obtained by IRMS (-27.77‰).

Conclusions

In this preliminary study, a methodology to analyze the stable isotope ratio of organic acids by ESI-Orbitrap MS has been development. At this moment, the connections and tune method were adjusted to improve the number of the ions, stability of the spray as well as the data treatment. In addition, benzoic acid was successfully analyzed by ESI-Orbitrap MS resulting in a $\delta^{13}C_{sample/VPDB}$ of -28.09‰ which is very similar to the correct value obtained by IRMS. The next steps of this work will involve applying the developed method to geochemically important acids and subsequently analyzing real samples. By extending the application of the method to acids of geochemical significance, we aim to gain valuable insights into the composition and isotopic ratios of organic acids in various environmental samples. This will enable us to further understand the geochemical processes and dynamics involved, contributing to a more comprehensive understanding of petroleum systems and their implications.

Acknowledgements

The authors acknowledge the financial support from Petróleo Brasileiro SA-Petrobras, CAPES, and CNPq.

References

Eiler, J., Cesar, J., Chimiak, L., Dallas, B., Grice, K., Griep-Raming, J., Juchelka, D., Kitchen, N., Lloyd, M., Makarov, A., Robins, R., Schwieters, J., 2017. Analysis of molecular isotopic structures at high precision and accuracy by Orbitrap mass spectrometry. International Journal of Mass Spectrometry 422, 126–142.

Eiler, J.M., 2007. “Clumped-isotope” geochemistry-The study of naturally-occurring, multiply-substituted isotopologues. Earth and Planetary Science Letters 262, 309–327.

Hilkert, A., Böhlke, J.K., Mroczkowski, S.J., Fort, K.L., Aizikov, K., Wang, X.T., Kopf, S.H., Neubauer, C., 2021. Exploring the Potential of Electrospray-Orbitrap for Stable Isotope Analysis Using Nitrate as a Model. Analytical Chemistry 93, 9139–9148.

Mueller, E.P., Sessions, A.L., Sauer, P.E., Weiss, G.M., Eiler, J.M., 2022. Simultaneous, High-Precision Measurements of δ2H and δ13C in Nanomole Quantities of Acetate Using Electrospray Ionization-Quadrupole-Orbitrap Mass Spectrometry. Analytical Chemistry 94, 1092–1100.

Neubauer, C., Crémière, A., Wang, X.T., Thiagarajan, N., Sessions, A.L., Adkins, J.F., Dalleska, N.F., Turchyn, A. V., Clegg, J.A., Moradian, A., Sweredoski, M.J., Garbis, S.D., Eiler, J.M., 2020. Stable Isotope Analysis of Intact Oxyanions Using Electrospray Quadrupole-Orbitrap Mass Spectrometry. Analytical Chemistry 92, 3077–3085.

Zeichner, S.S., Wilkes, E.B., Hofmann, A.E., Chimiak, L., Sessions, A.L., Makarov, A., Eiler, J.M., 2022. Methods and limitations of stable isotope measurements via direct elution of chromatographic peaks using gas chromotography-Orbitrap mass spectrometry. International Journal of Mass Spectrometry 477, 116848.

XVI LATIN AMERICAN CONGRESS ON ORGANIC GEOCHEMISTRY
9 - 11 AUGUST, 2023
ARACAJU, SERGIPE, BRAZIL

Isótopos de Enxofre ($\delta^{34}S$) Inorgânico e Orgânico na Caracterização de Rochas Geradoras do Brasil

[1]NAVAS, G. A.,[1]SALAZAR, J. M., [1]MOREIRA, M., [2]FERREIRA, A., [2]SOUZA, I., [1]DÍAZ, R.

1. Programa de Geociências (Geoquímica), Universidade Federal Fluminense, Niterói, Brazil.

2.. Centro de Pesquisas da Petrobras (CENPES)

*Corresponding author: gracenavas@id.uff.br

Introdução

Um elemento que pode estar associado às rochas geradoras é o enxofre (S), o que favorece a formação de óleos com um alto conteúdo de enxofre. O enxofre pode ser liberado na forma de sulfeto de hidrogênio (H_2S) durante o processo de produção de petróleo e devido a suas características corrosivas e tóxicas, o H_2S, representa um sério problema para as instalações petroleiras, à saúde dos trabalhadores e ao meio ambiente, o que pode afetar a produção e interrompê-la até o ponto de causar riscos econômicos [1]. Neste sentido, a avaliação das fontes de enxofre, inorgânico e orgânico, é de muita importância para a caracterização dos sistemas petrolíferos com o intuito de diminuir os riscos de exploração e produção, e assim reduzir custos ao longo do tempo [2].

Nesse contexto, a geoquímica do enxofre: inorgânica (sulfetos voláteis ácidos, do inglês *Acid Volatile Sulfide* - AVS, e enxofre redutível por cromo, do inglês *Chromium Reducible Sulfide*, CRS), orgânica (compostos orgânicos sulfurados) e isotópica ($\delta^{34}S$) tem sido utilizada como ferramenta na reconstrução das condições redox de ambientes de sedimentação antigos, como indicadora paleoambiental e das variações do conteúdo de oxigênio dissolvido na coluna da água, assim como entender a biogeoquímica do enxofre, incluindo fontes de enxofre e mecanismos de incorporação na matéria orgânica [3].

O estudo do S em rochas geradoras de bacias sedimentares brasileiras é raramente realizado. Assim, o presente trabalho utilizou a composição isotópica (^{34}S) nas frações inorgânica e orgânica de rochas geradoras do Brasil, com o intuito de auxiliar na interpretação do ambiente de sedimentação da rocha geradora, ajudar no entendimento dos processos associados ao ciclo do enxofre e sua interação com os sistemas petrolíferos, assim como contribuir para a compreensão dos mecanismos envolvidos na geração de H_2S.

Metodologia

Foram estudadas 26 amostras de rochas geradoras de diferentes formações localizadas em onze bacias sedimentares brasileiras. O enxofre nas rochas geradoras foi extraído utilizando o método de redução por cromo (CRS: Chromium Reducible Sulfur). O método é realizado em duas etapas continuas (I= AVS; II= CRS), em um sistema de destilação, em atmosfera de N_2 e com temperatura controlada. de 80°C. O CRS (FeS_2 + S_0) é liberado como H_2S e precipitado como sulfeto de zinco (ZnS) [4]. Finalmente o ZnS é precipitado como sulfeto de prata (Ag_2S) utilizando uma solução de nitrato de prata ($AgNO_3$, 0,1M), onde foi determinado o $\delta^{34}S$ no sulfeto ($\delta^{34}S_{CRS}$). Por outro lado, a rocha que fica como resíduo resultante na extração inorgânica, foi secada, pulverizada e peneirada, para posteriormente determinar o $\delta^{34}S$ na fração orgânica da rocha. Análises feitas por meio de combustão em espectrômetro de massa acoplado a um analisador elementar na Universidade de Brasilia.

Resultados e Discussão

A incorporação de enxofre reduzido na matéria orgânica geralmente gera compostos orgânicos de enxofre que apresentam empobrecimento em ^{34}S em relação com o sulfato marinho e um enriquecido em comparação com a pirita. Isto é consequência da cinética de reação, a qual favorece a reação entre o sulfeto e ferro reativo prioritariamente à incorporação do sulfeto na matéria orgânica. O qual é consequência do fracionamento isotópico que ocorre durante a formação de pirita e de compostos organosulfurados a partir de sulfeto produzido pelas reações de redução dissimilatória [3] [5]. Sendo provável que este processo tinha sido predominante no ambiente sedimentar, onde foram

geradas as rochas geradoras B1, B2, B3, B4, B13, B14, B18, B19, B20, B21, B22, B23, B24, B25 e B26. Estas amostras apresentaram empobrecimento em ^{34}S tanto na pirita (-36,75‰ a -14,61‰) como na fração orgânica (-16,18‰ a +6,75‰) (Tabela 1), que sugerem que a fonte do sulfeto é de tipo bacteriano [5] [6].

Por outro lado, em sistemas abertos onde existe um aporte constante de sulfato, os valores de $\delta^{34}S$ em piritas são próximos de -45‰. No entanto, em ambientes mais restritos com baixas concentrações de sulfato ou fontes limitadas de sulfato, podem ser gerados sulfetos menos empobrecidos em ^{34}S durante a sulfato redução [5] [6]. Nesta mesma linha de ideias, a pirita empobrecida em ^{34}S em relação à matéria orgânica circundante, mas em um rango próximo, sugere um ambiente deposicional com aporte de sulfato restrito [6], o que parece ser o caso das rochas geradoras B6 ($^{34}S_{CRS}$: -5,39‰; $^{34}S_{Org}$: +7,05‰), B7 ($^{34}S_{CRS}$: +4,44‰; $^{34}S_{Org}$: +8,60‰, B8 ($^{34}S_{CRS}$: +4,58‰; $^{34}S_{Org}$: 7,33‰), B9 ($^{34}S_{CRS}$: -2,08‰; $^{34}S_{Org}$: +11,41‰), B15 ($^{34}S_{CRS}$: -8,08‰; $^{34}S_{Org}$: +7,03‰) e B16 ($^{34}S_{CRS}$: +4,59 ‰; $^{34}S_{Org}$: +7,97 ‰) (Tabela 1).

Por outro lado, uma composição isotópica da pirita e do enxofre orgânico próxima ao sulfato da água do mar, podem ser produto de reações de redução termoquímica de sulfatos (TSR). A qual gera pirita secundaria, a qual teria uma composição isotópica similar ao $CaSO_4$ (enriquecida em ^{34}S), já que durante a redução termoquímica de sulfatos o fracionamento isotópico é depreciável [3] [7] [8]. O que parece ser o caso das amostras B11 e B12, ambas da Formação Codó da Bacia São Luís, onde os valores da razão isotópica do CRS apresentaram uma composição isotópica na pirita de 15,30‰ e 20,89‰ (Tabela 1).

		Amostra	Bacia Sedimentar	Formação	Tipo de Seção Geradora	Período (Idade)	Isotopos $\delta^{34}S_{CRS}$ ‰ ±0,2‰	Isotopos $\delta^{34}S_{RO}$ ‰ ±0,2‰
Intracratônicas	Área continental	B1	Amazonas	Barreirinha	Marinho	Devoniano	-21,6	1,99
		B2	Amazonas	Barreirinha	Marinho	Devoniano	-21,0	-4,12
		B3	Parnaíba	Pimenteiras	Marinho	Devoniano	-36,75	-3,40
		B4	Parnaíba	Pimenteiras	Marinho	Devoniano	-32,99	-0,44
		B5	Paraná	Ponta Grossa	Marinho	Devoniano	-20,28	5,53
		B6	Paraná	Ponta Grossa	Marinho	Devoniano	-5,39	7,05
		B7	Paraná	Irati	Marinho Evaporítico	Permiano	4,44	8,60
		B8	Paraná	Irati	Marinho Evaporítico	Permiano	4,58	7,33
Riftes Interiores	Margem Equatorial	B9	Potiguar Terra	Alagamar	Transicional	Cretacico (Aptiano)	-2,08	11,41
		B10	Potiguar Mar	Alagamar	Transicional	Cretacico (Aptiano)	-15,00	7,38
		B11	São Luís	Codó	Transicional	Cretacico (Aptiano)	15,3	13,54
		B12	São Luís	Codó	Transicional	Cretacico (Aptiano)	20,89	15,83
Margem Passiva	Margem Equatorial	B13	Pará-Maranhão	Gr. Caju Indiviso	Marinho Carbonático	Cretacico (Albiano)	-23,04	6,75
		B14	Pará-Maranhão	Gr. Caju Indiviso	Marinho Carbonático	Cretacico (Albiano)	-20,24	5,10
		B15	Ceará	Ubarana	Marinho Siliciclástico	Cretacico (Turoniano)	-8,08	7,32
	Margem Leste	B16	Sergipe Terra	Muribeca	Transicional	Cretacico (Aptiano)	4,59	7,97
		B17	Sergipe Mar	Muribeca	Transicional	Cretacico (Aptiano)	-15,94	4,20
		B18	Sergipe Mar	Cotinguiba	Marinho Siliciclástico	Cretacico (Turoniano)	-23,26	-16,18
		B19	Sergipe Mar	Cotinguiba	Marinho Siliciclástico	Cretacico (Turoniano)	-14,61	-7,31
		B20	Alagoas Mar	Cotinguiba	Marinho Siliciclástico	Cretacico (Turoniano)	-18,69	-1,51
		B21	Espírito Santo Mar	Regência	Marinho Carbonático	Cretacico (Albiano)	-25,78	1,34
		B22	Espírito Santo Mar	Regência	Marinho Carbonático	Cretacico (Albiano)	-30,7	-11,03
		B23	Santos	Itanhaem	Marinho Carbonático	Cretacico (Albiano)	-33,95	-10,41
		B24	Santos	Ariri	Marinho Carbonático	Cretacico (Albiano)	-35,53	-12,69
		B25	Santos	Itajaí-Açu	Marinho Siliciclástico	Cretacico (Turoniano)	-29,47	-2,60
		B26	Santos	Itajaí-Açu	Marinho Siliciclástico	Cretacico (Turoniano)	-28,98	-5,18

Tabela 1. Teores de enxofre total (ST), enxofre da fração inorgânica (CRS), enxofre da fração orgânica (Sorg) e composição isotópica da fração inorgânica e orgânica.

Conclusões

A composição isotópica da pirita e da fração orgânica ($\delta^{34}S$) permitiu estabelecer a fonte do sulfeto incorporado nas frações inorgânica e orgânica das rochas geradoras, a qual foi principalmente associada com as reações de sulfato redução microbianas ocorridas no ambiente de sedimentação. Tendo como a exceção a Formação Codó, onde a composição isotópica permitiu identificar outra fonte de enxofre, possivelmente, os sulfatos presentes nos evaporitos, como a gipsita e anidrita identificadas nesta formação, que sofreram redução termoquímica de sulfato que afetaram o sinal isotópico dessas frações, resultando em um $\delta^{34}S$ similar à encontrada no sulfato dissolvido na água do mar.

Agradecimentos

Obrigado pelo suporte à agencia de fomento CAPES, ao Programa de Geociências (Geoquímica) da UFF e ao Centro de Pesquisas da Petrobras (CENPES).

Referências

[1] Hyne, N. Nontechnical guide to petroleum geology, exploration, drilling and production. 2. ed. Tulsa: Penn Well Corp, 2001. 598 p.

[2] Mccarthy, K.; Niemann, M.; Palmowski, D.; Peters, K.; Stankiewicz, A. La geoquímica básica del petróleo para la evaluación de las Rocas Generadoras. Oilfield Review Services, v. 23, n. 2, p. 36-47, 2011.

[3] Amrani, A. Organosulfur compounds: molecular and isotopic evolution from Biota to oil and gas. Annual Review of Earth and Planetary Sciences, v. 42, p. 733–768, maio 2014.

[4] Fossing, H.; Jørgensen, B. Measurement of bacterial sulfate reduction in sediments: evaluation of a single-step chromium reduction method. Biogeochemistry, Holland, v. 8, p. 205-222, 1989.

[5] Canfield, D. Isotope fractionation by natural populations of sulfate-reducing bacteria. Geochimica et Cosmochimica Acta, v. 65, p. 1117-1124, 2001.

[6] Cai, C.; Li, K.; Anlai, M.; Zhang, C.; Xu, Z.; Worden, R.; Wu, G.; Baoshou, Z.; Chen, L. Distinguishing cambrian from upper Ordovician source rocks: evidence from sulfur isotopes and biomarkers in the Tarim Basin. Organic Geochemistry, v. 40, 2009a.

[7] Cai, C.; Worden, R.; Wolff, G.; Bottrell, S.; Wang, D.; Li, X. Origin of sulfur rich oils and H2S in Tertiary lacustrine sections of the Jinxian Sag, Bohai Bay Basin, China. Applied Geochemistry, v. 20, p. 1427-1444, 2005.

[8] Zhu, G.; Zhang, S.; Liang, Y.; Dai, J.; Li, J. Isotopic evidence of TSR origin for natural gas bearing high H2S contents within the Feixianguan Formation of the northeastern Sichuan Basin, southwestern China. Science in China Series D: Earth Sciences, v. 48, n. 11, p. 1960-1971, 2005.

PRELIMINARY CARBON AND OXYGEN ISOTOPE CHEMOSTRATIGRAPHY OF A CARBONATIC SUCCESSION (ILHA DE SANTANA AND PIRABAS FORMATIONS) ON THE BRAZILIAN EQUATORIAL MARGIN

ZONEIBE LUZ[1]*, NICOLÁS STRIKIS[1], HAMILTON SANTOS GAMA FILHO[2], MARCELINO JOSE DOS ANJOS[2], MAURO GERALDES[3], DAYANA ALVARADO SIERRA[4], BEATRIZ TEIXEIRA GUIMARÃES[4], ORANGEL AGUILERA[1]

1. Fluminense Federal University (UFF), Institute of Geochemistry/Institute of Biology, 24020-140/24210-201, Niterói, Rio de Janeiro, Brazil*;
2. Rio de Janeiro State University (UERJ), Institute of Physics Armando Dias Tavares, CEP 20550-013, Rio de Janeiro, Brazil;
3. Rio de Janeiro State University (UERJ), Faculty of Geology, CEP 20550-013, Rio de Janeiro, Brazil;
4. Federal University of Pará (UFPA), Geoscience Institute, Belém, Pará, Brazil.

*correspondent author: zoneibe.luz@gmail.com

Introduction

Situated between the North and Northeast regions, the Brazilian Equatorial Margin (BEM) has an inherent potential for oil exploration [1]. A succession of offshore carbonates that compose the Great Amazon Reef System [1] can be found at the border of the northern Brazilian platform. The carbonates were formed by coralline algae, and among the structures the most notably are the Rhodolith beds [1], which covers the seafloor serving as a substrate and ecosystem. Within the succession, the rocks have a permeability that resembles other carbonate successions of western neighboring countries, such as Guyana and Suriname [2]. To complement a paleoecological and paleoenvironmental perspective of the BEM, samples from a sedimentary core (500 to 3500 m) from a Well by Petrobras (Fig. 1) will be characterized through a comprehensive chemostratigraphy study involving multiple isotope and geochemical methods. Sediment, Rhodoliths and calcareous microfossils will be sampled. Here we present the preliminary results from sediments which were analyzed semi-quantitatively by X-ray diffraction (XRD) and had their inorganic carbon ($\delta^{13}C$) and oxygen ($\delta^{18}O$) isotope values measured.

Experimental

Fifty-three carbonate powder samples from depths between 510 to 1500 m (Fig. 2A) were used for XRD and isotopic analysis. To the XRD, the samples were mounted into acrylic sampling disks and analyzed by a D2 Phaser (BRUKER) at the Laboratory of Electronic Instrumentation and Analytical Techniques (LIETA) of the UERJ. To measure the $\delta^{13}C$ and $\delta^{18}O$ compositions, the samples were put into glass vials and analyzed by a Gasbench coupled to a Delta (Thermo Scientific) mass spectrometer at the Stable Isotope Laboratory (CPGeo-LES) of the USP. In addition, two foraminifera from 600 and 900 m had their U/Pb ages measured. The samples were prepared into resins and analyzed by a Neptune plus (Thermo Scientific) mass spectrometer at the Environment and Materials Multiuser Laboratory (MULTILAB) of the UERJ.

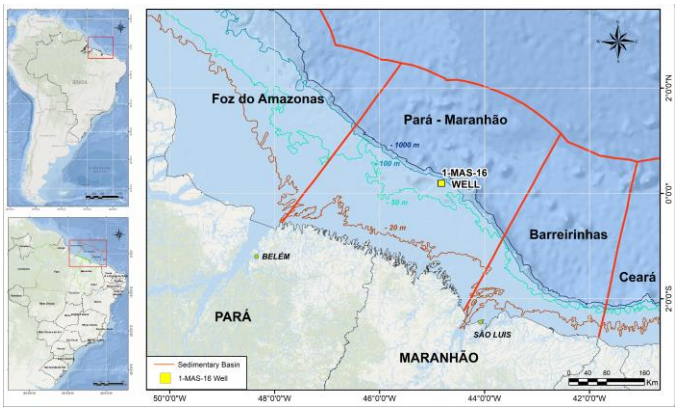

Figure 1. Location of the studied site in South America, Brazil, and within the Brazilian Equatorial Margin.

Results and Discussion

All results are summarized in Fig. 2. At the left (Fig. 2A), the $\delta^{13}C$ values ranged from -1.6 to 1.6 ‰ (VPDB), having a smaller variation than the $\delta^{18}O$ values, which ranged from -5.4 to -0.5 ‰ (VPDB). The noted offset between the isotopic excursions may be explained by the environmental dynamics recorded in the sediments. While to the carbon isotopes, the noted positive and negative shifts are related to the carbon cycle [3], the oxygen isotope shifts should be a combination of seawater temperature oscillations as well as eustatic fluctuations [3]. Both isotopic compositions correlated well to global climatic events (Fig. 3C). In addition, the large offset in the oxygen isotope values when compared to offshore sections (e.g., [4]) suggest that regional processes, such as the tidal range in the tropics, have also influenced the $\delta^{18}O$. The semi-quantitative XRD measurements also corroborated the isotopic excursions (Fig. 2B). The Ankerite mass

fractions (%, m/m) were up to 73, alternating with the predominant Calcite, which were as low as 27. The alternance between both seems to be correlated with glaciation periods (Fig. 2) during sea-level drops, hinting that Ankerite formed not in high-temperature conditions but rather in low-temperatures.

Conclusions

The XRD measurements and the carbon and oxygen isotope compositions of carbonate sediments from 53 samples distributed around the Eocene-Miocene provided robust results. The XRD and isotope shifts are likely correlated to global climatic events. However, the large offset of the oxygen isotope values may be also influenced by regional processes (e.g., tidal range) given their larger offset. Additional analyzes from the sedimentary core provided will further give insights about the paleoenvironmental, paleoecological and paleoclimatic conditions of the Brazilian Equatorial Margin.

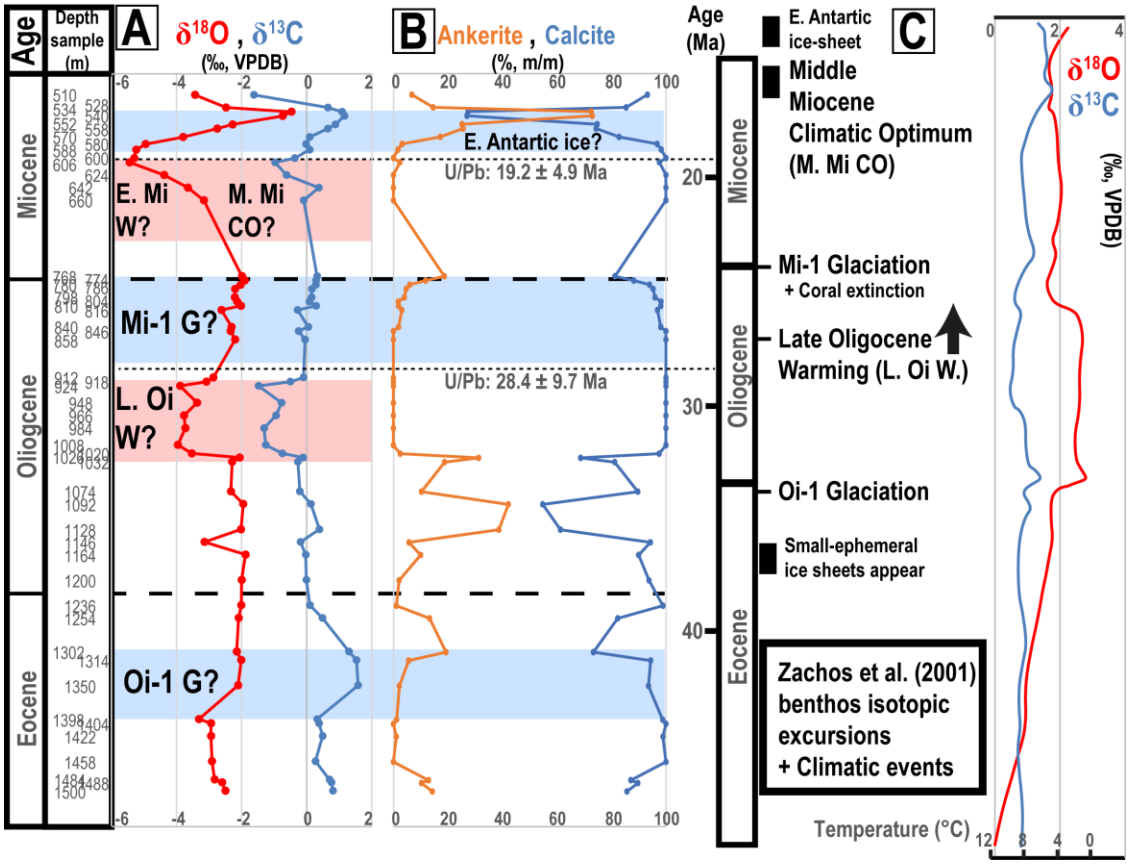

Figure 2. In the left, the isotope chemostratigraphy **(A)** and the XRD semi-quantitative measurements **(B)** from 500 to 1500 m depth of the 1-MAS-16 Petrobras Well are shown. In the right **(C)**, the isotope chemostratigraphy and estimated paleotemperatures compiled by [3] are shown, with the climatic events and one biotic event (Coral extinction) remarked. The two U/Pb ages in **(A)** and **(B)** measured in 600 and 900 m are correlated with the geological scale of [3] in **(C)**. The possible climatic events accounted to the noted geochemical shifts in **(A)** are suggested, and their full captions are given in **(C)**.

Acknowledgements

The authors thank to Veronica Ramirez and other contributors to the laboratorial support; to the Petrobras for granting the samples; and to the Universidade Federal Fluminense and the Universidade de Sao Paulo for the infrastructure.

References

[1] Francini-Filho, R., Asp, N., Siegle, E., Hocevar, J., Lowyck, K., D'Avila, N., et al. 2018. Perspectives on the Great Amazon Reef: Extension, Biodiversity, and Threats. Front. Mar. Sci.**5**, 142.

[2] Nemčok, M., Rybár, S., Ekkertová, P., Kotulová, J., Hermeston, S., Jones, D., 2016. Transform Margins: Development, Controls and Petroleum Systems. Geol. Soc. Spec. Publ.**431**, 199-217.

[3] Zachos, J., Pagani, M., Sloan, L., Thomas, E., Billups, K., 2001. Trends, Rhythms, and Aberrations in Global Climate 65 Ma to Present. Science**292**, 686-293.

XVI LATIN AMERICAN CONGRESS ON ORGANIC GEOCHEMISTRY
9 - 11 AUGUST, 2023
ARACAJU, SERGIPE, BRAZIL

Gas Hydrate Studies in Brazil: Future Perspectives

LUIZ FREDERICO RODRIGUES[a*], JOÃO MARCELO KETZER[b], JOSÉ A. CUPERTINO[c], ADOLPHO H. AUGUSTIN[c], DANIEL PRAEG[d*]

[a]UNIVERSIDADE FEDERAL DO RIO GRANDE, [b]LINNAEUS UNIVERSITY, [c]UNIVERSIDADE DO VALE DO RIO DOS SINOS, [d]GEOAZUR

[*]e-mail: luizfrederico.rodrigues@gmail.com

Introduction

Gas hydrates are energy resources whose organic carbon mass is greater than all other fossil fuels combined and are considered an alternative energy source [1]. In addition to their importance as an energy resource, studies of gas hydrates also provide important information about the Earth's carbon cycle and climate change. Changes in ocean water temperature conditions can cause the dissociation and release of large amounts of methane and carbon dioxide into the atmosphere. Massive destabilization of the gas hydrate system can also cause large underwater mass movements, with potential impact on subsea installations such as oil or even major catastrophes in coastal areas such as generation of tsunamis [2]. The existence of gas hydrates in Brazilian territory was confirmed in the Pelotas Basin [3] and in the Amazon fan [4].

Experimental

The Amazon deep-sea fan is approximately 250 km from the mouth of the Amazon River and extends 700 km seaward from the outer edge of the continental shelf to water depths of over 4,000 m in the Demerara Abyssal Plain [5]. The Rio Grande Cone is located in the southern portion of the Pelotas Basin and has a water depth between 200 and 3,000 m, 200 km from the city of Rio Grande. It has been deposited since the lower Miocene [6].

Results and discussion

The gas hydrates from Amazon deep-sea fan present in their composition CH_4 (95%), CO_2 (4%) and C_2H_6 (1%); methane isotope analysis ($\delta^{13}C$ between -61.7 and -59.2‰ and δD between -206 e -205‰) and ethane ($\delta^{13}C$ between -31.5 and -30.8‰). These results indicate a biogenic origin with possible thermogenic contamination. This mixing may have occurred during the vertical migration of thermogenic gases through the sediments, until reaching the microbial gas deposits at shallower depths. The thermogenic influence is possibly related to the connection provided by faults connecting deep gas sources to surface deposits. (Figure 1A). In the Rio Grande Cone, the gas in the hydrate is mostly methane with trace amounts of ethane. Isotopic analysis of methane carbon indicates a microbial origin, whose values varied between $\delta^{13}C$ from -69,3 to -66,7 (Figure 1B). Likewise, studies of free gases in sediments were produced by the product of microbial methanogenesis, that is, gaseous hydrocarbons were mainly generated by the microbial reduction of CO_2 [7].

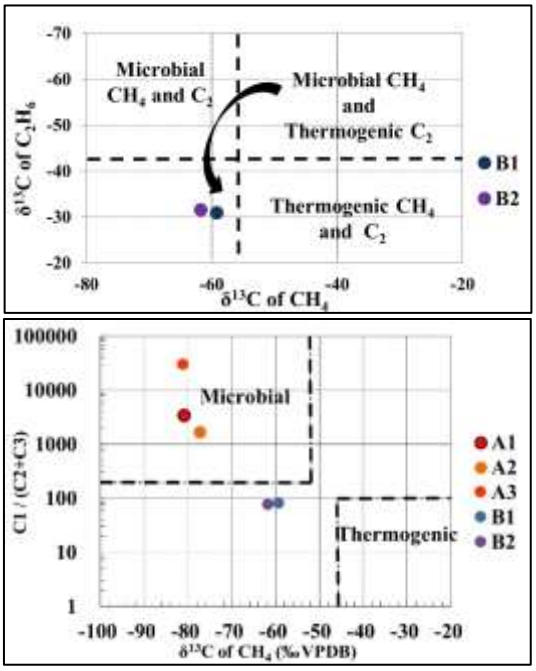

Figure 1. a) Graph showing the relationship between the compositions of C1/(C2+C3) versus ^{13}C of gases from hydrates, plumes and gases dissolved in sediments from Amazon deep-sea fan. b) Relationship between the values of $\delta^{13}C_2H_6$ e $\delta^{13}CH_4$ for samples from different areas of the Rio Grande Cone.

Conclusion

These discoveries in Brazilian territory aroused the need to carry out additional research that foster the understanding of its occurrence and the future use of this resource in other sedimentary basins. Recently, the works

resulting from these analyzes have aroused the interest of the world scientific community due to the importance of hydrates not only as an alternative energy resource but also for their importance for understanding the carbon cycle and its impacts on climate change. In the Amazon deep-sea fan, a cooperation project is being carried out between Brazilian universities (FURG, PUCRS, UFRGS, UNISINOS, USP, UFF, UERJ and UFESP), Linnaeus University, in Sweden, and French research institutes (IFREMER, GEOAZUR and LSCE). The objective of this project is to study the past climate history of the equatorial margin of Brazil over the last million years, to determine the behavior of gas hydrates in relation to submarine landslides of great impact and to evaluate the extent of gas leaks in the Amazon.

Acknowledgment

The authors would like to thank Petrobras S/A for financial support, Sens Ltda for supporting research and the Pos-Graduate Program in Technological and Environmental Chemistry at FURG.

Referências

[1] Collett, T.S.; Johnson, A.H.; Knapp, C.C.; Boswell, R. Natural Gas hydrates: a review. In: Collett, T.; Johnson, A.; Knapp, C.; Boswell, R. (eds.). Natural Gas Hydrates: Energy Resource Potential and Associated Geologic Hazards, AAPG Memoir 89, 2009, p. 146-219.

[2] Mienert, J.; Vanneste, M.; Haflidason, H.; Bünz, S. Norwegian margin outer shelf cracking: a consequence of climate- -induced gas hydrate dissociation? Int. J. Earth Sci. (Geol Rundsch) 99 (Suppl. 1), 2010.S207eS225.

[3] Miller, D. J.; Ketzer, J. M.; Viana, A. R.; Kowsmann, R.O.; Freire, A. F. M.; Augustin, A.H.; Lourega, R.V.; Rodrigues, L. F.; Natural gas hydrates in the Rio Grande Cone (Brazil): A new province in the western South Atlantic. Marine and Petroleum Geology, v. 67, 2015, p. 187-196.

[4] Ketzer, J.M.; Augustin, A.; Rodrigues, L.F.; Oliveira, R.; Praeg, D.; Pivel, M.A.; Gas seeps and gas hydrates in the Amazon deep-sea fan. Geo-Marine Letters, v. 38, 2018. 429-438.

[5] Figueiredo, J.; Hoorn, C.; Van der Ven, P.; Soares, E. Late Miocene onset of the Amazon River and the Amazon deep-sea fan: Evidence from the Foz do Amazonas Basin. Geology, 2009, 37, 619-622.

[6] Fontana, R.L.; Mussumeci, A. Hydrates offshore Brazil. In: Annals of the New York Academy of Sciences, International Conference on Natural Gas Hydrates 715, 1994. p. 106 e 113.

[7] Rodrigues, L.F.; Ketzer, J.M.; Oliveira, R.R..; Augustin, A.H.; Cupertino, J.A.; Viana, A.R.; Molecular and isotopic composition of hydrate-bound, dissolved and free gases in the Amazon deep-sea fan and slope sediments, Brazil. Geosciences 9, 2019, 73.

ALE

ENVIRONMENTAL GEOCHEMISTRY

Aromatic carotenoids by GC×GC-TOFMS in organic-rich shale from Irati Formation, Paraná Basin, Brazil

Vitor Hugo S. Goes[a], Mirella Castilho[a], Vinícius B. Pereira[a], Laércio L. Martins[b,c], Anderson José Maraschin [d], Hélio J.P.S. Ribeiro[b], Georgiana F. da Cruz[b], Débora A. Azevedo[a]

[a]**Federal University of Rio de Janeiro, Brazil;** [b]**North Fluminense State University;** [c]**Federal University of Ceará,** [d] **Pontifícia Universidade Católica do Rio Grande do Sul**

vitorhugo.santosgoes@eq.ufrj.br

Introduction

The Irati Formation (Early Permian) in the Paraná Basin is characterized by intervals of organic-rich shales from evaporitic layers in a marine and anoxic environment (Reis et al., 2018).

Recently, Martins et al. (2020) and Nascimento et al. (2021) detected aryl isoprenoids (AI) ranging from C_{13} to C_{31} in Irati samples but restrained their findings in monoaromatic carotenoids. Aromatic carotenoids (e.g., AI) are suggestive of the contribution of green and sulfur bacteria present in a lacustrine environment. These organisms thrive in photic euxinic environments and may also represent water column stratification (Summons et al., 1984; Araújo et al., 2020).

In this context, the present work describes the application of two-dimensional gas chromatography-time of flight mass spectrometry (GC×GC-TOFMS) to identify a greater range of aromatic carotenoids in extracts from the Irati Formation, Paraná Basin (Brazil). In addition, it is the aim of comparing their distribution between the northeast and southeast of the Paraná Basin.

Experimental

Three Irati rock samples, one from São Paulo state (ISP), and two from Rio Grande do Sul state (IRSA and IRSB) were crushed and pulverized prior to a 48-hour extraction with 300 mL of dichloromethane using a Soxhlet system. Asphaltenes were precipitated from approximately 50 mg of soluble organic matter. The maltenes were concentrated and separated into saturate, aromatic, and NSO fractions (Martins et al., 2021, Nascimento et al., 2021).

Aromatic hydrocarbons were thereafter analyzed by GC×GC-TOFMS (Leco Corporation, USA) using a RTX-5 (10 m × 0.18 mm, 0.20 µm) as a primary column and a DB-17HT (1.0 m × 0.25 mm, 0.15 µm) as the secondary column.

Results and Discussion

Identification of aryl-isoprenoids was achieved by the extracted ion chromatogram *m*/*z* 134 (Fig. 1). This ion is characteristic of carotenoid compounds due to cleavage of the aliphatic side-chain. The Irati extracts assessed herein presented two homologous series, the aryl-isoprenoids compounds (compounds I-VI), constituted of one aromatic ring with an aliphatic sidechain, and the diaryl-isoprenoids (VII-IX), with two aromatic rings connected by an aliphatic chain.

The aryl-isoprenoids and diaryl-isoprenoids are products of the diagenetic and catagenetic breakdown of their precursors, such as isorenieratene, okenone, and chlorobactene (Summons et al., 1986) and point to the presence of photic zone euxinia (PZE) during deposition of the irati black shales (Nascimento et al., 2021). Extracts IRSA and ISP presented compounds ranging from C_{14} to $C_{40,}$ while extract IRSB presented C_{13} to C_{40}.

The diaryl carotenoids and extended monoaromatic, in addition to their potential precursors isorenietane and chlorobactane, are reported for the first time in the Irati samples in this work.

Quantitative assessment of the aromatic carotenoids in the Irati shales showed that the ISP sample presented a higher concentration of these compounds in comparison to both samples collected from the Rio Grande do Sul state, as presented in Fig. 2. From these results it could be inferred that the PZE occurring in the São Paulo region of the Irati Formation was more significant that in the Rio Grande do Sul.This agrees with the shallower marine associated with higher salinity and reducing conditions of the Irati samples from the northeastern in relation to the samples from the central eastern and southern basins (Martins et al., 2020).

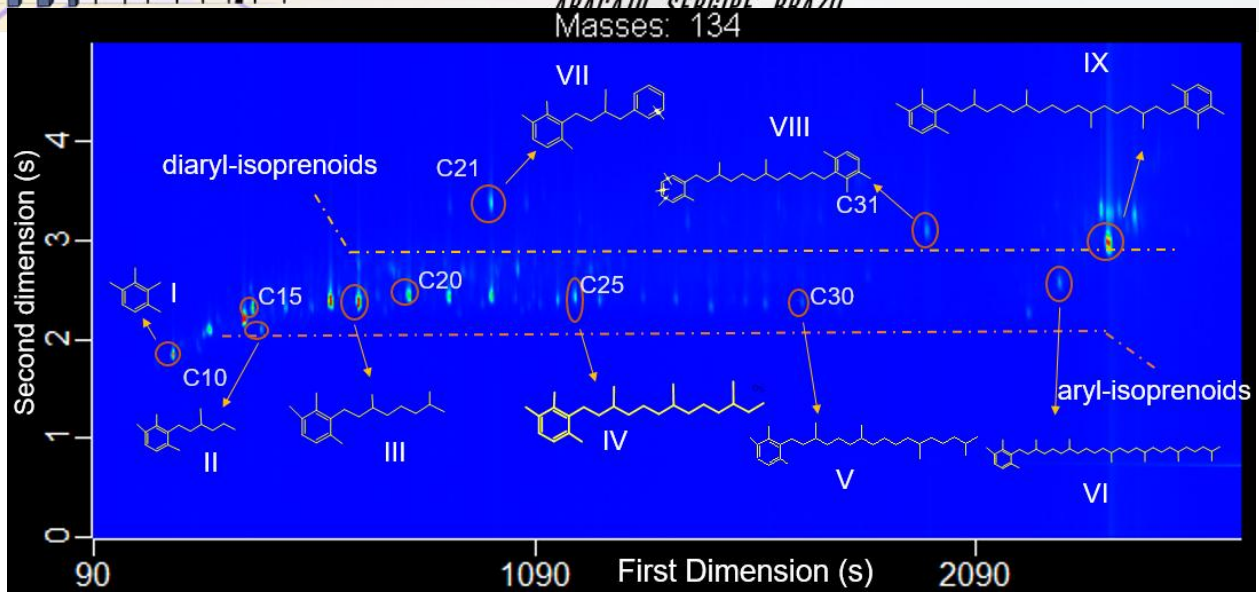

Fig. 1. Chromatogram (*m*/*z* 134) of the extract ISP showing the distribution of aryl carotenoids.

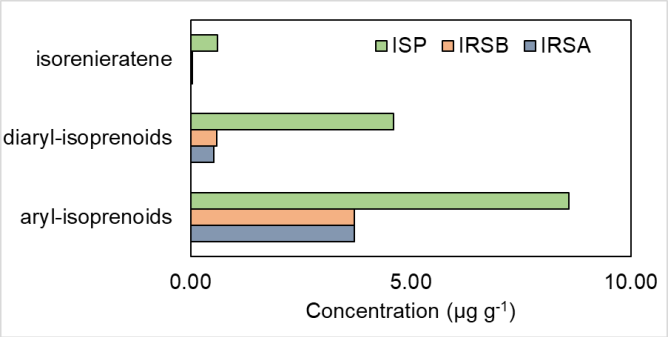

Fig. 2. Graphical representation of the summed concentration of aryl and diaryl isoprenoids, and individual concentration isorenieratane in the shales from the Irati Formation.

Conclusion

Aryl- and diaryl-isoprenoids were identified in organic extracts from the Irati Formation collected in São Paulo and Rio Grande do Sul states, Brazil. The distribution of these compounds in the extracts indicates a more intense anoxic event in the São Paulo region of the Irati Formation. The detection of diaryl carotenoids, extended monoaromatic, and potential precursors isorenietane and chlorobactane were reported for the first time in these samples, showing the efficiency of GC×GC-TOFMS.

Acknowledgements

The authors thank Capes, CNPq and FAPERJ for fellowships and financial support.

References

Araújo, B.Q., Pereira, V.B., Aquino Neto, F.R., Azevedo, D.A. 2020. Biomarkers of photosynthetic sulfur bacteria in Lower Cretaceous crude oils, East Brazilian marginal basin. Organic Geochemistry 148, 104083.

Martins, L.L., Schulz, H.M., Ribeiro, H.J.P.S., Nascimento, C.A., Souza, E.S., Cruz, G.F. 2020. Organic geochemical signals of freshwater dynamics controlling salinity stratification in organic-rich shales in the Lower Permian Irati Formation (Paraná Basin, Brazil). Organic Geochemistry 140, 103958.

Martins, L.L., Schulz, H.M., Noah, M., Poetz, S., Severiano Ribeiro, H.J.P., Cruz, G.F. 2021. New paleoenvironmental proxies for the Irati black shales (Paraná Basin, Brazil) based on acidic NSO compounds revealed by ultra-high resolution mass spectrometry. Organic Geochemistry 151, 104152.

Nascimento, C.A., Souza, E.S., Martins, L.L., Severiano Ribeiro, H.J.P., Santos, V.H., Rodrigues, R. 2021. Changes in depositional paleoenvironment of black shales in the Permian Irati Formation (Paraná Basin, Brazil): geochemical evidence and aromatic biomarkers. Marine and Petroleum Geology 126, 104917.

Reis, D.E.S., Rodrigues, R., Moldowan, J.M., Jones, C.M., Brito M., Cavalcante, D.C., Portela, H.A. 2018. Biomarkers stratigraphy of Irati Formation (Lower Permian) in the southern portion of Paraná Basin (Brasil). Marine and Petroleum Geology 95, 110-138.

Summons, R.E., Powel, T.G. 1986. Identification of aryl isoprenoids in source rocks and crude oils: Biological markers for the green sulphur bacteria. Geochimica et Cosmochimica Acta Vol. 51, pp. 557-566

Biomarker assessment in recent sediment from coastal ecosystem in Jurubatiba National Park (Rio de Janeiro, Brazil)

Manoel Mendes Alves Junior, Vinícius Barreto Pereira, Raquel Vieira Santana da Silva, Débora de Almeida Azevedo

LADETEC - Instituto de Química - Universidade Federal do Rio de Janeiro - Rio de Janeiro - 21941-598 – Brazil

manoelmaj@gradu.iq.ufrj.br

Introduction

The Jurubatiba Restinga National Park (PARNA Jurubatiba) is an ecological reserve that comprises a coastal ecosystem with 18 lagoons of great ecological interest, which have different degrees of salinity, origin, and perenniality (Martin and Domingues, 1994; Enrich-Prast et al., 2003).

Coastal lagoons are important aquatic ecosystems, formed by sedimentation of bays or river estuaries, separated from the ocean by sandbars. They provide excellent basis for the studies of processes controlling the evolution of the coastal zone, and are under the influence of both terrestrial and marine inputs (García and Muñoz-Vera, 2015). Therefore, each lagoon presents a unique organic matter signature and is of great importance for the understanding of transitional environments.

This work reports the application of two-dimensional gas chromatography coupled with time-of-flight mass spectrometry (GC×GC-TOFMS) for the identification and quantification of molecular biomarkers in recent sediment from the PARNA Jurubatiba.

Experimental

Superficial sediment was collected from the Visgueiro lagoon, a hypersaline intermittent waterbody from the PARNA Jurubatiba. The sediment was lyophilized, weighted (4.0 g), and extracted using ultrasonic agitation with 3 × 50 mL of dichloromethane/methanol solution (9:1) in an ultrasonic bath for 30 min. The extract was saponified and neutral lipids were extracted using 3 × 3 mL of hexane. These were fractionated into aliphatic hydrocarbons, aromatic hydrocarbons, and nonsaponifiable polar compounds using activated silica liquid chromatography. The analyses were carried out using two-dimensional gas chromatography coupled with time of flight mass spectrometry (GC×GC-TOFMS) Pegasus 4D using a non-polar/polar column set (DB5/BPX-50). The identification analysis was performed based on mass spectrum interpretation, literature comparison, and elution order.

Results and Discussion

n-Alkanes distribution presented a typical odd-even pattern, with ratios between terrigenous and aquatic material (TAR) and a carbon preference index (CPI) indicating natural input of alkanes with no anthropic contribution (Table 1). The evaluation of hopanoids showed the prevalence of ββ stereoisomers, confirmed by ββ/(αβ + ββ) ratio. These ratios are commonly used to identify the contribution of terrestrial vegetation in aquatic environments, to correlate anthropogenic actions, as well to provide information on the origin of sedimentary organic matter.

The TAR value combined with the proportion of sterols with 27, 28, and 29 carbon atoms, indicates an estuarine environment. The CPI indicates the preservation of the environment, reflecting a pristine environment, confirmed by αβ and ββ ratio.

Table 1. Reference ratios values that assist to provide information on the origin of sedimentary organic matter in the Visgueiro lagoon.

Ratio	
n-Alkanes	
TAR	3.61
CPI	2.88
Hopanes	
ββ/αβ+ββ	0.78
Steroids	
%C27	30%
%C28	16%
%C29	53%

Besides that, tricyclic and tetracyclic terpene and terpane homologous series were identified (Figure 1) with a total concentration of 112.38 ng g^{-1} and 28.61 ng g^{-1}, respectively. Saturated and unsaturated compounds were detected. Mass spectrum evaluation and the presence of C_{25+} compounds indicate that these compounds are consistent with extended tricyclic terpenes, rather than traditional tricyclic diterpenes found in recent environments, such as abietanes.

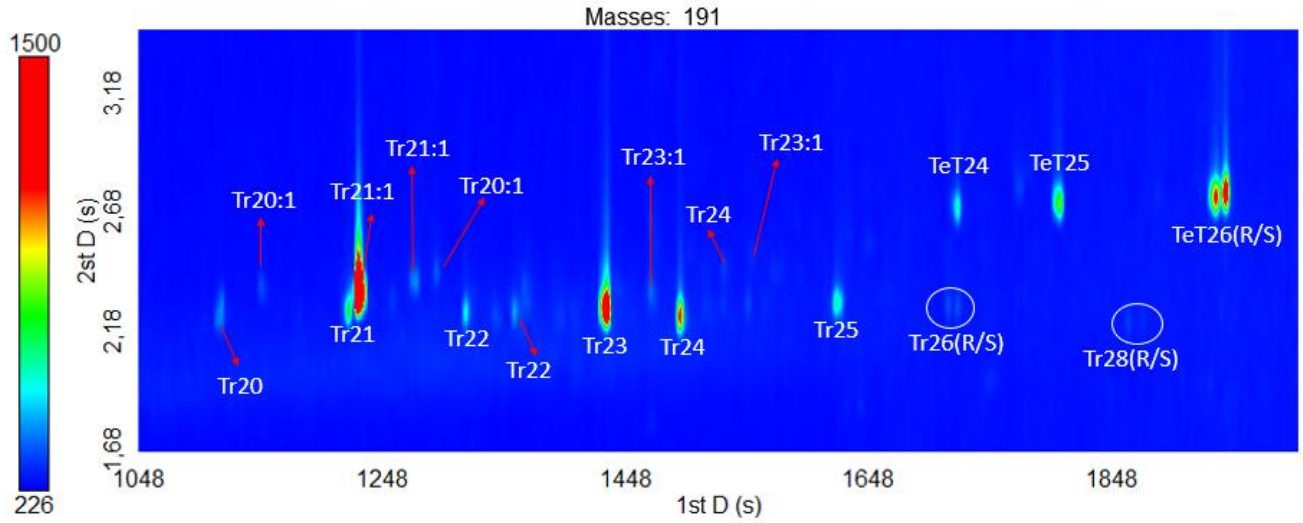

Figure 1. Extracted ion chromatogram *m/z* 191 from the Visgueiro lagoon extract illustrating the series of tricyclic terpanes and terpenes characterized from C_{20} to C_{28}, and tetracyclic terpanes (TeT) characterized from C_{24} to C_{26}.

Extended tricyclic terpanes are natural constituents of sediments, rocks, and petroleum, being widely used as biomarkers in geochemical studies (De Grande et al., 1983). Many of the published studies have related the presence of tricyclic terpanes and diagenetic derivatives with *Tasmanites* algae. However, the presence of tricyclic terpanes in geological samples is not exclusive of *Tasmanites* contribution since studies on the composition of kerogen in rocks rich in algae of the genus *Leiosphaeridia* have also been identified (Dutta et al., 2006).

The presence of extended tricyclic terpanes in microorganisms is poorly understood, and the presence of these compounds in recent sediments is generally associated with anthropic contribution and petroleum contamination. However, since the traditional ratios of biomarkers presented in Table 1 showed a pristine environment, combined with the presence of unsaturated compounds, uncommon in petroleum, the fossil origin of these compounds is disregarded, indicating a potential phytoplanktonic contribution.

Conclusions

The evaluation of these results shows a rare natural occurrence of tricyclic terpanes in recent sediments. In this study, it was observed that the determination of specific classes of compounds contributes to the identification of different types of organic material present in the sediment. However, further research must be developed to find biological precursors related to the tricyclic terpene series identified in this specific lagoon.

Acknowledgments

The authors thank CAPES, FAPERJ, and CNPq (Brazilian research councils) for fellowships and financial support.

References

De Grande, S.M.B., Aquino Neto, F.R., Mello, M.R., 1993. Extended tricyclic terpanes in sediments and petroleum. Organic Geochemistry 20, 1039–1047.

Dutta, S., Greenwood, P.F., Brocke, R., Schaefer, R.G., Mann, U. 2006. New insights into the relationship between Tasmanites and tricyclic terpenoids. Organic Geochemistry 37, 17-127.

Enrich-Prast, A., Bozelli, R.L., Esteves, F.A., Meirelles, F.P., 2003. Lagoas costeiras da Reserva de Jurubatiba: descrição de suas variáveis limnológicas. In: Rocha, C.F.D., Esteves, F.A., Scarano, F.R. Pesquisas de longa duração na Restinga de Jurubatiba: ecologia, história natural e conservação. RiMa, 245-253.

García, G., Muñoz-Vera, A. 2015. Characterization and evolution of the sediments of a Mediterranean coastal lagoon located next to a former mining area. Marine Pollution Bulletin 100, 249-263.

Martin, L., Dominguez, J.M.L. 1994. Geological history of coastal lagoons. In: B. Kjerfve (ed), Coastal lagoon processes. Elsevier Oceanography Series 60: 243-286.

Peters, K.E.; Walters, C.C.; Moldowan, J.M. 2005. The Biomarker Guide; Cambridge University Press: Cambridge, UK.

EVALUATION OF SOIL ORGANIC MATTER FROM DIFFERENT PRODUCTION SYSTEMS IN THE ATLANTIC FOREST BIOME

P. A. D. OLIVEIRA [a*]; R. A. R. RODRIGUES [a]; L. J. SILVA[b] ; M. T. Furtado [a]

[a] **Programa de Pós-Graduação em Geoquímica, Universidade federal Fluminense (UFF)/ [b] Universidade de São Paulo (USP)**

pa_dias@id.uff.br

Introduction (ARIAL 11 BOLD)

In Brazil, from 1976 to 2014 there was a productivity gain of 229% per hectare. As a result, the Southeast region of Brazil faces problems of high soil degradation. Allied to this scenario, the transformation of a natural system into agricultural areas represents, in tropical regions, an important factor that contributes to the increase in the concentration of atmospheric CO_2, with effects on climate change on a global scale. Under these conditions, it is necessary to use conservationist agricultural practices.

The contribution of SOM is not restricted to its quantity but also depends on its quality. However, most studies on the intervention of the type of management adopted on soil quality are limited to the quantitative assessment of organic matter.

Given the assumption, this study aimed to determine the structural quality of soil organic matter under different management systems using spectroscopic and thermoanalysis.

Experimental

The experimental area was in the José Henrique Bruschi Experimental Field, belonging to Embrapa Gado de Leite, Coronel Pacheco, Minas Gerais State, Brazil (21º 33'S, 43º 06'W) (Figure 1).

Three walls of each treatment were sampled at tree depths (0-10, 30-40, and 80-100 cm) Soils were classified as Red-yellow Latosol dystrophic with clay texture and wavy relief

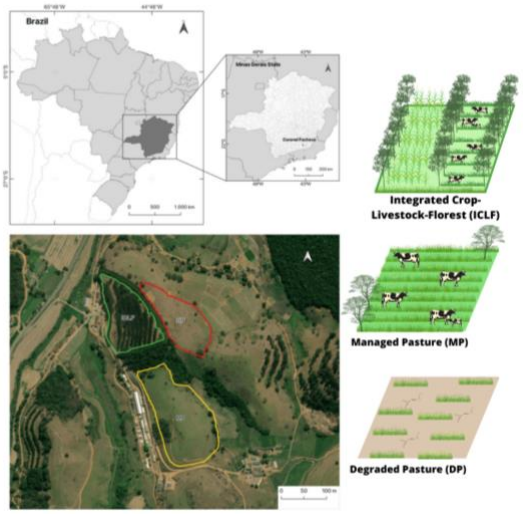

Figure 1: Experimental area in Coronel Pacheco, MG, Brazil.

Demineralization with HF 10 cL L-1 solution and elemental analysis

Determined according to Gonçalves et al. (2003).

Spectroscopic Analysis

Determined according to Gonçalves et al. (2003) and (Chefetz et al., 1996).

Thermogravimetric Analysis

Determined according to Plante et al. (2005).

Results and Discussion

Spectroscopic Analysis

The spectra obtained for all systems showed the same pattern (Figure 1).

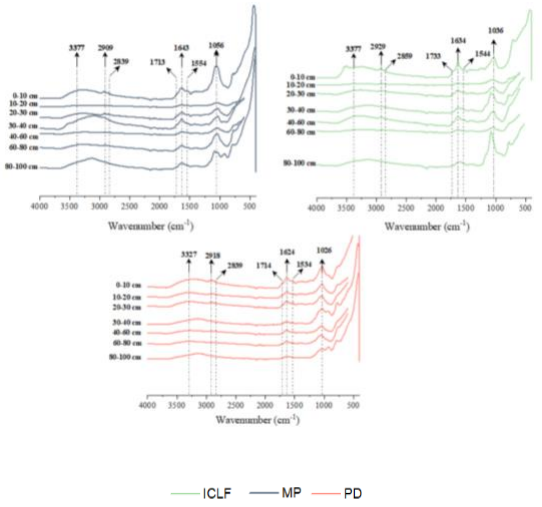

Figure 2: FTIR spectra of the different soil management

The prominent bands observed in the spectra were: 3417 cm-1, attributed to O-H bond stretching; 2918 and 2850 cm-1, related to the C-H stretching of aliphatic groups; 1720 cm-1, due to C=O stretching of the carboxylic group; 1630 cm-1, referring to C=C stretching of aromatic groups; 1540 cm-1, due to the N-H deformation and the C=N stretching; 1072 cm-1, attributed to C-O binding of carbohydrates.

The relative intensity referring to the aliphatic groups was more evident in MP, indicating the presence of more hydrophobic material in this system. In addition to the peak referring to the aliphatic groups, the MP also indicated higher relative intensities for RI 1630 and RI 1710, indicating the functionalization of aromatic compounds in this system by carboxylic groups.

The relative intensity around 1072 (RI 1072), referring to C=O groups of carbohydrates, tended to decrease in depth in MP and DP, while in the ICLF system, there was a tendency to increase in depth. Where can be explained by the entry of polysaccharides via root exudation.

When observing the IA, the highest values found in the PD suggest a more recalcitrant SOM in this management, probably having the presence of alkyls and carbonaceous compounds.

Thermogravimetric Analysis

In general, the SOMHF of the three treatments showed the same thermal-decomposition curve pattern and four main temperature intervals were identified (Figure 2).

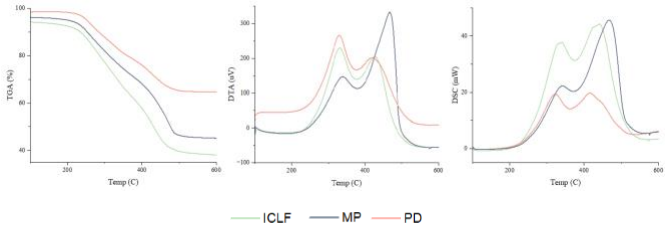

Figure 3: Thermoanalysis curves in 0-10 cm depth. (A) TGA curve and (B) DSC curve.

Most of the weight loss in DTG occurred in the labile pool; the recalcitrant pool accounted only for about 25% of total SOM (mean: 25,27± 2.9). The percentage of recalcitrant pool was very homogeneous; no significant effect of either the land use.

The thermogravimetric index (TGI), which informs the proportion between the less thermolabile and more thermostable structures, was higher in the MP and lowest in the DP.

Conclusions

The spectroscopic analysis indicated the presence of more hydrophobic material in the managed pasture, high content of polyphenols or lignin in the active soil layer and root exudation of the tree component in the ICLF and more recalcitrant organic matter in the degraded pasture. The thermogravimetric analysis indicated greater mass losses related to the labile carbon fraction and corroborated with the content and spectroscopy data.

Acknowledgements

The authors thank CNPq (Brazilian research council) for fellowships and the FAPERJ for financial support.

References

Chefetz, B., Hatcher, P. G., Hadar, Y., & Chen, Y. (1996). *Chemical and biological characterization of organic matter during composting of municipal solid waste* (Vol. 25, No. 4, pp. 776-785). American Society of Agronomy, Crop Science Society of America, and Soil Science Society of America

Gonçalves, C. N., Dalmolin, R. S., Dick, D. P., Knicker, H., Klamt, E., & Kögel-Knabner, I. (2003). The effect of 10% HF treatment on the resolution of CPMAS 13C NMR spectra and on the quality of organic matter in Ferralsols. *Geoderma*, *116*(3-4), 373-392

Plante, A. F., Pernes, M., & Chenu, C. (2005). Changes in clay-associated organic matter quality in a C depletion sequence as measured by differential thermal analyses. *Geoderma*, *129*(3-4), 186-199

XVI LATIN AMERICAN CONGRESS ON ORGANIC GEOCHEMISTRY
9 - 11 AUGUST, 2023
ARACAJU, SERGIPE, BRAZIL

INTEGRATED CROP-LIVESTOCK-FOREST AND WELL-MANAGED PASTURES INCREASE SOIL CARBON STOCKS IN THE BRAZILIAN ATLANTIC FOREST BIOME

P. A. D. OLIVEIRA [a*]; R. A. R. RODRIGUES [a]; L. J. SILVA[b]

[a] Programa de Pós-Graduação em Geoquímica, Universidade federal Fluminense (UFF)/ [b] Universidade de São Paulo (USP)

pa_dias@id.uff.br

Introduction

In recent decades, agriculture in Brazil has experienced rapid growth, mainly in tropical regions, where the expansion and intensification of agricultural land is seen as an opportunity to achieve food security for the world's population. region of Brazil faces problems of high soil degradation due to the adoption of traditional practices and inadequate management

According to (Hott et al., 2016), about 1.2 million hectares (32%) of the land in the Zona da Mata (MG) are used for pasture. Of these, about 60% have some degree of soil degradability. Under these conditions, it is necessary to use conservationist agricultural practices, such as proper management of pastures and the adoption of integrated systems (for example, Crop-Livestock-Forest), which make it possible to reduce soil disturbance, preserving the reserves of organic matter and nutrients (Pereira et al., 2018).

Given the assumption, this study aimed to determine the carbon and nitrogen contents of the soil under different types of management and, at the same time, to investigate the benefits of conservationist practices for the preservation of soil organic matter.

Experimental

The experimental area was the José Henrique Bruschi Experimental Field, belonging to Embrapa Gado de Leite, Coronel Pacheco, MG, Brazil (21º 33'S, 43º 06'W) (Figure 1).

The soils were classified as Dystrophic Red-Yellow Latosol with clayey texture and wavy relief. Three walls of each treatment were sampled at three depths (0-10, 30-40, and 80-100 cm).

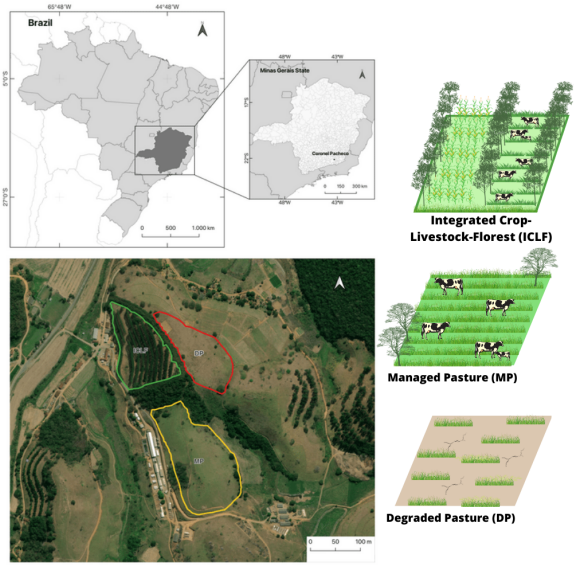

Figure 1: Experimental area in Coronel Pacheco, MG, Brazil.

Physical fractionation of soil

Determined according to (Cambardella & Elliott, 1992), with adjustments in the sample weight used as described in (Bayer et al., 2004).

Soil organic carbon and nitrogen contents

Described by (Nelson & Sommers, 1996) with adjustments from (Blair et al., 1995).

Carbon management index (CMI)

Determined according to Blair et al., (1995).

Results and Discussion

The granulometric analysis indicated that the use and management did not interfere with the soil texture. The

lower levels of clay in the DP indicate a more advanced stage of soil degradation.

Soil organic carbon and nitrogen contents

The SOC content showed a decrease in depth in the three systems evaluated, but the MP system (34.3±1.59 g kg-1) showed the highest levels of SOC followed by ICLF (26±1.35 g kg-1) and DP (19.2±1.67 g kg-1) (Table 2).

Table 1: C, N and C/N (mean ± standard deviation) content of different soil management in Coronel Pacheco-MG.

Management Type	Depth	SOC	C labile	C/N	C Sand	C Clay
	(cm)	(g Kg^{-1})	(g Kg^{-1})		(g kg^{-1})	(g kg^{-1})
ICLF	0-10	26,09	1,69	15,11	2,03	24,34
	30-40	15,88	*0,45*	13,56	0,4	12,16
	80-100	12,02	*0,04*	11,71	1,41	9,37
Mean ±SD		16,97±4,6	*0,96±0,4*	*13,5±1,4*	*0,69±0,6*	*12,16±4,9*
Managed Pasture	0-10	29,03	2,21	13,09	3,0	25,78
	30-40	16,87	*0,41*	14,1	1,31	12,68
	80-100	15,13	*0,02*	10,44	0,62	8,82
Mean ±SD		19,36±4,7	1,11±0,63	13,09±1,6	0,94±0,8	12,68±5,0
Degraded Pasture	0-10	19,63	1,26	14,79	0,58	18,94
	30-40	14,43	*0,57*	11,09	0,31	12,67
	80-100	12,13	*0,13*	13,33	0,3	8,45
Mean ±SD		14,85±2,5	1,01±0,2	12,15 ±1,8	0,36 ±0,1	12,67 ±3,1

SOC= Soil Organic Carbon; C-labile= labile carbon content; C/N= Elementary relation; Csand= carbon associated with the sand fraction; Cclay= carbon associated with the clay fraction.

Regarding the data for C_{labile}, it can be observed that the type of soil management influenced the contents mainly in the active soil layer (0-10 cm). The MP showed the highest levels (1.11 ±0.62 g kg^{-1}), followed by DP (1.01±0.21 g kg^{-1}) and ICLF (0.96±0.41 g kg^{-1}).

Carbon management index (CMI)

The variation in CMI values between the systems is interpreted as soil quality between the studied areas. There was a tendency to decrease in-depth, and the highest values were attributed to MP and ICLF (177 and 133, respectively) (Figure 2).

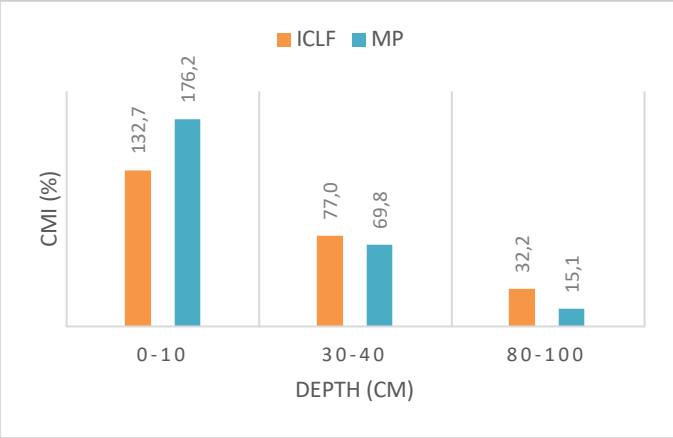

Figure 2: Carbon Management Index (CMI) considering Degraded Pasture as a reference.

The highest levels of SOC and C labile evidence the ability of these systems to improve soil quality and promote system sustainability, providing C as a source of energy for soil fauna and microbial activity.

Conclusions

The highest SOC content confirms our hypothesis that these systems could improve soil quality and increase SOM levels in the Atlantic Forest biome.

Acknowledgements

The authors thank CNPq (Brazilian research council) for fellowships and the FAPERJ for financial support.

References

Bayer, C., Martin-Neto, L., Mielniczuk, J., & Pavinato, A. (2004). Armazenamento de carbono em frações lábeis da matéria orgânica de um Latossolo Vermelho sob plantio direto. *Pesquisa Agropecuária Brasileira*, *39*, 677-683

Blair, G. J., Lefroy, R. D., & Lisle, L. (1995). Soil carbon fractions based on their degree of oxidation, and the development of a carbon management index for agricultural systems. *Australian journal of agricultural research*, *46*(7), 1459-1466

Cambardella, C. A., & Elliott, E. T. (1992). Particulate soil organic-matter changes across a grassland cultivation sequence. *Soil science society of America journal*, *56*(3), 777-783

Hott, M. C., Carvalho, L. M. T. D., Antunes, M. A. H., Santos, P. A. D., Arantes, T. B., Resende, J. C. D., & Rocha, W. S. D. D. (2016). Vegetative growth of grasslands based on hyper-temporal NDVI data from the Modis sensor. *Pesquisa Agropecuária Brasileira*, *51*, 858-868

Nelson, D. A., & Sommers, L. (1983). Total carbon, organic carbon, and organic matter. *Methods of soil analysis: Part 2 chemical and microbiological properties*, *9*, 539-579

Pereira, L. F., Ferreira, C. F. C., & Guimarães, R. M. F. (2018). Manejo, qualidade e dinâmica da degradação de pastagens na Mata Atlântica de Minas Gerais-Brasil. *Nativa*, *6*(4), 370-379

XVI LATIN AMERICAN CONGRESS ON ORGANIC GEOCHEMISTRY
9 - 11 AUGUST, 2023
ARACAJU, SERGIPE, BRAZIL

Distribuição de *n*-Alcanos em Sedimentos e Tecidos Vegetais de *Rhizophora mangle* em Manguezais da Baía de Paranaguá, PR (Brasil)

Stephani Tiné Didoni [a]; Ana Caroline Cabral [a,b*]; César de Castro Martins [a,b,c*]

[a] Centro de Estudos do Mar - UFPR; [b] Pós-Graduação em Sistemas Costeiros e Oceânicos – UFPR; [c] Universidade de São Paulo - USP

ana.ccabral2@gmail.com; ccmart@usp.br; ccmart@ufpr.br

Introdução

O manguezal é um dos ecossistemas mais produtivos do planeta, com impactos significativos na qualidade de vida humana e marinha. Em escala global, tem relevância no sequestro e estoque de carbono, atuando como agente regulador do clima e mitigador do aquecimento global. Espécies de mangue, como *Rhizophora mangle,* contribuem de forma significativa para o *pool* de matéria orgânica (MO) deste ecossistema. Por isso, integrar perfis de marcadores geoquímicos, como *n*-alcanos, de sedimento e tecidos vegetais desta espécie pode auxiliar na compreensão do papel dos manguezais no ciclo da MO em sistemas costeiros, bem como em estudos de ecofisiologia e paleoceanografia [1-2]. Sendo assim, neste estudo, investigou-se a distribuição de *n*-alcanos em tecidos vegetais de *R. mangle* e sedimento adjacente em manguezais do Complexo Estuarino de Paranaguá-PR (CEP) (Fig. 1), a fim de estabelecer o perfil de *n*-alcanos individuais em folhas, raiz e galhos e a contribuição destes tecidos na MO encontrada nos sedimentos.

Amostragem e método analítico

As coletas foram realizadas em fevereiro/2022, em seis pontos ao longo do eixo leste – oeste do CEP (Fig. 1).

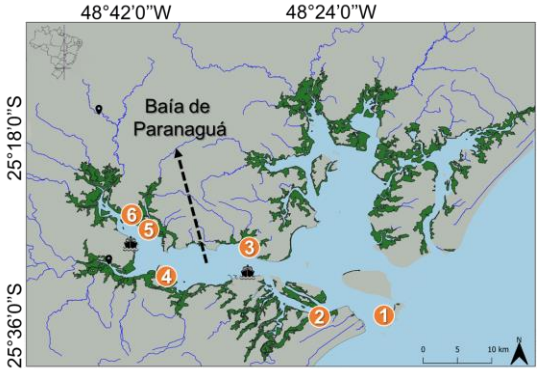

Figura 1. Mapa da área de estudo com os pontos de coleta indicados em laranja. Destaques em verde correspondem a áreas de manguezal.

Para a determinação dos *n*-alcanos, as amostras foram liofilizadas, trituradas/desagregadas, e uma alíquota de 2g por amostra foi extraída em ultrassom. Os extratos foram fracionados e purificados em cromatografia líquida de adsorção em coluna de vidro com sílica e alumina (5% desativadas), e eluição de 10 mL de *n*-hexano. A análise instrumental foi realizada em cromatógrafo gasoso acoplado a um espectrômetro de massas.

Resultados e Discussão

Sedimento e folhas apresentaram as maiores concentrações para *n*-alcanos totais (23,0 ± 20,8 e 128,4 ± 34,7 μg g^{-1}, respectivamente). Ambas as matrizes apresentaram perfis de *n*-alcanos equivalentes entre si, com predominância de cadeias longas e ímpares (*n*-C_{27} a *n*-C_{31}) (Fig. 2 e 3). Os *n*-alcanos de cadeias longas (> C_{26}) são comuns em ceras foliares de plantas vasculares, com importância fisiológica na regulação da transpiração da planta e proteção contra o estresse hídrico [3].

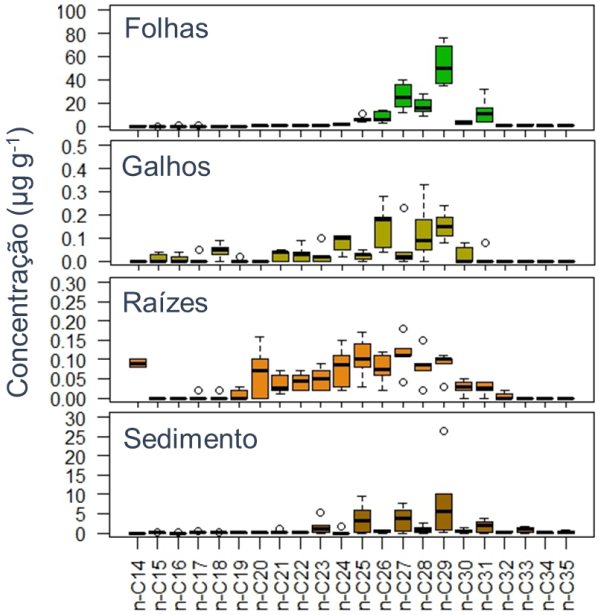

Figura 2. Perfil de *n*-alcanos (*n*-C_{14} a *n*-C_{35}) nas diferentes matrizes analisadas.

Por outro lado, raízes e galhos apresentaram concentrações para *n*-alcanos totais inferiores (< 1,0 µg g^{-1}) em relação a sedimento e folhas, com contribuições de cadeias médias e longas equivalentes entre si (Fig. 3), e sem predominância aparente entre cadeias pares ou ímpares. Em galhos, inclusive, verificou-se uma contribuição relevante de *n*-C_{26} e *n*-C_{28} (Fig. 2).

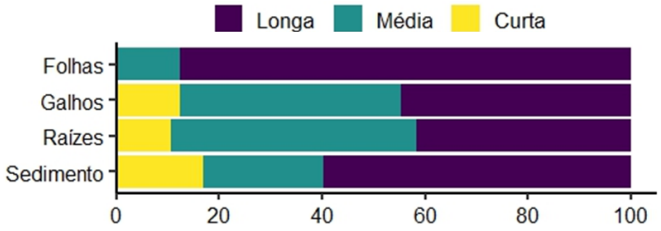

Figura 3. Perfil dos comprimentos de cadeia de *n*-alcanos em cada matriz analisada. Curta = *n*-C_{15} - *n*-C_{20}; Média = *n*-C_{21} - *n*-C_{26}; Longa = *n*-C_{27} a *n*-C_{32}.

Os parâmetros de avaliação de origem de MO 'Índice Preferencial de Carbono (IPC)', 'Razão Terrígeno/Aquático (RTA)' e 'Índice de Comprimento Médio de Cadeia (ICM)' foram aplicados para complementar a avaliação da assinatura de *n*-alcanos nas diferentes matrizes. Sedimento e folhas apresentaram IPC > 4,0 e RTA > 3,0, típicos de MO terrígena, como esperado, enquanto raízes e galhos apresentaram valores inferiores. Valores de ICM (~ 28,0) são indicativos de predominância de cadeias longas nas quatro matrizes.

Os resultados obtidos nas diferentes matrizes foram integrados em uma análise de componentes principais (ACP) (Fig. 4).

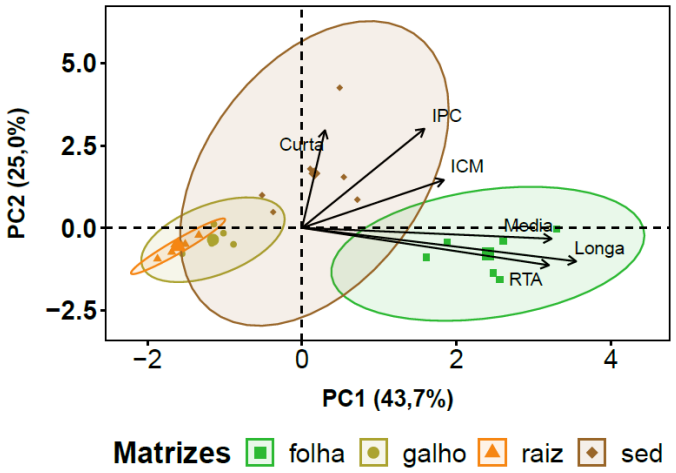

Figura 4. Análise de Componentes Principais (ACP) integrando resultados dos sedimentos e tecidos vegetais

Nesta ACP é evidenciada a separação das matrizes em três grupos principais: (i) sedimento; (ii) folhas, e; (iii) galhos e raízes. Amostras de folhas foram caracterizadas por altos valores de RTA e *n*-alcanos de cadeias médias e longas, enquanto as amostras de galho e raiz localizam-se no extremo oposto a estas variáveis. A maior dispersão das amostras de sedimentos na ACP pode ser relacionada à formação de MO sedimentar por *n*-alcanos proveniente de uma variedade de fontes, incluindo antrópicas, mesmo que folhas de *R. mangle* respondam por uma parcela significativa da MO sedimentar.

Conclusões

A equivalência das assinaturas de *n*-alcanos entre folhas e sedimento evidenciou a relevância das folhas de mangue na composição da MO sedimentar. Raízes e galhos, no entanto, apresentam menor contribuição, visto as menores concentrações e diferenças no perfil de *n*-alcanos em relação ao sedimento. Dados inéditos de *n*-alcanos em raízes e galhos de *R. mangle* são disponibilizados neste estudo, e as diferenças encontradas em relação às demais matrizes sugerem a necessidade de ampliar a gama de matrizes ambientais analisadas em manguezal para marcadores geoquímicos, a fim de identificar os principais contribuintes da MO para o ecossistema manguezal.

Agradecimentos

Os autores agradecem ao CNPq pelas bolsas de Pós-Doutorado Júnior de A.C. Cabral (Processo: 164390/2020–0), e de iniciação científica de S.T. Didoni (Processo: 133814/2022-0).

Referências

[1] Belligotti, F. M., Carreira, R. S., Soares, M. L. G., 2007. Contribuição Ao Estudo Do Aporte De Matéria Orgânica Em Sistemas Costeiros: Hidrocarbonetos Biogênicos em Folhas de Mangue. Geochimica Brasiliensis **21**, 71–85.

[2] Albergaria-Barbosa, A. C. R., Schefuß, E., Taniguchi, S., Santos, P. S., Cunha-Lignon, M., Tassoni-Filho, M., Figueira, R. C. L., Mahiques, M. M., Bícego, M. C., 2023. Characterization of the organic matter produced by Atlantic Rainforest plants and its influence in the surface sediments deposited in a protected subtropical Estuarine–Lagoon system. Regional Studies in Marine Science **57**, 102728.

[3] Eglinton, G., Hamilton, R. J., 1967. Leaf epicuticular waxes. Science **156**, 1322–1335.

XVI LATIN AMERICAN CONGRESS ON ORGANIC GEOCHEMISTRY
9 - 11 AUGUST, 2023
ARACAJU, SERGIPE, BRAZIL

VARIATIONS OF HYDROCARBON COMPOSITION IN SURFACE SEDIMENTS IN AMAZON FLOODPLAIN LAKES

ALEXANDER A. LOPES[a,*], VINÍCIUS B. PEREIRA[a], LEONARDO AMORA-NOGUEIRA[b], LUCIANE S. MOREIRA[b], RENATO C. CORDEIRO[b], HUMBERTO MAROTTA[b], GABRIELA VANINI[a], DÉBORA A. AZEVEDO[a]

[a] Federal University of Rio de Janeiro, Brazil
[b] Federal Fluminense University, Brazil

*alexander.silva@iq.ufrj.br

Introduction

Aquatic systems' organic matter (OM) can originate from autochthonous or allochthonous sources (Hobbie, 2000). Therefore, the characterization of OM can be used as a record of processes that happen in the water column and the transport processes suffered by the deposited material. The preserved OM allows the proposal of several parameters to determine its source (Killops and Killops, 2005). The study of the composition of organic sediment materials is difficult to achieve, in most cases, due to the heterogeneity and the different levels of preservation of the compounds that form organic materials, originating from the most different types of sources. Lipid markers (*n*-alkanes, hopanes, and plant triterpenes) were investigated to understand and reconstruct environmental regimes in short cores of floodlplain lakes from different types of water: the Taparí Lake (Tapajós River, clearwater), Comprido Lake (Amazon River, whitewater), Puruzinho Lake (Madeira River, whitewater), and Barro Preto Lake (São Manuel River, blackwater) in the Amazon Basin.

Experimental

Four short cores with 10-12 cm were collected from Taparí Lake (Tapajós River), Comprido Lake (Amazon River), Puruzinho Lake (Madeira River), and Barro Preto Lake (São Manuel River) in the Amazon Basin. The sample was sectionated at 2 cm interval, freeze-dried and kept at -20 ºC until analysis. Samples were weighted (ca. 1.0 g) and extracted) as described in Lopes et al. (2021). The extract was then dried, and added 1 mL of KOH 0.1 mol L^{-1} (methanol:H_2O 9:1). Samples were saponified and neutral lipids were extracted using 3×3 mL of hexane. These were fractionated into aliphatic hydrocarbons (F1), aromatic hydrocarbons (F2) and neutral polar compounds (F3) using activated silica liquid chromatography, eluded with *n*-hexane, *n*-hexane:dicloromethane (9:1) and dicloromethane: methanol (8:2), respectively.

F1 fractions were analyzed by GC-FID, GC/MS, and GC/C/IRMS, with a HP-5MS (5% phenyl-95% methylsiloxane, 30 m, 0.25 mm i.d., 0.25 µm df).
Qualitative analysis was performed based on mass spectrum interpretation, literature comparison and retention order, and individual concentration of compounds was achieved by semiquantitation based on internal standards concentration in ng g^{-1}.

Results and Discussion

The four cores presented distinct *n*-alkane origin profiles. Barro Preto Lake presented bimodal profile with an odd/even prevalence on the entire chromatographic fingerprint, pointing to a predominance of higher plants. The Puruzinho Lake profile was bimodal with even/odd carbon predominance in the range of *n*-C_{16} to *n*-C_{22} with C_{max} at *n*-C_{18}, suggesting the presence of non-photosynthetic bacteria, as well as for the Taparí Lake (FIG.2). Comprido Lake presented a bimodal profile (*n*-C_{23} to *n*-C_{35}) indicating the contribution of terrestrial plants. The presence of des-A-terpenes was revealed by GC/MS (Fig.2A). These are strong indicatives of vascular plants of C3 type, in which the cleavage of the A ring of the original precursor is usually associated with anoxic environments.

The analysis of hopanes, bacterial triterpenes, presented both biological ββ and thermally-mature αβ and βα isomers. Besides that, diploptene was detected in high concentrations in the samples, specially for the Barro Preto.

The Barro Preto and Comprido Lake sediments showed the highest concentrations of des-A-terpenes (average 34 ng g^{-1} TOC^{-1} and 23 ng g^{-1} TOC^{-1}, respectively), whereas Taparí Lake and Puruzinho presented the lowest values(average 3 ng g^{-1} TOC^{-1} and 10 ng g^{-1} TOC^{-1}).

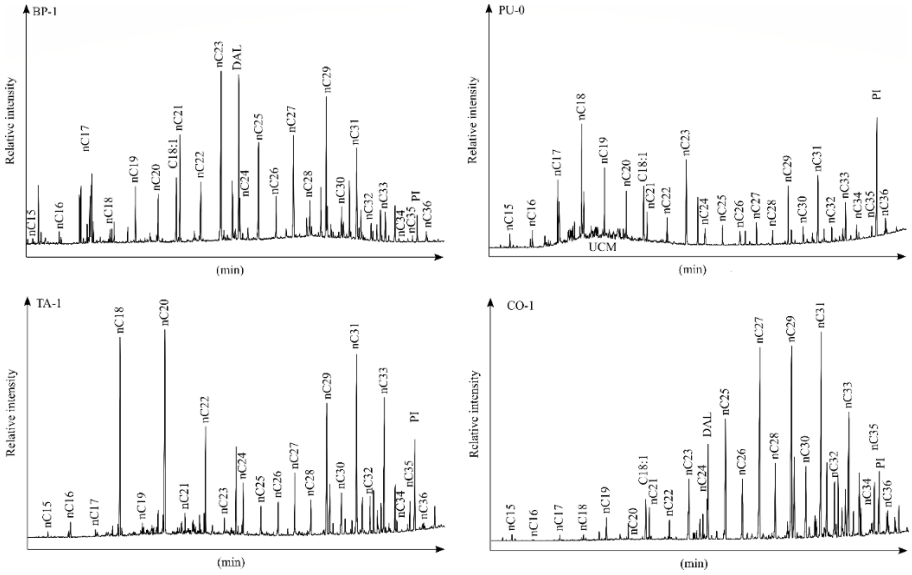

Figure 1. GC-FID chromatograms for the uppermost segments of the studied cores with n-alkane identifications.

The values for $\delta^{13}C$ isotopic composition of individual *n*-alkanes C_{27}-C_{31} of the 4 cores varied between -32 and -38 ‰ indicating the contribution of C3 higher plants, while depleted values of $\delta^{13}C$ from -42 to -52 ‰, determined for C_{20}-C_{27} *n*-alkane, pointed to incorporation of depleted ^{13}C from methane oxidation, in the Barro Preto core, as well as the - 42 ‰ value for the diploptene.

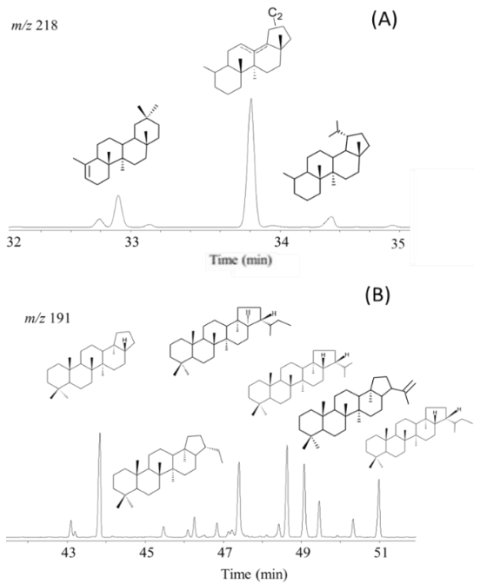

Figure 2. Extracted ion chromatograms (EIC) from Comprido Lake: (A) *m/z* 218 highlighting plants des-A-terpenes; (B) *m/z* 191 for hopanes.

Conclusions

The *n*-alkanes contribution was evaluated, and it was possible to determine the vegetation type and origin of the predominant organic matter, although it is not possible to determine if there is a relationship with the type of water, since the organic matter may be of lentic (from the lake itself) or lotic origin (transported by the river in the flooded season). The analysis of terpenes, more specifically des-A-terpenes, can be applied to differ blackwater lakes, which may be related to anoxic sediments, since Barro Preto and Comprido Lake presented the highest relative concentrations of des-A-terpenes.

Acknowledgments

The authors thank Capes, CNPq and FAPERJ for fellowships and financial support.

References

HOBBIE, J. E., Ed. Estuarine Science - a synthetic approach to research and practice. Covelo: Island Pressed. 2000.

KILLOPS S.D., KILLOPS, V.J. 2005. An Introduction to Organic Geochemistry. 2° Ed. EUA: Logman Scientific & Technical.

LOPES, A. A. ; PEREIRA, V. B. ; AMORA-NOGUEIRA L. et al., 2021. Hydrocarbon sedimentary organic matter composition from different water-type floodplain lakes in the Brazilian Amazon. Organic Geochemistry 159, 104287.

XVI LATIN AMERICAN CONGRESS ON ORGANIC GEOCHEMISTRY
9 - 11 AUGUST, 2023
ARACAJU, SERGIPE, BRAZIL

SOURCE AND WEATHERING OF SPILLED OILS ON THE COAST OF THE STATE OF CEARÁ, NORTHEAST BRAZIL, IN EARLY 2022

Rufino N.A. Azevedo[a*], Kamylla M.M. Bezerra[a], Ronaldo F. Nascimento[a], Robert K. Nelson[b], Christopher M. Reddy[b], Adriana P. Nascimento[a], Danielle M.M. Franco[c], Taynara R. Covas[c], Boniek G. Vaz[c], André H.B. Oliveira[a], Rivelino M. Cavalcante[a], Laercio L. Martins[a,d]

[a]Federal University of Ceará (UFC), [b]Woods Hole Oceanographic Institution (WHOI), [c]Federal University of Goiás (UFG), [d]North Fluminense State University (UENF)

*email: rufinoneto04@gmail.com

Introduction

In January 2022, the coastline of the state of Ceará, Northeast Brazil, was impacted by the arrival of approximately 8,000 liters of oil along 400 km and 65 beaches. Molecular biomarkers assessed by Gas chromatography demonstrated that these oils do not share the same source as the large spill that occurred in August 2019 on the Northeast coast of Brazil [1]. With this, this study aims to extend the investigation of the oil spilled early 2022 on the coast of Ceará, assessing the geochemical origin and the type of product, crude or refined oil, as well as, to evaluate the influence of weathering processes on its chemical composition.

Experimental

Six oil samples (P01#22 to P06#22) were collected from beaches along 130 km of the east coast of the State of Ceará. These samples were analyzed using one-dimensional gas chromatography techniques, GC-FID, to assess *n*-alkanes and isoprenoids, and GC-MS, for analysis of polycyclic aromatic hydrocarbons (PAHs), in addition to comprehensive two-dimensional gas chromatography (GC×GC-HRT and GC×GC-FID), for analysis of biomarkers. Furthermore, acidic compounds were analyzed by Fourier transform ion cyclotron resonance mass spectrometry (FT-ICR MS) using the electrospray ionization source in negative mode [ESI(-)].

Results and Discussion

Biomarker compounds are traditionally used in oil spill studies to assess geochemical information, including the maturity and depositional environment of their source rocks [2]. In the maturity assessment, the values obtained using the ratio C31HH 22S/(22S+22R) were close among the samples (~0.56), but outside the main phase of oil generation (0.57-0.62). However, the values for the ratio C32HH 22S/(22S+22R) (~0.59) and the values obtained for the ratio C30M/C30H (0.10-0.11) indicate that the main generation phase was reached [3]. In the depositional environment assessment, the high values of the ratio C31 HH/C30H (0.49-0.50), C35/C34 HH (1.12-1.22), C29/C30 H (0.98-1.00), and the C35 HH index (14.40-15.50 %), together with the low values of the Pr/Ph ratio (0.31-0.45), suggest that this oil was generated from marine carbonate source rocks, probably in an anoxic depositional environment [3].

Additionally, new evidence obtained through the PAHs indicates that the oil may have undergone thermal alteration processes, in the case of a refined product. The 2- and 3-methylphenanthrene (MP) isomers, more thermally stable, are found in greater abundance in refined products when compared to the 9/4-MP and 1-MP isomers, as was observed in this study (**Figure 1**). Anthracene (An) and its methylated compounds, especially 2-methylanthracene (MA), present in the analyzed oils (**Figure 1**), are generally absent or in very low abundance in crude oils. However, during rapid heating and cooling in some refining processes (e.g., cracking) these compounds can be formed [2].

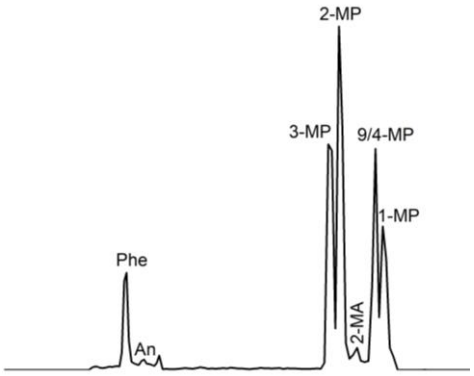

Figure 1. Representative chromatogram *m/z* 178 + 192 showing the An, Ph, and their methylated compounds present in aromatic fraction of the oil spilled in early 2022 in the state of Ceará.

Zhang et al., 2016 suggested new ratios using An, phenanthrene (Ph), 2-MA, and MP to distinguish crude oils from heavy fuel oils (HFOs), which share some physicochemical similarities. In the present study, the ratios that use 2-MA, such as the ratio 2-MA/∑MP (0.01-0.03), were below the values observed for HFOs (0.04-0.09). These ratios may be affected by photooxidation, which preferentially reduces the abundance of 2-MA over MP isomers [2]. Three of the six samples presented values for the ratio An/(An+Ph) (0.03-0.07) consistent with the values observed in HFOs (0.05-0.37) and all samples presented values for the ratio (3- + 2-MP)/(9- + 1-MP) (1.60-2.14) characteristic of HFOs >1.50 [4].

The weathering processes, also evaluated in this work (**Figure 2**), such as evaporation, biodegradation, and photooxidation, affect the chemical composition of spilled oils and must be considered in a forensic analysis [2].

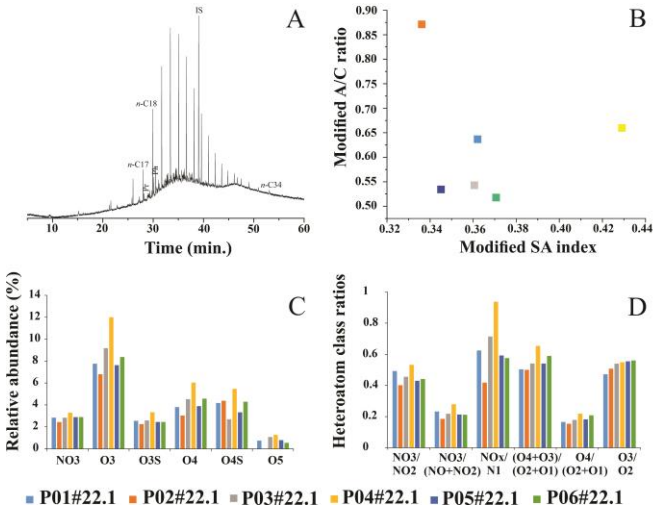

Figure 2. Evaluation of weathering effects: Evaporation through GC-FID chromatograms (representative for the samples) (a); Biodegradation by the A/C ratio and modified SA index (b), Photooxidation from the distribution of oxygenated classes (c) and ratios calculated from these classes (d).

Evaporation, which occurs in the first few hours after a spill, removing lighter compounds [4], was probably responsible for the absence of low molecular weight *n*-alkanes <*n*-C16 (**Figure 2A**). The low values obtained for the Pr/*n*C17 (0.26-0.41), Ph/*n*C18 (0.18-0.35) ratios together with the high values obtained for the A/C ratio (0.77-1.26), modified A/C ratio (0.52-0.87), and the low values of the modified SA index (0.35-0.43) are consistent with an oil that is non- to slight biodegraded [2;5]. The presence of classes with more than two oxygen atoms (e.g., O_3, O_4, and O_5, **Figure 2C**), indicates that these samples were intensely affected by photooxidation [6]. Furthermore, the presence of these classes in greater abundance, together with the higher values of the ratios suggested by Lima et al. (2021), which tend to increase with photooxidation (**Figure 2D**), are indications that the P04#22 sample was probably the most affected by photooxidative processes.

Conclusions

The biomarker ratios indicated that the oil spilled on the coast of the state of Ceará in January 2022 is mature and was generated from marine source rocks, probably in an anoxic depositional environment. The presence of anthracene and 2-methylanthracene, generally absent in crude oil, together with ratios obtained through PAHs, do indicate the possibility that this oil is a heavy fuel or blended mixture of a refinery product with crude oil. The ratios Pr/*n*C17, Ph/*n*C18, modified A/C, and modified SA index are consistent with low or non-biodegraded oil. However, the presence in greater abundance for the oxygenated compounds with more than two oxygen atoms (e.g., O_3, O_4, and O_5 classes), together with the values obtained for the ratios that use these compounds, indicate that the samples undergone significant photooxidation, in which the sample P04#22 was the most affected.

Acknowledgements

The authors thank Higher Education Personnel Improvement Coordination (CAPES); Chemistry Graduate Program (PGQUIM)-UFC; LEA-UFC; LACOR-UFC; LAT-UFC; Chemistry Institute-UFG, and MC&G-WHOI.

References

[1] Azevedo, R.N.A, Bezerra, K.M.M., Nascimento, R.F., Nelson, R.K., Reddy, C.M., Nascimento, A.P., Oliveira, A.H.B., Martins., L.L., Cavalcante, R.M., 2022. Is there a similarity between the 2019 and 2022 oil spills that occurred on the coast of Ceará (Northeast Brazil)? An analysis based on forensic environmental geochemistry. Environmental Pollution 314, 120283.

[2] Stout, S., Wang, Z., 2016. Standard handbook oil spill environmental forensics: fingerprinting and source identification. Academic press.

[3] Peters, K. E., Walters, C. C., & Moldowan, J. M., 2007. The biomarker guide: Volume 2, Biomarkers and isotopes in petroleum systems and earth history. Cambridge University Press.

[4] Zhang, H., Wang, C., Zhao, R., Yin, X., Zhou, H., Tan, L., Wang, J., 2016. New diagnostic ratios based on phenanthrenes and anthracenes for effective distinguishing heavy fuel oils from crude oils. Marine Pollution Bulletin 106, 58-61.

[5] Martins, L. L., Pudenzi, M. A., da Cruz, G. F., Nascimento, H. D., & Eberlin, M. N., 2017. Assessing biodegradation of Brazilian crude oils via characteristic profiles of O1 and O2 compound classes: petroleomics by negative-ion mode electrospray ionization Fourier transform ion cyclotron resonance mass spectrometry. Energy & Fuels 31, 6649-6657.

[6] Lima, B. D., Martins, L. L., de Souza, E. S., Pudenzi, M. A., da Cruz, G. F., 2021. Monitoring chemical compositional changes of simulated spilled Brazilian oils under tropical climate conditions by multiple analytical techniques. Marine Pollution Bulletin 164, 111985.

COMPOSITION OF PAHs IN WATER, SEDIMENTS AND OIL SLICKS FROM THE BRAZILIAN COAST TO ASSESS THE IMPACT OF THE 2019 OIL SPILL

ANTÔNIA M. CORRÊA [a*], MARCUS F. TENÓRIO [b], KÁTIA Z. LEAL [c], FELIPE F. CAMPOS [d], CARLOS D. PÉREZ [d], FABIANO THOMPSON [e], CARLOS E. de REZENDE [f], MARCELO C. BERNARDES [a,b]

[a]PROGRAMA DE PÓS-GRADUAÇÃO EM QUÍMICA, UFF, NITERÓI, RJ, BRASIL; [b]PROGRAMA DE PÓS-GRADUAÇÃO EM GEOQUÍMICA, UFF, NITERÓI, RJ, BRASIL; [c]DEPARTAMENTO DE FÍSICO-QUÍMICA, UFF, NITERÓI, RJ, BRASIL; [d]NÚCLEO DE BIOLOGIA, UFPE, VITÓRIA DE SANTO ANTÃO, PE, BRASIL; [e]INSTITUTO DE BIOLOGIA, UFRJ, RIO DE JANEIRO, RJ, BRASIL; [f]LABORATÓRIO DE CIÊNCIAS AMBIENTAIS, UENF, CAMPOS DOS GOYTACAZES, RJ, BRASIL.

* e-mail: antoniacorrea@id.uff.br

Introduction

Marine oil spills cause a series of damages to the environment and organisms, mainly due to the toxicity of petroleum hydrocarbons [1]. In August 2019, an unprecedented oil spill was identified on the Brazilian coast, reaching more almost 3,200 km of coastline from the extreme Northeast to the Southeast. In 2020 and 2021, the oil slick intermittently reappeared after intense oceanographic events [2–4]. The recovered oil had a dark, bituminous appearance, high viscosity and density greater than seawater, suggesting that it underwent a weathering process that altered its original composition [2]. In addition to the spilled oil characterization, it is important to determine petroleum hydrocarbons in environmental matrices to assess their impact, distribution and persistence [1]. PAHs are used for monitoring weathering and biodegradation and source identification [5]. This work evaluated the composition of the 16 priority PAHs in sediments, seawaters and oil slicks from the Brazilian Northeastern coast.

Experimental

Sediments and waters were sampled on 4 beaches from Pernambuco state, with mangrove or reef ecosystems, in 3 campaigns: 0.5, 1 and 1.5 years after the spill. Oil slicks were collected on affected beaches from Alagoas state. Sediments were lyophilized and extracted using dichloromethane (DCM) in an ultrasonic bath (3 cycles; 15 min each). The extract was centrifuged and re-eluted in n-hexane. Oils were dissolved in DCM and centrifuged. Sediment extracts and dissolved oils were fractionated using open column liquid chromatography with activated silica as stationary phase. Saturated fraction was eluted with n-hexane, and the aromatic one, with n-hexane/DCM (1:1 %v/v). PAHs in water samples were extracted using automated solid-phase microextraction coupled to GC-MS (SPME-GC-MS) with a 65 µm PMDS/DVB fiber. Extraction time and heating block temperature were optimized at 50 min and 60 °C, respectively. Analyzes were performed in an Agilent 7890A/5975C GC-MS. Samples were injected in splitless mode at 260 °C. An HP5-MS column was used (30 m x 0.25 mm i.d. x 0.25 µm), with oven temperature program: 55 °C (1 min); 7 ºC/min until 300 ºC (10 min). Hydrogen was used as carrier gas at 1.2 mL/min. Data acquisition used selective ion monitoring for the base peaks of each PAH. Ion source temperature was 290 ºC.

Results and Discussion

A similar distribution of PAHs was observed for the 3 oil slick samples, especially for compounds with higher molecular weight (fig. 1). Samples from Francês beach (A and B) had the highest concentrations of PAHs. The high concentrations of phenanthrene, pyrene, benzo[a]anthracene and chrysene in all samples stand out. A greater predominance of lighter compounds could indicate a less intense weathering process in Francês A.

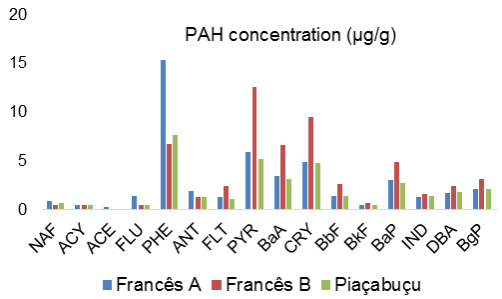

Figure 1. Priority PAHs in the oil slick samples.

A specific signature of PAHs was observed in the sediment samples (fig. 2), that was different from the oil samples. Phenanthrene was quantified in high concentrations, especially in Ariquindá (ARI) and Maracaípe (MAR), locations with mangrove ecosystem. There was a greater abundance of light to medium chain PAHs in the sediments. There is a higher concentration of PAHs in the 1st campaign that decreases with time, which can be a result of a greater input of hydrocarbons in the studied areas by the spill, which decreased over time due to weathering process, that forms alkylated PAHs [1]. Ariquindá had the highest concentration of

PAHs in all sampling campaigns, so there may be a chronic input of these compounds in the location, given that it was indirectly affected by the spill. Further biomarker studies are necessary, since several sources can contribute to the distribution of PAHs in sediments.

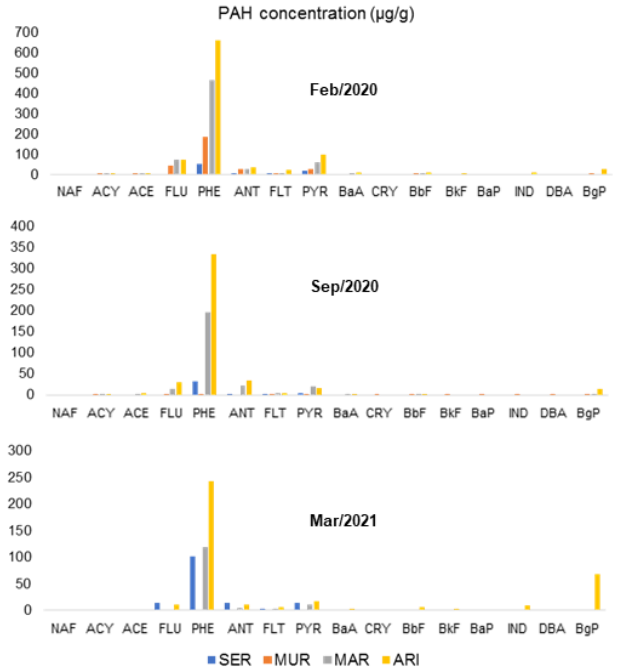

Figure 2. Dispersion and concentrations (µg/g) for the priority PAHs in the sediment samples.

From studying the area ratios of a PAH with an internal standard, it is observed that the water samples also showed a characteristic signature (fig. 3), which is different from the obtained for oil slick and sediment samples. Higher molecular weight PAHs were most abundant in these samples, as well as naphthalene due to its high solubility. Naphthalene abundance was higher in samples from the 2nd campaign (1 year), while the concentration of other PAHs was equivalent. In Maracaípe there was a significant increase in the PAHs from the 2nd to the 3rd sampling campaigns.

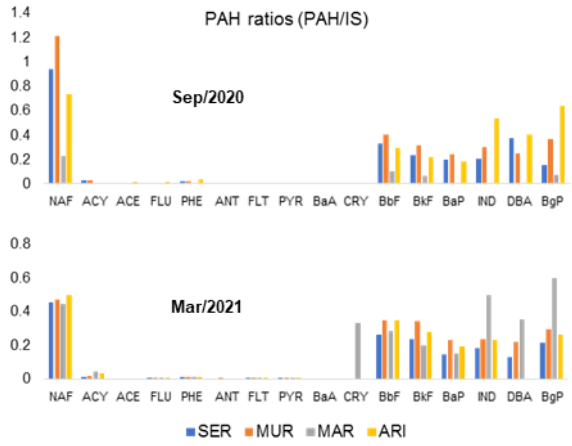

Figure 3. Dispersion and ratios (A_{PAH}/A_{IS}) for the priority PAHs in the water samples.

Conclusions

The oil slicks had hydrocarbon distributions similar to light crude oils, and evidence of low weathering. The results indicate that the 3 samples share the same source [5, 6]. Some minor differences, as the preservation of lighter compounds, may indicate a lighter weathering.

Both sediment and water samples had individual PAH signatures, different from the oil slicks. Phenanthrene was quantified in high concentrations in sediments and oils, and naphthalene in waters. Sediment samples from the 1st sampling campaign (0.5 year) showed higher concentrations of hydrocarbons and there was a decrease of total PAHs with time. In seawater samples, the quantity of heavier compounds was equivalent in the 2nd and 3rd campaigns (1 and 1.5 year), and naphthalene showed a decrease in relative abundance. Sediments showed a higher predominance of low molecular weight PAHs, that could be associated with a petrogenic origin. In water samples, on the other hand, the predominance of high molecular weight PAHs is consistent with a pyrogenic origin [5]. The results gave important initial insights of the spill, by evaluating the temporal-spatial distribution of PAHs in environmental matrices from the Brazilian coast.

Acknowledgements

CAPES (Code 001 PPG-Geoquímica-UFF and PPG-Química-UFF), CAPES Entre Mares (88887.469807/ 2019-00), FAPERJ (E-26/010.101117/ 2018, E-26/210.745/ 2021), FACEPE (APQ-0641-2.05/ 19) and CNPq (Proc. 309474/ 2022-1).

References

[1] Wang, Z.; Stout, S.A.; Fingas, M.; 2006. Forensic fingerprinting of biomarkers for oil spill characterization and source identification. Environmental Forensics **7**, 105–146.

[2] Lourenço, R.A.; Combi, T.; Alexandre, M. R.; Sasaki, S.T.; Zanardi-Lamardo, E.; Yogui, G.T.; 2020. Mysterious oil spill along Brazil's northeast and southeast seaboard (2019–2020): Trying to find answers and filling data gaps. Marine Pollution Bulletin **156**, 111219.

[3] Reddy, C.M.; Nelson, R.K.; Hanke, U.M.; Cui, X.; Summons, R.E.; Valentine, D.L.; Rodgers, R.P.; Chacón-Patiño, M.L.; Niles, S.F.; Teixeira, C.E.P.; Bezerra, L.E.A.; Cavalcante, R.M.; Soares, M.O.; Oliveira, A.H.B.; White, H.K.; Swarthout, R.F.; Lemkau, K.L.; Radović, J.R.; 2022. Synergy of Analytical Approaches Enables a Robust Assessment of the Brazil Mystery Oil Spill. Energy and Fuels **36**, 13688–13704.

[4] de Oliveira O.M.C.; de S Queiroz A.F.; Cerqueira J.R.; Soares S.A.R.; Garcia K.S.; Filho A.P.; de L da S. Rosa M.; Suzart C.M.; de L Pinheiro L.; Moreira Í.T.A.; 2020. Environmental disaster in the northeast coast of Brazil: Forensic geochemistry in the identification of the source of the oily material. Marine Pollution Bulletin **160**, 111597.

[5] Wang, Z.; Fingas, M.; Page, D.S.; 1999. Oil spill identification. Journal of Chromatography A **843**, 369–411.

[6] Peters, K.E., Walters, C.C., Moldowan, J.M., 2005. The Biomarker Guide, 2nd ed, The Biomarker Guide. Cambridge University Press, New York.

Evaluation of the anthropogenic contaminants in the atmospheric particulate matter over an ecotouristic area of Rio de Janeiro, Brazil

Manoel Mendes Alves Junior[a]*, Mateus Maurício de Oliveira[a], Raquel Vieira Santana da Silva[a], Denise de Almeida Gonzalez [b], Debora de Almeida Azevedo [a], Celeste Yara dos Santos Siqueira [a]

[a]LADETEC - Instituto de Química - Universidade Federal do Rio de Janeiro – Ilha do Fundão, Rio de Janeiro - 21949-900 – Brazil
[b] PPGeo- UERJ -Programa de Pós-graduação em Geografia - Universidade Estadual do Rio de Janeiro, Rio de Janeiro – Brazil

manoelmaj@gradu.iq.ufrj.br

Introduction

Air pollution is the main environmental risk factor for health worldwide, not only because of its impact on climate change, but also because of its impact on public and individual health. There are many pollutants that are major disease factors in humans. Among them, particulate matter (PM), volatile and semi-volatile organic compounds as dioxins and polycyclic aromatic hydrocarbons (PAHs) are all considered harmful air pollutants to humans (Manisalidis *et al.*, 2020; Cecinato *et al.*, 2022).

This research presents the analysis of the environmental impact of traffic and flower production on the atmospheric environment of the districts of São Pedro da Serra and Mury in Nova Friburgo city/RJ, a very popular region for ecotourism. Part of São Pedro da Serra district is located in the EPA (Environmental Protection Area) of *Macaé de Cima* and is a popular tourist destination along with the nearby district of Lumiar. Thus, the goal of this study was to present the results of the qualitative and semi-quantitative analyses by comprehensive two-dimensional gas chromatography coupled to time-of-flight mass spectrometry (GC×GC-TOFMS) of volatile and semi-volatile organic compounds extracted of PM collected by ambient air sampling carried out in three different locations in the mountainous region of the state of Rio de Janeiro.

Experimental

The collection of PM was carried out at three different outdoors points: (1) in Mury, next to a road, to evaluate the impact of traffic on the air quality of the Padre Franca State School and the surrounding region. In the district of São Pedro da Serra, outside (2) and inside (3) the EPA, to assess the impact on air quality due to the use of pesticides in the flower's cultivation (Figure 1).

The extraction was performed with 3×50 mL of dichloromethane/methanol (9:1) solution in an ultrasonic bath for 20 min. The extracts were concentrated by rotary evaporation, solubilized in internal standards solution and analyzed by GC×GC-TOFMS. The data process was acquired by LECO ChromaTOF® software.

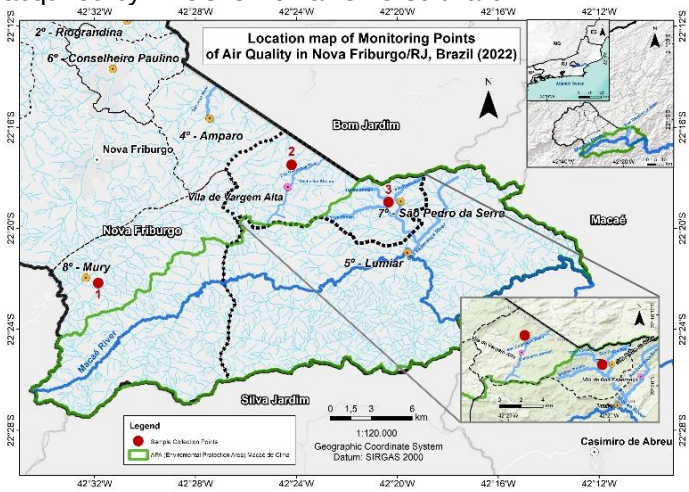

Figure 1: Study area indicating the three air quality monitoring sampling points: 1 - Padre Franca State School in Mury; 2 - Flower Greenhouse in Vargem Alta Village; and 3 - Rose Garden in São Pedro da Serra.

Results and Discussion

In the atmospheric PM over Padre Franca State School in Mury, the majority of the compounds detected are from biogenic origin. However, a minor anthropogenic contribution from petrogenic and pyrogenic contribution were detected. *n*-Alkanes (23.5 ng m^{-3}) in the C_{15}-C_{31} range were detected, with their maximum concentration centered between C_{19}-C_{26}, with C_{max} in C_{23} and carbon preference index (CPI_{25}) of 1.18, indicating anthropogenic input. Moreover, hopanes (0.79 ng m^{-3}), molecular biomarkers characteristic of petroleum (Figure 2), toluene (0.67 ng m^{-3}) and PAHs in low concentrations (0.08–0.01 ng m^{-3}) (Figure 3) were detected, indicating the contribution of petroleum derivate emission (Cecinato *et al.*, 2022). Levoglucosan (33.5 ng m^{-3}), a typical tracer for wood/vegetation combustion also were detected, indicating that the atmospheric PM over Padre Franca State School has at least two sources of contamination.

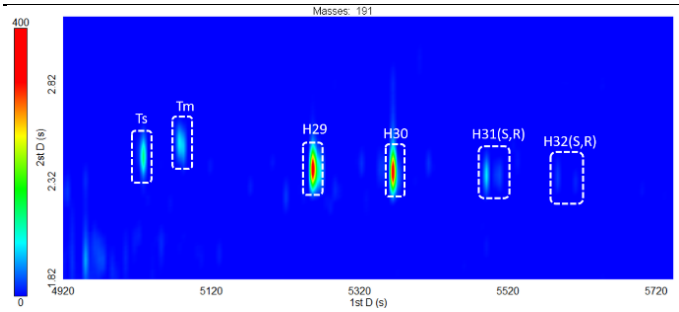

Figure 2: Extracted ion chromatogram *m/z* 191, characteristic of terpanes, e.g., hopanes, obtained in the sample of Padre Franca State School in Mury.

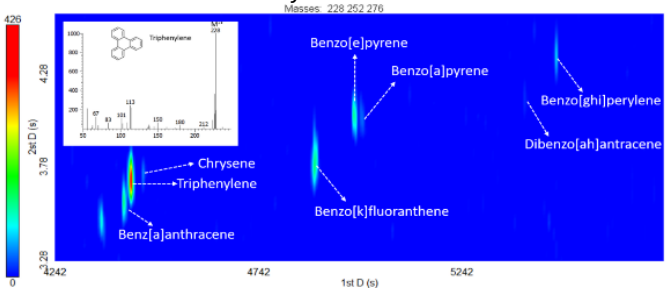

Figure 3: Extracted ion chromatogram *m/z* 228 + 252 + 276 of the aromatic hydrocarbons, showing the detection of PAHs, and triphenylene mass spectrum, obtained in the sample of Padre Franca State School in Mury.

n-Alkanes (32.9 ng m^{-3}) in the atmospheric PM over Flower Greenhouse in Vargem Alta Village were detected in the C_{15}-C_{29} range, with C_{max} in C_{21}, and CPI_{25} of 0.73 and indicate biogenic with anthropogenic emission (Cecinato *et al*. 2022), but petroleum biomarkers were not detected. A higher concentration of levoglucosan (407.0 ng m^{-3}) can be associated with a typical combustion of a hardwood (Cecinato *et al*. 2022) and less external air circulation. Among PAHs only pyrene (PY) and fluoranthene (FA) were detected in low concentrations (0.05 and 0.06 ng m^{-3}, respectively). The FA/PY ratio of 1.3 indicates waste fumes as source to these PAHs. No pesticides typically used on plantations were detected, but some toxic organochlorine substances (4.87 ng m^{-3}) that may be by-products of reactions of pesticides in the atmosphere have been detected, as: allyl chloride; Propane, 3-chloro-1,1-dimethoxy-; 2-Propanol, 1-chloro-, phosphate; and 3-azabicyclo[3.1.0]hexane-2,4-dione, 3-(3,5-dichlorophenyl)-1,5-dimethyl-. In addition, phthalates (107.8 ng m^{-3}) with known toxicity and identified as anthropogenic priority pollutants by the United States Environmental Protection Agency (US EPA, 2019) were identified.

The Rose Garden in São Pedro da Serra (open field), located in the EPA, 60 organic compounds were identified in the atmospheric PM, with alkanes (41.2 ng m^{-3}), alcohols (4.83 ng m^{-3}), and phthalates (23.0 ng m^{-3}) being the most abundant. Toxic organochlorine substances as allyl chloride (0.26 ng m^{-3}), 2-propanol, 1-chloro-, phosphate (1.06 ng m^{-3}) and phthalates (23.0 ng m^{-3}) also were detected in low concentration, but petroleum biomarkers and PAHs were not detected. *n*-Alkanes (27.9 ng m^{-3}) were identified in the C_{15}-C_{29} range, with C_{max} in C_{21}. Perhaps one of the aspects relevant to this fact is the weather conditions during the collection period of air particles, as the weather was cloudy and with light rain for a few hours.

Conclusions

In the three evaluated sites only in the Padre Franca State School atmospheric PM, compounds associated with fossil fuel pollutants were identified, but at low concentrations. No pesticides typically used on plantations were detected in the atmospheric PM over Flower Greenhouse in Vargem Alta Village and Rose Garden in São Pedro da Serra, but some toxic organochlorine substances, and phthalates were detected at trace levels. Moreover, the PAH levels in the three sites are well below the maximum permitted limit (1000 ng m^{-3}) for considering an environment polluted (US Environmental Protection Agency. 2019). Thus, the results indicate that the studied region is little impacted by anthropogenic activities, and the levels found are acceptable related to a non-polluted environment. Despite this, its traces can be a cumulative occurrence over time. Consequently, this is a factor that must be controlled and analyzed to avoid higher concentrations of components that are harmful to health.

Acknowledgments

The authors thank CNPq, PROFAEX, and FAPERJ (Brazilian research councils) for fellowships, and CAPES for financial support.

References

Cecinato, A., Bacaloni, A., Romagnoli, P., Perilli, M., & Balducci, C. (2022). Molecular signatures of organic particulates as tracers of emission sources. *Environmental Science and Pollution Research*, *29* (44), 65904-65923.

Manisalidis, I., Stavropoulou, E., Stavropoulos, A., & Bezirtzoglou, E. (2020). Environmental and health impacts of air pollution: a review. *Frontiers in public health,* 14.

US Environmental Protection Agency. (2019). Polycyclic Aromatic Hydrocarbons (PAHs) - Ambient Air Quality Standards (AAQS). Retrieved from https://www.epa.gov/air-pollution-transport-and-climate-change-overview/polycyclic-aromatic-hydrocarbons-pahs-ambient.

XVI LATIN AMERICAN CONGRESS ON ORGANIC GEOCHEMISTRY
9 - 11 AUGUST, 2023
ARACAJU, SERGIPE, BRAZIL

USE OF *N*-ALKANES IN THE RECOGNITION OF ENVIRONMENTAL CHANGES IN SUBTROPICAL ESTUARIES

MARINES M. WILHELM[a,b,*], ANA C. CABRAL[a], ANA LÚCIA L. DAUNER[a,c], MARINA R. GARCIA[a], CÉSAR C. MARTINS[b,d*]

[a] GRADUATE PROGRAM IN COASTAL AND OCEANIC SYSTEMS (PGSISCO), FEDERAL UNIVERSITY OF PARANÁ, BRAZIL

[b] CENTER FOR SEA STUDIES, CAMPUS PONTAL DO PARANÁ, FEDERAL UNIVERSITY OF PARANÁ, BRAZIL

[c] ECOSYSTEMS AND ENVIRONMENT RESEARCH PROGRAM, UNIVERSITY OF HELSINKI, FINLAND

[d] OCEANOGRAPHIC INSTITUTE, UNIVERSITY OF SÃO PAULO, BRAZIL.

e-mail *, * wilhelm.marines@gmail.com, ccmart@usp.br

Introduction

Estuaries are transition zones between terrestrial and marine ecosystems. Thus, estuarine sediments present sedimentary organic matter (SOM), mainly derived from terrigenous material originating from drainage basins and autochthonous aquatic organisms [1]. Local geomorphology, relief, altitude, climatic aspects, soil composition and other secondary factors are recorded through molecular 'signatures' in estuarine sedimentary systems. [2]. Thus, alterations caused by climatic and anthropogenic events can be identified by geochemical organic markers. Therefore, this study evaluated the influence of climatic and anthropogenic events on SOM composition in two subtropical estuarine systems in Brazil, Paranaguá Estuane System (PES) and Guaratuba Bay (GB), applying *n*-alkanes as geochemical markers. The PES is considered a natural heritage designed by UNESCO, and the GB is part of the Guaratuba Environmental Protection Area and the RAMSAR site, listed as one of wetlands with international importance.

Material and Methods

This study analysed two sediment cores from PES (AC and PC, sampled in November/2013) and one core from GB (GC, sampled in November/2010). (Fig. 1). Each core was subsampled into 2 cm sections, which were freeze-dried and disaggregated. The sedimentation rate was obtained from the determination of the radionuclides ^{210}Pb and ^{137}Cs, resulting in 0.49 ± 0.05 (AC), from 0.26 ± 0.03 (PC) [3] and 0.36 ± 0.02 cm y^{-1} (GC) [4]. The periods covered by the respective sedimentary cores were from 1960-2012 (AC), 1912-2010 (PC) and 1925-2008 (GC). The analytical procedure for the determination of *n*-alkanes followed the method described by Winieski et al. [5]. The determination of *n*-alkanes was performed on a gas chromatograph (*Agilent GC System 7890A Series*) equipped with a flame ionization detector (*FID*), using H_2 as carrier gas.

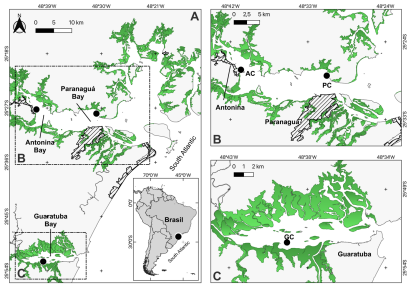

Figure 1. Map of the study area indicating the two subtropical estuaries (A). Sampling sites (black dots) where samples were collected in the respective bays: Antonina (AC) and Paranaguá (PC) (B), and Guaratuba (GC) (C). Cities are shown as shaded areas.

Results and Discussion

The highest concentrations of total *n*-alkanes were detected in the AC core (28.1 to 44.0 μg g^{-1}), followed by PC (6.0 to 13.0 μg g^{-1}) and GC (4.0 to 8.8 μg g^{-1}). Based on the analysis of the *n*-alkane profiles, a predominance of terrigenous MO (AC) or mixture of sources (PC and GC) was verified (Fig. 2). These results are related to the location of the collected cores, since AC is under strong fluvial influence from the main rivers in the region. In contrast, PC and GC were collected in an middle sector of the Paranaguá and Guaratuba Bays, respectively, with marine and fluvial influence.

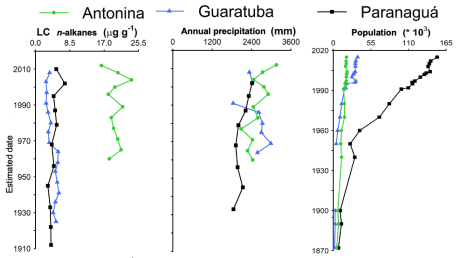

Figure 2. Profile of long-chain *n*-alkanes (> C_{24}), precipitation and population for the three analysed cores.

Land use and occupation

The municipality of Paranaguá had the most significant population growth, mainly from the 1950s onwards (Fig. 2). Antonina and Guaratuba present more stable rates, with a slight jump in Guaratuba around 1990 and stabilized afterwards. However, no statistical relationship was observed between the evolution of population growth and the oscillation of the analysed variables. The economic transition after the end of World War II and infrastructure improvements in the cities surrounding the PES carried out from 1945 onwards, such as the installation of marinas and nautical facilities on the banks of the estuary, improvement of the Paranaguá port and dredging activities, can have contributed to environmental changes in the region, causing, for example, a greater introduction of terrigenous material into the PES, identified with the increase in long-chain *n*-alkanes from this period. Regarding Guaratuba Bay, higher values of long-chain *n*-alkanes before 1965 may be related to the suppression of *Ilex paraguariensis* vegetation for economic purposes, activity intensified between 1930 and 1950. This event caused extensive deforestation, which may have resulted in the decrease of terrigenous MO entries in the following years (>1970).

El Niño - Southern oscillation events

In ENSO years, increased terrigenous MO input is expected due to increased continental runoff. The expected influence of the ENSO events on the oscillation of the analysed variables was not observed in the time interval covered by the AC, PC and GC cores. There was no significant variation in the introduction of terrigenous material into these estuaries, which is also evidenced by the absence of a correlation between precipitation and long-chain *n*-alkanes in the three cores. Other factors related to geographic characteristics and relief (i.e., estuaries located between the Atlantic Ocean and Serra do Mar with altitudes that reach 1800m) cause interactions with atmospheric systems that can affect the pluviometric dynamics and the amplitude thermal of the region. In addition, climate variability and interactions between the Pacific and Atlantic basins may intensify or attenuate the influence of ENSO in South America [6].

Conclusions

Recent anthropogenic activities have interfered with the composition and entry of terrigenous MO in Antonina and Paranaguá bays during the last century. Changes in the 1950s may be associated with land use due to the intensification of occupation in coastal drainages, adjacent basins, and port activities in the Paranaguá Bay. In the Guaratuba Bay, moderate impacts from plant extraction seem to have a greater influence than the population increase in the region. Physiographic characteristics of the area may attenuate the effect of ENSO events on the SOM composition of the Paraná estuaries.

Acknowledgements

The authors are grateful to Coordenação de Aperfeiçoamento de Pessoal de Nível Superior (CAPES) by the scholarship of M.M.Wilhelm, and to Conselho Nacional de Desenvolvimento Científico e Tecnológico (CNPq) for financial support (441265/2017-0).

References

[1] Sikes, E.L., Uhle, M.E., Nodder, S.D., Howard, M.E. (2009). Sources of organic matter in a coastal marine environment: evidence from n-alkanes and their $\delta^{13}C$ distributions in the Hauraki Gulf, New Zealand. Marine Chemistry, 113(3-4), 149-163.

[2] Rullkötter, J. (2006). Organic matter: the driving force for early diagenesis. Marine Geochemistry, 125-168.

[3] Martins, C.C., Doumer, M.E., Gallice, W.C., Dauner, A.L. L., Cabral, A.C., Cardoso, F.D., Dolci N.N, Camargo, L.M., Ferreira, P.A.L., Figueira, R.C.L., Mangrich, A.S. (2015). Coupling spectroscopic and chromatographic techniques for evaluation of the depositional history of hydrocarbons in a subtropical estuary. Environmental Pollution, 205, 403-414.

[4] Combi, T., Taniguchi, S., Figueira, R. C. L., de Mahiques, M. M., & Martins, C. C. (2013). Spatial distribution and historical input of polychlorinated biphenyls (PCBs) and organochlorine pesticides (OCPs) in sediments from a subtropical estuary (Guaratuba Bay, SW Atlantic). *Marine Pollution Bulletin*, *70*(1-2), 247-252.

[5] Wisnieski, E., Ceschim, L.M., & Martins, C.C. (2016). Validação de um método analítico para determinação de marcadores orgânicos geoquímicos em amostras de sedimentos marinhos. Química Nova, 39, 1007-1014.

[6] Cai, W., McPhaden, M.J., Grimm, A.M., Rodrigues, R.R., Taschetto, A.S., Garreaud, R.D., Dewitte B., Poveda, G., Ham Y-G., Santoso, A. Ng B., Anderson, W., Wang, G., Geng, T., Jo, H-s., Marengo, J.A., Alves, L.M., Osman, M., Li, S., Wu, L., Karamperidou, C., Takahashi, K., Vera, C. (2020). Climate impacts of the El Niño–southern oscillation on South America. Nature Reviews Earth & Environment, 1(4), 215-231.

XVI LATIN AMERICAN CONGRESS ON ORGANIC GEOCHEMISTRY
9 - 11 AUGUST, 2023
ARACAJU, SERGIPE, BRAZIL

INFLUENCE OF A WEATHER EVENT ON THE TRAJECTORY AND DEGRADATION LEVELS OF TARBALLS SAMPLES FROM AN OIL SPILL OCCURRED IN THE CAMPOS BASIN, RIO DE JANEIRO

ELIANE S. DE SOUZA, LUCAS R. TAVARES, NIVALDO S. FERREIRA

[a]**UNIVERSIDADE ESTADUAL DO NORTE FLUMINENSE DARCY RIBEIRO**

e-mail: eliane@lenep.uenf.br

INTRODUCTION

The entry of oil into the sea can have different sources: natural exudations, offshore oil E&P activities, transport of oil by pipelines and by tankers, as well as illegal activities involving the washing of tanks with the discharge of oil on the high seas [1]. Oil spilled into the sea undergoes various degradation processes known as weathering. Hydrocarbons with lower molecular weight normally evaporate, and the rest remain on the sea surface and undergo various biological, chemical and physical processes, such as the formation of water-in-oil emulsions. Over a period of time, the oil slick spilled into the sea will disintegrate into smaller fragments, which will eventually be transported via ocean currents to beaches and mangroves. These fragments, when they reach the coast are called tarballs [2].

The occurrence of tarballs on beaches on the coast of Rio de Janeiro is very rare, considering the meteorological and oceanographic conditions normally observed in this region. This is justified by the strong presence of the ocean current, known as the Brazil Current, which flows from North to South to the coast of Uruguay [3]. This current normally takes oil spills, resulting from spill accidents in the Campos Basin region, to the southern region of the country. However, between April 2 and 4, 2019, tarballs were found on beaches in the Região dos Lagos, Rio de Janeiro, from a real spill of 122 m³ of oil that occurred after a failure in the oil-water separation system of the P-53 oil production located in the Marlim Leste field, Campos Basin. The present work aimed to characterize, through the use of diagnostic ratios of oil-saturated biomarker compounds, the degree of weathering of tarball samples that arrived in the Região dos Lagos. And yet, to evaluate the influence of atypical meteorological events, observed in the oil E&P region of the Campos Basin during the spill period, on the trajectory and time of permanence of the oil spilled in the sea.

EXPERIMENTAL

Six tarball samples were collected from Praia Brava in Armação de Búzios and Prainha, Arraial do Cabo, Região dos Lagos (Rio de Janeiro) to geochemical analyzes. The tarballs samples were submitted to liquid chromatography for the separation of the fractions of saturated, aromatic, and polar compounds. The *n*-alkane, pristane and phytane concentrations were measured in the saturated fraction by GC-FID, using 5 α-androstane as an internal standard. The saturated biomarkers, tricyclic and pentacyclic terpanes (*m/z* 191) and steranes (*m/z* 217) were subjected by GC/MS analyzes. The compiled data of meteorological conditions, observed in the oil production region of the Campos Basin, at the time of the real spill, were acquired by consulting the website of the National Institute of Meteorology (INMET).

RESULTS AND DISCUSSION

Results showed that the concentrations of lighter *n*-alkanes (*n*-C_{17} to *n*-C_{22}) and isoprenoids in the samples from Arraial do Cabo are higher than those observed for the tarball samples collected in Armação de Búzios. Based on these residual concentrations, it was possible to calculate the weathering index of the samples collected on both beaches (Fig.1). Note that the average referring to the weathering indices for the samples from Armação de Búzios was 1.67 (±0.03) and for the samples collected in Arraial do Cabo was 1.23 (±0.11), and it can be inferred that the samples from Arraial do Cabo were less exposed to weathering agents. The increase in the weathering index was also observed in oil samples collected from a simulated spill in the first five days of exposure [4]. The saturated biomarker diagnostic ratios results showed little difference for the percentage values of C_{29} steranes (S+R) and for the ratio of C_{30} Hopane/C_{27} αααα (S+R). However, for the samples from Arraial do Cabo, the average values were higher for the ratio of Tr_{21}/Tr_{23} (0.67) when compared to those from Armação de Búzios (0.58), which may indicate that the samples from Arraial do Cabo

are more preserved and, consequently, they spent less time exposed to weathering processes after the spill.

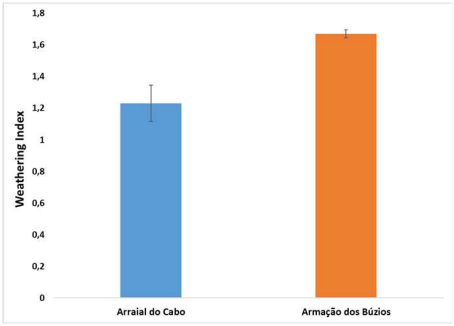

Figure 1. Average values of the weathering index of samples from Arraial do Cabo and Armação de Búzios. Weathering Index = (∑ n-C23-n-C31)/ (∑ n-C17-n-C22).

According to the ANP bulletin, the spill of 122m^3 of oil from the P-53 platform at Marlim Leste field in Campos Basin, occurred between March 24 and 25, 2019 [5]. In Figure 2a, it is possible to observe the map made by the Petroleum and Gas Production Coordination (COPROD/CGMAC/IBAMA) and the satellite image showing the oily feature of the slick with a clockwise trajectory, adrift between the 25th and 26th of March 2019, with an indication of the origin of an oil leak.

a) b)

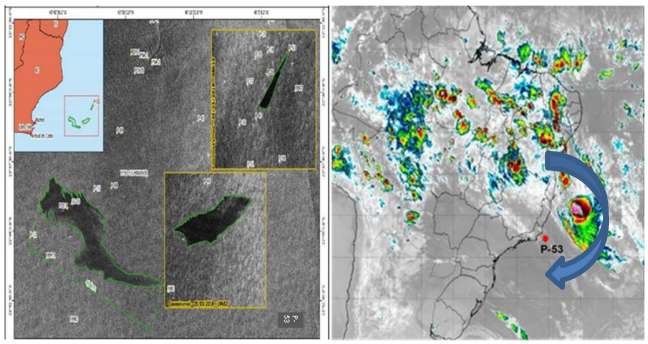

Figure 2. Map and satellite photos showing the oily feature of the slick, adrift between March 25 and 26, 2019, with an indication of the source of the oil leak (a). Satellite image of storm Iba showing the clockwise direction of the winds and the approximate location of platform P-53 (b).

In the same period of time that the oil slick was adrift in the ocean, tropical storm Iba had its highest intensity window recorded between March 24 and 25, 2019. On March 24, the storm reached maximum speed winds of 35 knots (65 km/h) and central pressure estimated at 1008 hPa, rotating clockwise [6]. In Figure 2b, the satellite image of tropical storm Iba, recorded by the National Institute of Meteorology (INMET) website, is located on the northern limit of the Campos Basin, close to the P-53 platform.

CONCLUSIONS

It was concluded that, with the use of different diagnostic ratios of *n*-alkanes, isoprenoids and tricyclic terpanes, it was possible to detect that the tarball samples collected at Prainha in Arraial do Cabo showed lower levels of weathering, having reached the beach earlier, probably on April 2, than those collected at Praia Brava in Armação de Búzios. It is also concluded that the formation of tropical storm Iba, with clockwise winds and a speed of 65 km/h, on the same day that 122 m^3 of oil was spilled from the P-53 platform, was decisive for the oil slick reached, in rare occurrence, in Arraial do Cabo after 7 days and in Armação de Búzios after 9 days of drifting at sea. Due to these results, we suggest that the change in the North-South direction of the oil slick trajectory, due to the increase in the frequency and intensity of meteorological events resulting from climate change, should be considered in the mathematical/computational models of slick trajectory in future accidents that may occur in the oil E&P regions of the Campos, Santos and Espírito Santo basins.

ACKNOWLEDGMENTS

This work was supported by the Darcy Ribeiro North Fluminense State University (UENF). We thank PIBIC for the scientific initiation scholarship of Lucas R. Tavares.

REFERENCES

[1] Zhang, B., Matchinski, E., Chen, B., Ye, X., Jing, L., Lee, K. (2019). World Seas: An Environmental Evaluation (Second Edition) Volume III: Ecological Issues and Environmental Impacts, Pages 391-406. Chapter 21 - Marine Oil Spills—Oil Pollution, Sources and Effects.

[2] Suneel, V.; Vethamony, P.; Zakaria, M.; Naik, B.; Prasad, K. (2013). Identification of sources of tar balls deposited along the Goa coast, India, using fingerprinting techniques. Marine Pollution Bulletin, v. 70, p. 81–89.

[3] Evans, D., Signorini, S. (1985). Vertical structure of the Brazil Current. Nature, 315, 48–50.

[4] Lima, B., Martins, L., Souza, E., Pudenzi, M., da Cruz, G. (2021). Monitoring chemical compositional changes of simulated spilled Brazilian oils under tropical climate conditions by multiple analytical techniques. Marine Pollution Bulletin Volume 164, 111985

[5] ANP-IBAMA (2020). Relatório de Investigação de Incidente FPU P-53 (Vazamento de óleo com toque na costa).

[6] Reis, J., Gonçalves, W. (2019). Análise sinótica da tempestade tropical Iba. VIII Simpósio Internacional de Climatologia. De 11 a 14 de novembro em Belém do Pará, Brasil, 1-13.

XVI LATIN AMERICAN CONGRESS ON ORGANIC GEOCHEMISTRY
9 - 11 AUGUST, 2023
ARACAJU, SERGIPE, BRAZIL

POSSIBLE IMPACT AND CONSEQUENCES OF CURRENT OCEAN ACIDIFICATION ON RHODOLITH BEDS ON THE SOUTH AMERICAN SHELF

GABRIELA O. ROSÁRIO[a*] / MIRIAN C.O COSTA[a*] / EMMANOEL V. SILVA FILHO [a*]

[a]**GEOSCIENCE (GEOCHEMISTRY) GRADUATE PROGRAM, UNIVERSIDADE FEDERAL FLUMINENSE, 24020-141, NITERÓI, RJ, BRAZIL**

rosariogabi@gmail.com, mirian.michelli@gmail.com, emmanoelvieirasilvafilho@id.uff.br

Introduction

Rhodoliths constitute carbonate beds formed by more than 50% of non-geniculated red coralline algae of the subclass Corallinophycidae, associated with several other species (Bosellini and Ginsburg, 1971). These carbonate layers occur in various marine regions around the world and are important biogeochemical components in the global carbon cycle (Oliveira et al., 2001). The rhodoliths occur in Brazil between latitudes 0º50'S to 27º17'S, mainly in the mesophotic zone, between 30 and 150 meters deep in the seawater column (Amado-Filho et al., 2007). Non-geniculated red algae predominantly consist of high-Mg calcite (>4% Mg), the most soluble form of $CaCO_3$ (Morse et al., 2006), with a concentration of 80 and 90% of its mass (Horta et al., 2016). However, the Mg content can change due to changes in the chemical composition and temperature of seawater (Sletten et al., 2017). Currently, the acidification of the oceans represents a risk to the formation of these carbonate banks, this considering the decrease of 0.1 pH units of the ocean surface, since pre-industrial times (Doney et al., 2009). The impact on the stability of the banks by acidification can influence the geochemical carbon balance, the shelf sedimentary balance and the equilibrium of marine ecosystems.

Experimental

The study was carried out on a rhodolith bank, outcrops in the intertidal zone of Parati beach, located in the south of the state of Espírito Santo, between latitudes 20°48'20.63"S and 20°49'27.35"S and longitudes of 40°36'0.39"W and 40°36'56.39"W. In this study, three (3) blocks of the outcropping carbonate bank were collected, with the extraction of ten (10) samples, which underwent a process of mechanical disaggregation and spraying for SEM-EDS and XRD analysis, and the preparation of two (2) thin section for identification and description under a petrographic microscope.

Results and Discussion

The rhodoliths analyzed are predominantly constituted by non-geniculate algae (74% of the biogenic content), which occur as thin continuous and intercalated sinuous laminae, 1 to 2 mm thick and 5 to 30 cm long, with the set of laminae reaching 0 .7 cm, filled with carbonate cement, manly by magnesian calcite abiotic (Fig.1).

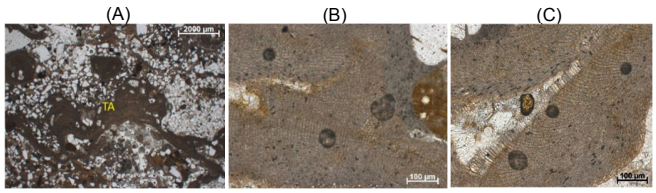

Figure 1. Images under petrographic microscope: (A) sinuous shape of algal mats (TA), surrounded by monocrystalline quartz grains; (B) detail of the encrusting non-geniculated algae thallus filaments; (C) filling with carbonate cement in the contact between the stalks.

The algae mats are composed mainly of magnesium calcite (Fig. 2), with a high molar concentration of Mg, from 10% to 16% by mass of $MgCO_3$ (EDS) (Fig. 3), which is different from the composition of geniculate algae, predominantly formed by calcite and aragonite (Menandro, 2018).

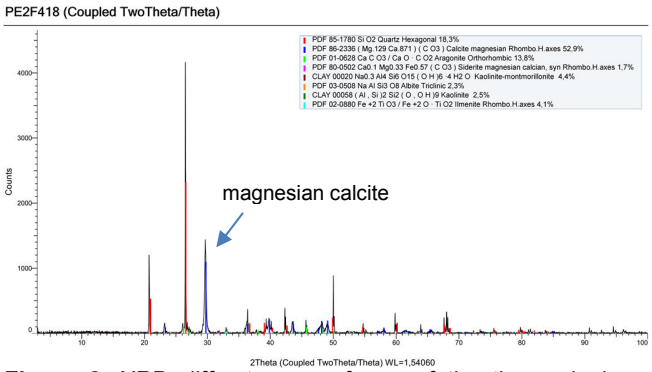

Figure 2. XRD diffractogram of one of the three algal mat samples analyzed.

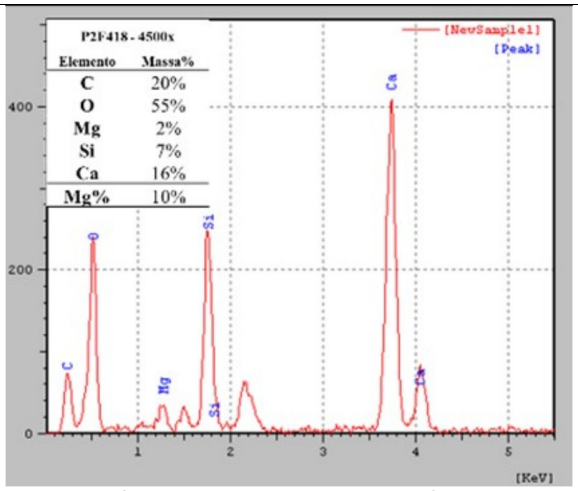

Figure 3. EDS microanalysis spectrum of cryptocrystalline magnesium calcite.

Magnesian calcite occurs as anhedral crystals of cryptocrystalline calcite, 0.5 to 3.0 µm long and 0.2 to 2.0 µm wide (Fig. 4).

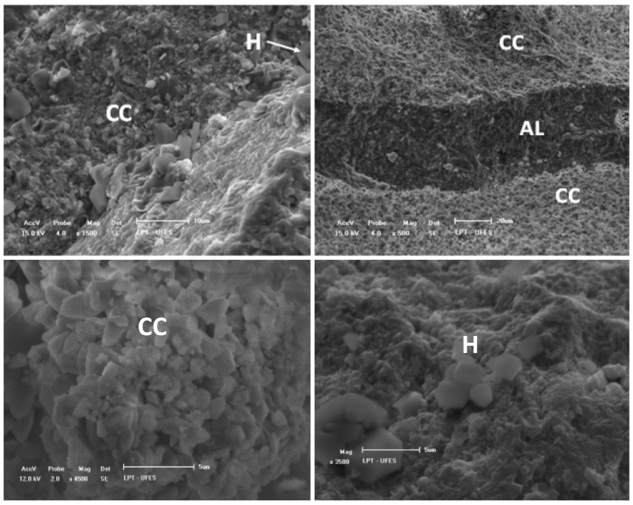

Figure 4. Images of cryptocrystalline magnesium calcite (CC), with anhedral crystals, associated with halite crystals (H) in algae mats (AL).

According to Morse et al. (2006), high Mg calcite (>4% Mg) is more soluble than aragonite, which is more soluble than low Mg calcite (<4% Mg). In acidification experiments, the calcareous algae showed dissolution and growth inhibition when subjected to pH 6.0 and 5.5, this in the first week, and demonstrating ideal formation conditions between pH 8.0 and 7.5 (Amancio, 2007). Current ocean acidification can lead to greater solubility of rhodoliths, responsible for $CaCO_3$ production of 0.025 tons/year and growth of around 1.0 mm/year on the Abrolhos platform, the most extensive in the world (Amado-Filho et al., 2007). Also, the carbonate banks of the coast of Espírito Santo consist of one of the main inputs of sediment in the shallow platform and are fundamental in the sedimentary balance regarding coastal erosion.

Conclusions

In this study, the rhodolith beds on the beach of Parati (ES), constituted by mats of non-geniculated algae, are predominantly formed by anhedral crystals of cryptocrystalline calcite with high magnesium, between 10 and 16% by mass of $MgCO_3$. Currently these banks consist of one of the main components in the sedimentary dynamics and sustainability of marine ecosystems on the shelf of southeastern Brazil. Therefore, ocean acidification can lead to greater solubility and growth inhibition of these banks, thus causing the intensification of coastal erosion and the decline of marine biodiversity.

Acknowledgements

We are grateful for the support of the teams at the LDRX of the UFF and SEM-LMC-LPT/LEMAG of the UFES. This study was financed in part by the CAPES – Finance Code 001. This research is an output of the INCT-TMCOcean supported by CNPq through Procs. Nos. 573.601/2008-9 and 465.290/2014-0), and FAPERJ currently financially support Mirian C. O. Costa with a scholarship (Grant E-26/ 210.745/2019 - 250464).

References

Amado-Filho, G. M.; Maneveldt, G. W.; Manso, R. C. C.; Marins-Rosa B. V.; Pacheco M. R; Guimarães S. M. P. B., 2007. Structure of rhodolith beds from 4 to 55 meters deep along the southern coast of Espírito Santo State, Brazil. Cienc. Marinas **33**(4): 399–410.

Amancio, C. E., 2007. Precipitação de $CaCO_3$ em algas marinhas calcárias e balanço de CO_2 atmosférico: os depósitos calcários marinhos pode atuar como reservas planetárias de carbono? Dissertação. Inst. Biociências - USP.

Bosellini, A.; Ginsburg, R. N., 1971. Form and internal Geol.**79**: 669-682.

Bastos, A. C.; Quaresma, V. S.; Marangoni, M. B.; D'Agostini, D. P.; Bourguignon, S. N.; Cetto, P. H.; Silva, A. E.; Amado-Filho, G. M.; Moura, R. L.; Collins, M., 2015. Shelf morphology as an indicator of sedimentary regimes: a synthesis from a mixed siliciclastic-carbonate shelf on the eastern Brazilian margin. Journal of South American Earth Sciences**63**:125-136.

Doney, S. C.; Fabry, V. J.; Feely, R. A.; Kleypas, J. A., 2009. Ocean acidification: the other CO_2 problem. Annual Review of Marine Science**1**:169–192.

Ginsberg, R. N.; Marszalek, D. S.; Schneidermann, N. I., 1971. Ultrastructure of carbonate cements in a Holocene algal reef of Bermuda. Journal of Sedimentary Petrology**41**(2): 472-482.

Menandro, T. F., 2018. Análise da composição e estrutura interna de rodolitos da Cadeia Vitória Trindade. Tese do PPG em Oceanografia Ambiental - UFES.

Oliveira, E. C.; Horta, P. A.; Amancio, C. E.; Sant'Anna, C. L., 2001. Algas e angiospermas marinhas bênticas do litoral brasileiro. In: Ministério do Meio Ambiente (org.). Macrodiagnóstico da Zona Costeira do Brasil. Rio de Janeiro.

Morse, J. W.; Andersson, A. J.; Mackenzie, F. T., 2006 Initial responses of carbonate-rich shelf sediments to rising atmospheric pCO_2 and "ocean acidification": Role of high Mg calcites. Geochim. Cosmochim. Acta**70**(23): 5814-5830.

Análise hidrográfica do Distrito Federal (DF): desenvolvimento de metodologia e levantamento isotópico

Campos S. M. [1], Costa A. C.J [1]

[1]Instituto de Geociências, Universidade de Brasília, Brasília (DF), Brasil

e-mail: suellen.campos@usp.br

Introduction

A água é um recurso natural essencial não só em relação à vida, mas também necessária para garantir o desenvolvimento econômico e social (WOLKMER, PIMMEL, 2013), dessa forma se fazem necessárias práticas de monitoramento e análise de águas. Assim este estudo, tomando como base a resolução n°357 do CONAMA, analisou em corpos hídricos do Distrito Federal os teores catiônicos de Na+, Ca2+, Mg2+, NH4+, e aniônicos de Cl-, NO2-, NO32-, SO42-, PO43-, juntamente com os valores de δ18O e δ13C do carbono inorgânico dissolvido das mesmas amostras para um maior entendimento dos corpos hídricos do DF além da realização de possíveis correlações de razões isotópicas e iônicas das águas do DF.

Experimental

Foram coletadas 11 em pontos distintos do Lago Paranoá e do córrego Sobradinho no mês de fevereiro de 2022, e posteriormente analisadas em cromatografia iônica e espectrometria de massas. No Laboratório de Química e Física Forense, as amostras coletadas foram analisadas para quantificação dos íons. A determinação do δ13C do carbono inorgânico dissolvido (DIC - dissolved inorganic carbon) na água foi realizada no Laboratório de Geocronologia da UnB. Para as análises isotópicas do DIC.

Results and Discussion

Destes dados foram analisados os teores encontrados, separados em grupos e constatadas correlações positivas entre os íons NO32-, e Cl-, e Ca2+ e Mg2+, Sendo NO32 e Cl- bons indicadores de poluição. Com os valores de δ18O e δ13C foram feitas correlações climáticas, há uma correlação negativa entre nitrato e δ13C, nos leva a sugerir uma possível origem biológica para o carbono inorgânico dissolvido, em detrimento do intemperismo de rochas carbonáticas

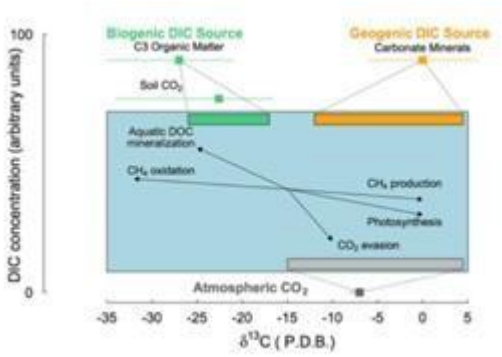

Figura 1. Gráfico dos valores $\delta^{13}C$ do carbono orgânico dissolvido de fontes biogênicas e geogênicas. (Campeau et al., 2017)

Conclusions

Observou-se um maior valor de nitrato nas amostras coletadas no ponto de amostragem próximo à Estação de Tratamento de Esgoto Norte. Neste ponto também ocorre um dos valores mais negativos de δ13C. Sugerese que existe uma relação entre despejo de esgoto e valores de δ13C mais negativos, de origem biológica, em detrimento de valores próximos a 0 de origem geológica. No entanto, nos pontos 2 e 11, os valores de δ13C são semelhantes ao ponto 4, mas os valores de nitrato não são tão elevados. Pretendemos ainda ampliar a área de amostragem e complementar as análises isotópicas com dados de δ13C do carbono orgânico dissolvido, para se avaliar melhor quais fatores controlam a assinatura isotópica de carbono nas águas do DF.

References

A.Campeau; M.B. Wallin; R. Giesler; etal. Multiple sources and sinks of dissolved inorganic carbon across Swedish streams, refocusing the lens of stable C isotopes. Rev Scientific reports 7: 1-14, 2017.

BRASIL. CONSELHO NACIONAL DO MEIOAMBIENTE– CONAMA. Resolução nº 357, Dispõesobre a classificação dos corpos de água e diretrizesambientais para o seu enquadramento, bem comoestabelece as condições e padrões de lançamento deefluentes, e dá outras providências de 17 de março de 2005.Brasília, 2005. Disponível em:<http://www2.mma.gov.br/port/conama/legiabre.cfm?codlegi=459>. Acesso em: 15 mar. 2021.

M.F.S. Wolkmer; N.F. Pimmel. Política nacional de recursos hídricos: governança da água e cidadania ambiental. Rev. Sequência 67:165-198, 2013.

XVI LATIN AMERICAN CONGRESS ON ORGANIC GEOCHEMISTRY
9 - 11 AUGUST, 2023
ARACAJU, SERGIPE, BRAZIL

VEGETABLE LOOFAH COATED WITH MAGNETIC NANOPARTICLES (FE_3O_4 AND FE_3O_4/CTBA) FOR REMOVAL OF OIL SPILLS

Luana Cecília M. Cantagesso [a], Gustavo Escher P. Mendes [a], Aryane Tofanello [b], Georgiana F. da Cruz [a]*

[a]Universidade Estadual do Norte Fluminense Darcy Ribeiro (UENF); [b]Universidade Federal do ABC (UFABC)

*georgiana@lenep.uenf.br

Introduction

Recent studies have shown that superparamagnetic nanoparticles demonstrated excellent results in removing oil, mainly due to their particle size, stable nature, magnetic properties and rapid response to the magnetic field, in addition to their good dispersion in oils [1, 2]. Nanomaterials such as aerogels, foams, sponges and polymers coated with nanoparticles are some examples of how the use of this technology has been studied to remove oil from water and soils [1]. In this context, this project focuses on the use of vegetable loofah (*Luffa aegyptiaca*) functionalized with magnetite (Fe_3O_4) nanoparticles in oil spill simulations aiming at the effective and low-cost remediation of areas contaminated by oil.

Experimental

The oil-in-water spill simulation was conducted with a 30,000 ppm NaCl solution and with two Brazilian oils with API 25 (oil 1) and 20 (oil 2). The vegetable loofahs were coated with two types of nanoparticles, pure magnetite (Fe_3O_4, A) and magnetite functionalized with CTAB (cationic surfactant cetyltrimethylammonium bromide, B). The nanoparticles were synthesized according to the method described by Calmon et al., (2012) [3]. The oil retention capacity (k) of nanoparticles was determined by k = (x - y)/x, where x is the weight (g) of the vegetal loofah and y is the weight (g) of the oil adsorbed material recovered from the artificial oil spill. All spill simulations were carried out in triplicates.

Results and Discussion

The scanning electron microscopy images (SEM) (Figure 1) depict the morphology of the untreated vegetable loofah, as well as the pristine magnetic composites, and their appearance after oil spill simulation in water. The untreated sponge (Fig. 1a) is composed of interwoven fibers that form non-rough lamellar structures. When modified with nanoparticles A and B, the reticular structure remains intact, indicating that the fibers were not damaged during the process (Fig. 1b). The Fe_3O_4 clusters anchored throughout the sponge are highlighted by the arrows (Fig. 1c) and contribute to an increased roughness of the arrays. X-ray energy dispersive spectroscopy (EDS) was employed to determine the surface elemental compositions of as-prepared Fe3O4@vegetable loofah. The EDS showed the presence of C, O and Fe elements. Remarkably, after the oil spill simulations, the microstructure of the sponges in both cases remained largely unchanged, with only a slight degree of fragmentation (Fig. e,f).

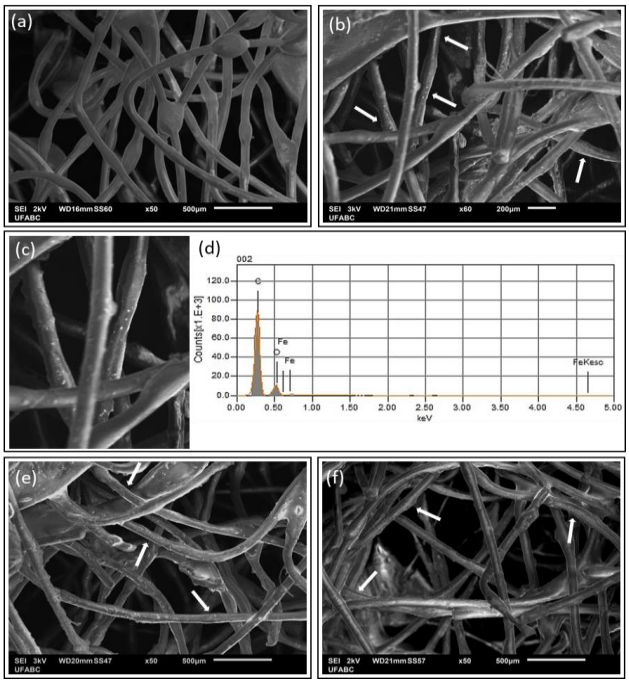

Figure 1. SEM images of the pure vegetable loofah (a), the as-prepared Fe_3O_4@ vegetable loofah and its EDS before (b,c) and after the A and B oil spill simulation, respectively (e,f).

Oil 1 showed a higher relative abundance of *n*-alkane compounds than oil 2. On the other hand, oil 2 showed higher TAN and $\%O_2$, properties indicative of a higher proportion of polar compounds (Figure 2).

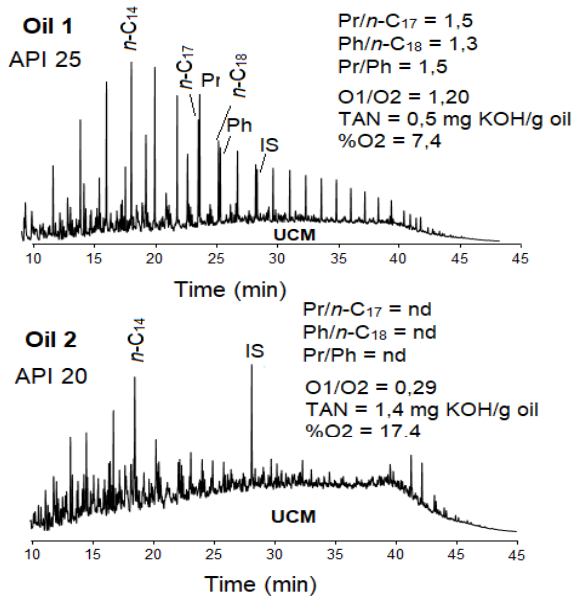

Figure 2. GC-FID Chromatograms for oil 1 and 2.

The remediation capabilities of vegetable loofah are shown in Figure 3. For oil 1 (API 25), nanoparticle B was more efficient for removing oil from water, with a removal capacity of 74.8%, while nanoparticle A showed removal capacity of 69.2%. However, nanoparticle A was more efficient for removing oil 2 (API 20) (88.8%). Nanoparticle B showed a capacity of 78.4%. The removal capacity of pure vegetable loofah for both oils was 32,1%.

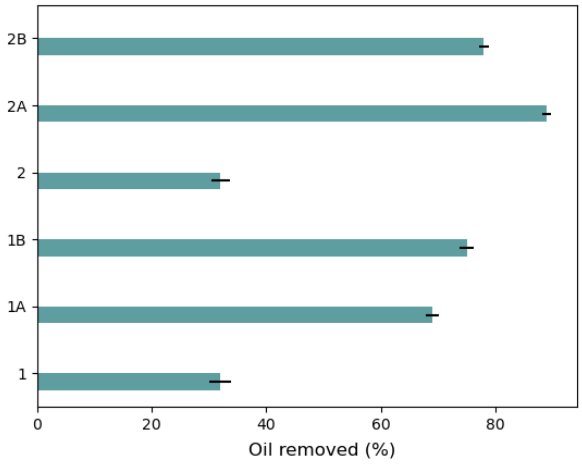

Figure 3. Mean and standard deviation of the amount of oil removed with nanoparticles A and B used in the study.

Oils containing higher contents of polar compounds (such as oil 2), are considered the most challenging to remove from the environment in the event of oil spills. Surprisingly, regardless of the type of nanoparticle used in this study, a higher oil removal capacity was observed for oil 2. This phenomenon can be attributed to the formation of a ternary complex (polar compounds/CTAB/Fe_3O_4 nanoparticles, Figure 4) [4]. Such complex formation facilitates the adsorption of the polar compounds onto the surface of the functionalized loofah, thereby improving the overall oil removal efficiency.

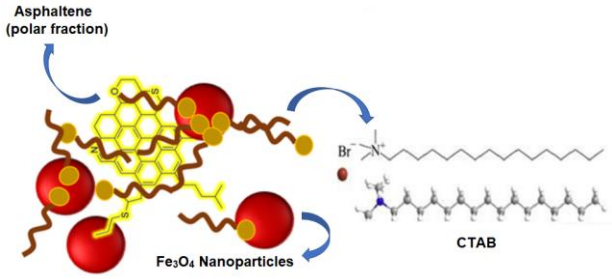

Figure 4. Ternary complex of polar compounds/CTAB/Fe3O4 nanoparticles formed during oil spill removal (Adapted from Toledo et al., 2022) [4].

Conclusions

This study has demonstrated that a vegetable loofah coated with magnetic nanoparticles is a promising material for effective oil spill removal for oils with different API. The findings suggest that this material may also be used for oil remediation in conjugation with other available technologies. These results highlight the potential of this innovative technology for improving the efficiency of oil spill remediation efforts, which is crucial for minimizing the environmental impact of such incidents.

Acknowledgments

The authors are grateful to FAPERJ and CAPES for providing the resources needed to conduct this research. We also thank the support of UFABC Multiuser Central (CEM) facilities in the experimental characterizations.

References

[1] Debs, K. B., Cardona, D. S., Silva, H. D. T., Nassar, N. N., Carrilho, E. N. V. M., Haddad, P. S., Labuto, G. 2019. Oil spill cleanup employing magnetite nanoparticles and yeast-based magnetic bionanocomposite. Journal of Environmental Management 230, 405-412.

[2] Singh, H., Bhardwaj, N., Arya, S. K., Khatri, M. 2020. Environmental impacts of oil spills and their remediation by magnetic nanomaterials. Environmental Nanotechnology, Monitoring & Management 14, 1–23.

[3] Calmon, M. F., Souza, A. T., Candido, N. M., Raposo, M. I. B., Taboga, S., Rahal, P. 2012. A systematic study of transfection efficiency and cytotoxicity in Heka cells using iron oxide nanoparticles prepared with organic and inorganic bases. Colloids and Surface B: Biointerfacces 100, 177-184.

[4] Toledo, G. F. G., Almeida, J. M., Brito, A. M. M., Batista, C. C. S., Andrade, L. S., Araújo, D. R., Icimoto, M. Y., Brochsztain, S., Nantes, I. L. 2022. Harvesting of Surfactant-Solubilized Asphaltenes by Magnetic Nanoparticles. Energy & Fuels 36, 11839-11848.

XVI LATIN AMERICAN CONGRESS ON ORGANIC GEOCHEMISTRY
9 - 11 AUGUST, 2023
ARACAJU, SERGIPE, BRAZIL

Geochemical and environmental assessment of marine sediments after the 2019 oil spill in Pernambuco state, Brazil

Bianca M. M. G. Acioli[a*], Thayane C. S. Moreira[a*], Alex. S. Moraes[a*], Jandyson M. Santos[a*]

[a]**Chemistry Department, Federal Rural University of Pernambuco (UFRPE), Recife, PE, 52171-900, Brazil**

*Correspondence: biancammga@gmail.com, cthayane36@gmail.com, alex.moraes@ufrpe.br, jandyson.machado@ufrpe.br

Introduction

The exploration of oil resources aims the production needs of an extensive energetic chain, but this activity also has a high probability of causing damage to the environment. One of the most dangerous environmental disasters is the oil spills in aquatic systems. For example, the 2019 oil spill was the biggest environmental disaster in Brazil involving oils, and after that, it has become essential to monitor petroleum hydrocarbons to study the contamination in the affected environments. The most abundant biomarkers are the aliphatic (AHs) and polycyclic aromatic (PAHs) hydrocarbons classes [1], which have various biological implications in the ecosystem, especially the 16 PAHs monitored by the USEPA[2]. Herein, we aim to evaluate the total concentrations of AHs and PAHs in a geochemical and environmental assessment of marine sediments collected after the 2019 oil spill in Pernambuco state coast, Brazil.

Experimental

A total of twenty-five samples (Figure 1) were collected along the coastal of Pernambuco state in summer season of 2021. The samples were stored at 4 °C, and then freeze-dried, after were macerated, sieved (2 mm mesh) and stored. The organic extract was obtained using 5.0 g of freeze-dried sample and 15.0 mL of dichloromethane:methanol (2:1, *v/v*). The mixture was subjected to vortex-type agitation and an ultrasonic bath for 30 minutes. Phase separation was accelerated by centrifugation at 5000 rpm, and the supernatant was removed with the aid of a glass Pasteur pipette and transferred to a round bottom flask. This process was repeated three times. The organic extract from all extractions was unified and concentrated in a rotary evaporator at 45 ± 5 ºC. After, the extract was fractionated on open glass column chromatography filled with 5.0 g of silica gel and 1.0 g of alumina, and the AHs were eluted using 40 mL of *n*-hexane and PAHs were eluted with 30 mL mixture of *n*-hexane:dichloromethane (1:1, *v/v*).

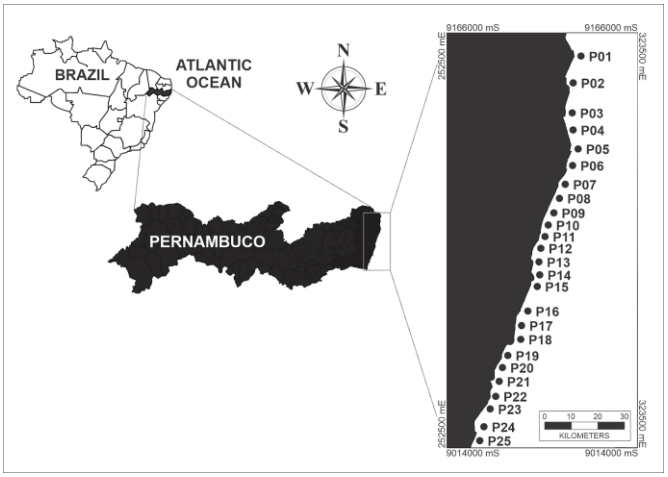

Figure 1 - Study area on the coast of the state of Pernambuco in northeastern Brazil and the 25 collection points.

GC/MS were performed in a quadrupole gas chromatograph-mass spectrometer (GCMS-QP2010 SE, Shimadzu Co., Japan), operated with electronic ionization (EI) at 70 eV, coupled to an autosampler (AOC-6000 Plus, Shimadzu). The temperatures of the injector, transfer line, and the EI were 280, 300, and 200 ºC, respectively. The injection mode was splitless and the injection volume was 1.0 µL. Detection of both classes was carried out in SIM mode by monitoring a list of *m/z* referring to the molecular ions of the AHs and PAHs. The quantification of the AHs was performed through an internal standardization analytical curve with concentrations ranging from 2.5 to 50 µg mL^{-1}. For PAHs, the concentrations ranged from 1 to 500 ng mL^{-1}. The internal standards used were hexadecane-d_{34} (10 µg mL^{-1}) for AHs and p-terphenyl-d_{14} (500 ng mL^{-1}) for PAHs.

Results and Discussion

We have quantified HAs in all samples with range from C_{11} to C_{36}, and the ∑HAs ranged from 0.613 to 9.828 µg g^{-1}, with the highest value for P13 and the lowest for P14 (Figure 2). P13 is located on Enseada dos Corais beach,

which has a high population and tourism rate in the summer period.

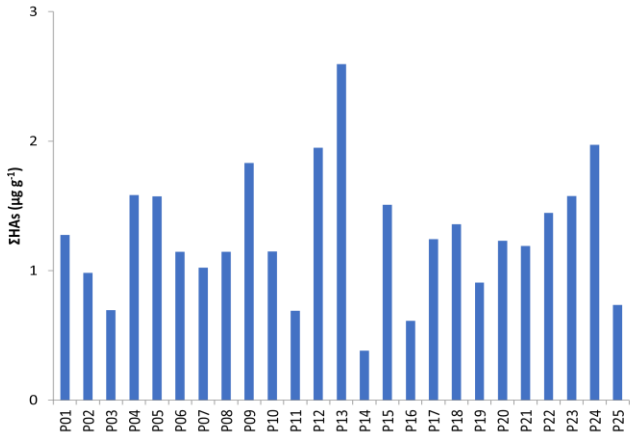

Figure 2 - ∑HAs (µg g^{-1}) for marine sediments collected on the coast of Pernambuco State, Brazil.

We have calculated the Pr/Ph, Pr/C_{17} and Ph/C_{18} diagnostic ratios. For Pr/Ph, all samples presented values close to 1, which may be indicative of petroleum hydrocarbons in the sedimentary organic matter. The Pr/C_{17} and Ph/C_{18} ratio indicates the occurrence of oil recently introduced into the environment [3], and the source is possibly related to the mysterious oil spill that affected the coast of Pernambuco state in 2019.

We were able to quantify 16 PAHs priority defined by USEPA in all samples, and the ∑PAH ranged from 1.26 to 3696.93 µg g^{-1}. The highest ∑PAH was found for the P05 sample, which represents a high level of contamination. The P05 is located on Janga Beach that is in the metropolitan area of Recife, in an area in front of a marina that receives boats and other marine vehicles, where there is the possibility of the introduction of these compounds into the aquatic environment. The P05 presented.

We also have calculated diagnostic ratios using the most important PAHs, which were: Flu/(Flu+Pyr), BaA/(BaA+Chry) and LMW/HMW. The Flu/(Flu+Pyr) ratio pointed to pyrolytic sources, which means combustion of grass, charcoal, and/or wood as source of organic matter in all samples. For BaA/(BaA+Chry) ratio, we also found values that indicates biomass combustion, present in all collected samples, except P15. We have found a value < 1 for LMW/HMW ratio in P05 sample, which indicating pyrolytic sources.

Conclusions

We were able to quantify AHs and PAHs in twenty-five sediments and obtained diagnostic ratios that were calculated to assess the sources and levels of contamination of marine sediments from the coast of Pernambuco state, Brazil. In general, the AHs results indicated the presence of petroleum hydrocarbons as biodegraded oil residues in most of the samples. In addition, the analysis of PAHs allowed the identification of petroleum-related and biomass combustion sources in the sedimentary organic matter. The sources may include oil spills, waste discharge, and shipping activities in the region. These findings contribute to the understanding of potential contamination and could assist in the development of appropriate mitigation strategies to protect the marine environment.

Acknowledgements

The authors thank CAPES and FACEPE for fellowships, and Petroleum, Energy and Mass Spectrometry Research Group (PEM) at UFRPE.

References

[1] He, M., Moldowan, M.J., and Peters, K, 2018, Biomarker: Petroleum. 2018. Ed. Encyclopedia of Geochemistry, Springer's Earth Science Encyclopedia. DOI: 10.1007/978-3-319-39312-4_170.

[2] Kinzer, G., R. Riggin, T. Bishop, M. Birts, And P. Strup. Epa (Envionmental Protection Agency) Method Study 20, Method 610--Pna's (Polynuclear Aromatic Hydrocarbons). U.S. Environmental Protection Agency, Washington, D.C., Epa/600/4-84/063.

[3] COIMBRA, M. A. C. Avaliação dos resultados analíticos de hidrocarbonetos como instrumento jurídico em caso de derrames de petróleo: mangue de Bertioga. Apresentado como dissertação de mestrado em ciências, Universidade de São Paulo – USP, 2006

XVI LATIN AMERICAN CONGRESS ON ORGANIC GEOCHEMISTRY
9 - 11 AUGUST, 2023
ARACAJU, SERGIPE, BRAZIL

METAL RATIO DISTRIBUTION IN SURFACE SEDIMENTS FROM A TROPICAL HYPERSALINE LAGOON

CLEUZA LEATRIZ TREVISAN[a]*; JAVIER SALAZAR[a]; MURILO DE CARVALHO VICENTE[a]; TERESA CRISTINA GUIMARÃES[a]; MANUEL MOREIRA-RAMIREZ[a]; RUT DÍAZ[a]; JULIO C. WASSERMAN[a]

[a]**Programa de Pós-Graduação em Geoquímica Ambiental, – UFF, Niterói, Brazil**

*correspondence: cltrevisan@id.uff.br

Introduction

The source of metals in coastal areas is from natural or anthropogenic origin, reaching these areas through different routes (river runoff, atmospheric deposition or human activities). The fate and effects of metals on humans and life in general depend on the environmental physicochemical conditions [1]. Elements such as Ca, Fe and Ti are suitable to describe sediment sources [2], being Ca associated with carbonates [3], Fe and Ti for siliciclastic content and terrigenous fraction [4]. Fe/Ca and Ti/Ca ratios are used as proxies for terrigenous origin while Ti/Al identifies granulometric variation [5]. Araruama Lagoon (AL) is a choked hypersaline lagoon [6], and its geological origin is related to sea level variations during Holocene and Pleistocene [7]. The objective of this work was to identify the origin of sediments and the association with granulometric classes using elemental ratios. The results show a prevalent terrigenous input with a slightly marine contribution and sediments dominated mainly by sandy grains.

Experimental

Two sampling campaigns in March (C1) and July (C2) 2020 were done to collect surface (10 cm) sediment samples in AL (Figure 1). A Van-Veen grab was used, and samples were frozen and stored in bags for later analysis. Samples were ground to150 µm mesh and analyzed by XRF with a Panalitica model Elipson 3x. Granulometry was determined using a digital particle analyzer CAMSIZER Retsch® and class sizes were plotted in a ternary diagram using Gradistat® software. Excel was used to generate the graphs of ratios (Fe/Ca, Ti/Ca, and Ti/Al) from the 10 stations that were discussed in the following section.

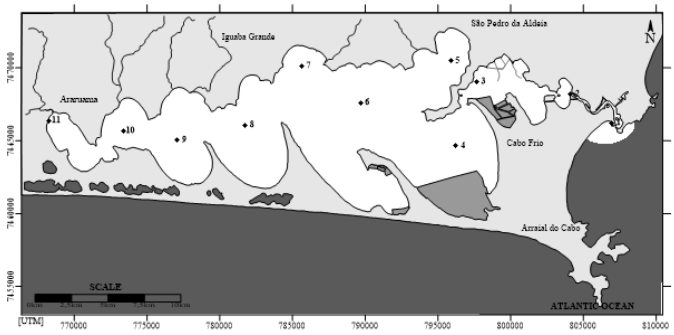

Figure 1. Sampling stations at Araruama Lagoon (2-11). Control station 1 was not included in the analyses.

Results and Discussion

The data (figures 2a and 2b), demonstrate a terrigenous origin for sediments from AL which agrees with the lagoon geological history [8]. Weathering and erosive processes due to sea level rising have nourished the lagoonal plain, while waves constructed sandy bars that enclosed the lagoon when sea levels fell. However, station 10 presented a very high Fe/Ca ratio that could not be explained. Riverine flows from watersheds are usually low and could not provide such large amount of material.

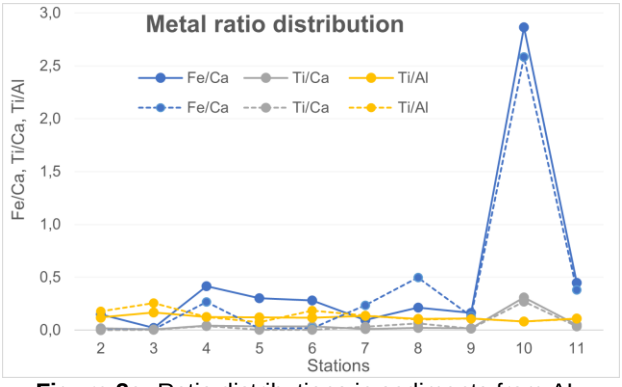

Figure 2a. Ratio distributions in sediments from AL.

Figure 2b. Ternary diagram of granulometry.

The hypersalinity of water column is associated with the high concentration of calcium and the presence of marine mollusks in the AL.

Conclusions

Erosive processes and geological characteristics in surrounding areas of the AL supplied material during variation in sea level. Further studies with elemental ratios could improve the understanding of natural and anthropogenic processes.

Acknowledgements

The authors thank FAPERJ, CAPES and CNPq for financial support, UFF for infrastructure and ProLagos for supporting field campaigns.

References

[1] United States Environmental Protection Agency. 2007. Framework for Metals Risk Assessment 120/R-07/001. www.epa.gov/osa.

[2] Dias, G. P. 2018. Avaliação das condições redox das águas intermediárias do Oceano Atlântico Sudoeste nos últimos 40 mil anos. Instituto Oceanográfico - Universidade de São Paulo, Brasil.

[3] Peterson, L. C., G. H. Haug, K. A. Hughen, and U. Rohl 2000. Rapid changes in the hydrologic cycle of the tropical Atlantic during the last glacial, Science, 290 (5498), 1947–1951. doi:10.1126/science.290.5498.1947.

[4] Arz, H. W., J. Pätzold, and G. Wefer. 1998. Correlated millennial-scale changes in surface hydrography and terrigenous sediment yield inferred from last-glacial marine deposits off northeastern Brazil, Quat. Res., 50(2), 157–166. doi:10.1006/qres. 1998.1992.

[5] Tisserand, A., B. Malaizé, E. Jullien, S. Zaragosi, K. Charlier, and F. Grousset. 2009. African monsoon enhancement during the penultimate glacial period (MIS 6.5. 170 ka) and its atmospheric impact. Paleoceanography. 24, PA2220. doi:10.1029/2008PA001630.

Archer, D. E. 1996. An atlas of the distribution of calcium carbonate in sediments of the deep sea, Global Biogeochem. Cycles, 10(1), 159–174. doi:10.1029/95GB03016.

[6] Kjerfve, b. 1986. Comparative oceanography of coastal lagoons. In: Wolfe, D. A., ed. (ed.). Eastuarine variability. New York: Academic Press. P. 63-81.

[7] knoppers, b.; kjerfve, b. 1999.coastal lagoons of southeastern brazil: physical and biogeochemical characteristics. In: perillo, g. M. E.;piccolo, m. C., et al (ed.). Estuaries of south america: their geomorphology and dynamics. Berlin, heidelberg: springer berlin heidelberg. P. 35-66.

[8] Turcq, b.; Martin, l.; Flexor, J.; Suguio, K. et al. 1999. Origin and evolution of the quaternary coastal plain between Guaratiba and Cabo Frio, state of Rio de Janeiro, Brazil. Environmental geochemistry of coastal lagoon systems, 6, p. 25-46.

EVALUATION OF URBAN POLLUTION IN A TROPICAL LACUSTRINE ECOSYSTEM BY USING N-ALKANES AND STEROLS AS BIOMARKERS

RODRIGO DE LIMA SOBRINHO[1], GABRIEL DA COSTA PEÇANHA[1], THALLIS MARTINS DE SOUZA[2], LUIZ CARLOS COTOVICZ JUNIOR[1,3], LUCIANA OLIVEIRA VIDAL[4], ANNIBAL DUARTE PEREIRA NETTO[2,5], MARCELO CORRÊA BERNARDES[1,2]

[1]Programa de Pós-Graduação em Geoquímica, Instituto de Química, Universidade Federal Fluminense, Niterói, RJ, Brazil

[2]Programa de Pós-Graduação em Química, Instituto de Química, Universidade Federal Fluminense, Niterói, RJ, Brazil

[3]Leibniz Institute for Baltic Sea Research, Germany

[4]Laboratório de Ciências Ambientais, Centro de Biociências e Biotecnologia Universidade Estadual do Norte Fluminense, Campos dos Goytacazes, RJ, Braziil

[5]Programa de Pós-Graduação em Alimentos e Nutrição, Universidade Federal do Estado do Rio de Janeiro, Rio de Janeiro, RJ, Brazil

e-mail*: limasobrinho@hotmail.com*

Introduction

The Jacarepaguá Lagoon System (JLS) receives industrial and domestic waste in an urban area with high population density and intense economic activity (Figure 1). The hydrography of the lagoons favours the sedimentation of particulate material transferred from the drainage basin. Water engineering, such as channel dredging and subsea outfall, did not satisfactorily mitigate pollution effects. Therefore, the environment is highly eutrophic, presents frequent blooms of algae and generates high emissions of greenhouse gases. There is no record in the literature on the analysis of organic compounds in the water compartment. The present work applies sterols as biomarkers to quantify the degree of pollution caused by biogenic compounds in riverine and lacustrine water of the JLS. n-Alkanes were applied to estimate the fractions of petrogenic contaminants.

Experimental

Nine sampling stations in four seasons were selected for in situ measurements and surface water sampling. Four of them were in the main rivers that flow into the JLS and five stations in the lagoon. Temperature (°C), dissolved oxygen (mg L^{-1}), salinity, pH, Eh and conductivity (µS cm^{-1}) were measured *in situ* using a YSI multiprobe.
n-Alakanes and Sterols wer identified and quantified by gas chromatography with flame ionization detection (GC-FID Agilent 7890A) using a DB-5 capillary column (30 m x 0.32 mm x 0.25 µm).

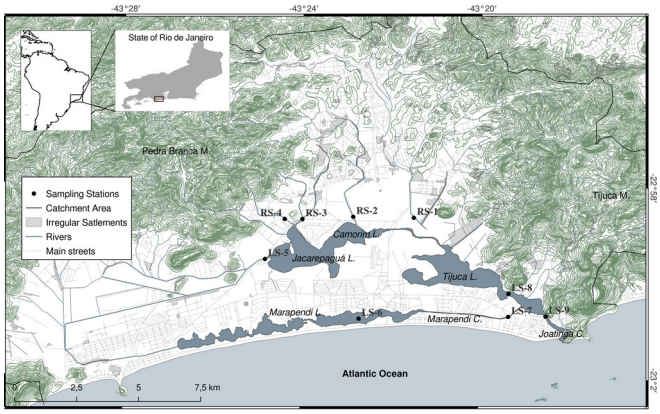

Figure 1. Map showing the riverine and lacustrine sampling stations of the Jacarepaguá Lagoon System.

Results and Discussion

The sums of n-alkanes and sterols analysed had average concentrations of 21 ± 20 µg L^{-1} and 10 ± 8 µg L^{-1}, respectively, in the river samples and 235 ± 156 µg L^{-1} and 30 ± 28 µg L^{-1}, respectively, in the lagoon samples. The work also showed that the organic compounds inside the lagoons are evenly distributed, and approximately 7% of them are transferred to the marine ecosystem. Biogenic biomarkers and the absolute concentrations of sterols showed that sewage contaminants transferred by the rivers are partially decomposed in the lagoons. The correlations between indices and physicochemical parameters indicated that the degradation of organic compounds in the lagoons

occurs mainly in the sediment compartment under anoxic conditions. The indices for sewage indicate that the ecosystem has exceeded its carrying capacity. The indices based on n-alkanes reported strong contamination at all sampling stations and inferred that 75–100% of these compounds were derived from petrogenic sources. These indices did not show any difference between rivers and the lagoon, which demonstrates the resilience of these compounds in the ecosystem.

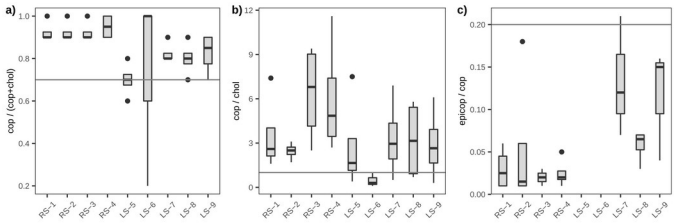

Figure 2. Box plots of the mean values of biogenic pollution indices at riverine and lacustrine sampling stations in the Jacarepaguá Lagoon System. a) coprostanol/(coprotanol + cholesterol), b) coprostanol/cholesterol, c) epicoprostanol/coprostanol (Bujagic et al., 2016).

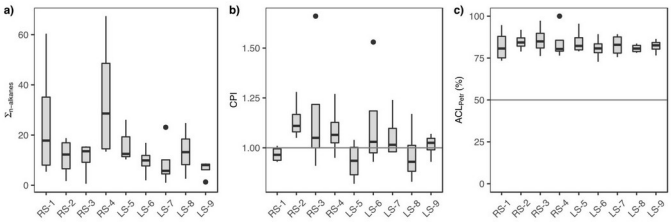

Figure 3. Box plots of mean values of total n-alkanes (µg L-1) and n-alkanes-based indices in riverine and lacustrine sampling stations of the Jacarepaguá Lagoon System. a) Sum of total n-alkanes, b) Carbon Preference Index (CPI), c) Percentage of pretrogenic source according to the end member approach applying Average Chain Lenght (ACL) (Jeng et al., 2006; Mille et al. 2007; Zakaria et al., 2008; Bush and McInerney, 2013; Omokpariola et al., 2022)

Conclusions

As main conclusions, the results showed that the quantified contaminants found in the JLS water samples originate in the urbanized drainage basin. Biogenic pollution indices such as cop/(cop + chol), cop/chol and epicop/cop presented results above the reference values, indicating highly polluted conditions at all sampling stations (Figure 2). Similarly, the CPI and ACL results indicated strong petrogenic contamination (Figure 3). The results also showed that biogenic and petrogenic contaminants are transported by rivers and distributed in lagoons as a result of their hydrodynamics. Fresh wastewater is the main source of biogenic contaminants. This group of compounds is partially degraded in lacustrine sediment under anoxic conditions. Petrogenic contaminants correspond to most aliphatic hydrocarbons and showed resilience to decomposition in the lacustrine environment. Therefore, increasing the entry of saline water into the lagoon system has no direct effect on the metabolic efficiency of the microbial community and, consequently, on mitigating the effects of urban areas.

Acknowledgements

We are grateful for financial support from CAPES Finance Code 001 PPG-Geoquímica-UFF, FAPERJ (Procs. E-26/010.101117/2018, E-26/210.745/2021) and CNPq (Proc. 420351/2016-7). MCB and ADPN thank CNPq for individual research grants (308535/2016-2 and 312288/2017-4). FAPERJ financially supported RLS with a PD scholarship (Proc. E-26/202.796/2016).

References

Bujagic I.M., GrujiS., JaukoviZ., Lausevi M., 2016. Sterol ratios as a tool for sewage pollution assessment of river sediments in Serbia. Environm. Pollut. 213, 76-83.

Bush R.T, McInerney F.A., 2013. Leaf wax n-alkane distributions in and across modern plants: Implications for paleoecology and chemotaxonomy. Geochim. et Cosmochim. Acta 117, 161–179.

Jeng, W-L., 2006. Higher plant n-alkane average chain length as an indicator of petrogenic hydrocarbon contamination in marine sediments. Mar. Chem. 102, 242-251.

Mille G., Asia L., Guiliano M., Malleret L., Doumenq P., 2007. Hydrocarbons in coastal sediments from the Mediterranean sea (Gulf of Fos area, France). Mar. Pollut. Bull. 54, 566–575.

Omokpariola, D.O., Nduka, J.K., Kelle, H.I. et al., 2022. Chemometrics, health risk assessment and probable sources of soluble total petroleum hydrocarbons in atmospheric rainwater, Rivers State, Nigeria. Sci Rep 12, 11829.

Zakaria M.P., Bong C.-W., Vaezzadeh V., 2018. Fingerprinting of Petroleum Hydrocarbons in Malaysia Using Environmental Forensic Techniques: A 20-Year Field Data Review in Oil Spill Environmental Forensics case Studies. Elsevier. Oxford, United Kingdom. 345-372

XVI LATIN AMERICAN CONGRESS ON ORGANIC GEOCHEMISTRY
9 - 11 AUGUST, 2023
ARACAJU, SERGIPE, BRAZIL

ENVIRONMENTAL GEOCHEMISTRY EVALUATION OF THE WEATHERING IMPACTS IN OILS FROM THE MYSTERIOUS 2019 SPILL

Isabelle F. S. de Lima,[1*] Ignes R. dos Santos,[1] Marília Gabriela A. Pereira,[1] Jhonattas de C. Carregosa,[2] Tarcísio M. Santos,[2] Alberto Wisniewski Jr.,[2] Jandyson M. Santos[1]

[1]Research Group in Petroleum, Energy and Mass Spectrometry (PEM), Department of Chemistry, UFRPE, Recife-PE, Brazil; [2]Research Group in Petroleum and Biomass Energy (PEB), Department of Chemistry, UFS, São Cristóvão- SE, Brazil

*E-mail: isabellefarias91@gmail.com

Introduction

On August 30, 2019, an oil spill was officially reported on the coast of Brazil, spreading over 4,334 kilometers in length by November 22, 2019, mainly encompassing Northeastern states, in a total of 120 municipalities and 724 localities.[1] The choice of efficient analytical methods can help identify the origin of spilled oil by promoting chemical characterization.[2] Gas Chromatography coupled to Mass Spectrometry (GC/MS) and Fourier Transform Mass Spectrometry (FT-MS) techniques have been used for oil spill geochemical studies.[3] These techniques can be applied to understand the chemical modifications in spilled oils that suffered weathering impacts such as biodegradation, evaporation, and photo-oxidation.[4] Herein, we aim to evaluate the chemical modifications of 2019 spilled oils that were naturally exposed in different environments, through samples collected on the coast of Pernambuco, Brazil.

Experimental

We studied three samples: 1) Oil sample collected immediately after the reported spill on September 2019 (SO); 2) Oil sample collected in January 2021, after naturally remaining in the marine aquatic environment (SA); and 3) Oil sample collected on April 2021, after naturally remaining in the terrestrial environment (ST). The SO and SA samples were collected at Praia de Enseada dos Corais, whereas, the ST sample was collected at Praia de Itapuama, Pernambuco state, Brazil. The samples were extracted according to the methodology used by Carregosa et al. (2021).[5]

For the GC-MS analyses, the samples were diluted in *n*-hexane to a concentration of 10 mg mL^{-1} and inserted into a GC-MS/MS model TQ8040 (Shimadzu Co., Japan), with a triple quadrupole analyzer and electron impact ionization (EI) source at 70 eV, in the multiple reaction monitoring (MRM) acquisition modes. The sample injection volume was 1 µL, in splitless mode, and the injector, ion source, and interface temperatures were 300, 280, and 290 °C, respectively.

For the FT-MS analyses, the samples were diluted in a mixture of toluene and methanol (3:1 v/v) with concentrations of 0.1 mg/mL^{-1} and inserted into an HCD Exactive Plus (FT-Orbitrap MS) system (Thermo Scientific, Germany), using electrospray ionization (ESI) in negative acquisition mode to access the acid polar compounds. The samples were injected directly with the aid of an auxiliary syringe pump and data were acquired using Xcalibur 2.0 and PetroMS software.

Results and Discussion

The GC-MS/MS analyses allowed assignments of twenty-three different petroleum biomarker compounds of terpenes (*m/z* 191) and steranes (*m/z* 217) classes. Thus, we have calculated twenty-two diagnostic ratios, whose resulting values are shown in **Figure 1**. It is possible to note a trend of similarity between the values of the ratios, as the graph lines form a profile that overlaps, with small variations in the three samples. The diagnostic ratios identify parameters related to the similarities between the oils and provide chemical and geochemical information, such as thermal maturity, deposition environment, and precursor organic matter. So, it can be said that the pattern of similarity between the values resulting from the twenty-two diagnostic ratios corroborates the fact that the three samples are from the same geochemical origin, and which are from the 2019 oil spill. The result shows that even after the spilled oil underwent weathering in different environments, it maintained the proportion between the main biomarkers, and these ratios can be safely used in investigations involving oil spills.

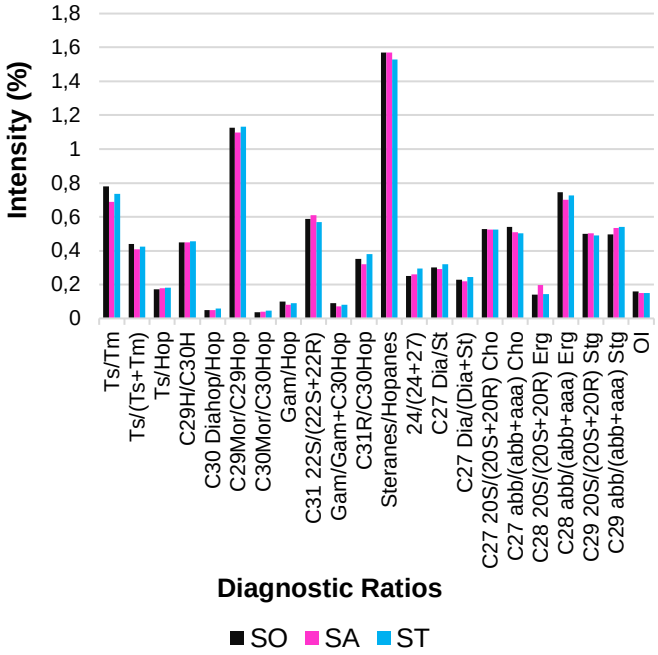

Figure 1. Diagnostic ratios of the petroleum biomarkers identified for the SO, SA, and ST samples by GC-MS/MS analyses in MRM mode.

For the *n*-alkanes profiles (*m/z* 85) we have found a gradual decrease in the intensities of *n*-alkanes from C_{14} to C_{40} for the SA and ST samples collected in 2021 when compared to the SO sample collected in 2019 (**Figure 2)**. The SA and ST oils were subjected to one and a half years of contact with different environments, aquatic and terrestrial, respectively, and continuous loss of *n*-alkanes can be justified by weathering processes such as biodegradation, evaporation, and/or photooxidation.

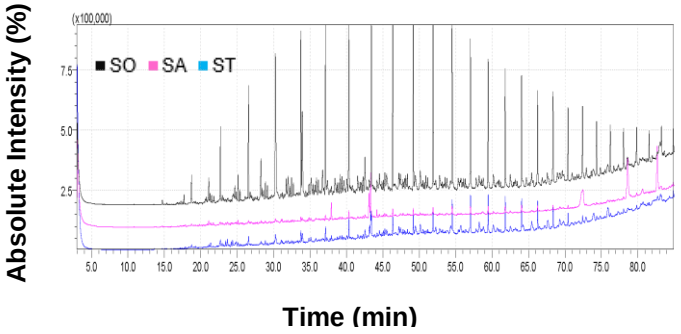

Figure 2. GC-MS/MS for *m/z* 85 related to *n*-alkane class for the SO, SA, and ST samples.

We have found by ESI(-) FT-MS different classes of molecular formulas (N_1, O_4S_1, O_2, O_1N_1, O_3, N_1S_1, O_2N_1, O_1, O_2S_1, O_4S_2, O_4, O_3S_1) for the three samples (**Figure 3**). It is possible to see that the time of exposure of the oily material to the spill mainly affects the intensity of classes that contain oxygen, in special the highest intensity of O_2 class in the SA sample, when compared with SO and ST. This can be explained by the weathering processes of biodegradation and photooxidation, but also due to the most time contact with the aquatic environment of the SA sample.

Figure 3. Class distribution for the SO, SA, and ST samples obtained by ESI(-) FT-MS.

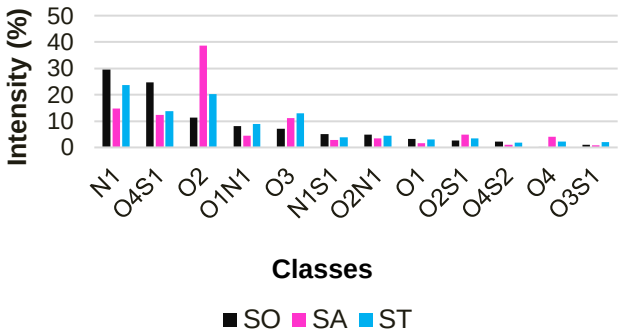

Conclusions

We were able to conclude that the twenty-two diagnostic ratios obtained for the biomarker compounds of terpenes and steranes classes have not suffered environmental chemical weathering. Then, these diagnostic ratios are safe to use as reference values for geochemical studies in environmental disasters involving oil spill events. As expected, the *n*-alkanes were the most susceptible classes affected by weathering, specifically biodegradation in the SA and ST samples. The acid polar organic compounds such as naphthenic acids (NA) may have been responsible for the increased intensity of the O_2 class identified in the analysis of the SA sample by ESI(-) FT-MS analyses. Therefore, the SA and ST samples underwent temporal chemical modifications due to the prevailing chemical weathering in different environments when compared to the SO sample.

Acknowledgments

This study was funded by Fundação de Amparo à Ciência e Tecnologia do Estado de Pernambuco (FACEPE BIC-1056-1.06/22). The authors are grateful to the Center of Multi-users Chemistry Laboratories (CLQM) at the Federal University of Sergipe.

References

[1] PENA, *et al.* Public Health Journal, v.36, n.2, 2020.
[2] RADOVIC, J. R. *et al.* Mar. Pollut. Bull., 79, 268–277, 2014.
[3] LIMA BD, *et al.* Mar. Pollut. Bull., 189, 114744, 2023.
[4] HOFFMANN, 3rd ed., 2007.
[5] Carregosa, *et al.* Anais da Acad. Bras. De Ciên., v.93, 2021.

XVI LATIN AMERICAN CONGRESS ON ORGANIC GEOCHEMISTRY
9 - 11 AUGUST, 2023
ARACAJU, SERGIPE, BRAZIL

Geochemical forensic evaluation of recently appearing tar balls on the northeast coast of Brazil and their relationship with the mysterious 2019 oil spill

Marília Gabriela A. Pereira[a*], **Ignes R. dos Santos**[a], **Isabelle F. S. de Lima**[a], **Jhonattas C. Carregosa**[b], **Alberto Wisniewski Jr**[b], **Jandyson M. Santos**[a],

[a]Petroleum, Energy and Mass Spectrometry Research Group (PEM), Chemistry Department, Federal Rural University of Pernambuco (UFRPE), Recife, PE, 52171-900, Brazil
[b]Petroleum and Energy from Biomass Research Group (PEB), Chemistry Department, Federal University of Sergipe (UFS), São Cristóvão, SE, 49100-000, Brazil

***e-mail:** marilia-gap@hotmail.com

Introduction

In August 2019, an oil spill was reported on the coast of northeastern Brazil, causing contamination, damage to the ecosystem and socioeconomic impacts (Magalhães *et al.*, 2020; Araújo *et al*., 2020). The oil was described as a viscous and dark material and reappeared in the years of 2020, 2021 and 2022 (Reddy *et al*., 2022; G1, 2022). The material that appeared in the half of 2022 was characterized as tar balls. Since then, studies have been carried out with the aim of understanding the chemical composition of the oils, using various analytical techniques to characterize the sample at the molecular level (Carregosa *et al*., 2021; Reddy *et al*., 2022). The present study aims to characterize the spilled oils and investigate any possible relationships between samples from 2019 and 2022, using organic geochemical evaluation with analytical techniques by gas chromatography/mass spectrometry (GC/MS) and ultrahigh-resolution MS (FT-MS).

Experimental

We have studies an oil sample collected in 09/2019 named of Sample2019 (Enseada Beach: 8°18'56"S; 34°56'52"W), and an tarball sample collected in 08/2022 named of Sample2022 (Candeias Beach: 8°12'34.8"S; 34°55'03.8"W), both sampling were performed in the state of Pernambuco, Brazil. The extraction of samples was performed as described by Carregosa *et al*. (2021) to obtain a 1 mg mL^{-1} solution prepared in *n*-hexane (HPLC grade, Merck) for GC/MS analysis.

GC/MS analyzes employed a quadrupole gas chromatograph/mass spectrometer (GCMS-QP2010 SE, Shimadzu, Japan), operated with electronic ionization (EI) at 70 eV, coupled to an autosampler (AOC-6000 Plus, Shimadzu). The sample injection volume was 1 µL, in split mode (1:20), and the injector, ion source, and interface temperatures were 300, 250, and 300 °C, respectively.

An HCD Exactive Plus (FT-Orbitrap MS) system (Thermo Scientific, NJ, USA) equipped with a heated electrospray ionization (H-ESI) probe was used for the analysis of polar compounds. Samples were prepared in a 60:30 (*v/v*) methanol:toluene ratio containing 0.5% formic acid (HPLC grade) for positive mode acquisition. Samples were introduced into the direct infusion, and data were acquired in scan mode from 180-1000 *m/z* with the instrument operated at a resolution of 140,000 (@200 *m/z*).

Results and Discussion

The GC/MS fingerprinting in scan mode provided the *n*-alkanes and isoprenoids distributions (Fig. 1), which were very different for the two samples. For Sample2019 we have found a unimodal medium-chain *n*-alkanes (*n*-C_{12} to *n*-C_{34}) distribution, whereas Sample2022 presented a bimodal profile of long-chain *n*-alkanes (*n*-C_{12} to *n*-C_{41}), which is known to be associated with paraffinic deposits in crude oil storage tanks (Boukadi *et al*., 2005).

The profiles of terpanes distribution were similar, but there was a subtle difference in steranes when compared Sample2019 versus Sample2022 (Peters *et al*., 2005a, 2005b). Diagnostic ratios of biomarkers were calculated to assess oil formation parameters, and showed similarities in Pr/*n*-C_{17} and CPI values, but slight differences in Ph/n-C18 and Pr/Ph values due to higher Ph content in Sample2022. Terpane and sterane biomarkers also showed similar values for both samples when we compared the diagnostic ratios (Tab. 1), indicating a similar geological origin. Additionally, the presence of characteristic biomarkers of the oil from the 2019 spill was also observed in Sample2022, suggesting

similar geological origins for the samples (Carregosa *et al*., 2021).

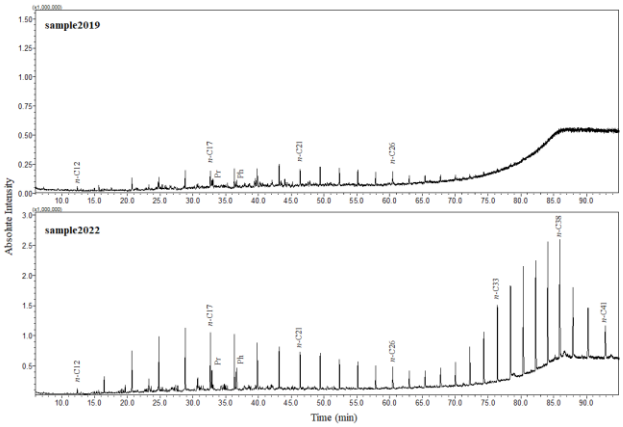

Figure 1. GC/MS profiles obtained in scan mode for Sample2019 and Sample2022, collected on the coast of Pernambuco, showing the distributions of n-alkanes (n-C12 to n-C41) and the isoprenoids pristane (Pr) and phytane (Ph).

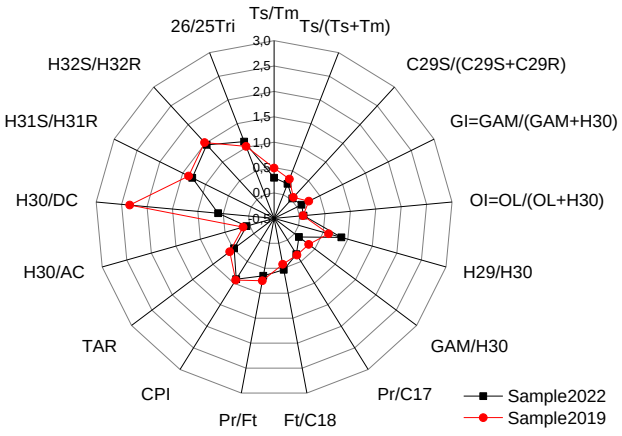

Figure 2. Crude oil biomarkers and diagnostic ratios obtained from GC/MS analysis in SIM mode at *m/z* 191 and *m/z* 217, for comparing Sample2019 and Sample2022 collected on the coast of Pernambuco.

Determination of basic polar compounds by ESI(+) FT-MS revealed differences in the *m/z* distributions (Fig. 3). For Sample2022, the most abundant ions were found for compounds with molecular weights between 200 and 400 Da, while for Sample2019 the highest abundance ions were centered in higher molecular weights (400-700 Da), according to the highest molecular weight numerical average (Mn) and average molecular weight (Mw) values (Santos *et al*., 2020). These results indicated that Sample2019 was composed of higher molecular weight basic polar components compared to Sample2022. This finding also indicated that Sample 2022 has the characteristics of a virgin crude oil from storage tanks, due to the lower content of polar compounds with lower molecular mass and high content of paraffinic *n*-alkanes (as observed in Fig. 1).

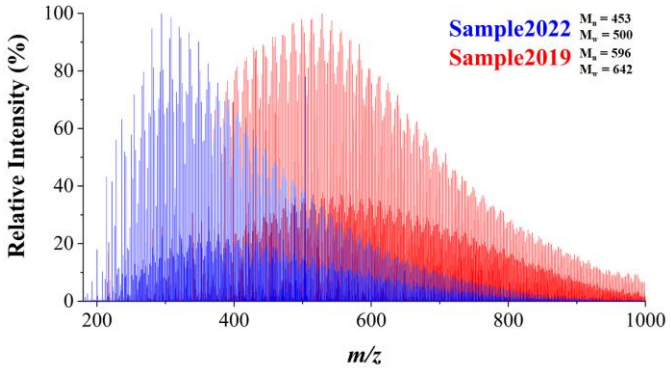

Figure 3. ESI(+) FT-MS of the Sample2022 and Sample2019 collected on the coast of Pernambuco and the values of Mn e Mw.

Conclusions

The results indicate differences in the composition of low molecular weight compounds between the tar ball (Sample2022) and the oil from the 2019 spill (Sample2019), suggesting that Sample2022 is characterized as a virgin/unprocessed oil. However, there are indications of a possible geological relationship between the two samples based on the distribution of steranes and terpanes. FT-Orbitrap MS results also show distinct profiles of polar compounds across samples. Based on the hypothesis of a World War II shipwreck as the source of the 2019 spill that was described by Reddy *et al.* (2022), it is suggested that the source of the spill may be the same shipwreck, carrying processed oil corresponding to Sample2019 and crude oil from storage tanks corresponding to Sample2022. However, it would be unlikely that the same vessel could transport all of these materials, thus further investigations are needed to confirm the sources of these oils/tarballs and the possibility that the tarballs are prone to a new spill event.

Acknowledgements

This study was funded by Fundação de Amparo à Ciência e Tecnologia do Estado de Pernambuco (FACEPE APQ-0036-1.06/20 and IBPG-1124-1.06/22). The authors are grateful to the Center of Multi-users Chemistry Laboratories (CLQM) at Federal University of Sergipe and PEB Group.

References

Carregosa, *et al.* Anais Da Acad. Bras. de Ciên., v.93, 2021.
Magalhães, K. M., *et al.,* Sci. of the Tot. Env. v. 764, 2021
Reddy, C. M., *et al.,* Ener. & Fue., v. 36, 2022.
Araújo, M. E. DE, *et al.,* Cader. de Saú. Públ. v. 36, 2020
Lourenço, R. A., *et al.,* Mari. Poll. Bull. v. 764, 2020.

XVI LATIN AMERICAN CONGRESS ON ORGANIC GEOCHEMISTRY
9 - 11 AUGUST, 2023
ARACAJU, SERGIPE, BRAZIL

Sources of sedimentary organic matter in the Río de la Plata estuary: A molecular and compound-specific isotope approach

Lígia Dias de Araujo[a], Satie Taniguchi[a], Leticia Burone[b], Michel Michaelovitch de Mahiques[a], Marcia Caruso Bícego[a]

[a] **Instituto Oceanográfico da Universidade de São Paulo, Praça do Oceanográfico, 191, São Paulo 05508-120, Brazil**

[b] **Instituto de Ecología y Ciencias Ambientales, Facultad de Ciencias, Universidad de la República, Iguá 4225, Montevideo 11400, Uruguay**

e-mail: ligiad.araujo@gmail.com

Introduction

Organic matter deposited in estuarine and coastal sediments is a major component of the global carbon cycle, as it retains significant quantities of natural and anthropogenic organic matter under the interactions of a series of physical, chemical, and biological processes. Sedimentary organic matter contains an abundance of various lipids, including so-called straight chain alkanes (*n*-alkanes), which are derived from terrestrial plant waxes, marine phytoplankton and bacteria, as well as biomass combustion and diagenetic transformation of biogenic precursors [1]. Carbon cycling in the coastal waters that connect terrestrial and oceanic systems, including rivers, estuaries and the continental shelf, is acknowledged to be a major component of global carbon cycle and budget [2].

The Río de la Plata (RdlP), South America's second-largest fluvial system, annually supplies $80x10^6$ t $year^{-1}$ of sediment to the ocean, with some sediment passing along the SE Uruguayan coast [3]. The RdlP estuary is route for a large number of ships that arrive at Montevideo Bay (Uruguay) to load and unload products [4]. In this context, the present study aims to characterize *n*-alkanes in surficial sediments to estimate the sources of organic matter, whether natural or anthropogenic, along the RdlP estuary.

Experimental

The study conducted an analysis of 14 sediment samples collected in the Rio de la Plata estuary (Uruguay) between 2008 and 2010, using a Smith-McIntyre bottom sampler, to identify and quantify *n*-alkanes and specific stable carbon isotopes (Figure 1).

The sediment samples were lyophilized, homogenized, and then subjected to an analytical procedure for *n*-alkanes, which involved extracting 20 grams of sediment in Soxhlet for 8 hours using dichloromethane/*n*-hexane solution. The extracts were purified by adsorption chromatography on a column using 5% deactivated alumina. The *n*-alkanes were then identified and quantified by injecting the extract into an Agilent™ gas chromatograph with a flame ionization detector (GC-FID).

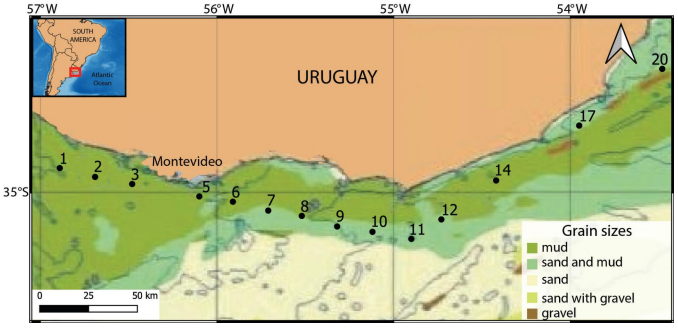

Figure 1. Sampling sites and spatial distribution of mud, sand and gravel. Adapted from (FREPLATA, 2005) [5]

Stable carbon isotope analysis of specific *n*-alkanes was performed on eight selected surface sediment samples using gas chromatograph coupled to an isotope ratio mass spectrometer (GC-IRMS). Prior to analysis, a purification step was necessary to remove unsaturated compounds that interfere with the analysis of target compounds. The procedure involved packing glass columns with silica gel impregnated with silver nitrate ($AgNO_3$) and eluting the *n*-alkanes with *n*-hexane. The stable carbon isotope analysis of *n*-alkanes was conducted using a Thermo Scientific Trace Ultra GC coupled to a Thermo Finnigan GC Combustion III with a combustion interface.

Results and Discussion

Total *n*-alkane concentrations varied from 1.35 to 12.20 µg g^{-1}. In general, the highest contents were observed in samples from the upper estuary. Terrigenous organic matter was present in all samples (Figure 2), represented by the presence of odd and high molecular weight *n*-alkanes (*n*-C29, *n*-C31, and *n*-C33). Throughout the Rio de la Plata estuary, it has been observed a lack of predominance of odd low molecular

weight *n*-alkanes over the even ones, indicating a possible recent introduction of petroleum derived products [6]. In some samples (samples 1, 2, and 20), the highest concentrations were found for medium-chain *n*-alkanes (*n*-C23, *n*-C24, and *n*-C25), possibly indicating the introduction of petroleum derived products with a higher degree of degradation.

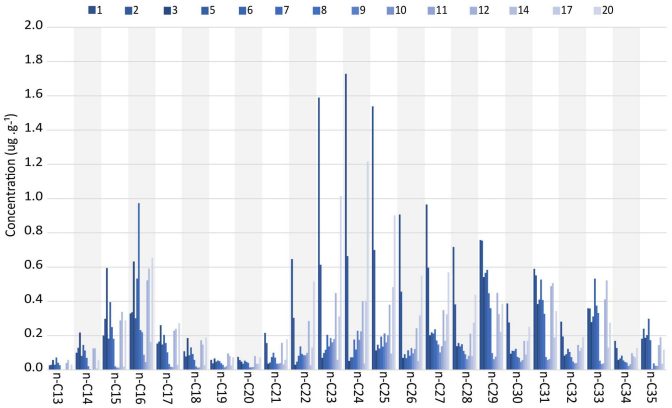

Figure 2. Distribution of *n*-alkanes in sedimentary samples.

The $\delta^{13}C$ values of the *n*-alkanes *n*-C27 to *n*-C33 ranged from -33.3 to -26.9‰ (Figure 3). Most samples showed $\delta^{13}C$ values between -31 and -29‰ for *n*-C27 to *n*-C32 homologues. These values are typically found in odd *n*-alkanes of high molecular weight of terrigenous origin, mainly from C3 plant sources. However, the anthropogenic input may be influencing the signature of the natural contribution by lowering its $\delta^{13}C$ values, as anthropogenic organic matter typically exhibits depleted $\delta^{13}C$ signatures [7]. Samples 2 and 3 show the most depleted values of all samples, with $\delta^{13}C$ values lower than -31‰. These samples are located in the uppermost region of the estuary and may be more strongly influenced by the input of petroleum derivate products.

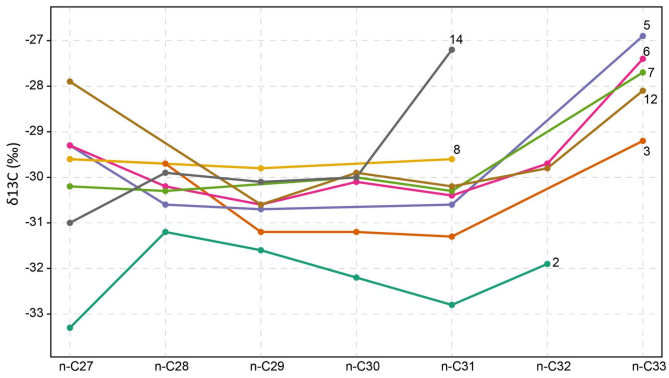

Figure 3. Profiles of *n*-alkane isotopic composition (from *n*-C27 to *n*-C33) in surficial sediments from the RdlP estuary

The $\delta^{13}C$ values of *n*-C33 are enriched compared to the other homologues. Considering that *n*-C33 is one of the primary *n*-alkanes synthesized by C4 plants, these plants may also be contributing to the sedimentary OM.

Conclusions

The analysis of *n*-alkane concentrations and $\delta^{13}C$ values in sediment samples from the RdlP estuary provided insights into the composition and sources of organic matter. Anthropogenic contributions were evident in most samples, indicated by the lack of predominance of odd *n*-alkanes over even ones (low and medium molecular weights). Terrigenous organic matter was present in all samples, identified by the presence of odd and high molecular weight *n*-alkanes. The $\delta^{13}C$ values suggested a primary origin from C3 plants and a secondary contribution from C4 plants. However, petrogenic inputs may be influencing the $\delta^{13}C$ values, complicating the identification of natural sources. Overall, these findings reveal the presence of both terrigenous and anthropogenic contributions to organic matter in the RdlP estuary. Further research and monitoring are necessary for a comprehensive understanding of the factors influencing organic matter dynamics in this complex environment.

Acknowledgements

The authors thank CNPq (Brazilian research council; 304274/2018-6; 152565/2022-1) and the fostering agency of the State of São Paulo (FAPESP 2015/17763-2; 2016/18348-1) for financial support and the Dirección Nacional de Recursos Acuáticos (DINARA).

References

1. Gogou, A., Bouloubassi, I., and Stephanou, E. G. 2000. Marine organicgeochemistry of Eastern Mediterranean: Aliphatic and polyaromatichydrocarbons in Cretean Sea surficial sediments. Marine Chemistry 68:265–282.

2. Bauer, J.E., Cai, W.-J., Raymond, P.A., Bianchi, T.S., Hopkinson, C.S., Regnier, P.A.G., 2013. The changing carbon cycle of the coastal ocean. Nature 504, 61–70.

3. Gilberto, D.A., Bermec, C.S., Acha, E.M., Mianzan, H., 2004. Large-scale spatial patterns of benthic assemblages in the SW Atlantic: the Rio de la Plata estuary and adjacent shelf waters. Estuarine Coastal Shelf Science 61, 1–13

4. García-Alonso, J., Lercari, D., and Defeo O., 2019. "Río de la Plata: a neotropical estuarine system." Coasts and Estuaries. Elsevier. 45-56.

5. FREPLATA, 2004. “Análisis Diagnóstico Transfronterizo del Río de la Plata y su Frente Marítimo”. Documento Técnico. Proyecto Protección Ambiental del Río de la Plata y su Frente Marítimo. Proyecto PNUD/GEF/RLA/99/G31

6. Simoneit, Bernd RT. Hydrothermal alteration of organic matter in marine and terrestrial systems, 1993. Organic geochemistry: principles and applications. 397-418.

7. Maioli, O., Rossi, C., Sasso, M., Madureira, L., Azevedo, D., Radler, F., 2012. Evaluation of the organic matter sources using the δ13C composition of individual *n*-alkanes in sediments from Brazilian estuarine systems by GC/C/IRMS. Estuar. Coast. Shelf Sci. 114, 140-147.

USING DIAGNOSTIC RATIOS FOR CHARACTERIZATION OF NATURAL ORGANIC MATTER FROM THE BERTIOGA MAGROVE, SÃO PAULO.

Daniela Gomes Moreira[a]* / Márcia Caruso Bícego[a] / Rafael André Lourenço[a]

[a]University of São Paulo - Oceanographic Institute

e-mail: *danielamoreira@usp.br;

Introduction

1.1 General aspects

The mangrove is an ecosystem that represents the transition between the terrestrial and oceanic environments (SCHAEFFER NOVELLI, 1989). It develops in tropical and subtropical regions, near the mouth of rivers, coastal lagoons, and estuaries. Its features extend along the intertidal zone, including both high and low tides.

With arboreal vegetation, and growing in brackish or salty water environments, the mangrove is an immensely important environment for the marine ecosystem, from the sequestration and storage of carbon in soil and biomass to the curious support of trees in muddy sediment, which efficiently slows down the hydrodynamic flow, generating protection and stability against erosion for tropical coastal zones, which are vulnerable to climate change.

1.2 n-alkanes

N-alkanes are linear saturated hydrocarbons that exhibit high resistance to degradation and stability, which can be preserved in the environment for thousands of years in sediment. They are biomarkers commonly found in sedimentary organic matter and are an important tool for environmental reconstruction studies. Their origin can be attributed to marine sources such as algae and phytoplankton, exhibiting short carbon chains (n-C14 to n-C24) and vascular plants, which have long-chain n-alkanes with odd carbon numbers (n-C25, n-C27, n-C29, n-C31, n-C33, n-C35) (EGLINTON and HAMILTON, 1967).

These plants show differentiation both in the carbon isotopic fractionation and in the compositional concentrations of n-alkanes, which allows for differentiation of the contribution of C3 and C4 plants in the sediment and the correlation of this contribution with the spatial distribution of these vegetation types on continents.

According to the literature, C3 plants produce higher amounts of n-C27 and n-C29 compared to C4 plants, which produce more n-C31 and n-C33 (SCHEFUß et al., 2003).

The use of ratios between individual n-alkanes as sensitive parameters to vegetation type and environmental conditions such as temperature and precipitation are employed in several studies, which follow some indices.

Study area

Located on the southeast coast, along the banks of the Guanabara River, this locality features a humid climate with average annual temperatures of 20°C. The area is home to three species of mangroves: *Rhizophora mangle* (red mangrove), *Laguncularia racemosa* (white mangrove), and *Avicennia schaueriana* (black mangrove).

The genus *Rhizophora mangle* anchors itself through branching structures that form as the pneumatophores penetrate the substrate. On the other hand, *Laguncularia racemosa* has underground roots (radial roots) that spread horizontally over the substrate, forming a support system in loosely consolidated soil. Additionally, the white mangrove has non-functional glands in the upper base of the red petiole. The genus *Avicennia schaueriana* also possesses underground roots, albeit more developed than those of the white mangrove. Another characteristic of this type of mangrove is the presence of pneumatophores, which emerge from the radial roots and grow vertically, aiding in the necessary gas exchange for the tree's survival.

2.1 Sediment collection

Twenty sediment samples were collected in the Bertioga mangrove between April and May 2022. These samples were stored in aluminum trays, labeled, immediately frozen, and subsequently lyophilized.

Experimental

The analysis followed the methodology described in UNEP (1992) and LOURENÇO et al. (2016) with small adaptations as described later.

In the first step, approximately 15 g of sediment was weighed, added to sulfate (Na_2SO_4), and transferred to a cartridge, followed by continuous extraction of hydrocarbons in a Soxhlet for 8 hours. Then, the organic extracts obtained were taken to the TurbVap concentrator, where they were concentrated to 1 ml for 30 minutes. Subsequently, the extracts were taken to the alumina column to purify the concentrated extracts. Later, the purified extracts were taken again to the TurbVap concentrator for 8 minutes, with the addition of an internal standard (hexadecene).

For the analysis of n-alkanes, the Agilent Technologies 6890 gas chromatograph equipped with a flame ionization detector (GC-FID) was used. The separations were performed on a capillary column with dimensions of 50m x 0.32mm x 0.17µm, using a stationary phase composed of 5% diphenyl and 95% dimethylpolysiloxane. The carrier gas used was helium, and the injector temperature varied according to the column heating. The injection mode employed was *splitless*.

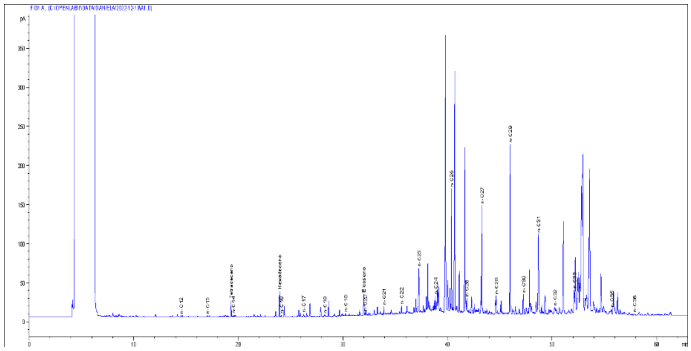

Figure 2. Chromatogram obtained after analysis of n-alkane

Results and Discussion

The total concentration of total HAs ranged from 0.12 ng g^{-1} to 11.80 ng g^{-1}. The preferential carbon index (CPI) had an average value of 11.59, indicating a higher dominance of higher plants. The norm31 index had an average value of 0.29, indicating a predominance of C3-type plants, typical of humid climates. Additionally, the average chain length was greater than 29, characterizing an environment with high temperature. It was also possible to observe and identify a strong predominance of compounds with an odd number of carbon in the chains (n-C29 and n-C31), indicating the input of terrigenous material.

Table 1: Interpretation of the results obtained

Index	Average	Standard deviation
Index norm31	0,29	0,14
CPI	11,59	3,11
TMC	196,09	76,08

Description	
Norm31	Humid climate and/or type C3
CPI	Higher plants
TMC	Lower humidity and higher temperature plants

Conclusions

The application of diagnostic ratios, based on n-alkane concentrations in the Bertioga mangrove, allowed the characterization of organic matter and provided information about the environmental conditions associated with the environment.

Acknowledgements

DG Moreira thanks CNPq for the PIBIC scholarship 2022/1773.

References

LOURENÇO, R.A., MAHIQUES, M.M., WAINER, I.E.K.C., Rosell-Melé, A., Bícego, M.C., 2016.. **Organic biomarker records spanning the last 34,800 years from the southeastern Brazilian upper slope: links between sea surface temperature, displacement of the Brazil Current, and marine productivity.** Geo-Mar Let., 36, 361-369. https://doi.org/10.1007/s00367

UNEP (1992). **Determinations of Petroleum Hydrocarbons in Sediments, Reference Methods for Marine Pollution studies** 20, 77pp.

Evaluation of the Organic Matter Maturity on Admiralty Bay Sediment, King George Island, Antarctic, During 2019-2020 Summer

Maria Julia Vieira Ventura [a]*, César de Castro Martins [a], Rafael André Lourenço [a]*

[a] **Instituto Oceanográfico da Universidade de São Paulo (IO-USP), São Paulo, Brazil**

* Corresponding authors: mariajulia_vventura@usp.br, rafaell@usp.br

Introduction

Marine sediments play a fundamental role in the storage of organic matter. Due to its inherent capacity it is possible to evaluate the organic matter trapped in the sediments for various purposes, such as determining its maturity, which shows whether the organic matter is fresh or degraded. This work aimed to assess the maturity of the organic matter in the sediments from the Admiralty Bay, Antarctica, based on proteins, carbohydrates, chlorophyll, and phaeopigments data obtained from 11 sediment samples.

The Admiralty Bay is a well-studied subantarctic marine environment. Hydrographic studies have been conducted in the region since 1980, by scientists from the Polish Arctowski Research Station, [1] and [2], and brazilian researchers from the Ferraz Station, [3]. The results presented here aim to contribute to the comprehension of the organic carbon cycle in the Antarctic marine environment. The ratios proteins/carbohydrates, and chlorophyll/phaeopigments can be calculated through its concentrations, is an information that may help to understand the process of production and degradation of organic matter by primary producers which is associated with the sequestration of organic carbon in the marine environment. That is possible due to the fact that proteins are remineralized faster than carbohydrates. Phaeopigments are the product of chlorophyll degradation. Therefore, in both cases, larger ratios reflect fresh production of organic matter higher than its degradation, while smaller ratios are a reflection of the opposite.

Experimental

The sediment samples were collected during the summer of 2019/2020 using a Van Veen grab sampler.

The instrumental technique used to determine the total compounds concentrations was molecular absorption spectrophotometry. The carbohydrates were determined according to Dubois et al [4], optimized to sediments by Gerchacov & Hatcher [5]. This is a colorimetric method based on the reaction between sugars and phenols in the presence of sulfuric acid, due to the sensibility of sugars to strong acids and high temperatures. The proteins were determined following the method described by Hartree [6] and Rice [7]. In an alkaline condition, the bivalent copper ion (Cu^{2+}) forms complexes with the peptidic bonds of proteins and it's reduced to its monovalent form (Cu^{+}). The Cu^{+} and the amino acids radical groups react with Folin-Ciocalteau (a phosphomolybdate and phosphotungstate mixture) forming a blue product. The determination of chlorophyll and phaeopigments was done according to the method described by Golterman et al [8]. The method is based on the extraction of these compounds with acetone and the conversion of chlorophyll into pheophytin, which is achieved through the addition of acid, that removes the magnesium from the chlorophyll molecule [9]. The maximum of the absorption spectrum of chlorophyll is also applicable to pheophytin. Therefore, the concentration of chlorophyll is calculated based on the variations in absorbance when the sample is acidified.

Results and Discussion

The analysis of the organic compounds was performed in 11 sediment samples from Admiralty Bay, collected in the Martel Inlet (points 8 to 13) and in the Ezcurra Inlet (points 13 to 18) (Fig. 1). The locations of the sampling stations are presented in Table 1, while the concentrations and ratios are presented in Table 2.

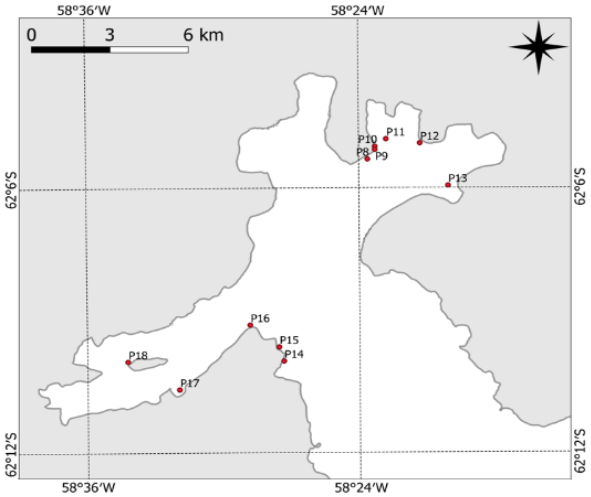

Figure 1. Spatial distribution of the sampling points in the study area.

Sampling point	Latitude (S)	Longitude (W)
P8	62°05.350'	58°23.617'
P9	62°05.133'	58°23.286'
P10	62°05.063'	58°23.286'
P11	62°04.893'	58°22.798'
P12	62°04.988'	58°21.311'
P13	62°05.949'	58°20.080'
P14	62°09.920'	58°27.343'
P15	62°09.600'	58°27.554'
P16	62°09.102'	58°28.822'
P17	62°10.562'	58°31.951'
P18	62°09.926'	58°34.216'

Table 1. Sampling points geographic coordinates.

Sampling point	Concentration (mg. g-1)				Ratio	
	Proteins	Carbohydrates	Chlorophyll	Phaeopigments	Proteins and Carbohydrate	Chlorophyll and Phaeopigments
P8	5,3	1,4	14,1	26,5	3,8	0,5
P9	5,1	1,4	15,5	58,5	3,7	0,3
P10	4,5	1,3	3,3	51,3	3,5	0,1
P11	5,0	2,7	65,3	60,6	1,8	1,1
P12	4,9	<LOD	50,8	94,9	-	0,5
P13	2,8	0,7	35,8	14,7	4,0	2,4
P14	0,2	0,2	2,1	0,1	0,9	19,9
P15	0,2	0,4	4,2	<LOD	0,4	-
P16	0,9	0,5	19,5	<LOD	2,0	-
P17	5,4	1,2	30,2	11,8	4,7	2,6
P18	4,0	0,8	13,6	15,3	5,2	0,9

Table 2. Total concentration data of carbohydrates, proteins, chlorophyll, phaeopigments, and its ratios in the sediment samples.

Although the concentrations of carbohydrates in P12 and phaeopigments in P15 and P16 turn out to be below the limit of detection of the analytical method, those significatively small numbers if quantitated would contribute to extremely large ratios that would indicate fresh organic matter. The proteins/carbohydrates ratio suggests that only in the samples for P14 and P15, the outermost sampling points of the bay, seem to be degraded. Similarly, mostly chlorophyll/phaeopigments ratios suggest fresh organic matter in the sediments.

Conclusions

In summary, the analysis of sediment samples suggests the presence of fresh organic matter based on the observed ratios of proteins/carbohydrates and chlorophyll/phaeopigments. Degradation of organic matter appears to be more pronounced in samples collected from the outermost points of the bay. These findings provide valuable insights into the composition of organic matter in the studied area and warrant further investigation to understand its implications in the ecosystem.

Acknowledgements

The authors acknowledge the Brazilian National Research Council (CNPq grant no. 126512/2022-1). The samples used for the development of this study were available due to the fact that this project is inserted in the CarbMet Project (CNPq), which is a part of the Brazilian Antarctic Program (PROANTAR). Therefore the authors also acknowledge their support.

References

[1] Rakuza-Swazczewski, S. 1980. Environmental conditions and functioning of Admiralty Bay (South Shetland Islands) as part of the Nearshore Antarctic Ecosystem. Polish Polar Research, 1: 11-27.

[2] Lipski, M. 1987. Variations of physical conditions, nutrients and chlorophyll a contents in Admiralty Bay (King George Island, South Shetland Islands, 1979). Polish Polar Research, 8(4): 307-332.

[3] Brandini, F. P. & Rebello, J. 1994. Wind field effect on hydrograph and chlorophyll dynamics in the coastal pelagial of Admiralty Bay, King George Island, Antarctica. Antarctic Science, 6(4): 433-442.

[4] Dubois, M.; Gilles, K.; Hamilton, J. K.; Rebers, P. A.; Smith, F. 1956. Colorimetric method for determination of sugars and related substances. Anal. Chem. 28: 350-356.

[5] Gerchacov, S. M. & Hatcher, P. G. 1972. Improved technique for analysis of carbohydrates in the sediment. Limnology and Oceanography. 17, 938-943.

[6] Hartree, E. F. 1972. Determination of proteins: a modification of the Lowry method that give a linear photometric response. Analytical Biochemistry. 48: 422-427.

[7] Rice, D. L. 1982. The detritus nitrogen problem: new observations and perspectives from organic geochemistry. Marine Ecology Progress Series. 9: 153-162.

[8] Golterman, H. L.; Clymo, R. S.; Ohnstad, M. A. M. 1978. Methods of Physical and Chemical Analysis of Fresh Waters. Blackwell Scientific Publications, Oxford, 214 p.

[9] Lorenzen, C. J. 1967. Determination of chlorophyll and pheo-pigments: spectrophotometric equations. Limnology and Oceanography, 12, 343–346.

XVI LATIN AMERICAN CONGRESS ON ORGANIC GEOCHEMISTRY
9 - 11 AUGUST, 2023
ARACAJU, SERGIPE, BRAZIL

BIODEGRADATION OF THE SPILLED OIL ON THE BRAZIL'S NORTHEAST COAST OVER TIME (2019-2021) ASSESSED BY HIGH-RESOLUTION TECHNIQUES

Laercio L. Martins[a,b,*], Bárbara D. Lima[a], Vinícius B. Pereira[c], Danielle M.M. Franco[d], Ignes R. dos Santos[e], Jandyson M. Santos[e], Boniek G. Vaz[d], Débora A. Azevedo[c], Georgiana F. da Cruz[a]

[a]Universidade Estadual do Norte Fluminense Darcy Ribeiro (UENF); [b]Universidade Federal do Ceará (UFC); [c]Universidade Federal do Rio de Janeiro (UFRJ); [d]Universidade Federal de Goiás (UFG); [e]Universidade Federal Rural de Pernambuco (UFRPE)

*laercio@lenep.uenf.br

Introduction

The oil spill that reached the Brazilian coast in 2019 is the largest and most severe environmental disaster ever recorded in the history of Brazil, which recorded thousands of tons of crude oil contaminating more than 980 beaches and affecting several marine ecosystems. More than a year and a half after the first appearance, spill oil samples still appeared on the beaches of Brazil [1]. In this context, the aim of this study is to assess the biodegradation extension and its effects in two spill oil samples collected on beaches in the Northeast of Brazil, in 2019 and 2021, through acid profiles assessed by GCxGC-TOF MS and ESI(-) FT-ICR MS.

Experimental

Two spilled oil samples, one collected in 2019 and one collected in 2021 at Gaibu and Itapuama beach, respectively, at the State of Pernambuco, Brazil, were submitted to Soxhlet-extraction with dichloromethane as the solvent, for a period of 12h. After this process, the samples were subjected to asphaltene precipitation using mixing 20 µL of dichloromethane with 2 mL of *n*-hexane in 0.05 g of oil and the solution was submitted to an ultrasonic bath for 10 min. The solvent was dried and maltene fraction was carried out to liquid chromatography using a column with activated silica gel and hexane, hexane:dichloromethane (4:1 v/v), and dichloromethane:methanol (9:1 v/v) as eluents to fraction the extract into saturated, aromatic, and polar compounds, respectively. The polar compounds were fractionated to obtain a carboxylic acid enriched fraction, which was derivatized using BF_3/MeOH 14%. Firstly, the saturated fraction was assessed by GC-FID and GC-MS, and the aromatic fraction was assessed by GC-MS. Then, applying high-resolution techniques, the acid fraction was analyzed by GCxGC-TOF MS, and a whole oil sample was analyzed by ESI(-) FT-ICR MS to assess acid compounds.

Results and Discussion

Diagnostic ratios based on terpane, steranes, tetracyclic polyprenoids, and triaromatic steroids, which are resistant to weathering effects, were similar to the Gaibu and Itapuama oil samples, pointing out the same source for both spilled oils. However, the less resistant hydrocarbon compounds, such as *n*-alkanes, isoprenoids, and *n*-alkylcyclohexanes, were highly affected by the process of evaporation, photooxidation, and mostly biodegradation (details in [1]).

From the ES(-) FT-ICR MS results, there was an increase in the abundance of classes with more than two oxygens ($O_{x>2}$; $SO_{x>2}$), such as O_2, O_3, O_4, O_5, SO_2, SO_3, SO_4, SO_5, and SO_6 (), while the N class and other classes with only one oxygen (e.g., O and SO classes) decreased when comparing the samples collected in 2019 and 2021 (**Figure 1a**). These results indicate biodegradation affecting the spilled oil since this process generates carboxylic acids. Based on that, three new ratios are suggested to assess this microbial process over oil spill time: $O_{x>2}$/O, SO_x/SO, and SO_x/N. These ratios increase with the progression of biodegradation (**Figure 1b**).

In addition, there was an increase in the abundance of DBE 2 (monocyclic acids), 3 (bicyclic acids), 4 (tricyclic acids), 5 (tetracyclic and monoaromatic acids), and 6 (pentacyclic and monoaromatic acids) of O_2 class over time, which is characteristic of the microbial degradation process of hydrocarbons. These results are highlighted by diminishing the A/C and modified A/C ratios and the rising of the modified SA index (**Figure 1c**) over time. Furthermore, the increasing predominance of even-to-odd preference for acyclic oxygenated species suggests a biological contribution [2]. Previous works showed that linear fatty acids with a preference for even-to-odd can be

a result of the biodegradation of hydrocarbons by anaerobic microorganisms [3].

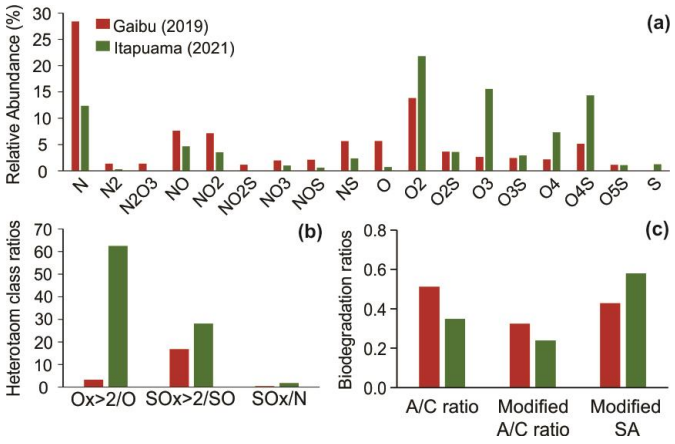

Figure 1. (a) Heteroatom class distribution obtained by ESI(-) FT-ICR MS; (b) Variation of the new heteroatom class ratios proposed to assess biodegradation; (c) Variation of the biodegradation parameters A/C ratio, modified A/C ratio, and modified SA index for the oil samples collected in 2019 (at Gaibu Beach) and 2021 (at Itapuama Beach).

According to GCxGC TOF MS results, both spilled oils are enriched in monocarboxylic acids, with a contribution of oxo-carboxylic and dicarboxylic acids. Based on the distribution of carboxylic acids obtained by GC×GC, ratios were calculated to assess the distribution of this class (**Figure 2a** and **b**). UC16/C16 and UC18/C18 were calculated to evaluate the weathering through time. Both ratios varied greatly over time, suggesting a considerable advance in biodegradation since works show that unsaturated carboxylic acids are found in biodegraded oils, and their concentration increases as biodegradation enhances [4].

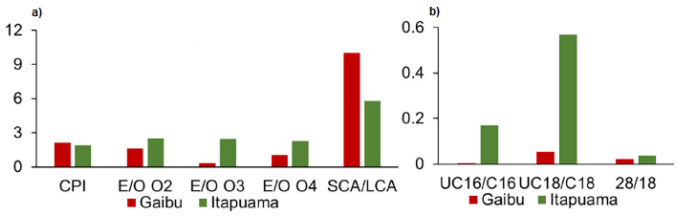

Figure 2. Ratios applied for carboxylic acids detected by GC×GC of the spilled oils collected at Gaibu and Itapuama beaches. CPI (carbon preference index): 2 × (C28/C27 + C29); E/O: even/odd carboxylic acids of monocarboxylic acids (O_2 class), oxo-carboxylic acids (O_3 class), and dicarboxylic acids (O_4 class); SCA/LCA: ratio between short-chain carboxylic acids and long-chain carboxylic acids; UC16/C16: unsaturated hexadecanoic acid/saturated hexadecanoic acid; UC18/C18: unsaturated octadecanoic acid/octadecanoic acid; 28/18: C28/C18 acids ratio.

E/O ratios for the identified classes (O_2, O_3, and O_4) showed a preference for even carboxylic acids over odd ones, with an increasing tendency from 2019 to 2021, which was also observed in results obtained by FT-ICR MS. Furthermore, SCA/LCA showed a decreasing tendency from 2019 to 2021, and the 28/18 ratio increased, indicating that the contribution of LCA increased over 1.5 years. This is consistent with evidence that extensive biodegradation of hydrocarbons increases the concentration of higher molecular weight (>C20) carboxylic acids over time [5].

Conclusions

We conclude that biodegradation was an effective weathering process on the spilled oils on Brazilian beaches over 1.5 years (2019-2021). High-resolution techniques showed the increase of acid compounds with two or more oxygens. By ESI(-) FT-ICR MS, it was suggested three new ratios using heteroatom classes to evaluate the progress of the biodegradation process over time: $O_{x>2}/O$, SO_x/SO, and SO_x/N ratios. The results from the GC×GC-TOFMS show a higher abundance of mono- and dicarboxylic acids in the oil sampled in 2021 than in the oil collected in 2019, corroborating the biodegradation as an important weathering process that changes the chemical composition of the oil. The broad chemical evaluation by high-resolution techniques presented herein can offer powerful tools for better understanding the chemical composition changes that beached spilled oil undergoes due to the biodegradation process.

Acknowledgements

The authors thank Capes (Finance code 001), FAPERJ, PRH-ANP and FACEPE for grants and financial support.

References

[1] Lima, B.D., Martins, L.L., Pereira, V.B., Franco, D.M.M., Santos, I.R., Santos, J.M., Vaz, B.G., Azevedo, D.A., Cruz, G.F., 2023. Weathering impacts on petroleum biomarker, aromatic, and polar compounds in the spilled oil at the northeast coast of Brazil over time. Marine Pollution Bulletin 189, 114744.

[2] Cheung, S.G., Wai, H.Y., Shin, P.K.S., 2010. Fatty acid profiles of benthic environment associated with artificial reefs in subtropical Hong Kong. Marine Pollution Bulletin 60, 303–308.

[3] Da Cruz, G.F., Marsaioli, A.J., 2012. Natural processes of petroleum biodegradation in reservoirs. Química Nova 35, 1628–1634.

[4] Jaffé, R., Gallardo, M.T., 1993. Application of carboxylic acid biomarkers as indicators of biodegradation and migration of crude oils from the Maracaibo Basin, Western Venezuela. Organic Geochemistry 20, 973–984.

[5] Kristensen, M., Johnsen, A.R., Christensen, J.H., 2021. Super-complex mixtures of aliphatic- and aromatic acids may be common degradation products after marine oil spills: A lab-study of microbial oil degradation in a warm, pre-exposed marine environment. Environmental Pollution 285, 117264.

XVI LATIN AMERICAN CONGRESS ON ORGANIC GEOCHEMISTRY
9 - 11 AUGUST, 2023
ARACAJU, SERGIPE, BRAZIL

Higher PCBs concentrations in suspended particulate matter of Admiralty Bay, Antarctica Peninsula, in the late summer of 2023

AMANDA CÂMARA DE SOUZA[a,*] / JOSILENE DA SILVA[a] / SATIE TANIGUCHI[a] / TATIANE COMBI[b] / CÉSAR DE CASTRO MARTINS[a,c] / RAFAEL ANDRÉ LOURENÇO[a]

[a]INSTITUTO OCEANOGRÁFICO, UNIVERSIDADE DE SÃO PAULO, BRASIL; [b]DEPARTAMENTO DE OCEANOGRAFIA, UNIVERSIDADE FEDERAL DA BAHIA, BRASIL; [c]CENTRO DE ESTUDOS DO MAR, UNIVERSIDADE FEDERAL DO PARANÁ, BRASIL

*amandacamaradesouza@gmail.com

Introduction

Polychlorinated biphenyls (PCBs) are Persistent Organic Pollutants with historical use in industrial and urban activities. Despite the worldwide restrictions, they are still detected in several environmental compartments, even in areas where they have never been produced, such as Antarctica [1]. Coastal regions of Antarctica experience abrupt climatic variations during the austral summer, characterized by a rise in temperature and glacier melting. This results in an increase in freshwater and suspended particulate matter (SPM) which carries organic matter, contaminants, and nutrients to the marine environment [2]. Thus, this study aimed to determine the concentrations of PCBs in the water column of Admiralty Bay, located on King George Island, Antarctic Peninsula, in a short time scale perspective (during late spring to late summer), to understand how these pollutants vary with the gradual increase in temperature in this period.

Sampling and PCBs determination

Sampling was performed in five campaigns during the 2022/2023 summer at 16 sites in Admiralty Bay (Fig. 1).

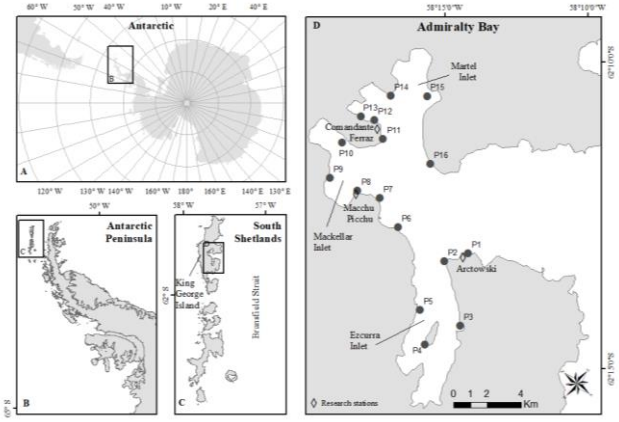

Figure 1. Map of the location of the study area showing the sampling sites of Admiralty Bay, Antarctica Peninsula.

Approximately 20 L of surface water was vacuum filtered through GF/F Whatman® (0.7 µm) filters to obtain the SPM. Samples were extracted in Soxhlet apparatus. Total PCBs ($\sum_{51}$PCBs) identification and quantification were performed using an Agilent gas chromatograph model 7890B coupled to an Agilent triple quadrupole TQMS model 7010B operating in multiple reaction monitoring.

Results and Discussion

PCBs contents in SPM from Admiralty Bay varied from 2.64 to 78.15 ng g^{-1} (26.03 ± 19.37 ng g^{-1}). These values are higher than the detected in sediments of the bay (<DL to 2.92 ng g^{-1}) [1]. Higher contents of organic pollutants and molecular markers in SPM relative to sediments also was detected in a subtropical estuary [3-4].

The campaigns of November and December 2022 were statistically different from the campaigns of January to March 2023 (Kruskal-Wallis non-parametric test and Dunn's post hoc test; $p < 0.01$). PCBs concentrations were higher in the last campaigns (Fig. 2), coinciding with the increase of the freshwater input related to the warmer temperatures in the late summer, represented by the rise in sea surface temperature during the five campaigns (Fig. 3).

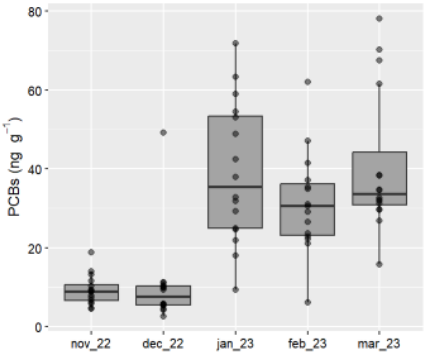

Figure 2. Boxplot distribution of total PCBs in SPM samples of Admiralty Bay, Antarctica Peninsula in the 2022/2023 summer campaigns.

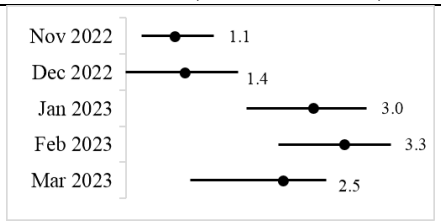

Figure 3. Minimum, maximum, and mean surface temperatures (°C) of the 16 sites detected in the 2022/2023 summer campaigns.

Casal et al. [2] also detected increasing organic pollutants values in the water column of another coastal region of the Antarctica Peninsula. In general, PCBs presented higher concentrations in all 16 sites in the last three campaigns (Fig. 4).

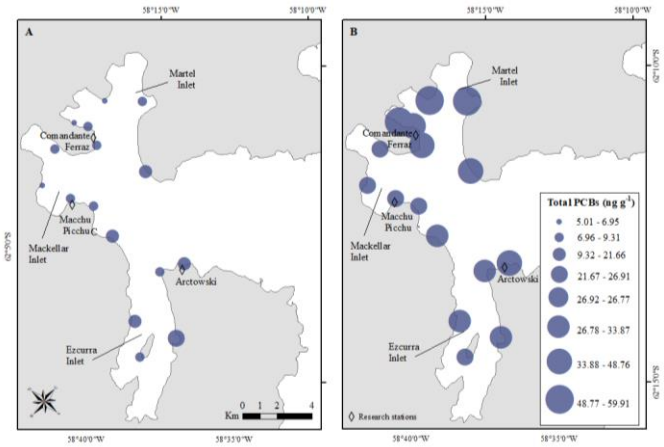

Figure 4. Total PCBs distribution in SPM of the Admiralty Bay, Antarctica Peninsula. A: mean values of the November and December 2022 campaigns. B: mean values of January to March 2023 campaigns.

Spatially, the higher values were detected near the Comandante Ferraz and Arctowski research stations. Historically these regions have experienced the highest human occupation of Admiralty Bay and where the highest contributions of high-chlorinated PCBs (penta- and hexa-CBs) were detected (Fig. 5), which suggests a local source input for these sites.

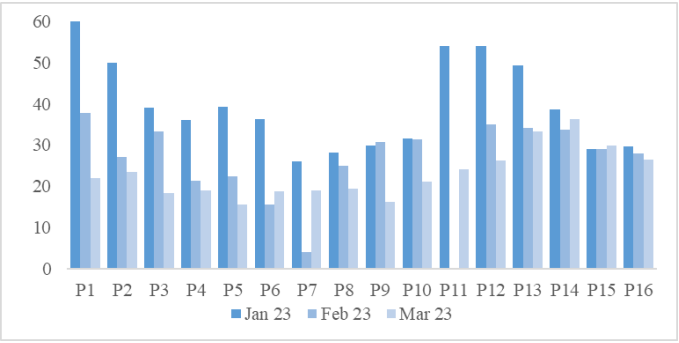

Figure 5. % of high-chlorinated PCBs in the 16 sites detected in the 2023 summer campaigns.

Conclusions

Despite the distance from large urban centers, the Antarctica environment is not exempt from the input of contaminants related to human activities. The detection of PCBs in SPM is a risk to vulnerable and endemic species from Antarctica once they become available to primary producers and, consequently, other marine organisms when present in the water column.

This study contributed to the scientific basis for the understanding of PCBs cycles in marine environments, as data on PCBs in SPM are still scarce. Considering that the Antarctica continent has been facing accelerated warming in recent decades, the increase of PCBs with temperature in this short period can contribute to understanding the possible effects of global climate changes on a local scale.

Acknowledgments

The authors thank CNPQ, MCTI, SECIRM, and PROANTAR for providing financial and logistical support to the CARBMET project (The multiple faces of organic carbon and metals in the sub-Antarctic ecosystem: space-time variability, connections with environmental factors and the transfer between compartments - Edital CNPq/MCTIC/CAPES/FNDCT – N° 21/2018). A.C. Souza thanks FAPESP (2020/15701-8) for the Ph.D. Scholarship.

References

1. Combi, T., Martins, C.C., Taniguchi, S., Leonel, J., Lourenço, R.A., Montone, R.C., 2017. Depositional history and inventories of polychlorinated biphenyls (PCBs) in sediment cores from an Antarctic Specially Managed Area (Admiralty Bay, King George Island). Marine Pollution Bulletin 118, 447–451.

2. Casal, P., Cabrerizo, A., Vila-Costa, M., Pizarro, M., Jiménez, B., Dachs, J., 2018. Pivotal Role of Snow Deposition and Melting Driving Fluxes of Polycyclic Aromatic Hydrocarbons at Coastal Livingston Island (Antarctica). Environmental Science and Technology 52, 12327–12337.

3. Cabral, A.C., Stark, J.S., Kolm, H.E., Martins, C.C., 2018. An integrated evaluation of some fecal indicator bacteria (FIB) and chemical markers as potential tools for monitoring sewage contamination in subtropical estuaries. Environmental Pollution 235, 739–749.

4. Cardoso, F.D., Dauner, A.L.L., Martins, C.C., 2016. A critical and comparative appraisal of polycyclic aromatic hydrocarbons in sediments and suspended particulate material from a large South American subtropical estuary. Environmental Pollution 214, 219–229.

XVI LATIN AMERICAN CONGRESS ON ORGANIC GEOCHEMISTRY
9 - 11 AUGUST, 2023
ARACAJU, SERGIPE, BRAZIL

EVIDÊNCIA DE MUDANÇAS AMBIENTAIS POR MEIO DE PIGMENTOS FOTOSSINTETIZANTES SEDIMENTARES

EVIDENCE OF ECOSYSTEMS CHANGES USING SEDIMENTARY PHOTOSYNTHETIC PIGMENTS

SHEILA CARDOSO-SILVA*[1]/ OLGA KRAMER[2]/ MARCELO POMPÊO[3]/ RUBENS CÉSAR LOPES FIGUEIRA[4], VIVIANE MOSCHINI-CARLOS[1], EDUARDO VICENTE[2]

[1] UNESP Postdoctoral Program PROPE, Institute of Science and Technology, State University of Sao Paulo (UNESP), Sorocaba, SP, Brazil

[2] Department of Microbiology and Ecology, University of Valencia, Valencia, Spain

[3] Ecology Department, Biosciences Institute, University of São Paulo (USP), São Paulo, SP, Brazil

[4] Oceanographic Institute, University of São Paulo (USP), São Paulo, SP, Brazil

*correspondência: e-mail: she.cardosos@gmail.com

Introduction

Paleolimnological studies focused on trophic state reconstruction present better results when associating a biological component to the analysis. This is because the levels of P, a key element in eutrophication, can be released to the water column and do not predict properly the water body trophy. Among the biological proxies, photosynthetic pigments have the advantage over diatoms, as they do not require microscopy analysis, which is time-consuming and requires a broad domain of taxonomy. In the tropics, few studies focus on the analysis of pigments in reservoir sediments [1, 2]. Higher temperatures and faster metabolism in these areas can make it difficult to preserve pigments [3]. In addition, the complex sedimentation patterns of the reservoirs make it difficult to use the paleolimnological approach. The objective of this work is to investigate the temporal heterogeneity of chlorophyll-a and pheopigment contents, indicators of algal biomass, in sedimentary profiles of three reservoirs in the state of São Paulo/Brazil. These data will shed light to better discuss the history of eutrophication.

Experimental

Sedimentary profiles were sampled in two areas of the Barra Bonita reservoir (BB) located in the Middle Tietê Basin (SP/ Brazil). An area under the influence of the incoming waters of the Piracicaba River (BB-Pir -22,6016 -48,3028) and another with the influence of the waters of the Tietê River (BB-Ti -22,6692 -48,3374) (November 2022). And in an area in the cascade reservoirs Jaguari (JG- -46.4356875 -22.9716) and Jacareí (JC- -46.4156088 -22.9167), belonging to the Cantareira System (located in the Piracicaba basin-SP/Brazil) (December 2022). Three cores were collected at each sampling point, which were sliced at 2 cm intervals. The sediments were evaluated for the presence of organic matter by the ignition method (460°C -6 hours). The extraction of pigments occurred according to Lorenzen's recommendations [4]. A solution of 50% acetone 90%-DM50 was used as solvent, so that there was disruption of cells and release of photopigments. Three extractions were performed with the addition of 3 and 2 ml of solvent to ~ 0.2 g of sediment. The extract was used to read the levels of chlorophyll-a and pheophytin in spectrophotometry. For pheophytin analysis, 2 drops of 1N HCL were added to the sample used to chlorophyll-a analysis in a spectrophotometric method (Ultraviolet-visible-UV-vis, Varian. Cary 4000). The entire procedure was performed under low light conditions.

Results and Discussion

The absorbance ratios of 430:410 nm indicate the level of preservation of pigments. Thus, the closer to 1, the better the preservation [5]. The average values for the 430:410 nm ratio in the reservoirs were: BB- Pir 0.78 ± 0.05; BB Ti 0.83 ± 0.04; JG 0.95 ± 0.08 e JC 0.86 ± 0.08 indicating, therefore, a good preservation. The sediments were classified as organic with organic

matters contents greater than 10%: JG 14.28 ± 2.96%; JC 15.44 ± 4.05%; BBPir 16.87 ± 2,65%; BBTi 12.96 ± 4.86%. Chlorophyll-a contents were lower than those of pheophytin (Fig. 1 and 2) at all sampled points. This result is expected since chlorophyll is a pigment that tends to be easily degraded [2] and pheophytin is the product of this degradation.

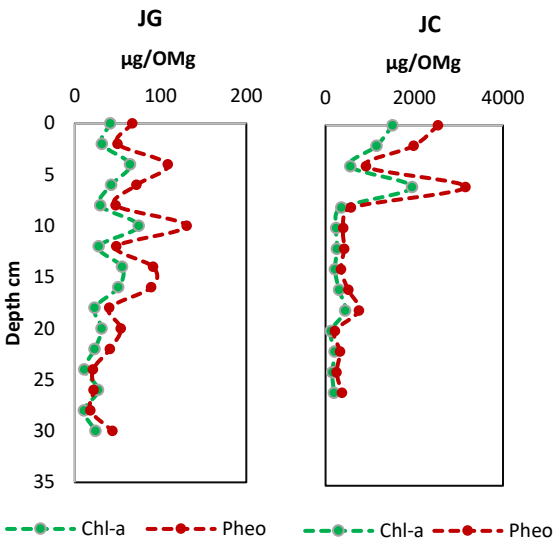

Figure 1. Sedimentary profiles of chlorophyll-a and feoftin levels in Jaguari (JG) and Jacareí (JC) reservoirs.

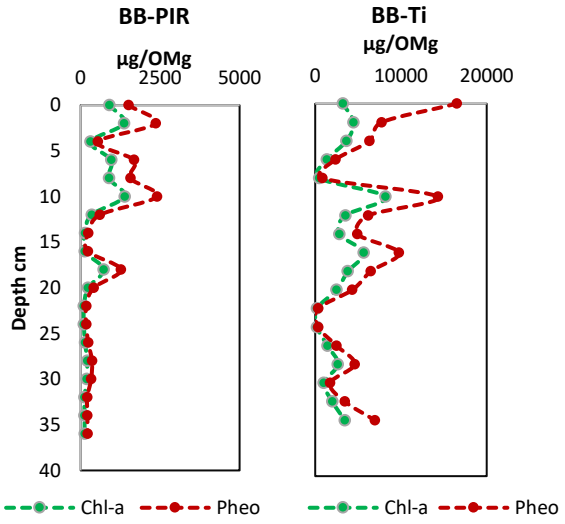

Figure 2. Sedimentary profiles of chlorophyll-a and feoftin levels in Barra Bonita reservoir.

Kruskal Wallis test with a significance level of 0.05 shows that there are significant differences for chlorophyll-a and pheophytin contents among all sampled points. Algal biomass tends to be higher in the BB reservoir compared to JC and JG, thus suggesting a higher primary productivity in BB (Fig. 2). In JC and in both points sampled in BB, a more accentuated increase in chlorophyll-a and pheophytin contents is observed (Figs 1 and 2), in the upper layers, suggesting an increase in eutrophication over time. The results in JG and JC oppose the theory of cascade reservoirs where it is expected that the upstream reservoirs present a lower trophy [6]. The lower percentage of forest cover present in the Jacareí basin may make the area more susceptible to anthropic uses, favouring a greater supply of nutrients. The BB Reservoir under the influence of the Tietê River tends to present higher trophic conditions than in BB-Pir.

Conclusions

Partial results show a clear tendency of increase in pigment contents. This increase is associated with the increase eutrophication in the BB and Jacareí watersheds due to low due to low coverage in effluent treatment and use of fertilizers. The geocronology and sedimentation rates as well as the analysis of carotenoid pigments, C, N and P will provide more information for the reconstitution of the trophy in these environments.

Acknowledgements

The authors are grateful to the University of Valencia, to the UNESP Postdoctoral Program PROPE-ICTS, to the Ecology Department of the Institute of Biosciences and The Institute of Oceanography, at the University of São Paulo. Financial support for this work was provided by FAPESP (Fundação de Amparo à Pesquisa do Estado de São Paulo 21/11283-0, and 21/10637-2 and UNESP Projet 4443).

.

References

[1] Halac, S.; Mengo, L.; Guerra, L.; et al. 2020 Paleolimnological reconstruction of the centennial eutrophication processes in a sub-tropical South American reservoir. J S Am Earth Sci **103**:102707

[2] Cardoso-Silva, S.; Mizael, J. S. S.; et al. 2022. Geochemistry and sedimentary photopigments as proxies to reconstruct past environmental changes in a subtropical reservoir. Environ. Sci. Pollut. Res., **29**, 1.

[3] Buchaca, T.; Kosten, S.; Lacerot, G.; et al. 2019. Pigments in surface sediments of South American shallow lakes as an integrative proxy for primary producers and their drivers. Freshw Biol **64** (8),1437–1452

[4] Lorenzen C.J. 1967. Determination of chlorophyll and phaeopigments spectrophotometric equations. Limnol Oceanogr **12,** 343–347.

[5] Lami, A., Musazzi, S., Marchetto, A., et al., 2009. Sedimentary pigments in 308 alpine lakes and their relation to environmental gradients. Adv. Limnol. 62, 217–238.

[6] Pompêo, M.; Moschini-Carlos V, Lopez-Doval JC, et al. 2017. Nitrogen and phosphorus in cascade multisystem tropical reservoirs: water and sediment. Limnol Rev **17**(3),133–150.

HETEROGENEIDADE ESPACIAL E TEMPORAL EM UM MULTISSISTEMA DE RESERVATÓRIOS EM CASCATA

SPATIAL AND TEMPORAL HETEROGENEITY IN CASCADE MULTISYSTEM RESERVOIRS

SHEILA CARDOSO-SILVA* [1]/ TAILISI HOPPE TREVIZANI[2] / RUBENS CÉSAR LOPES FIGUEIRA[2] / MARCELO POMPÊO[3]/ VIVIANE MOSCHINI-CARLOS[1]

[1] UNESP Postdoctoral Program PROPE, Institute of Science and Technology, State University of Sao Paulo (UNESP), Sorocaba, SP, Brazil

[2] Oceanographic Institute, University of São Paulo (USP), São Paulo, SP, Brazil

[3] Ecology Department, Biosciences Institute, University of São Paulo (USP), São Paulo, SP, Brazil

* correspondência: e-mail: she.cardosos@gmail.com

Introduction

The ecological theory of cascade reservoirs (interconnected reservoirs constructed along the same river) predicts that element contents, such as those related to the eutrophication process, tend to decrease towards the reservoirs located downstream [1]. In this study, we seek to understand whether the theory also applies to cascade multisystem reservoirs (interconnected reservoirs that have origins in different rivers) and to establish the historical trends in metal contamination and eutrophication through a paleolimnological perspective. The extent of contamination was also assessed applying criteria such as enrichment factor (EF) and sediment quality guidelines (SQGs). This research contributes to improving understanding of the dynamics of metals, total Phosphorus (TP) and pigments in cascade multisystem reservoirs, which to date has been insufficiently studied.

Experimental

Surface and core sediments were sampled in the cascade reservoirs Jaguari (JG) and Jacareí (JC) (Cantareira System, Piracicaba basin- SP/Brazil) (December 2022). Surface sediments were sampled in triplicates, in an area of ~2.5 km nearby the dam zone of the reservoirs. Three cores were collected at each sampling point in Jaguari (JG: -46.4356875 -22.9716) and Jacareí (JC: -46.4156088 -22.9167) and were sliced at 2 cm intervals. The sediments were evaluated for the presence of Cr, Cu, Ni, Pb, Zn, Al, Fe, K, Mn, V and Ti, and TP through a partial digestion [2] and analysed by ICP-OES. Chl-a and Pheo were extracted according to Lorenzen's recommendations [3]. A solution of 50% acetone 90%-DM50 was used as solvent. The extract was used to read the levels of pigments in a spectrophotometric method (Ultraviolet-visible-UV-vis, Varian. Cary 4000). Data were evaluate using descriptive statistical and Principal Component Analysis (PCA). Enrichment factor [4] and 'The empirical Sediment Quality Guideline' (SQG) (CCME 2001), TEL (Threshold Effect Level) or ISQG (Interim Sediment Quality Guideline) and PEL (Probable Effect Level) were applied. In the SQG model, for each contaminant there is a range of values, where above a given concentration (PEL), a toxic effect is likely to occur, while below a given value, TEL effects are unlikely. Values between TEL/ISQG and PEL, the effects are uncertain [5].

Results and Discussion

Surface sediments

Mean values for most metals in surface sediments were higher in Jaguari than Jacareí reservoir, according to the cascade reservoir theory (Pompeo et al, 2018). On the other hand, Chl-a and Pheo concentrations were higher in Jacareí reservoir (JG: Chl-a 45.99 ± 51.15 µg/g and Pheo 78.51 ± 86.11 µg/g; and JC: Chl-a 75.66 ± 74.41 µg/g and Pheo 130.6 ± 128.51 µg/g). No enrichment (EF < 2) was observed, and values were lower than ISQG, indicating toxicity is unlikely to occur. In the PCA (Fig. 1), the two principal components (PC) explained 60.52% of the total variability of data.

The PC 1 influenced the distribution of the JG samples and the concentrations of Cr (0.800), Ni (0.791) and Pb (0.855); elements of ecotoxicological interest that were mainly from geological sources.

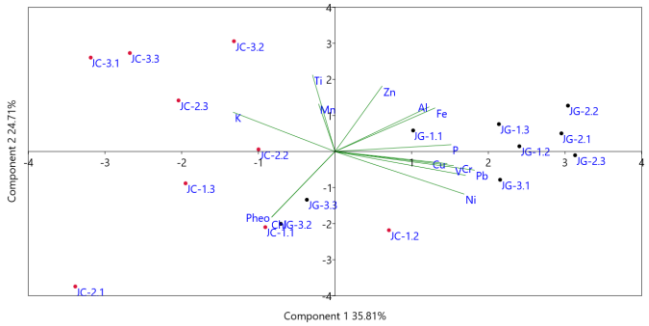

Figure 1. PCA for metals, TP, Chl-a and Pheo in surface sediments sampled in the Jaguari (black) and Jacareí (red) reservoirs (SP-Brazil).

The PC2 was influenced by Chl-a (-0.710) and pheophytin (-0.710) concentrations, suggesting the presence of a higher algal biomass in JC reservoir and one sample in JG. Therefore, the PCA suggested a clear separation of the JC and JG reservoirs. The JG with higher metal concentrations and the JC with higher algal biomass.

Core samples

In the sampled cores EF was < 2 indicating the absence or minimal enrichment of metals. The metals values were below the ISQG. In the PCA the PC1 and PC2 explained 58.98% of the total data variability.

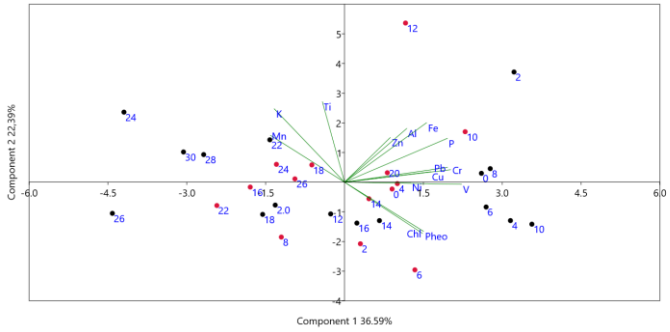

Figure 2. PCA for metals, TP, Chl-a and Pheo in sediments of a core sampled in the Jaguari (black) and Jacareí (red) reservoirs (SP-Brazil), numbers indicate the sample depth (cm).

The PC1 influenced the arrangement of the upper layers of both reservoirs, the variables responsible for the result were the contents of Cr (0,792), V (0.866), Pb (0.743) and P (0.745). The PC2 was influenced by the concentrations of major elements and of terrigenous origin like K (0.748) and Ti (0.830), responsible for arranging samples from the lower layers in JG and JC; and by the Chl-a (-0.529) and Pheo (-0.510) contents, also responsible for the arrangement of the upper layers. The PCA shows, therefore, that despite the evidence of a very low or absent enrichment for metals of toxicological interest (eg. Cr, Cu, Ni, Pb, Zn), these elements tend to present higher values in the upper layers of the sedimentary profiles. Also, TP and the pigments indicative of algal biomass tended to show higher values in the most recent layers. These data are suggestive of an increase in the eutrophication process.

Conclusions

The metal concentration in JG and JC are in accordance with the theory of cascade reservoirs except for the Chl-a and Pheo. The highest levels for these pigments were recorded in the downstream reservoir. The lower percentage of forest cover present in the Jacareí basin may make the area more susceptible to anthropic uses, favouring a greater supply of nutrients. Despite the good condition of the reservoir for metals, the data draw attention to the increase in elements especially in algal biomass over time, indicating an increase in pressures in the watershed of the reservoirs.

Acknowledgements

The authors are grateful to the University of Valencia, to the UNESP Postdoctoral Program PROPE-ICTS, to the Ecology Department of the Institute of Biosciences and The Institute of Oceanography, at the University of São Paulo. Financial support for this work was provided by FAPESP (Fundação de Amparo à Pesquisa do Estado de São Paulo 21/11283-0, and 21/10637-2 and UNESP Projet 4443).

References

[1] Pompêo, M.; Moschini-Carlos V, Lopez-Doval JC, et al. 2017. Nitrogen and phosphorus in cascade multisystem tropical reservoirs: water and sediment. Limnol Rev **17**(3),133–150.

[2] US EPA United States Environmental Protection Agency.1996. Method 3050B. Acid digestion of sediments, sludges and soil. Revision 2. December.

[3] Lorenzen C.J. 1967. Determination of chlorophyll and phaeopigments spectrophotometric equations. Limnol Oceanogr **12,** 343–347.

[4] Sutherland, R.A. 2000 Bed sediment-associated trace metals in an urban stream, Oahu, Hawaii. Environ Geol **39**(6):611-627.

[5] CCME. 2001. Canadian Sediment Quality Guidelines for the Protection of Aquatic Life - Protocol for the derivation of Canadian Sediment Quality Guidelines for the Protection of Aquatic Life (CCME EPC-98E). 35 p.

ASSINATURA MOLECULAR DA VEGETAÇÃO DE MANGUEZAL LOCALIZADA SOB DIFERENTES CONDIÇÕES CLIMÁTICAS E PRESSÕES ANTROPOGÊNICAS

Mylena Dias Diniz [a*], Samires Moura Malaquias Pinheiro [a], Ana Cecília Rizzatti de Albergaria Barbosa [a]

*e-mail: mylenadiasdiniz@gmail.com

a. Laboratório de Geoquímica Marinha e LEPETRO, Instituto de Geociência, Universidade Federal da Bahia

Introdução

Os manguezais fornecem uma infinidade de bens e serviços, e um desses está ligado com a sua grande capacidade de armazenamento de matéria orgânica (MO) alóctone e autóctone em seus sedimentos[1]. O estudo dessa MO é uma ferramenta importante na compreensão dos processos biogeoquímicos e das mudanças naturais/antrópicas que ocorrem nesses ecossistemas. Para esta investigação, pode-se usar os *n*-alcanos, que são marcadores orgânicos que possuem alta estabilidade físico-química e uma grande variedade estrutural das suas moléculas, apresentando fontes variadas e específicas[2]. No entanto, as condições bioquímicas da vegetação e as características ambientais da região onde essa está localizada podem influenciar na proporção dos compostos produzidos. Assim, este estudo objetiva identificar se há mudanças na composição dos *n*-alcanos presentes nas folhas de três gêneros típicos de vegetação de manguezal, no intuito de observar se há diferenças entre os compostos produzidos pela vegetação coletada em diferentes regiões, com distintos graus de antropização e em períodos com diferentes características climáticas.

Materiais e métodos

As amostras de folhas foram coletadas em manguezais preservados e impactados do estado do Maranhão e São Paulo. Na Bahia, foram coletadas apenas na área preservada (Figura 1). Foram analisada 30 amostras de folhas, onde os *n*-alcanos foram extraídos através do uso de um ultrassom e quantificados por meio de um cromatógrafo a gás acoplado a um detector de ionização de chamas. Foram avaliados também o teor de carbono orgânico total (COT), de nitrogênio total (NT), o $\delta^{13}C$ e $\delta^{15}N$ das folhas. Para este fim, as alíquotas foram submetidas a análise elementar e isotópica em um analisador elementar acoplado a um detector de espectrometria de massa de razão isotópica (EA-IRMS) (modelo Costech Instruments Elemental System e Thermo Finnigan Delta Plus, respectivamente).

Figura 1. Localização das áreas amostradas no presente estudo

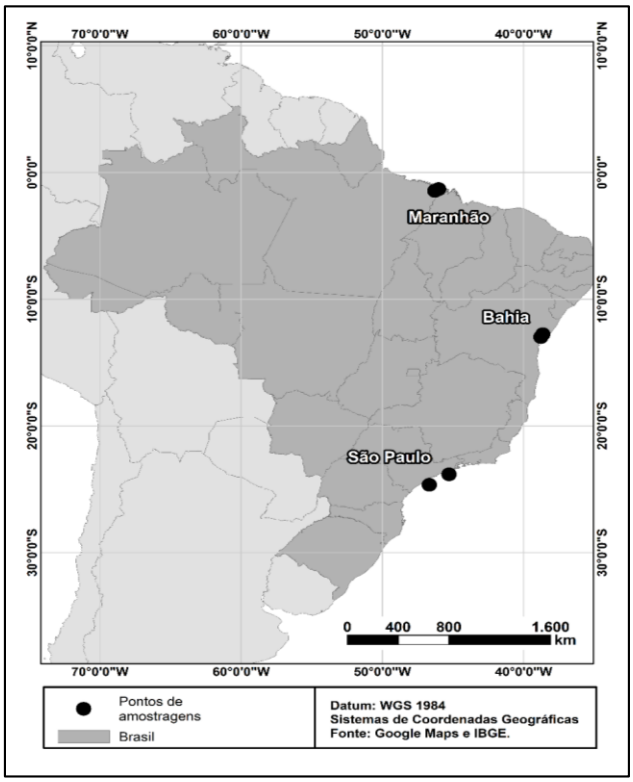

Resultados e Discussão

Os valores de COT, NT, $\delta^{13}C$ e $\delta^{15}N$ variaram respectivamente de 10,7 a 65,7%, 0,14 a 4,79%, -39 a -24‰ e -4,9 a 7,0‰. Não houve variações significativas entre os diferentes gêneros amostrados e nem entre as

áreas impactadas e preservadas do Maranhão e São Paulo. Considerando os *n*-alcanos individualmente, *Avicennia* apresentou concentrações de compostos mais pesados com dominância do *n*-C_{31} e *n*-C_{33}. *Rhizophora* apresentou predominância do *n*-C_{31} e *n*-C_{29}. Em *Lagunculária*, predomínio do *n*-C_{29} e *n*-C_{27} (Figura 2).

Figura 2. Distribuição média dos *n*-alcanos encontrados nas amostras de folha dos gêneros *Rhizophora*, *Avicennia* e *Lagunculária* nas áreas do Maranhão, São Paulo e Bahia

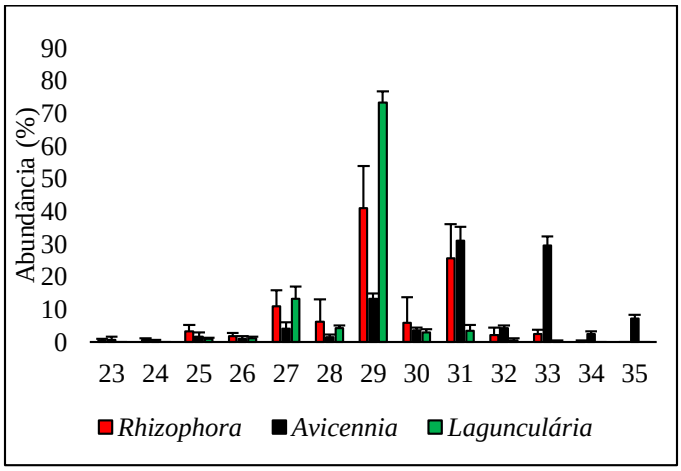

Essas diferenças foram influenciadas pelas características fisiológicas e morfológicas dos gêneros amostrados. *Avicennia* mostra-se mais tolerante à radiação solar.

Algumas razões diagnósticas foram calculadas, o Tamanho médio de cadeia (TMC_{23-33}), a razão de concentração do *n*-C_{29} sobre o *n*-C_{31} (Norm31), o índice de produção aquática (PAQ) e o IPC variaram, respectivamente, de 29 a 31, 0,01 a 0,16, 0,02 a 0,79 e 2,6, a 37. *Avicennia* exibiu valores maiores do TMC, diferenciando-se assim, dos gêneros *Rhizophora* e *Lagunculária*. Essa diferença pode indicar que apesar de crescerem nas mesmas condições, os gêneros possuem adaptações morfológicas e fisiológicas individuais já fixadas, tais com, espessamento foliar, aumento do tempo de retenção do nitrogênio e eficiência no uso da água, que faz com que elas possuam diferentes padrões de distribuição de compostos entre elas. *Avicennia* também apresentou valores de Norm31 maiores que 0,5, o que segundo a literatura indica plantas com o padrão fotossintético do tipo C_4[3]. Entretanto, ela possui o padrão do tipo C_3. Isso demonstra a importância em se estudar os padrões de distribuição de *n*-alcanos em plantas de regiões tropicais para se aplicar dados mais reais com a realidade de cada local, evitando caracterizar essas áreas de forma errônea. Em relação aos valores de PAQ, L*agunculária* apresentou diferenças significativas com Avicennia e *Rhizophora.* Essa diferença se dá, porque *Lagunculária* apresenta pouquíssima ou nenhuma concentração de compostos com cadeias médias (23 e 25), possuindo apenas predominância do C_{29} e C_{27}, cadeias mais leves quando comparada com as biossintetizadas pela *Avicennia* e a *Rhizophora*. Assim, em estudos associados aos manguezais, valores de PAQ iguais ou menores a 0,01 podem ser associadas ao gênero *Lagunculária* e valores de PAQ iguais ou maiores a 0,04 podem indicar fontes de *Avicennia* e *Rhizophora* para o ambiente. Já o IPC, não exibiu variações significativas entre os gêneros amostrados. Seus menores valores estiveram relacionados com a presença de compostos de cadeia pares no gênero *Rhizophora* na Região de Mutá, que possivelmente ocorreu devido a uma variação no início da biossíntese de ácidos graxos.

Conclusão

A composição dos *n*-alcanos difere entre os distintos gêneros de vegetação de mangue. As razões não apresentaram variações relacionadas a localização geográfica e nem aos períodos sazonais, mostrando que a composição molecular da vegetação de mangue é influenciada principalmente pelas características intraespecíficas de cada gênero. Dentre os compostos de alta massa molecular, produzidos pela vegetação superior, *Avicennia* biossintetiza maiores proporções de compostos mais pesados (*n*-C_{31} e *n*-C_{33}), enquanto *Rhizophor*a produz maiores proporções de compostos intermediários (*n*-C_{29} e *n*-C_{31}) e *Laguncularia* maiores proporções de compostos mais leves (*n*-C_{29} e *n*-C_{27}). Essas diferenças podem ser usadas na identificação dos gêneros para a matéria orgânica depositada em manguezais.

Agradecimento

O presente trabalho foi realizado com apoio da Coordenação de Aperfeiçoamento de Pessoal de Nível Superior - Brasil (CAPES) - Código de Financiamento 001.

Referências

[1] ROVAI, A. S. et al. Macroecological patterns of forest structure and allometric scaling in mangrove forests. **Global Ecology and Biogeography**, v. 30, n. 5, p. 1000-1013, 2021.

[2] VOLKMAN, John K. Lipid markers for marine organic matter. **Marine organic matter: biomarkers, isotopes and DNA**, p. 27-70, 2006.

[3] ZHANG, Z.et al. Leaf wax lipids as paleovegetational and paleoenvironmental proxies for the Chinese Loess Plateau over the last 170 kyr. **Quaternary Science Reviews**, v. 25, n. 5/6, p. 575-594, 2006.

Paleo-oxygenation of the Equatorial Atlantic using pores in benthic foraminifera over the past 30,000 years

Fernanda Pessanha Alvarenga Costa[a]; Cátia Fernandes Barbosa[b].

[a]Universidade Federal do Rio de Janeiro, Instituto de Química, Ilha do Fundão, Rio de Janeiro, RJ, 21941-909, Brazil

[b]Universidade Federal Fluminense – UFF, Instituto de Química, Valonguinho, Niterói, RJ, 24020-150, Brazil

e-mail: fpac@iq.ufrj.br

Introduction

The Western Equatorial Atlantic (AEO) comprises part of the AMOC (Atlantic Meridional Overturning Circulation), which is one of the most important components in the heat distribution of the oceans and plays an important role in regulating and maintaining the climate on the planet (ARZ, 1999). During the Heinrich Events (HE) weakening in the formation of the NADW (North Atlantic Deep Water) occurred and, consequently, disruption in the ocean circulation system. It is known that weakening of the oceanic circulation leads to a decrease in the O_2 content of the bottom waters, causing disturbance to benthic organisms (ZHANG, 2016). The distribution of foraminifera is influenced by several factors, especially the O_2 content. Studies point out that, in environments where this content is low, the tests of foraminifera tend to have larger pores and vice-versa (PETERSEN *et. al*, 2016).

Experimental

Core sample MD09-3243CQ, the object of study of this paper, was collected at 656 m depth on the slope of the Brazilian continental margin. A chronological model for the core was generated by radiocarbon dating on carbonaceous sediment and planktonic foraminifera using an Accelerator Mass Spectrometer (AMS). Analysis of the benthic foraminiferal assemblage was also carried out, using a resolution of 6 cm, totaling 34 sub-samples. They were weighed, washed, sieved and dried, then quartered and sorted, reaching at least 300 specimens with the help of a binocular magnifying glass. After the identification, at the genus level, the samples were imaged in SEM - Scanning Electron Microscope - and the data obtained were statistically treated by cluster analysis in PRIMER 6 software. Regarding the pore analysis, the system proposed by Petersen et al. (2016) was adopted and the resolution adopted was 2 cm, totaling 103 subsamples. An average of three individuals of the species *Cibicides pseudoungeriana* CUSHMAN, 1922, larger than 125 µm, were screened from each of the subsamples. In total, 348 specimens were taken to the SEM and had their penultimate chamber imaged from the dorsal side at 1000x magnification. These images were processed in ImageJ software, generating data such as number of pores, total pore area, average pore area, porosity, perimeter and circularity.

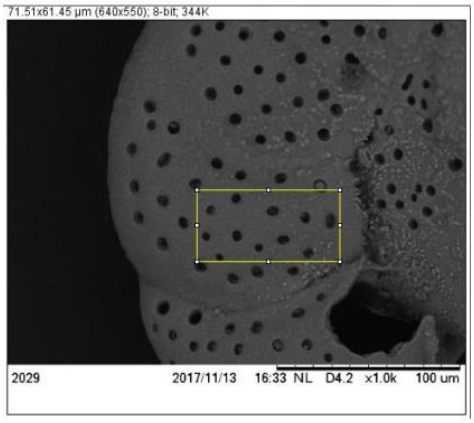

Figure 1: Example of positioning the frame inside the penultimate chamber of a *Cibicides pseudumgeriana*.

Results and Discussion

As a result, it was obtained that during the interglacial period there was an increase in photosynthetic rates, causing a higher concentration of O_2 and, consequently, a lower mean pore area of the tests. Besides, an assemblage more abundant in epifaunals. During Heinrich 1 (H1), two phases were observed, in the first one, the weakening of the AMOC implied in lower rates of O_2 and in response, the average area of the pores increased. Regarding the assembly, it exhibited the

highest abundance of infaunals in relation to the epifaunals. Already during the 2nd phase, it was understood that with the resumption of AMOC, the background oxygenation increased and, with this, the pore areas of the tests decreased. At this stage, the assemblage had fewer infaunals than the first. During the glacial, smaller photosynthetic rates were found, as a consequence, the average area of the pores increased relatively and the assemblage showed predominance of epifaunals, showing that O_2 concentrations were not as low as in H1. Thus, the variation in pore size was understood as an ecophenotypic characteristic that occurs first, as a form of defense or adaptation of foraminifera to changes in the oxygenation pattern of the environment and, only in more extreme cases, with a significant drop in O_2 levels, the fauna configuration is effectively disturbed. In addition, the porosity data were correlated to ^{231}Pa / ^{230}Th data in order to verify the correspondence between low AMOC intensity and the increase in porosity in *Cibicides pseudoungeriana* tests, in this way, such relationship was proven and showed to be evident around 16,000 years BP.

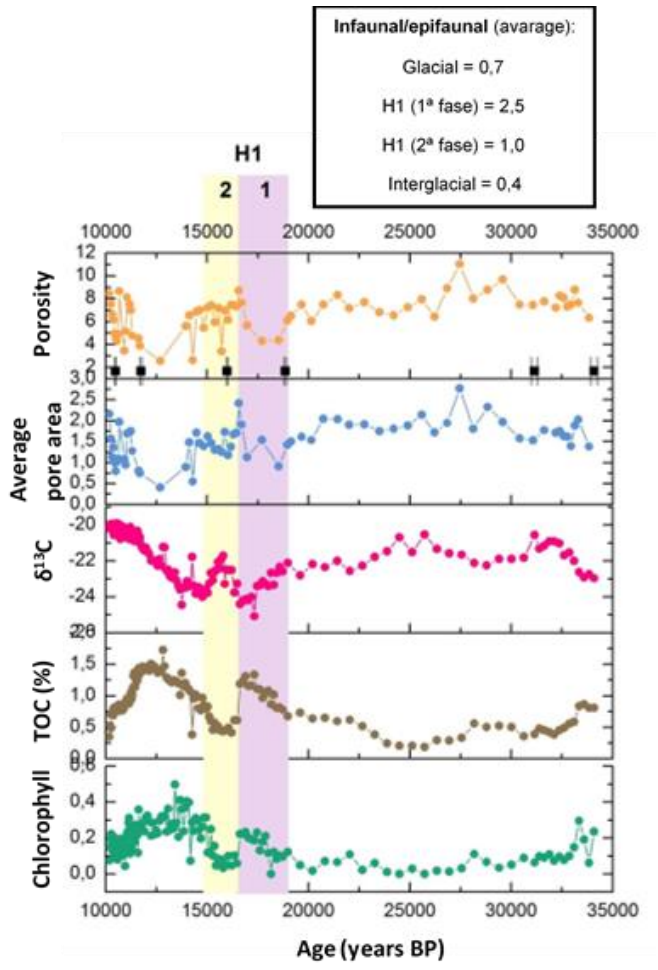

Figure 2: Graphical representation of organic matter data as chlorophyll, TOC, $\delta^{13}C$ (MAIA, 2016) and of the average pore area and porosity data by age.

Conclusions

The results generated from the pore analysis showed that the variation in the porosity pattern of the *Cibicides pseudoungeriana* tests correlated directly with previous organic matter data and also with the groupings of the benthic foraminifera assemblage, responding as expected to the hypothesis of the work, throughout the phases found in the core, especially during the Heinrich 1 event. It was concluded that when it comes to subtle variations in oxygenation, tests porosity is a more sensitive indicator than the infaunal/epifaunal ratio. The change in pore size may be an initial ecophenotypic variation of defense and/or adaptation of foraminifera that occurs before the changes in the community structure. That is, only in more severe cases of low oxygenation the fauna conformation is, in fact, altered. The porosity data found for the benthic foraminifera from the core deposit also correlated directly with the ^{231}Pa / ^{230}Th ratio values from other Atlantic cores, supporting the proposal that the AMOC presented a greater weakening during the 1st phase of H1, around 16,000 years BP, and re-circulated at the end of the 2nd phase, around 15,000 years BP. Furthermore, the pore analysis methodology was attested for the species *Cibicides pseudoungeriana* in a known oligotrophic deep-sea environment. Unlike previous work on this subject which has focused on restricted environments and/or oxygen minimum zones (OMZ), where oxygenation variations are usually more evident.

Acknowledgements

The authors thank CNPq (Brazilian research council) for fellowships for financial support.

References

ARZ, H. W.; PÄTZOLD, J.; WEFER, G. The deglacial history of the western tropical Atlantic as inferred from high resolution stable isotope records off northeastern Brazil. Earth and Planetary Science Letters, Bremen, v. 167, p. 105–117, 1999.

BROECKER, W. S. Massive iceberg discharges as triggers for global climate change. Nature, Nova Iorque, v. 372, p. 421 – 424, 1994.

MAIA, C. S. R. Pelagic paleoproductivity and sedimentary geochemistry of the Brazilian equatorial margin in the Late Pleistocene. Niterói. 99 f. Dissertation (Master in Geosciences) - Institute of Chemistry. Universidade Federal Fluminense, Niterói, 2016.

PETERSEN, J.; RIEDEL, B.; BARRAS, C.; PAYS, O.; GUIHÉNEUF, A.; MABILLEAU, G.; SCHWEIZER, M.; MEYSMAN, F. J. R.; JORISSEN, F. J. Improved methodology for measuring pore patterns in the benthic foraminiferal genus Ammonia. Marine Micropalentology, França, v. 128, p. 1-13, 2016.

XVI LATIN AMERICAN CONGRESS ON ORGANIC GEOCHEMISTRY
9 - 11 AUGUST, 2023
ARACAJU, SERGIPE, BRAZIL

Origin and distribution of sterols at the Southern and Southeastern Continental Shelf of Brazil

Alana P. Silva[a*], Ligia D. Araújo[a], Satie Taniguchi[a], Rafael A. Lourenço[a], Michel M. Mahiques[a], Marcia C. Bícego[a]
[a]Instituto Oceanográfico da Universidade de São Paulo (IO-USP)
*alanaparanhos@usp.br

Introduction

The Southern Continental Shelf of Brazil is characterized by the presence of elongated mudbelts deposits, which represent important reservoirs of organic matter (OM) in the oceans. These formations along Brazilian coast are strongly associated to the input of the La Plata River, which is transported northward by the Brazilian Coastal Current and influences the region up to approximately 24°S [1].

Assessing variables that characterize OM in the marine environment provides insights into its origin, distinguishing between marine and terrigenous sources. The TOC/TN (Total Organic Carbon/Total Nitrogen) ratio and the organic carbon isotopic ratio are widely used to differentiate sedimentary OM origins [2]. Besides those ratios, several compounds, called biomarkers, present in sediments can be used as tracers for the origin of organic matter. Sterols are particularly useful due their widespread in organisms and their stability in sediments [3]. Therefore, the analysis of sterol concentrations and their distribution in surface sediments samples from mudbelts of the South and Southern Continental Shelf of Brazil was used to evaluate the origin of the sedimentary organic matter in these deposits.

Experimental

The analysis was conducted on 27 surface sediment samples, collected from mudbelts of the South and Southeast Brazilian Continental Shelf using a Multiple Corer. The following analyses were conducted: grain size, total organic carbon (TOC) content, total nitrogen (TN), and organic carbon isotopic ratio (δ13C), and the quantification of five sterols (β-sitosterol, cholesterol, dinosterol, stigmasterol, and campesterol). Sterol determination in the sediments, followed a protocol that involves extraction, purification, sample derivatization, and gas chromatography analysis [4].

Results and Discussion

In general, samples showed high levels of mud content, exceedding 70%. Most samples exhibit high levels of TOC with values greater than 0.5%. A distinct pattern becomes apparent, showing higher TOC concentrations to the southernregion of the study area, wich is situated near the mouth of the La Plata River, which plays a significant role as sediment source for the area. The TOC/TN ratio ranged from 2.46 and 23.14 (Fig. 1). Only two samples exceeded 20, considered the reference limit for terrigenous OM.

Most samples were in the range of 4 and 10, indicative of marine OM [2]. The $\delta^{13}C$ values varied from -24.32 to -17.40 ‰ (Fig. 1). Values ranging from -23 to -16‰ are indicative of sedimentary organic matter from marine algae, while values lower than -23‰ are associated with terrigenous organic matter. Most of the analyzed samples presented values corresponding to OM of marine origin [2]. However, they were values close to the reference limits for OM of continental origin. This may be indicative of the mixture of terrigenous and marine sources.

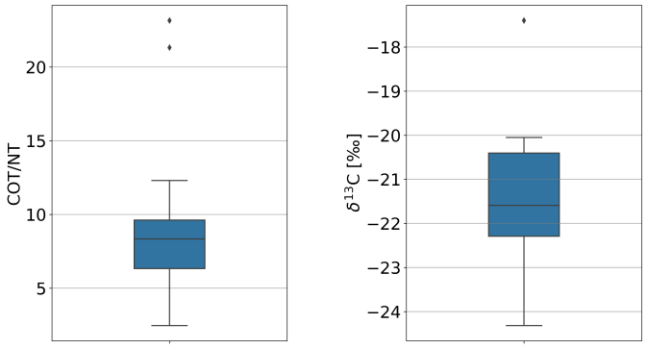

Figure 1. Boxplots of TOC/NT ratios (left) and organic carbon isotope ratios (right)

Total sterol concentrations ranged from 0.82 and 11.45 $\mu g.g^{-1}$, wich is consistent with observed in other regions of the continental shelf [5]. The highest concentrations tended to occur at the south of the study area, between 34°S and 32°S (Fig. 2). In the central portion of the region, concentrations showed greater variability, with higher contents observed closer to the coast and in the mid-shelf region. Towards the northern region beyond 24°S, wich is considered the the limit of the influence of the La Plata River [1], lower concentrations of sterols were observed.

The relatively high concentrations of sterols in the southernmost portion and in the coastal regions of the study area can be attributed to the significant influence of the La Plata River in these areas. The impact of the plume is linked to the supply of terrigenous material and

nutrients, resulting in an increase in primary production within the area [6].

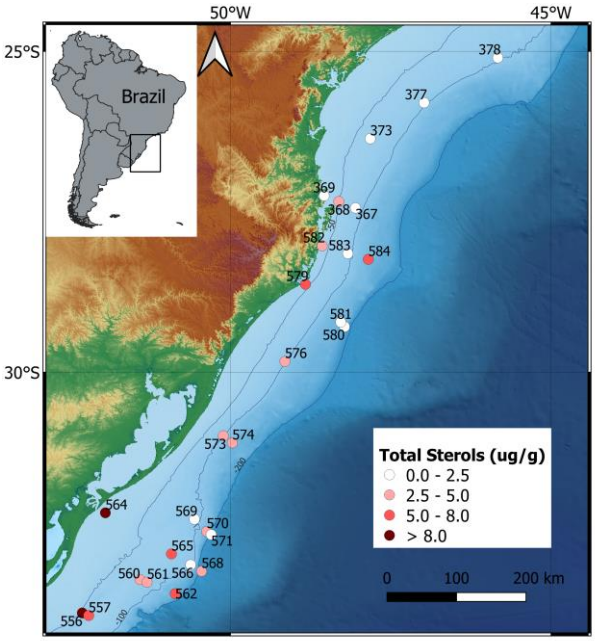

Figure 2. Map of distribution of total sterols concentrations along the study area.

Among the quantified sterols, β-sitosterol and cholesterol showed the highest concentrations throughout the studied area (Fig. 3), ranging from 0.23 to 3.69 $\mu g.g^{-1}$ and 0.06 to 3.63 $\mu g.g^{-1}$ respectively. Cholesterol, being the primary sterol produced by marine planktonic organisms, serves as an indicator of OM of marine origin. β-sitosterol, differently, is typically associated with terrigenous OM, although it can also be produced by marine organisms [3]. Dinosterol (0.06 to 1.42 $\mu g.g^{-1}$), stigmasterol (0.09 to 1.34 µg.g-1) and campesterol (0.04 to 1.95 $\mu g.g^{-1}$) showed relatively lower concentrations, but were present in all samples. Dinosterol is produced by marine planktonic organisms. While stigmasterol and campesterol are mainly produced by terrestrial vascular plants, although they can also be found in marine plankton [3].

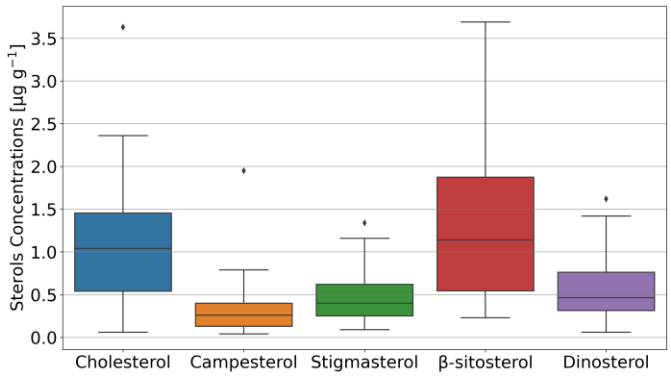

Figure 3. Boxplots of analyzed sterols concentrations.

Conclusions

The analysis of sterols concentrations provided insights into the distribution of sedimentary organic matter along the southern continental shelf of Brazil. The data revealed a predominance of marine organic matter, although the influence of terrigenous was also observed. The significant contribution of the La Plata River was evident in the distribution of sterols concentrations along the continental shelf, with its strongest influence verified up to 33°S, gradually decreasing towards the northeast.

Acknowledgements

The authors thank PUB/USP and CNPq (304274/2018-6) fellowships; ANP (Brazilian Petroleum Agency), Petrobras S/A and PGQu – UFRJ for financial support and fostering agency of the State of São Paulo - FAPESP 2015/17763-2 and 2016/18348-1; and the crew of the oceanographic research vessel Alpha Crusis for the support during the sampling process.

References

1. Nagai RH, Sousa SHM, Mahiques MM. The southern Brazilian shelf. Geol Soc Mem. 2014;41(1):47–54.

2. Meyers PA. Preservation of elemental and isotopic source identification of sedimentary organic matter. Chem Geol. 1994;114(3–4):289–302.

3. Volkman JK. A review of sterol markers for marine and terrigenous organic matter. Org Geochem. 1986;9(2):83–99.

4. Lourenço RA. Aplicação de Marcadores Orgânicos Moleculares em Estudos Oceanográficos e Paleoceanográficos : Estudo de Caso na Margem Continental Superior do Sudeste do Brasil. 2007.

5. Pang SY, Tay JH, Suratman S, Simoneit BRT, Mohd Tahir N. Input of organic matter in Brunei Bay, East Malaysia, as indicated by sedimentary steroids and multivariate statistics. Mar Pollut Bull. 2020;156(May).

6. De Mahiques MM, Tessler MG, Maria Ciotti A, Da Silveira ICA, E Sousa SHDM, Figueira RCL, et al. Hydrodynamically driven patterns of recent sedimentation in the shelf and upper slope off Southeast Brazil. Cont Shelf Res. 2004;24(15):1685–97.

Characterization of Polycyclic Aromatic Hydrocarbons (PAHs) contamination in mud depocenter from the southern Brazilian shelf

Alexandre Santos de Andrade*[a]; Satie Taniguchi[a]; Rafael André Lourenço[a]; Michel Michaelovitch de Mahiques[a]; Rubens César Lopes Figueira[a]. Márcia Caruso Bícego[a]

[a]Instituto Oceanográfico da Universidade de São Paulo

*email: a.andrade@usp.br.

Introduction

Continental shelf is a dynamic environment where sedimentary processes and human impacts interact. As consequence, sediments that contain materials derived from human activities can be used as indicators of that impact on the continent (Ya et al., 2017). Polycyclic aromatic hydrocarbons (PAHs) are a significant group of contaminants in marine environments. Extensive research has been conducted to comprehend their sources, behavior, fate due to their toxic properties. PAHs are predominantly associated with fine-grained, organic-rich sediments and therefore these sediments are an important reservoir for these pollutants. The objective of this study is to characterize anthropogenic polycyclic aromatic hydrocarbons (PAHs) in a sediment core obtained from a mud depocenter located in the southern Brazilian inner shelf, near the outlet of Patos Lagoon, located in the state of Rio Grande do Sul, in southern Brazil and considered one of the largest in the South America (Niencheski, et al 2006,).

Experimental

Sampling Collection

The core 564 (60 cm sediment record) was collected from the inner shelf using a piston corer at a depth of 18 m during a research cruise onboard the *Alpha Crucis* RV in January 2019 (Figure 1). The core was subsampled at 2 cm fractions and the samples were frozen for subsequent freeze-drying.

Age-depth model

Samples were analyzed by Gamma spectrometry to determine ^{210}Pb and ^{137}Cs activity in accordance with Figueira et al. (2007) guidelines.

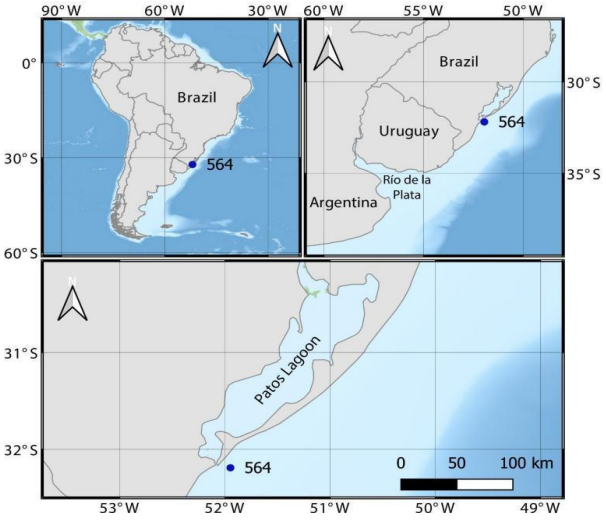

Figure 1: Sampling site in the Southern Brazilian Inner Continental Shelf.

PAH extraction and analysis

The 16 analyzed PAHs were based on the priority compounds outlined by the USEPA (2014). Figure 2 presents the main steps of the analytical procedure (UNEP,1992) for the analytical procedure.

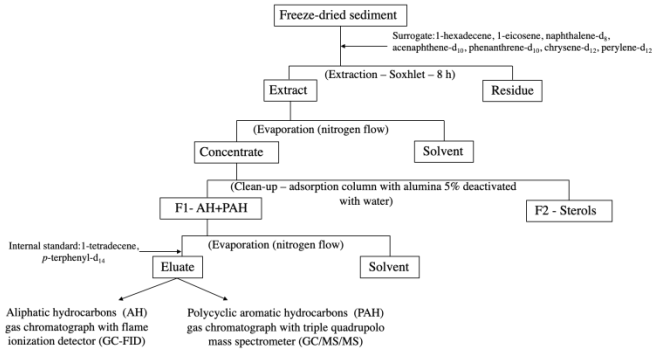

Figure 2: Analytical procedure of the 16 priority PAHs in sediment samples.

Results and Discussion

According to the results of sedimentation rate given by the applied model, the age of the core involves the interval between the years of 1792 and 2019 (sampling year). The total PAH concentrations and the ratio between Low molecular weight and High molecular weight are shown in Figure 3. The most of the 16 analysed PAHs were detected in all core subsamples.

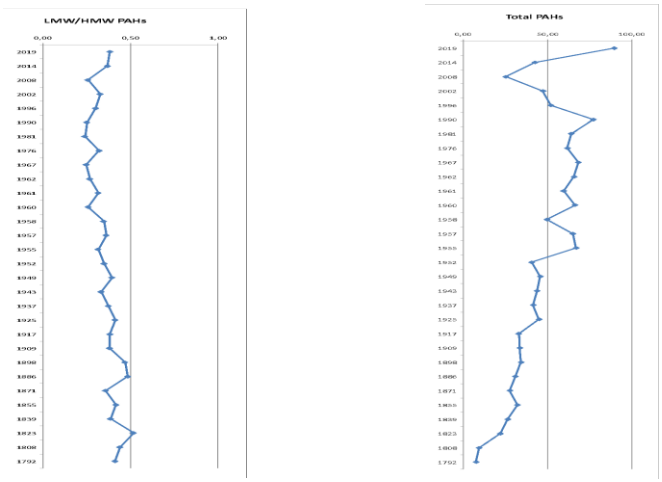

Figure 3: Vertical distribution of the ratio between Low molecular weight and High molecular weight PAH (LMW/HMW PAH) and the distribution of the concentration of total PAHs.

The PAH identified in this study show similarities to those found in regions with limited human influence, such as Laranjeiras Bay, Brazil (Martins et al., 2012), and exhibit lower levels compared to heavily polluted areas like the Santos estuary, Brazil (Bicego eta al, 2006). The observed PAH concentrations are comparable to those reported in other mud depocenter regions, such as the East China Sea (Timoszczuk, et al., 2021). According to the data presented in the graphs, there is a tendency towards an increase in the total concentration of PAHs over time. The difference in total PAHs concentrations, between the bottom and the top of the core, can be 10 times greater for the most recent dating. The profile of PAH in Fig.3 suggests that the increase in the introduction of PAHs anthropic origin in the vicinity of Patos Lagoon, coincides with the construction of the Port of Rio Grande (1910), inaugurated in 1915.

Conclusions

The increase in PAH input, mainly in the early 20th century, is directly related to the development of the Rio Grande city region with the beginning of anthropic activities such as port and industrial activities and the consequent increase in the local population.

Acknowledgements

The authors thank CNPq (Brazilian research council) for fellowships (304 274/2018-6) and financial support (404001/2021-1); ANP (Brazilian Petroleum Agency), Petrobras S/A and PGQu – UFRJ for financial support and fostering agency of the State of São Paulo - FAPESP 2015/17763-2 and 2016/18348-1.

References

Bícego,M.C., et al. 2006 Assessment of contamination by polychlorinated biphenyls and aliphatic and aromatic hydrocarbons in sediments of the Santos and São Vicente Estuary System, São Paulo, Brazil Mar. Pollut. Bull., 52 1804-1816;

Figueira, R.C.L., et al., 2007 Is there a technique for the determination of sedimentation rates based on calcium carbonate content? A comparative study on the southeastern Brazilian shelf. Soils Found., 47 pp. 649-656;

Martins, C.C. et al. 2012. Multi-molecular markers and metals as tracers of organic matter inputs and contamination status from an Environmental Protection Area in the SW Atlantic (Laranjeiras Bay, Brazil) Sci. Total Environ. 417:158-168;

Niencheski, L.F.H et al. 2006. Patos Lagoon: indicators of organic pollution. Journal of Coastal Research, SI 39 (Proceedings of the 8th International Coastal Symposium), 1356 - 1359. Itajaí, SC, Brazil;

Timoszczuk, C.T.,et al. 2021 Historical Deposition of PAHs in Mud Depocenters from the Southwestern Atlantic Continental Shelf: The Influence of Socio-Economic Development and Coal Consumption in the Last Century. Environmental Pollution 284: 117469;

UNEP,1992 Determinations of Petroleum Hydrocarbons in Sediments, Reference Methods for Marine Pollution Studies. Washington DC (USA);

USEPA(2014). U.S. EPA EPA Appendix A to 40 CFR, Part 423-126 Priority Pollutants;

Ya, M., et al. 2017 Transport of terrigenous polycyclic aromatic hydrocarbons affected by the coastal upwelling in the northwestern coast of South China Sea. Environ. Pollut. 229:60-68.

IS THERE A CORRELATION BETWEEN THE WAXY TARBALLS STRANDED ON THE COAST OF NORTHEAST BRAZIL IN LATE 2022 WITH PREVIOUS OIL SPILLS?

Adriana P. do Nascimento[a], Rufino Neto A. Azevedo[a], Marília Gabriela A. Pereira[b], André Henrique B. Oliveira[a], Jandyson M. Santos[b], Rivelino M. Cavalcante[a], Laercio L. Martins[a,c]

[a]Federal University of Ceará; [b]Federal Rural University of Pernambuco; [c]North Fluminense State University

e-mail: adrianapn@alu.ufc.br

Introduction

In late 2022 tens of tons of mysterious tarballs stranded on the northeast coast of Brazil, contaminating many marine and seashore areas (MCTI, 2022). The first oiled materials were found in the State of Pernambuco in late August, reaching the states of Alagoas, Sergipe, Bahia, Paraiba, Rio Grande do Norte, and Ceará in the following weeks in an extension of more than 2,000 km. Oil spills affecting Northeast Brazil have been an immeasurable social, economic, and ecological problem due to their high frequency, high amount of oil, and because they have been affecting large geographic extension, impacting a broad number of coastal communities and protected areas (Soares et al., 2022).

In this context, this work aims to investigate the mysterious tarballs that reached the northeast coast of Brazil in late 2022. Forensic Environment Geochemistry using gas chromatography techniques was applied to assess the possible correlation between the tarballs collected in late 2022 with the spilled oils collected in early 2022 (Azevedo et al., 2022) and in 2019 (Reddy et al., 2022).

Experimental

The set of samples encompasses 20 spilled oil samples, including 16 tarballs collected from August to October 2022 (2022.2) on different beaches of the states of Bahia, Sergipe, Alagoas, Rio Grande do Norte, and Ceará, northeast of Brazil, and two oil samples collected in January 2022 (2022.1) in the State of Ceará (Azevedo et al., 2022) and two samples from the 2019 oil spill event also from Ceará (Reddy et al., 2022). The oil was extracted from the material collected on the beaches using dichloromethane by vortexing followed by centrifugation. Asphaltenes were precipitated from approximately 300 mg of oil using *n*-hexane and the obtained maltenes were separated into saturate, aromatic, and NSO fractions by liquid chromatography. The saturate fraction was analyzed by GC-FID to assess *n*-alkanes and isoprenoids, and the maltene fractions were analyzed by GC-MS to assess saturate and aromatic biomarkers.

Results and Discussion

The 2022.2 tarballs have a roughly spherical appearance, ranging from small (< 1 cm) to large materials (>10 cm). They are soft and black with an oil smell, which fluctuates on the seawater. The precipitation of a considerable amount of wax in the aliphatic fraction after the fractionation by liquid chromatography pointed out their waxy characteristics. They have physical aspects distinct from the oils beached in previous events, which have more liquid aspects of oil.

The GC-FID chromatograms of the 16 tarball samples collected in late 2022 shows a similar bimodal profile, with *n*-alkanes ranging from C12 to C40, maximizing at C17 and C33. The high abundance of long-chain *n*-alkanes (C31 to C40) corroborates their waxy characteristic, and together with no detection of UCM (unresolved complex mixture), points to little-weathering tarballs. Similar characteristics were observed by Edwards et al. (2018) in the stranding waxy tarballs in southern Australia. In addition, their GC-FID chromatograms have notable distinct profiles from the chromatograms of the 2019 and 2022.1 spilled oils (**Figure 1a**), these last two already presented by Reddy et al. (2022) and Azevedo et al. (2022). These differences suggest distinct sources for these three groups of spilled oils. However, as the diagnostic features from the GC-FID profiles are influenced by weathering, more resistant molecular biomarkers are needed to assess possible similarities among these spilled oils.

The radar plots of the diagnostic ratios based on resistant biomarkers, assessed by GC-MS, for all 16

tarballs show good similarity, corroborating the GC-FID results, with the relative standard deviation (RSD) lower than 10% to 25 of the total of 28 ratios. Exceptions are the ratios 21/23 Tri, 23/24 Tri, and Tet24/26Tri, which can be explained due to the possible susceptibility of tricyclic terpanes to weathering processes.

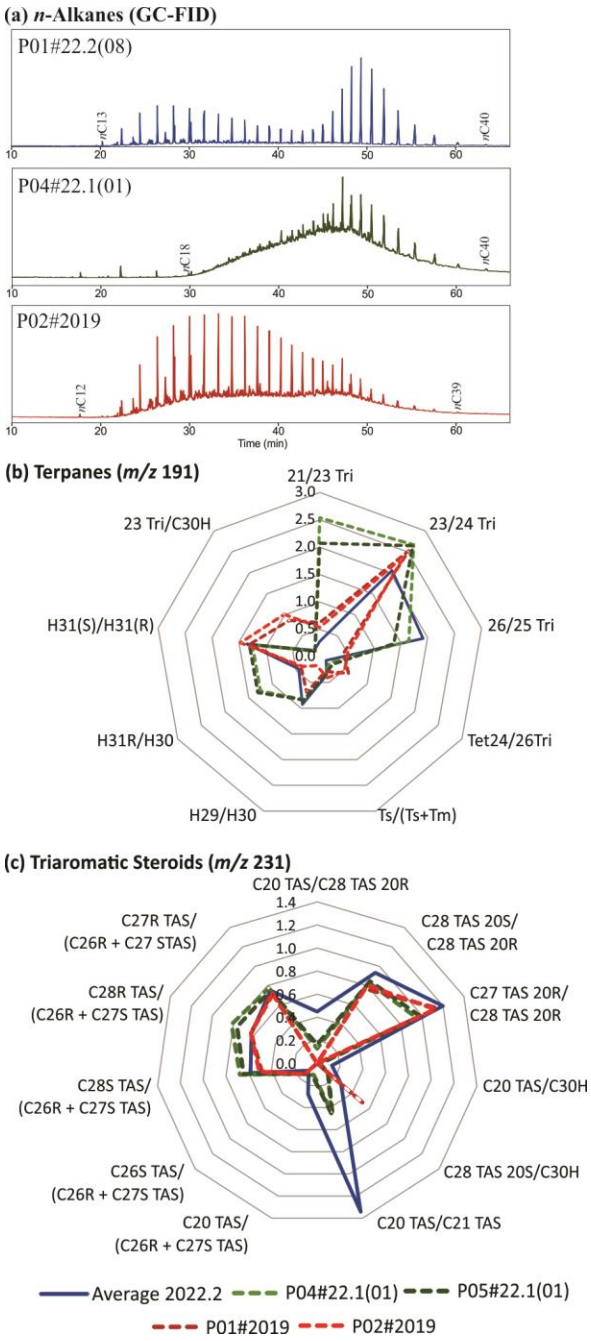

Figure 1. GC-FID chromatograms representative for the tarballs (2022.2), the 2022.1, and 2019 spilled oils (a); radar plots comparing the diagnostic ratios of tricyclic and pentacyclic terpanes (b) and triaromatic steranes (c) for the average of the tarballs and the 2022.1 and 2019 spilled oils.

The similarity among the 16 tarball samples confirms the great extension of the Brazilian coast affected by this oil spill in the states of Northeast, from Bahia to Ceará.

However, the radar plots of the diagnostic ratios for the average of the 16 tarballs (2022.2) and the 2022.1 and 2019 spilled oils are remarkably different (**Figure 1b** and **c**), clearly indicating that these sets of samples originated from a distinct source and different events. The RSDs considering all 20 environmental oil samples are considerably higher than the RSD only of the 16 tarballs, reaching values up to 38.9% to the TAS and up to 106.5% to the terpanes.

Conclusions

This work reports the waxy characteristics of the tarballs beached in the Northeast of Brazil in late 2022. Geochemical investigation showed that the tarballs collected from 16 beaches in five states of Brazil have the same sources, highlighting the large extension of the Brazilian coast affected by them, from the state of Bahia to Ceará. Finally, these tarballs have distinct source from the spilled oils stranded in 2019 and early 2022 at the State of Ceará, indicating different events.

Acknowledgements

This work was supported by the Federal University of Ceará (UFC) and performed with financial support provided by Fundação de Amparo à Ciência e Tecnologia do Estado de Pernambuco (FACEPE APQ APQ-0036-1.06/20) and Coordenação de Aperfeiçoamento de Pessoal de Nível Superior (CAPES), Brazil.

References

Azevedo et al., 2022. Is there a similarity between the 2019 and 2022 oil spills that occurred on the coast of Ceará (Northeast Brazil)? An analysis based on forensic environmental geochemistry. Environmental Pollution 315, 120283.

Edwards et al., 2018. Waxy bitumen stranding in southern Australia: A geochemical study of multiple oil families and their likely origins. Organic Geochemistry 118, 132-151.

MCTI, 2022. Resíduos de óleo encontrados em agosto no litoral do Nordeste. https://www.gov.br/mcti/pt-br/acompanhe-o-mcti/noticias/2022/09/nota-tecnica-a-imprensa-residuos-de-oleo-encontrados-em-agosto-no-litoral-do-nordeste (Accessed 19 April 2022).

Reddy et al., 2022. Synergy of Analytical Approaches Enables a Robust Assessment of the Brazil Mystery Oil Spill. Energy Fuel 36, 13688–13704.

Soares et al., 2022. The most extensive oil spill registered in tropical oceans (Brazil): the balance sheet of a disaster. Environmental Science and Pollution Research 29, 19869–19877.

XVI LATIN AMERICAN CONGRESS ON ORGANIC GEOCHEMISTRY
9 - 11 AUGUST, 2023
ARACAJU, SERGIPE, BRAZIL

Characterization of natural aliphatic hydrocarbon in a mud depocenter from the southern Brazilian shelf

Giovanna Piccini*[a]; Satie Taniguchi[a]; Felipe Rodrigues dos Santos[a], Rafael André Lourenço[a]; Michel Michaelovitch de Mahiques[a]; Rubens César Lopes Figueira[a]. Márcia Caruso Bícego[a]

[a]Instituto Oceanográfico da Universidade de São Paulo

e-mail: giovannapiccini@usp.br

Introduction

The continental shelf is a complex system that plays a crucial role in the transport and storage of organic and inorganic materials from the continent. Previous studies have identified mud belt deposits in these areas as primary sites for the deposition of compounds originating from land sources (Dias et al., 2023). The objective of this study is to characterize natural aliphatic hydrocarbons in a sediment core obtained from a mud depocenter located in the southern Brazilian inner shelf, near the outlet of Patos Lagoon. The Lagoon's discharge represents a significant local contribution to the suspended sediment budget of the southern Brazilian inner shelf (Niencheski et al., 2006; Marques et al., 2010).

Experimental

Sampling Collection

The core 564 (60 cm length) was collected from the inner shelf using a piston core sampler at an 18 m depth during a research cruise onboard the *Alpha Crucis* RV in January 2019 (Figure 1). The core was subsampled at 2 cm fractions and the samples were frozen for subsequent freeze-drying.

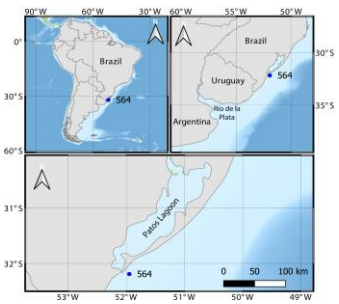

Figure 1: Map of the southern Brazilian shelf.

Age-depth model

Samples were analyzed by Gamma spectrometry to determine ^{210}Pb and ^{137}Cs activity following Figueira et al. (2007) guidelines.

Extraction and Analysis

Figure 2 presents the main steps of the analytical procedure (UNEP,1992) for the analysis of the aliphatic hydrocarbon

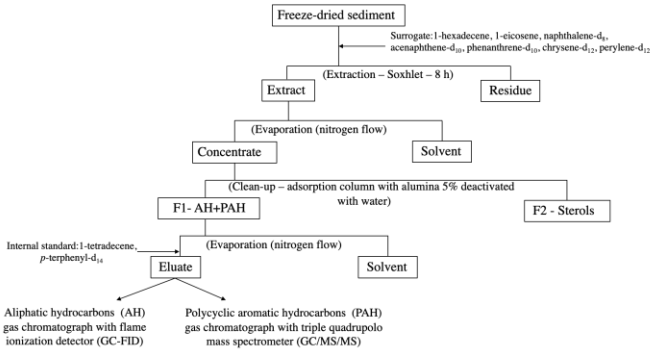

Figure 2: Main steps of the analytical procedure for the analysis of aliphatic hydrocarbons.

Results and Discussion

According to the age model results, the sediment core 564 covers the interval between 1792 and 2019 CE (sampling year).

Diagnostic ratios were applied to aliphatic hydrocarbon to evaluate the variations of the marine and terrigenous input in the region. Table 1 presents the ratios used for this evaluation and Figure 3 presents the diagnostic ratios results.

Index	Values	Predominant Source	Reference
CPI	1-2	Algeae Predominance	(EGLINTON *et al*., 1962; BI *et al*., 2005)
	>3	Superior Plants Predominance	(RAO *et al*., 2009)
AI	<0,5	C3 Plants Predominance	(ZHANG *et al*., 2006)
	>0,5	C4 Plants Predominance	
TAR	Higher	Predominance of Terrigenous Input	(Peters *et al*., 2005)
	Lower	Predominance of Aquatic Input	

Table 1. Values of CPI, AI and TAR ratios used for interpretation.

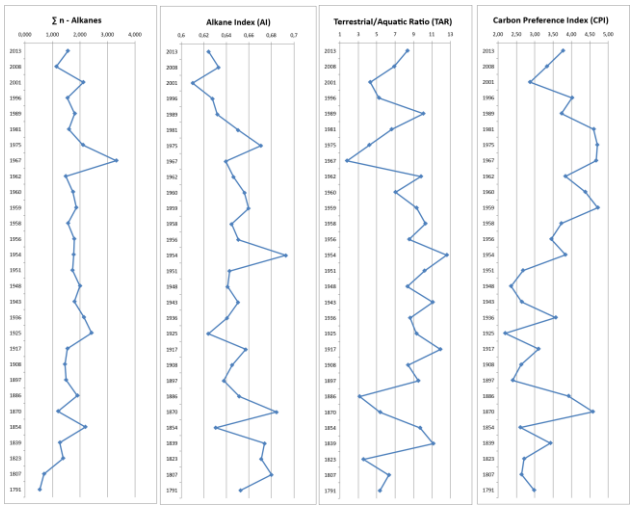

Figure 3: Profiles of ∑n-Alkanes, AI, TAR and CPI results of the 564 core.

The ∑n-Alkanes, AI, TAR and CPI varied from 0,5 to 3.3 µg g^{-1}, 0.60 to 0.69, 1,8 to 12.6 and 2.2 to 4.7, respectively. The AI values showed a constant profile with its lower variation around the average value of 0,65 ± 0.05. The ∑n-Alkanes lower variability suggests that no intense change in marine and terrigenous organic matter input occurred in the last 230 years. In addition, the AI ratio also suggests that no intense climatic or/and vegetation change occurred in the last 230 years, with a predominance of C4 or grasslands vegetation in the Patos Lagoon drainage basin.

The TAR ratio presented no well-defined variation pattern, varying from 1.8 to 12.6. The CPI ratio ranged from 2.2 to 4.7, indicating the predominance of marine and non-degraded organic matter. The CPI values >2 also indicate that the main alkane source is from natural and biogenic material, mainly terrigenous input. CPI values presented two phases. The first phase from 1791 to 1951 is represented by relatively lower values, except from 1876 and 1880 which showed higher values. The second phase is from 1951 to 2019, represented by higher CPI values. These higher values suggest an increase in the terrigenous material, which may be caused by rainfall amount in continent.

Conclusions

The southern Brazilian Shelf associated with Patos Lagoon is characterized by the influence of terrestrial sediment. The predominance of terrigenous input may provide the understanding of the anthropogenic impact resulting by the local occupation process.

Acknowledgements

The authors thank CNPq (Brazilian research council) for fellowships (304 274/2018-6) and financial support (404001/2021-1); ANP (Brazilian Petroleum Agency), Petrobras S/A and PGQu – UFRJ for financial support and fostering agency of the State of São Paulo - FAPESP 2015/17763-2 and 2016/18348-1.

References

Dias *et al.,* 2023. “Geochemical Characterization and Assessment of Contamination in Mud Depocenters from the Southern Brazilian Shelf.” Continental Shelf Research 257

Figueira *et al.,* Is there a technique for the determination of sedimentation rates based on calcium carbonate content? A comparative study on the southeastern Brazilian shelf. 2007 Soils Found., 47 pp. 649-656,

Mahiques M.M. *et al.,* 2015 Mud depocentres on the continental shelf: a neglected sink for anthropogenic contaminants from the coastal zone. Environ. Earth Sci., 75 (1)

Marques, *et al.*, 2010, Dynamics of the Patos Lagoon coastal plume and its contribution to the deposition pattern of the southern Brazilian inner shelf, J. Geophys. Res., 115,

Niencheski, *et al.,* 2006. Patos Lagoon: indicators of organic pollution. Journal of Coastal Research, SI 39 (Proceedings of the 8th International Coastal Symposium), 1356 - 1359. Itajaí, SC, Brazil, ISSN 0749-0208

UNEP,1992 UNEP Determinations of Petroleum Hydrocarbons in Sediments, Reference Methods for Marine Pollution Studies. Washington DC (USA)

XVI LATIN AMERICAN CONGRESS ON ORGANIC GEOCHEMISTRY
9 - 11 AUGUST, 2023
ARACAJU, SERGIPE, BRAZIL

Assessment and spatial distribution of Polycyclic Aromatic Hydrocarbons (PAH) in the surface sediment of the Santos Estuary, Brazil

Lucas Costa Pereira[a*], Satie Taniguchi[a]; Rafael André Lourenço[a]; Michel Michaelovitch de Mahiques[a]; Rubens César Lopes Figueira[a], Márcia Caruso Bícego[a]

[a]INSTITUTO OCEANOGRÁFICO DA UNIVERSIDADE DE SÃO PAULO - IOUSP

[*]correspondência: lucas897costa897@usp.br

Introduction

The Santos Estuary, situated on the southern coast of São Paulo, Brazil, encompasses the largest port complex in Latin America, the Port of Santos (CODESP, 2011). This area is subject to the introduction of a significant amount of pollutants due to the port activities and their proximity to the industrial complex of Cubatão and the high level of urbanization in the surrounding regions (Martins et al., 2011). The aim of this study is the assessment of the spatial distribution and source of toxic and carcinogenic polycyclic aromatic hydrocarbons (PAH) in the surface sediments throughout the estuary.

Experimental

Sixteen surface sediment samples were collected between the months of June and August 2022 using a sediment grab sampler, following the distribution shown in Figure 1.The sampling date of each station is provided in Table 1.

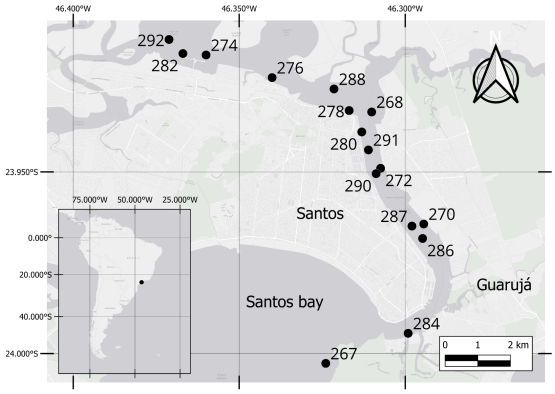

Figure 1. Sampling stations along the Santos Estuary.

Station	Date
268, 267	6/1/2022
270	6/8/2022
272	6/13/2022
274	6/15/2022
276	6/22/2022
278	6/23/2022
280	7/6/2022
282	7/7/2022
284	7/20/2022
286, 287, 288	8/17/2022
290, 291, 292	8/24/2022

Table 1. Sampling date of each station.

Figure 2 presents the main steps of the analytical procedure (UNEP,1992) for the determination of the PAH.

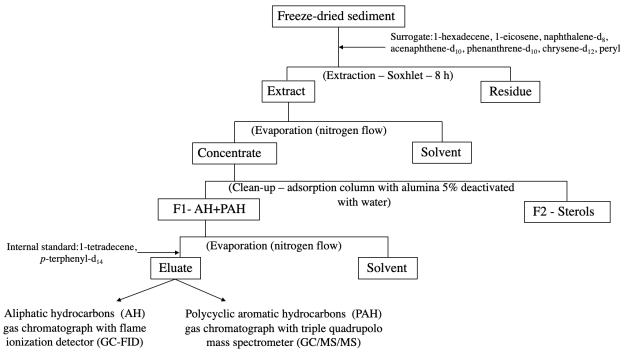

Figure 2. Analytical procedure for PAH.

Results and Discussion

The total PAH concentration ranged from 74.6 to 3943 ng g^{-1}. Figure 3 presents the spatial distribution of total PAH in each sampling station.

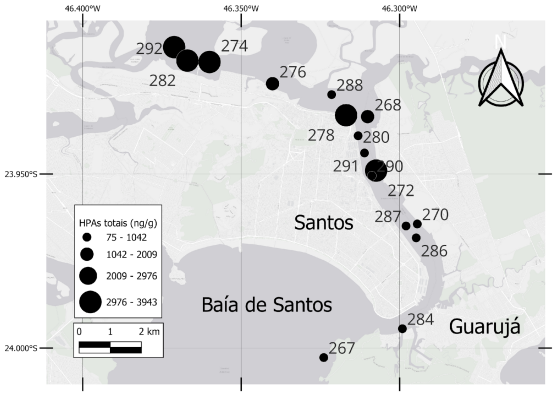

Figure 3. Spatial distribution of total PAH (ng g^{-1}) in each sampling station.

The highest concentrations were observed at stations 292, 282 and 274, located close to the industrial complex of Cubatão, at stations 268 and 278, which are nearby the petroleum and derivatives storage facilities on Barnabé Island, and at Station 272, situated near a densely urbanized area. Concentrations were above threshold effects level (TEL) index (Macdonald et al, 1996) in all these stations, except for 268. The station with the lowest concentration was station 267, located at the outlet of the Santos Port channel.

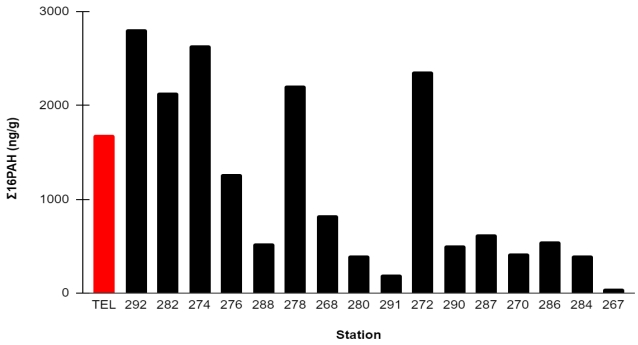

Figure 4. Values for Σ16PAH calculated for the stations (black) and TEL index (red).

The PAH concentrations identified in this study show similarities to those found in a prior study at that same area (Netto et al, 2022) and in heavily polluted areas (Kılıç, et al. 2023).

Source evaluation of studied PAH diagnostic ratios to indicate whether the origins of hydrocarbons are pyrogenic or petrogenic were used for the core sediment samples (Yunker et al, 2002). Except for station 267, which showed relatively higher concentrations of alkylated homologues from petrogenic sources, the majority of them indicated a stronger influence of pyrogenic PAH.

Conclusions

The operations related to the industrial and port activities, in addition to urban and industrial sewage, are the main sources of PAHs to the sediment of Santos Estuary. That area also covers a huge touristic hub, mainly in the summer, which can also contribute to higher input of those compounds in that environment.

Acknowledgements

The authors thank CNPq (Brazilian research council) for fellowship (304 274/2018-6) and financial support (404001/2021-1); ANP (Brazilian Petroleum Agency), Petrobras S/A and PGQu – UFRJ for financial support and fostering agency of the State of São Paulo - FAPESP 2015/17763-2 and 2016/18348-1.

References

CODESP 2011 (Companhia Docas do estado de São Paulo) Porto de Santos: Relatório anual.

Martins, C C. M. C. Bícego, M. M. Mahiques, R. C.L. Figueira, M. G. T., R. C. Montone 2011. Polycyclic aromatic hydrocarbons (PAHs) in a large South American industrial coastal area (Santos Estuary, Southeastern Brazil): Sources and depositional history, Marine Pollution Bulletin,63:452-458.

Netto, A. A.; Souza, P.F., Lima, L.S., Vieira, K.S., Delgado, J.F., Menezes, C.R., Neves, C.V., Baptista Neto, J.A., Fonseca, E.M., 2022. Distribution dynamics and potential sources of polycyclic aromatic hydrocarbons for surface sediments and bivalves from a highly anthropized estuary. Revista S&G 17, 1.

Kılıç, S. Kılıç, Ö., M. Belivermiş, H.A. Ergül,2023 Chronology of PAH and PCB pollution using sediment core in the Golden Horn estuary (Sea of Marmara), Marine Pollution Bulletin,187

Yunker, M. B.; Macdonald, R. W.; Vingarzan, R.; Mitchell, R. H.; Goyette, D.; Sylvestre, S., 2002. PAHs in the Fraser River basin: a critical appraisal of PAH ratios as indicators of PAH source and composition. Organic Geochemistry, 33.

Macdonald, D.D., Carr, R.S., Calder, F.D., Long, E.R., Ingersoll, C.G., 1996.Development and evaluation of sediment quality guidelines for Florida coastal waters, Ecotoxicology, 5: 253-278

XVI LATIN AMERICAN CONGRESS ON ORGANIC GEOCHEMISTRY
9 - 11 AUGUST, 2023
ARACAJU, SERGIPE, BRAZIL

ASSESSMENT OF PETROGENIC HYDROCARBONS IN LEPAS ANATIFERA FIXED ON BEACHED TARBALLS ON THE NORTHEASTERN COAST OF BRAZIL IN 2022

ANTÔNIA D.F. LIMA[a*], LUIZA C. MELLO[a], BEATRIZ DINIZ[a], ADRIANA P. NASCIMENTO[a], LAERCIO L. MARTINS[a,b], RIVELINO M. CAVALCANTE[a]

[a] Postgraduate Program in Tropical Marine Sciences (PPGCMT)/Federal University of Ceará (UFC); [b]North Fluminense State University (UENF)

aduci.flima@gmail.com

Introduction

From the end of August 2019, occurrences of oily stains appeared on several beaches in northeastern Brazil, taking on greater dimensions in the following months, thus being considered one of the most serious incidents ever to occur in the country (Soares et al., 2020). New oil spill events occurred in the following years, including the event that started at the end of August 2022 in the State of Ceará, this time with a peculiarity, in which most of the oil material like tarballs contained some marine organisms attached to it, the crustacean of the species *Lepas anatifera* (Cirripedia, Lepadomorpha). Studies of these occurrences are important because they support the classification of species as ecological indicators, more specifically as bioindicators of environmental impact. In this context, the purpose of this study is to evaluate the contamination of lepas, fixed on surfaces of tarballs sampled at beaches from the state of Ceará and Rio Grande do Norte, Brazil, through the identification and quantification of chemical markers (aliphatic hydrocarbons, HAs; and Polycyclic aromatic hydrocarbons, HPAs) and their sources.

Experimental

Oil samples like tarballs containing *Lepas anatifera* were collected at Ceará beaches (Futuro, Icaraí, Cumbuco, Pecém, and Almofala) in September and October 2022, and at Rio Grande do Norte beaches (Baía Formosa and Tabatinga) in September 2022, both states in Northeastern Brazil. Samples of coconut with the same species fixed on them as substrate were also collected at Praia do Futuro in October 2022 and used as a control or blank sample.

A chemical analysis was conducted to quantify the compounds of interest by the QUECHERS method, in which extraction and clean-up of the samples were made. For identification and quantification of the HPAs, GC-MS were used, while the aliphatics were analyzed by GC-FID.

Results and Discussion

The studied Lepas presented sizes ranging from 0.122 to 2.20 cm, indicating that the tarballs used as a substrate have been floating on the ocean at least for a month.

All organic extracts from the Lepas have GC-FID profiles of HAs characteristic of oil (Figure 1), including C_8 to C_{40} *n*-alkanes and isoprenoids pristane (Pr) and phytane (Phy), and a pronounced UCM (unresolved complex mixture) evidencing petrogenic origin (Farrington and Quinn, 2015). Except for the sample collected from the coconut (G5), used as a control.

UCM is considered a benchmark for environmental contamination by petroleum hydrocarbons and is therefore noted as one of the main geochemical indications of petroleum contamination (Reddy et al., 2000; Farrington and Quinn, 2015). In this way, the result obtained for UCM evidencing petrogenic origin, except for the sample collected from the coconut (G5) used as a control (**Figure 1**)

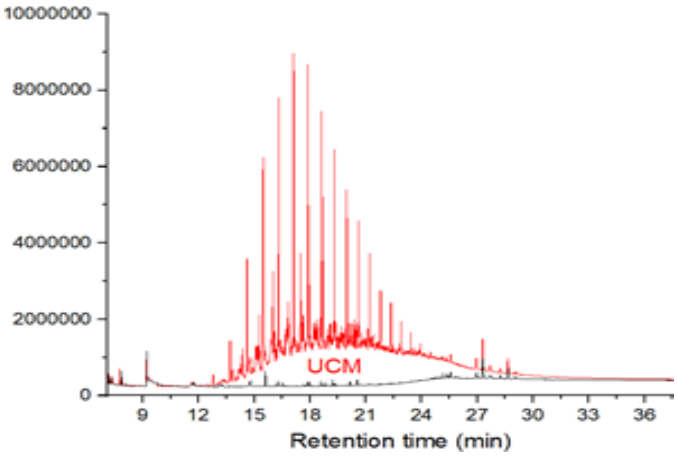

Figure 1. GC-FID chromatogram: red representing lepas (G1) with oil and black representing control sample (G5).

The pristane over phytane ratio (Pri/Phy) ranged from 0.78 to 0.92. The values of the ratios Pri/*n*C17 and Phy/*n*C18 range from 0.38 to 0.51 and from 0.49 to 0.72, respectively. Therefore, these results corroborate the petrogenic origin of the Has, since the ratio values are characteristic of crude oils.

In addition to HAs, 21 PAHs were analyzed in the organic extracts, in which the sum ranged from 476.33 to 3816.53 ng g^{-1}. Among these aromatic compounds are the 16 EPA (United States Environmental Protection Agency) priority PAHs, and also 1-methylnaphthalene, 2-methylnaphthalene, dibenzothiophene, benzo[e]pyrene, and perylene. Such compounds exhibit toxic, mutagenic, carcinogenic, and teratogenic characteristics (US EPA, 2014).

The following diagnostic ratios were evaluated to identify sources of PAH in Lepas: Fln/(Fln + Py) < 0.5, Fln/Pyr < 1 and ΣLMW/ΣLMW > 1, IP/ (IP + B(ghi)P) < 0. 5, Phe/Ant > 15, Naph/Phe > 1, Ant/(Ant + Phe) < 0.1, B(a)A/(B(a)A + Chry) < 0.2. These ratios and their values are associated with petrogenic inputs (Yunker et al., 2002; Budzinski et al., 1997; Stogiannidis and Lane, 2015). The petrogenic origin of the quantified PAHs was confirmed in at least 2 ratios proposed in the **Figure 2**.

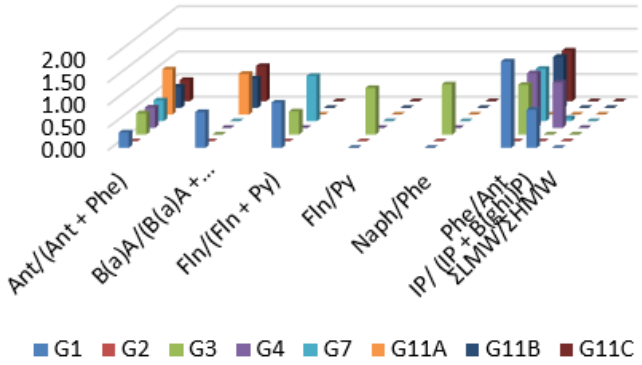

Figure 2. PAHs diagnostic ratios for the *Lepas anatifera*. Naph – naphthalene, Phe – phenanthrene, Ant – anthracene, Fln – fluoranthene, Py – pyrene, B(a)A – benz(a)anthracene, Chry – chrysene, IP - indeno[1.2.3-cd]pyrene, B(ghi)P - benzo[ghi]perylene. ΣLMW= PAHs with 2–3 rings/ ΣHMW = PAHs with 4–6 rings.

As highlighted by the results (**Figures 1** and **2**), the analyzed crustaceans presented contamination with compounds likely from the tarballs, whose toxicity levels can be extended to other organisms in the food chain when ingested (Rand et al., 1995; Gray, 2002).

Conclusions

This paper presents, to the best of our knowledge, the first report of the occurrence of *Lepas anatifera* in tarballs scattered along the Atlantic Ocean coast. The analysis of chemical markers allowed us to confirm the source of petrogenic origin, characterized mostly by the high concentration of low molecular weight PAH and also by the presence of UCM and some HA indicators of this source. This toxicity can be transferred to other individuals who feed on this Lepas species.

Acknowledgements

The authors thank PQ-2 Grant (308216/2017-2-CNPq), INCT-AmbTropic phase II (CNPq Process 465634/2014-1), and project “Dispersants and adsorbents for remediation of coastal areas affected by crude oil spills (Coast of Ceará, Northeast Brazil)” (440868/2020–3), both linked to MCTI Emergency Action to Combat the Oil Spill (2020), as well as Lemae/Finep/CNPq (380975/2022–0).

References

Budzinski, H., Jones, I., Bellocq, J., Pierard, C., Garrigues, P., 1997. Evaluation of sediment contamination by polycyclic aromatic hydrocarbons in the Gironde estuary. Mar. Chem. 58, 85–97.

Farrington, J. W., Quinn, J. G., 2015. “Unresolved Complex Mixture” (UCM): a brief history of the term and moving beyond it. Mar. Pollut. Bull. 96, 29–31.

Gray, J.S., 2002. Biomagnification in marine systems: the perspective of an ecologist. Mar. Pollut. Bull. 45, 46–52.

Yunker, M. B. et al. PHAs in the Fraser River basin a critical appraisal of PHA ratio as indicators of PAH source and composition. Organic Geochemistry, v.33, p. 489-515, 2002.

Rand, G.M., Wells, P.G., McCarthy, L.S., 1995. Introduction to aquatic ecology. In: Rand, G.M. (Ed.), Fundamentals of AquaticToxicology. Taylor and Francis, London, pp. 3–53.

Reddy, C.M., Eglinton, T.I., Palic, R., Benitez-Nelson, B.C., Stojanovic, G., Palic, I., Djordjevic, S., Eglinton, G., 2000. Even carbon number predominance of plant wax n alkanes: a correction. Org. Geochem. 31, 331–336.

Soares, M. O., Teixeira, C. E. P., Oliveira, A. H. B., Cavalcante, R. M., et. al. (2020). Oil spill in South Atlantic (Brazil): Environmental and governmental disaster. Marine Policy 115, 103879

Stogiannidis, Efstathios & Laane, Remi. (2015). Source Characterization of Polycyclic Aromatic Hydrocarbons by Using Their Molecular Indices: An Overview of Possibilities. Reviews of environmental contamination and toxicology. 234. 49-133.

US EPA. (2014). EPA’s priority pollutants List. United States Environmental Protection Agency, 1-2.

XVI LATIN AMERICAN CONGRESS ON ORGANIC GEOCHEMISTRY
9 - 11 AUGUST, 2023
ARACAJU, SERGIPE, BRAZIL

CAFFEINE AND CARBAMAZEPINE AS INDICATORS OF WASTEWATER CONTAMINATION IN THE BASIN OF PAQUEQUER RIVER (TERESÓPOLIS, RJ, BRAZIL)

ELINE S. GONÇALVES[a*]; MARCELO C. BERNARDES[a]; SARA RODRIGUEZ-MOZAZ[b,c]; MERITXELL GROS[b,c]; DAMIÀ BARCELÓ[b,d]; SILVANA V. RODRIGUES[a]; RICARDO E. SANTELLI[e]

[a]FEDERAL FLUMINENSE UNIVERSITY (UFF, NITERÓI, BRAZIL); [b]CATALAN INSTITUTE FOR WATER RESEARCH (ICRA-CERCA, GIRONA, SPAIN);[c]GIRONA UNIVERSITY (UdG, GIRONA, SPAIN) [d]INSTITUTE OF ENVIRONMENTAL ASSESSMENT AND WATER RESEARCH (IDAEA-CSIC, BARCELONA, SPAIN); [e]FEDERAL UNIVERSITY OF RIO DE JANEIRO (UFRJ, RIO DE JANEIRO, BRAZIL).

*e-mail: elinesg@gmail.com

Introduction

Water contamination is one of the environmental impacts that most affects human health and quality of life, and it is related to the provision of basic sanitation, which includes not only the proper disposal and treatment of domestic and industrial sewage, but also the provision of networks for clean water supply and its treatment. This issue becomes even more significant in situations of water scarcity faced by many people around the world [1].

Emerging contaminants have been arousing the interest of the scientific community and the general public due to their widespread use by the population in their day-to-day lives (as they are present in the composition of food, medications, personal care products such as creams, sunscreens, and even in the coatings of cookware) and their occurrence in the environment.

Caffeine is probably the most consumed stimulant in the world, although a small portion of the population consumes caffeine in pharmaceutical formulations, a large part of this alkaloid is ingested in the form of beverages and other food items. Several authors have proposed the use of caffeine as a tracer for domestic sewage effluents [2].

Carbamazepine is an anticonvulsant medication used in the treatment of epilepsy and neuropathic pain, has been frequently detected in the aquatic environment due to its resistance to degradation [3].

The objective of this study was to determine and compare the concentrations of caffeine and carbamazepine in natural water bodies with total dissolved nitrogen (TDN) and HPO_4^{2-} loads and evaluate their use as indicators of domestic sewage contamination.

Experimental

Study Area: The study area of this work involves the Paquequer River basin (Figure 1), in the municipality of Teresópolis, in the mountainous region of the state of Rio de Janeiro, Brazil. The headwaters of the Paquequer River are located within the Serra dos Órgãos National Park (PARNASO), and along its course, it passes through the entire urban zone of the municipality of Teresópolis, receiving loads of non-treated domestic sewage and impacted tributaries as well.

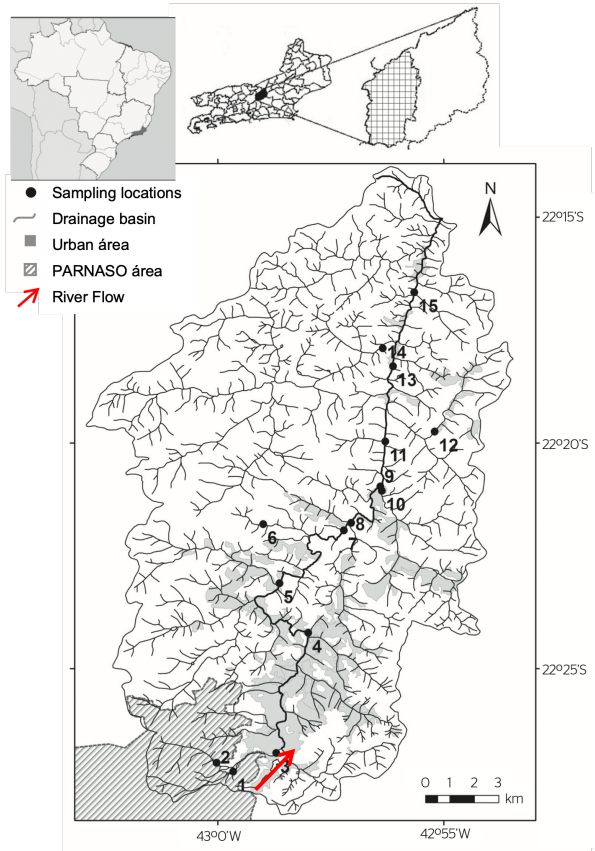

Figure 1. Sampling locations in Paquequer River Basin. Source: ALVIM et al. [4].

Sampling was carried out during the dry season (August 2010) at nine points along its main channel (P1, P3, P4, P5, P7, P9, P11, P13, and P15) and six points in some of its main tributaries (P2, P6, P8, P10, P12, and P14), considering the different land uses.

Caffeine and carbamazepine analysis: Extraction of the target compounds was done using solid-phase extraction cartridges (Strata-X^{TM}, 3 mL, 500 mg, Phenomenex). Instrumental analysis was carried out using a Waters Acquity Ultra-Performance^{TM} liquid chromatograph (UHPLC) system coupled to mass spectrometry using a 5500 QTRAP hybrid triple quadrupole-linear ion trap mass spectrometer (Applied Biosystems, Foster City, CA, USA) and controlled by Analyst 1.5.1 software.

Total Dissolved Nitrogen (TDN) and HPO_4^{2-} loads: These data were obtained and previously published by Alvim et al. [4] and Queiroz et al. [5].

Results and Discussion

The caffeine concentrations ranged from 13.6 ng L^{-1} (P2) to 26.9 µg L^{-1} (P4), being found in all analyzed samples. Carbamazepine was found in values very close to the quantification limit of the method at points within PARNASO (P1, P2, P3) and in some tributaries (P6, P10, P12), and the maximum value found at point P9, in the concentration of 74.5 ng L^{-1}.

The integration between the river discharge of each sampling location with the mass of an analyte allows to determine its river load along the basin, in a punctual and instantaneous way, but which can be predicted for a dry season [5]. The result of this analysis (Figure 2) shows the highest loads of contaminants coming from the urban area (P4, P5, P7), and the lowest in the most preserved areas and some tributaries (P1, P2, P3, P6); after the urban zone, a slight decrease in concentrations is observed, followed by constant levels until the end of the basin.

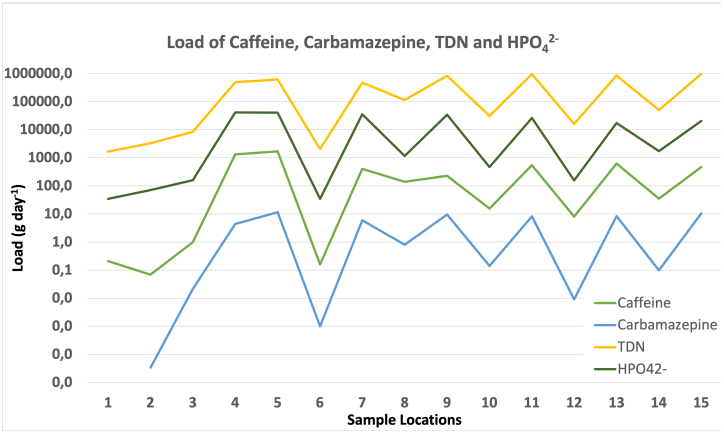

Figure 2. Load (g day^{-1}) in logarithm scale of caffeine, carbamazepine, TDN and HPO_4^{2-} in the sampling locations in Paquequer River Basin.

The river loads of caffeine and carbamazepine were compared to TDN and HPO_4^{2-} loads to assess the representativeness of these two compounds as indicators of domestic sewage. The results show that the loads of both compounds behave similarly along the basin, however in different orders of magnitude. The river loads found for carbamazepine are a thousand times less than the caffeine load.

Obviously, this difference between carbamazepine and caffeine is related to the wide and diverse consumption of caffeine by the population. Thus, these data corroborate even more with the establishment of the use of caffeine as an indicator of sewage.

Conclusions

The results obtained show the applicability of caffeine as a sewage indicator in concentration ranges close to other commonly used indicators, such as nitrogen and phosphorus. Its presence within preserved areas deserves further studies that consider possible natural sources. Carbamazepine, even present in low concentrations, may be more unambiguous as to human origin.

Acknowledgements

The authors wish to thank to Dr. William Z. Mello e Dr. Carla S. Silveira for providing the samples for this study. The fellowships were supported by the Coordenação de Aperfeiçoamento de Pessoal de Nível Superior (CAPES); This work was support by the Economy and Knowledge Department of the Catalan Government through a Consolidated Research Group (ICRA-ENV – 2021 SGR 01282); and the Spanish Ministry of Science and Innovation through CERCAGINYS program.

References

[1] Kiguchi, O.; Sato, G.; Kobayashi, T., 2016. Source-specific sewage pollution detection in urban river waters using pharmaceuticals and personal care products as molecular indicators. Environ Sci Pollut Res, 23, 22513-22529.

[2] Gonçalves, E. S.; Rodrigues, S. V.; Silva-Filho, E. V., 2017. The use of caffeine as a chemical marker of domestic wastewater contamination in surface waters: seasonal and spatial variations in Teresópolis, Brazil. Rev. Ambient. Água, 12, 192-202.

[3] Zind. H.; Mondamert, L.; Blancart-Remaury, Q.; Cleon, A. Karpel Vel Leitner, N.; Labanowski, J., 2021. Occurrence of carbamazepine, diclofenac, and their related metabolites and transformation products in a French aquatic environment and preliminary risk assessment. Water Research, 196, 117052-117064.

[4] Alvim, R. B.; Mello, W. Z.; Silveira, C. S.; Kligerman, D. C.; Ribeiro, R. P., 2014. Emissões de óxido nitroso em águas fluviais não poluídas e poluídas da Bacia do Rio Paquequer (Teresópolis, Rio de Janeiro). Eng. Sanit Ambient, 19, 471-472.

[5] Queiroz, L. A. V; Siveira, C. S.; De Mello, W. Z.; Alvim, R. B.; Vieira, M. D., 2012. Hidrogeoquímica e poluição das águas fluviais da bacia do rio Paquequer, Teresópolis (RJ). Geociências, 31, 606-621.

PHYSICO-CHEMICAL CHARACTERIZATION OF SEPETIBA AND ILHA GRANDE BAYS IN RIO DE JANEIRO.

NASCIMENTO, L.[a], BRANDINI, N. [a], ERBAS, T. [a], OLIVEIRA, B. [a], ABRIL, G. [a,b], MACHADO, W. [a], BERNARDES, M. [a]

[a]PROGRAMA DE PÓS-GRADUAÇÃO EM GEOCIÊNCIAS (GEOQUÍMICA), UNIVERSIDADE FEDERAL FLUMINENSE, NITERÓI, RJ, BRAZIL.
[b]BIOLOGIE DES ORGANISMES ET ECOSYSTÈMES AQUATIQUES (BOREA), UMR 7208, MUSÉUM NATIONAL D'HISTOIRE NATURELLE, CNRS, SU, UCN, UA, IRD, PARIS CEDEX 05, FRANCE

lorenasn@id.uff.br

Introduction

Coastal zones play a crucial role in biogeochemical cycles and have great ecological importance. However, in Brazil, most rivers that flow into coastal systems, such as bays and estuaries, have some impact that alters the quality and quantity of material transported from the continent to the oceans[1].

The excess of nutrients from anthropogenic sources, mainly linked to agricultural, domestic and industrial effluents, can result in environmental problems such as eutrophication[3].

Eutrophication is the process of enriching nutrients and organic matter in aquatic bodies that favor primary productivity[2, 5].

This work aimed to investigate the spatial variability of physico-chemical parameters of water quality in an estuarine complex formed by the Ilha Grande (IGB) and Sepetiba (SB) bays, located in the State of Rio de Janeiro.

Experimental

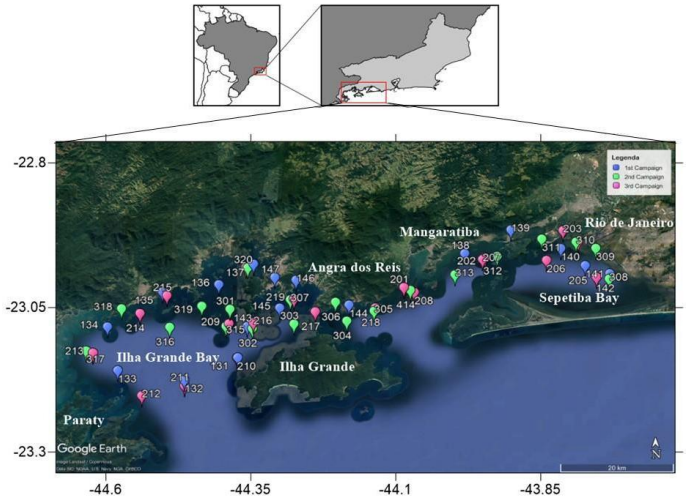

Figure 1. Study area and sampling stations for each campaign.

- Three campaigns were carried out (Sep/2021, Apr/2022, Sep/ 2022) resulting in 63 sampling points;
- N:P: Grasshoff et al., (1983);
- Chlorophyll: Strickland and Parsons (1972);
- SPM: Grasshoff et al., (1983);
- DO: Winkler's iodometric principle;
- Temperature, salinity and pH were measured with a Hanna HI9829 multiparameter probe, with a precision of: ± 0,15ºC (temperature), ± 0,01 (salinity) and ± 0,02 (pH).

Results and Discussion

Table 1 Mean and standard deviation of the analyzed parameters (secchi, salinity, temperature, pH, dissolved oxygen, MPS, chlorophyll-a and N:P ratio) for Ilha Grande Bay (IGB) and Sepetiba Bay (SB) in each campaign.

Campaigns	Secchi (m)	Sal	T (°C)	pH
SEP100	1.92 ± 0.69	29.69 ± 2.48	23.83 ± 1.23	8.47 ± 0.16
SEP200	4.19 ± 3.69	31.45 ± 2.65	26.01 ± 0.59	8.32 ± 0.08
SEP300	3.28 ± 2.24	32.32 ± 2.55	21.97 ± 0.16	8.32 ± 0.10
BIG100	7.32 ± 2.43	32.57 ± 1.52	24.12 ± 1.33	8.30 ± 0.05
BIG200	12.72 ± 4.16	33.81 ± 1.01	26.66 ± 0.85	8.26 ± 0.02
BIG300	6.40 ± 1.82	34.68 ± 0.62	21.68 - 0.55	8.23 ± 0.09

Campaigns	DO % Sat	SPM (mg/ L)	Chl-*a* (µg/m³)	N:P
SEP100	117.74 ± 26.94	7.35 ± 3.53	17.39 ± 12.95	34.01 ± 53.74
SEP200	118.81 ± 13.59	8.68 ± 6.81	9.99 ± 8.51	54.03 - 118.57
SEP300	99.01 ± 4.31	9.05 ± 7.28	8.13 ± 9.94	10.62 ± 15.60
BIG100	93.52 ± 17.84	2.19 ± 0.49	1.33 ± 1.02	7.38 ± 3.96
BIG200	105.58 ± 5.76	2.06 ± 0.65	0.63 ± 0.54	12.37 ± 11.00
BIG300	100.46 ± 4.64	6.32 ± 3.30	0.90 ± 0.28	2.70 ± 2.25

According to CONAMA resolution 357/2005, Sepetiba and Ilha Grande's bays are saline (>30). All campaigns had a pH consistent with the references established by CONAMA for saline water standards (8.3 - 8.7), with the exception of campaigns 200 and 3 in IGB. Ilha Grande bay presented DO% close to saturation in all campaigns, while SB presented means that indicated supersaturation in the first and second campaigns, which characterizes environments with high primary activity.

The SPM showed homogeneity between the 3 campaigns for SB, while the IGB was marked by an increase in the SPM in the third campaign, which can be explained by sediment resuspension due to rain during this sampling period.

Low concentrations of chlorophyll-a were found in IGB (<2.00 µg/L), while SB showed higher values, which can be related to more favorable conditions for phytoplanktonic growth due to nutrient availability and low circulation (>8 µg/L).

The mean N:P ratio was higher than the Redfield ratio (16:1) in campaigns 100 and 200 in Sepetiba bay, indicating a P limitation for primary production. For the bay of Ilha Grande it was shown that N was the limiting nutrient in every campaign, which is common in saline waters.

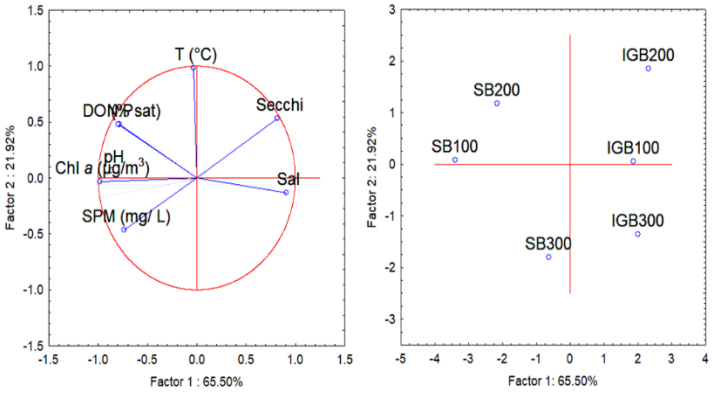

Figure 1. PCA performed with median of normalized data at the surface in the bays of Sepetiba and Ilha Grande: salinity (Sal), dissolved oxygen saturation (%DO), chlorophyll (Chl-*a* ug/L), of the ratios for N and P (N:P), suspended organic matter (SPM), secchi, temperature (T °C) and pH.

In figure 1 it is possible to see a PCA with the averages of each parameter for each campaign and bay. The first two components (PC1: 65.50% and PC2: 21.92%) accounted for 87.42% of the total variance. Secchi and Salinity parameters are related to all IGB campaigns while the other variables are related to SB. The main relationships correspond to factor 2 with the Sepetiba bay. DO and N:P parameters are positively related to each other and related to the SB200 campaign, as well as pH and chlorophyll-a are for SB100, which was characterized as a campaign in a rainy period.

Conclusion

The physico-chemical parameters of the bays presented a descriptive record during three campaigns. With the characterization applied, the BIG homogeneity and a good state of conservation were observed. Regarding SB, a higher primary production was identified by oxygen supersaturation and high chlorophyll values, with P as a limiting factor, probably due to a eutrophication process in the area.

This characterization in the SB highlights the need for public policies and public awareness of the threat posed by the process of eutrophication of coastal ecosystems.

Acknowledgements

The authors thank CAPES (PPG-Geoquímica-UFF), FAPERJ (Protocols: E-26/010.101117/2018, E-26/210.745/2021), CNPq (Proc. 309474/2022-1) and the VELITROP project.

References

[1] Barletta, M., Lima, A. R., & Costa, M. F., 2019. Distribution, sources and consequences of nutrients, persistent organic pollutants, metals and microplastics in South American estuaries. Science of the Total Environment, 651, 1199-1218.

[2] Cloern, J. E., 2001. Our evolving conceptual model of the coastal eutrophication problem. Marine ecology progress series, 210, 223-253.

[3] Dagg, M., Benner, R., Lohrenz, S., & Lawrence, D., 2004. Transformation of dissolved and particulate materials on continental shelves influenced by large rivers: plume processes. Continental shelf research, v. 24, n. 7-8, p. 833-858, 2004.

[4] Grasshoff, K; Ehrardt, M; Kremling, K., 1983. Methods of Seawater Analysis. Weinhein: Verlag Chemie.

[5] Nixon, S. W., 1995. Coastal marine eutrophication: a definition, social causes, and future concerns. Ophelia, 41(1), 199-219.

[6] Rybczyk, J. M., Day Jr, J. W., Yanez-Arancibia, A., & Cowan, J. H., 2012. Global climate change and estuarine systems. Estuarine Ecology, p. 497-518, 2012.

[7] Strickland, J. D. H., & Parsons, T. R., 1972. A practical handbook of seawater analysis.

Transport of terrigenous organic matter to the ocean related to precipitation events during the last 18,000 years in the Amazon Basin.

GOMES, S. G. [a*]/ **RODRIGUES, A.M. S.** [a] / **VENANCIO, I. M.** [a]/ **BERNARDES, M. C.** [a]

[a]**Programa de Pós-Graduação em Geoquímica Ambiental, Universidade Federal Fluminense, Niterói, Brazil**.

e-mail: gabrielasg@id.uff.br

Introduction

Paleoclimate reconstructions in the Amazon Basin provide us with crucial information on how changes in climate (i.e. temperature and precipitation) altered vegetation and affected the transport of organic matter (O.M.) to the ocean {6}. However, the heterogeneity of the basin makes it difficult to understand these processes as the different study sites are not representative for the whole basin, the lack of continuity in the records and the different topographic settings {1}. Thus, an approach that integrates large-scale climate events is necessary, such as the use of proxies that help understand changes in the dynamics of transport of materials from the continent to the ocean. This work evaluated the main events that have occurred over the last 18,000 years in the Amazon Basin, related to climate change and its influence on the transport of terrestrial organic matter to the ocean.

Experimental

This work is centered on the study of core GL-1251 (1°06.83'N; 45°08.0'W) (Fig. 1), provided by Petrobrás for the ASpECTO project which is part of the IODP - CAPES program. GL-1251 is 20 meters long and was collected in an area with a water column of 1,968 meters. It is located in the area of influence of the Amazon mouth sedimentary basin, and comprises the last 18,000 years approximately. The Ti intensities of the core were obtained by scanning the core surface of the half-file with the X-ray Fluorescence Core Scanner II (AVAATECH Serial No. 2) at MARUM, University of Bremen (Germany).

For the characterization of phenols originating from lignin in sediment samples, oxidative degradation in a basic medium with copper oxide (CuO) {5}. The analyses were performed on an Agilent 7890A gas chromatograph coupled to a flame ionizing detector (GC-FID) and HP-5 capillary column (30 meters long, 0.32 mm internal diameter, 0.25 µm film thickness). The results of the amount of lignin - λ8 (mg/100 mg CO^{-1}) are expressed as mg per 100 mg Organic Carbon of the sample.

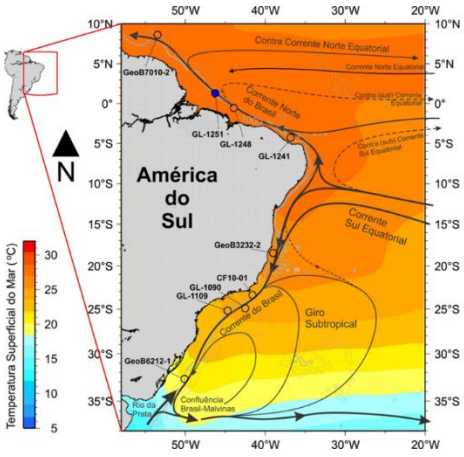

Figure 1. Location map of GL-1251, at the mouth of the Amazon River (blue dot).

Results and Discussion

The Ti records (Fig 2a.) obtained from the GL- 1251 core, show increasing values during the Heinrich Stadial 1 (HS1) event, with a peak during 14,000 years, which can be characterized as a wet period and with intense precipitation events {4, 9}. These values are accompanied by a maximum of 1.4 % total organic carbon (TOC) (Fig. 2b), and increase in lignin (λ8) values (Fig. 2c) which shows a peak of 1.9 mg/100mgCO at the end of this period. A higher Ti/Ca content reflects a higher terrigenous input from river runoff, indicating periods of higher precipitation {9; 6}. In this period some authors have reported that there was an expansion of the Amazon forest with a possible stabilization of vegetation {2, 3}. At the end of the YD, a change from wetter to drier climate occurs, which directly influenced the vegetation, as well as there was a decrease in precipitation, which has been recorded in studies on lower lake levels in this period {3, 9}, which can be seen in Fig 2, where the Ti and lignin data show

a decrease only at the end of the YD, while carbon decreases at the very beginning, in about 13,000 years, which can be explained as this climate change response and which influences the quality of the transported TOC {9} .

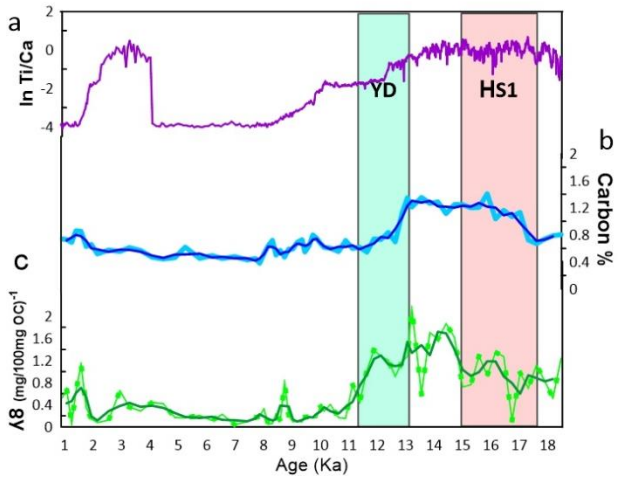

Figure 2. Relation of Titanium and Calcium in purple (a). Terrestrial organic carbon in light blue and medium in dark blue (b). Lignin in green light and medium in dark green (c). YD (blue rectangle) and HS1 (pink rectangle) events.

Between 10,000-6,000 low TOC and lignin values can be observed, probably because of the large surface drag from the intense precipitation, which may have remobilized the carbon that was already incorporated in the soil, characterized by the decrease of lignin and because the vegetation was not yet consolidated {1, 2, 9}. Increasing Ti/Ca values were observed after 4,000 years, accompanied by a small increase in lignin, which was indicated by some studies that in this period of the Holocene pollen studies in Amazonian lakes and vegetation modifications indicated that there was an expansion and modification of the forest, with an increase in precipitation {3, 8}.

Conclusions

The data obtained from the sedimentary core show that abrupt climatic variations generate changes in the precipitation regime in the Amazon Basin thus influencing changes in terrigenous organic carbon transport, which was presented by high values of Ti/Ca, TOC, and lignin highlighting periods of greater erosion during HS1. In the YD occurs a change from humid to dry climate, as well as lower precipitation values that influence the transport of TOC, demonstrating high chemical weathering through high Ti/Ca values, thus presenting the importance of these climatic changes in the burial of carbon.

Acknowledgements

The authors thank CAPES cod. (PPG-Geoquímica-UFF); FAPERJ (Procs. E-26/010.101117/2018, E-26/210.745/2021); CNPQ (Proc. 309474/2022-1).

References

Absy, M. L.; Silva, S. A. F. 2009. Registros Palinológicos das Mudanças Climáticas na Amazônia Brasileira Durante o Neógeno. p. 9.

Arruda D. M; Schaefer C.E.G.R; Fonseca R.S, Solar; R.R.C, Fernandes-Filho EI. 2011.Vegetation cover of Brazil in the last 21 ka: New insights into the Amazonian refugia and Pleistocenic Behling H. Holocene environmental dynamics in coastal, eastern and central Amazonia and the role of the Atlantic sea-level change. Geographica Helvetica. 6 (3): 208-216.

Behling, H., 2002. Carbon storage increases by major forest ecosystems in tropical South America since the last glacial maximum and the early Holocene. Glob. Planet. Change 33, 107-116.

Cruz, F. W.; Vuille, M.; Burns, S. J.; Wang, X.; Cheng, H.,Werner, M.; Edwards, R. L., Karmann, I.; Auler, A. S.; Nguyen, H.. 2009. Orbitally driven east–west antiphasing of South American precipitation. Nature Geoscience, v. 2, n. 3, p. 210–214, mar.

Goñi, M.A.; Hedges, J.I. 1990. Cutin-derived CuO reaction products from purified cuticles and tree leaves. Geochimica et Cosmochimica Acta, v. 54, p.3065-3072.

Govin, A.; Holzwarth, U., Heslop, D., Ford Keeling, L., Zabe, M. l, Mulitza, S., Collins, J. A.; Chiessi, C. M. 2012. Distribution of major elements in Atlantic surface sediments (36°N–49°S): Imprint of terrigenous input and continental weathering, Geochem. Geophys. Geosyst., 13.

Jennerjahn, T. C., Ittekkot, V., Arz, H. W., Behling, H., Patzold, J., & Wefer, G. 2004. Asynchronous terrestrial and marine signals of climate change during Heinrich events. Science, 306 (5705), 2236-2239.

Fontes, D.; Cordeiro, R.C.; Martins, G.S.; Behling, H.; Turcq, B.; Sifeddine, A.; Seoane, J.C.S.; Moreira, L.S.; Rodrigues, R.A. 2017. Paleoenvironmental dynamics in South Amazonia, Brazil, during the last 35,000 years inferred from pollen and geochemical records of Lago do Saci. Quaternary Science Reviews, v. 173, p. 161-180.

Zhang, Y., Chiessi, C. M., Mulitza S., Zabel M., Trindade, R.I.F., Hollanda, M. H. B.M., Dantas, E. L., Govin, A., Tiedemann, R., Wefer G. 2015. Origin of increased terrigenous supply to the NE South American continental margin during Heinrich Stadial 1 and the Younger Dryas. Earth and Planetary Science Letters, v. 432, p. 493-500.

XVI LATIN AMERICAN CONGRESS ON ORGANIC GEOCHEMISTRY
9 - 11 AUGUST, 2023
ARACAJU, SERGIPE, BRAZIL

Iron and Trace Metals Geochemistry in Marine Sediments from Continental Shelf of Doce and Jequitinhonha Rivers, Brazil

[1]SALAZAR, J. M. [1]NAVAS, G. A., [1]MOREIRA, M., [1]NÓBREGA, G., [2]ALBUQUERQUE, A. L., [3]BAHR, A., [1]DÍAZ, R.

1. Programa de Geociências (Geoquímica), Universidade Federal Fluminense, Niterói, Brazil.

2. Departamento de Geologia e Geofísica da Universidade Federal Fluminense, Niterói, Brazil.

3. Institute of Earth Sciences, Heidelberg University, Heidelberg, Germany.

*Corresponding author: javiersalazar@id.uff.br

Introduction

On November 5, 2015, one of the worst environmental accidents in Brazil history occurred, because of the collapse of the Fundão tailings dam (Minas Gerais state, SE-Brazil). The tailings flow reached the Doce river (DR), which is one of the main sediment sources for the continental shelf (148-ton km^2 / year). The tailings reached the Atlantic Ocean, on November 22 (2015). The collapse contributed with $60x10^6m^3$ of tailings, which are generated mainly by the iron minerals extraction (mostly crystalline Fe oxyhydroxides like hematite and goethite) [1][2].

Consequently, the mining tailings' arrival on the coastal environment, may have increased iron, manganese and trace metals concentrations, also modifying the dynamics of marine sediments. Where the study of their distribution in coastal sediments is essential for pollution and bioavailability determination [3][4][5].

In this sense, Fe, Mn and trace metals, have their bioavailability and behavior controlled mainly by the redox conditions and organic matter content [5][6]. In this context, this work evaluated the sedimentary geochemistry of Fe, Mn and trace metals, to evaluate the mining tailings effect on the fractionation and bioavailability of trace metals in marine sediments from Doce river discharge zone.

Experimental

The marine sediment core was collected on the continental shelf, in the Doce river discharge zone, during the research vessel R/V Meteor trip number M125 [7]. The depth and length of the core were 24 m and 29 cm respectively. The core was sliced every 1 cm and preserved in zinc acetate.

Sequential Extraction: The method proposed by [3] was used, obtaining two operationally defined fractions: reactive and pyritic.

Briefly, the reactive fraction was extracted using HCl 1M, and the extract was collected after centrifugation. To the residue from the HCl extraction, HF 10 M was added agitated to remove the silicate phase. Subsequently, the solid residue from the previous extraction was treated with concentrated H_2SO_4 to remove the organic matter. Finally, the extraction of the pyrite fraction was performed by adding concentrated HNO_3 to the sediment residue and shaking. The fractions were analyzed using the Optical Emission Spectrometry with an Inductively Coupled Plasma source (ICP - OES).

Acid volatile sulfides (AVS) and Chromium-reducible sulfide (CRS) Extraction: Were extracted the AVS, using 1g of wet samples, in an inert atmosphere, carried out at room temperature with HCl (6M), where the released H_2S was precipitated as zinc sulfide (ZnS) [8]. The sulfide concentration was measured in a UV spectrophotometer [9].

Results and Discussion

The highest concentrations for the Doce river core, were found above 16 cm depth for all metals studied, iron and trace metals. With a tendency throughout the core to increases the concentration with depth (Figure 1a, 1b e 1c). These results suggest that significant amounts of iron oxyhydroxides associated with tailing were delivered after dam rupture, where the trace metals are associated with the oxyhydroxides present in the reactive fraction.

These metals might be released from the oxyhydroxides to the water column or interstitial water as a result of changes in redox conditions, increasing their availability to be incorporated into other mineral phases such as AVS, organic matter and/or pyrite, according on their availability, organic matter reactivity, redox conditions and the metal thermodynamics [3][10][11].

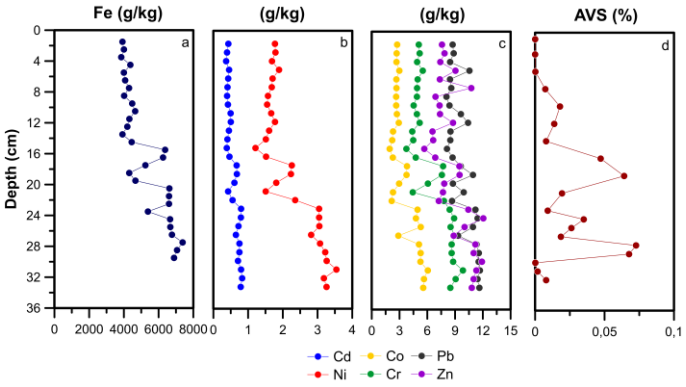

Figure 1. Fe (a) and Trace Metals (b,c) content in Reactive Fraction and AVS (d) concentration with depth for Doce River.

In this sense, the content of iron monosulfides or AVS, can be directly related to the metal's behavior found in the reactive fraction. Since the AVS have two accumulation zones, especially one at 16 cm deep (Figure 1d). Where this accumulation zone may be associated with the reactive iron arrival and its subsequent sulfurization, forming iron monosulfides and indicating in turn the tailings influence on the sediments [12]. Furthermore, there is no depletion of Fe at this point, as consequence of the constant supply of reactive iron to the environment from the tailings.

The second accumulation zone of AVS about 26cm depth), can be related to monosulfides that have not yet been transformed into pyrite [13]. Furthermore, AVS can be preserved in recent sediments as a consequence of rapid sedimentation [14][15], as reported in Kau Bay, Indonesia [15] and Saguenay Fjord, Canada [14] and probably the Doce River discharge zone, as a consequence of the tailings arrival, which increased suspended particulate material (SPM) from 100 mg L^{-1} to 9000 mg L^{-1}, according to [16].

Conclusions

The arrival of mining tailings to the Doce river discharge zone, as consequence of the *Fundão* dams rupture, brought high concentrations of reactive iron and trace metals to the coastal sediments, affecting the redox conditions and favored the formation of iron monosulfides (AVS), which are evidence the effect on the dynamics of the sediments present at the discharge zone from Doce river by arrival of the mining tailings.

Acknowledgements

Thanks to the support by CAPES and FAPERJ, the Geosciences Program (Geochemistry) from Universidade Federal Fluminense (UFF) and Anthropocene Geochemistry and Oceanography and Paleoceanography laboratories from UFF.

References

[1] Marta-Almeida, M.; Mendes, R.; Amorim, F.; Cirano, M.; Dias, J., 2016. Fundão Dam collapse: Oceanic dispersion of River Doce after the greatest Brazilian environmental accident. Marine Pollution Bulletin 112, 359 - 364.

[2] Queiroz, H., Ferreira, T., Barcellos, D., Nóbrega, G., Antelo, J., Otero, X., Bernardino., 2021a. From sinks to sources: The role of Fe oxyhydroxide transformations on phosphorus dynamics in estuarine soils. Journal of Environmental Management 278, 111575.

[3] Huerta-Díaz, M.; Morse, J. A., 1990. Quantitative Method for Determination of Trace Metal Concentrations in Sedimentary Pyrite. Marine Chemistry 29, 199–144.

[4] Tessier, A.; Fortin, D.; Belzile, N.; Devitre, R.; Leppard, G., 1996. Metal sorption to diagenetic iron and manganese oxyhydroxides and associated organic matter: Narrowing the gap between field and laboratory measurements. Geochimica et Cosmochimica Acta 60, 387–404.

[5] Buccolieri, A.; Buccolieri, G.; Cardellicchio, A.; Dell´Atti, A.; Di Leo, A.; Maci, A., 2006. Heavy metals in marine sediments of Taranto Gulf (Ionian Sea, Southern Italy). Marine Chemistry 99, 227 – 235.

[6] Berner, R.,1984 Sedimentary Pyrite Formation: An update. Geochimica et Cosmochimica Acta 48, 605 – 615.

[7] Bahr, A. *et al.,* 2016. South American Hydrological Balance and Paleoceanography during the Late Pleistocene and Holocene (SAMBA). METEOR-Berichte 125.

[8] Fossing, H.; Jørgensen, B., 1989. Measurement of Bacterial Sulfate Reduction in Sediments: Evaluation of a Single-Step Chromium Reduction Method. Biogeochemistry 8, 205 – 222.

[9] Cline, J., 1969. Spectrophotometric Determination of Hydrogen Sulfide in Natural Waters. Limnology and Oceanography, Baltimore 14, 454 – 458.

[10] Álvarez-Iglesias, P.; Rubio, B., 2008. The degree of trace metal pyritization in subtidal sediments of a mariculture area: Application to the assessment of toxic risk. Marine Pollution Bulletin 56, 973–983.

[11] Díaz, R. *et al*., 2012. Early diagenesis of sulfur in a tropical upwelling system, Cabo Frio, southeastern Brazil. Geology 40, 879-882.

[12] Queiroz *et al*., 2018. The Samarco mine tailing disaster: a possible time-bomb for heavy metals contamination?. Science of the Total Environment, 637 – 638.

[13] Wijsman, J.; Middelburg, J.; Herman, P.; Böttcher, M.; Heip, C., 2001. Sulfur and iron speciation in surface sediments along the northwestern margin of the Black Sea. Marine Chemistry 74, 261–278.

[14] Gagnon, C.; Mucci, A.; Pelletier, E., 1995. Anomalous accumulation of acid-volatile sulphides (AVS) in a coastal marine sediment, Saguenay Fjord, Canada. Geochimica et Cosmochimica Acta 59, 2663 – 2675.

[15] Middelburg, J., 1991. Organic carbon, sulphur, and iron in recent semi-euxinic sediments of Kau Bay, Indonesia. Geochimica et Cosmochimica Acta 55, 2663 – 2675.

[16] Quaresma, V. *et al.,*2015. Modern sedimentary processes along the Doce river adjacent continental shelf. Brazilian Journal of Geology 45, 635 – 644.

Ulva lactuca phytoremediation of nitrogen and phosphorus compounds of an eutrophic tropical coastal lagoon

Tácila Oliveira Pinto De Freitas* (PG)[a], Vinícius Latgé Meira (IC)[a], Vinícius Peruzzi De Oliveira (PQ)[b,c], Wilson Thadeu Machado (PQ)[a], Julio Cesar Wasserman (PQ)[a]

[a]Programa de Pós-Graduação em Geoquímica - Universidade Federal Fluminense; [b]Departamento de Biologia Marinha - Instituto de Biologia - Universidade Federal do Rio de Janeiro; [c]Unidade Multiusuário de Análises Ambientais - Universidade Federal do Rio de Janeiro
*tacilafreitas@id.uff.br

Introduction

Coastal lagoons are important water bodies that can be indicators of environmental quality, because they are sensitive and vulnerable to human activities. The anthropic impacts often lead to a decrease in their biodiversity and degradation of the quality of their waters [1]. Due to the disposal of domestic sewage and the consequent nutrient enrichment, the lagoon of Marapendi – Rio de Janeiro has suffered from intense eutrophication process, displaying bad to awful situation according to the INEA (Regional Environmental Agency) classification index [2]. Therefore, aiming the improvement of the water quality, an *in vitro* experiment was performed using *Ulva lactuca* as a bioremediator agent to reduce the nutrients concentrations in the eutrophic water.

Experimental

Water samples were collected from the lagoon of Marapendi/RJ (lat:-23.007477; long:-43.3853893) and seaweeds were collected from Praia Vermelha/RJ beach's rocky shores. The experiment carried out at 24.4 ± 0.8 ºC and salinity was 13 PSU in cultivation chambers at UFRJ. The experiment followed the proportion 1 (g) of fresh biomass for 1 (L) water, performed in triplicates, with controls for 12 days long (Figure 1).

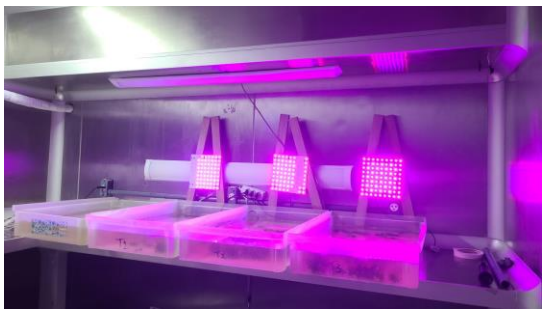

Figure 1. Experiment performed in cultivation chamber at Federal University of Rio de Janeiro.

Results and Discussion

The mean concentrations of nutrients in the water in time 0 (beginning of the experiment) were respectively 71.74 ± 1.42 µmol L^{-1}, 1.57 ± 0.17 µmol L^{-1}, 0.99 ± 0.08 µmol L^{-1}, 19.25 ± 0.11 µmol L^{-1} for NH_4^+, NO_3^-, NO_2^- and PO_4^{3-} (Figure 2).

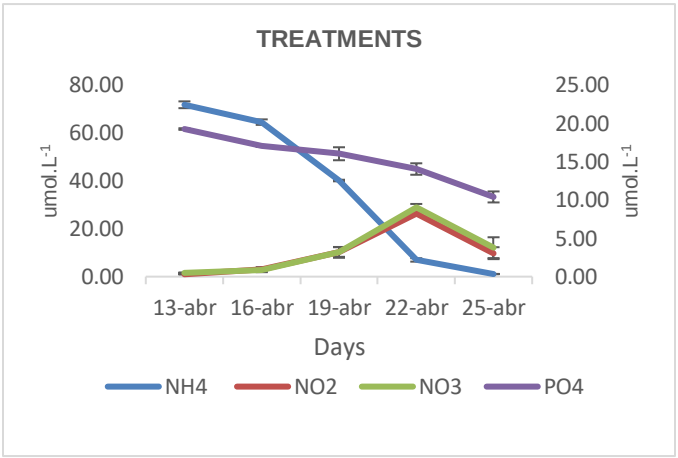

Figure 2. Consumption of nitrogenous and phosphorous compounds by *U. lactuca* in water of lagoon on a 12 days experiment.

Ammonium was the most rapidly consumed species which reinforces the idea that, as Ulva is considered an ammoniophilic genus [3, 4]. Besides, NH_4^+ reduces the uptake and assimilation of nitrite and nitrate. This pattern was also observed in the literature [5], which tested petroleum field wastewater. The efficiency of nutrient removal after the experiment was 99.96%, 58.16%, 62.73% and 80.05% for NH_4^+, NO_3^-, NO_2^- and PO_4^{3-}, respectively. From the nutrient concentrations decay curves, it was possible to notice that two processes occurred simultaneously in the system: the natural oxidation of NH_4^+ to NO_3^- and NO_2^- and the nitrification of

NH_3 by the macroalgae. Ammonium absorption occurred quickly, so that on the nineth day of the experiment, the concentration had already reached a minimum value. The decrease in NH_4^+ concentration was followed by an increase of NO_3^- and NO_2^- concentrations in tanks so the peaks of NO_3^- (28.91 ± 1.43 µmol.L^{-1}) and NO_2^- (26.29 ± 0.05 µmol.L^{-1}) were associated with low ammonium values (6.97 ± 0.73 µmol.L^{-1}). The N/P ratio in the water can heavily influence the nutrient uptake of aquatic environments, and the algae requirement for N is higher than P [6]. The N/P ratio in water samples at time 0 was 3.86, indicating a severe nitrogen limitation. As NO_3^- and NO_2^- become the most abundant nitrogen forms, the consumption of these nutrients by the macroalgae started and soon reached exhaustion, while NH_4^+ continued to be naturally oxidized. PO_4^{3-} absorption was also measured over the days. Low N/P ratios are indicative of environment eutrophication since the growth of macroalgae becomes limited by the restricted availability of N, while the growth of species capable of fixing atmospheric N_2 is favored, promoting cyanobacterial blooms [7].

Conclusions

Despite the stressful environmental conditions in which the algae were cultivated (low O_2 concentration, low salinity water), *U. lactuca* performed well as a phytoremediating agent and was able to remove high concentrations of nutrients from the lagoon of Marapendi water in just a few days of cultivation. Future analyses of the CNP contents will be realized in the treatment and control filters for a better understanding of the processes that occurred in the system.

Acknowledgements

The authors thank the financial support and scholarships of CAPES (Coordenação de Aperfeiçoamento de Pessoal de Nível Superior - Brazilian research funding agency) (Grant # 001). JCW also thanks CNPq (Conselho Nacional de Desenvolvimento Científico e Tecnológico) for a fellowship (grant # 310425/2020-4).

References

[1]Christelle Audouit, Vanina Pasqualini , Rutger De Wit, Hervé Flanquart, Philippe Deboudt, Caroline Rufin-Soler. 2019. Comparing social representation of water quality in coastal lagoons with normative use of ecological indicators. Marine Policy, Volume 101, 137-146**.**

[2] Instituto Estadual do Ambiente – INEA. Secretaria do Ambiente e Sustentabilidade. LAGOAS DE JACAREPAGUÁ - Boletim nº 4 - Outubro de 2021 (medição em 05/10/2021). Rio de Janeiro, 2021.

[3] D'Elia, C. F., and J. A. DeBoer. 1978. Nutritional studies of two red algae. II. Kinetics of ammonium and nitrate uptake. J. Phycol. 14:266–272

[4] Schuenhoff, A., L. Mata, and R. Santos. 2006. The tetrasporophyte of Asparagopsis armata as a novel seaweed biofilter. Aquaculture 25, 2:3–11.

[5] Vinícius Peruzzi de Oliveira, Nuno Tavares Martins, Pâmela de Souza Guedes, Ricardo César Gonçalves Pollery and Alex Enrich-Prast. 2016. Bioremediation of nitrogenous compounds from oilfield wastewater by Ulva lactuca (Chlorophyta). Bioremediation Journal, 20:1, 1-9.

[6] Liu Junzhuo, Vyverman Wim. 2015. Differences in nutrient uptake capacity of the benthic filamentous algae *Cladophora* sp., *Klebsormidium* sp. and *Pseudanabaena* sp. under varying N/P conditions. Bioresource Technology**,** 179, 234-242.

[7] Cotovicz Júnior, L. C., Brandini, N., Knoppers, B. A., Mizerkowski, B. D., Sterza, J. M., Ovalle, A. R. C., Medeiros, P. R. P. 2013. Assessment of the trophic status of four coastal lagoons and one estuarine delta, eastern Brazil. Environmental Monitoring and Assessment, 185, 3297-3311.

XVI LATIN AMERICAN CONGRESS ON ORGANIC GEOCHEMISTRY
9 - 11 AUGUST, 2023
ARACAJU, SERGIPE, BRAZIL

SPATIAL DISTRIBUTION OF THE COASTAL REGION OF RIO DE JANEIRO: NITROGEN AND PHOSPHORUS IN SEPETIBA AND ILHA GRANDE BAYS

***[1]BRANDINI, N.; [1]OLIVEIRA, G.B.; [2]ERBAS, T.; [1]NASCIMENTO, L.S.; [1]KNOPPERS, B.A.; [1]BERNARDES, M.C.; [1]MACHADO, W.T.V.; [3]ABRIL, G.**

[1]PROGRAMA DE PÓS-GRADUAÇÃO EM GEOCIÊNCIAS (GEOQUÍMICA), UNIVERSIDADE FEDERAL FLUMINENSE, NITERÓI, RJ, BRAZIL. [2]PROGRAMA DE PÓS-GRADUAÇÃO EM BIOLOGIA MARINHA E AMBIENTES COSTEIROS, UNIVERSIDADE FEDERAL FLUMINENSE, NITERÓI, RJ, BRAZIL. [3]LABORATOIRE DE BIOLOGIE DES ORGANISMES ET ECOSYSTÈMES AQUATIQUES (BOREA), MUSÉUM NATIONAL D'HISTOIRE NATURELLE, CNRS, PARIS, FRANCE

e-mail: nbrandini@id.uff.br

Introduction

Coastal systems, such as estuaries and bays, are water bodies surrounded by land that have oceanic water input, shelter diverse ecosystems, and have high biodiversity, in addition to being often conducive to the development of economic activities[1]. Among the factors that impact coastal aquatic systems, eutrophication is one of the most recurrent processes that cause significant changes at different levels of the trophic chain, as it alters the biogeochemical cycles of carbon, nitrogen and phosphorus[2]. Nitrogen (N) and phosphorus (P) are the main nutrients needed for the growth of all organisms, such as plants and phytoplankton in the oceans[3]. N and P can be present in inorganic, organic, dissolved and particulate forms, and the cycling of these nutrients is dependent on hydrodynamics, circulation, and residence time, acting on the intensification and remineralization of the different forms of organic matter (OM). The dissolved and organic forms of nutrients in seawater are part of the metabolic processes in coastal systems, contributing to the production and regeneration of OM, which can undergo degradation through an oxidation process as it reaches the sediment layer4. The objective of this study was to evaluate the spatial distribution of nutrients in nitrogen and phosphate forms in three campaigns (n=120, surface and bottom) distributed in the Sepetiba (SEP) and Ilha Grande (BIG) bays located in the state of Rio de Janeiro (RJ) on the SE coast of Brazil.

Material and methods

The bays of Sepetiba (SEP) and Ilha Grande (BIG) are in the coastal region of the State of Rio de Janeiro. The SEP (22º53'S – 23º05'S and 43º35'W – 44º03'W; As= 447 km^2; Z m= 8.6 m; Ab= 2711 km^2) has a drainage basin with about half a million inhabitants and a large industrial area. The BIG (23º00'S – 23º18'S and 44º00'W – 44º40'W; As= 800 km^2; ZM = ± 20 m; Ab= 1740 km^2) is in a region of great influence from the sea, with area conservation, and its drainage basin has the approximate presence of 205 thousand inhabitants.

The data analyzed are from the Brazil/France agreement project (VELITROP - International Research Project CNRS-INEE), and the campaigns (VLT100/Nov/21, VLT200/Apr/22 and VLT300/Sep/22) were carried out with surface and bottom water sampling using a 5L Niskin bottle. Some parameters (T, salt, pH and %DO) were obtained in situ using the HANNA-HI9829 probe. In the laboratory, the analysis of inorganic (DIN, DIP) and organic nutrients (DON, DOP) were executed after filtration, following the methodology of[5], Chlorophyll contents (GF/F 0.7 µm) was evaluated according to[6].

Preliminary Results

The data distribution of the variables (salt, %DO, Cl-a, and N:P, DON:DOP, TN:TP ratios) in surface and deep waters in the VLT100, VLT200 and VLT300 campaigns are shown in Fig. 1. Differences between surface and bottom, were observed in all campaigns. As for the N:P ratio of the dissolved form (organic and total), according to Redfield (1934) of 16N:1P, the BIG campaigns indicate that the waters have nitrogen as a limiting nutrient and a low concentration of chlorophyll. On the other hand, the SEP showed decreasing values near the coast for the total phosphorus ratios with an increase in the chlorophyll concentration, indicating a limitation of DIP mainly in the VLT100 and VLT300 campaigns (Fig. 1). Concerning the inorganic, organic and dissolved and total fractions for the DIN:DIP, DON:DOP and TN:TP ratios, it suggests a tendency for the entry mainly of dissolved organic forms by the contribution of continental drainage in Sepetiba Bay, which is corroborated by chlorophyll contents and %OD. On the other hand, BIG with low chlorophyll content, low N:P ratio and high

*[1]BRANDINI, N.; [1]OLIVEIRA, G.B.; [2]ERBAS, T.; [1]SAMPAIO, L.; [1]KNOPPERS, B.A.; [1]BERNARDES, M.; [1]MACHADO, W.T.V.; [3]ABRIL, G.

salinity with oligotrophic characteristics, suggests a greater influence of oceanic waters.

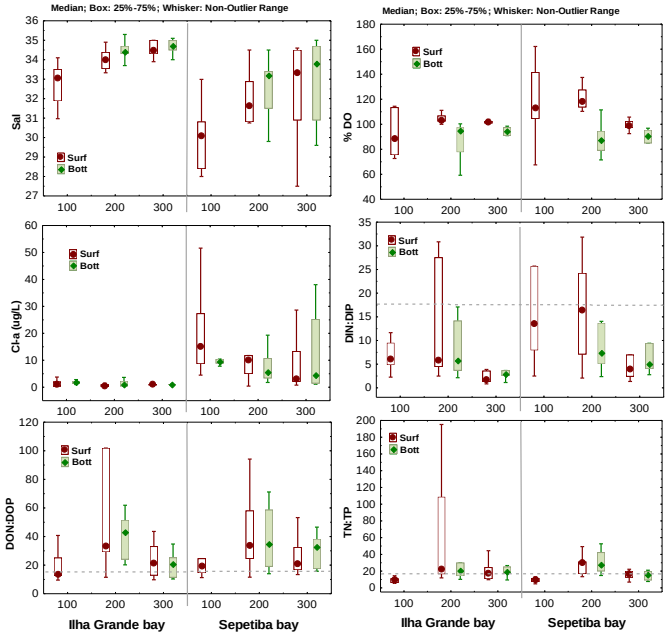

Figure 1. Median values at the surface (● Surf) and bottom (o Bott) in the bays of Sepetiba and Ilha Grande: salinity (Sal), dissolved oxygen saturation (%DO), chlorophyll (Cl-a ug/L), of the ratios for N and P (inorganic, organic and dissolved). Vertical lines separate the SEP and BIG bays, and the dashed lines are the ratio of Redfield ratios (16N:1P).

Principal component analysis (PCA), was performed to identify the dominant factors that contributed to the variation in the data set separating the bays7 (Canuel, 2001), which presented two main factors (F1 and F2), totaling 72.57%, which made it possible to separate the SEP bay on the left side and the BIG on the right side, the variables (n=13) used were: Secchi, Salt, T(ºC), pH, %DO, Cl-a, TP, DOP, DIP, TN, DON, DIN, N:P. The data obtained were normalized and evaluated by PCA statistical analysis using the STATISTICA program, version 10, StatSoftInc, USA (Fig. 2). Evaluating the PCA mean data in Figure 2, the variables Secchi (8.63 ± 3.9 m), Salinity (33.6 ± 1.41) and DIP (0.20 ± 0.11 uM), which were related to Ilha Grande bay (BIG - surface and bottom) for all campaigns, while nutrients, in general, were referred to Sepetiba bay (SEP). In the upper left quadrant, pH (8.4 ± 0.14), DOP (0.65 ± 0.35 uM), DIN (5.69 ± 10.5 uM), TP (1.58 ± 12.5 uM) and chlorophyll (ug/L) were mainly related to the VLT100 campaign because it was a rainy season.
In the lower left quadrant, the TN (22.9 ± 15.3 uM), %DO (111.8 ± 19.8), DON (17.2 ± 10.8 uM), and the N:P ratio is mainly related to campaigns VLT100 and VLT200 (SEP - 32.2 ± 72.51) while BIG presented an N:P ratio of 7.62 ± 7.74. The VLT200 campaign had a more pronounced difference between the surface and the background, as it was a period of little rain and higher temperatures compared to the other campaigns.

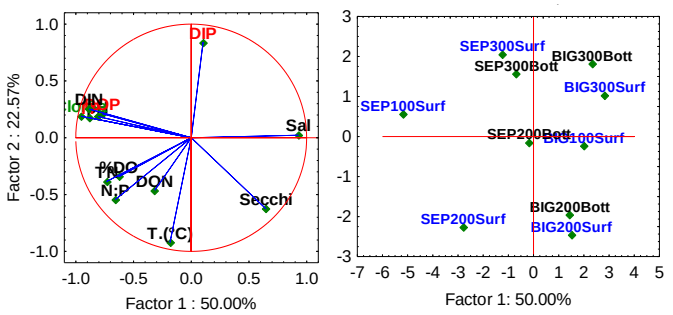

Figure 2. Principal component analysis (PCA) showing the direction and magnitude of correlations between parameters, using data media normalized for 13 variables: Secchi, Salinity, T.(°C), pH, %DO, Cl-a, TP, DOP, DIP, TN, DON, DIN and N:P, on the BIG and SEP surface (S) and bottom (B).

Sepetiba Bay suggests a tendency towards greater anthropic impact (large drainage, industrial and urbanization area), unlike the BIG, which has a greater influence on oceanic waters and is relatively better preserved.

Acknowledgements

This article was supported by the Graduate Program in Environmental Geochemistry (CAPES/PNPD/UFF); Laboratory of Marine Biogeochemistry at UFF; Funded by the VELITROP project (CNRS INEE, France) and the FAPERJ-FAPESP/2023 program.

References

[1] Cloern, J.E. Our evolving conceptual model of the coastal eutrophication problem. Marine Ecology Progress Series, v. 210, p. 223–253, 2001.
[2] Bricker, S.B. et al. Effects of nutrient enrichment in the nation's estuaries: A decade of change. Harmful Algae, v. 8, n. 1, p. 21–32, dez. 2008.
[3] Day, J.W. et al. (EDS.). Estuarine Ecology. Hoboken, NJ, USA: John Wiley & Sons, Inc., 2012.
[4] Andersen, J.H., Carstensen, J., Holmer, M., Krause-Jensen, D., Richardson, K., eds. (2020). Research and Management of Eutrophication in Coastal Ecosystems. Lausanne: Frontiers Media SA. doi: 10.3389/978-2-88963-432-3
[5] Grasshoff, K. et al. Methods of Seawater Analysis. Weinhein: Verlag Chemie, 1983.
[6] Strickland, J.D.H.; Parsons, T.R.A Practical Hand Book of Seawater Analysis. 2nd. ed. Ottawa: Fisheries Research Board of Canada, 1972.
[7] Canuel, E.A., 2001. Relations between river flow, primary production, and fatty acid composition of particulate organic matter in San Francisco and Chesapeake Bays: a multivariate approach. Organic Geochemistry 32, 563–583.

XVI LATIN AMERICAN CONGRESS ON ORGANIC GEOCHEMISTRY
9 - 11 AUGUST, 2023
ARACAJU, SERGIPE, BRAZIL

EVALUATION OF EUTROPHICATION IN ESTUARIES IN BRAZIL: ROTEIRO, MUNDAÚ, MANGUABA AND SÃO FRANCISCO RIVER (NORTHEAST); GUANABARA BAY (SOUTHWEST); GUARATUBA AND LARANJEIRAS BAYS (SOUTH)

[a]BRANDINI, N.; [b]MELO-MAGALHAES, E.M.; [b]SANTOS JR, R.C.; [a]KNOPPERS, B.A.; [c]MACHADO, C.M.; [d]CAVALCANTE, G. P.R.P.; **[b]MEDEIROS, P.R.P.**

[a]PROGRAMA DE PÓS-GRADUAÇÃO EM GEOCIÊNCIAS (GEOQUÍMICA/UFF), NITERÓI, RJ, BRAZIL. [b]UNIVERSIDADE FEDERAL DE ALAGOAS, PRÓ-REITORIA DE PÓS-GRADUAÇÃO E PESQUISA, LABMAR. [b]INSTITUTO DE GEOGRAFIA DESENVOLVIMENTO E MEIO AMBIENTE, UNIVERSIDADE FEDERAL DE ALAGOAS, BRAZIL, [c]INSTITUTO DE OCEANOGRAFIA, UNIVERSIDADE FEDERAL DO RIO GRANDE, RIO GRANDE, RS, BRAZIL. [d]INSTITUTO DE CIÊNCIAS ATMOSFÉRICAS, UNIVERSIDADE FEDERAL DE ALAGOAS, BRAZIL.

nbrandini@id.uff.br

Introduction

In estuaries, spatial variability becomes pronounced when freshwater inputs are significant, forming well-defined salinity gradients. The meteorological regime, geomorphological characteristics and anthropogenic impacts establish the characteristics of each region on coastal areas[1]. Eutrophication in an aquatic environment, can be characterized by the degree of or trophic state level[2]. Nixon (1995)[3] proposed the classification of four trophic states for estuarine and coastal marine ecosystems based on primary productivity: oligotrophic, mesotrophic, eutrophic and hypertrophic. The TRIX[4] index includes factors related to primary productivity (chlorophyll-*a*), nutrients availabiliity in the system (nitrogen and phosphorus) and dissolved oxygen saturation. This study aimed to apply the TRIX[4] index to estuarine systems located in the coastal regions of northeast, southeast and south of Brazil. The index includes parameter factors related to primary productivity (chlorophyll-a), nutritional factors (N and P) and dissolved oxygen saturation.

Experimental

Study Area: The estuary of the São Francisco River (**RSF**)[5,6], classified as oligotrophic and impacted by dams with little urban influence. The Lagoa dos Roteiro (**ROT**)[7] with mangroves, impacted by tourist and the Lagoon Estuarine Complex Mundaú (**Mun**)[7] and Manguaba (**Man**)[7] (CELMM), with restricted drainage system influenced by cultivation of sugar cane, and impacted by urban pollution. The Guanabara Bay (**BG**)[8], affected by untreated sanitary and industrial sewage. The bays of Laranjeiras (**LARJ**) and Guaratuba (**GUA**)[9] considered environments with little impact, surrounded by environmental protection reserves and a large presence of mangroves[9]. The study addressed published data from projects developed by FAPEAL[7], UFAL/AL[5], UFF/RJ[8] and CEM/UFPR[9], totaling n= ≈ 2000, distributed by rainy and dry periods for each system. The TRIX[4] index applies a linear combination of factors using scalar coefficients to set minimum and maximum limits with a scale extension varying from 0 to 10 units. The variables used: Depth (m), Temperature (°C), Salinity, pH, %DO, N:P ratio, DIN and DIP (uM), Chl-a (µg/l). **Location:** Laranjeiras (**Lar**j): (25°16'S-48°17'W) AS: 612 km^2; Zm: 2.5 m; Ab: 1443 km^2; QR: 5.108 m^{3}s^{-1}. Guaratuba (**Gua**): (25º52'S–48º39'W) AS: 48 km^2, Zm: 3 m; Ab: 1,700 km^2; Qr: 53.66 m^{3}s^{-1}. Guanabara Bay (**GB**): (23º45'S-44º45'W) AS = 384 m²; Zm = 5.7 m; Ab= 4080 km^2; Qr= 100±59 m^{3}s^{-1}). São Francisco River estuary (**RSF**): (10°15S-36°36W) AS: 19 km^2; Zm: 3m; Ab: 639,210 km^2, Qr: ±2000 m^{3}s^{-1}. Lagoa do Roteiro (**Rot**): AB: 624 km^2. Lagoa de Manguaba (**Man**): (9º46'-35º58') AS: 43; Zm: 2.1m; Ab: 3718; Qr: 57.2±15.9 m^{3}s^{-1}. Lagoa de Mundaú (**Mun**): (9º35'S-35º44'W) Zm: 1.5m; Ab: 4126 m^2; Qr: 65.9±14.1 m^{3}s^{-1}.

Results and Discussion

The TRIX index (NID, PID, OD% and Chl-a) detected seasonal and spatial variability in all systems. Salinity ranged from 29.6 (± 4.4) in the BG to 1.31 (± 4.8) in the RSF estuary. The PCA (n= 14) separated the quadrants on the left side for systems such as BG, Man and Mun, related to nutritional factors, which highlighted the Guanabara Bay, Manguaba and Mundaú, about nitrogen and phosphates high levels, NID: 29.8 (± 25.0), 13.9 (± 18.7) and 9.42 (± 16.7), and for the PID: from 2.21 (± 2.37), 0.98 (± 1.1) and 1.33 (± 1.26), respectively. The quadrant on the right was related to less eutrophic

environments (RSF, Gua, Larj and Rot) in the MPS variables, N:P ratio, depth (m) and water transparency.

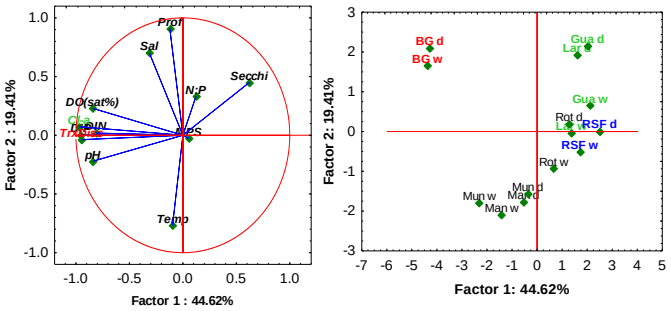

Figure 1. Figure 1. Principal component analysis (PCA) showing the direction and magnitude of correlations between parameters, using normalized mean for 14 variables: Secchi, Salinity, T (°C), pH, %DO, Cl-a, N:P, DIN, DIP, MPS, and TRIX, on the BG, Man, Mun, RSF, Rot, Gua, Lar. Rainy and dry season.

Conclusions

The characterization of the trophic state by TRIX indices demonstrated the variability between the systems (Figure 2). The color scale classified the trophic state as Ultra oligotrophic (blue: < to 2), Oligotrophic (green: 2 to 4), Mesotrophic (yellow: 4 to 5), Mesotrophic to Eutrophic (orange: 5 to 6), Eutrophic (red: 6 to 10). However, it was found that ammoniacal nitrogen was predominant in the dissolved inorganic nitrogen fraction (NID), while PID was more present in Guanabara, Manguaba and Mundaú bays.

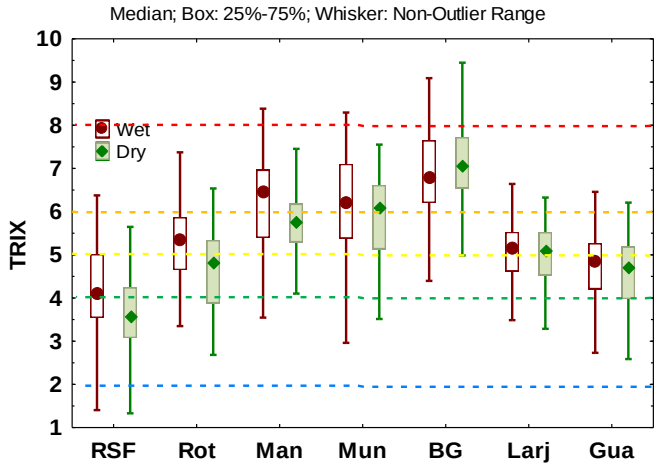

Figure 2. Median values at the Rainy and dry season. Estuário do Rio São Francisco (RSF), Lagoas do Roteiro (Rot), Manguaba (Man) e Mundaú (Mun), baias de Guanabara (BG), Laranjeiras (Larj) e Guaratuba (Gua).

The estuary of the RSF was considered excellent with small oscillating between the classification of ultra- to Oligotrophic, in the sequence follows the bay of Laranjeiras, Guaratuba and the lagoon of Roteiro considered as moderate to Mesotrophic.

Acknowledgements

This article was funded by the Graduate Program in Geochemistry Environmental (CAPES/PNPD/UFF); Research Support Foundation of the State of Alagoas (FAPEAL/CNPq), Integrated Laboratory of Marine and Natural Sciences (LABMAR/UFAL) and Center for Marine Studies (CEM/UFPR).

References

1 Libes, S.M. An Introduction to Marine Biogeochemistry. New York John Wiley and Sons, Inc., 1992, 734 p.

2 Bricker, S. B. et al. Effects of nutrient enrichment in the nation's estuaries: A decade of change. Harmful Algae, v. 8, n. 1, p. 21–32, dez. 2008.

3 Nixon, S. W. Coastal marine eutrophication: A definition, social causes, and future concerns. Ophelia, v. 41, n. 1, p. 199–219, 20 fev. 1995.

4 Vollenweider et al., 1998. Characterization of the trophic conditions of marine coastal waters with special reference to the NW Adriatic Sea: proposal for a trophic scale, turbidity and generalized water quality index. Environmetrics, v. 9, n. 3, p. 329–357.

5 Medeiros, P.R.P; Cavalcante, G.H.; Melo, E.R.; Brandini, N. 2018. The são Francisco river (NE): review on the interannual loading of particulate matter suspended to the ocean and impacts of dams. International Journal of Hydrology. Int J Hydro. MedCrave, 2018;2(2):190–193.

6 Abril, G.; Libardoni, B.G.; Brandini, N.; Cotovicz Jr, L.; Medeiros, P.P.; Cavalcante, G.H.; Knoppers, B.A. 2021. Thermodynamic uptake of atmospheric CO2 in the oligotrophic and semiarid Sao ˜ Francisco estuary (NE Brazil). Marine Chemistry 233 (2021) 103983. https://doi.org/10.1016/j.marchem.2021.103983

7 FAPEAL: Fundação de Amparo à Pesquisa do Estado de Alagoas. Projeto edital 08/2015 PDCR (2016-2019).

8 Cotovicz JR., L.C.; Knoppers, B.A.; Brandini, N.; Costa Santos, S.J.; Abril, G. 2015. A strong CO2 sink enhanced by eutrophication in a tropical coastal embayment (Guanabara Bay, Rio de Janeiro, Brazil). Biogeosciences, v. 12, p. 6125-6146.

9 Brandini, N.; Machado, E.C.; Sanders, C.J.; Cotovicz, L.C.; Bernardes, M.C.; Knoppers, B.A. Organic matter processing through an estuarine system: Evidence from stable isotopes (δ13C and δ15N) and molecular (lignin phenols) signatures.

Evaluation of naphthenic acids in water/oil interface using ESI-Orbitrap MS

Júlia G. de Souza [a], Lays I. Rodrigues [a], Jussara V. Roque [a], Iris Medeiros Júnior [b], Rogério M. de Carvalho [b], Boniek G. Vaz [a], Gabriel F. dos Santos [a*]

[a] Chemistry Institute, Federal University of Goiás, Goiania, Gois, 74690-900, Brazil

[b] CENPES, PETROBRAS, Rio de Janeiro, RJ, 21941-915, Brazil.

E-mail: julia2@discente.ufg.br

Introduction

Produced water is a natural by-product formed by different organic and inorganic compounds, where the chemical composition change according to geographical and geological factors (Jiménez et al., 2018). Organic compounds are usually classified into aromatic hydrocarbons, phenolic compounds, and organic acids, while inorganic compounds mainly consist of dissolved salts and heavy metals (De Figueredo et al., 2014; de Araújo et al., 2022).

Naphthenic acids (NAs) are natural organic acids found in crude oils and produced water, and their concentration can significantly change according to the oil source. The NAs are formed in crude oil due to insufficient deposit catagenesis or incomplete hydrocarbon oxidation by microbial degradation. These compounds comprise a complex mixture of acyclic, cycloaliphatic, and aromatics carboxylic acids with the general formula $C_nH_{2n+z}O_2$ (de Aguiar et al., 2021; de Araújo et al., 2022).

NAs have been noted for their high toxicity to marine biota, causing damage to several organisms, such as fishes, plants, microorganisms, and others (Bartlett et al., 2017). They are also related to corrosion in refinery units, emulsion formation, and precipitate in pipes, affecting oil production and causing substantial economic losses (Madill et al., 2001)]. Given the significant environmental and economic impacts caused by NAs, understanding the distribution of naphthenic acid in the water/oil interface has been crucial. This study reports the naphthenic acids distribution in water/oil emulsions in two different crude oils and the influence of salt concentration and pH on this distribution.

Experimental

This study was performed with two crude oils (Oil A and Oil B). Artificial seawater (ASW) was prepared following the literature (de Araújo et al., 2022) for simulating the produced water. The experiment evaluated the relationship between salt concentration and pH variations in the distribution of ANs for a system consisting of crude oil and ASW. An experimental design (Doehlert matrix) with two variables (salt concentration and pH) and five replications at the central point was used (Doehlert, 1970). Salt concentration was evaluated at five levels and pH at three levels, as shown in Table 1.

Table 1. Levels and independent variables studied in the Doehlert matrix.

Variables	Levels				
Salt concentrations (g L^{-1})	3.00	19.75	36.50	53.50	70.00
pH		2.0	6.0	10.0	

For sample preparation, 25 mL of crude oil and 25 mL of ASW were stirred in a vortex for 2 minutes, followed by the addition of a methanol solution of cyclopentanecarboxylic acid, benzoic acid, cyclohexanebutyric acid, 1-naphthoic acid, decanoic acid, 3,5-dimethyladamantane-1-carboxylic acid, 9-anthracenecarboxylic acid, pentadecanoic acid and 2-methyloctadecanoic acid analytical standards (5 µg mL^{-1}). Samples were shaken for an additional 2 minutes and centrifuged at 15000 rpm for 30 minutes. After this process, 25 mL of ASW was separated and acidified to pH 2 with HCl 2.0 mol L^{-1}, and a liquid-liquid extraction was performed with 25 mL of dichloromethane three times. The drying of the organic phase with anhydrous sodium sulfate, and its filtration to later concentrate it in the retroevaporator, was followed. The resulting extracts were analyzed in the Q-Exactive Orbitrap mass spectrometer with a commercial electrospray source in negative ionization mode (ESI(−)-Orbitrap MS).

Results and Discussion

After analyzing the extracts by ESI(−)-Orbitrap MS, experimental results were obtained from the absolute intensities of the NAs standards of *m/z* 113.06; 121.03; 169.12; 171.05; 171.14; 207.14; 221.06; 241.22; and 297.28. Then, *p*-values were calculated for the linear

and quadratic effects of the salt concentration and pH variables and the interaction effect between them. The effects significance was calculated at 95% confidence level by using the pure error of replications at the central point. The ions of *m/z* 169.12; 171.14; 207.14; 171.04, and 221.22 was significant and positive to pH values which means that their intensities increase with the increase of pH. Meanwhile, the opposite occurred to the ion *m/z* 297.28, where the effect was significant and negative on oil B.

Regarding the varying salt concentrations, only oil A resulted in significant values, which showed us that, with the increase in the concentration, the greater the signal intensity is in the ions.

Lastly, a desirability function was applied to include all the response variables obtained by the absolute intensities of the NAs samples, so we could better see the effects of the two variables (Derringer and Suich, 1980). Thus, obtaining a general measure called global desirability, represented in Figure 1, shows the response surfaces concerning salt concentration and pH for the best desirability found for oils A and B, with red representing the highest intensities of the NAs when the standards were in the highest pH ranges and with the highest salt concentrations.

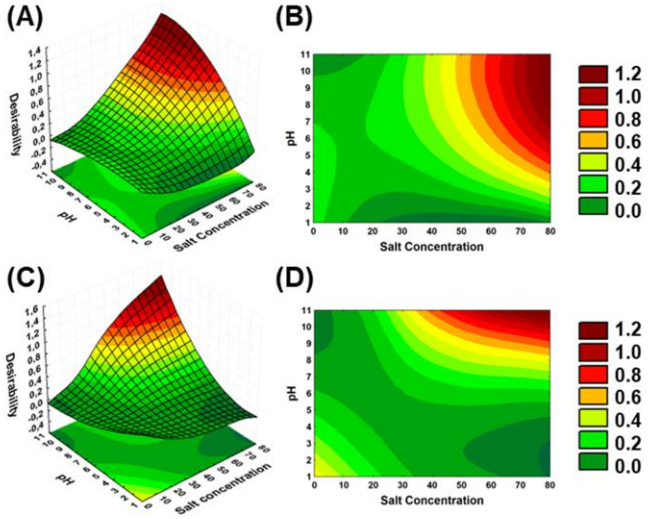

Figure 1. Desirability response surface for oils A and B. (A) and (B) 3D and 2D response surface, respectively, for oil A; (C) and (D) 3D and 2D response surface, respectively, for oil B.

Conclusions

From the experimental design of the Doehlert matrix type, it was possible to evaluate the effect of salt concentration and pH on the intensity of nine NAs standards in a system consisting of crude oil and ASW. Hence, we conclude that the intensity of NAs increases linearly with the concentrations of salts and pH to the most number of ions.

Acknowledgments

The authors acknowledge the financial support from Petróleo Brasileiro SA-Petrobras, CAPES, and CNPq.

References

Bartlett, A.J., Frank, R.A., Gillis, P.L., Parrott, J.L., Marentette, J.R., Brown, L.R., Hooey, T., Vanderveen, R., McInnis, R., Brunswick, P., Shang, D., Headley, J. V., Peru, K.M., Hewitt, L.M., 2017. Toxicity of naphthenic acids to invertebrates: Extracts from oil sands process-affected water versus commercial mixtures. Environmental Pollution 227, 271–279.

de Aguiar, D.V.A., da Silva, T.A.M., de Brito, T.P., dos Santos, G.F., de Carvalho, R.M., Medeiros Júnior, I., Simas, R.C., Vaz, B.G., 2021. Chemical characterization by ultrahigh-resolution mass spectrometry analysis of acid-extractable organics from produced water extracted by solvent-terminated dispersive liquid-liquid microextraction. Fuel 306, 121573.

de Araújo, G.L., dos Santos, G.F., Martins, R.O., Lima, G. da S., de Carvalho, R.M., Júnior, I.M., Simas, R.C., Sgobbi, L.F., Chaves, A.R., Gontijo Vaz, B., 2022. Electromembrane Extraction of Naphthenic Acids in Produced Water Followed by Ultra-High-Resolution Mass Spectrometry Analysis. Journal of the American Society for Mass Spectrometry. doi:10.2139/ssrn.4057238

De Figueredo, K.S.L., Martínez-Huitle, C.A., Teixeira, A.B.R., de Pinho, A.L.S., Vivacqua, C.A., da Silva, D.R., 2014. Study of produced water using hydrochemistry and multivariate statistics in different production zones of mature fields in the Potiguar Basin - Brazil. Journal of Petroleum Science and Engineering 116, 109–114.

Derringer, G., Suich, R., 1980. Simultaneous Optimization of Several Response Variables. Journal of Quality Technology 12, 214–219.

Doehlert, D.H., 1970. Uniform Shell Designs. Journal of the Royal Statistical Society. Series C (Applied Statistics) 19, 231–239.

Jiménez, S., Micó, M.M., Arnaldos, M., Medina, F., Contreras, S., 2018. State of the art of produced water treatment. Chemosphere 192, 186–208.

Madill, R.E.A., Orzechowski, M.T., Chen, G., Brownlee, B.G., Bunce, N.J., 2001. Preliminary risk assessment of the wet landscape option for reclamation of oil sands mine tailings: Bioassays with mature fine tailings pore water. Environmental Toxicology 16, 197–208.

FOOD SAFETY OF SEAFOOD OF THE CEARÁ COAST (NORTHEAST, BRAZIL) AFTER THE OIL SPILL (2019-2020)

BEATRIZ DINIZ LOPES[a*], RIVELINO M. CAVALCANTE[a]

[a] Postgraduate Program in Tropical Marine Sciences (PPGCMT)/Federal University of Ceará (UFC)

beatrizdiniz.lopes@gmail.com

Introduction

In late August 2019 to August 2020, the most extensive oil spill and the most severe environmental disaster ever recorded in Brazil and the South Atlantic Ocean occurred. Among the 11 states affected, 9 are from the Northeast region, which has unique demographic characteristics such as diverse tropical ecosystems associated with tourism and subsistence fishing. Polycyclic Aromatic Hydrocarbons (PAHs) are an important constituent of petroleum, which stand out for their wide distribution and their mutagenic, toxic, and carcinogenic characteristics. In addition to impacting biodiversity, the oil spill severely affected traditional fishing communities, since the fish resources that constitute most of their income and diet could not be sold or consumed. Thus, the impacts of the oil spill on fish resources and human health safety on the coast of Ceará were investigated. The concentration and composition of PAHs were evaluated in fish species of commercial interest.

Experimental

The 84 fish samples were acquired from artisanal fishermen from four tourist beaches (Extractive Reserve (RESEX) Prainha do Canto Verde, Icapuí, Cumbuco, and Jaguaribe) in September 2021. The biometry of the fish was performed and later their muscle was removed for analysis, since it is the part that is consumed by humans. The analysis of the 16 priority HPAs was done using the QUECHERS method and for the identification and quantification of the HPAs, GC-MS were used under the following conditions, from Agilent Technologies, model 7890B GC System/5977B. The capillary chromatography column used was the Agilent 19091S-433 HP-5ms (30 m x 250 µm x 0.25 µm).

To assess the food safety of the seafood, the levels of concern published by the National Health Surveillance Agency (ANVISA, 2019 [1]) during the time of the spill were used. The cancer risk for individual PAHs after seafood consumption by humans was based on the toxic equivalence (TEQ) approach relative to benzo[a]pyrene.

Results and Discussion

The total concentrations of PAHs ($\sum 16_{PAHs}$) ranged from Not Detected (N.D.) to 10.0 ng g^{-1} ww in the fish tissues. The noncarcinogenic PAHs with the highest concentrations in the samples were Naphthalene, Fluoranthene, Phenanthrene, and Fluorene, respectively. Regarding carcinogenic PAHs, the most found were Benzo[k]fluoranthene, Benzo[b]fluoranthene and Chrysene, respectively (Figure 1). Low molecular weight (LMW) compounds were predominant, because LMW HPAS are not as metabolized as high molecular weight (HMW) (Figure 2). Animals with well-developed mixed function hepatic oxygenase (MFO) systems do not accumulate petroleum hydrocarbons for long (Saadoun, 2015 [2]).

Figure 1. Individual PAHs concentrations in fish samples**.**

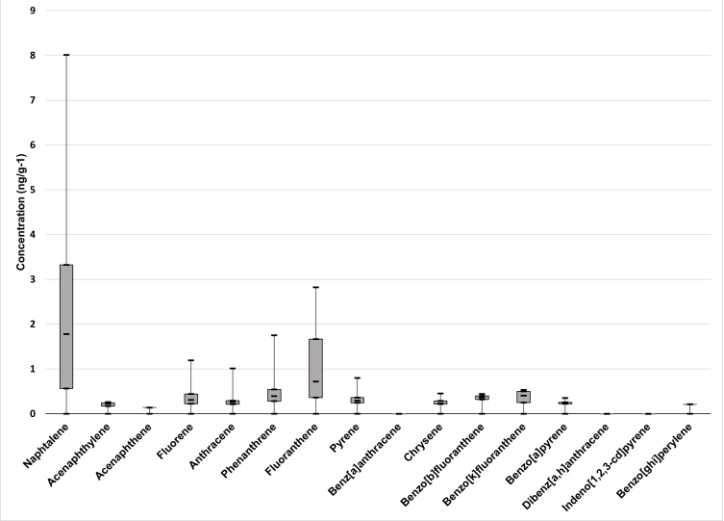

Figure 2. Means of the concentrations for each site and sum of the means for Low Molecular Weight and High Molecular Weight PAHs.

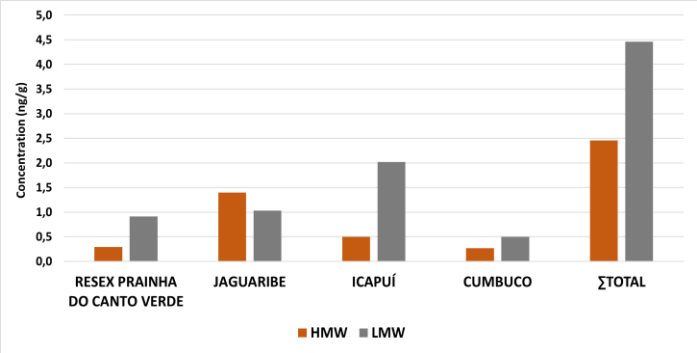

Regarding seafood safety, PAHs were separated into two groups (non-carcinogenic and carcinogenic) based on the regulations issued by the Brazilian authorities, where levels of concern (LOC) were established for individual PAHs and a benchmark based on their carcinogenic activity in relation to Benzo[a]Pyrene. The concentrations of non-carcinogenic and carcinogenic PAHs were below the levels of concern established for oil spill events in Brazil (2019 accident) (Table 1).

Table 1. Comparison between the concentration ranges (ng g-1) found in the samples and the levels of concern (ng g-1) published by ANVISA.

PAHS	SAMPLES	LOC (BRAZIL)
NON-CARCINOGENIC		
NAPHTHALENE	<0,20 – 8,01	6670
ACENAPHTHENE	<0,01 – 0,14	20000
FLUORENES (C0-C3)	<0,20 – 1,19	13330
ANTHRACENES (C0-C4)	<0,20 – 1,01	100000
PHENANTHRENES (C0-C4)	<0,20 – 1,75	
FLUORANTHENES (C0-C2)	<0,20 – 2,82	13330
PYRENES (C0-C2)	<0,20 – 0,80	10000
CARCINOGENIC		
BENZ[A]ANTHRACENE	<0,20	44
CHRYSENE	<0,04 – 0,45	1453
BENZO[B]FLUORANTHENE	<0,10 – 0,44	46
BENZO[K]FLUORANTHENE	<0,07 – 0,53	91
BENZO[A]PYRENE	<0,10 – 0,35	6
DIBENZ[A,H]ANTHRACENE	<0,14	6
INDENO[1,2,3-CD]PYRENE	<0,14	28
BENZO[GHI]PERYLENE	<0,08 – 0,21	291

All concentration levels of PAHs were converted in B[a]P equivalents to evaluate the carcinogenic risk of fish from the study areas. Using the toxicity equivalent factor (TEF) values (ANVISA, 2019 [1]), the toxic equivalent quotient (TEQ) was determined for fish. In terms of benzo[a]pyrene equivalent (BaPeq), the levels of concern issued by ANVISA specifically for the 2019 Brazil oil spill were set as 6 ng g^{-1} w.w. for fish. Considering all 84 samples analyzed, the limit was not exceeded (Table 2).

Table 1. TEQ (ng/g) value of each location and sum of TEQs.

LOCAL	TEQ (ng/g)
RESEX Prainha do Canto Verde	0,15
Icapuí	0,044
Cumbuco	0,16
Jaguaribe	0,16
TOTAL	0,514

Conclusions

Considering that the samples analyzed had low concentrations of PAHs and were compared with the seafood regulations published by ANVISA, it is unlikely that the Brazilian oil spill event would negatively impact the health of the human population immediately following the event. This finding, however, does not negate the need for long-term monitoring, as the amount of oil remaining in the local marine and estuarine environment is still unknown. Short-term monitoring (i.e., three months after the spill) of fish indicated a clear sign of exposure to oil residues, evidenced by the presence of LMW PAHs, particularly naphthalene, fluoranthene, phenanthrene, and fluorene. However, contrary to expectations, the seafood was safe for consumption immediately after the spill, as none of the samples posed a risk to human health.

Acknowledgements

The authors would like to thank CAPES for funding this research.

References

[1] ANVISA, 2019. Riscos a saúde humana decorrentes do consumo de pescados oriundos das praias contaminadas por oleo cru na Regiao Nordeste do Brasil. Agencia Nacional de Vigilancia Sanitaria, Nota Tecnica nº 27/2019/SEI/GGALI/DIRE2/ ANVISA, Processo nº 25351.940364/2019-93, 5p.

[2] Saadoun, I.M.K., 2015. Impact of oil spills on marine life. In: Larramendy, M.L., Solonesky, S. (Eds.), Emerging Pollutants in the Environment- Current and Further Implications. IntechOpen Publishing, pp. 75–103. https://doi.org/10.5772/60455.

XVI LATIN AMERICAN CONGRESS ON ORGANIC GEOCHEMISTRY
9 - 11 AUGUST, 2023
ARACAJU, SERGIPE, BRAZIL

Composição elementar e de *n*-alcanos em sedimento de lago da bacia do Rio Negro, Amazônia Brasileira: um estudo preliminar

Fernanda S. Pinto[a*], Luciane M. Silva[a], Renato C. Campello[a], Bruno J. Turcq[b], Debora de A. Azevedo[c], Vinicius B. Pereira[c], Juliano H.F.Soares[a]

[a] **Universidade Federal Fluminense (UFF),** [b] **Instituto Institut de Recherche pour le Développement** [c] **Universidade Federal do Rio de Janeiro**

e-mail: fernandapinto@id.uff.br

Introdução

A capacidade de análise a nível molecular é de grande importância para estudos geoquímicos, pois suas características estruturais fornecem informações mais especificas sobre as condições ambientais do passado, quando comparado aos indicadores geoquímicos do material sedimentar bruto (*bulk*). Os biomarcadores moleculares fornecem informações como a origem da matéria orgânica, diferenciação entre fontes de organismos (autóctones e alóctones), além de fornecer informações sobre as fontes não biogênicas de matéria orgânica e/ou contaminações provenientes de combustíveis fósseis (PEREIRA, 2021). O interesse nos estudos realizados a nível molecular está na capacidade de separação dos componentes terrestres, aquáticos e sedimentares, além de investigar as condições ambientais, tanto da coluna d'agua como da bacia de drenagem, simultaneamente.

O objetivo deste trabalho é fornecer uma breve discussão sobre a origem da matéria orgânica presente em testemunho lacustre do Lago do Cabeçudo localizado no Baixo Rio Negro utilizando como indicador de fonte de matéria orgânica os *n*-alcanos e também os marcadores elementares, visando uma reconstrução paleoambiental.

Experimental

No presente trabalho foi estudado o Lago do Cabeçudo, localizado no complexo fluvial de Anavilhanas, na bacia do Rio Negro (Região Amazônica, Norte do Brasil). Um testemunho de 6 metros foi coletado, aberto, descrito, fatiado e quantificado os teores de carbono orgânico total (TOC), Nitrogênio total (NT) e assinatura isotópica de carbono ($\delta^{13}C$) em um analisador elementar acoplado a um espectrômetro de massa de razão isotópica (IRMS) na Southern Cross University, Austrália. A datação de diferentes profundidades foi realizada no *Laboratoire de Mesure du carbone* (LMC14C-França). Para determinação de *n*-alcanos, cerca de 4g de sedimento foram liofilizados e os lipídios foram extraídos com diclorometano e metanol 9:1 (suprasolv Merck) e três frações (F1, F2, F3) de lipídios foram separadas através de cromatografia líquida em coluna de sílica, utilizando solventes de polaridade distintas. A fração 1 composta por hidrocarbonetos alifáticos foi analisada por GC-FID. As frações 2 e 3, respectivamente, de hidrocarbonetos aromáticos (F2) e compostos orgânicos polares não saponificáveis (F3) foram armazenadas.

Resultados e Discussão

Os valores de TOC variaram entre 0,27% e 6,99%, enquanto os valores de NT variaram entre 0,04% e 0,52%, com maiores valores de TOC quantificados para o período a partir de 5420 BP, enquanto os maiores valores de NT medidos para períodos anteriores a 510 BP. A razão C/N (Figura1) variou entre o mínimo de 6,19 (473cm) e o máximo 26,82 (265cm). Os altos valores médios da razão C/N no testemunho indicam o aporte de matéria orgânica predominantemente oriunda de plantas vasculares, que contém elementos estruturais refratários como celulose e lignina. Valores de C/N acima de cerca de 15 geralmente indicam predominância de plantas vasculares terrestres (MEYERS; EADIE, 1993). Corroborando com este indicador, o diagrama $\delta^{13}C_{bulk}$ × C/N (Figura 2) mostra que a contribuição vegetal está majoritariamente associada à vegetação de tipo C_3, tipicamente angiospermas (MEDINA et al., 2005).

Foram identificados *n*-alcanos com cadeias entre *n*-C_{17} e *n*-C_{35}. O testemunho apresentou predominância ímpar-par e maior concentração de *n*-alcanos de cadeia longa, atingindo os maiores picos em n-C_{29} e n-C_{31} (Figura 3), indicam que as plantas superiores foram a principal fonte de *n*-alcanos nesse registro (EGLINTON; HAMILTON, 1967). Não foram observadas quantidades significativas de *n*-C_{17}, sugerindo que a produção de algas e cianobactérias é baixa e/ou a preservação desse indicador na amostra foi insuficiente. As algas aquáticas e bactérias produzem preferencialmente

cadeias curtas, com 15 a 19 carbonos, enquanto as plantas terrestres possuem majoritariamente *n*-alcanos de cadeia longa (*n*-C_{29} a *n*-C_{33}) (EGLINTON; HAMILTON, 1967), que constituem as ceras cuticulares e conferem proteção contra a perda de água (BRASSEL, 1993).

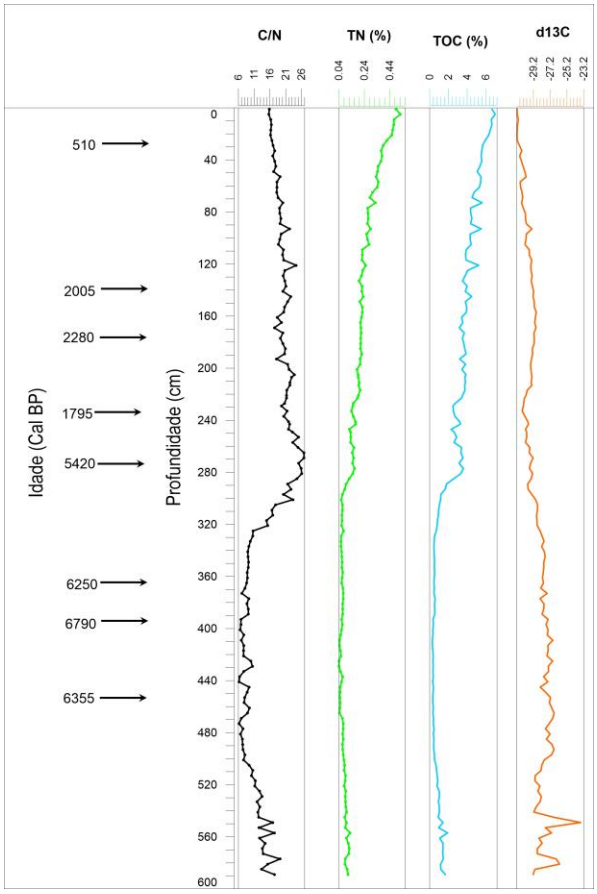

Figure 1. Distribuição dos dados geoquímicos

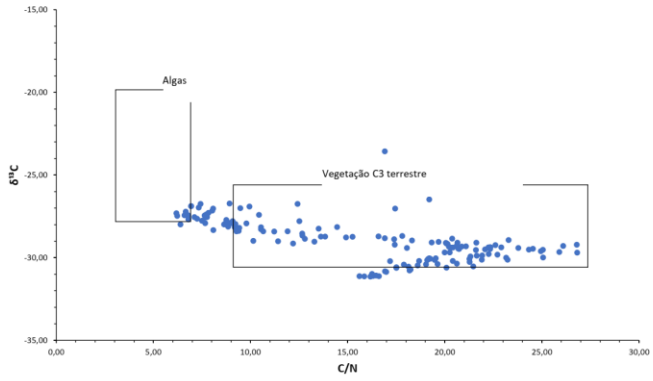

Figure 2. Diagrama δ13C × C/N

Algumas amostras apresentam mistura complexa não resolvida (UCM,*unresolved complex mixture*) representada por um amplo aumento da linha base devido à presença de compostos não resolvidos por cromatografia, o que pode indicar um retrabalho microbiano e, geralmente é considerado uma mistura de vários compostos de estruturas complexas (BOULOUBASSI; SALIOT, 1993).

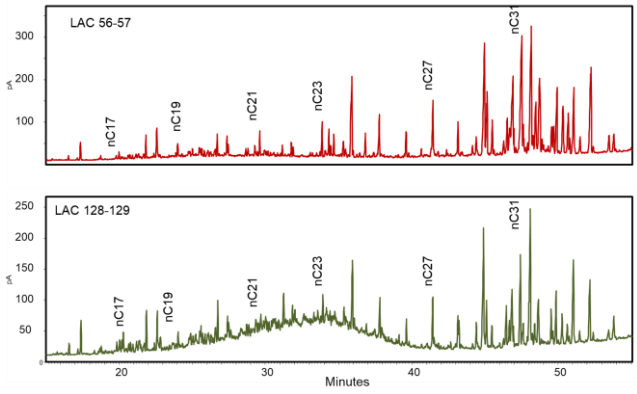

Figura 3: Seleção de cromatogramas da fração de hidrocarbonetos alinfáticos

Conclusões

O presente estudo apresenta alguns resultados preliminares que serão aprofundados com a continuidade do trabalho. Diante da relevância de identificar as fontes de matéria orgânica, foram efetuadas coletas da vegetação na área de estudo para realização da calibração das abundâncias relativas de *n*-alcanos e da composição isotópica da vegetação atual.

Agradecimentos

Os autores agradecem a Fundação de Amparo à Pesquisa do Estado do Rio de Janeiro (FAPERJ), CNPq, Programa de Pós-graduação em Geociências (Geoquímica Ambiental) UFF.

Referências

BOULOUBASSI, I., SALIOT, A., 1993. Investigation of anthropogenic and natural organic inputs in estuarine sediments using hydrocarbon markers (NAH, LAB, PAH). Oceanologica Acta 16, 145–161.

BRASSELL, S. C., Applications of biomarkers for delineating marine paleoclimatic fluctuations during the Pleistocene, in Topics in Geobiology, vol. 11, Organic Geochemistry, Principles and Applications, pp. 699-738, New York, 1993.

EGLINTON, G.; HAMILTON, R. J. Leaf epicuticular waxes. Science, v.156, n. 3780, p.1322–1335, 1967.

MEDINA, E.; FRANCISCO, M.; STERNBERG, L.; ANDERSON, W. T. Isotopic signatures of organic matter in sediments of the continental shelf facing the Orinoco Delta: Possible contribution of organic carbon from savannas. Estuarine, Coastal and Shelf Science, v. 63 p. 527–536, 2005.

MEYERS, P.A., EADIE, B.J. 1993. Sources, degradation and recycling of organic matter associed with sinking particulares in Lake Michigan. Organic Geochemistry 20, 4-56.

PEREIRA, V. B. Biogeoquímica molecular da matéria orgânica em testemunho do Lago Jacundá, Amazônia Brasileira. Dissertação de mestrado, UFRJ, 2021.

Evaluation of the molecular chemical profile of Brazilian oils for forensic studies and investigation of environmental crimes

Flavia R. Alvares (PG)[a]*, Vinícius B. Pereira (PG)[b], Ana Luiza B. S. Silva (IC)[a], Luiz Augusto de O. Costa (PQ)[c], Débora de A. Azevedo[b], Francisco R. de Aquino Neto (PQ)[a], Gabriela V. Costa (PQ)[a]*

[a] Núcleo de Análises Forenses (NAF), Instituto de Química, UFRJ; [b] Laboratório de Geoquímica Orgânica, Molecular e Ambiental (LAGOA), Instituto de Química, UFRJ; [c] Instituto Brasileiro do Meio Ambiente e dos Recursos Naturais Renováveis (IBAMA)

flavia.rodriguesa@hotmail.com; gabrielavanini@iq.ufrj.br

Introduction

The growing increase in offshore oil production in Brazil results in the recording of several oil spills and the need for geochemical characterization of these spilled oils, as distinct aspects of molecular composition are essential for understanding the contribution of organic matter, thermal evolution, and biodegradation. In this study, the molecular analysis of seven spilled oils from different sites in Brazil (four in Fernando de Noronha and three in Ceará) was performed using comprehensive two-dimensional gas chromatography with time-of-flight mass spectrometry (GC×GC-TOFMS) and high-resolution mass spectrometry (Orbitrap-HRMS) to investigate geochemistry biomarkers. The main objective was to apply efficient methods to monitor and classify biomarkers and polar compounds present in spilled oils from different sites in Brazil using advanced analytical techniques to facilitate investigations of environmental accidents involving this type of samples.

Experimental

Oil samples were extracted using Soxhlet, followed by asphaltenes precipitation procedure. Maltenes were thereafter fractionated by liquid chromatography, separated them into saturated, aromatic, and polar compounds. Cyclic and branched hydrocarbons (C/B) were concentrated in the saturated fraction using urea adduct by removal of *n*-alkanes. C/B compounds were then analyzed by GC×GC-TOFMS and the analytical data evaluated by ChromaTOF™ to identify nonpolar molecules. Crude spilled oils were analyzed by high-resolution Orbitrap mass spectrometry in order to identify polar compounds and the analytical data was evaluated by Composer™ and XCalibur™ softwares.

Results and Discussion

The biodegradation of the oils can be classified according to the presence of 25-nor-hopane (25-NH), 25,28-bis-nor-hopane (25,28-BNH), 25,30-bis-nor-hopane (25,30-BNH) and 25,28,30-tris-nor-hopane (25,28,30-TNH) and their geochemical ratios with 17α(H),21β(H)-29-hopane (H29) and 17α(H),21β(H)-30-hopane (H30). Spilled oils from Fernando de Noronha, the biodegradation parameters had average values: 25NH/H30= 0.12; 25,28BNH/H30= 0.02; 25,30BNH/H29= 0.02; 25,28,30TNH/H29= 0.01; 25,28,30TNH/H30= 0.01. These parameters indicate that these oils are severely degraded or constitute a mixture of oils **(Figure 1).** Oils from Ceará did not present these compounds, indicating a lower biodegradation. Geochemical evaluation can also be performed using origin parameters. Hopanes and steranes gives information to distinguish source rocks in different oil reservoirs. The geochemical ratio H30/Est27 > 7 is related to the lacustrine origin and can be regard as a common characteristic of all oil samples.

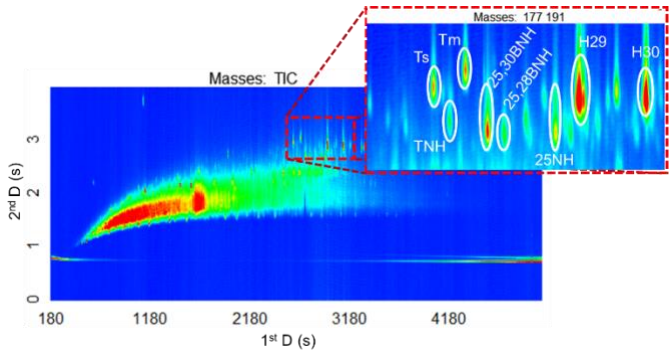

Figure 1. TIC and EIC (*m/z* = 177 + 191) of spilled oil from Fernando de Noronha.

Thermal maturity parameters evaluate the heat level received by the deposited organic matter to enable its

transformation into oil. The ratio of C27ααα S/(R+S) steranes varied between 0.50 and 0.65 and C27[αββ/(ααα+αββ)] was between 0.35 and 0.48 in oils from Fernando de Noronha. In oils from Ceará, C27ααα S/(R+S) varied between 0.44 and 0.63 and C27[αββ/(ααα+αββ)] was between 0.44 and 0.67. From these results it is possible to infer that oils from Ceará have greater thermal maturity than those from Fernando de Noronha.

Crude spilled oils were also analyzed by ESI (±)-Orbitrap-HRMS to identify the high boiling point polar substances. For this analysis the identified species in the spilled oils corresponded to the N[H], N_2[H], N_2O_2[H], N_3O_2[H], N_3O_3[H], NO[H], NO_2[H] and NS[H] classes in positive mode and HC[H], N_2O[H], N_2[H], N_2O_2[H], N_2O_3[H], O_2[H], O_3[H], NO_2[H], N_2OS[H], N_2S[H] and S[H] classes in negative mode.

ESI (+) and ESI (-) mass spectra in the analysis of polar compounds (N, S and O) in crude oil samples were assessed. The double bond equivalents (DBE) distribution in function of carbon number (CN) was obtained for the crude oils (**Figure 2**). It was possible to detect about 11.000 substances in ESI (+) and about 13.000 substances in ESI (-) in the spilled oils.

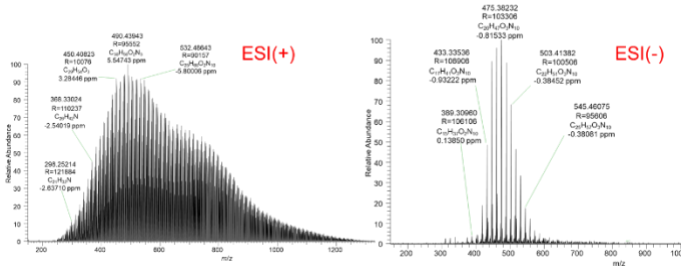

Figure 2. ESI (+) and ESI (-) mass spectra.

The most abundant class in positive mode is the nitrogen class in all spilled oils analyzed, which can be related to thermal evolution and aromaticity levels in crude oils. The higher thermal evolution causes more aromatic rings to form and generates higher DBE levels for crude oils. In negative mode, the most abundant class in oils from Fernando de Noronha is N_2O_3[H] class

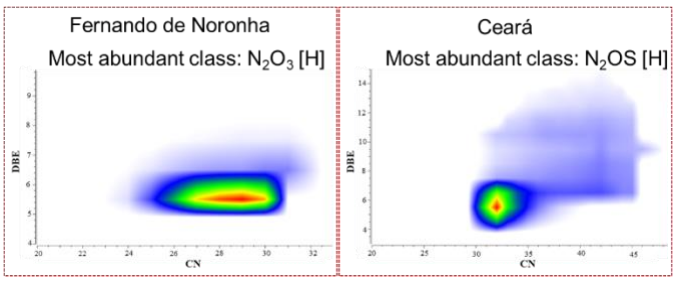

and in oils from Ceará is N_2OS[H] class **(Figure 3)**.

Figure 3. DBE *versus* CN graphics.

Conclusions

Advanced analytical techniques used in a complementary way allowed the characterization of spilled oil samples. Two-dimensional chromatography allowed the identification and semiquantification of biomarkers, and biomarker ratios were applying to differentiate oils. High-resolution mass spectrometry allowed the detection of about 26 thousand analytes in each sample. Based on these results, spills from Ceará and Fernando de Noronha are inconsistent among themselves, indicating multiple spills in Brazilian coast. This set of information is prone to become an important tool for the discrimination of oils involved in spills, as it brings elements related to their origins. The next step of this work involves the development of a chemometric model to identify different types of oils involved in environmental impacts investigations.

Acknowledgements

The authors gratefully acknowledge the financial support from the IBAMA (Brazilian Institute for the Environment and Renewable Natural Resources), PRH-ANP (Human Resources Program – Brazilian Petroleum Agency), Finep (Financier of Studies and Projects), CNPq (Brazilian research council) and CAPES finance code 0001 (Higher Education Personnel Improvement Coordination).

References

VANINI, G. et al., 2020. Characterization of Nonvolatile Polar Compounds from Brazilian Oils by Electrospray Ionization with FT-ICR MS and Orbitrap-MS. **Fuel 282**, 118790.

WANG, Z. et al., 2006. Forensic Fingerprinting of Biomarkers for Oil Spill Characterization and Source Identification. **Environmental Forensics**, 7:105-146.

SOARES, R. F. et al., 2013. Comprehensive Two-Dimensional Gas Chromatography Coupled to Time of Flight Mass Spectrometry: New Biomarker Parameter Proposition for the Characterization of Biodegraded Oil. **Journal of the Brazilian Chemcal Society**, 24:1570-1581.

MELLO, M. R. et al., 1988. Organic geochemical characterization of depositional paleoenvironments of source rocks and oils in Brazilian marginal basins. **Organic Geochemistry 13**, 31-45.

LIMA, B. D. et al., 2023. Weathering impacts on petroleum biomarker, aromatic, and polar compounds in the spilled oil at the northeast coast of Brazil over time. **Marine Pollution Bulletin**, 189, 114744.

SANTOS, J. M. et al., 2017. Advanced Aspects of Crude Oils Correlating Data of Classical Biomarkers and Mass Spectrometry Petroleomics. **Energy & Fuels**, 2:31, 1208–1217.

USE OF GEOCHEMICAL BIOMARKERS AS SEWAGE SOURCE TRACERS IN *NODIPECTEN NODOSUS* SCALLOP CROPPING

JÉSSICA DE MEDEIROS SOARES[1*]; ANTONI FELIPE OLIVEIRA DE ANDRADE[1*]; MARCELO CORRÊA BERNARDES[1*]; NÍVIA DE MELLO NASCIMENTO[1*], BRUNO CESAR SILVA ROCHA[1*]; RICARDO O'REILLY VASQUES[2*]; ELINE SIMÕES GONÇALVES[1*]; WILSON THADEU VALLE MACHADO[1*].

[1]* DEPARTMENT OF GEOCHEMISTRY, INSTITUTE OF CHEMISTRY, FEDERAL FLUMINENSE UNIVERSITY (UFF), CENTER, NITERÓI, RJ, BRAZIL, CEP 24020-141; [2]* UNIVERSITY OF GRANDE RIO, RUA JOSE DE SOUZA HENDY, DUQUE DE CAXIAS, RJ, BRAZIL, CEP 25071-202.

e-mail: jessicams@id.uff.br

Introduction

The inadequate disposal of domestic effluents into aquatic ecosystems, in addition to contributing to organic enrichment of the water column, has negative effects on biodiversity. Among the contaminants that cause severe damage to the marine environment, petroleum hydrocarbons stand out. Considering the growth of aquaculture in the last decade, it is necessary to monitor the areas where fishery resources are extracted, cultivated, and/or commercialized. Among these resources, we can highlight pectiniculture. Scallops are widely cultivated organisms in Brazil and worldwide, with high commercial value where demand often exceeds supply. On the other hand, due to their specific physiology that allows them to filter water, these organisms are used as bioindicators of environmental quality. In this context, this study aims to evaluate n-alkanes and sterols as biomarkers of marine pollution in *Nodipecten nodosus* scallops on a pectiniculture farm located in the municipality of Armação dos Búzios, on the coast of the state of Rio de Janeiro (Brazil), where it is possibly under the influence of anthropogenic contamination.

Experimental

Two collections were carried out considering the period of summer and winter (January and July 2015, respectively). On each trip, 15 individuals were selected in the Ilha Rasa region (Búzios, RJ, Brazil). After removal of the epifauna, the organisms were placed in aquariums containing local water, where they were tolerated for 24 hours to purify the stomach contents and then frozen. subsequently, the soft tissue was separated from the shell, being lyophilized, macerated, homogenized and identified. Of the 30 individuals collected, 6 composite exceptions were generated, containing 5 individuals each. Then, 0.5g of each sample was weighed and the monitoring step began, following the methodology of [2]. For fractionation, liquid chromatography columns adapted from the EPA-8270E method in pauster pipettes were used. After obtaining the two fractions of interest F1 (n-alkanes) and F3 (sterols), both were dried under N2 flow, being stored at -2 ºC until analysis. In F3, derivatization was performed with N,O-Bis (trimethylsilyl) trifluoroacetamide with trimethylchlorosilane (BSTFA/TMCS 9:1). Analyzes of aliphatic hydrocarbons (F1) and sterols (F3) were performed using gas chromatography coupled to an ionizing flame detector (GC-DIC Agilent 6890) following the protocol based on the EPA-8015C method. The peaks were quantified using the Cerity – QAQC software from the company Agilent Technologies.

Results and Discussion

In the *Nodipecten nodosus* scallop samples collected at the mariculture farm, alkanes from n-C_{12} to n-C_{40} were identified. Considering the need for a more precise result and the scarcity of studies described in the literature, the following diagnostic criteria were employed to assess the presence of petroleum hydrocarbons in the studied coastal area: Carbon Preference Index (CPI), Terrestrial and Aquatic Ratio (TAR), and Aquatic Plant Proportion Index (Paq). The CPI values were above one (Figure 1) in both analyzed periods, indicating a biogenic source (CPI > 1). The Paq values ranged from 0.4 in summer to 0.6 in winter, indicating the presence of n-alkanes from submerged or floating macrophytes (Figure 1).
The values of TAR, both in summer and winter, were above one, characterizing a higher contribution of terrestrial source compounds (allochthonous) [3].

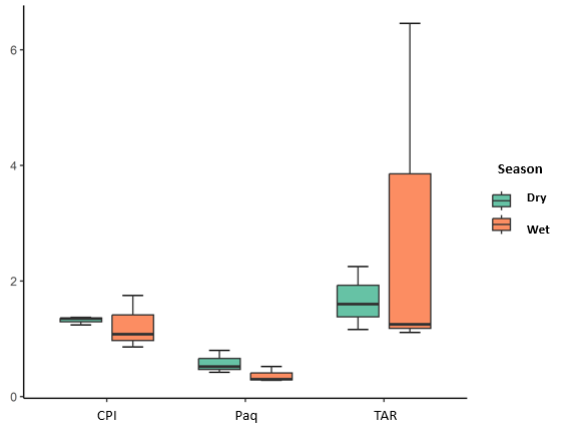

Figure 1. Preferential Carbon Index (CPI), Aquatic Plant Proportion Index (Paq), in μg.g^{-1}, and Terrestrial and Aquatic Ratio (TAR).

MCNR was detected in 75% of the samples, with concentrations exceeding 100 μg.g^{-1}, characterizing contamination by petrogenic derivatives, especially in winter.

Other diagnostic reasons were also employed to assess domestic sewage inputs in coastal areas.

One reason used to assess sewage contamination in water and sediment samples collected in the coastal region of Spain was the ratio between coprostanol and cholestanone ketone.

The results obtained in this study were above 0.3 and less than 0.7 in both periods and could not be classified regarding their level of fecal contamination using this diagnostic ratio (Figure 2). Proposed a modification to the previous ratio, employing the compound cholestanol instead of cholesterol [1]. However, the values of the ratio ([5β/(5α+5β)]) applied to the organisms were below 0.3, indicating a higher proportion of cholestanol compared to coprostanol and therefore the absence of fecal contamination classification.

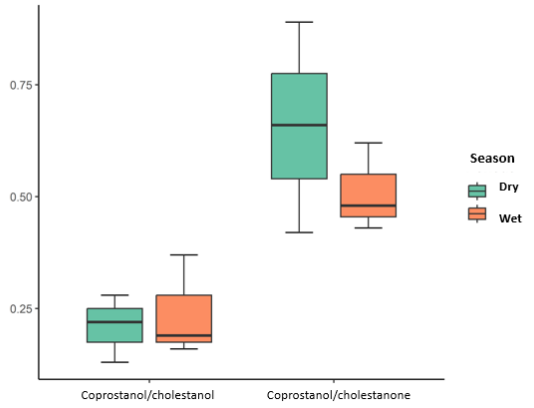

Figure 2. Ratio between coprostanol and cholestanone acetone, and ratio between coprostanol and cholestanol.

Conclusions

The use of diagnostic ratios in this study was effective in identifying the origin of organic matter in the monitored area. The CPI ratio demonstrated biogenic influence, as the maximum carbons (n-C24 and n-C26) were removed and the values remained above one. The TAR showed good applicability, indicating a terrestrial origin contribution, meaning the ratio is greater than one in all periods. The Paq indicated the presence of submerged/floating macrophytes in the region. The ratios [5β/(5α-ona+5β)] and [5β/(5α+5β)] require reformulation for better applicability in living organisms. However, the MCNR values indicated the impact of degraded petroleum contamination.

Acknowledgements

To the Dean of Research, Graduate Studies and Innovation (PROPPI) of the Fluminense Federal University (UFF); It is to the development agencies: CNPq, CAPES 01 and FAPERJ (E-26/210.745/2021).

References

[1] CARREIRA, R. S.; SANTOS, E. S.; KNOPPERS, B. A. Sedimentary sterols as indicators of environmental conditionsin southeastern Guanabara Bay, Brazil. Brazilian Journal of Oceanography, São Paulo, v. 56, n. 2, p. 97-113, 2008.

[2] COPEMAN, L. A.; PARRISH, C. C. Lipids Classes, Fatty Acids, and Sterols in Seafood from Gilbert Bay, Southern Labrador. Journal of Agricultural and Food Chemistry, v. 52, n. 15, p. 4872-4881, 2004.

[3] JAFFÉ, R.; MEAD, R.; HERNANDES, M. E.; PARALBA, M. C.; DI GUIDA, O. A. Origin and transport of sedimentary organic matter in two subtropical estuaries: a comparative, biomarker-based study. Organic Geochemistry, Oxford, v. 32, n. 4, p. 507-526, 2001.

GEOCHEMICAL AND MICROPALEONTOLOGICAL CHARACTERIZATION OF THE PIRABAS FORMATION (PARÁ, BRAZIL): A PALEOENVIRONMENTAL APPROACH

BEATRIZ TEIXEIRA GUIMARÃES[1*], ORANGEL AGUILERA[2], ANA PAULA LINHARES[3], SABRINA PINTO RAMOS[1], RUT DÌAZ[4], MANUEL MOREIRA[4], HAMILTON SANTOS GAMA FILHO[5], MARCELINO JOSE DOS ANJOS[5], VINICIUS KÜTTER[1]

1. Federal University of Pará (UFPA), Geoscience Institute, 66075-110, Belém, Pará, Brazil*;
2. Fluminense Federal University (UFF). Institute of Biology, 24210-201, Niterói, Rio de Janeiro, Brazil;
3. Museu Paraense Emilio Goeldi (MPEG), Earth Sciences and Ecology Coordination, 66077-830, Belém, Pará, Brazil;
4. Fluminense Federal University (UFF), Institute of Chemistry, 24020-150, Niterói, Rio de Janeiro, Brazil;
5. Rio de Janeiro State University, Institute of Physics Armando Dias Tavares, CEP 20550-013, Rio de Janeiro, Brazil

* correspondent author: beatriz.97.guimaraes@gmail.com

Introduction

The Pirabas Formation [1] is found in coastal outcrops and quarries in the Pará state in north Brazil. It is distinguished by a mixture of carbonate-siliciclastic deposits in shallow water from the late early to late middle Miocene [2;3;4]. The shallow-water inner marine heterozoan reef deposits of the Pirabas Formation were influenced by hurricanes and high-intensity coastal storms during the Neogene. Petrography, micropaleontology, and geochemistry were used to investigate a chaotic superposition of benthic infauna and epifauna, as well as demersal and pelagic species in the same area, in order to comprehend sedimentary and paleoenvironmental processes.

Material and Methods

Eleven samples were collected at two outcrops from the type locality of the Pirabas Formation at Ilha de Fortaleza, São João de Pirabas, Pará state, Brazil (Ponta do Castelo, (0°40'55.69" S, 47°10'13.30" W, and Fazenda, 0°42"43.79" S, 47°9'58.65"W) (Fig. 1). These outcrops are mostly composed of packstone layers and present approximately 4 m thick. For micropaleontology recuperation, 1 kg each was disaggregated and processed using 500, 250, 125, and 63 µm mesh sizes. The images were obtained using an electronic microscope. Six thin petrographic sections from the Ponta do Castelo and Fazenda outcrops were prepared. The samples were fixed on 76 x 26 mm glass slides and polished to a thickness of 30 µm. The mineral characterization of carbonate rock conducted from Ilha de Fortaleza was compared to those of Pirabas Formation reference samples (Fig. 3). For the X-ray diffraction analysis (XRD) all samples were pulverized in a stainless-steel ball mill for 10 min and subsequently packed into a specific acrylic sample holder fixed in the Spinner system for analysis. For elemental quantification (XRF) the pulverized samples were mixed with lithium tetraborate and funded. The ignition losses were performed at 1,020 °C for 2 h. Quantitative analyses in carbonate rock over the detection level included CaO, MgO, SiO2, Al2O3, Fe2O3, Na2O, K2O, P2O5, TiO2, SrO, MnO, and S.

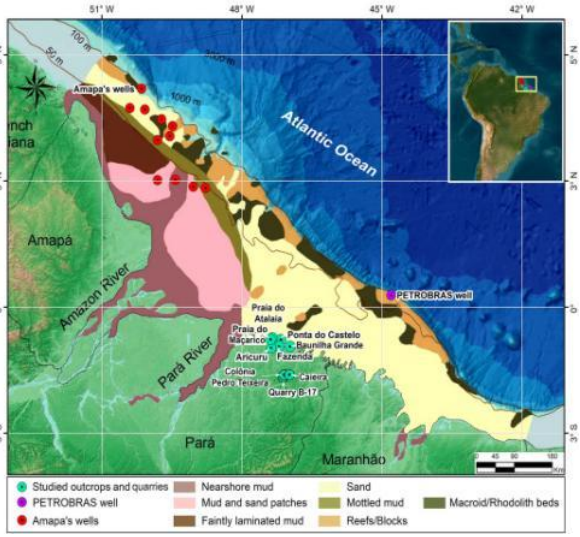

Figure 1. Map of the northwestern Brazilian platform modified of [5;6]. Light green circle: Ponta do Castelo and Fazenda outcrops studied from Ilha de Fortaleza and reference samples from other outcrops of the Pirabas Formation.

Results and Discussion

A high concentration and diversity of microfossils, bioclast remains, and grains were recorded in the thin sections (Fig. 2). This comprises fragments of echinoderms, bryozoans, mollusks, large benthic foraminifera, red and green calcareous algae, and ostracods. The assemblages of benthic and planktonic foraminifera comprise shallow water rotaliid of *Amphistegina*, *Elphidium*, *Cibicides*, and *Discorbis*, which inhabit coralline algae and coral reefs. Nearshore and lagoon foraminifera are represented by miliolids and comprise *Pyrgo* and *Quinqueloculina*, and *Archaias*. Shallow water to open ocean species, including the *Lagena* and *Oolina*, and neritic to pelagic planktonic included *Globigerina*, *Globigerinella*, *Globigerinoides*,

and *Globoturborotalita*. The ostracods comprise Cytherellidae, Bairdiidae, Pontocyprididae, Bythocytheridae, Xestoleberididae, Cushmanideidae, Cytheruridae, Cytheridae, Cytherettidae, Hemicytheridae, and Trachyleberididae that inhabit the inner and mid-outer shelfs.

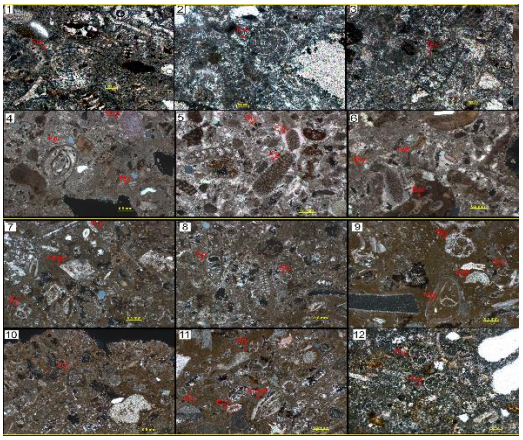

Figure 2. Microphotograph of microfossils from Ilha de Fortaleza outcrops, São João de Pirabas, Pará State, Brazil. The Ponta do Castelo outcrop comprises: 1, *Amphistegina* (Amph); 2, *Pyrgo* (Pyr); 3, *Textularia* (Tex); 4, *Spiroloculina* (Spi) and *Textularia* (Tex); 5, coralline algae (Alg), bryozoan (Bry), and echinoids spines of Cidaridae (Ech); 6, asteroid paxila (Ast), bryozoan (Bry), and balanid (Bal). The Fazenda outcrop comprises: 7, *Amphistegina* (Amph) and bryozoan (Bry); 8, *Textularia* (Tex) and bryozoan (Bry); 9, ophiuroids ossicles of Gorgonocephalidae (Ech), aff. *Margaretta*) (Bry), and bivalve (Mol) 10, planktonic foraminifera (For); 11, *Amphistegina* (Amph) and aff. *Nellia* (Bry); 12, *Globorotalia*/*Globigerina* (For).

The mineralogical composition (Fig. 3) of the oldest outcrops (late early Miocene) from the Ilha de Fortaleza comprises calcite and ankerite in the most basal layer. They are almost pure carbonates and thus represent an exposed part of the Bragantina platform. Referential outcrops from the Pirabas Formation like Praia de Atalaia, Praia do Maçarico, and Aricuru are rich in siliciclastic and thus they are close to the coast. The element concentrations testify to the fact that Ponta do Castelo and Fazenda represent an exposed part of the platform. The facies α is dominated by CaO (Ponta do Castelo and Fazenda outcrops, and in the referential Capanema B-17 quarry). The facies ß shows inputs of terrigenous sources of SiO2, Al2O3, and Fe2O3 including other referential outcrops (Praia do Atalaia, Praia do Maçarico, Aricurú, and Baunilha Grande), and the Y is characterized by MgO involved in the diagenesis processes (basal section of Praia do Atalaia).

Conclusions

According to geochemical and micropaleontological data, the outcrops at Ponta do Castelo and Fazenda depict an open marine environment, while the other Pirabas Formation reference outcrops are found close to the coast. The fossil disposition is chaotic, and the fossil assemblage consists of a combination of components from several paleoenvironments. The Pirabas Formation paleoenvironmental set provides clear evidence of high-energy storms throughout the early to middle Miocene.

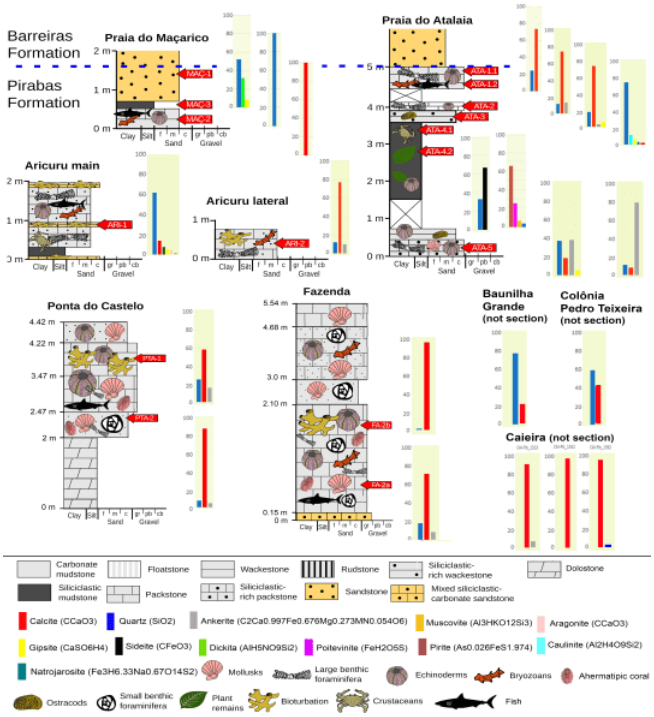

Figure 3. Simplified stratigraphic logs from the Pirabas Formation outcrops and quarry (modified from Aguilera et al., 2022), showing the mineral characterization and the semi-quantitative percent analyzed by X-Ray Diffraction.

Acknowledgments

The authors thank CNPq for financial support; to the National Mining Agency of Brazil and PETROBRAS for granting the samples; to UFF MPEG for the infrastructure.

References

[1] Maury, C.J., 1925. Fósseis terciários do Brasil com descrição de novas formas Cretáceas. Serviço Geológico e Mineralógico do Brasil, Monografia 4, 665 p.

[2] Aguilera et al., 2022. Palaeoenvironment of the Miocene Pirabas Formation mixed carbonate–siliciclastic deposits, Northern Brazil: Insights from skeletal assemblages. Marine and Petroleum Geology, 145, 105588. https://doi.org/10.1016/j.marpetgeo.2022.105855.

[3] Aguilera et al., 2023. Miocene tropical storms: Carbonate framework approaches and geochemistry proxies in a reservoir model. Marine and Petroleum Geology, 106333. https://doi.org/10.1016/j.marpetgeo.2023.106333.

[4] Gomes et al., 2023. Biostratigraphy and paleoenvironments of the Pirabas Formation (Neogene, Pará state-Brazil) Mar. Micropaleontol., 180, 102218. https://doi.org/10.1016/j.marmicro.2023.102218.

[5] Banha et al., 2022. The great Amazon reef system: a fact Front. Mar. Sci., 9, 088956. https://doi.org/10.3389/fmars.2022.1088956.

[6] Vale et al., 2022. Distribution, morphology and composition of mesophotic 'reefs' on the Amazon Continental Margin Mar. Geol., 447, 106779. https://doi.org/10.1016/j.margeo.2022.106779.

Characterization of terrestrial organic carbon during the last glacial from marine core in the western equatorial Atlantic

Alice Maria da S. Rodrigues[1]*, Rodrigo de L. Sobrinho[1], Patrícia Piacsek[6], Ioanna Bouloubassi[2], Arnaud Huguet[5], Ana Luiza S. Albuquerque[3], Igor M. Venancio[1], Joana F. Cruz[1], Mercedes Mendez[4], Marcelo C. Bernardes[1]

[1]Department of Geochemistry, Federal Fluminense University, Niterói, Brazil.
[2]Sorbonne Université, CNRS, IRD, MNHN, Laboratoire d'Océanographie et du Climat: Expérimentations et Approches Numériques, LOCEAN, IPSL, F-75005, Paris, France.
[3]Department of Geology and Geophysics, Federal Fluminense University, Niterói, Brazil.
[4]IRD, SU, CNRS, MNHN, IPSL, LOCEAN: Laboratoire d'Océanographie et du Climat: Expérimentations et Approches Numériques, Bondy, France.
[5]Milieux Environnementaux, Transferts et Interactions dans les Hydrosystèmes et les Sols (METIS), Sorbonne Université, Campus Pierre et Marie Curie, Paris, France.
[6]Centro de Geociencias, Universidad Nacional Autónoma de México, Campus UNAM Juriquilla, Querétaro, Oro, México, 76230.

e-mail: alicemsrodrigues@gmail.com

Introduction

The continental margins prompeted by rivers contribute significantly to the sedimentation of organic carbon (OC) and are crucial for the burial process in the global carbon cycle (2). The sedimentary organic carbon (SOC) is mainly produced on the continent by terrestrial plants and subsequently transferred to the marine environment via river systems (1). Therefore, disturbances in vegetation cover on drainage basins alter continental organic carbon (OCcont) sedimentation in coastal areas, consequently affecting the global carbon budget. Therefore, the links between past climate changes, the continental vegetation, and the burial of organic carbon in marine sediments for a specific region have been a relevant issue in paleoclimate research (5). This study aims to investigate how precipitation changes alter the dynamics of OCcont quality, transport, and preservation through the application of multiple biomarkers (lignin phenols, n-alkanes, and brGDGTs) in the marine sediment core GL - 1248 (0° 55.2' S, 43° 24.1' W) in northeastern Brazil (NEB). The scope of this work is limited to marine isotope stages 4 and 3 and their paleoclimatic events and their impact on the Parnaíba River Basin.

Experimental

This core was provided by the Brazilian oil company Petrobras and consists with 1,929 cm long. The method applied for the identification and quantification of lignin phenols consists of the oxidation with copper oxide (CuO) in a basic, inert medium and high temperature (3). Quantification was performed using Agilent 7890A gas chromatography coupled to ionizing flame detector (GC-FID) and HP-5 capillary column. Lipids were extracted from dry-frozen sediments (7-8g) by 3 times of ultrasonication using a solvent mixture of dichloromethane/methanol, 3:1 (v:v). Total lipids were fractionated by silica gel column chromatography using solvent mixtures of increasing polarities. The hydrocarbons were analyzed on an Agilent 6890N gas chromatography coupled to a flame ionization detector (GC-FID). The GDGT analyses were performed by high-pressure liquid chromatography (HPLC-MS) using Shimadzu LCLS-2020 equipment.

Results and Discussion

The Heinrich Stadials (HSs) during the glacial periods MIS4 and MIS3 have been associated with wet phases in NEB, known as HS6, HS5, HS4, and HS3 (8). However, repercussions of the dry season length within the HSs on the ecosystem composition/vegetation cover in NEB have been recently debated (6), possibly affecting the transport of OC_{cont}. The Ti/Ca ratio and Total Organic Carbon (TOC) values of the GI-1248 showed a decrease during the MIS4-MIS3 transition (Figures 1A and B). These results are followed by low concentrations of total lignin (Σ8), long-chain *n*-alkanes ($\sum C_{27}$-C_{35}), and brGDGTs (Figures 1C, D, and E, respectively) until the end of HS5a, where it reached its lowest value. Along MIS3, they increased during Heinrich stadials (HS5, HS4, and HS3). Thus, despite their differences, the biomarkers confirm changes in continent-ocean transport at the MIS4-MIS3 transition and during the HSs of MIS3. The MIS4-MIS3 transition was marked by the predominance of the woody OCcont source. We assumed that the predominance of more refractory compounds displayed during the MIS3, such as lignin phenols, favored its burial, even in the low supply of n-alkanes (HS5a and HS3) to the SOC. Low insolation seems to have dictated reduced ocean-continent transport, increasing the length of dry seasons,

reflected in the low n-alkane burial during HS5a and HS3 (Figure 1D) (6). On the other hand, lignin phenols and long-chain n-alkanes (∑C27-C35) also showed positive intrusions in HS5 and HS4, suggesting a high contribution of precipitation events to the burial and preservation of OCcont during this period. We suggest that HS events, especially HS5 and HS4, facilitated both the change in OCcont quality and transport and burial, thus leading to more significant OCcont sequestration in coastal environments.

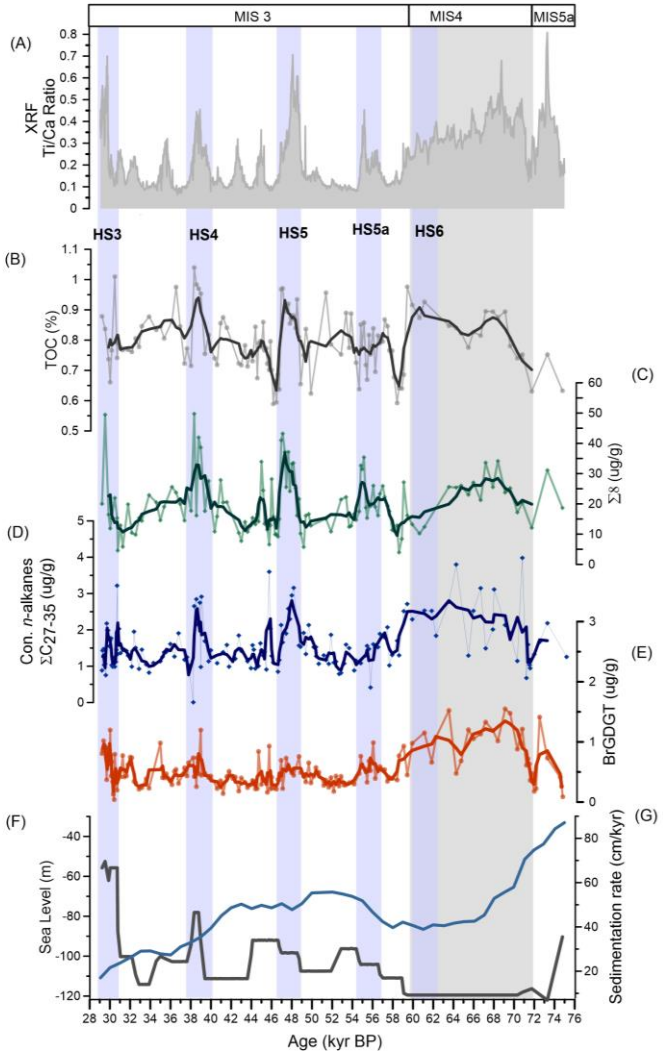

Figure 1. Data from the marine sediment core GL-1248 produced in the present work and found in the literature. (A) Ti/Ca record (7); (B) Total organic carbon - TOC (%) (Fadina et al., 2019); (C) Total lignin phenols per dry weight of sediment (∑8 ug/g); (D) Concentration of long-chain odd *n*-alkanes ∑C27-35; (E) BrGDGT, as a source of COterr from soil, as BrGDGTs are mainly derived from soil bacteria. (F) Sea level (m) (Waelbroeck et al., 2002); (G) Sedimentation rate (cm/Kyr) (7). The vertical bars in blue mark the Heinrich Stadial (HSs) distribution during MIS4 and MIS3, the MIS4 is marked in gray. For parameters C, D, E, and F, a 3-point moving average (thick lines) was assigned to accentuate trend variations.

Conclusions

The change in OCcont quality perceived during the precipitation anomalies in NE Brazil, along with facilitated transport along HS events, likely influenced OCcont production and burial along the HS, especially during HS5 and HS4 events, resulting in greater OCcont sequestration in the coastal environment.

Acknowledgements

The authors thank CAPES cod. (PPG-Geoquímica-UFF); FAPERJ (Procs. E-26/010.101117/2018, E-26/210.745/2021); CNPQ (Proc. 309474/2022-1); CAPES/Paleoceano Project (23038.001417/2014-7); CAPES-IODP/Aspecto Project (88887.091731/2014-01) and CAPES/Programas Estratégicos (88881.145911/2017-01).

References

[1] Atwood TB, Witt A, Mayorga J, Hammill E and Sala E. Global Patterns in Marine Sediment Carbon Stocks. Front. Mar. Sci, (2020).

[2] Bradley, J.A., Hülse, D., LaRowe, D.E. et al. Transfer efficiency of organic carbon in marine sediments. Nat Commun 13, 7297 (2022).

[3] Goñi, M.A.; Hedges, J.I. Cutin-derived CuO reaction products from purified cuticles and tree leaves. Geochimica et Cosmochimica Acta, v. 54, p.3065-3072, 1990.

[4] Jennerjahn, T.C.; Ittekkot, V.; Arz, H.W.; Behling, H.; Patzold, J.; Wefer, G. Asynchronous terrestrial and marine signals of climate change during Heinrich Events. **Science**, v.306 (5705), p. 2236-2239, (2004).

[5] Korasidis, V. A., Wing, S. L., Shields, C. A., & Kiehl, J. T. Global changes in terrestrial vegetation and continental climate during the Paleocene-Eocene Thermal Maximum. Paleoceanography and Paleoclimatology, 37, e2021PA004325, (2022)

[6] Piacsek, P.; Behling, H.; Strílis, N. M.; Ballalai, J.M.; Venancio, I. M.; Rodrigues, A. M.S.; Albuquerque, A. L. S. Response of vegetation to hydroclimate changes in northeast Brazil over the last 130 kyrs, Palaeogeography, Palaeoclimatology, Palaeoecology, v. 605, (2022).

[7] Venancio I. M.; Mulitza S.; Govin A.; Santos T. P.; Lessa D. O.; Albuquerque A. L. S.; Chiessi C. M.; Titedemann R.; Vahlenkamp M.; Bickert T.; Schulz M. Millennial- to orbital-scale responses of western equatorial Atlantic thermocline depth to changes in the trade wind system since the Last Interglacial. **Paleoceanography and Paleoclimatology**, v. 33, n. 12, p. 1490-1507, (2018).

[8] Wang, X.; Auler, A. S.; Edwards, R. L.; Cheng, H.; Cristalli, P. S.; Smart, P. L.; Richards, D. A.; Shen, C.-C. Wet periods in northeastern Brazil over the past 210 kyr linked to distant climate anomalies. **Nature**, v. 432, p. 740–743, (2004).

APPLICATION OF PENTACYCLIC TRITERPENOL METHYL ETHERS IN RECENT SEDIMENTS: A NEW PALEOENVIRONMENTAL INDEX?

Vinícius B. Pereira, Karen T. Stelzer, Rafael S. Xavier, Alexander A. Lopes, Raquel V. S. Silva, Débora A. Azevedo

Federal University of Rio de Janeiro (UFRJ), Rio de Janeiro, Brazil

*e-mail: viniciuspereira@iq.ufrj.br

Introduction

Coastal lagoons are important aquatic ecosystems, formed by sedimentation of bays or river estuaries, separated from the ocean by sandbars. They provide excellent basis for the studies of processes controlling the evolution of the coastal zone, and are under the influence of both terrestrial and marine inputs (García and Muñoz-Vera, 2015). Therefore, each lagoon presents an unique organic matter signature and are of great importance for the understanding of transitional environments.

Pentacyclic triterpenol methyl ethers (PTME) are biomarkers of specific higher plant subspecies, generally associated with Gramineae input. These compounds appear to be more resistant to environmental alteration in comparison to their alcohol counterparts, whose diagenesis involves oxidation, dehydratation, ring opening and aromatization consequent of removal of the C-3 hydroxyl group (Oyo-Ita et al., 2010). Despite its relevance to limnological and environmental studies, few reports of PTME in plants from tropical environments have been assessed.

Thus, this work aims to investigate occurrence of PTME structures present in the sediment core from Garças lagoon, located in the Jurubatiba Sandbank National Park, located in northern Rio de Janeiro State, Brazil. This lagoon is located in a *restinga* between dunes with flat areas which allows the formation of perennial pools, resistant during drought seasons and maintained by groundwater (Enrich-Prast et al., 2004).

Experimental

A 40 cm core was collected near the margin of the lagoon (-22°,21'35.1"S; -41°99'07.8"W) using 50 cm corer and sectioned at 2 cm each, which were subsequently lyophilized. Approximately 2 g of each section was extracted using dichloromethane/methanol mixture using an accelerated solvent extractor, ASE 350 (Dionex, USA).

The extracts were concentrated, followed by saponification using 1 mL KOH 0.1 mol L^{-1} in methanol/water 9:1 at 80 °C for 3 h, and by liquid-liquid extraction (3×3 mL *n*-hexane) to obtain neutral lipids.

The neutral lipids fraction was diluted in 500 µL dichloromethane and analyzed using GC/MS system, consisted of an Agilent Technologies 7890A gas chromatograph coupled to a 4000C mass spectrometer. The GC was equipped with a HP-5MS (5% phenyl-95% methylsiloxane, 30 m, 0.25 mm i.d., 0.25 µm df; Agilent Technologies) as stationary phase.

Results and Discussion

PTME identification (Fig 1) was achieved monitoring extracted ion chromatogram (EIC) *m*/*z* 440.8 ($M^{+\bullet}$) and characteristic ions, such as *m*/*z* 425 $(M-15)^+$,408 $(M-32)^{+\bullet}$ and 393 $(M-32-15)^+$.

Six compounds were identified with individual concentration varying from 0.05 to 4.89 µg g^{-1} in all the core sections. Compound II was identified as taraxer-14-en-3β-ol ME, and compounds IV-VI present fragmentation patterns consistent with fernene or arborene-based structures, with intense peaks at *m*/*z* 273. They were assigned as isomers of fern-9(11)-en-3β-ol methyl ether (ME), and retention times shift are associated with α-β isomerization at positions C14, 15 and 17.

The disappearance of structures IV and V in the most recent segments of the core hints to a diagenetic origin of these compounds. These compounds are most likely originated from the structural rearrangement of VI structure, present in all the segments. Structure I also present *m*/*z* 273 fragment, but retention time consistent with tetracyclic triterpenol. Ions at *m*/*z* 163, 191, 205 and 206 in the mass spectrum most likely point to lanostedien-3β-ol ME (Jacob et al., 2005), whereas *m*/*z* 191 as base peak in structure III has not been previously associated with any known compound.

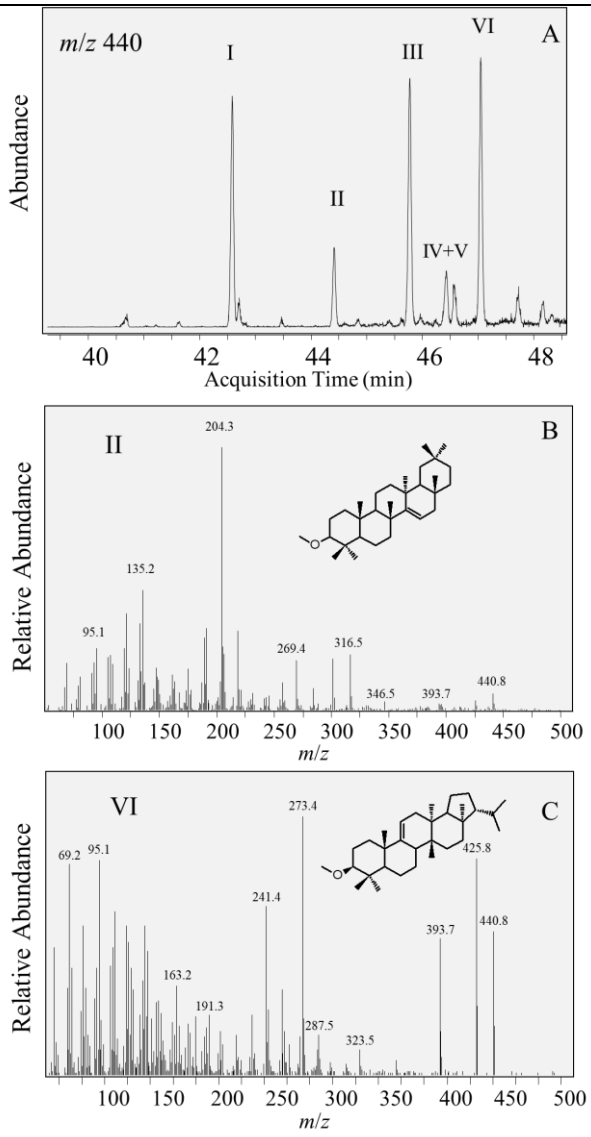

Fig 1. (A) EIC *m/z* 440, revealing PTME structures in the 28 cm depth sample, and mass spectra assigned as (B) taraxer-14-en-3β-ol ME (structure II) and (C) fern-9(11)-en-3α-ol ME (structure VI).

The overall concentration of these compounds varied greatly among the samples, with maximum at 8 cm depth (Table 1). This would be associated with a stronger contribution of Gramineae to the organic matter input in this section. Given the nature of the Garças lagoon, the appearance of Gramineae in most recent periods hints to a decrease in water content in the lagoon, allowing for these plants to grow.

This result agrees with *n*-alkane distribution and terrigenous over aquatic ratio (TAR), a classic proxy applied on organic matter origin studies, which present highest value at 8 cm (TAR = 31.0).

Table 1. Individual concentration of PTME detected in the core and TAR value of each depth

Depth (cm)	Concentration (μg g^{-1})						TAR
	I	II	III	IV	V	VI	
2	1.72	0.67	0.51	n.d.	n.d.	0.81	12.5
8	0.14	4.89	0.43	n.d.	n.d.	0.79	31.0
16	0.49	0.79	0.39	0.04	0.05	0.21	4.8
28	0.70	0.42	0.57	0.05	0.05	0.05	6.7

TAR = (C_{27} + C_{29} + C_{31}) / (C_{15} + C_{17} + C_{19}); n.d. – not detected

Conclusions

Six PTME have been identified in the Garças lagoon, one of the 19 coastal lagoons from the Jurubatiba Sandbank National Park, Rio de Janeiro State, Brazil. These compounds are specific higher-plant biomarkers of Gramineae input in sediments, and their quantity can be applied in future indexes of paleoenvironmental reconstructions for modern environments, in comparison to classic ratios largely used in geochemical records. This is, to the best of our knowledge, the first assessment of PTME compounds in recent sediments from SE Brazil.

Acknowledgements

The authors thank Capes, CNPq and FAPERJ for fellowships and financial support.

References

Enrich-Prast, A., Bozelli, R.L., Esteves, F.A., Meirelles, F.P. 2004. Lagoas costeiras da Restinga de Jurubatiba: Descrição de suas variáveis limnológicas. In Pesquisas de longa duração na Restinga de Jurubatiba – Ecologia, história natural e conservação (C.F.D. Rocha, F.A. Esteves & F.R. Scarano, eds). RiMa, São Carlos, 245-253).

García, G., Muñoz-Vera, A. 2015. Characterization and evolution of the sediments of a Mediterranean coastal lagoon located next to a former mining area. Marine Pollution Bulletin 100, 249-263.

Oyo-Ita, O.E., Ekpo, B.O., Oros, D.R., Simoneit, B.R.T. 2010. Occurrence and Sources of Triterpenoid Methyl Ethers and Acetates in Sediments of the Cross-River System, Southeast Nigeria. International Journal of Analytical Chemistry 2010, 1-8.

Jacob, J., Disnar, J.R., Boussafir, M., Albuquerque, A.L.S., Sifeddine, A., Turcq, B. 2005. Pentacyclic triterpene methyl ethers in recent lacustrine sediments (Lagoa do Caçó, Brazil). Organic Geochemistry 36, 449-461.

Determination of renewable content in aviation kerosene samples using carbon-14

Marcos Felipe C. Silva[1], Kita Chaves Damasio Maracrio[1], Carla Regina Alves Carvalho[1], Fabiana Monteiro de Oliveira[1], Renata Magalhães Jou[1], Marco Antonio Teixeira[1], Joana Artiles Escudine[1]

[1]Laboratório de Radiocarbono, Instituto de Física, Universidade Federal Fluminense, Av. Gal. Milton Tavares de Souza, s/n, Niterói, 24210-346, Rio de Janeiro, Brazil

mfcostasilva@id.uff.br

Introduction

Due to growing environmental concerns, there has been a significant effort to avoid the excessive use of petroleum-based fuels, which has been causing extensive environmental degradation. All over the world, research is being conducted to explore and develop alternative sources, such as biodiesels or fuels blends with biogenic carbon content. These fuels are produced by volumetrically mixing fossil and renewable sources during the production process. Although these options effectively reduce greenhouse gas emissions, it is crucial to maintain the same chemical composition and energy efficiency. Radiocarbon analysis is a highly precise and accurate method used to determine the biogenic fraction, enabling the distinction between fossil and modern carbon. In this study, aviation kerosene samples were analyzed in quintuplicate at LAC-UFF using the 14C-AMS technique.

Experimental

The samples were frozen in liquid nitrogen under vacuum prior to combustion. Graphitization was the performed using sealed Pyrex tubes using the zinc and Titanium hydride method. Renewable content was determined according to the ASTM-D6866-21 guidelines. The results are presented in following:

Table 1: Renewable content for samples using 14C-AMS.

Samples	Biogenic fraction	pMC (means)
1	1 ± 3	1,024 ± 0,028
2	1 ± 3	1,307 ±0,028
3	1 ± 3	1,267 ± 0,028
4	1 ± 3	1,087 ± 0,040

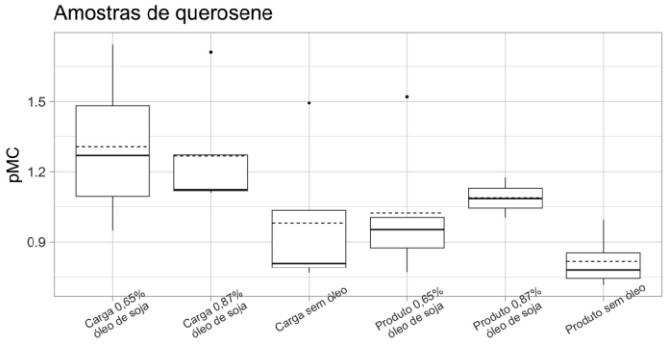

Figure 1. Comparison between pMC means of all sample results from kerosene.

Results and Discussion

The use of biogenic feedstocks in biofuel production and the efficiency of their presence on commercially significant products require differentiation among sources of materials with similar chemical characteristics. Due to the indistinguishable chemical composition of each product, the solution lies in utilizing natural markers.

The renewable content in a material can be quantified through the analysis of the isotopic ratio of carbon-14, calculated according to ASTM-D6866-21 (Standard Test Methods for Determining the Bio-based Content of Solid, Liquid, and Gaseous Samples Using Radiocarbon Analysis). The material that presents this ratio similar to that of the current atmosphere is considered as 100% biogenic.

In the analyses of the samples in this study, the 14C technique by Accelerator Mass Spectrometry (14C-AMS) was used, which is extremely efficient as it allows the direct counting of carbon atoms.

Aviation kerosene is a fuel that requires several physical-chemical quality criteria for its proper use. The 14C-AMS technique is the most commonly used method in the world to determine the biogenic fraction. However, when

working in the range below 1% of renewable load in fuel blends, the detection limit can be compromised or may not be very accurate. The samples sent by Petrobras had loads of renewable content between 0.65% and 0.87% of soybean oil. Figure 1 shows a variation in pMC values with the addition of renewable load.

Conclusions

With the results, questions about accuracy and precision in the analyses proved to be of great importance, indicating a characterization technique surrounded by advantages, which is directed towards market expectations. The knowledge generated in the study was intended to improve the determination of the biogenic fraction of fuels by the 14C-AMS technique and at the same time the processes used for the production of biofuels, especially those aimed at aviation.

Acknowledgements

The authors thank FEC-UFF, CAPES and CNPq (Brazilian research councils) for fellowships; Petrobras S/A and PPG Geo – UFF for financial support.

References

Pinto, A.C. et al. (2005). Biodiesel: An overview. Journal of the Brazilian Chemical Society. DOI: 10.1590/S0103-50532005000800003

Reddy, C.M. (2008). Determination of Biodiesel Blending Percentages Using Natural Abundance
Radiocarbon Analysis: Testing the Accuracy of Retail Biodiesel Blends. Environ. Sci. Technol. 42:
2476–2482.

Dijs, I.J. et al. (2006). Quantitative determination by 14 C analysis of the biological component in fuels,
Radiocarbon 48 (3): 315–323.

Jou et al. 2015. Biogenic fraction in the synthesis of polyethylene terephthalate. International journal of mass
spectrometry. 388: 65-68.

Macario et al. 2013. The Brazilian AMS Radiocarbon Laboratory (LAC-UFF) and the intercomparison of results with CENA and UGAMS. Radiocarbon. 55:325 – 330.

ALF
BIOGEOCHEMISTRY

XVI LATIN AMERICAN CONGRESS ON ORGANIC GEOCHEMISTRY
9 - 11 AUGUST, 2023
ARACAJU, SERGIPE, BRAZIL

HIGH SPATIAL VARIABILITY OF AEROBIC CARBON DIOXIDE PRODUCTION IN AMAZONIAN FLOODED SOILS (MADEIRA RIVER, BRAZIL)

ANA LUISA FONSECA*[a], FAUSTO MACHADO-SILVA[b], ROBERTA BITTENCOURT PEIXOTO[b], JASQUELIN PEÑA[c], TORSTEN VENNEMANN[c], LEONARDO AMORA-NOGUEIRA[a], GUILHERME QUINTANA[ac], INGO WAHNFRIED[d], MATHIEU MARTINEZ[c], JORGE ALMEIDA DE MENEZES[d], AMAZONINO LEMOS DE CASTRO[d], CARLOS BARBOSA PESSOA[d], PETRUS MAGNUS AMARAL GALVÃO[ac], HUMBERTO MAROTTA*[a]

[a]PROGRAMA DE PÓS-GRADUAÇÃO EM GEOQUÍMICA (GEOCIÊNCIAS) – UFF, [b]UNIVERSITY OF TOLEDO, [c]UNIVERSITY OF LAUSANNE, [d]UNIVERSIDADE FEDERAL DO AMAZONAS (UFAM)

analuisaoliveira@id.uff.br
humbertomarotta@id.uff.br

Introduction

The Amazon floodplain has long been considered an important carbon sink (C) and biological control of greenhouse gases (GHGs) [2][3]. Seasonal variations of drought and flooding determine substantial fluctuations in the balance between biological synthesis [4] and remineralization of organic matter (OM) [5], which affects the production of GHGs and especially carbon dioxide (CO_2) [6].

In addition, climatic extremes events are increasingly frequent due to anthropogenic causes in the Amazon rainforest [7][8]. The dynamics of droughts and floods highlights the need for studies on the rates of degradation of OM in soils influenced by the seasonal flooding of rivers. However, the spatial heterogeneity of the most efficient pathway of CO_2 production by OM degradation, which occurs under aerobic conditions [9], is still poorly understood in vast floodable areas. Thus, the present study aims to evaluate the spatial heterogeneity of aerobic CO_2 production in flooded soils of the Amazon river plain, from areas closer to distant from the main channel (Madeira River, Brazil).

Methodology

Soil cores (~10 cm deep and ~20 cm^2 of area) were collected in three sites (P1, P2 and P3) in the plain of the Madeira River, ~2 km upstream of the city of Humaitá (AM). P1 was the lowest annual frequency of flooding and the driest site, while P3 was closest to the lake and wet. P2 was intermediate between P1 and P3.

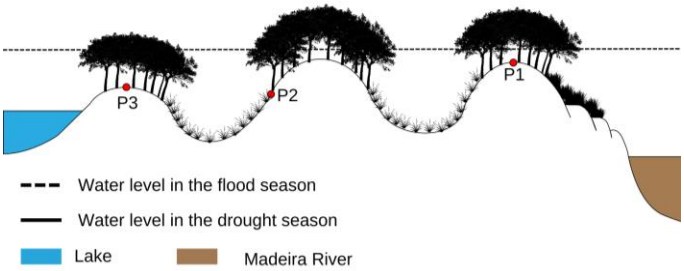

Figure 1. Representation of collection sites. The red circles represent the collection sites.

In the laboratory, intact soil cores were dried in an oven at 25°C for ~24 hours. Before incubation, river water was added to a water column ~2 cm above the surface [10], resulting in headspace ~250 mL. The incubation flasks were closed with atmospheric air at pressure at sea level. The CO_2 concentrations inside each flask were measured using a gas chromatograph (Agilent, model 7890B) equipped with a TCD detector at intervals of 3 to 10 minutes for ~1 hour, until the reduction of the production of this gas was achieved. Thus, we determined the aerobic production rates by the variation of the CO_2 concentration within the incubation core under experimental conditions.

Results and Discussion

The results showed significant differences in CO_2 production between points P1 and P3, while P2 did not obtain difference for either of the two points (one-factor ANOVA followed by Tukey's post-test, $p<0.05$). The rates of aerobic CO_2 production in flooded soils reached on average ~10887(±1628) $mgC\text{-}CO_2 m^{-2} d^{-1}$, or ~2 times the P1 value.

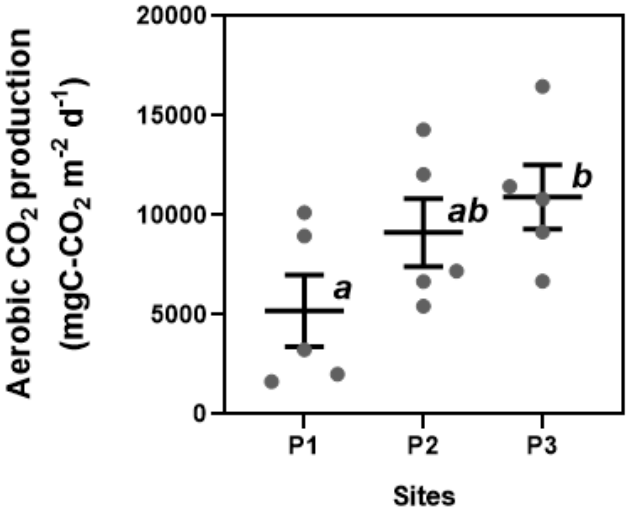

Figure 2. Aerobic production of CO^2 (mgC-$CO^2m^{-2}d^{-1}$) in P1, P2 and P3. The bars represent the averages and each gray circle a replica. Equal letters indicate non-significant difference (one-factor ANOVA followed by Tukey's post-test, p<0.05)

In the present study, soils that were inland and more frequently submerged by depositional aquatic ecosystems (i.e., P3 by the lake) showed higher aerobic CO_2 production rates than those closer to the river channel (i.e., P1). The lacustrine waters can favor the production of labile aquatic OM, associated with algae and aquatic macrophytes in less turbulent conditions [11] [12]. This labile OM could be a substrate for CO_2 production by aerobic decomposition. On the other hand, the P1 site could present a more erosive characteristic in a higher area next to the high-energy river, contributing to reduce the deposition of OM both terrestrial [13] and aquatic [14].

Conclusion

The study highlights a variation in aerobic CO_2 production by an order of magnitude at collection sites situated a relatively short distance in the Madeira River plain. Aerobic CO_2 production can be highly spatially variable, which highlights the need to understand the heterogeneity of C cycling in the floodplain in equatorial forests.

Acknowledgements

The authors thank the CAPES funding institutions and CNPq, as well as the GAS-UFF Multiuser Unit for the analyses.

References

[1] Amora-Nogueira, L.., et al., 2022. Tropical Forest as drivers lake carbon burial. Nature communications 13, 1-7.

[2] Sanders, L.M., et al., 2017. Carbon accumulation in Amazonian floodplain lakes: A significant component of Amazon budgets. Limnology and oceanography letters 2, 29-35.

[3] Moreira-Turcq, P., et al., 2013. Seasonal variability in concentration, composition, age, and fluxes of particulate organic carbon exchanged between the floodplain and Amazon River. Global Biogeochemical Cycles 27, 119–130.

[4] Santoro, M., et al., 2021. The global forest above-ground biomass pool for 2010 estimated from high-resolution satellite observations. Earth System Science Data 13, 3927-2950.

[5] Pangala, S., et al., 2017. Large emissions from floodplain trees close the Amazon methane budget. Nature 552, 230–234.

[6] Marengo,J.A., 2016. Extreme seasonal drought and floods in Amazonia: causes, trends and impacts. Int. J. Climatol.36: 1033 – 1050.

[7] Machado-Silva, F., Peres, L.F., Gouveia, C.M., 2021. Drought Resilience Debt Drivers NPP Decline in the Amazon Forest. Global Biogeochemical Cycles 35, 1-19.

[8] BASTVIKEN, D., 2010. Methane. In: Encyclopedia of Inland Waters. v. 2, p. 783-805.

[9] Sánchez-Garcia, C., et al. 2020. Water repellency reduces soil CO2 efflux upon rewetting, Science of the Total Environment 708, 1-31.

[10] Fasching, C., et a., 2014. Microbial degradation of terrigenous dissolved organic matter and potential consequences for carbon cycling in brown-water streams. Scientific Reports 4, 1-70.

[11] Kumar, S.S., et al., 2022. Impact of climate change on soil health. International Journal of Environmental Science 7, 70-90.

[12] Sanders, L.M., et al., 2017. Carbon accumulation in Amazonian floodplain lakes: A significant component of Amazon budgets. Limnology and oceanography letters 2, 29-35.

[13] Ciemer, C., et al., 2019. Higher resilience to climatic disturbances in tropical vegetation exposed to more variable rainfall. Nature Geocience 12, 174-179.

SUBSURFACE METHANE PRODUCTION IN THE SEDIMENT OF AN AMAZONIAN FLOODPLAIN LAKE (HUMAITÁ, AM)

ANA LUISA FONSECA*[ab], THAIRINY FONSECA[ab], MANUELA LIMA CARVALHO[b], DOUGLAS DA MOTTA PIO[b], LEONARDO AMORA-NOGUEIRA[ab], GUILHERME QUINTANA[abd], LUIZA MACHADO[bc], HELENA BOMFIM[b], DANIELA FRANÇA[b], HUMBERTO MAROTTA*[abc]

[a]PROGRAMA DE PÓS-GRADUAÇÃO EM GEOQUÍMICA (GEOCIÊNCIAS) - UFF, [b]UNIDADE DE MULTIUSUÁRIO EM GEOQUÍMICA DE GASES, ÁGUA E SEDIMENTOS DA UNIVERSIDADE FEDERAL FLUMINENSE, [c]PROGRAMA DE PÓS-GRADUAÇÃO EM GEOGRAFIA – UFF, [d]UNIVERSITY OF LAUSANNE

analuisaoliveira@id.uff.br
humbertomarotta@id.uff.br

Introduction

In recent decades, studies have been highlighted that show the strong contribution of lakes in carbon cycling (C) [1][2]. These ecosystems receive important inputs of organic matter (OM) from the forest in vast areas in the drainage basin [3], as well as from the autochthonous processes themselves [4]. Thus, the lacustrine sediments become important sites of deposition [5] subsequent biological remineralization [6] of OM. The high consumption of oxygen in thin surface layers contributes to anoxia, favoring the occurrence by anaerobic pathways of degradation of OM, including the production of methane (CH_4), one of the most important greenhouse gases [6].

In tropical forests, due to year-round warm conditions, methanogenesis from OM remineralization in lake sediments can be intensified [7]. The Amazon is the most productive forest on the planet [8], located in the river basin with the largest volume of water [9]. Although potentially important in anoxic subsurface sedimentary layers, its potential for CH_4 production is still poorly known. In this sense, the present study aims to determine the rate of CH_4 production at different depths of bottom sediment of an Amazon floodplain lake.

Methodology

Lake Puruzinho is located in the municipality of Humaitá-AM, floodplain of the Madeira River. In its depocenter, a sedimentary core of ~1.1 m was collected (Figure 1). Throughout the hydrological cycle, it is influenced by the black waters of the forest and white waters of the river channel, which are characterized by the acidic pH associated with the high concentrations of dissolved OM, and neutral-basic with high content of suspended material, respectively [10]. For anaerobic incubation conditions, the core was sliced in the depths: 0-15cm, 15-35cm, 35-55cm, 55-75cm, 75-95cm, 95-110cm. All sediment manipulation was performed in a glove box with dinitrogen gas atmosphere. After incubation, the flasks with sediment were kept in a thermal bath at 25°C for 24 days of experiment and analysis intervals of 1-3 days. CH_4 concentrations were measured by an Agilent Gas Chromatograph (7890B) equipped with methanizer and FID detector. The production rates of CH_4 were determined by the variation of this gas over the experimental time, assuming the maximum inclination and a minimum of 3 consecutive measurements and R^2>0.80 [11].

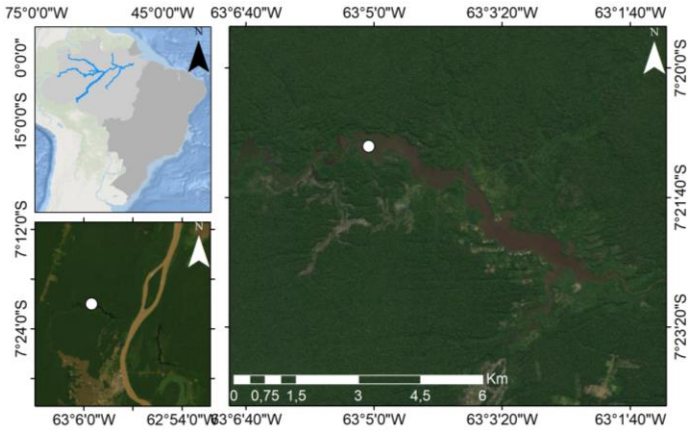

Figure 1. Geographical location of Lake Puruzinho.

Results and Discussion

The present study identified a higher mean production of CH_4 in the subsurface layer of 15-35 cm, ~1.440(±0.2312) mmolC-CH4 $m^{-2}d^{-1}$, reaching values ~3 times higher than the surface of 0-15 cm. Even deeper layers of 55-75 cm and 75-95 cm showed methanogenesis rates ~60% compared to those found on the surface.

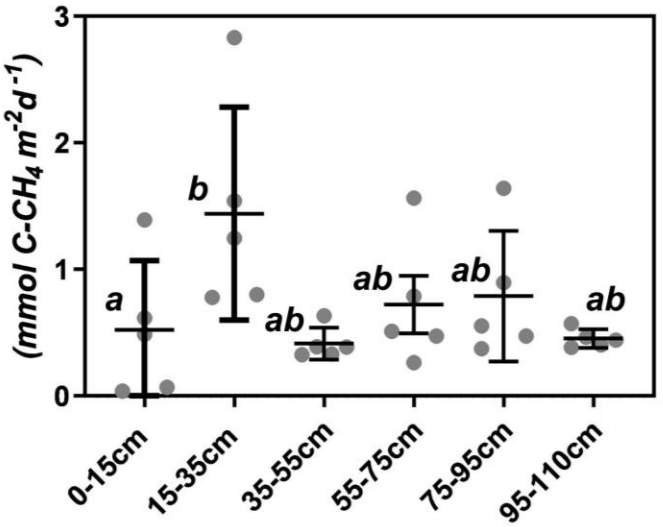

Figure 2. Production of CH_4 (mmol C-CH_4 $m^{-2}d^{-1}$) in each sedimentary depth of Lake Puruzinho. The bars represent the averages and each gray circle a replica. Equal letters indicate non-significant difference (one-factor ANOVA followed by Tukey's post-test, p<0.05)

These results contrast to the vast evidence described in the literature for freshwater over the past few decades, describing the most superficial benthic fraction as the most active for metabolic pathways that produce CH_4 [12]. Although with higher CH_4 production in layers even deeper than 15 cm, this pattern of subsurface increment is commonly found in marine sediments, attributed to the presence of electron acceptors that favor MO degradation pathways that compete with methanogenesis and that becomes reduced in depth [13]. In this sense, the lower rates of methanogenesis in the superficial benthic layer could be attributed to the typical presence of ions in the Amazonian white waters [10] since the variability of such acceptors can affect them significantly [14]. Another factor that may contribute to this difference along the vertical sedimentary profile is the burial of labile OM itself after storms or erosive events, contributing to increase the availability of organic substrates to biological remineralization in deeper layers of the sedimentary profile [15].

Conclusion

The study revealed that there is vertical variation in CH_4 production in tropical lake sediments. In addition, it was possible to observe non-superficial layers presenting a higher production than the top of the sediment, something little found in the freshwater literature. Therefore, the results demonstrated that subsurface sediment layers need to be an active OM remineralization site. The heterogeneity of CH_4 production along the benthic vertical profile is a potentially important component to understand the dynamics of C cycling in tropical forest basins.

Acknowledgements

The authors thank the Multiuser Unit in Geochemistry of Gases, Water and Sediments of the Fluminense Federal University for the analyses.

References

[1] Cole, J.J., et al., 2007. Plumbing the global carbon cycle: Integrating inland waters into the terrestrial carbon budget. Ecosystems 10, 171–184.
[2] Alin, S.R., 2007. Carbon cycling in large lakes of the world: A synthesis of production, burial, and lake-atmosphere exchange estimates. Global Biogeochemical Cycles 21, 1-12.
[3] Drake, T.W., 2018. Terrestrial carbon inputs to inland waters: A current synthesis of estimates and uncertainty. Limnology and Oceanography 3, 132-142.
[4] Attermeyer, K., et al., 2018. Organic Carbon Processing During Transport Through Boreal Inland Waters: Particles as Important Sites. JGR Biogeosciences 123, 2412-2428.
[5] Amora-Nogueira, L., et al., 2022. Tropical Forest as drivers lake carbon burial. Nature communications 13, 1-7.
[6] Val, K.J., et al., 2019. Estimates of the remineralization and burial of organic carbon in Lake Baikal sediments. Journal of Great Lakes Research 46, 102-114.
[7] BASTVIKEN, D., 2010. Methane. In: Encyclopedia of Inland Waters. v. 2, p. 783-805.
[8] Marotta, H., Pinho, L., Gudasz, C., 2014. Greenhouse gas production in low-latitude lake sediments responds strongly to warming. Nature Climate Change 4, 11–14.
[9] Malhi, Y., 2012. The productivity, metabolism and carbon cycle of tropical forest vegetation, 65–75.
[10] Junk, W., et al., 2011. A classification of major naturally-occuring Amazonian lowland wetlands. Wetlands 3, 623-640.
[11] MOREIRA-TURCQ, P. et al., 2004. Carbon sedimentation at Lago Grande de Curuai, a floodplain lake in the low Amazon region: Insights into sedimentation rates. Palaeogeography, Palaeoclimatology, Palaeoecology 214, 27–40.
[12] Segarra, K.E.A., et al., 2015. High rates of anaerobic methane oxidation in freshwater wetlands reduce potencial atmospheric methane emissions. Nature Communications 6, 1-12.
[13] Yin, X., et al., 2021. Sulfate reduction and its important role in organic carbon mineralization in sediments of the Pearl River Estuary. Estuarine, Coastal and Shelf Science 260, 1-11.
[14] Mach, V., et al., 2015. Methane production potentials, pathways, and communities of methanogens in vertical sediment profiles of river Sitka. Front. Microbiol 6, 506
[15] Bodmer, P., Wilkinson, J., Lorke, A., 2019. Sediment Properties Drive Spatial Variability of Potential Methane Production and Oxidation in Small Streams. JGR Biogeosciences 125, 1-15.

LABILE ORGANIC MATTER IN A MARINE SEDIMENT CORE AT SOUTHEASTERN BRAZILIAN MARGIN

CAROLINA SANTOS REIS DE ANDRADE DA SILVA[a]*, BRUNA BORBA DIAS[b]*, ANA LUIZA S ALBUQUERQUE[c]*, ELISAMARA SABIDINI-SANTOS[a]*, ANDRÉ BAHR[d]*, RUT AMELIA DÍAZ RAMOS[a]*

[a]Programa de Geoquímica Ambiental, Universidade Federal Fluminense/ [b] Escola de Artes, Ciências e Humanidades, Universidade de São Paulo/ [c]Departamento de Geofísica e Geologia, Universidade Federal Fluminense/ [d] Institute of Earth Sciences, Heidelberg University.

carolinasras@id.uff.br, brunaborbadias@id.uff.br, *ana_albuquerque@id.uff.br, esabidini@id.uff.br, andre.bahr@geow.uni-heidelberg.de*, *rutdiaz@id.uff.br

Introduction

Organic carbon degradation in marine sediments is a critical component of the global carbon cycle and is intricately linked to Earth's climate. Regarding the Brazilian continental margin, the knowledge of biogeochemical processes, as well as the main factors that act in the degradation of organic matter in sediments, have increased in the last decade, but it is still poorly understood [2,3]. Despite the wide application of lipid biomarkers, the quantification of major compounds classes of sedimentary organic matter – such as proteins, carbohydrates, and lipids – has not yet been addressed in Brazilian marginal sediments. Furthermore, the effects of environmental conditions that can alter the bioavailability and biodegradation of these biopolymers are unknown.

Experimental

The sediment core analyzed were collected at 430m depth at the continental shelf on the Southeastern Brazilian margin The first 10 cm of each sediment core was analyzed considering a resolution of 1 cm, excepting the first top centimeter which was sliced at 0.5 cm resolution. The total carbohydrate (CHO) concentrations were measured spectrophotometrically using the phenol sulfuric acid assay for sediment samples [5,7]. PRT concentrations were determined according to [8] modified by [11]. Total lipids (LIP) were extracted by direct elution with chloroform and methanol following the procedure of [1] and analyzed according to [9]. All biochemical analyses were carried out in three replicates, with a maximum coefficient of variation of 15 %. The sum of the carbon equivalents of CHO, PRT, and LIP was referred as biopolymeric carbon (BPC) considering the conversion factors of 0.40, 0.49, and 0.75 mgC.mg-1, respectively [6].

Results and Discussion

Downcore depth profile of the evaluated organic compounds is shown in Figure 1. Regarding the functional role of proteins, [10] defined it as a limiting factor for benthic organisms, while [4] related to the high levels of primary production. The prevalence of PRT content may reflect the supply of high-quality food, as suggested by the higher contribution of proteins compared to carbohydrates.

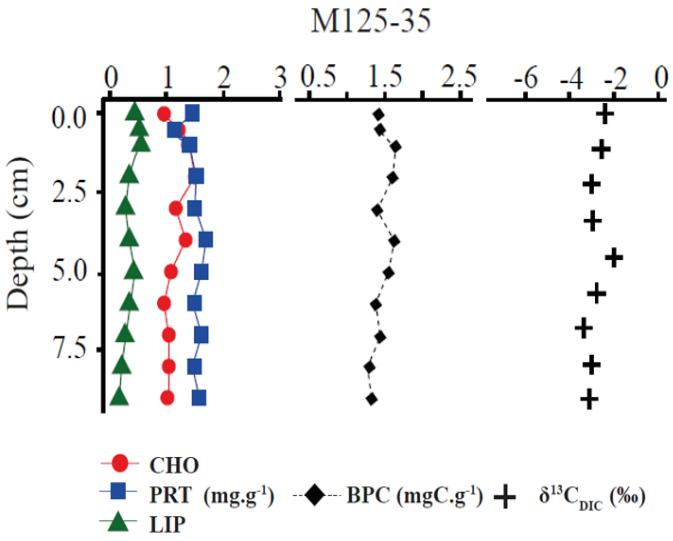

Figure 1. Depth profile of organic compounds in the sediments of investigated core M125-35: biopolymeric carbon (BPC), total carbohydrates (CHO), total proteins (PRT), total lipids (LIP) concentration and $\delta^{13}C_{DIC}$ values.

Considering that a relatively low rate of primary production is observed on the Brazilian margin [12], the highest values of PRT found in the M125-35 does not necessarily mean freshly accumulated organic matter,

but it could be related to slow organic matter recycling due to less heterotrophic activity. Also, the presence of high-quality organic matter in the sediments could be related to some differentiated sedimentation patterns triggered by local oceanographic dynamics. The downslope transport of sand to the depths around 300 – 450 m was reported for the region by the action of Brazil Current and South Atlantic Central Water flows reworking the shelf-derived sand due to the ocean-atmosphere changes and to the local physiography [13].

Conclusions

Here we evaluated the biopolymers distribution in a sediment core from the Southeastern Brazilian margin The presence of sediments with high-quality organic matter is attributed to a local downslope transport of the sand sediments that combines protective processes involving adsorption to mineral surfaces and preventing the heterotrophic consumption in the upper slope.

Acknowledgements

Carolina Santos R. de A. da Silva acknowledges the scholarship from Coordenação de Aperfeiçoamento de Pessoal de Nível Superior (CAPES) and Conselho Nacional de Desenvolvimento Científico e Tecnológico (CNPq). Bruna B. Dias appreciates financial support from Fundação de Amparo à Pesquisa do Estado de São Paulo (FAPESP, grant 2020/11452-3). Ana Luiza S. Albuquerque is a senior scholar from CNPq (grants 302521-2017-8 and 429767/2018-8). We also acknowledge the partial support from CAPES – Finance Code 001. Dataset from this work will be available on PANGAEA database.

References

1.Bligh, E.G., Dyer, W.J., 1959. A rapid method of total lipid extraction and purification. Canadian Journal of Biochemistry and Physiology 37, 911–917.

2.Carreira, R.S., Cordeiro, L.G.M.S., Oliveira, D.R.P., Baêta, A., Wagener, A.L.R., 2015. Source and distribution of organic matter in sediments in the SE Brazilian continental shelf influenced by river discharges: An approach using stable isotopes and molecular markers. Journal of Marine Systems, Biogeochemistry-ecosystem interaction on changing continental margins in the Anthropocene 141, 80–89.

3.Cordeiro, L.G.M.S., Wagener, A.L.R., Carreira, R.S., 2018. Organic matter in sediments of a tropical and upwelling influenced region of the Brazilian continental margin (Campos Basin, Rio de Janeiro). Organic Geochemistry 120, 86–98.

4. Dell'Anno, A., Mei, M.L., Pusceddu, A., Danovaro, R., 2002. Assessing the trophic state and eutrophication of coastal marine systems: a new approach based on the biochemical composition of sediment organic matter. Marine Pollution Bulletin 44, 611–622.

5. DuBois, Michel., Gilles, K.A., Hamilton, J.K., Rebers, P.A., Smith, Fred., 1956. Colorimetric Method for Determination of Sugars and Related Substances. Analytical Chemistry 28, 350–356.

6. Fabiano, M., Danovaro, R., Fraschetti, S., 1995. A three-year time series of elemental and biochemical composition of organic matter in subtidal sandy sediments of the Ligurian Sea (northwestern Mediterranean). Continental Shelf Research 15, 1453–1469.

7.Gerchakov, S.M., Hatcher, P.G., 1972. IMPROVED TECHNIQUE FOR ANALYSIS OF CARBOHYDRATES IN SEDIMENTS1. Limnology and Oceanography 17, 938–943.

8.Hartree, E.F., 1972. Determination of protein: A modification of the lowry method that gives a linear photometric response. Analytical Biochemistry 48, 422–427.

9. Marsh, J.B., Weinstein, D.B., 1966. Simple charring method for determination of lipids. Journal of Lipid Research 7, 574–576.

10. Pusceddu, A., Sarà, G., Armeni, M., Fabiano, M., Mazzola, A., 1999. Seasonal and spatial changes in the sediment organic matter of a semi-enclosed marine system (W-Mediterranean Sea). Hydrobiologia 397, 59–70.

11. Rice, D., 1982. The Detritus Nitrogen Problem: New Observations and Perspectives from Organic Geochemistry. Marine Ecology Progress Series 9, 153–162.

12. Rossi-Wongtschowski, C.L.D.B., Madureira, L.S.P., 2006. O Ambiente oceanográfico da plataforma continental e do talude na região sudeste-sul do Brasil. EdUSP.

13. Viana, A.R., 2001. Seismic expression of shallow- to deep-water contourites along the south-eastern Brazilian margin. Marine Geophysical Researches 22, 509–521.

Mercury and Selenium in biological pump under upwelling-downwelling influence, South Atlantic Ocean, Cabo Frio shelf, Brazil.

Alina Criane de Oliveira Pires[1*], Sabrina Pinto Ramos[2], Orangel Aguilera[1,3], Jeremie Garnier[4], Silvia Keiko Kawakami[2], Eduardo Vianna Almeida[5], Emmanoel Vieira Silva-Filho[6], Ana Luiza Spadano Albuquerque[7], Vinicius Tavares Kütter[1],

1- Programa de Pós graduação em Geologia e Geoquímica, Universidade Federal do Pará, Rua Augusto Corrêa, 1, Campus Guamá, PA 66075- 110, Brasil;
2- Laboratório de Oceanografia Química, Universidade Federal do Pará, Rua Augusto Corrêa, 1, Campus Guamá, PA 66075- 110, Brasil
3- Universidade Federal Fluminense (UFF), Laboratório de Paleoecologia e Mudanças Globais, Campus Gragoatá, Bloco M, No. 110, CEP: 24210-200, Niterói, Rio de Janeiro, Brasil
4- Universidade de Brasília, Instituto de Geociências, Campus Darcy Ribeiro, L2, Asa Norte, Brasília, Distrito Federal, Brasil.
5- Universidade Federal do Rio de Janeiro, Instituto de Biologia Departamento de Zoologia Centro de Ciências da Saúde Av. Carlos Chagas Filho, n. 373 CEP 21941-902 Cidade Universitária Rio de Janeiro
6- Programa de Geoquímica, Universidade Federal Fluminense, Niterói, RJ 24020-150, Brasil;
7- Programa de Pós-Graduação Dinâmica dos Oceanos e da Terra, Universidade Federal Fluminense, Niteroi 24210346, Brasil

e-mail:alinapires16@gmail.com

Introduction

In the last 600 years, the concentration of mercury (Hg) in the deep waters of the South Atlantic Ocean has increased [1]. This element is extremely harmful to human health due to its methylmercury form found mainly in the marine environment, as it accumulates in top predators due to biomagnification and organification that occurs along the trophic web [2]. On the other hand, selenium (Se) is an essential element for living beings and acts as a protective agent by reducing the availability of methylmercury through complexation with aminoacids. Antagonistic effects between Se and Hg in organisms have been frequently observed [3].

Upwelling areas are important sites for investigating the biogeochemical cycles of Hg and Se due to higher marine productivity and the mixture of surficial and deep waters. Due to this phenomenon that occurs in the southeast region of Brazil, the state of Rio de Janeiro is considered the third-largest national producer of marine fish (79,000 tons/year) [4]. This leads to a greater risk of contamination of the ecosystem and human health due to the increase in fish production.

Considering the biomagnification capacity and toxicity of Hg, and a hotspot of this element in the region, the present study proposes the investigation of the distribution of Hg and Se in the planktonic community under the influence of the upwelling-downwelling system at Cabo Frio coast, southeastern Brazil.

Experimental

A total of 79 plankton samples (fractions > 20µm, >64 µm, >150 µm and >300 µm) were collected on the Cabo Frio Continental Shelf during 7 oceanographic cruises in 2012 (Figure 1). The determination of total Hg and Se concentration was performed according to the methodology proposed by [5]. The determination of Selenium and Aluminum was performed by Inductively Coupled Plasma Mass Spectrometer (ICP-MS) (Thermo Fisher Xseries II). Biomagnification factor (BMF) was calculated using the equation BMF = CD/CP, according to [6]. The Shapiro-Wilk test and later the Kruskal-Wallis test was carried out with Statistica® Version 12.

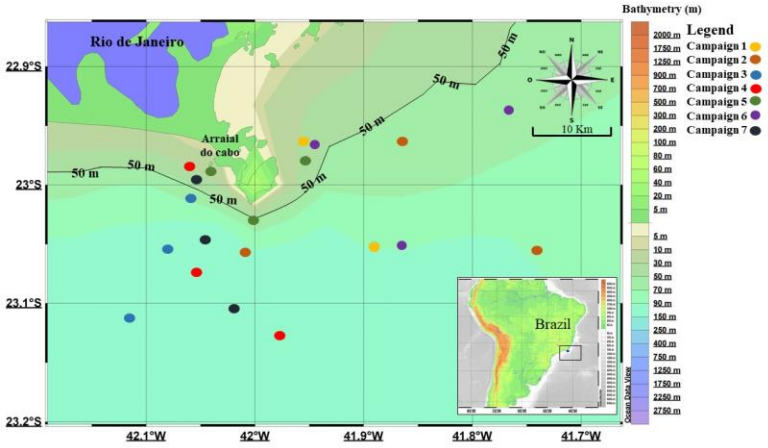

Figure 1: Sampling site at Cabo Frio coastal shelf.

Results and Discussion

Higher averages of Hg in marine plankton were found in the zooplankton fraction compared to phytoplankton (Table 1), and demonstrate that there was a process of biomagnification between organisms from phytoplankton to zooplankton. zooplankton have a diet mostly composed of smaller organisms such as phytoplankton or their fecal pellets, and thus can serve as a Hg transport route and

bioaccumulate this element, as in several studies in southeastern Brazil [7;8]. [9] present upwelling as a key factor for the entry of Hg into planktonic organisms, since in addition to the fertilization of the upper layer, which is done through upwelling carrying benthic species to the trophic layer, there is an increase in biodiversity caused by the increase in primary production and, consequently, an increase in trophic levels.

Tabela 1:Biomagnification Factor in plankton from Cabo Frio Shelf.

Fractions	HgT BMF (MEAN±SD)	Se BMF (MEAN±SD)
300/64 µm	1.29 ±0.02	0.98± 1.34
300/20 µm	2.30±0.05	0.97±1.90
150/64µm	1.56±0.04	1.04± 3.04
150/20µm	2.79±0.07	1.03± 2.47

Higher concentrations of Se were observed in phytoplankton than in the zooplankton fraction, indicating a possible antagonism between Hg and Se, related to the antioxidant properties of Se against exogenous metals, including Hg (Figure 2). Previous studies [10;11] demonstrated how it acts by binding to HgT, reducing and even inhibiting its toxicity.

Se:Hg molar ratios greater than 1 indicate protection of Se against Hg toxicity in the food chain [12;13]. We found Se:Hg ratios greater than 1 for all fractions, evidencing the availability of Se to participate in Hg detoxification.

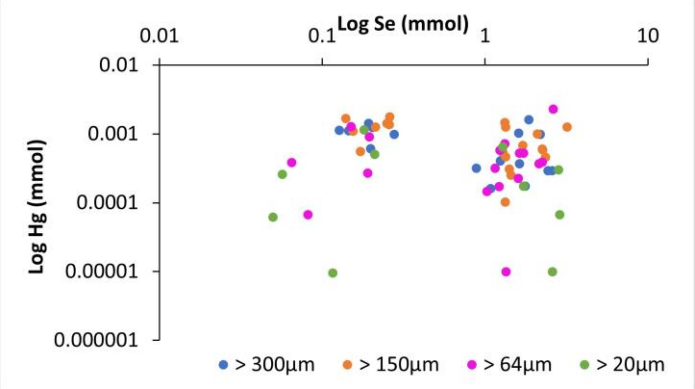

Figure 2: The Se:Hg ratio in the planktonic community of Cabo Frio according to the 20, 64, 150 and 300 µm meshes

Conclusion

We observed an excess of the Se:Hg ratio in plankton and high concentrations of Se in phytoplankton, which may be indicative of reduced Hg toxicity. Upwelling influenced the concentrations of Hg and Se, once for Se, it resuspended these elements from the Sediment and made it available for biota, while for Hg, it recirculated along the biological pump, making these elements available for organisms studied.

Acknowledgment

The PETROBRAS/Cenpes and the National Petroleum Agency (ANP), within the scope of the Upwelling Project (Projeto Ressurgência) and National Council for Research and Development (Cnpq, Brazil). The authors would like to thank CAPES.

References

[1] Zhang, Y.X., Jaegle, L., Thompson, L., Streets, D.G., 2014. Six centuries of changing oceanic mercury. Global Biogeochemical Cycles **28**, 1251–1261.

[2] Batrakova, N., Travnikov, O., Rozovskaya, O., 2014. Chemical and physical transformations of mercury in the ocean: a review. Ocean Science **10,** 1047–1063.

[3] Manceau, A., Gaillot, A.C., Glatzel, P., Cherel, Y., Bustamante P., 2021. In Vivo Formation of HgSe Nanoparticles and Hg-Tetraselenolate Complex from Methylmercury in Seabirds-Implications for the Hg-Se Antagonism. Environmetal Science Technology **55,**1515–1526.

[4] Ministro de Estado da Pesca e Aquicultura-MPA. IBGE. Equipe Técnica (org.), 2011. Boletim Estatístico da Pesca e Aquicultura: Brasil 2011. Brasília, DF, MPA, 60 p.

[5]Malm, O., Pfeiffer, W.C., Bastos, W.R., Souza, C.M.M., 1989. Utilização Do Acessório De Geração De Vapor Frio Para Análise De Mercúrio Em Investigações Ambientais Por Espectrofotometria De Absorção Atômica. Revista Ciência e Cultura, **1,** 88–92.

[6] Gray J. S., 2002. Biomagnification In Marine Systems: The Perspective of An Ecologist. Marine Pollution Bulletin, **45**, 1-12

[7] Silva-Filho, E.V., Kütter, V.T., Figueiredo, T.S., Tessier, E., Rezende, C.E., Teixeira, D.C., Donard, O.F.X., 2014. Mercury speciation in plankton from the Cabo Frio Bay, SE - Brazil. Environmental Monitoring and Assessment, **186,** 8141–8150.

[8] Kehrig, H.A., Seixas, T.G., Palermo, E.A., Baêta, A.P., Castelo-Branco, C.W., Malm, O., Moreira, I., 2009. The Relationships Between Mercury and Selenium In Plankton And Fish From A Tropical Food Web. Environmental Science and Pollution Research, **16,** 10–24.

[9] Manhães, B.M.R., Picaluga, A.S., Bisi, T.L., Azevedo, A., Torres, J.P.M., Malm, O., Lailson-Brito, J., 2020. Tracking mercury in the southwestern Atlantic Ocean: the use of tuna and tuna-like species as indicators of bioavailability. Environmental Science Pollution Research, **27**, 6813–6823.

[10] Ralston, N.V., Ralston, C.R., Blackwell, J.L., Raymond, L.J., 2008. Dietary and tissue elenium in relation to methylmercury toxicity. Neurotoxicology, **29**, 802-811.

[11] Khan, M.A., Wang, F., 2009. Mercury-selenium compounds and their toxicological significance: Toward a molecular understanding of the mercury-selenium antagonism. Environmental Toxicology and Chemistry: An International Journal, **28**, 1567-1577.

[12] Arcagni, M., Campbell, L., Arribére, M.A., Marvin-DiPasquale M., Rizzo, A., Guevara, S.R., 2013. Differential mercury transfer in the aquatic food web of a double basined lake associated with selenium and habitat. Science of the total environment, **454,** 170-180.

[13] McCormack, M.A., Jackson, B.P., Dutton, J., 2020. Relationship between mercury and selenium concentrations in tissues from stranded odontocetes in the northern Gulf of Mexico. Science of The Total Environment, **749,** 141350.

XVI LATIN AMERICAN CONGRESS ON ORGANIC GEOCHEMISTRY
9 - 11 AUGUST, 2023
ARACAJU, SERGIPE, BRAZIL

BIOGENIC OR THERMOGENIC? THAT IS THE QUESTION ! TERPENOID HYDROCARBONS IN THE SEDIMENTS OF MANGROVE SWAMPS IN A BRAZILIAN SUBTROPICAL ESTUARINE SYSTEM

MARINA REBACK GARCIA[a,b,c,*]; **RICHARD PAUL PHILP**[c]; **CÉSAR C. MARTINS**[a,d,*]

[a] Centro de Estudos do Mar, Universidade Federal do Paraná, Brazil
[b] Programa de Pós-Graduação em Sistemas Costeiros e Oceânicos (PGSISCO), Universidade Federal do Paraná, Brazil
[c] School of Geology and Geophysics, The University of Oklahoma, Norman, OK, 73019, USA
[d] Instituto Oceanográfico, Universidade de São Paulo, Brazil.

E-mail adresses: marinareback@gmail.com (M.R. Garcia); ccmart@usp.br (C.C. Martins)

Introduction

'Natural' and 'anthropogenic' inputs may co-exist in sediments with a high content of OM, such as mangrove swamps that have the appropriate conditions for the accumulation of hydrophobic compounds. The high level of natural terpenoids found in mangrove sediments may pose a challenge in the identification of the thermogenic compounds in the same matrix because the structures of the biogenic molecules are very similar and provide a similar spectral signature (e.g., primarily relatively intense signals in the m/z 191 from total ion chromatograms, TIC), which may lead to identification errors.

Therefore, the present study aimed to (1) characterize the natural background of cyclic aliphatic hydrocarbons from Paranaguá Estuarine System (PES); (2) map the chronic low-level inputs of thermogenic terpanes and hopanes under a high biogenic background to identify anthropogenic inputs; (3) associate the occurrence of selected biogenic and anthropogenic hydrocarbons as tracers of OM ('blue carbon') accumulation in mangrove swamps.

Experimental

The PES is a subtropical estuary (25°30′S; 48°25′W) surrounded by Atlantic rainforest in a Natural World Heritage site: 'The Atlantic Forest South-East Reserves'. It is threatened by intensive tourism, urban development, and harbor activities, with high risk of organic and inorganic contamination.

Samples of superficial sediments were obtained from 36 sites. Bulk data were obtained *in situ* (temperature, Eh and pH). The sediments were frozen (−20 °C), freeze-dried and stored in cleaned glass jars until analysis. The extraction was performed in Soxhlet apparatus (8 h, DCM and *n*-hexane 1:1) with activated copper [1]. The extract was purified via adsorption column chromatography (5% deactivated alumina and silica) eluted by *n*-hexane obtaining the fraction 1: aliphatic hydrocarbons and petroleum biomarkers).

The extracts of five samples with the highest mass of extractable OM were molecular-sieved for removal of *n*-alkanes with the adsorbent S-115 (Honeywell/UOP, dry at 85 °C) packed into a glass pipette (~ 2 g, eluted 3 x 5 mL of *n*-pentane). The five molecular-sieved extracts were injected in full scan mode (GC-MS), and site #9 was used to primarily characterize the natural/thermogenic compounds, comparing the mass spectra and retention times from known thermogenic compounds found in Lower Pennsylvanian Morrow shale and published data [2, 3, 4].

Instrumental analyses were performed in a GC Agilent 7890A paired with an Agilent 5975C MSD quadrupole with a DB-5 column with manual in splitless mode in the multiple ion detection mode. The estimated concentrations of the compounds (semi-quantitative analysis) were based on the integrated areas of specific ions (m/z 191 for the hopanes and m/z 221 for the surrogate 5α-cholestane-d_4).

Results and Discussion

Results were published in Garcia *et al*. [5]. The identified molecules exhibited high abundance of 22 or 24 carbons and different degrees of unsaturation, showing an early stage of degradation/diagenesis (des-A configuration), deriving from the microbial degradation of plant triterpenoids (unsaturated oleananoids, ursanoids and lupanoids) under anoxic conditions.

Terpanes that elute in the hopane retention time include natural and thermogenic compounds with similar signal intensities in the TIC.

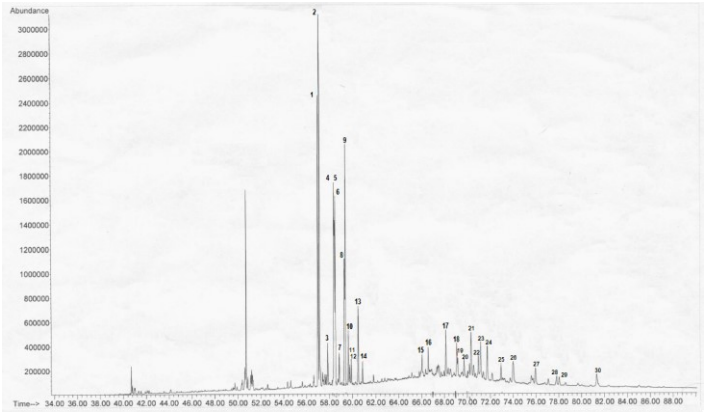

Figure 1. Total ion chromatogram (TIC) of branched and cyclic fractions of site #09.

Many of the natural compounds have similar structures with different stereochemical configurations, and many remain unidentified, but the partial identifications could differentiate between thermogenic and biogenic compounds and provide key information to assess the low-level anthropic inputs to the study area. Among the naturally occurring compounds, some six-carbon membered E-rings were identified, such as oleanane and taraxerane which are synthetized by high plants.

Several bacterially derived pentacyclic triterpenoid hopanoids were also identified. Thermogenic and biogenic compounds were distributed throughout the estuarine system, with higher concentrations observed in the E-W axis of the system (Antonina and Paranaguá bays). The two groups of compounds showed correlation to each other (R^2 = 0.66) and to TOC (R^2 ≈ 0.50), what may be interpreted as an indication of similar 'depositional behavior'. Therefore, the distribution of terpenoids likely depends on locally specific depositional conditions and TOC content, and do not show an evident relationship with the distance from the expected major sources, such as urban centers and ports.

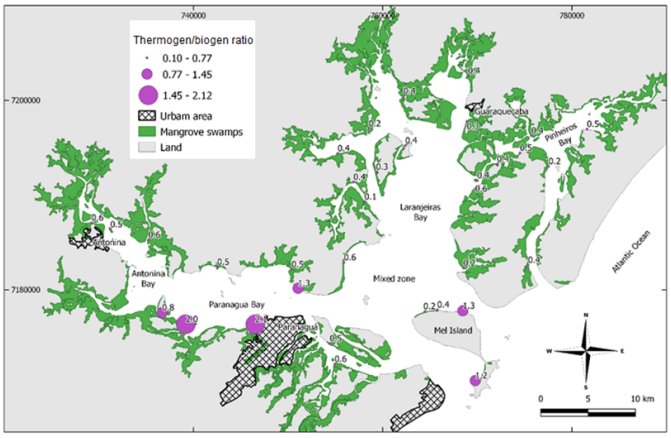

Figure 2. Thermogenic/Biogenic terpanes ratios calculated for the mangrove sediments of the Paranaguá Estuarine System, Brazil.

The ratio of thermogenic/biogenic terpanes (TRM/BIO) was proposed in this study as a proxy to distinguish the contribution of each of these two possible contributions of organic components to the mangrove sediments. There are no natural inputs of fossil fuels, such as crude oil seeps, in the study area. Therefore, this ratio should reflect anthropogenic sources of petroleum hydrocarbons. The TRM/BIO ratios for terpanes and hopanes were higher than 1.0 in five samples (Fig. 2). The highest values were observed near Paranaguá port and surroundings, in the Paranaguá bay area. The other two sites were in Mel Island, which is the main tourist destination in the PES.

Conclusions

The concentrations of thermogenic terpanes had a spatial distribution that was linked to the depositional conditions (TOC and fine sediments), with no major or point sources of evidenced (inputs predominantly diffuse, probably due to the maritime traffic).

The proposed ratio of thermogenic/biogenic terpenoids accurately assessed the low-level chronic inputs of anthropogenic hydrocarbons in the study area. This innovative approach may be applied to areas with a high natural input of OM where chronic low-level hydrocarbon inputs are not evident.

Acknowledgements

M.R. Garcia would like to thank CAPES (Coordenação de Aperfeiçoamento de Pessoal de Ensino Superior) for the Ph.D. and PDSE Scholarship. C.C. Martins was funded by CNPq (Brazilian National Council for Scientific and Technological Development) (306468/2017- 4) and Fundação Araucária de Apoio ao Desenvolvimento Científico e Tecnológico do Estado do Paraná (CP 09/2016, 47.395).

References

[1] Wisnieski, E., Ceschim, L.M.M, Martins, C.C., 2016. Validation of an analytical method for geochemical organic markers determination in marine sediments. Quim. Nova 38, 1007–1014.

[2] Philp, R.P., 1985. Fossil Fuel Biomarkers. Applications and Spectra. Elsevier, Amsterdam.

[3] Shiojima, K., Arai, Y., Masuda, K., Takase, Y., Ageta, T., Ageta, H., 1992. Mass spectra of pentacyclic triterpenoids. Chem. Pharm. Bull. 40, 1683–1690.

[4] Sinninghe-Damsté, J.S., Van Duin, A.C.T, Hollander, D., Kohnen, M.E.L., De Leeuw, J.W., 1995. Early diagenesis of bacteriohopanepolyol derivatives: formation of fossil homohopanoids. Geochem. Cosmochim. Acta 59, 5141–5157.

[5] Garcia, M.R., Philp, R.P., Martins, C.C., 2020. Biogenic and thermogenic terpenoid hydrocarbons as potential geochemical tools for the study of sedimentary organic matter in subtropical mangrove swamps. Applied Geochemistry, 122, 104726. https://doi.org/10.1016/j.apgeochem.2020.104726.

XVI LATIN AMERICAN CONGRESS ON ORGANIC GEOCHEMISTRY
9 - 11 AUGUST, 2023
ARACAJU, SERGIPE, BRAZIL

Elementary and isotopic characterization of sedimentary organic matter from the Oiapoque River (Brazil – French Guiana Border)

SCHÜTZ, YASMYM DE VINCENZI WERICH[a,b,*],, REZENDE, CARLOS EDUARDO DE[c],, SOUZA, FERNANDA MARIA DE[d], MARTINS, CÉSAR C.[b,e,*]

[a]FEDERAL UNIVERSITY OF RIO GRANDE,[b] FEDERAL UNIVERSITY OF PARANÁ, [c] STATE UNIVERSITY OF NORTHERN RIO DE JANEIRO, [d] INSTITUTE FOR SCIENTIFIC AND TECHNOLOGICAL RESEARCH OF THE STATE OF AMAPÁ, [e] UNIVERSITY OF SÃO PAULO,

e-mail:*yasmymsdvw@gmail.com, ccmart@usp.br*

Introduction

The Oiapoque River estuary is located on the Brazil-French Guiana border and is characterized as a pristine environment with an intense discharge of fluvial sediment and terrestrial organic matter (OM) [1]. The sedimentary OM on this estuary may reflects the biomass present in adjacent lands and the autochthonous production Environmental conditions (e.g., temperature, salinity) and physical dynamics (e.g., tides, local currents) of the coastal zones may influence the composition of OM [2]. In this sense, the aim of this study was to understand and distinguish the main sources of OM for this Amazon coastal zone estuary, using geochemical tools, such as the elementary and isotopic composition of OM. The percentage of Total Organic Carbon (TOC), Total Nitrogen (TN), and their relative ratio (C/N) such as their stable isotopic ratios ($\delta^{13}C$ and $\delta^{15}N$) were analyzed in order to evaluate the composition of OM in surficial sediment from the Oiapoque River estuary.

Experimental

Two sediment sampling campaigns were conducted: (i) in May 2018 (wet season, campaign A) and (ii) October 2018 (dry season, campaign B) (Fig. 1). Sampling sites covered the estuarine spatial gradient and the main channel of the estuary. About 8-10 mg of dry sediment from each site was used to determine the percentage of TN, the isotopic ratio ($\delta^{15}N$) and total carbon (TC). The same amount of sample was decarbonated by acid treatment with 1 mol L^{-1} HCl solution, in silver capsules, and this sample was used to determine the percentage of TOC and the $\delta^{13}C$ ratio. Sediments were weighed and analysed, through a Carlo Elba Flash 2000 elemental analyser coupled to the Conflo IV interface with an isotopic ratio mass spectrometer detector (Thermo Scientific Delta V Advantage Isotope ratio MS).

Precipitation data was obtained from INMET (National Institute of Meteorology). The grain size parameters were obtained after treated (desalted, decarbonated and oxidized) using a particle analyzer and the SysGran software. Statistical analyses were carried out (Pearson and Spearman correlation, Principal Components Analysis, among others), where the components and appropriate correlations were obtained for the studied parameters.

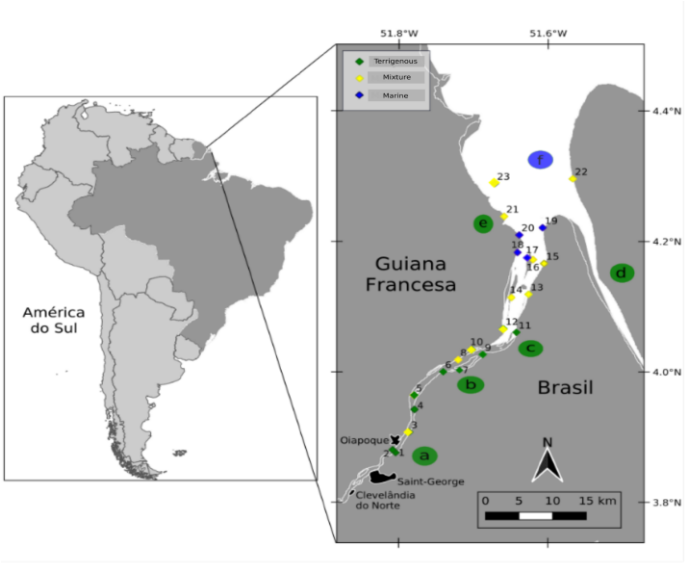

Figure 1. Map of the study area with the sources and influences to the sedimentary OM. Sectors are: (a) inner portion of the estuary; (b) Usina Taparabo; (c) Ponta dos Índios; (d) Uáça River; (e) Ouanary River; (f) mouth of the estuary.

Results and Discussion

Results of TOC and TN showed a strong correlation considering both sampling campaigns (Fig. 2). The C/N ratio showed the terrigenous input (~24) to the upstream sites, while marine input (~5 and 9) was detected in the downstream stites. The results indicate the presence of mixed sources, predominant in central portion of the estuary [3].

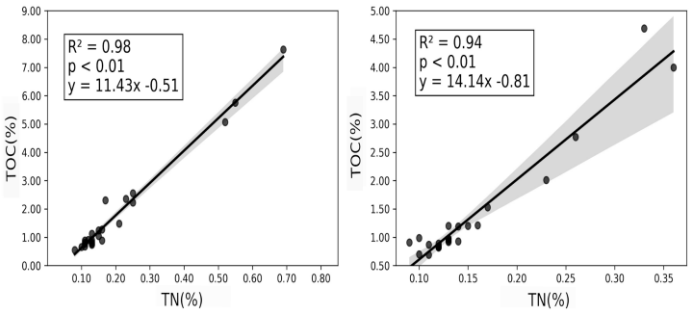

Figure 2. Linear regression (Pearson correlation) for TOC (%) vs. TN (%) to samples from campaigns A and B, respectively.

Results of $\delta^{13}C$ (‰) (Fig. 3) showed low variability along the estuary, with low values (~ -27 ‰, contribution from land and/or by C3-plants) in upstream sites and close to the estuary mouth. Intermediate values (~ -24 ‰), were related to mixed sources, obtained throughout the estuary, mainly in the central portion. The higher values (~ -22 ‰), related to marine input are found close to the mouth. The $\delta^{15}N$ (‰) presented values around ~3 ‰ (associated with terrestrial plants), being found mainly in the inner region, in the center of the estuary, and in its mouth, where there is the discharge of rivers [4].

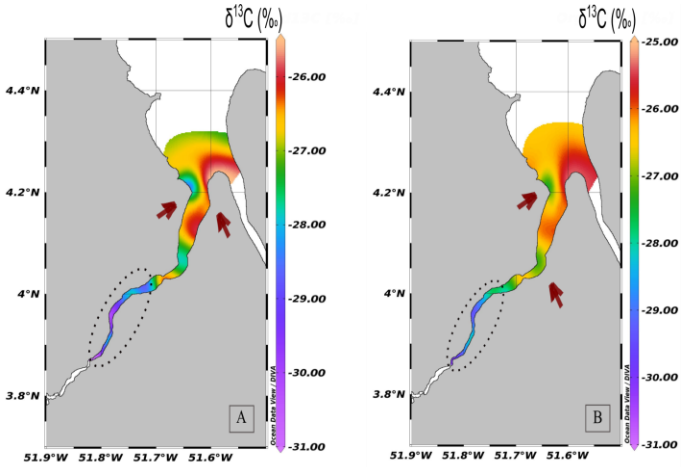

Figure 3. The $\delta^{13}C$ (‰) values over the study area (Oiapoque River Estuary) in campaigns A and B. The lower values are represented for the colors: purple, blue and green, and the dashed circles (-31 a -27 ‰); intermediate values presented in the color yellow (~ -26 ‰) and the higher values are red color and arrows (~ -27 ‰).

Conclusions

The elementary and isotopic composition of the sedimentary OM from Oiapoque River estuary indicated an estuary with influences of multiples sources, with a predominance of terrigenous OM (especially near the mouth of the estuary and in the region where the Uáça and Ouanary rivers flow). The estuarine dynamics (mainly rainfall and tidal currents) may influence the distribution of marine input and the mixture of allochthonous and autochthonous sources, which remains present throughout the estuary and flows from the mouth towards the upstream of the estuary.

Acknowledgements

The authors thank National Council for Scientific and Technological Development (CNPq, 432285/2016-4 and 310850/2020-7).

References

[1] Pichler, N., Souza, F.M., Santos, V.F., Martins, C.C., 2021. Polycyclic aromatic hydrocarbons (PAHs) in sediments of the amazon coast: Evidence for localized sources in contrast to massive regional biomass burning. Environmental Pollution 268, 115958.

[2] Sobrinho, R.L., Bernardes, M.C., de Rezende, C.E., Kim, J.-H., Schouten, S., Sinninghe Damsté, J.S., 2021. A multiproxy approach to characterize the sedimentation of organic carbon in the Amazon continental shelf. Marine Chemistry 232, 103961.

[3] Barros, G.V., Martinelli, L.A., Oliveira Novais, T.M., Ometto, J.P.H.B., Zuppi, G.M., 2010. Stable isotopes of bulk organic matter to trace carbon and nitrogen dynamics in an estuarine ecosystem in Babitonga Bay (Santa Catarina, Brazil). Science of The Total Environment 408, 2226–2232.

[4] Brandini, N., da Costa Machado, E., Sanders, C.J., Cotovicz, L.C., Bernardes, M.C., Knoppers, B.A., 2022. Organic matter processing through an estuarine system: Evidence from stable isotopes ($\delta^{13}C$ and $\delta^{15}N$) and molecular (lignin phenols) signatures. Estuarine, Coastal and Shelf Science 265, 107707.

XVI LATIN AMERICAN CONGRESS ON ORGANIC GEOCHEMISTRY
9 - 11 AUGUST, 2023
ARACAJU, SERGIPE, BRAZIL

GEOCHEMICAL CHARACTERIZATION OF BIOTIC CRISES FROM EARLY TO MIDDLE DEVONIAN IN PONTA GROSSA FORMATION, PARANÁ BASIN

ELIANE SOUZA[a], LUIZA ROCHA[a], HÉLIO SEVERIANO RIBEIRO[a], LUIS C. BERTOLINO[b], GEORGIANA F. DA CRUZ[a]

[a]UNIVERSIDADE ESTADUAL DO NORTE FLUMINENSE DARCY RIBEIRO (UENF/LENEP), [b]CENTRO DE TECNOLOGIA MINERAL (CETEM)

e-mail: eliane@lenep.uenf.br

INTRODUCTION

At the end of the Devonian, an approximate loss of 21% of marine life is recognized. However, some intervals, which preceded this extinction are considered biotic crisis events: Zilchov (Pragian - Emsian), Daleje (late Emsian), Choteč (Emsian - Eifelian), and Kačák (Eifelian-Givetian). The hypotheses that justify these events can be catastrophic, such as asteroid impact and volcanism, or gradual, showing progressive changes in paleoenvironment conditions such as oxygen levels, salinity, temperature, and sea-level oscillations [1]. In the present work, changes in the physicochemical conditions of the depositional paleoenvironment of Ponta Grossa Formation, Paraná Basin were evaluated by organic and inorganic geochemical analyzes with the aim of correlating them with significant biotic crises that preceded the great Devonian extinction event, culminating in the extinction of the Malvinokaffric fauna [2].

EXPERIMENTAL

Fifteen shale samples from Ponta Grossa Formation outcrops were characterized by organic geochemical parameters, such as Pristane/Phytane (Pr/Ph), *n*-alkanes, *n*-alkyl cyclohexanes, tricyclic index, gammacerane, αβ C_{30} hopane, tetrahydrophenanthrene, cadalene, tetramethyl naphthalenes (TeMN), triaromatic steroids, and perylene by GC/MS analyzes. In addition, inorganic geochemical parameters such as rare earth elements (REE), vanadium and nickel were evaluated by ICP-OES analyzes.

RESULTS AND DISCUSSION

In the Ponta Grossa Formation, a decrease in the Σ *n*-alkanes concentration from JG-05 to JG-06 (Fig.1A) and in the V/(V+Ni) values (Fig.1F) followed by the increasing of REE concentrations (Fig.1G) could indicate the occurrence of the **Zilchov biotic crisis** in the Pragian to Emsian transition [3]. The **Daleje biotic crisis** is considered significant and with international recognition of sea-level rise [1]. However, in this time interval, the Paraná Basin experienced regressive depositional sequences [4], described by biomarkers and PAH from PG-04 to PG-07. First, a decrease in the Σ *n*-alkanes concentration was observed. Then, Pr/Ph values increased, indicating more oxidizing conditions (Fig.1A), confirmed by the decreasing of V/(V+Ni) values (Fig.1F). Severe changes in depositional conditions were also detected by the increase in the αβC_{30} hopane (Fig.1B) and gammacerane concentration values, along with an increase of tetrahydrophenanthrene concentration (Fig.1C), suggesting water column stratification as a consequence of fresh waters incursions. The *n*-alkyl cyclohexanes series were also detected in high concentrations, especially in PG-06 and PG-07 (Fig.1B). This increasing was followed by the high concentration of aromatic steroids (Fig.1E). The **Choteč biotic crises** was characterized in its strata by a rapid transgression [4]. PG-08 points out this change with a drop of Pr/Ph values, suggesting a more anoxic condition, and the decrease in Σ *n*-alkanes concentration from PG-07 to PG-08 (Fig.1A). In addition, the non-detection of *n*-alkyl cyclohexanes and the decrease in αβC_{30} hopane (Fig.1B) and gammacerane concentration values indicated depositional paleoenvironment conditions changes (Fig.1C), especially related to the decrease in water column stratification and in the decrease in terrigenous input, observed by the decrease in cadalene and TeMN concentration values (Fig.1D) [3]. The **Kačák biotic crisis** is characterized by the deposition of black shales and changes in water temperature and oxidation level [1]. Rising sea level is another feature that characterized the Eifelian-Givetian interval and was experienced in a very expansive way in the Paraná Basin. Seawater anoxia resulting from this event can be observed by the drastic reduction in Pr/Ph values from PG-08 to PG-09 (Fig.1A), and by the increase of V/(V+Ni) values (Fig.1F) and of REE concentrations (Fig.1G). This biotic crisis was recorded by all biomarkers and PAH evaluated in sample PG-09. The Σ *n*-alkanes concentration was the smallest among the samples (Fig.1A), the *n*-alkyl cyclohexanes series was not detected (Fig.1B), and concentration values for αβC_{30} hopane, gammacerane and tetrahydrophenanthrene decreased from PG-08 to PG-

09. The TeMN, cadalene, and triaromatic steroids were also not detected. In addition, the soil drags resulting from this extensive marine connection could explain the detection of perylene, one of the products of plants metabolism by soil fungi, in the highest concentration value in PG-09 (Fig.1E) [3].

CONCLUSIONS

The geochemical analyses of changes detected in depositional paleoenvironment conditions were able to identify the Zilchov, Daleje, Choteč, and Kačák biotic crisis events. In the Pragian-Emsian interval, a decrease in the Σ *n*-alkanes, $\alpha\beta C_{30}$ hopane and gammacerane concentrations were observed, as well as an increase in change in depositional conditions, within water column Pr/Ph values, which could indicate a regressive interval related to **Zilchov event**, representing the first decline of the Malvinokaffric fauna. During the Late Emsian, severe stratification due to freshwater incursions, leading to the second decline in the Malvinokaffric fauna, which could be related to the **Daleje event**. During the Emsian-Eifelian interval, the detection of more anoxic conditions and the decrease in Σ *n*-alkanes concentration suggested the occurrence of **Choteč event**. During the Eifelian-Givetian, Paraná Basin experienced a very expansive sea-way as a result of the sea level rising. The seawater anoxia can trigger a biotic crisis, related to the **Kačák event**. This transgression conditioned marine connections between Paraná and Parnaíba basins with the entry of warmer water and fauna from Parnaíba Basin, promoting a dramatic ecological change and probably the disappearance of the Malvinokaffric fauna.

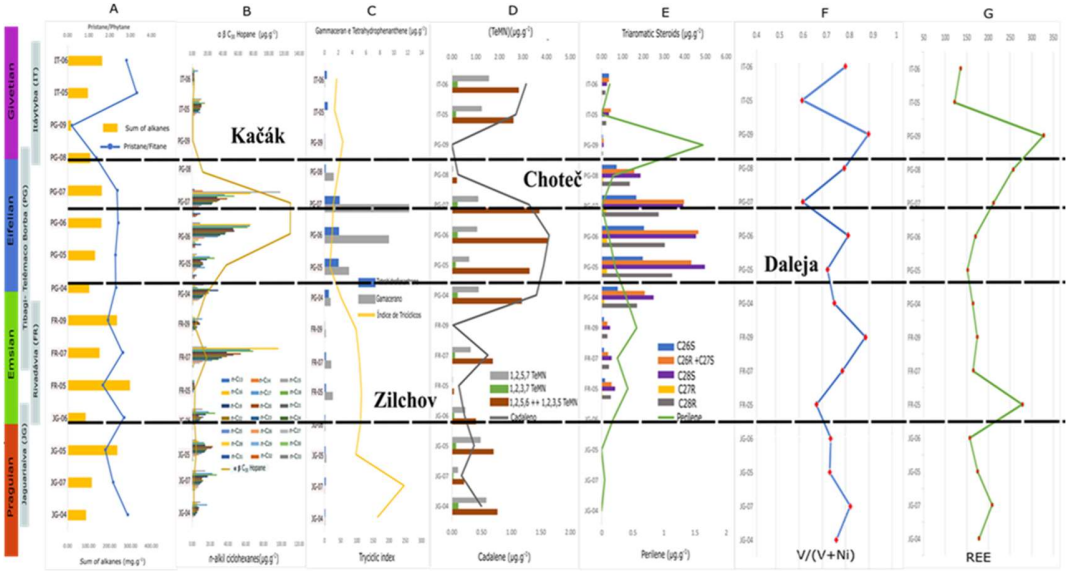

Figure 1. Summary of the main results that punctuated the positioning of the biotic crisis events. Σ *n*-alkanes concentration (mg.g^{-1}) and Pr/Ph values (A). *n*-alkyl cyclohexanes and $\alpha\beta C_{30}$ Hopane concentrations (µg.g^{-1}) (B). Gammacerane, tetrahydrophenanthrene concentrations (µg.g^{-1}) and tricyclic index distribution (C). TeMN and Cadalene concentration (µg.g^{-1}) distributions (D). Triaromatic steroids and Perylene concentration (µg.g^{-1}) distributions (E). V/(V+Ni) ratio values (F). Σ REE Concentration (µg.g^{-1}) (G).

ACKNOWLEDGEMENTS

The authors are grateful to Professor Elvio Bosetti, from Ponta Grossa State University, for helping by suggesting some outcrops for sample collecting during the field trip. We also thank CAPES for the doctoral scholarship of Luiza Rodrigues Rocha.

REFERENCES

[1] House, M. (2002). Strength, timing, setting and cause of mid-Palaeozoic extinctions. Paleogeography, Paleoclimatology, Paleoecology, 181, 5-25.

[2] Bosetti, E., Grahn, Y., Horodyski, R., Mauller, P. (2012). The first recorded decline of the Malvinokaffric Devonian fauna in the Paraná Basin and its cause; taphonomic and fossil evidences. Journal of South America Earth Sciences, 37, 228-241.

[3] Rocha, L., Souza, E., Severiano Ribeiro, H., Franco, D., Covas, T., Gontijo, B., da Cruz, G. (2023). Detection of Early-Middle Devonian biotic crises in East Gondwana, Paraná Basin, Brazil: an organic geochemical approach. Organic Geochemistry (*under review*).

[4] Vargas, M., da Silveira, A., Bressane, A., D'Avilla, R., Faccion, J., Paim, P. (2020). The Devonian of the Paraná Basin, Brazil: Sequence stratigraphy, paleogeography, and SW Gondwana interregional correlations. Sedimentary Geology, 408, 105768.

Land use and land cover change and the production of methane in the sediment of tropical coastal lagoons

LUIZA PEREIRA MACHADO[bc]*, ROBERTA. B PEIXOTO[ab] , MANUELA L. CARVALHO[b], DOUGLAS MOTTA PIO[b], ANA LUISA FONSECA[ab], LEONARDO AMORA-NOGUEIRA[ab], HELENA RODRIGUES DO BONFIM[b], DANIELA FRANÇA[b], GÉSSICA LOPES DE ABREU[b], HUMBERTO MAROTTA[abc]*

[a]**Programa de Pós-Graduação em Geoquímica (Geociências) - UFF,** [b]**Unidade de Multiusuário em Geoquímica de Gases, Água e Sedimentos da Universidade Federal Fluminense,** [c]**Programa de Pós-Graduação em Geografia – UFF**

*correspondência: luizapereira@id.uff.br

*correspondência: humbertomarotta@id.uff.br

Introduction

The greenhouse effect is the natural process of heat retention by the absorption of infrared radiation, intensified by human activities such as the burning of fossil fuels [1] and deforestation [2]. Methane (CH_4) is the greenhouse gas (GHG) that stands out for its ability to absorb infrared radiation is ~23 times higher than carbon dioxide (CO_2) over 100 years [3]. An important source of CH4 is the degradation of organic matter (OM) in lake sediments [4], ecosystems that are important destinations for organic [5], and inorganic [6] C inputs from the drainage basin. The upper layers of lake sediment may have the highest rates of methanogenesis due to the greater dispersibility of biomass labile to biological degradation [7]. Land use and land cover changes in the drainage basin, especially disordered urban expansion due to lack of wastewater treatment, can substantially increase nutrient and MO inputs, which favor CH4 production in more severe eutrophication and anoxia events [8].

Coastal lagoons with saline and brackish waters, as a consequence of marine influence, have a higher availability of electron acceptors, which favor more efficient MO degradation pathways that compete with methanogenesis (e.g., sulfate as a resource for sulfate reduction) [3]. However, previous evidence has increasingly highlighted the role of CH4 production in urbanized and eutrophic coastal lagoons, even those receiving high seawater inputs [9]. In this sense, the objective of the present study is to determine the methanogenesis rates in the surface layers of Maricá and Imboassica lagoons and to evaluate the relationship between land use and land cover.

Methodology

In 2017, surface layers (~15cm) were collected at the central point of the coastal lagoons of Maricá and Imboassica, located in the State of Rio de Janeiro (Fig.1). The anaerobic production of CH4 was determined by incubating the sediments in 120mL flasks in a controlled T Lauda bath (25°C), 3mL of air were removed from the flasks for analysis of CH4 concentrations in the Agilent Gas Chromatograph (model 7890B).

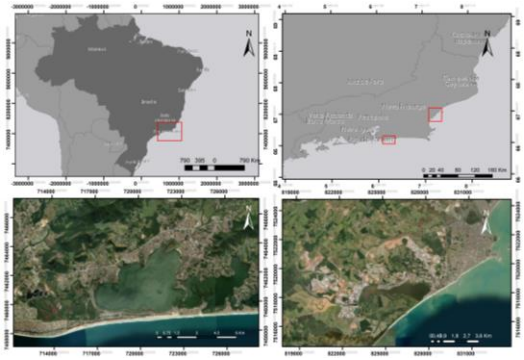

Figure 1: Location of core collection in Maricá and Imboassica Lagoons.

Results and Discussion

Table 1: CH_4 production (mg C-CH_4 m^{-3} d^{-1}) in the central region of Maricá and Imboassica lagoons (t-test, p<0.05).

Lagoon	Mean	Standard Deviation
Maricá	43,72	11,99
Imboassica	2659	732,6

In the surface layer (0-15 cm), the Imboassica lagoon had a CH4 production 60.8 times higher than the Maricá lagoon (T-test, p<0.05, Fig. 2), whose salinity differs on average 2.30±6.16‰ [10] to 11.3±19.12‰ [11], respectively. Between 1985 and 2019, the Maricá Lagoon

showed an urban expansion of 42km^2 from the reduction of forest, field and sandbank areas (Fig.3). In the Imboassica lagoon, the urban area grew by 11 km^2 in a period of ~50 years, advancing over the Forest and Field areas of the drainage basin (Fig.4).

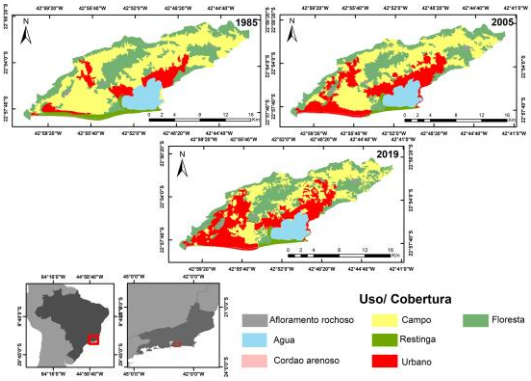

Figure 2: Land use and land cover in the Maricá Lagoon basins between the years 1985, 2005 and 2019. Landsat 5 and 9.

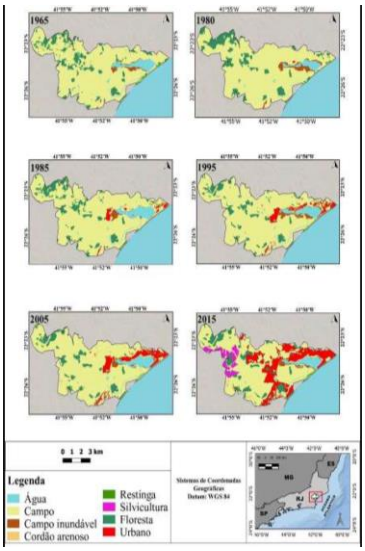

Figure 3: Land use and land cover in the Lagoa de Imbossica basin between the years 1965 to 2015. Landsat 5 and 9.

The Imboassica lagoon showed higher rates of methanogenesis. Despite the lower absolute expansion in the urban area of Imboassica in relation to Maricá, recent studies point out sewage discharge [12] and the eutrophication process. In addition, its waters may be less saline, with a greater presence of aquatic macrophytes in the surroundings. Periods of artificial opening and closing of the bar may further favor the entry of fresh water, reducing salinity and the availability of other electron acceptors [13].

Conclusions

The results suggest that land use and land cover are associated with a lack of wastewater treatment may favor CH4 production in aquatic sediments, even if urban expansion is not the highest. Less saline coastal lagoons may be even more susceptible to the intensification of methanogenesis subsidized by inputs of untreated urban effluents.

Acknowledgments

The authors thank the institutions CAPES and CNPq, the Laboratory of Global Change Ecology and the Multiuser Unit GAS-UFF. We are especially grateful to the technician Carlos Oliveira for the support at NAB-UFF.

References

[1] SANFORD, T. et al. The climate policy narrative for a dangerously warming world. **Nature Climate Change**, v. 4, n. 3, p. 164-166, 2014.
[2] KUMP, Lee R. Reducing uncertainty about carbon dioxide as a climate driver. **Nature**, v. 419, n. 6903, p. 188-190, 2002.
[3] Bastviken, D. Encyclopedia of Inland Waters. *Encycl. Virol.* **2008**, *4*, 359–365.
[4] FOURQUREAN, J. W. et al. Seagrass ecosystems as a globally significant carbon stock. **Nature geoscience**, v. 5, n. 7, p. 505-509, 2012.
[5] Cole, J. J et al. Carbon Dioxide Supersaturation in the Surface Waters of Lakes. **Science**, v. 265, n. 5178, p. 1568-1570, 1994.
[6] MAROTTA, H. et al. Long-term CO_2 variability in two shallow tropical lakes experiencing episodic eutrophication and acidification events. **Ecosystems**, v. 13, p. 382-392, 2010.
[7] THEBRATH, B. et al. Methane production in littoral sediment of Lake Constance. **FEMS microbiology ecology**, v. 11, n. 3-4, p. 279-289, 1993.
[8] D'AMBROSIO, Sofia L.; HARRISON, John A. Methanogenesis exceeds CH4 consumption in eutrophic lake sediments. **Limnology and oceanography letters**, v. 6, n. 4, p. 173-181, 2021.
[9] COTOVICZ, L. C. et al. Spatio-temporal variability of methane (CH_4) concentrations and diffusive fluxes from a tropical coastal embayment surrounded by a large urban area (Guanabara Bay, Rio de Janeiro, Brazil). **Limnology and Oceanography**, v. 61, p. S238– S252, 2016.
[10] FARIAS, R. N. DE. **De campo a cidade: urbanização e eutrofização artificial de um ecossistema aquático costeiro (Lagoa de Imbossica, RJ)**. Tese de Doutorado (Ciências Ambientais e Conservação). UFRJ-Macaé, 2018.
[11] BATISTA, S. A. **Diagnóstico geoambiental da Lagoa de Maricá (RJ) como subsídio as formas de uso e ocupação do litoral.** Dissertação (Mestrado em Geografia). Universidade do Estado do Rio de Janeiro, Rio de Janeiro, 97 p. 2018.
[12] BERALDI, G. F. et al. Assessment of a coastal lagoon metal distribution through natural and anthropogenic processes (SE, Brazil). **Marine pollution bulletin**, v. 146, p. 552-561, 2019.
[13] DOS SANTOS FONSECA, A. L. et al. Lagoas costeiras urbanas sujeitas a impactos antrópicos via aporte de efluentes: aspectos gerais e a concentração de metano na Lagoa Imboassica, Macaé, RJ. **Boletim do Observatório Ambiental Alberto Ribeiro Lamego**, v. 14, n. 1, p. 81-97, 2020.

XVI LATIN AMERICAN CONGRESS ON ORGANIC GEOCHEMISTRY
9 - 11 AUGUST, 2023
ARACAJU, SERGIPE, BRAZIL

From atoms to landscapes through time: Biogeochemical cycles and the chemical controls on carbonate precipitation in alkaline lakes

Raphael Pietzsch[a]

[a]Petrobras Research Centre, Av. Horácio Macedo 950, Cidade Universitária, Rio de Janeiro, 21941-915, Brazil.

e-mail: pietzsch@petrobras.com.br

Introduction

Atoms are the stuff that make up everything. A lump of rock, an outcrop, the landscape, an ecosystem. Atoms combine and dissociate, minerals are formed and dissolved, eventually triggering the formation of new minerals. Ultimately, this delicate balance enables biogeochemical cycles to initiate and to be maintained.

But how do minerals form? Here I will strive to cover our current understanding on the fundamental driving forces of carbonate mineral nucleation and growth.

This group of minerals comprise some of the most common sedimentary rock-forming constituents [**1**]. Importantly, to tell the story of ancient sedimentary carbonate rocks the processes driving their precipitation must be phenomenologically and mechanistically understood. Thermodynamic and kinetic effects will be discussed, with a special focus on alkaline lake water environments, known to be one of the most productive ecosystems on Earth today [**2,3**].

What are the mechanisms of carbonate mineral precipitation under these alkaline conditions? What processes are involved? What do we still not know? This discussion will follow a bottom-up approach, moving from the microscopic scale and will take us around a bigger picture, addressing some crucial element cycling that can take place in lake waters and sediment pore waters. Of great relevance is the interplay between carbon, calcium, magnesium, phosphorus and nitrogen, and potential feedback mechanisms amongst these essential components in such solutions enabling or hampering productivity, driving mineral formation and the evolution of alkaline lakes. These mechanisms ultimately build the landscape and connect the geo- and biospheres and may similarly have operated on the ancient Earth [**2**].

To address these questions, this study (1) mined data of published physicochemical properties of lakes from around the world, covering six continents and 16 countries, finding commonalities defining alkaline lakes; (2) Did thermodynamic calculations based on Pitzer equations to evaluate ion activity coefficients and ion speciation in high ionic strength solutions; (3) Investigated the roles of Mg^{2+} and ΣPO_4 (total phosphate), two important inhibitors of $CaCO_3$ nucleation and growth in natural and synthetic waters [**4,5**]. Importantly, because of its central role in biology, finding plausible physicochemical mechanisms able to concentrate soluble and labile phosphate, a relatively rare commodity on Earth, has been an active field of research [**3,6**]. Additionally, (4) constant composition experiments were run to observe the mechanisms influencing $CaCO_3$ mineral nucleation and/or growth, as well as its interaction with the ions above. Finally, (5) experimental and theoretical data were contrasted with geological material of the Barra Velha Fm (BVF), mostly represented by carbonate rocks and associated minerals, mainly deposited as sediments precipitated from alkaline lake waters, during the Early Cretaceous.

Experimental

A database of physical and chemical properties of alkaline lake waters from 16 countries was compiled, comprising n = 539 water samples.

An implementation of the Pitzer equations to explore carbonate geochemistry and the roles of inhibitors such as Mg^{2+} and ΣPO_4 was developed to more accurately calculate the dissociation constants and ion activity coefficients of phosphate species in natural and synthetic solutions.

Chem-stat experiments were run in chemical reactors filled with synthetic solutions (~1 L) prepared to mimic the composition of natural alkaline waters, with in situ and ex situ measurements of fluid and solid products.

Rock samples collected from a 198.1 m long core sampling the BVF were investigated using different and complementary methods. A set of 489 thin sections was investigated under the optical microscope, as well as using the SEM-EDS, QEMSCAN and electron probe microanalysis (EPMA). Bulk powdered samples were also analysed by X-ray diffractometry (XRD). Finally, 691 rock samples were analysed in an ICP-OES and ICP-MS, and a further subset of samples was analysed for $\delta^{13}C_{VPDB}$, $\delta^{18}O_{VPDB}$ and $^{87}Sr/^{86}Sr$ ratio.

Results and Discussion

The observations of natural lake water chemistry with new experimental results from Na-Ca-Mg-CO_2-Cl-PO_4 solutions mimicking alkaline waters support previous work pointing out that ΣPO_4 can reach high concentrations under high alkalinity [**3,7**]. Observations also unambiguously show that only 25 µmoles of phosphate suffice to inhibit $CaCO_3$ precipitation by one order of magnitude, compared to no phosphate in solution, maintaining supersaturation ≈70−100 [**2**].

Figure 1 illustrates the rationale and the workflow behind this study, as well as summarises the main results [**2**].

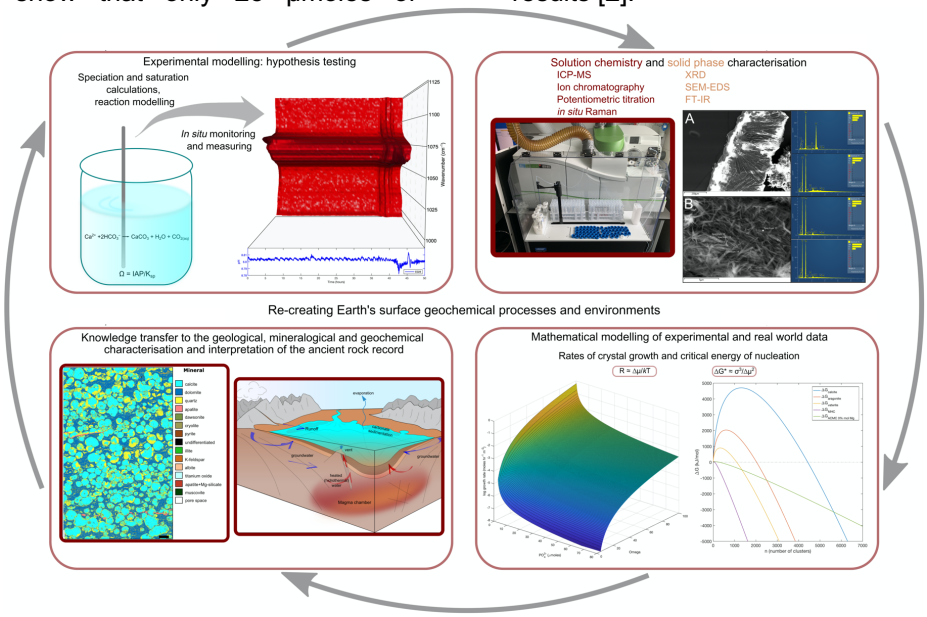

Figure 1. Summary of the main approaches used in this study and the iterative mode of investigation, comprising theory, empirical observation, experimentation, modelling and back to the laboratory [**2**].

Additionally, the analytical data from rock samples indicate that primary calcitic textures in the BVF are intimately associated with levels of P that tend to be higher than P concentrations reported in both biogenic and abiotic marine carbonates [**7**]. These data strongly support the presence of P (presumably as ΣPO_4) in Santos Basin waters at the time of sedimentation, although complexities with P incorporation during growth preclude meaningful estimates of corresponding ΣPO_4 concentrations.

In alkaline lakes high phosphate concentrations (as well as bioavailable nitrogen) are sequestered by photosynthesising organisms, thereby maintaining lower levels of ΣPO_4 than predicted by theoretical calculations [**2**]. Conversely, ammonia volatilisation, a phenomenon that may occur as a result of high alkalinity in some lakes, may result in nitrogen becoming the main limiting factor to productivity, thereby allowing dissolved phosphate levels to increase as they may not be efficiently mined from lake waters [**2**].

Conclusions

Inhibitors play a decisive role in influencing supersaturation in alkaline environments. This, in turn, favours the formation of metastable intermediates that can develop unusual crystal textures, and which can incorporate amounts of trace elements that depart from predictions assuming equilibrium precipitation. Importantly, the observations here provide additional evidence that high soluble phosphate concentrations may have been attained in alkaline settings on early Earth, with important implications for prebiotic chemistry scenarios, preceding biosynthesis of organic biomolecules. Additional research exploring antagonistic effects of ΣPO_4 and ions that promote/stabilise $CaCO_3$ clusters, such as dissolved SiO_2 [**2**] will be required to address and quantify these competing processes.

Acknowledgements

I am grateful to Petrobras for funding my PhD, enabling me to immerse in a fundamental and exciting research endeavour for four years, with clear implications in applied studies. I am also deeply thankful to my PhD supervisor Nicholas J. Tosca and several friends and colleagues for many discussions and for raising significant questions. I am specially indebted to Brooke Johnson, Clancy Zhijian Jiang, Matt Brady, Rosalie Tostevin, Sascha Roest-Ellis, Benjamin Tutolo, Julie Cosmidis, and numerous Petrobras colleagues for years of continuing discussions.

References

[**1**] Morse et al. 2007. Chem Rev 107, 342–381.
[**2**] Pietzsch, R., 2022. DPhil Thesis, University of Oxford.
[**3**] Toner, J., Catling, D., 2020. PNAS 117, 883−888.
[**4**] Purgstaller et al. 2019. CrysEngComm 21, 155–164.
[**5**] Dove, P.M., Hochella, M.F., 1993. GCA 57, 705–714.
[**6**] Brady et al. 2022. Nature Communications 13, 1–9.
[**7**] Ingalls et al. 2020. GRL 47, doi:10.1029/2020GL088804.

XVI LATIN AMERICAN CONGRESS ON ORGANIC GEOCHEMISTRY
9 - 11 AUGUST, 2023
ARACAJU, SERGIPE, BRAZIL

Quantitative estimations of preservation of organic carbon during Cretaceous Oceanic Anoxic Events in the Espírito Santo Basin

VENANCIO, I.M.[a*], SANTOS, T.P.[b], BELEM, A.L.[c], BERNARDES, M.C.[a], DIAZ, R.A.[a], CARREIRA, V.R.[c], MOREIRA, M.A.[c], SPIGOLON, A.L.D.[d], SOUZA, I.V.A.F.[d], ALBUQUERQUE, A.L.S.[c]

[a]PROGRAMA PÓS-GRADUAÇÃO EM GEOCIÊNCIAS (GEOQUÍMICA), UNIVERSIDADE FEDERAL FLUMINENSE, NITERÓI, BRASIL

[b]ESCOLA DE ARTES, CIÊNCIAS E HUMANIDADES, UNIVERSIDADE DE SÃO PAULO, SÃO PAULO, BRASIL

[c]PROGRAMA DE PÓS-GRADUAÇÃO DINÂMICA DOS OCEANOS E DA TERRA, UNIVERSIDADE FEDERAL FLUMINENSE, NITERÓI, BRASIL

[d]DIVISION OF GEOCHEMISTRY, PETROBRAS RESEARCH AND DEVELOPMENT CENTER (CENPES), RIO DE JANEIRO, BRAZIL

*correspondence: ivenancio@id.uff.br

Introduction

The oceanic anoxic events (OAEs) are characterized by an expansion and increased intensity of the oxygen minimum zones (OMZs) and enhanced accumulation of organic carbon in marine sediments [1]. These events were linked to global warming due to the release of CO2 to the atmosphere because of the degassing resultant of large-scale volcanism and dissociation of methane hydrates [2]. During OAEs, there is an interplay between production and preservation of organic carbon in the marine realm, but there is still a debate regarding which of these processes is more important for the accumulation of organic carbon. Recent studies have pointed out that preservation might be more important than production during these events [3]. However, few studies so far have focused on providing estimations on the fraction of organic carbon that was preserved. Studies have estimated ca. 2% of preservation of organic carbon during mid-Cretaceous anoxic events [4], but other findings have shown that these values can be even higher [5].

The majority of the investigations about OAEs are derived from sedimentary basins in the Northern Hemisphere [6]. Nevertheless, some studies have shown the occurrence of such events during the Cretaceous in Brazilian sedimentary basins [7]. However, to our knowledge, none of these studies from the Brazilian basins have presented quantitative estimations on the fraction of organic carbon that was preserved. Here, we present new data of organic carbon accumulation rate (OCAR) for several wells located in the Espírito Santo Basin during Cretaceous OAEs (OAE1d, ca. 100–98 Ma; and OAE2, ca. 94–92 Ma). These data allowed us to quantitatively estimate the preservation factor (PF) for these events, considering a range of possible values of primary productivity (PP).

Experimental

Wells are located in a bathymetric range from 1332 to 2081 m below sea level. The chronology of well ES-1 was built through astronomical tuning, and full details can be accessed in [8]. We then took advantage of the proximity among the wells investigated here to propagate the ES-1 astronomical age model. A total of 145 measurements of total organic carbon (TOC) is used in this study. Rock samples were dried at 40 °C and then grounded to a fine powder with subsequent carbonate dissolution with HCl and organic carbon combustion using a LECO WR 112 Carbon Analyzer to determine the TOC content. Density (RHOB) data were extracted from the log data of the wells. We calculated organic carbon accumulation rate (OCAR) and preservation factor (PF) for all the wells (OCAR = TOC x SR x ρ; PF = OCAR / PP).

Results and Discussion

Our results show that OCAR and PF were higher during OAE1d and OAE2, when compared to the modern conditions, confirming that organic carbon preservation was enhanced in the Espírito Santo Basin during these anoxic events (Figure 1). Our OCAR and PF values for OAEs are comparable to the ones reported by other studies [4,5]. Most notably, we were able to quantify, for the first time, the increase in preservation during OAEs for the Espírito Santo Basin. Considering mean values of PF from modern conditions and for OAEs, preservation was approximately eight times greater than modern conditions during OAE2 and approximately fourteen times greater during OAE1d. By comparing PF values from both OAEs, it is also possible to indicate that preservation during OAE1d was in general higher than OAE2, and by

considering mean PF values, the preservation was approximately two times greater during OAE1d compared to OAE2. In addition, the maximum PF during OAEs reached values of 5.14% for OAE2 and 8.64% for OAE1d, highlighting the higher potential of preservation during OAE1d compared to OAE2 for the Espírito Santo Basin. Our maximum PF value for OAE2 is very similar to the one reported by [5] for the southern part of the proto-North Atlantic. A possible explanation for the more intense preservation of organic carbon during OAE1d compared to OAE2 in the Espírito Santo Basin may reside on the important role of paleogeography preconditioning the ocean for organic carbon preservation. As pointed out by [9], land–sea configuration affects the ease with which OAEs can develop; thus, the more restricted Atlantic Basin during OAE1d compared to OAE2 may have been more favorable for low-oxygen conditions, causing higher quantities of organic carbon to be preserved in the oceans.

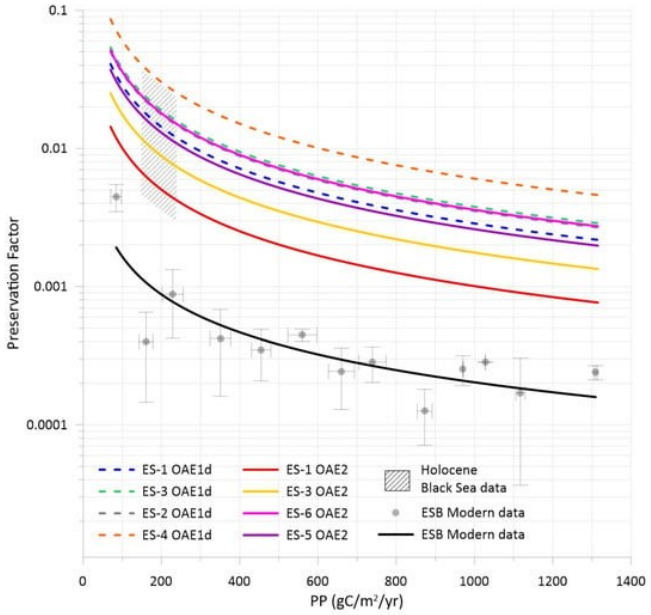

Figure 4. Preservation factors (fraction) for a range of primary productivities (PP) (gC/m2/yr). Preservation factors were calculated from modern data from the Espírito Santos Basin (ESB modern data), error bars are displayed, and a curve was fitted to the data (black solid line). For the wells located in the ESB, preservation factors were estimated based on the mean organic carbon accumulation rate (OCAR) for each oceanic anoxic event (OAE1d and OAE2) and a variable PP considering the modern range of PP for the ESB. Solid colored lines show the calculated values for OAE2, and the dashed colored lines show the calculated values for OAE1d. The y-axis is in log-scale. The rectangle with forward slash filling exhibits the values for the Black Sea during the Holocene.

Conclusions

Our results for the Espírito Santo Basin showed an increase in organic carbon accumulation during OAE1d and OAE2 compared to modern conditions. The high organic carbon accumulation rate values were associated to enhanced preservation due to the presence of bottom water with low O2 concentrations and not due to fast burial caused by high sedimentation rates. Furthermore, we provided quantitative estimations of preservation by calculating preservation factor (PF) values for the OAEs. The estimations showed that PF values could reach up to 8.6% during OAE1d and 5.1% during OAE2. These results led us to conclude that OAE1d was probably a more intense anoxic event than OAE2 at the Espírito Santo Basin. We highlight that our results are relevant for organic facies modelling studies, which need to provide quantitative estimations of the amount of carbon preserved for their model simulations.

Acknowledgements

The authors thank ANP (Brazilian Petroleum Agency), Petrobras S/A, UFF and Project PR4 for financial support.

References

[1] Jenkyns, H.C., 2010. Geochemistry of oceanic anoxic events: REVIEW. Geochemistry, Geophysics, Geosystems 11.
[2] Valle, B., Dal' Bó, P.F., Mendes, M., Favoreto, J., Rigueti, A.L., Borghi, L., De Oliveira Mendonça, J., Silva, R., 2019. The expression of the Oceanic Anoxic Event 2 (OAE2) in the northeast of Brazil (Sergipe-Alagoas Basin). Palaeogeography, Palaeoclimatology, Palaeoecology 529, 12–23.
[3] Tessin, A., Hendy, I., Sheldon, N., Sageman, B., 2015. Redox-controlled preservation of organic matter during "OAE 3" within the Western Interior Seaway. Paleoceanography 30, 702–717.
[4] Bralower, T.J., Thierstein, H.R., 1987. Organic carbon and metal accumulation rates in Holocene and mid-Cretaceous sediments: palaeoceanographic significance. Geological Society, London, Special Publications 26, 345–369.
[5] Kuypers, M.M.M., Pancost, R.D., Nijenhuis, I.A., Sinninghe Damsté, J.S., 2002. Enhanced productivity led to increased organic carbon burial in the euxinic North Atlantic basin during the late Cenomanian oceanic anoxic event: ENHANCED PRODUCTIVITY DURING C/T OAE-2. Paleoceanography 17, 3-1-3–13.
[6] Wilson, P.A., Norris, R.D., 2001. Warm tropical ocean surface and global anoxia during the mid-Cretaceous period. Nature 412, 425–429.
[7] Mello, M.R., Koutsoukos, E.A.M., Hart, M.B., Brassell, S.C., Maxwell, J.R., 1989. Late cretaceous anoxic events in the Brazilian continental margin. Organic Geochemistry 14, 529–542.
[8] Santos, T.P., Bione, F.R.A., Venancio, I.M., Bernardes, M.C., Belem, A.L., Lisboa, L.P., Franco, D.R., Díaz, R.A., Moreira, M., Leonardo, N.F., Souza, I.V., Spigolon, A.L.D., Albuquerque, A.L.S., 2022. Late Cretaceous astrochronology, organic carbon evolution, and paleoclimate inferences for the subtropical western South Atlantic, Espírito Santo Basin. Cretaceous Research 129, 105032.
[9] Donnadieu, Y., Pucéat, E., Moiroud, M., Guillocheau, F., Deconinck, J.-F., 2016. A better-ventilated ocean triggered by Late Cretaceous changes in continental configuration. Nature Communications 7, 10316.

XVI LATIN AMERICAN CONGRESS ON ORGANIC GEOCHEMISTRY
9 - 11 AUGUST, 2023
ARACAJU, SERGIPE, BRAZIL

Influence of eutrophication on different size classes of *Perna perna* mussels on the coast of Rio de Janeiro: preliminary results of an integrated approach based on carbon and nitrogen stable isotopes, and morphometry

ERBAS T.[1], MARQUES JR A.[1], SILVA E.[1], DUARTE M.[1], BRANDINI N.[2], CERDA M.[1], NASCIMENTO L.[2], LOPES M.[1] ABRIL G.[1,3]

[1] PROGRAMA DE PÓS-GRADUAÇÃO EM BIOLOGIA MARINHA E AMBIENTES COSTEIROS, UNIVERSIDADE FEDERAL FLUMINENSE, NITERÓI, RJ, BRAZIL.
[2] PROGRAMA DE PÓS-GRADUAÇÃO EM GEOCIÊNCIAS (GEOQUÍMICA), UNIVERSIDADE FEDERAL FLUMINENSE, NITERÓI, RJ, BRAZIL.
[3] LABORATOIRE DE BIOLOGIE DES ORGANISMES ET ECOSYSTÈMES AQUATIQUES (BOREA), MUSÉUM NATIONAL D'HISTOIRE NATURELLE, CNRS, PARIS, FRANCE

thaiserbas@id.uff.br

Introduction

Marine eutrophication is caused by the loading of organic matter and nutrients [1] that deeply affects biogeochemical cycles and metabolism of coastal ecosystems. These nutrients have a considerable variety of sources; in large urban centers with the Rio de Janeiro the nutrients come in majority from urban sewage [2]. Nutrient loading causes a rapid raise in the primary production of phytoplankton[3], and extensive changes other biological communities[4], such as bivalve mollusks living in eutrophicated areas. These suspension feeders' organisms can present metabolic responses according to the changes in the nature of suspended matter they use as food and energy source, which gives them a great potential for evaluating eutrophication[5]. The different levels of eutrophication influence the quality and quantity of phytoplankton and are likely to affect key aspects of the ecophysiology of filter feeder bivalves, such as the chemical composition of somatic body tissues[6, 7] and their morphometric characteristics[5, 8]. The objective of this work is to investigate the relationship between the composition of suspended matter, and the composition of mussel's soft tissues (hepatopancreas and muscle) and their morphometry along a gradient of eutrophication in the Region of Rio de Janeiro. We also compare the response of mussels to eutrophication according to their size in order to define the most appropriate animal size for biomonitoring purpose.

Materials and methods

Study area - Adults of *P. Perna* were collected from natural beds in three sites with different levels of eutrophication on the coast of the State of Rio de Janeiro (Saco do Mamanguá - October 2021, noted "MAM", Boa Viagem - June 2022, noted "BV" and Itaipu - July 2022, note "ITA") and transferred to the laboratory, where they were ranked according to their size, cleaned, and dissected for further analysis.

Environmental parameters - Water sampling was performed 4 days before mussel collection, at 15-13 points in an area of 2km diameters around each mussel sampling site. Water samples were filtrated through pre-combusted GF/F glass fiber filters (porosity 0.7 µm) to determine Suspended particulate matter (SPM) concentrations. δ13C and δ15N will be determined at the UC Davis Stable Isotope Facility using a Europe Hydra 20 / 20 mass spectrometer equipped with a continuous flow isotope ratio monitoring device (IRM). Chlorophyll a (Chl-*a*) concentration using the methodology of Strickland and Parsons (1972)[9]. In addition, total nutrients (nitrogen and phosphorus) of unfiltered samples were analyzed according to colorimetric methodologies described by Grasshoff et al. (1983)[10] and measured salinity, temperature with a Hidrolab - HL7 multiparameter probe.

Processing of biological samples - The sampled organisms were divided in 3 size class. For each size class 30 organisms were selected. On five organisms, soft tissues (muscle and hepatopancreas) were extracted, lyophilized, and stored frozen at -5 ◦C. The dry mass was used to determine δ13C and δ15N. In each size classes, 30 right valves were used for morphometric analysis[11]. Eleven linear measures of each valve were taken for 256 individuals, in addition to the weight.

Preliminary Results

Environmental parameters - The three study site had similar salinities (34.5) and temperature (22.5°C), but

strongly differed in terms of SPM, Chl-*a*, and nutrients concentrations confirming that the site MAM is oligotrophic whereas the sites BV and ITA are eutrophic (table 1). Chl-a and SPM showed highest concentrations in BV (23.9 µg/m^3 and 11.2 mg/ L and lower concentrations in MAM (1.26 µg/m^3 and 5.6 mg/ L). Mean Total nitrogen (TN) concentrations were highest in ITA (29.9 µmol/L) with maximus values as high as 119.7 µmol/L near the lagoon and minimum in MAM (8.9 µmol/L). The total phosphorus showed minimal concentrations in ITA (1.5 µmol/L) and a maximum in BV (2.2 µmol/L).

	MAM	BV	ITA
	oligotrophic	eutrophic	eutrohic
n	15	13	12
Sal	34.46 ± 0.92	34.32 ± 0.61	34.27 ± 5.84
T (°C)	22.04 ± 0.79	22.49 ± 0.36	22.39 ± 1.24
SPM (mg/ L)	5.62 ± 4.35	11.27 ± 4.85	9.15 ± 8.83
Chl a (µg/m^3)	1.26 ± 0.70	23.94 ± 14.73	9.35 ± 5.41
Feo (µg/m^3)	0.26 ± 0.19	2.64 ± 2.79	0.59 ± 0.49
TN (µmol/L)	8.96 ± 6.44	27.02 ± 5.44	29.97 ± 36.51
TP (µmol/L)	1.71 ± 0.84	2.24 ± 0.75	1.53 ± 2.03
N/P	4.21 ± 4.94	14.15 ± 8.55	22.80 ± 8.13

Table 1. Mean and standard deviation for environmental parameters: Sal, T, SPM, Chl a, Feo, TN, TP and N/P in MAM, BV and ITA.

***Morphometry* –** The analysis of the discriminant functions, for the three geographic populations, showed that the morphology was effective in identifying the populations. At cross-validation 97% of the individuals are classified in their origin group. Size class III (≤7.5 cm) had the best percentage of correct classifications (90%), while the worst was class I (75.6%). The Principal Components Analysis for the three geographic groups shows that 93.2% of the variation can be explained by the first two components (Axis 1: 89.5 %; Axis 2: 3.7%). Class III has the highest percentage of variance explained by the first component (47.5%), while the smallest was class II (34.1%).

A Multiple Factor Analysis applied to morphometric measurements in relation to environmental parameters the best result (Class III) showed a total explanation was 68.4% (Axis 1: 36.6 %; Axis 2: 31.7%). Among the 12 measures used, height (Hei) and distance from posterior adductor muscle to posterior shell margin (Pap) are negatively correlated with MPS and Chl-*a*. Umbo width (Hp) and width (Wid) are strongly correlated with TN and N/P. these results suggest that along the eutrophication gradient, food availability and quality is reflect in the mussel development. Stable isotopes measured in the SPM and in the soft tissue o *P. Perna* reveal that 15N is a good tracer of eutrophication and that transfer of isotopic signature occurs with no fractionation between the SPM and the hepatopancreas and with a small fractionation between the hepatopancreas and the muscle. The data also show that biggest animals are more representative of eutrophication state of the waters.

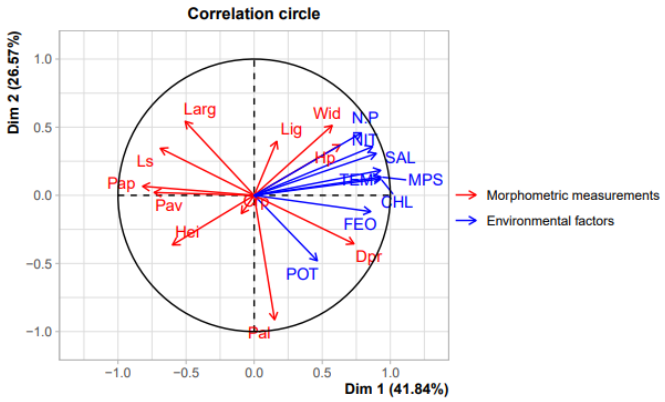

Figure 1. Multiple Factor Analysis applied to morphometric measurements in relation to environmental parameters.

Acknowledgements

The authors thank CAPES for fellowships; to the support of PBMAC. the Aquatic Biogeochemistry Laboratory. the Marine Genetics Laboratory. the Marine Biogeochemistry Laboratory at UFF. and the VELITROP project (CNRS INEE, France).

References

[1] Nixon, S. W., 1995. Coastal marine eutrophication: a definition, social causes, and future concerns. Ophelia, 41(1), 199-219.
[2] Jessen C., Bednarz VN, Rix L., Teichberg M., Wild C. (2015) Marine Eutrophication. Em: Armon R., Hänninen O. (eds) Indicadores Ambientais. Springer, Dordrecht.
[3] Drupp, P., Carlo, E.H., Mackenzie, F.T., Bienfang, P. and Kaneohe Bay, Hawaii. Aquatic Geochemistry, 17(4-5), 473-498.
[4] Carneiro, F.M., Nabout, J.C., Vieira, L.C.G., Roland, F. and Bini, L.M. Determinants of chlorophyll-a concentration in tropical reservoirs. Hydrobiologia, 740(1), 89-99.
[5] Resgalla, Jr C. et al., 2008. O mexilhão Perna perna (L.): biologia, ecologia e aplicações. Rio de Janeiro (RJ): Interciência, 324p.
[6] McKinney, R.A., J.L. Lake, M.A. Charpentier, and S. Ryba. 2002. Using mussel isotope ratios to assess anthropogenic nitrogen inputs to freshwater ecosystems. Environmental Monitoring and Assessment 74:167–192.
[7] Rogers, K. M. 2003. Stable carbon and nitrogen isotope signatures indicate recovery of marine biota from sewage pollution at Moa Point, New Zealand, Marine Pollution Bulletin, Volume 46, Issue 7, Pages 821-827.
[8] Alunno-bruscia, M.; Edwin, B. and Fréchette, M. (2001). Shell allometry and length-mass-density relationship for Mytilus edulis in an experimental food-regulated situation. Marine Ecology Progress Series (01718630), Vol. 219, P. 177-188. 219.
[9] Strickland, J. D. H., & Parsons, T. R., 1972. A practical handbook of seawater analysis.
[10] Grasshoff, K; Ehrardt, M; Kremling, K., 1983. Methods of Seawater Analysis. Weinhein: Verlag Chemie.
[11] Marques, H. 2003.Variação Morfológica em Perna perna (Linnaeus, 1758). Niterói, RJ – UFF, Instituto de Biologia.

XVI LATIN AMERICAN CONGRESS ON ORGANIC GEOCHEMISTRY
9 - 11 AUGUST, 2023
ARACAJU, SERGIPE, BRAZIL

Raman microspectroscopy as a tool for identifying biosignatures in speleothem microbialites

Gabriela Duarte [a], Ivo Karmann [a], Luana Morais [a], Patricio Munoz [a], Niklaus U. Wetter [b], Jessica Dipold [b], Anderson Z. Freitas [b]

[a] Institute of Geosciences – University of São Paulo (IGc-USP), Rua do Lago, 562, São Paulo, SP, 05508-080, Brazil.

[b] Nuclear and Energy Research Institute (IPEN-CNEN), Avenida Professor Lineu Prestes, 2242, São Paulo, SP, 05508000, Brazil.

e-mail: gduart@usp.br

Introduction

Raman spectroscopy [RS] is a non-destructive and high-resolution technique to detect molecules and mineral phases. This technique is effective in differentiating organic and inorganic compounds at a (sub-) micrometer scale [1]. Combined with other techniques (*e.g.,* Petrography, Scanning Electron Microscopy [SEM]) RS can be useful in identifying biosignatures in rocks.

The expected biosignatures in sedimentary rocks include fatty acids, amino acids, saccharides, and carbonaceous matter [2].

We used RS to investigate biosignatures in speleothems (calcite crusts) that are possible markers of microbial communities found in a cave system in Northeast Brazil. These crusts occur in the Catão cave, a 100-meter-long cave situated in São Desidério, west of the State of Bahia.

RS is a non-usual technique for this type of sedimentary deposits and shows efficient results in identification of organic compounds. This study aims to comprehend microbe-rock interactions in extreme environments (low-light incidence). Additionally, these speleothems might be examples of Holocenic microbialites that evolved in caves, elucidating biologically induced or mediated mineral precipitation in low temperature systems.

Methods

The samples of calcite crust from Gruta do Catão were partitioned in 8 petrographic thin sections, analyzed using a petrographic microscope with reflected and transmitted light and magnification up to 1000x with a coupled camera.

Samples were categorized into microfabrics, and filaments were identified in specific micritic layers. Thin section I7 was chosen due to the abundance of filaments in micritic layers. Filaments closer to the thin section's surface were selected as targets for RS.

Five targets were settled in a Raman Horiba microscope. Experiments were performed using laser length of 785 nm (IPEN). Equipment parameters were variable depending on the lens magnification and product obtained. Objectives of 10, 50 and 100x were used, with acquisition time varying between one and four seconds, and up to twenty accumulations. Incident energy on samples was 25 and 50 mW, and beam diameter ~1 µm.

Raman spectra processing was performed via baseline subtraction and smoothing in Origin. In addition, Raman spectra analysis included hierarchical clustering via the Hyperspec R-code. This clustering revealed data groups of similar spectral features, where peaks were identified using a non-linear iterative curve fitting code used in Matlab ® (peakfit of ISignal: https://terpconnect.umd.edu/~toh/spectrum/). This non-linear fit used a set of Lorentzian plus Gaussian peaks and yielded an error of ~3% regarding spectrum representative of cluster D.

Results and Discussion

Columnar microfabrics observed in thin sections contain fine laminations defined by intercalations of micritic and microsparitic layers. **Figure 1a** shows a caption of thin section I7 with arrows indicating micritic laminae. The targets indicated by squares show abundant filaments, which occur in micritic layers, with length varying from 10 to 50 µm. **Figure 1b** shows a filament encountered in target 3 (red in Figure 1a), where Raman spots were shot.

The spectra indicate calcite as the only mineral phase encountered in the specified targets (peaks: 155, 287, 712, 1087, 1437 cm^{-1} [3]. Although calcite peaks present the most intense signals, the interval between 1200 and 1700 cm^{-1}, where organic bounds vibrate, register numerous peaks.

Hierarchical clustering revealed three data groups of similar spectral features, presented in **Figure 2**. Spectra 01, 03 and 06 were grouped in Cluster A; spectra 02, 04 and 05 in Cluster B; spectrum 07 in Group C (outlier), and spectra 08, 09 and 10 in Cluster D.

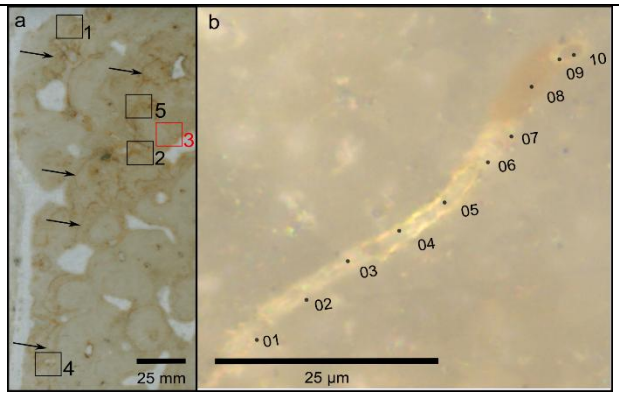

Figure 1. (a) caption of thin section I7, arrows indicate micritic laminae, squares indicate targets, red target indicate location for (b). (b) Filament showing Raman spots.

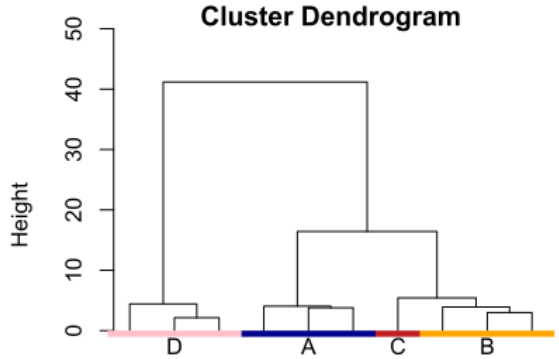

Figure 2. Cluster A: spectra 01, 03, 06; Cluster B: spectra 02, 04, 05; Cluster C: spectrum: 07; Cluster D: spectra 08, 09, and 10.

Deconvolution of Cluster D's medium curve revealed ten peaks in the range between 1200 and 1600 cm -1 (**Figure 3**, peaks: 1240, 1292, 1335, 1368, 1437, 1492, 1546, 1573 cm·¹).

We suggest that those peaks represent several organic bonds as found in [4], including: C-C-N bend, C-N stretch, N-H bend in amide III (1240 and 1292 cm·¹); (Metal) N-heterocycle ring vibration and/or calcite (1437 cm·¹); C-H antisymmetric deformation (peak 1492 ± 53 FWHM cm·¹ which includes 1483 cm·¹ peak from Wiemann et al., 2020); Pyridine-like ring stretch (1573 cm·¹). Peaks 1335, 1368, 1546 cm·¹, were not yet identified.

Based on these preliminary results, we suggest that the identified peaks correspond to peptides and/or proteins preserved in the filaments, which were not entirely altered by diagenesis. Similar Raman spectra were obtained in the porous carbonate micritic matrix, also indicating the presence of proteins.

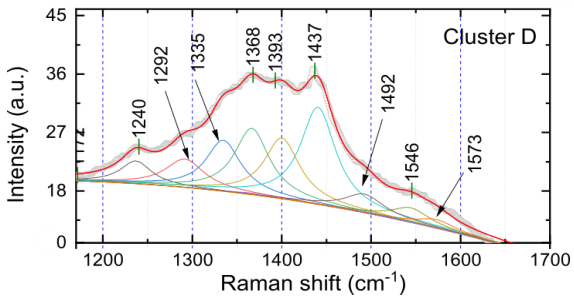

Figure 3. Medium baseline corrected Raman curve for Cluster D in gray; curve fit in red; defined peaks indicated by Raman shift number, with approximate error of ~3%.

Conclusions and future directions

The possible presence of peptides and/or proteins in the filaments and the micritic matrix suggests their biological origin. The matrix probably provided an organic substrate in which filaments evolved during deposition in subaqueous conditions.

The transport of the filaments and organic matter to the depositional site is unlikely due to their small size, high fragility and abundance, and the absence of associated detritic material. Diagenesis in surface-temperature and young age of the samples [5] could be the providers of good taphonomic conditions and material preservation.

As an on-going study, the characterization of alternative clusters and targets will provide additional data regarding filament and matrix composition. Therefore, Raman outputs advocate for application of different tools such as small-angle x-ray scattering to determine co-location of organics into porous matrices. Also, we will focus on quantification of OM via maldi-tof and SEM imaging.

Acknowledgements

The authors acknowledge IPEN and FAPESP which enabled the execution of RS (grant No. 17/50332-0 to Niklaus U. Wetter, Marcelo Linardi; grant No. 18/19240-5 to Anderson Z. Freitas, Niklaus U. Wetter).

References

[1] Foucher, F., 2019, Detection of Biosignatures Using Raman Spectroscopy, in Cavalazzi, B. and Westall, F. eds., Biosignatures for Astrobiology, Advances in Astrobiology and Biogeophysics, Springer Nature Switzerland AG, p. 267–282.

[2] De Gelder, J. De, Gussem, K. De, Vandenabeele, P., and Moens, L., 2007, Recent Advances in linear and nonlinear Raman spectroscopy I: Journal of Raman Spectroscopy, v. 38, p. 1538–1553, doi:10.1002/jrs.

[3] Buzgar, N.; Apopei, A. I.; Buzatu, A., 2009. Romanian Database of Raman Spectroscopy (http://rdrs.uaic.ro).

[4] Wiemann, J., Crawford, J. M., & Briggs, D. E., 2020. Phylogenetic and physiological signals in metazoan fossil biomolecules. *Science Advances*, *6*(28).

[5] Godinho, L.P. de S., 2020, Geoespeleologia, geomorfologia e geocronologia do sistema cárstico de São Desidério, Bahia, Brasil: Universidade de São Paulo.

ALG
ANALYTICAL TECHNIQUES

Orbitrap High Resolution Mass Spectrometry as an important toll for the characterization of crude oils

Thamara Andrade Barra*; Gabriela Vanini Costa; Débora de Almeida Azevedo

Universidade Federal do Rio de Janeiro, Instituto de Química, LAGOA-LADETEC, Rio de Janeiro, 21941-598

*thamara.barra@iq.ufrj.br

Introduction

The Orbitrap mass spectrometer is a high resolution (Orbitrap HRMS) and precision mass analyzer, and in a similar way to FT-ICR MS (Fourier transform ion cyclotron resonance mass spectrometry), allow the fingerprint of the polar non-volatile oil fraction composition.

The thermal maturation effect on polar constituents was investigated by FT-ICR MS [1,2]. It was reported that with increasing maturity: detected heteroatom classes reduced their relative abundances; the compounds became more aromatic; dealkylated species are enriched; the carbon number range became narrower; Ox compounds decrease, and nitrogen containing compounds (Nx) with high double bond equivalent (DBE) values grow. Regarding source aspects, lacustrine oils tend to be enriched with Nx compounds while marine oils have a preference for Ox compounds [3]. The O1 class was the second most abundant for both lacustrine and marine oils.

This study applied ESI(±)-Orbitrap HRMS for molecular geochemical characterization of the polar and heteroatomic compounds of six Brazilian crude oils, three from pre-salt reservoirs. These set of crude oils were analyzed previously by well stablished geochemical methods [4]. Here, the ESI(±)-Orbitrap HRMS provides enhanced insight and views, looking for better and in-deep characterization of each crude oil as complementary tool for geochemical assessment.

Experimental

Six post- and pre-salt oils from southeastern offshore Brazilian basins were supplied by the National Agency of Petroleum, Natural Gas and Biofuels (ANP). The oils were weighed and diluted with toluene/methanol (1:1 (v/v)) solutions with formic acid or ammonium hydroxide as additives (0,1% (v/v)). Mass spectra acquired by ESI(±)-Orbitrap HRMS were analyzed using the Xcalibur 2.2 program (Thermo Scientific, Bremen, Germany) and processed by the Composer 64 program (Sierra Analytics, USA).

Results and Discussion

The code, basin, reservoir, depth and API gravity of the crude oil samples are described in **Table 1**.

Table 1. Details of crude oil sample used in the study.

Code	Basin	Reservoir	Depth (m)	°API
TAB-7S	Santos	Pre-salt	5045/5112	29.4
TAB-7L	Santos	Pre-salt	5184/5232	27.9
TAB-6J	Campos	Pre-salt	4425/4556	29.4
TAB-6A	Campos	Post-salt	4424/4448	26.4
TAB-0Q	Espírito Santo	Post-salt	----------	29.6
TAB-4G	Espírito Santo	Post-salt	4533/4622	44.8

The ESI(±)-Orbitrap HRMS analyses provided mass spectra with homologous series detected in positive and negative modes, being possible to distinguish a variety of classes of heteroatomic polar compounds (NSO). The relative abundance percentage of the analyzed classes is represented in the diagram in **Figure 1**. The negative ionization mode had a greater number of different chemical classes compared to the positive mode, although in the later mode were detected more pseudo-molecular ions. The N1 class is the major one for both ionization modes. The Ox classes, mainly O1 and O2, were detected in the negative ionization mode, characterizing mainly the phenol and carboxylic acid classes, respectively. The O2 class was present in greater relative abundance mainly in the TAB-7S (35 %), TAB-7L (30 %), TAB-6A (16 %) and TAB-4G (24 %) among the studied crude oils. The relative abundances of N1, O1 and O2 classes, analyzed in the negative mode, were totally distinct among the six crude oils under study, but detected in all of them. The distribution of N1 and O1 classes, in the ESI(-) mode, sorted into groups of DBE pseudohomologs *versus* an intensity of class are shown in **Figure 2**.

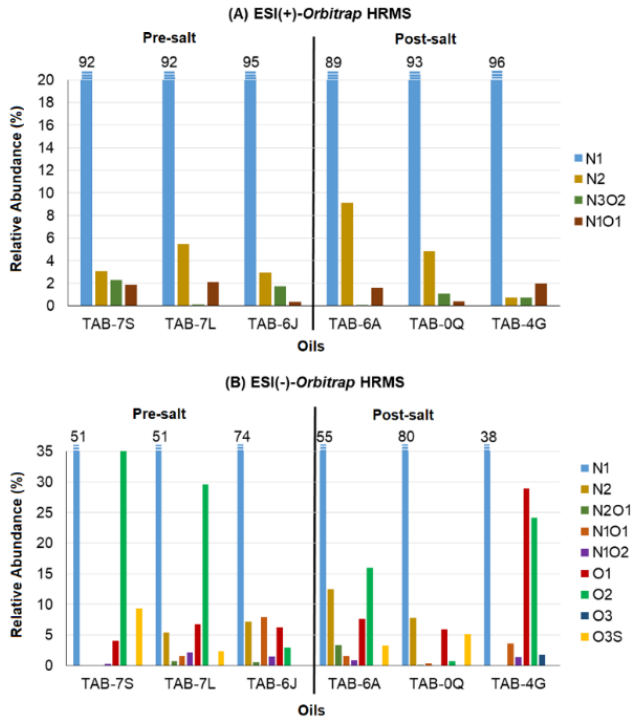

Figure 1. Class diagrams for pre- and post-salt oils obtained by: (A) ESI(+)-Orbitrap HRMS; (B) ESI(-)-Orbitrap HRMS.

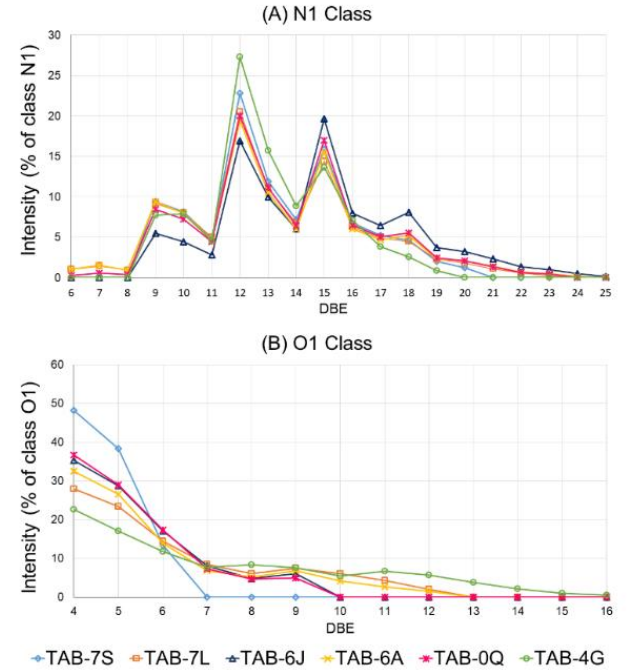

Figure 2. Distribution of N1 (A) and O1 (B) classes sorted into groups of DBE *versus* an intensity of class measured in ESI(-) mode for each oil.

The most prominent DBE value percent intensities for N1 class showed in **Figure 2A** were 9 (carbazoles), 12 (benzocarbazoles) and 15 (dibenzocarbazoles). The highest percentage intensities for O1 class occurred in DBE 4 and 5 (**Figure 2B**), indicating the presence of phenolic components and suggesting lacustrine depositional environment [3]. TAB-4G oil had the lowest relative intensity for DBE 4 and 5 values and was enriched with DBE from 8 to 16 species (**Figure 2B**). Two aspects can contribute to this fact: advanced thermal maturity stage, which increases aromatization [1]; and the contribution of marine organic matter, that tend to enrich the oil with Ox compounds, mainly with DBE from 8 to 17 species of O1 class [3].

Conclusions

The studied crude oils from pre-salt reservoirs and the TAB-6A and TAB-0Q oils from post-salt reservoirs were interpreted as lacustrines based on data from polar heteroatomic compound classes as well as the interpretation by the previously traditional analyses. The TAB-4G, post-salt reservoir oil, high relative percent intensities for DBE from 8 to 16 species of O1 class detected indicated to be marine, as well as biomarkers parameters.

The ESI(±)-Orbitrap HRMS encompassed the characterization of polar heteroatomic non-volatile compounds, that are in a smaller percentage in oil, allowing detailed molecular compounds evaluation and contributing to the geochemical characterization.

Acknowledgements

The authors thank Capes, CNPq and FAPERJ for the grants; ANP for providing the samples.

References

[1] Oldenburg, T.B.P., Brown, M., Bennett, B., Larter, S.R., 2014. The impact of thermal maturity level on the composition of crude oils, assessed using ultra-high resolution mass spectrometry. Organic Geochemistry **75**, 151–168.

[2] Rocha, Y., S., Pereira, R.C.L., Mendonça Filho, J.G., 2018a. Geochemical characterization of lacustrine and marine oils from off-shore Brazilian sedimentary basins using negative-ion electrospray Fourier transform ion cyclotron resonance mass spectrometry (ESI FT ICR-MS). Organic Geochemistry **124**, 29–45.

[3] Rocha, Y., S., Pereira, R.C.L., Mendonça Filho, J.G., 2018b. Negative electrospray Fourier transform ion cyclotron resonance mass spectrometry determination of the effects on the distribution of acids and nitrogen-containing compounds in the simulated thermal evolution of a Type-I source rock. Organic Geochemistry **115**, 32–45.

[4] Barra, T.A., Torres, C.L., Dal Sasso, M.A., Pereira, V.B.,Santos Neto, E.V., Azevedo, D.A., 2021. Deconvolution of post- and pre-salt petroleum sources in southeastern offshore Brazilian basins. Organic Geochemistry **152**, 104146.

XVI LATIN AMERICAN CONGRESS ON ORGANIC GEOCHEMISTRY
9 - 11 AUGUST, 2023
ARACAJU, SERGIPE, BRAZIL

Optimization of a gas chromatography triple quadrupole mass spectrometry method for quantification of organic sulfur markers in crude oils samples

[a] *FÁBIO XAVIER ANTUNES SAMPAIO, [b] KARINA SANTOS GARCIA, [b] ANTÔNIO FERNANDO DE SOUZA QUEIROZ [a,b] MARIA ELISABETE MACHADO

[a] DEPARTAMENTO DE QUÍMICA ANALÍTICA, PROGRAMA DE PÓS-GRADUAÇÃO EM QUÍMICA, UFBA; [b] LEPETRO, PROGRAMA DE PÓS-GRADUAÇÃO EM GEOQUÍMICA: PETRÓLEO E MEIO AMBIENTE, INSTITUTO DE GEOCIÊNCIAS, UFBA

e-mail: * fxsampaio@ufba.br; karina.ksg4@gmail.com; afsqueiroz.ufba@gmail.com; maria.e.pf@gmail.com;

Introduction

Dibenzothiophene (DBT), benzothiophene (BT) and benzonaphthothiophenes (BNT) are important classes of compounds present in low concentrations in petroleum. These compounds have been employed as geochemical markers (S-markers) to evaluate maturity, biodegradation and depositional environment [1]. Traditionally, the characterization of S-markers in crude oils and source rocks involves several steps of sample preparation based on separation by classes, according to polarity of the compounds and subsequent analysis of the separated fractions by GC-MS. Recently, triple quadruple mass spectrometry (GC-MS/MS) without prior sample separation has been a powerful tool for the detection of compounds at trace levels in complex matrices, such as petrochemical samples, and can effectively overcome some of the deficiencies of traditional procedures. This study aims to optimize a methodology by GC-MS/MS to quantify 14fourthen S-markers in crude oil samples from the Potiguar basin without prior fractionation.

Experimental

The GC-MS/MS (Agilent 7890B GC and 7000D triple quadrupole) method was optimized using a standard mix with fourteen standards of the BT, DBT and BNT classes. First, the instrument was operated in SCAN mode to obtain retention time and mass spectrum from each compound. After, analysis in SIM mode was employed for comparative study. Finally, the MS/MS was operated in MRM mode to define the optimum energies in the collision cell. The optimized method was applied to quantify eight crude oil samples after dilution in dichloromethane at a concentration of 0.02 mg μL^{-1} in a vial of 1.5 mL. The samples were provided by NUPPRAR from the UFRN and represent different points in the Potiguar basin.

Results and Discussion

Optimization of the GC-MS/MS

Collision energies (CEs) of 10eV to 50 eV at intervals of 10 eV aiming to obtain the best product ion transition signal and fine tuning of CE in the MRM mode for selection of highest intensity of MRM were optimized. The results, which were used to quantify the target compound (quantifier transition), and another one or two to confirm the identity of the compounds (qualifier transition) are summarized in Table 1.

Table 1. Optimized conditions for each S-marker in MRM mode from GC-MS/Ms.

Compounds	First transition - Quantification			Second transition - Confirmation		
	Precursor ion (m/z)	Product ion (m/z)	CE	Precursor ion (m/z)	Product ion (m/z)	CE
Benzothiophene - BT	134	89	20	134	108	20
3-metilbenzothiophene – 3-MBT	147	77	40	147	115	30
2,3-dimethylbenzothiophene – 2,3-DMDBT	162	147	20	162	128	40
'2,3,4-trimethylbenzothiophene – 2,3,4-TMBT	176	161	20	176	128	40
Dibenzothiophene - DBT	184	92	30	183	139	20
Phenantrene - Phen	178	152	30	178	176	40
4-methyldibenzothiophene – 4-MDBT	197	171	30	198	166	30
1- methyldibenzothiophene – 1-MDBT	197	171	30	198	166	30
4,6-dimethyldibenzothiophene – 4,6-DEDBT	212	197	20	212	178	40
2,4- dimethyldibenzothiophene – 2,4-DMDBT	212	197	20	212	178	40
1,4- dimethyldibenzothiophene – 1,4-DMDBT	212	197	20	212	178	40
2,4,7-trimethyldibenzothiophene – 2,4,7-TMDBT	226	211	20	211	178	20
4,6-diethyldibenzothiophene – 4,6-DEDBT	225	210	20	240	210	40
Benzo[b]naphtho[1,2-d]thiophene - BNT	234	189	40	234	208	30

The chromatogram in MRM mode, after optimization of the CE, is shown in Fig. 1.

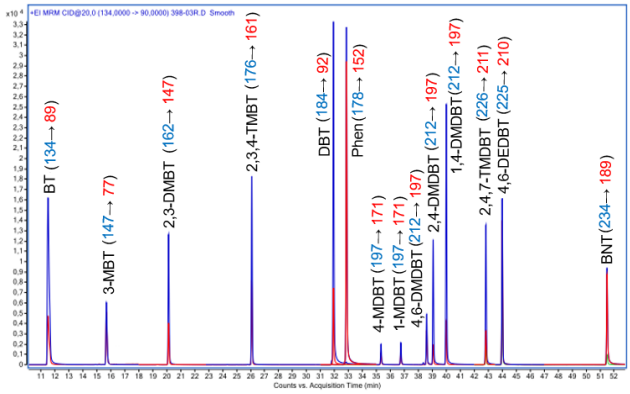

Figure 1. GC-MS/MS chromatogram in MRM mode for S-markers in mix standard at 0.25 mg L^{-1}. Primary transition in blue and secondary transition in red.

Method validation

Validation of the GC-MS/MS method was performed according to the guidelines established by the IUPAC. Analytical parameters, including linearity, recovery, intermediate precision (reproducibility), repeatability, limit of quantification (LOQ) and limit of detection (LOD), were evaluated. The LOD ranged from 0.005 µg mL^{-1} (BT) to 0.159 µg mL^{-1} (BNT) and LOQ from 0.014 µg mL^{-1} (4,6-DEDBT) to 0.53 µg mL^{-1} (BNT). Intraday precision was better than 20% in all cases. Recoveries ranged from 78.2% (1,4-DMDBT) to 117% (2,4,7-TMDBT).

Application in real samples

The applicability of the proposed methodology was proven by analyses of real samples. The concentrations in all samples were from 1.27 µg g^{-1} (1-MDBT) to 98.9 µg g^{-1} (BNT). The MRM approach proved to be very effective in the elimination of interferences by selecting adequate of the MRM transitions. An example of such an occurrence is shown in Fig. 2. For methyl-DBT, it is possible to observe the separation of three isomers of four possible isomers. 1-MDBT and 4-MDBT were quantified, and another peak with a characteristic transition refers to the sum of the 2 + 3-MDBT isomers (TR 35.9 min) [2][3].

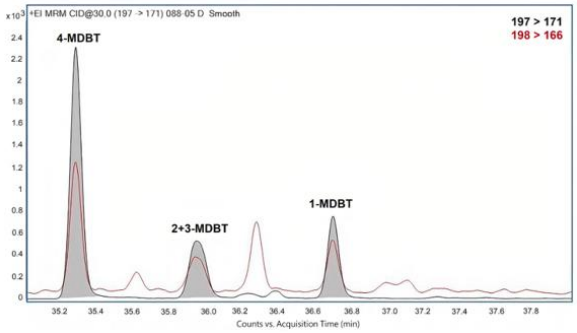

Figure 2. MRM chromatogram in region of elution for a sample of crude oil showing the evaluated methyldibenzothiophene isomers.

The use of ratios of the diagnostic S-markers, in particular determination of relative distribution of source-specific isomers has been used for geochemical assessment of maturity, biodegradation and depositional environment. The diagnostic ratios were calculated for the eight samples of crude oil from the Potiguar basin based on the individual concentrations (µg g^{-1}) of the target compounds obtained from quantitative analysis. According to results, all samples were mature oil range. Samples P4, P5, P6 and P7 have greater thermal maturity, P2 and P3, and P8 have intermediate maturation, and sample P1 has a discrepant value, attributed to a possible biodegraded sample (Fig. 3).

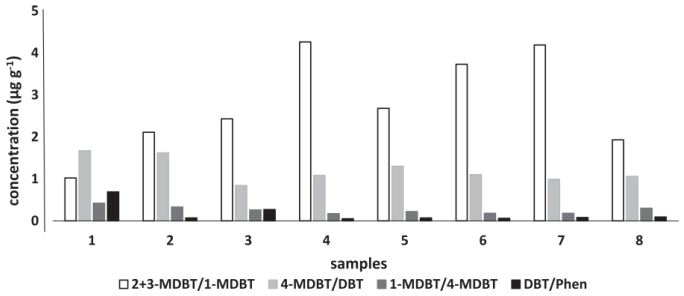

Figure 3. Bar graphs showing the diagnostic ratios used to evaluate biodegradation in the eight samples of crude oil.

Conclusions

The present study illustrated the optimization, quantification, and posterior application of an efficient and selective GC–MS/MS analytical method for the determination of S-markers in crude oil samples. GC–MS/MS increases the selectivity by using specific MRM transitions, eliminating or reducing interferences from petroleum content. The validation procedure was successfully employed in the quantification of 14 S-markers (BT, DBT, and BNT classes) without any kind of previous separation of the matrix compounds. The application of the method to crude oil samples showed its reliability in the detection in oils where these compounds are in low concentrations.

Acknowledgements

The authors thank the support from Shell Brasil through the project “Research in Petroleum Systems of Brazilian Sedimentary Basins” ANP 20075-8, the strategic support given by ANP through the R&D levy regulation, the CAPES and Núcleo de Processamento Primário e Reuso de Água Produzida e Resíduo (NUPPRAR) of UFRN by provide the samples.

References

[1] M. Mei, K. K. Bissada, T. B. Malloy, L. M. Darnell, and B. Szymcyk, 2018. Improved method for simultaneous determination of satured and aromatic biomarkers, organosulfur compounds and diamondoids in crude oils by GC-MS/MS. *Org. Geochem.* **116**, 35–50.

[2] F. A. Franchina, M. E. Machado, P. Q. Tranchida, C. A. Zini, E. B. Caramão, and L. Mondello, 2015 Determination of aromatic sulphur compounds in heavy gas oil by using (low-)flow modulated comprehensive two-dimensional gas chromatography-triple quadrupole mass spectrometry. *J. Chromatogr. A*, **1387**, 86–94.

[3] F. X. A. Sampaio, K. S. Garcia, A. F. de Souza Queiroz, and M. E. Machado., 2021. Determination of organic sulfur markers in crude oils by gas chromatography triple quadrupole mass spectrometry. *Fuel Process. Technol.* **217**,106813.

XVI LATIN AMERICAN CONGRESS ON ORGANIC GEOCHEMISTRY
9 - 11 AUGUST, 2023
ARACAJU, SERGIPE, BRAZIL

ANALYTICAL INNOVATION FOR THE CHARACTERIZATION OF LIGHT HYDROCARBONS FOCUSING ON RESERVOIR GEOCHEMISTRY

Daniela França[a], Dayane M. Coutinho [a], Clarisse L. Torres [a], Vinícius B. Pereira [a], Raquel V. S. da Silva [a]
Daniel S. Dubois[b], Joelma P. Lopes[b], Gabriela Vanini [a], Francisco R. Aquino Neto [a], Débora A. Azevedo [a]

[a]Universidade Federal do Rio de Janeiro, Instituto de Química, Ilha do Fundão, Rio de Janeiro, RJ 21941-909, Brazil
[b]Petrobras/CENPES/PDIEP/GEOQ, Cidade Universitária, Rio de Janeiro, RJ 21941-915, Brazil

e-mail: danimelf@yahoo.com.br

Introduction

Light hydrocarbons (LHs) are a significant portion of most crude oils and these compounds store essential geochemical information that represents a great potential for the optimization of exploration and production stages (Mango, 1997). Reservoir geochemistry is an area that employs LHs to understand the chemical composition of the oil inside the reservoir and try to relate it to the dynamics of interaction between rock and water (Larter & Aplin, 1995). The application of comprehensive two-dimensional gas chromatography coupled to time-of-flight mass spectrometry (GC×GC-TOFMS) in crude oil analysis has been extensively explored in the literature (Coutinho *et al*., 2022). However, LHs are typically analyzed using the normal configuration (nonpolar/polar) of columns in the first dimension (^{1}D), with lengths of 50-60 m and time-consuming chromatographic runs (~2.5 h) to achieve LHs separation. In the second dimension (^{2}D), columns of medium polarity are generally used, with lengths between 1.5 and 2.0 m and thinner film thicknesses (Xiangchun *et al*., 2017; Chang *et al*., 2017). This study aims to apply ^{1}D columns of shorter lengths (30 m) in a nonpolar/polar configuration, optimizing the temperature program, carrier gas flow and cold and hot modulator periods along the chromatogram, to optimize the analysis time of these light hydrocarbons, maintaining the chromatographic resolution necessary for their adequate quantification.

Experimental

This study employs a new approach for the detailed characterization of light hydrocarbons (C_4-C_{15}) using a 30 m column length and different modulation periods in a single crude oil analysis with minimal preparation. Several parameters were evaluated and adjusted, such as the modulation period (different periods and proportions of cold and hot jet), the temperature programme (35 °C (3 min) $\overset{1°C/min}{\text{-------}}$ 40 °C $\overset{3°C/min}{\text{---------}}$ 160 °C $\overset{20°C/min}{\text{----------}}$ 330 °C), and the carrier gas flow (1.0 mLmin^{-1}), in addition to evaluating different solvents (CH_2Cl_2 and CS_2).

Results and Discussion

The solubilization of the oil with CS_2 solvent showed better results when compared to CH_2Cl_2, because it allowed using ions characteristic of light hydrocarbons and spectral deconvolution to separate the analytes that elute in the region close to the solvent. The solvent volume was also adjusted. Its reduction facilitated the visualization of components that elute at retention times close to CS_2 (Figure 1). It is necessary to point out that the studies in the literature are applied to condensates or light oils. In contrast, the present study is applied to crude oil from the Santos Basin with intermediate API gravity (Xiangchun *et al*., 2017; Chang *et al*., 2017).

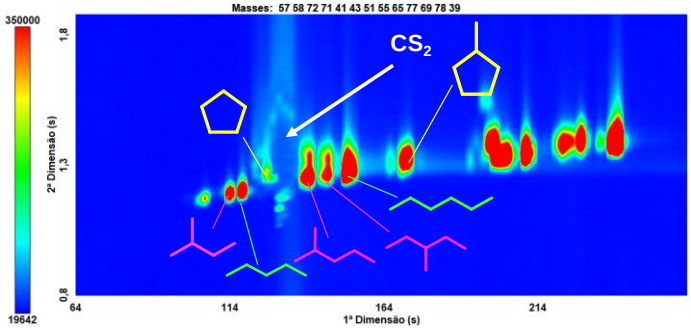

Figure 1. Extracted ion chromatogram (EIC; ∑ *m/z* 39 + 41 + 43 + 51 + 55 + 57 + 58 + 65 + 69 + 71 + 72 + 77 + 78) for a crude oil analysis diluted in carbon disulfide, using nonpolar/polar column set, highlighting the chemical structure of some identified classes: n-alkanes, branched alkanes, and cycloalkanes.

The analyzes were carried out in a temperature program with different ramps. Furthermore, the branched and linear alkane resolution was not adequate when using polar/nonpolar column set.

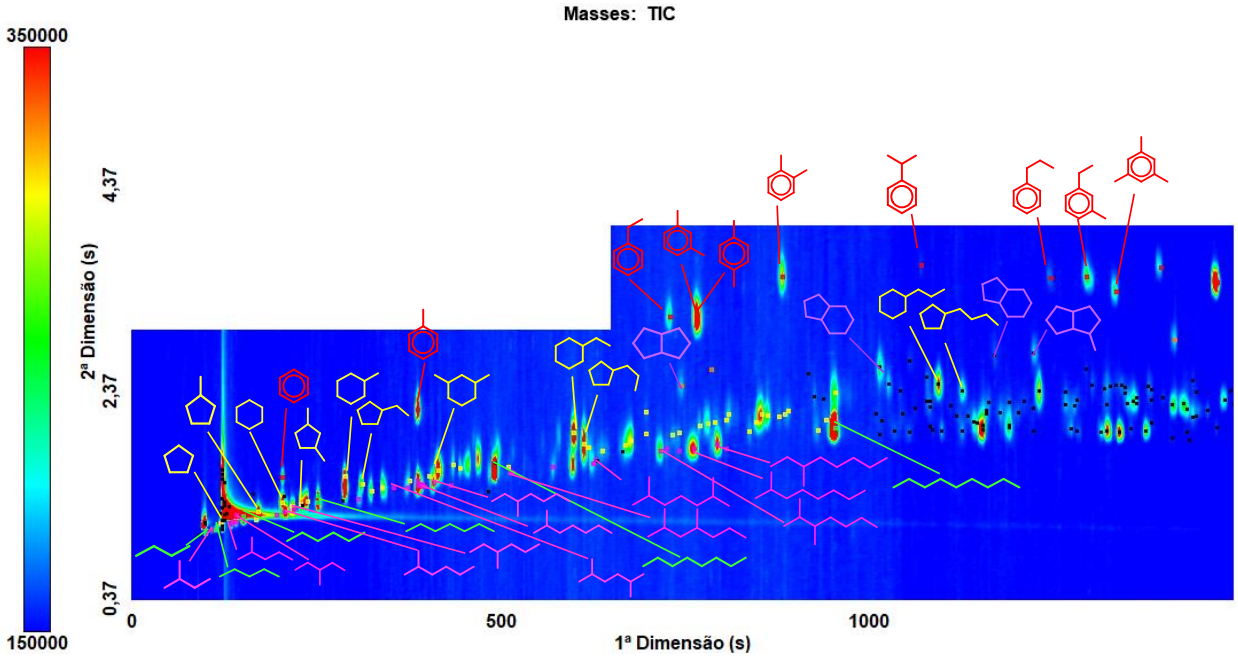

Figure 3. Total ion chromatogram using a ^{1}D 30 m column in a nonpolar/polar column set, of a reference oil highlighting, the chemical structure of typical analytes.

The analytical variables adjusted in this work allowed the identification of molecular diverse components of crude oils in over half the analysis time of current methods. Figure 3 presents only a few assigned substances besides considering their isomers. Furthermore, higher cold jet times in the modulation process were essential to improve the target compounds focusing on the second dimension and their peak shapes and widths.

Conclusions

The use of five distinct modulation periods combined with a shorter hot pulse duration allowed the optimization of the peaks of the most volatile compounds due to the increased trapping in the modulator. In addition, the fit of these parameters provided a chromatographic run with a shorter time, avoiding the loss of volatile compounds, maintaining the chromatographic resolution for the detailed characterization of the C_5-C_{15} range hydrocarbons present in the whole oil using a nonpolar/polar configuration column set. Thus, it was possible to develop a chromatographic method for identifying and subsequently quantifying light hydrocarbons up to C15 that can be applied to study the behavior of oil inside the reservoir.

Acknowledgements

The authors thank CNPq and FAPERJ (Brazilian research councils) for fellowships; Petrobras S/A (0050.0121394.22.9), and CAPES financial code 001, for financial support.

References

Mango, F. D. 1997. The light hydrocarbons in petroleum: a critical review. Organic Geochemistry, 26(7-8), 417-440.

Larter, S. R., & Aplin, A. C. 1995. Reservoir geochemistry: methods, applications and opportunities. Geological Society, London, Special Publications, 86(1), 5-32.

Coutinho, D. M., França, D., Vanini, G., Gomes, A. O., & Azevedo, D. A. 2022. Understanding the molecular composition of petroleum and its distillation cuts. Fuel, 311, 122594.

Xiangchun, C., Lixin, M., Youde, X., & Tiantian, L. 2017. C8 light hydrocarbon parameters to indicate source facies and thermal maturity characterized by comprehensive two-dimensional gas chromatography. Energy & Fuels, 31(9), 9223-9231.

Chang, X., Shi, B., Han, Z., Li, T., 2017. C5–C13 light hydrocarbons of crude oils from northern Halahatang oilfield (Tarim Basin, NW China) characterized by comprehensive two-dimensional gas chromatography. Journal of Petroleum Science and Engineering 157, 223–231.

ANALYSIS OF CARBONACEOUS ELEMENTS IN THE AGUAS ZARCAS CARBONACEOUS CHONDRITE METEORITE USING ELECTRON MICROPROBE TECHNIQUE.

DONATO, T.P. [a]/ TOSI, A. [a]/ ZUCOLOTTO, M. E. [a]/ PAIXÃO, C. [a]

[a] **FEDERAL UNIVERSITY OF RIO DE JANEIRO**

tatiane18.tpd@gmail.com

Introduction

The carbonaceous chondrite meteorites are extraterrestrial rocky bodies mainly composed of phyllosilicates, organic compounds, water, and chondrules. CCs can contain up to 20% water and between 2% and 7% organic matter. This assemblage is fragmented into a mixture of hydrocarbons and carbon associated with minerals, as observed in the Murchison meteorite (Mukhopadhyay et al., 2007).

The meteorite studied here is the Aguas Zarcas, which fell in Costa Rica in 2019. It was classified as CM2, with "M" referring to the name of the first identified specimen of the class (Mighei), and "2" representing the petrographic classification of the meteorite, indicating low thermal metamorphism, high aqueous alteration, and a significant presence of hydrated minerals (Heide & Wlotzka, 1995).

This study focuses on the analysis conducted using the Electron Microprobe technique on the chondrules of the Aguas Zarcas Meteorite in search of carbonaceous elements associated with minerals.

Chondrules are spherical structures formed during or before the formation of the solar system due to generalized thermal events. They adhere to a sedimentary matrix during cementation and are imprinted within the matrix of the rocky fragments. The original water content influences this parameter, which can lead to partial or complete dissolution of these formations (Brearley, 2006).

Experimental

The Aguas Zarcas meteorite used in this study was a native fragment acquired by the National Museum of Rio de Janeiro and donated by Dr. Maria Elizabeth Zucolotto (Figure 1) for the collection of analytical results. This meteorite was chosen for analysis due to its composition containing a significant amount of organic material.

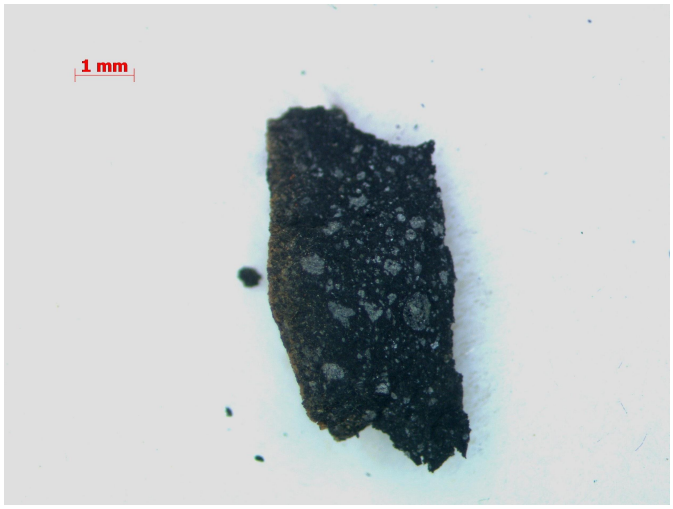

Figure 1: Fragment of the Aguas Zarcas Meteorite.

The analysis was performed using the Jeol JXA8230 Electron Microprobe (EPMA) available at the Labsonda laboratory of UFRJ (Federal University of Rio de Janeiro). No carbon coating was applied due to carbon contamination concerns. Only the analysis of the uncoated fragment placed on the sample stage was conducted. First, the electron beam emission voltage was calibrated to achieve satisfactory results considering the lack of coating. Next, points were selected within the chondrules' core and edges.

Semiquantitative analysis of the investigated phases was conducted using the Energy Dispersive Spectrometry (EDS) method. The beam conditions included an acceleration voltage of 10 keV, a beam current of 7 nA, and a 1 µm diameter for silicates.

Results and Discussion

Upon examination the chondrules of the Aguas Zarcas meteorite, significant percentages (wt.%) of carbon associated with important elements for phyllosilicates such as silica and magnesium were found, as described in the comparative Table 1.

When directing the electron beam at the brighter points in the matrix or chondrules, the same percentage of carbon was not found, only elements such as silica and magnesium, indicating only mineral compositions and not amorphous carbon.

The most impressive result was the discovery of potential carbonaceous elements incorporated into olivine present in the chondrules. These structures underwent high temperatures and pressure but acted as "protectors" for these compounds, as shown in points 002 and 004 of analysis 04AZ and point 010 of analysis 011AZ in Figure 2 and Table 1.

Another way to understand this formation is through aqueous alteration during high temperatures, which caused carbonaceous elements present in the matrix to percolate between minerals. Upon cooling, they became associated, as seen in points 004 and 006 of analysis 11AZ in Figure 2 and Table 1.

Points	Fe	O	C	Mg	Si	S	Ca
04 AZ-2	3.51	12.30	*65.04*	*4.66*	*12.32*	1.06	0.59
04 AZ-4	3.22	11.78	*61.99*	*2.31*	*18.81*	0.32	0.95
11AZ-010	5,01	19,56	*51,43*	*12,59*	*10,55*	0,34	0,22
11AZ-004	5.38	11.70	*52.87*	*1.85*	*24.74*	1.30	0.58
11AZ-006	7.69	13.47	*56.57*	*4.66*	*15.47*	0.70	0.60

Table 1: Comparison among semiquantitative analyses of the rich-carbon points by EDS/EPMA.
Concentration in wt.%.

Conclusions

Chondrules in carbonaceous meteorites can carry carbon elements or hydrocarbons associated with minerals. These elements can originate from the matrix or the formation of the chondrules.

Based on the present analyses and existing literature, it is evident that there is a possibility for these carbonaceous elements to be hydrocarbons, as it is described in the literature that insoluble and soluble hydrocarbons are present in the chemical structure of carbonaceous meteorites. Moreover, the applied analytical condition as well as the instrumentation allowed access to this important organic and inorganic chemical association in meteorites.

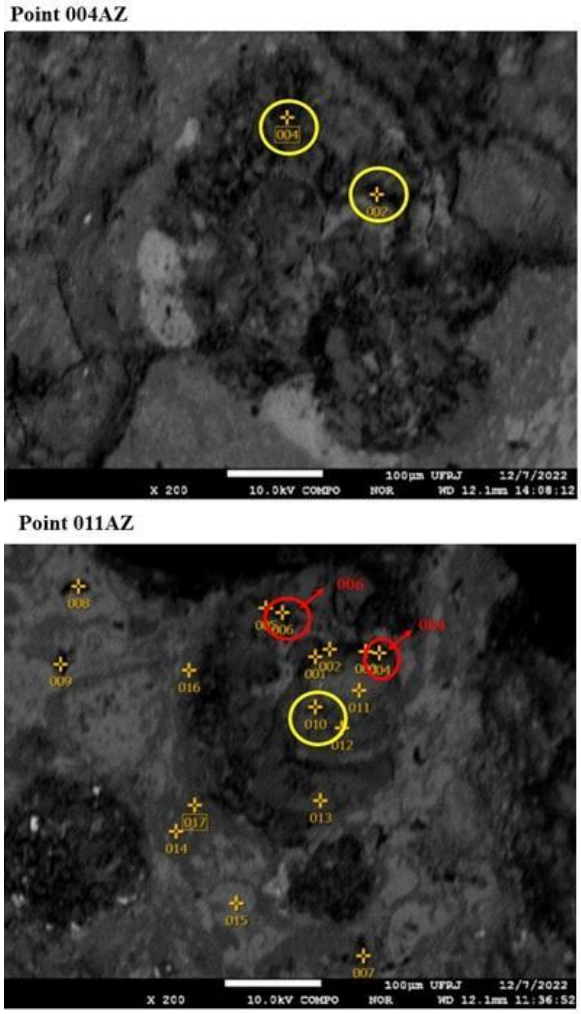

Figure 2: Microanalysis by EDS/EPMA of the selected points in chondrules 004 and 011.
Points labeled in red circles represent the chondrule edges.
Points labeled in yellow represent the cores of the analyzed chondrules.

References

Mukhopadhyay, P. K., Mossman, D. J., & Ehrman, J. M., 2007. The case for vestiges of Early Solar System biota in carbonaceous chondrites: petroleum geochemical snapshots and possible future petroleum prospects on Mars Expedition. In Instruments, Methods, and Missions for Astrobiology X (Vol. 6694, pp. 107-122). SPIE.

Heide, F., Wlotzka, F.,1995. The meteorites (pp. 97-168). Springer Berlin Heidelberg.

Brearley, A. J. 2006. The action of water. Meteorites and the early solar system II, 943, 587-624.

XVI LATIN AMERICAN CONGRESS ON ORGANIC GEOCHEMISTRY
9 - 11 AUGUST, 2023
ARACAJU, SERGIPE, BRAZIL

FRACTIONATION OF NSO COMPOUNDS FROM HIDROUS PYROLYSIS PRODUCTS BY H-MPLC AS A TOOL FOR EVALUATING CARBON ISOTOPIC COMPOSITION IN PETROLEUM GENERATION AND EXPULSION

RODRIGO CABRAL DA SILVA[a*], ANDRÉ LUIZ DURANTE SPIGOLON[a], TAYNARA RODRIGUES COVAS[b], NERILSON MARQUES LIMA[b], BONIEK GONTIJO VAZ[b]

[a] Petrobras Research Centre, Av. Horácio Macedo 950, Cidade Universitária, Rio de Janeiro, 21941-915, Brazil;
[b] Federal University of Goiás (UFG), Chemistry Institute, Av. Esperança S/N, IQ1, Campus Samambaia, Goiânia, 74.690-900, Brazil.

e-mail: rodrigocabral@petrobras.com.br

Introduction

Gas chromatography (GC), liquid chromatography (LC), physicochemical analyses and elemental analyses are among the most commonly employed techniques to characterize products generated through hydrous pyrolysis (HP) experiments (Spigolon et al., 2015).

These techniques play a crucial role in measuring a wide range of parameters that define the properties of these matrices, like gas/ oil ratio, gas/ bitumen/ oil composition, oil density, sulfur content, as well as Saturates (SAT), Aromatics (ARO), Resins (RES), and Asphaltenes (ASPH) compound content (Spigolon et al., 2015).

For the molecular characterization of the isolated fractions from HP bitumen and oils, the commonly used is LC which generate SAT and ARO fractions rich in biomarkers, subsequently analyzed using GC coupled with a mass spectrometer (GC-MS and GC MS/MS) (Radke et al.,1986).

In the context of monitoring the polar fraction (NSO) in HP bitumen and oils, the sub-fractionation based on polarity and chemical affinity has been accomplished the use of hetero-medium pressure liquid-chromatography (H-MPLC). It is a promising alternative for minimizing matrix complexity interferences in molecular and functional readings of techniques such as ESI FT-ICR MS (Covas et al., 2020).

In this study, a series of HP oils and bitumens derived from an immature source rock and subjected to varying temperatures were fractionated using H-MPLC. The resulting subfractions, distinguished by polarity, acidity, and basicity, were then subjected to Elementary Isotopic Ratio Analysis of Carbon (EA-IRMS). The primary objective of the study was to investigate whether these NSO subfractions, differentiated through H-MPLC, could serve as practical tools for monitoring the thermal evolution in HP experiments by providing isotopic profiles.

Experimental

Spigolon et al. (2015) provided details regarding the HP protocol and its products.

The isolation of NSO from HP samples was initially performed using a specific protocol for this isolation method can be found in the work of Willsch et al. (1997).

Each sample was dissolved in *n*-hexane and injected into a first thermally deactivated silica column (A). The SAT, and ARO were eluted with *n*-hexane trough a second thermally activated silica column (M), while the NSO were strongly retained in column A. After collecting the full SAT, the ARO fraction was eluted and collected from the top of column M through backflush.

Column A, which retained the NSO was coupled into the H-MPLC system containing additional columns arranged in series: two impregnated with KOH (B and D), one treated with HCl (C), and a larger one with pure silica (E), as depicted in Fig. 1.

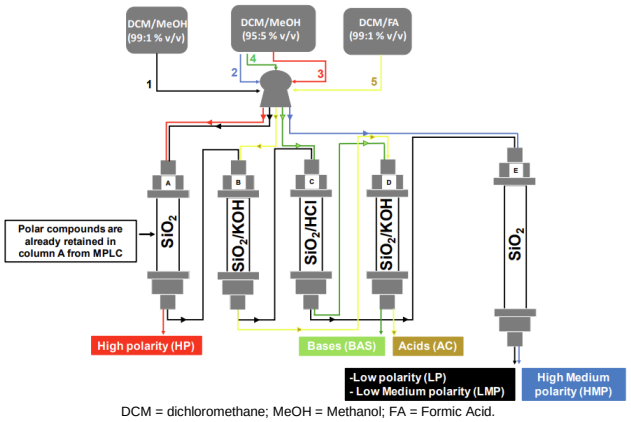

DCM = dichloromethane; MeOH = Methanol; FA = Formic Acid.

Figure 1. H-MPLC scheme. Three different mobile phases for the elution of polar compounds: phase I (DCM: MeOH, 99:1% v/v), phase II (DCM: MeOH, 95:5% v/v), and phase III (DCM: FA, 99:1% v/v) - (Covas et al., 2020).

Columns B, C, D, and E were pre-conditioned with Phase I. The low polarity (LP) fraction and low, medium polarity (LMP) fraction were sequentially eluted using Phase I through columns A, B, C, and E. Next, the high polarity fraction (HMP) was obtained by exclusively washing out the column E with Phase II. Subsequently, the high polarity fraction (HP) was directly recovered by percolating the Phase II trough column A.

Phase II was applied over column C and D to elute basic compounds (BAS) fraction. Additionally, an acid fraction (AC) was obtained from columns B and D using the Phase III.

Finally, all polar fractions obtained for each hydrous pyrolyzed Bitumen and oils were evaporated using nitrogen-blowing instrument system, weighted for mass balance calculations, and then analyzed on an EA-IRMS analyzer from Themo Fisher.

Results and Discussion

Mass balances of SAT, ARO, RES, ASPH, and total NSO present in the HP oil and bitumen (Bit) are presented in Table 1. The carbon isotopic ratio performed for all these whole materials and all NSO fractions collected by H-MPLC have been displayed in Fig. 2.

Temp(°C)	Time(h)	%SAT		%ARO		%RES		%ASPH		%POLARS	
		Oil	Bit.	Oil	Bit.	Oil	Bit.	Oil	Bit.	Oil	Bit.
Temperature series											
Unheated	**NA**	**NA**	**14.5**	**NA**	**23.0**	**NA**	**41.5**	**NA**	**21.0**	**NA**	**62.5**
280	**72**	**37.9**	**6.6**	**30.4**	**15.6**	**26.5**	**26.8**	**5.2**	**51.0**	**31.7**	**77.8**
300	**72**	**29.8**	**6.7**	**21.8**	**16.5**	**16.8**	**18.6**	**3.8**	**58.2**	**20.7**	**76.7**
310	**72**	**37.8**	**7.1**	**25.1**	**16.9**	**15.2**	**15.3**	**4.0**	**60.8**	**19.2**	**76.1**
320	**72**	**35.3**	**6.8**	**21.1**	**15.0**	**14.0**	**10.1**	**4.8**	**68.0**	**18.7**	**78.2**
325	**72**	**39.6**	**8.2**	**23.5**	**17.3**	**16.4**	**10.6**	**4.2**	**63.9**	**20.6**	**74.5**
330	**72**	**34.9**	**9.4**	**29.1**	**18.5**	**15.7**	**11.3**	**4.0**	**60.8**	**19.7**	**72.1**
340	**72**	**34.2**	**13.5**	**27.3**	**23.1**	**15.6**	**11.4**	**5.1**	**52.1**	**20.7**	**63.4**
345	**72**	**31.1**	**16.1**	**26.6**	**26.1**	**13.0**	**13.9**	**5.1**	**43.9**	**18.1**	**57.8**
350	**72**	**30.0**	**16.7**	**26.3**	**30.0**	**14.1**	**17.6**	**5.8**	**35.8**	**20**	**53.4**
355	**72**	**30.0**	**18.7**	**25.6**	**26.0**	**13.0**	**13.8**	**6.7**	**41.5**	**19.7**	**55.3**
360	**72**	**27.2**	**13.7**	**27.2**	**24.3**	**12.8**	**15.7**	**7.4**	**46.4**	**20.3**	**62.0**
365	**72**	**28.9**	**12.0**	**24.4**	**29.8**	**12.6**	**18.5**	**6.0**	**39.7**	**18.5**	**58.2**

Table 1. Mass balance for SAT, ARO, and NSO in HP products as a function of transformation ratio (Spigolon et al., 2015).

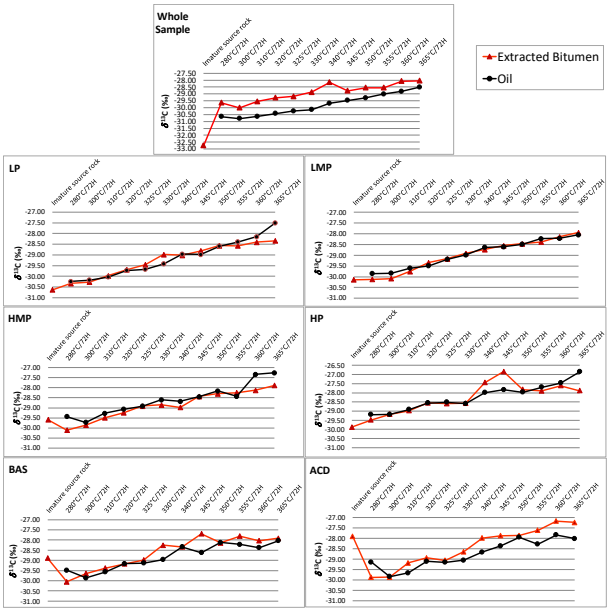

Figure 2. Carbon isotope ratio ($\delta^{13}C$) measured for total HP oils and bitumens and its polar fractions obtained in H-MPLC.

Notably, NSO exhibits a great decrease in the oil while this reduction in bitumen was relatively lower over the HP temperatures.

The HP experiments observed a significant carbon isotopic difference between bitumen and oils across all temperature gradient ranges. The bitumen consistently exhibited a higher abundance of ^{13}C compared to the corresponding oils. This highlights the genetic relationship between the transformation of bitumen into oil during the thermal cracking process, as predicted by Spigolon et al. (2015).

On the other hand, the isotopic composition for LP, LMP, HMP, and HP fractions showed nearly identical isotopic ratios between the fractions derived from both bitumens and oils at all pyrolysis temperatures. However, exceptions were observed in BAS and ACD fractions, particularly above 325°C, which kept the whole bitumen and whole oil behavior. These fractions exhibited behavior consistent with the overall Bitumen and oil compositions.

Conclusions

The integration of H-MPLC for fractionating HP products into its NSO portions has expandend the use of carbon isotopic data for chracterizing the compositional changes occuring during the thermal cracking process.

By employing carbon isotopic measurements over fractionated NSO, a more comprehensive understanding of the preferential isotopic pathways involved in the cracking reactions can be achieved for petroleum generation and expulsion studies.

Acknowledgments

The authors thank Petrobras S/A, CAPES and CNPq (Brazilian research council) for all support.

References

Covas, T.R.; Freitas, C.S.; Tose, L.V.; Dávila, J.A.V.; Rocha, Y. dos S.; Rangel, M.D.; Silva, R.C.; Vaz, B.G., 2020. Fractionation of polar compounds from crude oils by hetero-medium pressure liquid chromatography (H-MPLC) and molecular characterization by ultrahigh-resolution mass spectrometry. Fuel**267**, 117289.

Radke, M., Welte, D.H., Willsch, H., 1986. Maturity parameters based on aromatic hydrocarbons: influence of the organic matter type. Organic Geochemistry**10**, 51–63.

Spigolon, A.L.D.; Lewan, M.D.; Penteado, H.L.B.; Coutinho, L. F.; Mendonça Filho, J. G., 2015. Evaluation of the petroleum composition and quality with increasing thermal maturity as simulated by hydrous pyrolysis: A case study using a Brazilian source rock with Type I kerogen. Organic Geochemistry **83-84**, 27-53.

Willsch, H., Clegg, H., Horsfield, B., Radke, M., Wilkes, H., 1997. Liquid Chromatographic Separation of Sediment, Rock, and Coal Extracts and Crude Oil into Compound Classes. Analytical Chemistry **69**, 4203-4209.

XVI LATIN AMERICAN CONGRESS ON ORGANIC GEOCHEMISTRY
9 - 11 AUGUST, 2023
ARACAJU, SERGIPE, BRAZIL

Ultra-fast separation of biomarkers using The Average Theoretical Peak Time metric as a method development tool

Ellen Jessica Monteiro Pereira Campos[a], Rodrigo Silva Teixeira[a], Carlos Alberto Carbonezi[b], Carin von Mühlen[a]

[a] Faculdade de Tecnologia, Universidade do Estado do Rio de Janeiro

[b] Centro de Pesquisas, Desenvolvimento e Inovação Leopoldo Américo Miguez de Mello

e-mail: carin@fat.uerj.br

Introduction

The use of petroleum biomarkers, such as terpanes, is very important for quantifying weathering levels and to identify the source of oil spills (Xu *et al.,* 2020). Terpanes are an important class of cyclic compounds used as biomarkers. They have large number of homologous series, including bicyclic, tricyclic, tetracyclic and pentacyclic compounds. These compounds have as their main mass spectra characteristic the m/z 191 ion (Kruge *et al.,* 2018).

The Average Theoretical Peak Time (ATPT) can be defined as the time (in ms per peak) needed to elute a theoretical peak in a chromatographic system. It was proposed to define chromatographic speed in gas chromatography considering conventional and multidimensional separations (von Mühlen *et al.,* 2022).

The objective of this study was to evaluate the speed of comprehensive two-dimensional gas chromatography coupled with time-of-flight mass spectrometry (GC×GC/TOFMS) separations of petroleum biomarkers. ATPT was applied as a method development tool to evaluate fast and conventional separation methods using five selected terpanes as reference compounds.

Experimental

The SARA methodology was applied for a Brazilian crude oil sample fractionation (Kharrat *et al.,* 2007). Approximately 40 mg crude oil were deposited in the top of a dry silica gel column with length of 30 cm and then eluted with 15 mL of *n*-hexane for the elution of saturated fraction. The fraction was concentrated and the required amount of 1 ml solvent was added to adjust the final volume. The chemical analysis was accomplished using a GC×GC/TOFMS Pegasus 4D LECO Instruments, equipped with GC 7890A (Agilent Technologies, Santa Clara, CA, EUA) system, with consumable-free cryogenic thermal modulator and an Agilent 4513A autosampler. Conventional and fast separation were evaluated. To perform conventional GC×GC analysis a low polarity column with 30 m × 0.32 mm × 0.25 µm in first dimension and a medium polarity column with (2 m × 0.15 mm × 0.15 µm) in second dimension were used. For fast-GC × GC it was applied a column with the same stationary phase in ^{1}D with dimensions 10 m × 0.18 mm × 0.20 µm, and the same second dimension column. The conventional and fast separation methods were optimized and compared based on ATPT metrics.

Results and Discussion

The ATPT metric was calculated using the equation (1) as described by von Mühlen *et al.*(2022):

$$ATPT = (2.8\ {}^{1}w_{0.5}\ {}^{2}w_{0.5}/P_M) \quad (1)$$

In equation (1), ATPT for a GC×GC system depends on the average peak width at half height in first and second dimensions ($^{1}w_{0.5}$ and $^{2}w_{0.5}$, respectively), and the modulation period (P_M). To establish parameters of 1D peak, w_b was calculated utilizing curve fitting to a Gaussian profile. In this calculation the width at half height ($w_{0.5}$) will be considered as the peak has the ideal "Gaussian" shape, then $w_b = 1.7\ w_{0.5}$.

In table (1), the conventional and fast two-dimensional separations were classified on ATPT parameters. ATPT define chromatographic speed based on peak capacity and can be notice that both separations were classified as ultra-fast separations. For the fast separation, ATPT values were close to one third of the ATPT values of the conventional separation. The total run time were reduced in the same scale, from 81 min to 25,83 min.

In figures 1 and 2 it is possible to observe the color plot of the separation of terpane biomarkers in conventional and fast methods, the compound was identified based on Aguiar *et al.* (2010). As the ATPT reduced in the same scale of the total run time (with a faster temperature ramp), the resolution obtained in the conventional separation was preserved for those compounds.

Table 1. ATPT values calculated for conventional and fast GC×GC/TOFMS of selected terpanes.

No.	Compounds	Conv - ATPT (ms/peak)	Fast - ATPT (ms/peak)
1	17α(H),21β(H)-22,29,30-trisnorhopane (Tm)	0.0644	0.0269
2	17α(H),21β(H)-30-norhopane (H29)	0.1172	0.0529
3	17α(H),21β(H)-hopane (H30)	0.1863	0.0334
4	(22S)-17α(H),21β(H)-30-Homohopane (H31S)	0.1153	0.0380
5	(22R)-17α(H),21β(H)-30-Homohopane (H31R)	0.1117	0.0381
	Average	**0.1153**	**0.0380**

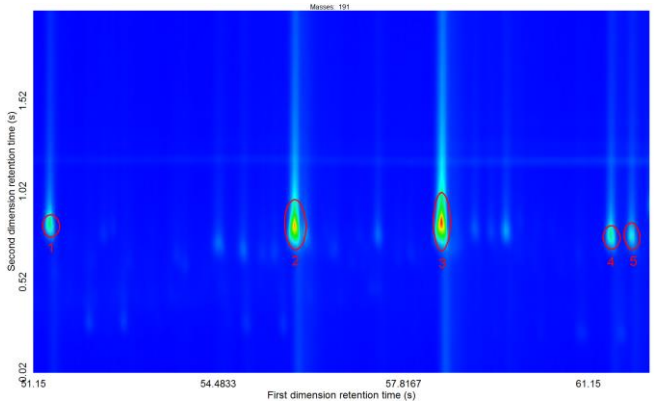

Figure 1. Color plot of the separation of selected terpanes biomarkers in a conventional GC×GC method.

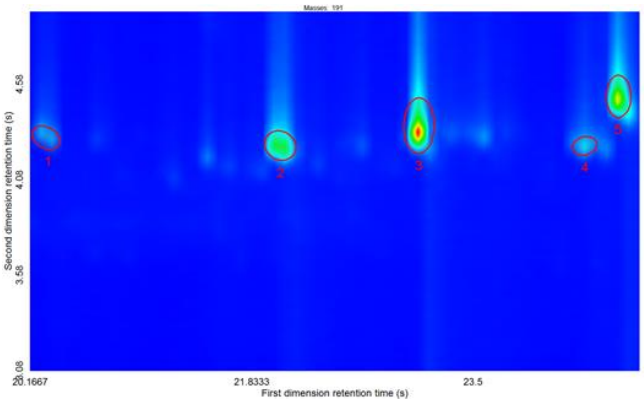

Figure 2. Color plot of the separation of selected terpanes biomarkers in a fast GC×GC method.

ATPT metrics was an effective metric to classify analytical methods in one-dimensional and multidimensional separations (Mazza *et al.,* 2023). With this metric it was possible to evaluate the efficiency of a multidimensional chromatographic separation considering all dimensions (von Mühlen *et al.,* 2022; Mazza *et al.,* 2023). GC×GC analysis of petroleum is commonly performed using a conventional column system. In this study the approach of fast chromatography resulted in a high-resolution separation with a higher chromatographic speed. In other words, fast two-dimensional gas chromatography preserved the chromatographic information from conventional two-dimensional gas chromatography, reducing the total analysis time in one third, using ATPT as a method optimization tool.

Conclusions

The ATPT metric was an important method development tool applied to evaluate the chromatographic separation in multidimensions. This metric was applied to improve the separation speed of terpanes, resulting in a method three times faster than a conventional separation, preserving the resolution obtained in a conventional GC×GC method.

.

Acknowledgements

The authors thank Petrobras S/A for financial support.

References

Aguiar, A., Silva Júnior, A.I., Azevedo, D.A., Aquino Neto, F.R., 2010. Application of comprehensive two-dimensional gas chromatography coupled to time-of-flight mass spectrometry to biomarker characterization in Brazilian oils. Fuel 89(10), 2760-2768.

Kharrat, A.M., Zacharia, J., Cherian, V.J., Anyatonwu, A., 2007. Issues with Comparing SARA Methodologies. Energy & Fuels 21(6), 3618-3621.

Kruge, M.A., Gallego, J.L.R., Lara-Gonzalo, A., Esquinas, N., 2018. Chapter 7 - Environmental Forensics Study of Crude Oil and Petroleum Product Spills in Coastal and Oilfield Setting: Combined Insights From Conventional GC-MS, Thermodesorption -GC-MS, and Pyrolysis-GC-MS. Oil Spill Environmental Forensics Case Studies,131-155.

Mazza, F.C., Sampaio, N.A.S., von Mühlen, C., 2023. Hyperspeed method for analyzing organochloride pesticides in sediments using two-dimensional gas chromatography–time-of-flight mass spectrometry. Analytical and Bioanalytical Chemistry 415(13), 2629-2640.

von Mühlen, C., Mangelli, L.N.R., Marriot, P.J., 2022. Average theoretical peak time as a metric to analytical speed in one dimensional and multidimensional gas chromatographic separations. Journal of Chromatography A 1667, 462887.

Xu, H., George, S.C., Hou, D., Cao, B.X., Chen, X.D., 2020. Petroleum sources in the Xihu Depression, East China Sea: evidence from stable carbon isotopic compositions of individual n-alkanes and isoprenoids. Journal Of Petroleum Science and Engineering 190, 107073.

XVI LATIN AMERICAN CONGRESS ON ORGANIC GEOCHEMISTRY
9 - 11 AUGUST, 2023
ARACAJU, SERGIPE, BRAZIL

Optimization of a methodology for plant wax investigation as geomarker in soil forensic analysis: a n-alkane study by GC-FID

Amanda P. Faillace*, Janaina de A. Matos [2], Lívia M. L. Teixeira [3], Gislaine N. S. Costa [4], Lucas M. Duarte [5], Silvana V. Rodrigues [6], Carla S. Silveira [7]

Postgraduate Program in Geochemistry, Department of Analytical Chemistry - Institute of Chemistry, Universidade Federal Fluminense, Niterói, RJ, Brazil

*Amanda P. Faillace: amandafaillace@id.uff.br

Introduction

Physical, chemical and mineralogical profiles enable the characterization of aspects that give uniqueness (fingerprint) to soil from a specific region, allowing for the geolocation of its origin even after transfer [1]. This helps to determine whether there is a connection between the suspects and the crime scene [2]. The creation of a georeferenced soil database, for forensic use in the Baixada Fluminense region of Rio de Janeiro, demanded the development of analytical methodologies for the analysis of soil fingerprint variables, including the profile of n-alkanes.

In forensic literature [3, 4], the profile of n-alkanes is used as a fingerprint marker due to their persistent characteristics in soils and sediments, providing a stable and reliable profile, along with information about the origin of the alkanes. Adapted versions of a published protocol [5] have been used in different studies involving the analysis of n-alkanes in soil for forensic purposes using gas chromatography with flame ionization detection (GC-FID) [3, 4, 6, 7]. However, these studies focused on the investigation of n-alkane profiles derived from vascular plant waxes (odd-chain n-alkanes, especially C27 to C33) in analytical runs that lasted for hours.

Considering an international trend to build a georeferenced soil database for forensic purposes [6, 7, 8], the present work describes an optimization of methodology for investigation of n-alkane profiles of soils from Baixada Fluminense by GC-FID intending to incorporate it, along with other soil parameters, to a soil database.

Experimental

A Thermo Trace Ultra GC-FID was used to conduct the analysis. The instrumental parameters proposed here are based on different methodologies [3,8,9], and are compared to a reference work [3] in Table 1. A standard mixture of C7-C40 was injected at a concentration of 10 µg mL^{-1} in heptane.

	Dawson et al. (2004)	Current methodology
Column	DB-1, 30 m x 0.75 mm x 1 µm	DB-5, 30 m x 0.25 mm x 0,25 µm
Carrier gas	He: 4,0 mL/min	He: 2,0 mL/min
FID gases	Synthetic air → 350,0 mL/min H_2 → 35,00 mL/min N_2 → 50,00 mL/min	Synthetic air → 350,0 mL/min H_2 → 30,00 mL/min N_2 → 30,00 mL/min
Injection	0,7 µL/Splitless	1 µL/Splitless
Temperature ramp	170 °C por 4 min 170 a 215 °C – 30 °C/min 215 a 300 °C – 6 °C/min, held for 3 min.	50 a 320°C - 6°C/min, held for 10 min.
Analysis time	22,7 min	22,7 min
Inlet temperature	280 °C	300 °C
Detector temperature	340 °C	320 °C

Table 1. Comparison of the initial method and the current optimized method.

The soil preparation followed the procedure proposed by Dawson et al (2004) [3]. The soil samples analyzed by GC-FID showed that adaptations in the sample preparation process are needed, due to the low concentration of n-alkanes and their distribution profile in urban soils [8].

Results and Discussion

When using the corresponding parameters from the reference methodology [3], it was observed that only n-alkanes starting from C12 were obtained, which is below the range of interest. Several tests for parameter modifications were performed using the same C7-C40 standard. The tests were performed according to Silva et al (2008), which achieved a range of C14-C30. However, hydrogen was used as carrier gas.

The first modification was the replacement of the 100% dimethylpolysiloxane column (DB1) for a 5% phenyl, 95% dimethylpolysiloxane (DB5), with appropriate mathematical corrections applied. Other modifications are described in Table 1.

The temperature of the detector and injector, as well as the detector gas flows, were kept as previously proposed [9], while the oven ramps were successively adjusted in order to achieve a wider and more qualified range of n-alkanes profiles.

Seven parameter modification tests were conducted, resulting in the best adjustment in the desired range (C11 to C40), sensitivity, resolution, and reduced analysis time (Figure 1).

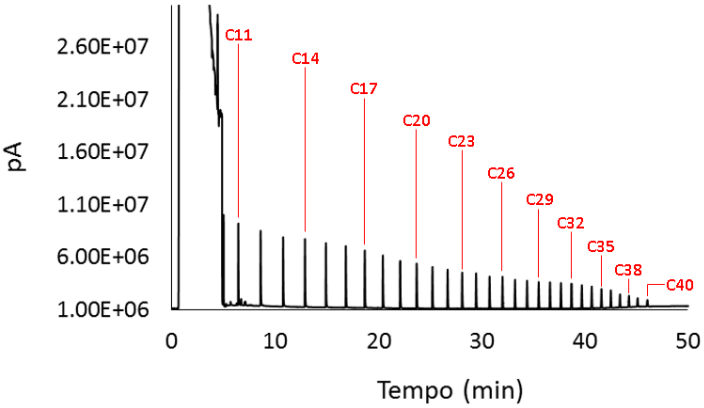

Figure 1. Chromatogram of the n-alkane standard mixture, identified C11 to C40.

Conclusions

The optimized parameters achieved the best fit for the desired range with good sensitivity, resolution and reduced analysis time. These parameters will be used for n-alkane profile analysis in soil of forensic interest in Rio de Janeiro.

Acknowledgements

The authors thank FAPERJ and PCERJ for the research scholarships and scientific support.

References

[1] MEASUREMENT OF SOIL CHARACTERISTICS FOR FORENSIC APPLICATIONS. Dawson, L. A.; Hillier, S.; 2010.

[2] CARACTERIZAÇÃO DE SOLOS DA REGIÃO DE LISBOA PARA APLICAÇÃO FORENSE. Pacheco, A.; 2017.

[3] THE USE OF PLANT HYDROCARBON SIGNATURES SOIL ORGANIC MATTER. Dawson, L. A., Towers, W., Mayes, R. W., Craig J., Väisänen, R. K., Waterhouse, E. C.; 2004.

[4] THE DISCRIMINATION OF GEOFORENSIC TRACE MATERIAL FROM CLOSE PROXIMITY LOCATIONS BY ORGANIC PROFILING USING HPLC AND PLANT WAX MARKER ANALYSIS BY GC. McCulloch, G., Dawson, L. A., Ross, J. M., Morgan, R. M.; 2018.

[5] PROTOCOL FOR THE ANALYSIS OF N-ALKANES AND OTHER PLANT-WAX COMPOUNDS FOR THEIR USE AS MARKERS FOR QUANTIFYING THE NUTRIENT SUPPLY OF LARGE MAMMALIAN HERBIVORES. Dove, H., Mayes, R. W.; 2006.

[6] ORGANIC MATTER CHARACTERIZATION OF SEDIMENTS IN TWO RIVER BEACHES FROM NORTHERN PORTUGAL FOR FORENSIC APPLICATION. Carvalho, A., Ribeiro, H., Mayes, R., Guedes, A., Abreu, I., Noronha, F., Dawson, L.; 2013.

[7] SOIL FORENSIC CHARACTERISATION IN FORENSIC CASE WORK. Dawson, L.; 2017.

[8] PEDOLOGIA E MINERALOGIA DE SOLO APLICADAS ÀS CIÊNCIAS FORENSES. Testoni, S. A.; 2019.

[9] DISTRIBUIÇÃO DE COMPOSTOS LIPÍDICOS EM SEDIMENTOS DA LAGOA DA CONCEIÇÃO, ILHA DE SANTA CATARINA, BRASIL. Silva, C. A, Oliveira, C. R., R. Oliveira, I. R. W. Z., Madureira, L. A. S. 2008.

XVI LATIN AMERICAN CONGRESS ON ORGANIC GEOCHEMISTRY
9 - 11 AUGUST, 2023
ARACAJU, SERGIPE, BRAZIL

Assessment of a potential biomarker for thermal evolution of oils from polar compounds analysis by ultrahigh-resolution mass spectrometry

Arquimedes Moraes Souza Coutinho[1*], Jhonnatas de Carvalho Carregosa[2], Wenes Ramos da Silva[2], Boniek Gontijo Vaz[3], Taynara Rodrigues Covas[3], Alberto Wisniewski Jr.[2], Jandyson Machado Santos[1]

[1]**Petroleum, Energy and Mass Spectrometry Group, Chemistry Department, Federal Rural University of Pernambuco – UFRPE, Recife, Pernambuco, Brazil;** [2]**Petroleum and Energy from Biomass Group, Chemistry Department, Federal University of Sergipe – UFS, São Cristóvão, Sergipe, Brazil;** [3]**Chemistry Institute, Federal University of Goiás - UFG, Campus Samabaia, Goiânia, Goiás, Brazil.**

*arquimedesmoraes@yahoo.com.br; jandyson.machado@ufrpe.br.

Introduction

Petroleum is an important and complex chemical mixture, composed of percentage above 90% of hydrocarbons and other organic compounds derived from S, N, O, halogens and metals [1]. It is formed from thermal process of animal and plant fossil sediments, which results in a mixture of undefined and varied composition [2]. The chemical composition of biomarkers is used to evaluated the geochemical characteristics of oils, one of the most important is the thermal evolution [2].

The gas chromatography/mass spectrometry (GC/MS) has been used for to identify biomarkers and calculate the ratios to obtain the level of thermal evolution, among it, Ts/Tm, Ts/(Ts+Tm), C32S/(C32S+32R) [3]. Although very efficient for this task, GC/MS has the disadvantage of a long analysis time and sometimes requires sample preparation. In the other hand, the ultrahigh-resolution mass spectrometry (FT-MS) allows the characterization of thousands of compounds existing in petroleum, due to ion cyclotron resonance analyzers (FT-ICR MS) or Orbitrap (Orbitrap MS), which coupled with electrospray ionization (ESI) has the advantage of direct insertion to achieve the polar compounds [3].

The study aims to evaluate a potential biomarker of the thermal evolution related to polar compounds obtained by ESI FT-MS in an investigation using pyrolysis (Py) process in crude oils, by correlation between FT-MS ratio and Ts/Tm, Ts/(Ts+Tm) and C32S/(C32S+32R) thermal evolution ratios.

Experimental

Fourteen commercial standards, which are from the classes of thiophenes, pyridinols, phenols, carboxylic acids, ketones and hydrocarbons were chosen based on the methodology used by [4]. The fourteen standard compounds described were submitted to Py, following the previous methodology [5], in which 10 mg of each compound was heated to a maximum temperature of 500 °C (in a borosilicate glass by Ni-Cr resistance). The inert gas used was N_2, in flow of 2 ml min^{-1} and 30 s of purge. The time total analysis was 3 minutes. The solvent used for final elution of the retained compounds was methanol:toluene mixture (1:1, *v/v*), to a final volume of 1 mL. The final solution was analyzed by ESI(-) FT-MS.

Four samples of crude oils (named A, C, S and P) were provided by Petroleum Brasileiro S.A. (PETROBRAS). The oils are from the Sergipe-Alagoas basin, located in northeastern Brazil.

Analysis of standards and oils were performed in a mass spectrometer with an Orbitrap analyzer (Exactive Plus Thermo Scientific, USA).The FT-MS conditions were: dissolution in toluene/methanol (1:1 *v/v*) to a final concentration of 1 mg mL^{-1}, and ammonium hydroxide in the proportion of 0.4% as an ionization promoter for the ESI(-) analyses at flow rate of 5 µL min^{-1}; capillary voltage at -3.2 kV in ESI(-) and capillary temperature at 280 °C, and N_2 as sheath, auxiliary and spare gases. The acquisition and interpretation of mass spectra were performed using Xcalibur 2.0 software (Thermo Scientific, USA) in a range of *m/z* 100-1000. FT-MS/MS was performed in a FT-ICR MS (9.4 T Solarix, Bruker Daltonics, Germany) in the ESI(-) mode acquisition using a collision energy of 25 V with similar conditions as described above.

For GC/MS analysis, oil samples were prepared from 5 g of crude oil that was first fractionated to obtain saturated fraction. The GC/MS operated in electron ionization (EI) mode, following the conditions of [6]. The *m/z* transitions were monitored as follow: Ts/Tm and Ts/(Ts+Tm) in transition of *m/z* 370>191 and C32S/(C32S+32R) in transition of *m/z* 412>191.

Results and Discussion

Among all standard analyzed, the evaluation of 2,6-dimetyl-pyridin-4-ol and its Py products indicated that

this compound when subjected to the thermal process produced new compounds, as shown in Fig. 1

Fig. 1 - ESI(-) FT-MS of 2,3-dimethyl-pyridin-4-ol with emphasis on the isotopic pattern (a) and Py (b).

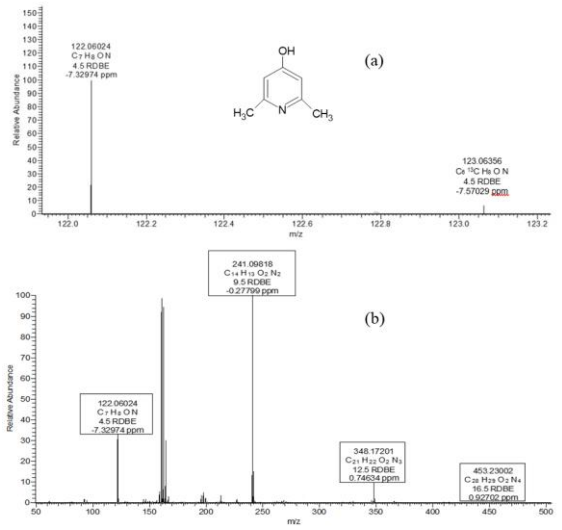

Thus, the presence of 2,3-dimethyl-pyridin-4-ol and its first pyrolysis product were verified in the oil samples. Thus, the MS ratio was calculated according to equation (1) and correlated with the calculated GC/MS ratios for the four oils, getting R^2 close to 1, as shown in Fig. 2.

MS Ratio = (Abundance of 2,3-dimetil-piridinol-4)/(Abundance of its first product of Py) **(eq. 1)**

Fig. 2 - Graphs of linear correlation between MS Ratio and Ts/Tm (a), Ts/(Ts+Tm) (b), C32S/(H32S+H32R) (c)

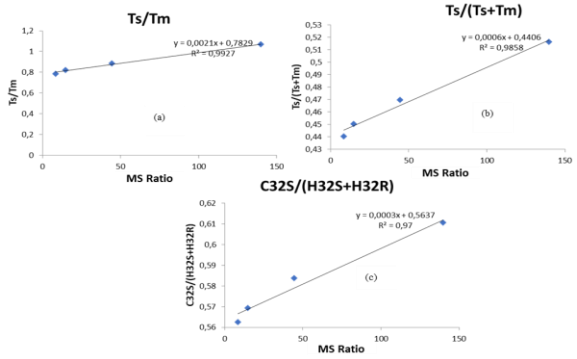

. The analysis of the pyrolysis of the potential biomarker at 200 ºC (temperature close to the catagenesis) led to a greater abundance of the original pattern compared to pyrolysis product, so that it was deduced that the MS ratio increases with thermal evolution. Thus, the same decreasing order of thermal evolution: A>P>C>S, as shown in Table 1, for both the techniques.

Tab. 1 – Results of MS Ratios and diagnostic ratios of biomarkers Ts/Tm, Ts/(Ts+Tm), C32S/(C32S+32R)

Diagnostic Ratio	Crude oil			
	A	P	C	S
MS Ratio	139.77	44.44	14.84	8.51
Ts/Tm	1.07	0.89	0.82	0.79
Ts/(Ts+Tm)	0.52	0.47	0.45	0.44
C32S/(C32S+32R)	0.61	0.59	0.58	0.56

Conclusions

2,3-dimethylpyridin-4-ol is an able candidate to thermal evolution biomarker by ESI-FT-MS, whose Eq.1 got linear correlations with ratios obtained by GC/MS.

Acknowledgements

CLQM/UFS, LABMAQ, LAMTESA/UFRPE, LaCEM/UFG.

References

[1] Triggia, A. A; Correia, C.A.; Veroti Filho, C. ; Xavier, J. A. D.; Machado, J. C. V.; Thomas, J. E.; De Souza Filho, J. E. ; De Paula, J. L.; De Rossi, N. C. M.; Pitombo, N. E. S.; Gouvea, P. C. V. de M.; Carvalho, R. de S.; Barragan, R. V. Fundamentos de Engenharia de Petróleo. Rio de Janeiro: Interciência, 2001.

[2] Peters, K. E.; Walters, C. C.; Moldovan, J. M. 2005. The biomarker guide – biomarkers and isotopes in petroleum exploration and earth history. New York: Cambridge University Press.

[3] Santos, J. M.; Santos, F. M. L.; Eberlin, M. N.; Wisniewski, A, 2017. Advanced Aspects of Crude Oils Correlating Data of Classical Biomarkers and Mass Spectrometry Petroleomics. Energy & Fuels, [s.l.], v. 31, n. 2, p. 1208–1217.

[4] Pudenzi, M. A.; Eberlin, M. N. 2016. Assessing Relative Electrospray Ionization, Atmospheric Pressure Photoionization, Atmospheric Pressure Chemical Ionization, and Atmospheric Pressure Photo- and Chemical Ionization Efficiencies in Mass Spectrometry Petroleomic Analysis via Pools and Pairs. Energy & Fuels, [*s.l.*], v. 30, n. 9, p. 7125–7133.

[5] Maciel, S. T. A.; Wisniewski, A.; De Souza, M. J. B, 2015. Use of micropyrolysis and TG to study the thermal catalytic conversion of onshore crude oil using the zeolite catalysts type Y and ferrierite. Journal of Thermal Analysis and Calorimetry, [*s.l.*], v. 122, n. 1, p. 369–377.

[6] Carregosa, J. C.; Santos, I. R., Sá, M. S., Santos, J. M., & Wisniewski Jr, A., 2021. Multiple reaction monitoring tool applied in the geochemical investigation of a mysterious oil spill in northeast Brazil. Anais da Academia Brasileira de Ciências, v. 93.

XVI LATIN AMERICAN CONGRESS ON ORGANIC GEOCHEMISTRY
9 - 11 AUGUST, 2023
ARACAJU, SERGIPE, BRAZIL

Application of fast GC×GC-TOFMS for the investigation of biomarkers from the Devonian sequence of the Parnaíba Basin, NE Brazil

Vinícius B. Pereira [a*], Vitor Hugo S. Góes [a], Raquel V. S. Silva [a], Helio J. P. S. Ribeiro [b], Georgiana F. da Cruz [b], Débora A. Azevedo [a]

[a] Federal University of Rio de Janeiro, Brazil; [b] Fluminense State University, Brazil; [c] Federal University of Ceará, Brazil; [d] Federal University of Espírito Santo, Brazil

viniciuspereira@iq.ufrj.br

Introduction

Comprehensive two-dimensional gas chromatography (GC×GC) has been extensively applied in geochemical evaluation of sedimentary organic matter. While it has promoted a more detailed evaluation and improved the discrimination of molecular biomarkers (Casilli et al., 2014), the methods usually take long times and require long processing. The advent of the application of faster and more efficient methods have recently allowed the identification and separation of multiple compounds with suitable resolution (Schena et al., 2020), but application of fast-GC×GC in geological samples has not been assessed. Due to the matrix complexity and the presence of multiple stereoisomers with varying concentration, evaluation of fast-GC×GC methods for geochemical assessments must be carefully conducted.

This work describes the application of GC×GC employing concepts of fast chromatography for the separation of aliphatic biomarkers present in extracts from the Pimenteiras Formation (Devonian) in the Parnaíba Basin (NE Brazil).

Experimental

The extracts of outcrops from Pimenteiras Formation (Devonian) were obtained by ultrasonic extraction. After elementary sulfur removal, extracts were fractionated into aliphatic and aromatic hydrocarbons, and polar compounds.

The aliphatic fraction was then analyzed by GC×GC-TOFMS (Leco Corporation, USA) using a RTX-5 (10 m × 0.20 mm, 0.18 µm) as primary column, and a DB-17HT (1.0 m × 0.25 mm, 0.15 µm) as secondary column. Methods were adjusted to obtain suitable separation of biomarkers, with final time at 30 minutes.

Results and Discussion

First, a performance evaluation of the method was assessed with authentic standards of multiple biomarkers. Low relative standard deviation (RDS <10%), and a good determination coefficient (r^2 >0.9) were obtained in the 1-20 µg mL^{-1} range.

The evaluation of organic extracts from Pimenteiras Formation show typical characteristics of immature organic matter, with multiple unsaturated biomarkers, including the hopenes, sterenes, and tri- and tetracyclic terpenes, along with high amounts of moretanes and ββ-hopanes. In addition to unusual biomarkers 3-methyl, and 3-ethyl-steranes, des-A-diasterenes, 2α-methyl-hopanes, methyl-diasterenes, and C16-C18 diterpanes commonly associated with terrestrial input, were found for the first time in extracts from the Pimenteiras Formation.

Fig 1. shows the extracted ion chromatograms obtained by fast-GC×GC-TOFMS showcasing hopanoids (*m/z* 191), and steroids (*m/z* 217).

The majority of the compounds were efficiently separated by the chromatographic conditions applied. Hopanoids and steroid compounds presented multiple isomers, with saturated and unsaturated moieties. Therefore, these families were applied to evaluate chromatographic parameters, such as resolution, selectivity and efficiency of the proposed method. Results in Table 1 show that most pairs presented suitable separation with Rs >1.5 and α ~ 1.5. Pairs with Rs > 1.0 presented separation higher than 80% in the first dimension, thus not hindering a reliable identification and geochemical assessment of the peaks. Besides that, a peak purity evaluation was performed, and the maximum peak overlap obtained for selected compounds was of 5%, which would not greatly affect the application of geochemical proxies .

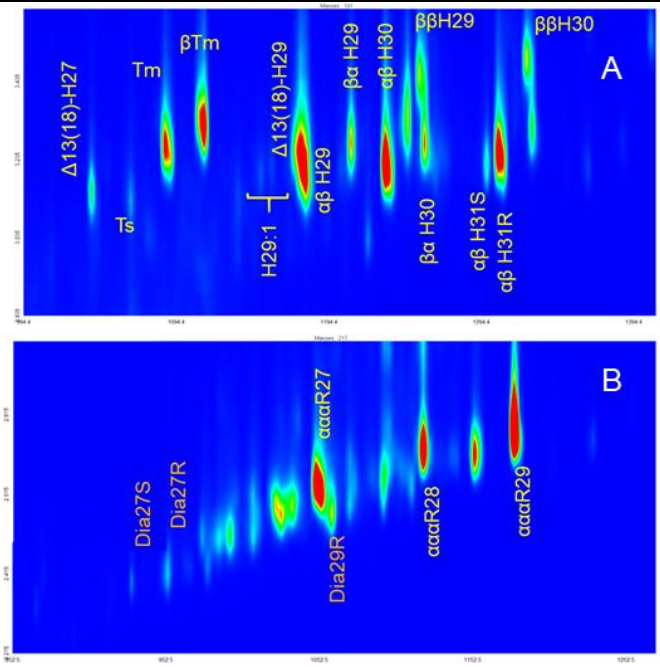

Figure 1. Extracted ion chromatograms (EIC) of (a) *m/z* 191 and (b) *m/z* 217

Table 1. Chromatographic parameters, relative retention index (RRI) and separation efficiency (%) for selected pairs of sterenes and hopenes present in extracts from the Paranaíba Basin

Compound	RRI	GC×GC Rs	GC×GC α	Separation (%)	
H29:1a	29.770	1.5	1.5	>99.7	**
H29:1b	29.879				
ββH29	31.198	0.9	1.5	87	63
βαH30	31.225				
ββH30	31.770	1.1	1.5	87	89
βαH31	31.768				
(14)C29:1	28.036	0.8	1.4	87	45
DiaC29R	28.089				
C27R	28.301	2.2	1.4	>99.7	**
Dia29S	28.457				
Unknown H29	31.141	1.5	1.4	>99.7	**
ββH29	31.198				
13(18)-H29	30.169	0.8	1.4	87	45
αβH29	30.227				

* compounds which coeluted in the first dimension;
** compounds fully separate in first dimension

Efficiency was calculated for a total 59 compounds with hopanoid skeleton, and 70 compounds presenting steroid moieties. Average height equivalent of a theoretical plate (HETP) obtained for hopanoids was $1.6x10^{-5}$, and $2.1x10^{-5}$ for steroids (Fig. 2). These values indicate a high peak capacity obtained for this method. We also observed that, in general, HETP was inversely proportional to retention time, and compounds with higher molecular weights presented higher efficiency.

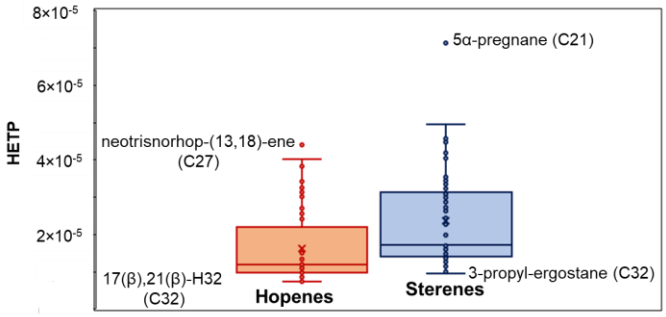

Fig 2. Efficiency evaluation of hopenes and sterenes, showing low HETP values for biomarker assessments.

Conclusions

The proposed 30 minutes faster GC×GC-TOFMS method applied in this study to a complex geochemical extract sample allowed the separationof multiple biomarker isomers and families, with adequate sensitivity and robustness. A suitable resolution and selectivity was obtained for most compounds. The low maturity of the extracts revealed a great number of unsaturated compounds, which were separated from their saturated counterparts, not hindering geochemical assessments.

Acknowledgements

The authors thank Capes, CNPq and FAPERJ for fellowships and financial support.

References

Casilli, A., Silva, R.C., Laakia, J., Oliveira, C.J.F., Ferreira, A.A., Loureiro, M.R.B., Azevedo, D.A., Aquino Neto, F.R. 2014. High resolution molecular organic geochemistry assessment of Brazilian lacustrine crude oils. Organic Geochemsitry 698, 61-70.

Schena, T., Bjerk, T.R., von Muhlen, C., Caramão, E.B. 2020. Influence of acquisition rate on performance of fast comprehensive two-dimensional gas chromatography coupled with time-of-flight mass spectrometry for coconut fiber bio-oil characterization. Talanta, 121186.

XVI LATIN AMERICAN CONGRESS ON ORGANIC GEOCHEMISTRY
9 - 11 AUGUST, 2023
ARACAJU, SERGIPE, BRAZIL

Performance of a high resolution, multi-collector, noble gas mass spectrometer Helix MC Plus installed at the São Paulo State University (UNESP-Brazil)

Hurtado,[a.b]* G. R.; Siqueira Ribeiro,[c*] M. C.; Sulato,[c] E. T.; Santos Neto,[d] E. V.; Luvizotto,[b,c] G. L.; Ferreira,[e,] A. A.; Morais,[e] E. T.; Lopes,[e] J. P.; Souza,[e] I. V. A. F.; Vieira,[e] A. J. M.

[a] São Paulo State University (Unesp), Institute of Science and Technology, São José dos Campos (SP), Brazil

[b] São Paulo State University (Unesp), Institute of Advanced Studies of the Sea, Rio Claro (SP), Brazil

[c] São Paulo State University (Unesp), Institute of Geosciences and Exact Sciences, Rio Claro (SP), Brazil

[d] Senior Advisor, Rio de Janeiro (RJ), Brazil

[e] Petrobrás - CENPES, Rio de Janeiro (RJ), Brazil

*correspondência: gabriela.hurtado@unesp.br / carina.siqueira@unesp.br

Introduction

The noble gas isotopic analysis laboratory was commissioned in 2022 and is part one of the research center of the Institute for Advanced Studies of the Sea "Professor Peter Christian Hackspacher". The main focus of the laboratory is to characterize geochemically natural gas samples focusing on noble gas. It is equipped with a Helix MC Plus Mass Spectrometer that is installed at the São Paulo State University (Unesp), Rio Claro (SP) (Brazil). Noble gas geochemical analyses is a useful technique to constrain physical behavior of hydrocarbon systems. This can be used to better characterize the subsurface fluid dynamics, such as processes during hydrocarbon generation, migration, and accumulation, oil/gas-water interactions, and residence time of fluids [1]. In order to report the performance of the laboratory, we present isotopic ratio data on atmospheric air and the Helium Standard Japan (HESJ).

This Thermo Fisher Scientific Helix MC Plus Noble Gas Mass Spectrometer is a 350 mm sector, 120° extended geometry, high resolution, multicollector mass spectrometer for the simultaneous acquisition of noble gas isotopic data, which provides substantial benefits in analytical precision and shortens the time of analysis. The detector array includes a fixed axial (Ax) detector, two adjustable high mass (H1 and H2) detectors, and two adjustable low mass (L1 and L2) detectors. Each detector is equipped with a Faraday/ion counting multiplier CFM (Combined Faraday and CDD (Compact Discrete Diode) Multiplier) collector.

Experimental

The Helix MC Plus Noble Gas Mass Spectrometer at the UNESP is equipped with an on-line noble gas extraction and purification system that operates at ultrahigh vacuum conditions with a base pressure better than 10E-09mbar. The gas handling system consists of a) two a gas purification system with SAES NP10, SAES C50, Ti bulk getters, standard gas pipette tanks, Nupro pneumatic valves, b) a Janis He cryogenic trap assembly (10 to 475 K), c) a quadrupole gas analyzer and d) a Photon-Machines Fusion 970 diode laser heating system. The system is controlled using Qtegra software platform of Thermo Fisher Scientific, which controls both the mass spectrometer and auxiliary devices.

An Air Gas standard and the HESJ helium standard [2] were analyzed in this work. The Air Gas standard was prepared in the noble gas laboratory at UNESP from a clean air sample collected at the site. One aliquot of the Air Gas standard contains 3.97×10^{-8} cc STP of ^{40}Ar and 7.02×10^{-11} cc STP of ^{20}Ne with atmospheric noble gas abundances. One aliquot of the HESJ helium standard delivers 6.87×10^{-8} cc STP of ^{4}He isotope. For He measurements, a full shot of the HESJ standard was used. For Ne measurements, 40 shots of the air standard were used, with LN_2 charcoal traps or the Janis cryogenic trap running to adsorb the heavier noble gases and other gases such as CO_2 and water.

Results and Discussion

The combination of different detectors (Faraday and Ion Counting multipliers), mass resolution, mass offset and integration time were used to improve the signal of the noble gas isotopes measured.

Our results of reproducibility of Ar and Ne ratios in the air standard are agree with the literature data (Table-1). To calculate the isotopic ratios, 10 measurements were made with 5 cycles of repetitions. The results are listed below.

Isotopic ratio	Value obtained (cc STP)	Isotopic ratio [3]
$^{36}Ar/^{40}Ar$	0.003403±0.08	0.003379
$^{38}Ar/^{40}Ar$	0.000657±0.26	0.000635
$^{38}Ar/^{36}Ar$	0.193207±0.29	0.188
$^{40}Ar/^{36}Ar$	293.8±0.08	295.989
$^{21}Ne/^{20}Ne$	0.002847±2.0	0.003
$^{22}Ne/^{20}Ne$	0.095659±2.0	0.10233
$^{21}Ne/^{22}Ne$	0.029917±2.0	0.02984
$^{20}Ne/^{22}Ne$	10.48±2.1	9.782

The $^{3}He/^{4}He$ ratio results from HESJ standard are listed in the Table 2.

$^{3}He/^{4}He$ (cc STP)	$^{3}He/^{4}He$ (R/Ra)
2.95E-05	21.81
2.76E-05	20.63
Average=2.86E-05	Average=21.22

The HESJ standard measurements show a slight R/Ra variation circa of the 2,8% compared to the value R/Ra (20.63) presented by Matsuda [2]. To monitor this variation, further measurements are routinely performed during the noble gas analysis.

Conclusions

Isotopic ratio data obtained for Ar, Ne and He the new noble gas laboratory UNESP are in well agreement with published values. Therefore, with the current setup, the laboratory can run state-of-the art analyses that can be used to investigate genetic and post-genetic processes occurring in petroleum systems, as well as, the fate of fluids in sedimentary basins. Such analyses will improve our understanding of noble gases showing how they can be used as tracers in the subsurface environment, providing a valuable geochemical results for the exploration and production of petroleum.

Acknowledgements

The authors thank Petrobras S/A to financial support to projects numbers SAP 4600661515 and SAP 4600544881, PROPe-UNESP and UNESPetro.

References

[1] Li, Y., Cao, C., Huang, H. 2022. The use of noble gas to constrain subsurface fluid dynamics in the hydrocarbon system. Frontiers in Earth Science 10, 1-12.
[2] Matsuda, J., Matsumoto, T., Sumino, H., Nagao, K., Yamamoto, J., Miura, Y., Kaneoka, I., Takahata, N., Sano, Y. 2002. The 3 He/ 4 He ratio of the new internal He Standard of Japan (HESJ). Geochemical Journal 36, 191-195.
[3] Sano, Y., Marty, B., Burnard, P., 2013. Noble gas in the atmosphere. In: Burnard, P. P. Burnard (Ed.), The Noble Gas as Geochemical Tracers, Advances in Isotope Geochemistry. Springer-Verlag Berlin-
Heidelberg, pp.17-31.

XVI LATIN AMERICAN CONGRESS ON ORGANIC GEOCHEMISTRY
9 - 11 AUGUST, 2023
ARACAJU, SERGIPE, BRAZIL

OPTIMIZATION AND CERTIFICATION OF THE QUECHERS METHOD FOR THE DETERMINATION OF PAHS AND ALKYLATED PAHS AND THEIR ASSOCIATED RISKS IN MARINE ORGANISMS FROM OILED AREAS

RIVELINO M. CAVALCANTE[a,b], MARILIA G.G. MENEZES[a], BEATRIZ D. LOPES[a], GABRIELLE M. FERNANDES[a].

[a] Organic Contaminant Assessment Laboratory (LACOr), Institute of Marine Sciences (LABOMAR), Federal University of Ceará (UFC);
[b] Environmental and Petroleum Chromatography Center (CECAMP/LABOMAR/UFC).

rivelino@ufc.br

Introduction

Studies have shown that some PAHs are genotoxic and carcinogenic (Jameson, 2019). According to the Scientific Committee of Food (SCF) of the 33 PAHs evaluated, 15 of them show evidence of genotoxicity, and of these, 14 show carcinogenic effects in experimental animals (SCF, 2002).

In this sense, the study was motivated due from 2019 to 2022, the northeast region was the target of 3 mysterious oil spills with volumes ranging from 5,000 to 12,000 tons (Azevedo et al., 2022; Reddy et al., 2022). Despite being considered one of the largest hazards in South America and tropical regions, few studies have been carried out to investigate the degree of impact on marine life as well as the risks to organisms and food safety. Therefore, in addition to the oil accident on the Brazilian coast, and also because oil impacts take decades, and some PAHs are highly deleterious to living organisms, the objective of the present study was to optimize and certify a method that offers a rapid response from levels of PAHs in a large volume of samples of marine organism samples.

Experimental

The study was developed in three stages. First, the best conditions of the instrumental method and the sample preparation method were validated by checking the analytical figures of merit, such as recovery tests and participation in Quality Assurance of Information for Marine Environmental Monitoring in Europe) laboratory proficiency (QUASIMEME, 2020). The certification and accreditation exercise consists of analyzing, using the developed or optimized analytical method, a standard sample of biota with a concentration unknown to the participants. Thus, the laboratory received four samples from the QUASIMEME proficiency study (samples code: QPH101BT to QPH104BT, Round 1 and 2, March–June 2021; Exercise 2021, BT4) and after collecting the results, QUASIMEME reports the bias and Z-scores for each participating laboratory, allowing the verification of the analytical efficiency as well as the accuracy of the method used in the analyses.

Secondly, for the determination of PAHs and alkylated PAHs, the best conditions of the method were used for analysis in fish captured in areas that received oil and transported to the laboratory at low temperature. Sample preparation followed an optimized and certified QuEChERS methodology (Anastassiades et al., 2003). Briefly, a mass of 5 grams of samples was added to 10 mL of Acetonitrile and stirred for 2 minutes. After, 4 grams of Magnesium Sulfate ($MgSO_4$) and 1 gram of Sodium Acetate were added to the analysis tube and stirred for 2 minutes and then centrifuged for 8 minutes at 2000 rpm. Extract purification was carried out in a 10 ml glass tube containing 150 mg of $MgSO_4$ and 150 mg of PSA. The total volume of clean extract was transferred to a vial, stored at -4°C for later analysis by gas chromatography (Fig. 1). The analysis of PAHs was performed on a GC/MS/MS^n Ion Trap instrument from Thermo Electronic Corporation using an Agilent J&W DB-5 capillary chromatography column (30 m x 0.25 mm x 0.25 µm).

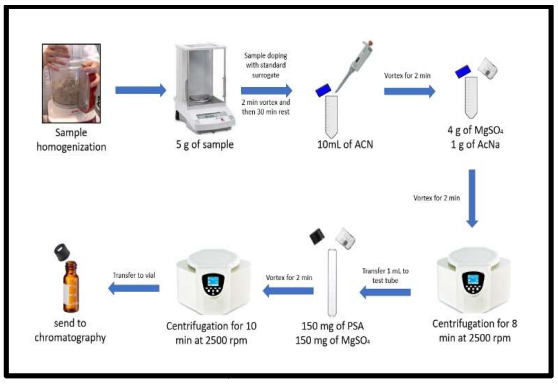

Figure 1. Steps of the QuEChERS method

To establish the safety of fish consumption following the oil spill in the Northeast region of Brazil were used the standard risk assessment methods for carcinogenic PAHs technical note (NT27/2019/SEI/GGALI/DIRE2/ANVISA) published by the National Health Surveillance Agency.

Results and Discussion

The optimized and certified QuChERS method proved to be easy to apply and able to prepare 20 samples for 8 hours with two people performing the respective sample preparation. A summary of all evaluated Z-scores is plotted in Figure 1, as can be observed on the basis of QUASIMEME Z-score quality requirements, more than 53% of the data of PAHs and alkylated PAHs were satisfactory (|Z|<2), 10% are questionable (2<|Z|<3) and about 32% are unsatisfactory (|Z|>3). However, when only parent PAHs are considered, more than 80% were satisfactory (|Z|<2) and the rest considered between questionable (13.7%) and unsatisfactory (6.5%). Another important fact, most methodologies in biological matrices are not efficient for the light PAHs, which were not observed using the developed protocol.

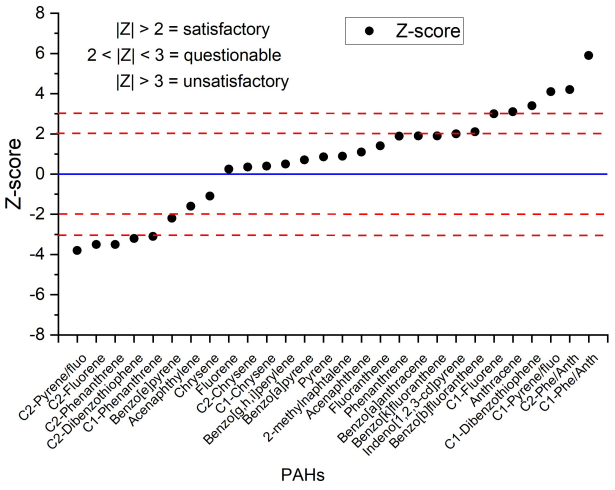

Figure 1. Z-scores for PAHs and alkylated PAHs in standard sample of biota

According to Gluschke (2006), |Z|<2 greater than 60% of parent PAHs is acceptable. And as for the low Z-score of the alkylated PAHs, this is probably due to the fact that they are quantified based on the calibration curves of their parent PAHs, since there are no analytical standards.

A total of 130 organisms: 110 mollusks, 50 crustaceans and 16 fish (gills, liver and muscle) were analyzed for PAHs concentrations in areas where oil was recorded in 2019. The overall mean sum of the 18 PAHs analyzed was 286.15 ± 742.20 ngg^{-1}, with a minimum of 3.21 ngg^{-1} and a maximum of 3960.04 ngg^{-1} and alkylated PAHs were not detected. In general, $\sum_{18HPAs}$ concentration levels were higher in sawfish, in the liver and gill organs. Regarding the levels of Σ_{18HPAs} in these tissues in sawfish and red snapper, the values between liver and gills are similar and higher than the values in muscle (gills~liver > muscle), this result is similar to that found by other studies with fish (Melo et al., 2022).

Regarding the human health risk assessment, non-carcinogenic PAHs were considered below the level of concern established by ANVISA in all analyzed organisms. However, when considering carcinogenic PAHs, despite the levels found in fish muscles being below the recommended level of concern (18 ngg^{-1} TEQBaP), the concentration levels in 6 samples of crustaceans and mollusks were above the limit (6 ngg^{-1} TEQBaP) ranging from 7.23 to 35 ngg^{-1}.

Conclusions

The optimized and certified method had an excellent analytical efficiency for the parent PAHs. Although there is still no consensus regarding the risk posed by alkylated PAHs, the analytical efficiency was considerable, demonstrating that efforts to improve analyzes must undergo advances.

The risk to marine biota and human health were low, but monitoring must be carried out effectively for years to check for changes in levels, ensuring ecological balance and food security in an area that received a significant amount of oil.

Acknowledgements

The authors thank PQ-2 Grant (315281/2020-0-CNPq), INCT-AmbTropic phase II (CNPq Process 465634/2014-1), and project “Dispersants and adsorbents for remediation of coastal areas affected by crude oil spills (Coast of Ceará, Northeast Brazil)” (440868/2020–3), both linked to MCTI Emergency Action to Combat the Oil Spill (2020), as well as Lemae/Finep/CNPq (380975/2022–0).

References

Anastassiades, M.; Lehotay, S. J.; Stajnbaher, D.; Schenck, F.J. Fast and easy multiresidue method employing acetonitrile extraction/partitioning and dispersive solid-phase extraction for the determination of pesticide residues in produce, *Journal of AOAC International*, vol. 86, no. 2, pp. 412–431, 2003.

Azevedo, R.A., Bezerra, K.M.M., Nascimento, R.F., Nelson, R.K., Reddy, C.M., Nascimento, A.P., Oliveira, A.H.B., Martins, L.L., Cavalcante, R.M. (2022). Is there a similarity between the 2019 and 2022 oil spills that occurred on the coast of Ceará (Northeast Brazil)? An analysis based on forensic environmental geochemistry. Environ. Pollut. 315, 120283. https://doi.org/10.1016/j.envpol.2022.120283

Gluschke, M. QUASIMEME results of laboratories involved in the German Marine Monitoring Programme for the North and Baltic Seas. Accred Qual Assur (2006) 11: 470–473. DOI 10.1007/s00769-006-0155-3.

Melo, A.P.Z., Hoff, R.B., Molognoni, L. *et al.* Determination of Polycyclic Aromatic Hydrocarbons in Seafood by PLE-LC-APCI-MS/MS and Preliminary Risk Assessment of the Northeast Brazil Oil Spill. *Food Anal. Methods* 15, 1826–1842 (2022). https://doi.org/10.1007/s12161-022-02252-z

QUASIMEME, 2021. QUASIMEME Laboratory Performance Studies, 34. BT-4 exercise 588. Polyaromatic Hydrocarbons in Biota (https://www.wepal.nl/en/wepal.htm).

Reddy, C.M., Nelson, R.K., Hanke, U.M., Cui, X., Summons, R.E., Valentine, D.L., Rodgers, R.P., Chacon-Patino, M.L., Niles, S.F., Teixeira, C.E.P., Bezerra, L.E.A., Cavalcante, R.M., Soares, M.O., Oliveira, A.H.B., White, H.K., Swarthout, R.F., Lemkau, K.L., Radovíc, J.R. (2022). Synergy of Analytical Approaches Enables a Robust Assessment of the Brazil Mystery Oil Spill. Energy Fuel. https://doi.org/10.1021/acs.energyfuels.2c00656

SCF (2002). Opinion of the scientific committee on food on the risks to human health of polycyclic aromatic hydrocarbons in food expressed on 4. December 2002. SCF/CS/CNTM/PAH/29/final. Brussels (Belgium).

XVI LATIN AMERICAN CONGRESS ON ORGANIC GEOCHEMISTRY
9 - 11 AUGUST, 2023
ARACAJU, SERGIPE, BRAZIL

GC-MS/MS applied for the identification of novel diaromatic compounds

BRUNO QUIRINO ARAÚJO [*a] ARKELLAU KENNED SILVA MOURA [b]; VINÍCIUS BARRETO PEREIRA [c]; DÉBORA DE ALMEIDA AZEVEDO [c], ANTÔNIA MARIA DAS GRAÇAS LOPES CITÓ [b]

[a] **Universidade Federal do Espírito Santo, Departamento de Química, NCQP - LABPETRO, Vitória, Espírito Santo, ES, 29075-910, Brazil**

[b] **Universidade Federal do Piauí, Campus Universitário Ministro Petrônio Portela, CCN, LAGO, Teresina, PI, 64049-550, Brazil**

[c] **Universidade Federal do Rio de Janeiro, Instituto de Química, LAGOA - LADETEC, Ilha do Fundão, Rio de Janeiro, RJ, 21941-598, Brazil**

* bquirinoa@gmail.com

Introduction

α,ω-bisaryl compounds (α,ω-BA) are homologous groups of aromatic hydrocarbons constituted by a linear alkyl chain with two alkyl-substituted or not, aromatic rings as end-groups that could be found in geological samples. Gorchs et al. (2003) tentatively identified based on GC–MS chromatogram and mass spectrum (EI, 70 eV), the C_{24} to C_{26} α,ω-diphenylalkanes, C_{25} to C_{27} α,ω-phenyl, toluyl-alkanes and C_{26} to C_{28} α,ω-phenyl, xylyl-alkanes in sulfur-rich coal (Cretaceous) from Maestrazgo Basin, Utrillas, Spain. Organic matter sources and the α,ω-BA geochemical significance are still unknown, although their occurrence has been related to marine organic matter, euxinia, and sulfur bacteria (Gorchs et al., 2003; Moura et al., 2019).
Recently, the advanced application of gas chromatography-tandem mass spectrometry (GC–MS/MS) and comprehensive two-dimensional gas chromatography-time-of-flight mass spectrometry (GC×GC–TOFMS) to petroleum aromatic fractions from Sergipe-Alagoas Basin Cretaceous crude oils, allowed beyond the identification of *n*-alkylaromatics hydrocarbons series, the attempt to tentatively identify α,ω-bis(aryl)alkanes series for the first time in both marine and lacustrine crude oils (Moura et al., 2019). In this context, GC−tandem MS (GC−MS/MS) was applied to identify the α,ω-BA diaromatic isomers in a crude oil samples (SEAL) from the Sergipe-Alagoas Basin, Brazil, using authentic standards.

Experimental

Aromatic fraction was separated from an aliquot of 100.0 mg of crude oil using liquid chromatography on silica gel (3.0 g;, 48 h dichloromethane Soxhlet extracted and activated at 120 °C/12 h; 0.063−0.200 mm, Merck, Darmstadt, Germany), and eluted with 10 mL *n*-hexane, 10 mL *n*-hexane/CH_2Cl_2 (8:2, v/v), and 10 mL CH_2Cl_2/MeOH (9:1, v/v) to yield saturated hydrocarbon (F(sat), 84,34 mg), aromatic hydrocarbon (F(aro), 6,94 mg), and polar compound (NSO, 6,08 mg) fractions, respectively. For the GC-MS/MS analysis, aromatic hydrocarbon fraction was dissolved in 500 µL of dichloromethane perdeuterated pyrene (C16D10) solution (5.9 ng µL-1, 98% D; CDN Isotopes). Chromatographic grade solvents were used in all geochemical preparation procedures (Tedia, Rio de Janeiro, RJ, Brazil).

The aromatic fraction was analyzed using a GC−MS/MS Agilent Technologies system, GC (7890A) equipped with an autosampler (AS7963) and a quadrupole/hexapole/quadrupole (QqQ 7000C) analyzer tandem mass spectrometer (MS/MS). The Agilent J&W HP-5MS column (5% phenyl – 95% methylpolysiloxane phase, 30 m, 0.25 mm i.d., 0.25 µm df). An aliquot of 1 µL of the sample was injected in pulsed splitless mode (40 psi pulsed by 30 s), the temperature of the injector was 310 °C, the temperature of the interface at 290 °C, and the time of purge was 3 min. The oven temperature program was 70 °C to 250 °C at 3 °C/min and then to 340 °C at 20 °C/min. Helium (99.9999%, White Martins) was the carrier gas used at a 1.5 mL/min constant flow. The mass spectrometer operated in multiple reaction-monitoring (MRM) mode with the ion-source temperature at 230 °C, EI at 15 eV, and solvent delay time of 5 min. The gases used in the collision cell were nitrogen as collision gas (1.5 mL/min) and helium as quenching gas (2.25 mL/min).

Analysis was performed by the MRM mode with the acquisition of chromatograms from precursor ion (molecular ion, M+•) → product ion transitions. MS/MS conditions in the MRM mode were: scan time 50 ms, a mass range of m/z 0.02, peak width in quadrupole 1 (Q1,

full width at half-maximum) of 0.7, collision energy of 15 eV.

Data treatment and MRM chromatograms acquisition were done in MassHunter Workstation Qualitative Analysis software (B.06.00, Agilent Technologies).

Results and Discussion

α,ω-BA series were identified based on authentic standards retention time; MS (EI, 70 eV) information such as F(aro) sample peaks mass spectra comparison diagnostic fragments at m/z 91/92, 105/106 and molecular ion (DBE = 8 for diaromatic compounds); GC-MS/MS selected monitoring reaction chromatograms (MRM: 224 → 92; 238 → 106 (Figure 1); 252 → 106); and authentic standards coinjection chromatographic analysis.

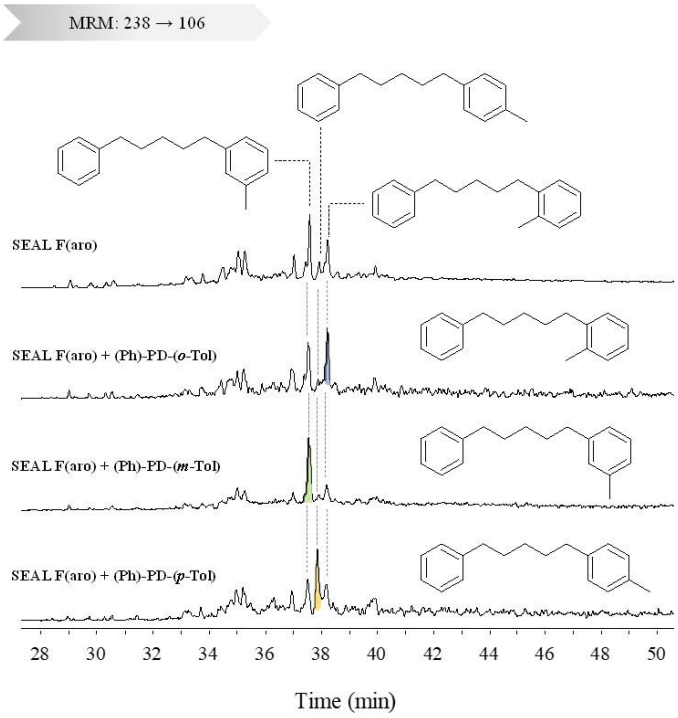

Figure 1. Spiked and non-spiked MRM 238 → 106 chromatograms of C_{19} α,ω-BA isomers for SEAL F(aro)

Despite that, analytes in the sample showed the same coeluting retention times of α,ω-BA standards. The coinjection experiments caused the corresponding peak areas of the analytes to increase 2 to 11 times, and fortunately allowed their identification in the SEAL oil sample.

Conclusions

GC−MS/MS target analysis and 10 synthetic authentic standards of α,ω-BA C_5-n-alkyl-chain isomers, allowed the unequivocal identification and assessment of α,ω-bis(aryl)alkanes series in the aromatic fraction of a lacustrine crude oil from Sergipe-Alagoas Basin. The mass spectra could not clearly differentiate isomers, despite some differences in the intensity of the fragments that could be helpful in isomers discrimination. The elution order of C_5-*n*-alkyl-chain α,ω-BA was established based on standards hydrocarbon profiles.

Acknowledgements

The authors thank CNPq (Brazilian research council), CAPES, FAPERJ and FAPES for fellowships and financial support.

References

Gorchs, R.; Olivella, M. a.; De Las Heras, F. X. C., 2003. New aromatic biomarkers in sulfur-rich coal. Organic Geochemistry **34**, 1627-1633..

Moura, A. K. S.; Ribeiro, D. O.; Do Carmo, I. S.; Araújo, B. Q.; Pereira, V. B.; Azevedo, D. A.; Citó, A. M. G. L., 2019. An Assay on Alkyl Aromatic Hydrocarbons: Unexpected Group-Type Separation of Diaromatic Hydrocarbons in Cretaceous Crude Oils from Brazilian Marginal Basin. Energy and Fuels **33**. doi:10.1021/acs.energyfuels.8b03268López,

ALH

DATA MINING & ARTIFICAL INTELIGENCE

IDENTIFICATION OF CHEMICALLY DISTINCT CRUDE OIL PROFILES FROM THE SERGIPE-ALAGOAS BASIN USING MULTIPLEX NETWORKS AND ESI(±) FT-ICR MS DATA FUSION

PEDRO G. C. LUCENA[a]*, JHONATTAS C. CARREGOSA[b], MARCOS N. EBERLIN[c], ALBERTO WISNIEWSKI JR[b], JANDYSON M. SANTOS[a]

[a]Grupo de Pesquisa em Petróleo, Energia e Espectrometria de Massas (PEM), Departamento de Química, Universidade Federal Rural de Pernambuco (UFRPE), Recife, PE, 52171-900, Brasil

[b]Grupo de Pesquisa em Petróleo e Energia da Biomassa (PEB), Departamento de Química, Universidade Federal de Sergipe (UFS), São Cristóvão, SE, 49100-000, Brasil

[c]Universidade Presbiteriana Mackenzie, São Paulo, SP, 01222010, Brasil

*e-mail: pedro.lucena@ufrpe.br

Introduction

Polar components such as asphaltenes and resins play a crucial role in crude oil physical-chemistry properties, such as wetting, corrosion, and emulsion stability (Covas et al., 2020). Thus, it is fundamental to associate molecular information with bulk oil properties for better understanding and predicting the properties of crude oils (França et al., 2021). In this scenario, the use of ultra-high-resolution technique such as Fourier-transform ion cyclotron resonance mass spectrometry (FT-ICR MS) provides a large amount of molecular information about polar species in oil analyses. However, due to the multiple ionization modes and enormous data acquisition, comparing samples and identifying cluster structures is a big challenge. To address this, a multiplex network approach was developed to unravel the cluster structure associated with SARA fractions of crude oils from the Sergipe-Alagoas basin based on FT-ICR MS data fusion for molecular composition obtained by electrospray ionization in both positive and negative modes - ESI(±), which is not readily available by conventional Hierarchical Clustering Analysis (HCA) when is used based on individual ionization modes.

Experimental

Fourteen crude oil samples from the Sergipe-Alagoas basin were studied. The fractions of saturates, aromatics, resins, and asphaltenes (SARA) were obtained using the method proposed by Vasquez and Mansoori (2000). In addition, polar compounds eluted with methanol after resins separation were also obtained. The analyses were performed by ESI(±) FT-ICR MS (LTQ FT Ultra mass spectrometer, Thermo Scientific, Bremen, Germany) of 7.2 T, and data acquisition was carried out over an *m/z* range of 200-1000 for ESI(-) and 200-1200 for ESI(+). To provide a suitable matrix for the multiplex network approach, first, the identified ions were filtered by intensity (>10% from the maximum intensity ion) and then binned at 0.01 Da. Subsequently, the Composite Score (Kellogg et al., 2020) and Manhattan distance were applied to each data matrix and were fused, providing a similarity matrix for each ESI acquisition mode. The similarity matrices were filtered using the modularity index, generating two adjacency matrices that were used to represent the multiplex network. On the other hand, we also evaluated the HCA processing using the individual ESI(+) and ESI(-) datasets with Ward clustering and Manhattan distance measurement methods. The chemometric analysis was carried out using R software (version 4.2.0).

Results and Discussion

Bulk oil composition had differences mainly in the resins, asphaltenes, and polar compounds fractions, which is demonstrated by the high coefficient of variation (CV) values of 32.4%, 43.3%, and 81.3%, respectively. The crude oils exhibited different similarities depending on the ionization mode, which led to the employment of a multiplex network approach to fuse the contrasting patterns and reveal new ones. This method is a mid-level data fusion model that was optimized using the

modularity parameter of the individual network from each ESI ionization mode. For the ESI(-) and ESI(+), the modularity values were 0.80 and 0.70, respectively. Figure 1 displays the filtered multiplex network, where the infomap algorithm identified five clusters based on molecular similarities of samples, revealing intra-cluster variability. It is evident that asphaltenes, resins, and polar compounds fractions better differentiated the clusters of oils.

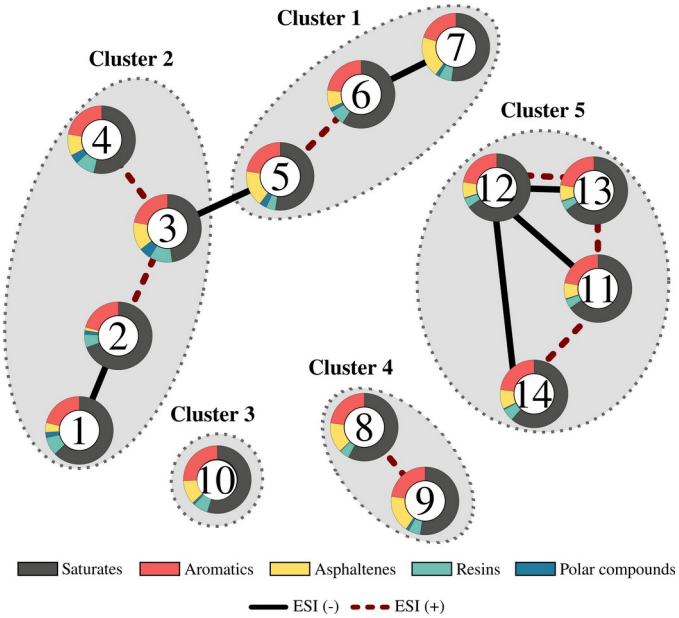

Figure 1. Filtered multiplex network of fourteen crude oil similarities, using 0.70 and 0.80 of modularity ESI(+) and ESI(-), respectively. The SARA was included for visual comparison of the clusters.

Figure 2 shows evidence of differences in the content of polar compounds and asphaltenes + resins among the clusters. Note that polar compounds played a crucial role in profile interpretation, with Clusters 1 and 2 having higher content when compared to the other clusters (>1.5%). Clusters 3, 4, and 5, had low polar compounds content (<1.5%). Additionally, Clusters 3 and 4 differed from Cluster 5 in terms of asphaltenes + resin content.
When we have applied the traditional HCA approach (data not displayed here), we have found a fragmented perception of the oil composition, and no trends associated with the SARA fractions were observed. These findings reinforce that the discovered patterns are effective for oil fingerprinting and guiding efforts and anticipating possible problems in exploration, production, and refining operations.

Conclusions

We proposed a mid-level data fusion based on a multiplex network and ESI(±) FT-ICR MS data fusion for enhanced identification of oil profiles. The method identified five profiles that are not readily observable using conventional HCA-based clustering methods. The profiles showed contrasting bulk and molecular composition. Thus, the proposed method is a supportive tool providing insights into the oil industry about its properties and potential uses.

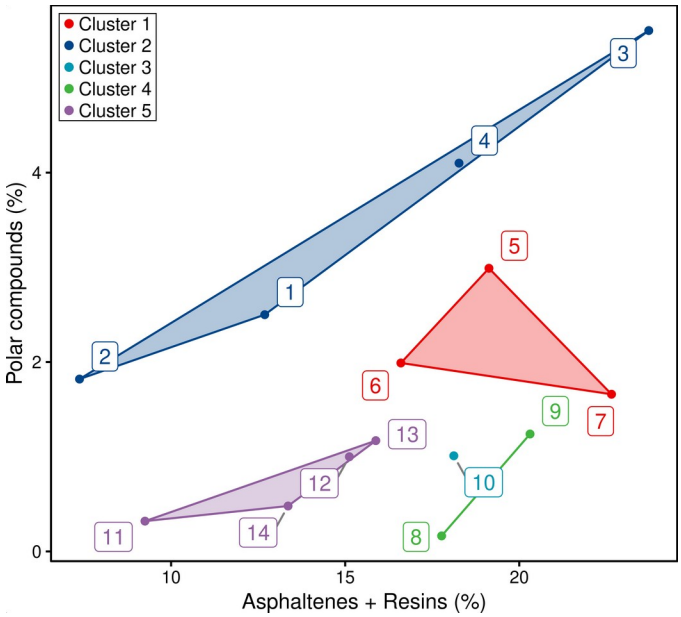

Figure 2. Discrimination of the clusters based on polar compounds and asphaltenes + resins classes for fourteen crude oils.

Acknowledgements

The authors thank CLQM/UFS, CNPq, FACEPE, CAPES, PRPG/UFRPE, PEM/UFRPE.

References

Covas, T.R., *et al*. Fuel 267, 117289, 2020.

França, D., et al. Fuel 293, 120474, 2021.

Kellogg, J.J., et al. Analytica Chimica Acta 1095, 38–47, 2020.

Vazquez, D., Mansoori, G.A., Journal of Petroleum Science and Engineering 26, 49–55, 2020.

XVI LATIN AMERICAN CONGRESS ON ORGANIC GEOCHEMISTRY
9 - 11 AUGUST, 2023
ARACAJU, SERGIPE, BRAZIL

Predictive Models to Distinguish Seepage Slicks from Oil Spills on Sea Surfaces employing SAR Sensors and Artificial Intelligence: Geometric Patterns Recognition under a Transfer Learning Approach

Fernando P. Miranda [a], Gil M. A. Silva [a], Ítalo O. Matias [b], Patrícia C. Genovez [b], Francisco F. A. Ponte [b], Sarah B. Torres [b], and Carlos H. Beisl [c]

[a] Petrobras Research, Development and Innovation Center (CENPES), Federal University of Rio de Janeiro, Av. Horácio Macedo 950, Cidade Universitária, Ilha do Fundão, Rio de Janeiro 21941-915, Brazil; [b] Software Engineering Laboratory (LES), Informatics Division, Pontifical Catholic University of Rio de Janeiro (PUC-Rio), R. Marquês de São Vicente, 225 - Gávea, Rio de Janeiro 22451-900, Brazil; [c] GeoSpatial Petroleum, R. Miguel de Farias, 92, Icaraí, Niterói, Rio de Janeiro 24220-002, Brazil.

e-mail: fmiranda@petrobras.com.br

Introduction

The development and application of predictive models to distinguish seepage slicks from oil spills are challenging, since Synthetic Aperture Radars (SAR) detect these events as dark spots on the sea surface (Brekke & Solberg, 2005; Alpers et al. 2017; Al-Ruzouq, 2020).

Traditional Machine Learning (ML) has been used to discriminate the Oil Slick Source (OSS) as natural or anthropic assuming that the samples employed to train and test the models in the source domain (D_S) follow the same statistical distribution of unknown samples to be predicted in the target domain (D_T) (Carvalho et al., 2018; Miranda et al., 2022; Matias et al., 2021; Genovez et al., 2023). When such assumptions are not held, Transfer Learning (TL) allows the extraction of knowledge from validated models and the prediction of new samples, thus improving performances even in scenarios never seen before (Daume & Marcu, 2006; Pan & Yang, 2009; Kouw & Loog, 2019).

The objective of this work is to disseminate the promising results achieved by Genovez et al. (2023) applying TL to discriminate the OSS considering samples detected in distinct geographic regions, using different satellites. To accomplish this, a huge and original database containing geometric patterns extracted from 6,279 oil slicks detected by multiple SAR sensors in the Gulf of Mexico (GoM) for 13 years was used as input. This rare and valuable dataset of labelled samples was field validated by PEMEX (Petróleos Mexicanos based on Ciudad del Carmen, Gulf of Mexico) and used to develop trustworthy and controlled predictive models for OSS identification in the GoM and its Mexican portion (GMex).

Innovatively, these well-trained models were applied to predict the OSS of unknown events in the GoM, the American (GAm) portion of the GoM, and in the Brazilian continental margin (BR).

Data Set and Methodology

Seven ML algorithms (Artificial Neural Network: ANN, Random Forest: RF, Gaussian Naive Bayes: GNB, Linear Discriminant Analysis: LDA, Support Vector Machine: SVM, Logistic Regression: LR, K Nearest Neighbour: KNN) were used to train and test predictive models in the D_S domain. The first one used 4,130 samples of seepage slicks and oil spills validated by Pemex in the GMex and detected by the RADARSAT-2 (RDS2) satellite. The second one compiled 6,279 samples of seepage slicks and oil spills detected in the GMex and GAm to train wider models over the entire GoM, employing RADARSAT-1 (RDS1) and RDS2 satellites.

The models were subsequently saved to transfer learning when predicting unknown oil slick samples in different D_T domains. Two TL methods were tested, Comon Data Shift (CDS) and Data Interpolation (DI). The performances achieved by all methods were compared to verify the transferability and generalization capacity of models to transfer-knowledge across different scenarios:

- **Study case 1 (GoM ⇥ GoM):** GoM models applied to predict the OSS of 698 new samples of seepage slicks and oil spills detected in the GoM. This scenario has similar domains ($D_S = D_T$) in terms of geographic regions (D_S ⇥ GoM; D_T ⇥ GoM) and satellites employed for detection (D_S ⇥ [RDS1, RDS2]; D_T ⇥ [RDS1, RDS2]);
- **Study case 2 (GMex ⇥ GAm):** GMex models applied to predict the OSS of 1,738 new samples of seepage slicks detected in the GAm. This scenario has different domains ($D_S \neq D_T$) in terms of geographic regions (DS ⇥ GMex; D_T ⇥ GAm) and satellites employed for detection (D_S ⇥ RDS2; D_T ⇥ RDS1);
- **Study case 3 (GoM ⇥ BR):** GoM models applied to predict the OSS of 421 new samples of seepage slicks and oil spills detected in the BR. This is the most

challenging scenario, comprising different domains ($D_S \neq D_T$) in terms of geographic regions ($D_S \twoheadrightarrow$ GoM; $D_T \twoheadrightarrow$ BR), and satellites employed for detection ($D_S \twoheadrightarrow$ [RDS1, RDS2]; $D_T \twoheadrightarrow$ [RDS1, RDS2, SENTINEL-1 (SNT1)]).

Results and Discussion

Results revealed not only the adaptability and responsiveness of these models to operate in different scenarios with outstanding performances, but also their limitations. The complete results and analysis can be found in Genovez et al. (2023). Since DI achieved the best performances than CDS in all cases, Figure 1 indicates the maximum global accuracies per scenario comparing traditional ML only with DI.

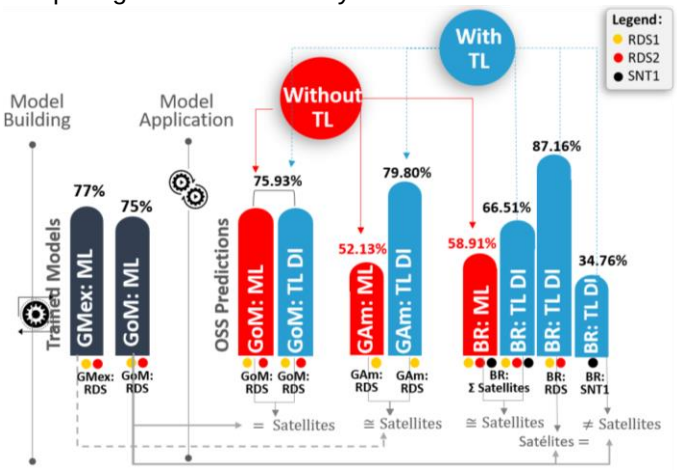

Figure 1. Maximum performances achieved by traditional ML and TL (DI) during the development and application phases.

When the D_S and D_T domains are similar (GoM↠GoM), the TL and generalization are null, being equivalent to the usual ML (75.93%). However, when domains are different but statically related, TL (GMex↠GAm: 79.80%; GoM↠BR: 66.51%) outdoes ML (GMex↠GAm: 52.13%; GoM↠BR: 58.91%), attaining 87.16% of global accuracy when using compatible SAR sensors in the D_S and D_T domains (GoM↠BR: RDS). Conversely, incompatible SAR sensors produce domains statistically divergent, causing negative transfers and generalizations as seen in GoM↠BR: SNT1 (34.76%).

Conclusions

The great performances achieved demonstrated the adaptability of these models to learn geometric patterns and transfer them to make accurate inferences on new samples from different locations.

From an operational standpoint, the generalization capacity of these models with TL saves time and budget, avoiding the collection of validated new training samples, as well as the models re-training from scratch, optimizing human resources and infrastructure.

When looking for new exploratory frontiers, automatic prediction is a value-added product that strengthens the knowledge-driven classifications and the decision-making processes. Moreover, the prompt identification of an oil spill can speed up the response actions to clean up and protect sensitive areas against oil pollution.

Lastly, as new oil slicks are considered in new cycles of training and testing, the predictive models increasingly become more effective in recognizing known and novel patterns, transferring knowledge between domains, thus improving the prediction accuracies. The continuous increment of the database with newly validated oil slick samples is a future priority for the project, embracing different regions of interest for the petroleum industry, as well as other SAR sensors.

Acknowledgements

The authors are grateful to Petróleo Brasileiro S.A. (Petrobras) for providing funds for this project. The authors would also like to acknowledge the Software Engineering Lab (LES) of PUC-Rio, for providing all in-house software used to process the dataset.

References

Alpers, W.; Holt, B.; Zeng, K., 2017. Oil spill detection by imaging radars: Challenges and pitfalls. Remote Sens. Environ., 201, 133–147.

Al-Ruzouq, R.; Gibril, M.B.A.; Shanableh, A.; Kais, A.; Hamed, O.; Al-Mansoori, S.; Khalil, M.A, 2020. Sensors, Features, and Machine Learning for Oil Spill Detection and Monitoring: A Review. Remote Sens., 12, 3338

Brekke, C.; Solberg, A.H.S., 2005. Oil spill detection by satellite remote sensing. Remote Sens. Environ., 95, 1–13.

Carvalho, G.D.A.; Minnett, P.J.; Paes, E.; De Miranda, F.P.; Landau, L, 2018. Refined Analysis of RADARSAT-2 Measurements to Discriminate Two Petrogenic Oil-Slick Categories: Seeps versus Spills. J. Mar. Sci. Eng., 6, 153.

Daume, H., III; Marcu, D., 2006. Domain Adaptation for Statistical Classifiers. *J. Artif. Intell. Res.*, *26*, 101–126.

Genovez, P.C.; Ponte, F.F.A.; Matias, Í.O.; Torres, S. B.; Beisl, C.H.; Mano, M.F.; Silva, G.M.A.; Miranda, F.P., 2023. Development and Application of Predictive Models to Distinguish Seepage Slicks from Oil Spills on Sea Surfaces Employing SAR Sensors and Artificial Intelligence: Geometric Patterns Recognition under a Transfer Learning Approach. Remote Sens., 15, 1496.

Kouw, W.M.; Loog, M., 2019. *Technical Report: An Introduction to Domain Adaptation and Transfer Learning*; Cornell University, USA; pp. 1–41.

Matias, I.O.; Genovez, P.C.; Torres, S.B.; Araújo, F.F.P.; Oliveira, A.J.S.; Miranda, F.P.; Silva, G.M.S, 2021. Improved Classification Models to Distinguish Natural from Anthropic Oil Slicks in the Gulf of Mexico: Seasonality and Radarsat-2 Beam Mode Effects under a Machine Learning Approach. Remote Sens., 13, 4568.

Miranda, F.P.; Silva, G.M.A.; Matias, I.O.; Genovez, P.C.; Torres, S.B.; Ponte, F.F.A.; Oliveira, A.J.S.; Beisl, C.H., 2022. Geometric Pattern Recognition Using Machine Learning: Predictive Models to Distinguish Natural from Anthropic Oil Slicks in The Gulf of Mexico. In Proceedings of the Rio Oil & Gas Expo and Conference 2022.

Pan, S.J.; Yang, Q., 2009. A Survey on Transfer Learning. *IEEE Trans. Knowl. Data Eng.*, *22*, 1345–1359.

Stochastic TOC modeling for East African Rift System Lakes, a possible pre-salt analogous.

CARREIRA, V.R. [a*], VENANCIO, I.M. [b], BELEM A.L. [c], NASCIMENTO, R.A.[a], SOUZA, I.V.A.F.[d], SPIGOLON, A.L.D[d], ALBUQUERQUE, A.L.S. [a]

[a]PROGRAMA DE PÓS-GRADUAÇÃO DINÂMICA DOS OCEANOS E DA TERRA, UNIVERSIDADE FEDERAL FLUMINENSE, NITERÓI, BRASIL

[b] PROGRAMA DE PÓS-GRADUAÇÃO EM GEOCIÊNCIAS (GEOQUÍMICA), UNIVERSIDADE FEDERAL FLUMINENSE, NITERÓI, BRASIL

[c] DEPARTAMENTO DE ENGENHARIA AGRÍCOLA E MEIO AMBIENTE (OBSERVATÓRIO OCEANOGRÁFICO), UNIVERSIDADE FEDERAL FLUMINENSE, NITERÓI, BRASIL

[d] CENTRO DE PESQUISA LEOPOLDO AMERICO MIGUEZ DE MELLO, CENPES PETROBRAS, RIO DE JANEIRO, BRASIL

*correspondence: victorcarreira@id.uff.br

Introduction

In Brazil, one of the key challenges concerning ultra-deepwater exploitation is the complete understanding of the paleoenvironment and its variables that compose Total Organic Content (TOC), in lake systems [1]. Brazilian geoscientists aim for the part of this goal by defining pre-salt sequence as sedimentary rich organic rocks formed in great rift lake systems during Lower Cretaceous Period [2]. According to the uniformitarianism principle, a structural pre-salt analogous is suggested, in this work, from TOC's studies of the East African Rift Lakes [3,4].

Fuzzy systems models are great metaheuristic tools that can enlighten TOC modeling while the lake's function is not known and its variables have a strong statistical dependence [5]. One case is the TOC's predictive modeling problem. In this case, it is possible to simulate over a sequence of different lakes scenarios of accumulation and preservation of the organic carbon before diagenetic processes, generating fundamental information about the potential lacustrine source rocks.

This work aims to validate a direct fuzzy model that predicts the Total Organic Content (TOC) inside Rift Lake Systems. In this sense, we use as a geological analogous to pre-salt Rift System the East African Lakes that have TOC data available and compare two different membership functions[7].

Experimental

For the total organic carbon simulation, we use a data set composed of lake variables such as dissolved oxygen (mg/L), sedimentation rate (cm/kyear), grain size deposit (mm), grain selection(mm), primary productivity (gC/m²/year), lake depth (m), and TOC (%) of five great African lakes known as Lakes Edward, Mobutu, Kivu, Tanganyika, and Victoria.

The methodology is described in Figure 1.

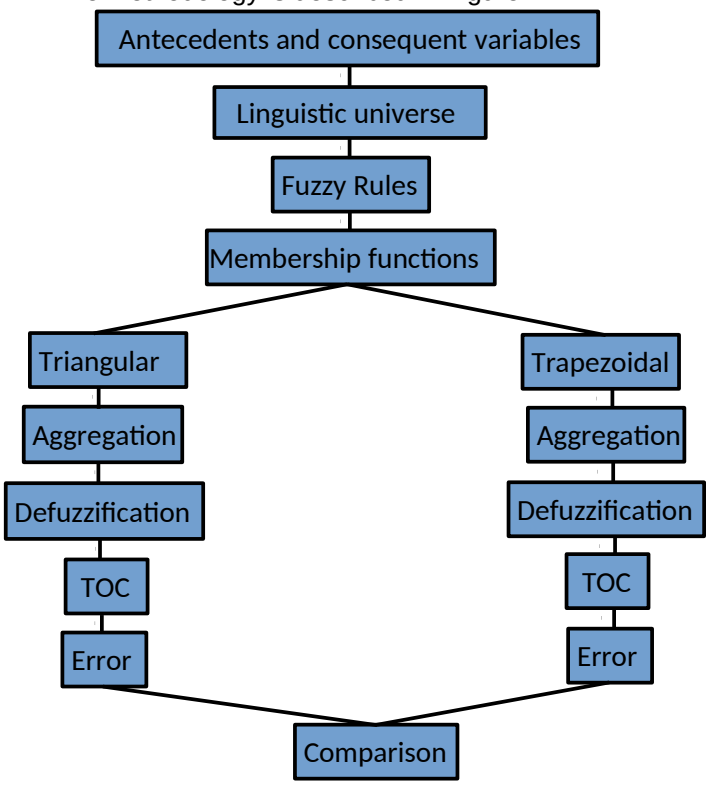

Figure 1. Methodological flowchart.

In the defuzzification stage, two membership functions (trapezoidal and triangular) were selected to

estimate the original TOC value. Defuzzification is the process in which a fuzzy set can be represented by a real number [6]. Figure 2 shows defuzzification the process for Victoria Lake.

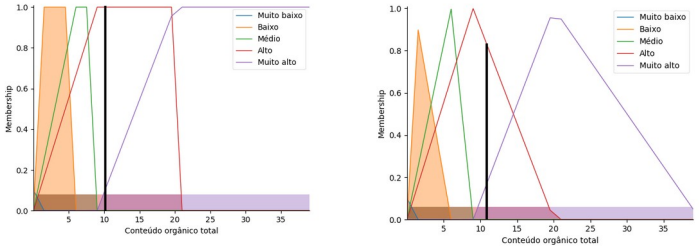

(a) (b)

Figure 2. (a) defuzzification process using a trapezoidal membership function. (b) defuzzification process using a triangular membership function.

The error was determined by the calculation of the Loss function between the observed TOC data and the calculated TOC fuzzy data.

Results and Discussion

The tests carried out with the previously selected lake data, in the East African Rift System show that the results obtained by the fuzzy model are in agreement with the measured TOC. In Lake Victoria, calculated TOC shows values up to 11%. This value coincides with the observed TOC.

In most of the lakes studied membership function tests show a better performance for triangular function. Victoria Lakes presents an error of 0.35% for the triangular function and 1.89% for the trapezoidal function.

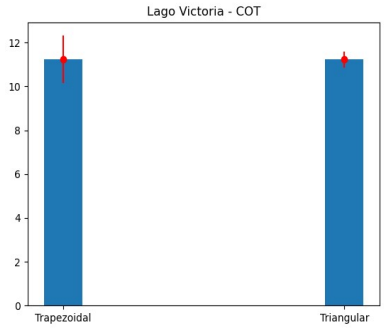

Figure 3. Predictive TOC comparison between two memberships functions in Victoria Lake.

Conclusions

The simulations held for the East African Lake Systems showed good results for TOC estimation when a lake TOC function is not known. The TOC concentration is better estimated when triangular membership functions are applied. The data indicates that the organic matter contents can be estimated considering important environmental variables such as primary productivity (maximum of 600 gC/m²/year) and dissolved oxygen, but also when geological parameters such as sedimentation rate, granulometry, and selection are considered.

Acknowledgments

The authors thank ANP (Brazilian Petroleum Agency), Petrobras S/A, UFF and PR4 project for financial support.

References

[1] Xue, Y.; Clarke, D.; Wang, K. 2022. Multiscenario-based deep learning workflow for high-resolution seismic inversion on Brazil presalt 4D. Second International Meeting for Applied Geoscience & Energy. https://doi.org/10.1190/image2022-3739686.1

[2] Neves, I., Lupinacci, W., Ferreira, D., Zambrini, J., Oliveira, L., Azul, M., Ferrari, A., Gambôa, L. (2019). Presalt reservoirs of the Santos Basin: Cyclicity, electrofacies, and tectonic-sedimentary evolution. Interpretation. 7. 1-37. 10.1190/int-2018-0237.1.

[3] Cazier, E. C., Bargas, C., Buambua, L., Cardoso, S., Ferreira, H., Inman, K., ... & Shinol, J. (2014, September). Petroleum geology of Cameia field, deepwater pre-salt Kwanza basin, Angola, West Africa. In *AAPG International Conference and Exhibition, Istanbul, Turkey. Actas* (Vol. 4, pp. 14-176)

[4] Reinterpreting the South Atlantic Pre-Salt 'Microbialite' reservoirs: petrographic, isotopic and seismic evidence for a shallow evaporitic lake depositional model (2018). First Break. https://doi.org/10.3997/1365-2397.n0094

[5] Siddig, O., Gamal, H., Soupios, P. Utilization of adaptive neuro-fuzzy interference system and functional network in prediction of total organic carbon content. *SN Appl. Sci.* **4**, 16 (2022). https://doi.org/10.1007/s42452-021-04899-5

[6] Jafelice, R. S. M., Fuzzy teory set applications (in Portuguese) – São Carlos, SP. SBMAC, 2012, 119p., v 17, second edition. ISBN: 978-85-86883-62-0

[7] Wright, P. and Tosca, N. A Geochemical Model for the Formation of the Pre-Salt Reservoirs, Santos Basin, Brazil: Implications for Understanding Reservoir Distribution, 2016. APPG Annual Convention and Exhibition.

XVI LATIN AMERICAN CONGRESS ON ORGANIC GEOCHEMISTRY
9 - 11 AUGUST, 2023
ARACAJU, SERGIPE, BRAZIL

Application of Deep Learning Methods for Sporomorph Subgroup Identification

Richard Bryan Magalhães Santos[a*], Karen Soares Augusto[a], Marcos Henrique de Pinho Maurício[a], Sidnei Paciornik[a], Leandra Costa Lages[b], Sizenando Bispo-Silva[b], André Luiz Durante Spigolon[b], Gil Marcio Avelino Silva[b], Taíssa Rêgo Menezes[c].

[a]**Dept. of Chemical and Materials Engineering, Pontifical Catholic University of Rio de Janeiro (DEQM/PUC-Rio), Rua Marquês de São Vicente, 225, Gávea, 22451-900 Rio de Janeiro, Brazil,** [b] **Division of Geochemistry, Petrobras Research and Development Center (CENPES), Av. Horácio Macedo, 950, Cidade Universitária, 21.941-915 Rio de Janeiro, RJ, Brazil,** [c] **PETROBRAS Exploração (EXP/TPGG/TDGEO)**

e-mail: rbryan2022@puc-rio.br

Introduction

The importance of determining the degree of thermal maturation in samples of source rocks led to the proposal to develop systems based on artificial intelligence for identifying palynomorphs and eventually determining the Spore Color Index (SCI) in slides.

The evaluation of the SCI is a method applied to palynomorphs (spores and pollens) to determine the degree of maturation and thermal evolution of kerogen in slides analyzed under an optical microscope in transmitted light [1]. A comparison is made between the coloration of spores and pollen grains found in the studied sample with a reference standard, where numerical values are attributed to the coloration variations.

This traditional method requires a considerable amount of time and effort from a dedicated human operator. This work aims to develop a deep learning method that could automatically identify palynomorphs, then significantly increasing the ability to generate and analyze data.

In present study, the Mask R-CNN [2], which is a neural network algorithm that is currently state-of-the-art for instance segmentation, was chosen to be tested on this problem.

Experimental

The SCI slides were prepared following a standard procedure. 2373 images (1292x968 pixels) were captured using a motorized transmitted light microscopy, with 20X lens, for 8 slides with SCIs ranging from 3.5 to 8.0.

The images had their spores and pollen grains manually delineated and later that “tagging” was validated by a specialist. The images were split into training and test sets; this split was made to preserve approximately a 80%/20% ratio for the annotated objects between the training and the test sets, respectively.

The images were used to train a Mask R-CNN model for palynomorphs identification. The training was executed for around 1500 epochs, approximately one weeklong with four graphics processing units (GTX 1080-TI GPUs), 2 Intel Xeon E5-2630 v4 CPUs and 192GB of RAM, with one image trained on each GPU at a time.

Results and Discussion

The model achieved recall and precision of 83% and 87.2%, respectively. That means the model was able to correctly identify 83% of every palynomorph that was annotated and that out of all identification attempts it has made, 87.2% were correct. Figures 1 and 2 show an image with an annotated object and the model’s correct attempt at segmenting the palynomorph.

This was a preliminary result, as deep learning methods rely on extensive and representative databanks. In order to improve the metrics obtained so far, it will be necessary to not only capture and prepare more images from the slides collected, but also expand the dataset to include a larger variety of samples from different wells. The more diversified the databank is, the more likely it will be for the model to learn the inherent morphological varieties of the palynomorphs. This would contribute to the model having a less restricted application, so it could work on samples and wells it has not learned from. Aside from expanding the databank, it will also be necessary to fine tune the training parameters to improve the results.

To maximize the applicability of our approach, special attention should be given to issues in the different measurement objects that will influence the final product and present some limitations of this technique: addressed by analyzing morphologically and taxonomically groups of sporomorphs according to the age range of the studied section. The problem of signal-dependent color variations includes the thickness of the sporoderm, the character of surface ornamentation, resistance to rework, and

abundance in the sample material. The thickness of the sporoderm was approached through the analysis of morphologically and taxonomically well-defined groups of sporomorphs, the type of sample from the sedimentary section.

In addition, any caved, reworked, microbially degraded, ruptured, or pyrite-filled specimens to avoid misleading results. Samples with exinal thickening will also be excluded. This, in combination with their high robustness to chemical and physical degradation, could potentially cause overrepresentation of reworked specimens in the evaluated assemblies, thus producing potentially misleading estimates of thermal change. After the measurements, a statistical analysis of different RGB parameters will indicate which component (Red/Blue/Green) is more sensitive to thermal maturation in contrast to the other proposed studies.

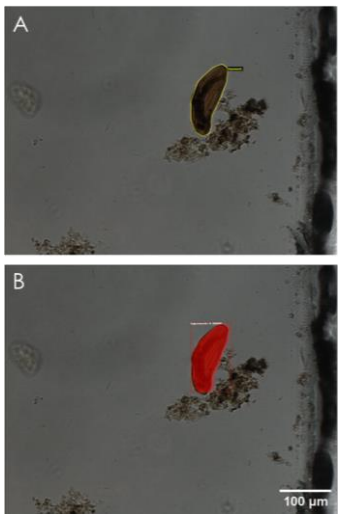

Figure 1. Manually annotated image containing a sporomorph (A), Model's segmentation output (B).

Conclusions

The proposed method has achieved a high performance based on the available metrics and has the potential to evolve even further. It is well-known that all deep learning algorithms are highly dependent on a good database of images. 2373 images are still considered a low number. Thus, efforts will be made to increase this databank, not only increasing the range of the covered SCI, but also by including samples from other wells. This would turn the data bank more representative, allowing the model to achieve a better performance on a wider variety of samples.

It should also be noted that fine tuning the training parameters will potentially provide a better performance, but such work should only be attempted once the databank collection is substantially improved.

After that work is fine-tuned, should the model continue to perform consistently, it would be possible to conceive a method to calculate the SCI directly from the segmented objects. Such calculation will require a thorough calibration of the optical microscope operational parameters using SCI standards.

Moreover, it is essential for the application based on artificial intelligence that the analytical limitations are remedied by associating the specialist's experience with the geological information: morphological and taxonomic identification of sporomorphs according to age group and evaluating parameters to reduce analytical errors: sporoderm thickness, surface ornamentation, resistance to rework, unambiguous identification caving, reworked particles and microbially degraded, disrupted, or pyrite-filled specimens to avoid misleading results.

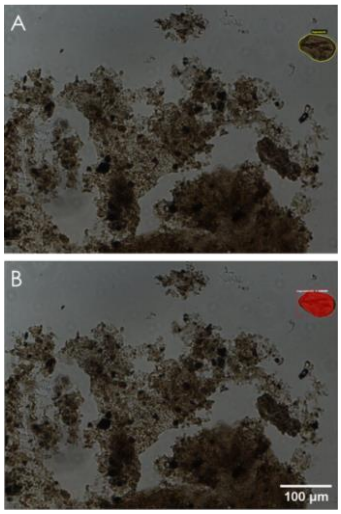

Figure 2. Manually annotated image containing a sporomorph (A), Model's segmentation output (B).

Acknowledgements

The authors thank CNPq (Brazilian research council) for fellowships; ANP (Brazilian Petroleum Agency) and Petrobras S/A for financial support.

References

Suarez-Ruiz, I.; Flores, D.; Mendonça Filho, J., G.; Hackley, P., C., 2022. Review and update of the applications of organic petrology: Part 1, geological applications International Journal of Coal Geology vol. 263, 104111

He, K.; Dolla, P.; Girshick, R.; Gkioxari, G. Mask R-CNN, arXiv:1703.06870v3 (2018), https://arxiv.org/abs/ 1703.06870, accessed on 25th September 2020

MACHINE LEARNING-BASED PREDICTION OF ORIGIN, THERMAL EVOLUTION, AND BIODEGRADATION OF CRUDE OIL SAMPLES BY FT-ICR MS

JUSSARA V. ROQUE[a], LIDYA C. SILVA[a], DANIELLE M.M. FRANCO[a], GESIANE S. LIMA[a], TAYNARA R. COVAS[a], BONIEK G. VAZ[a]

[a]**Chemistry Institute, Federal University of Goiás, Goiânia, Goiás, 74690-900, Brazil**

E-mail: jussara_roque@ufg.br

Introduction

Understanding the depositional environment (Rocha et al., 2018), the thermal evolution (Ren et al., 2020), and the biodegradation level (Head et al., 2003) of an oil sample is of utmost importance for petroleum exploration, reservoir characterization, and environmental studies.

Mass spectrometry (MS) can provide valuable insights into these geochemical parameters. For this, the positive ion-atmospheric pressure photoionization - APPI (+) and the negative ion-electrospray ionization - ESI (−) are commonly employed (Cornford, 2005). However, the advances in MS instrumentation resulted in the development of powerful mass analyzers, such as the Fourier transform ion cyclotron resonance (FT-ICR). As a result, the volume of data generated has increased, making data analysis indispensable (Pereira et al., 2019).

Therefore, this study aims to develop machine learning models to classify crude oils according to their origin, thermal evolution, and biodegradation levels.

Experimental

This study applied APPI (+) and ESI (−) FT-ICR MS analyses from 110 crude oil samples to build machine learning models to predict the origin, thermal evolution, and biodegradation.

The MS analyses were conducted using a 7T Bruker SolariX 2xR FTICR-MS instrument and the mass range was set from *m/z* 128 to 2000. The acquired mass spectra were processed using the Composer64 software (Sierra Analytics, CA, United States) version 1.5.3. for molecular assignment formulas.

The information regarding monoisotopic abundance, molecular formulas, *m/z*, and heteroatom classes was imported to Matlab R2020a software (Mathworks Inc) for data analysis. For each ionization source, unique molecular formulas were obtained for the 110 samples, with 17,226 in APPI (+) and 13,362 in ESI (−). Consequently, a data matrix containing the monoisotopic abundance values were built and named matrix **X**, representing the independent variables.

The 110 samples exhibit different origins (lacustrine, marine, and transitional), thermal evolution (low moderate, moderate, high moderate, high, and highest), and different levels of biodegradation (non-biodegraded, low, medium, and high). Thus, based on these different origins, thermal evolution, and biodegradation, partial least squares for discriminant analysis (PLS-DA) (Barker and Rayens, 2003) and ordered predictors selection from discriminant analysis (OPSDA) (Roque et al., 2019) were used to build classification models by using APPI (+) and ESI (−) FT-ICR MS data.

The classification models were evaluated using accuracy, which can be calculated by the ratio of the number of samples that were correctly classified to the total number of samples.

Results and Discussion

PLS-DA classification models with variables selected by OPSDA were built to predict the origin, thermal evolution, and biodegradation of crude oil samples. The accuracies for both APPI (+) and ESI (−) FT-ICR MS data were presented in Table 1.

Table 1. Models' accuracy for origin, thermal evolution, and biodegradation from APPI (+) and ESI (−) FT-ICR MS.

	APPI (+)	ESI (−)
Origin	100%	94%
Thermal Evolution	99%	79%
Biodegradation	100%	95%

The classification models with APPI (+) yielded accuracies >99%, while with ESI (−), several samples were misclassified, achieving lower accuracies than APPI (+) models. In this way, the PLS-DA OPSDA models obtained using APPI (+) demonstrate great potential for predicting the origin, thermal evolution, and biodegradation of crude oil samples.

In Figure 1, the most important variables are highlighted using a color scale representing their importance in a graph depicting the relationship between the carbon number and DBE (double bond equivalent). The most important variable in the classification models for origin using APPI (+) exhibited DBE values of 5 and 29 carbons for the HC class, DBE values of 11 and 53 carbons for the N class, DBE values of 8 and 14 carbons

for the O class, and DBE values of 12 and 16 carbons for the S class.

For thermal evolution, DBE values of 19 and 43 carbon atoms for the HC class, DBE values of 22 and 34 carbon atoms for the N class, DBE values of 10 and 28 carbon atoms for the O class, and DBE values of 9 and 15 carbon atoms for the S class.

In classification models for biodegradation, the most important variable exhibited DBE values of 8 and 15 carbon atoms for the HC class, DBE values of 20 and 31 carbon atoms for the N class, DBE values of 7 and 55 carbon atoms for the O class, and DBE values of 27 and 44 carbon atoms for the S class.

Conclusions

The findings demonstrated promising potential in utilizing APPI (+) FT-ICR MS for the classification of oil samples, as well as in identifying molecules that can serve as prospective markers for distinguishing oils based on their origin, thermal evolution, and biodegradation characteristics.

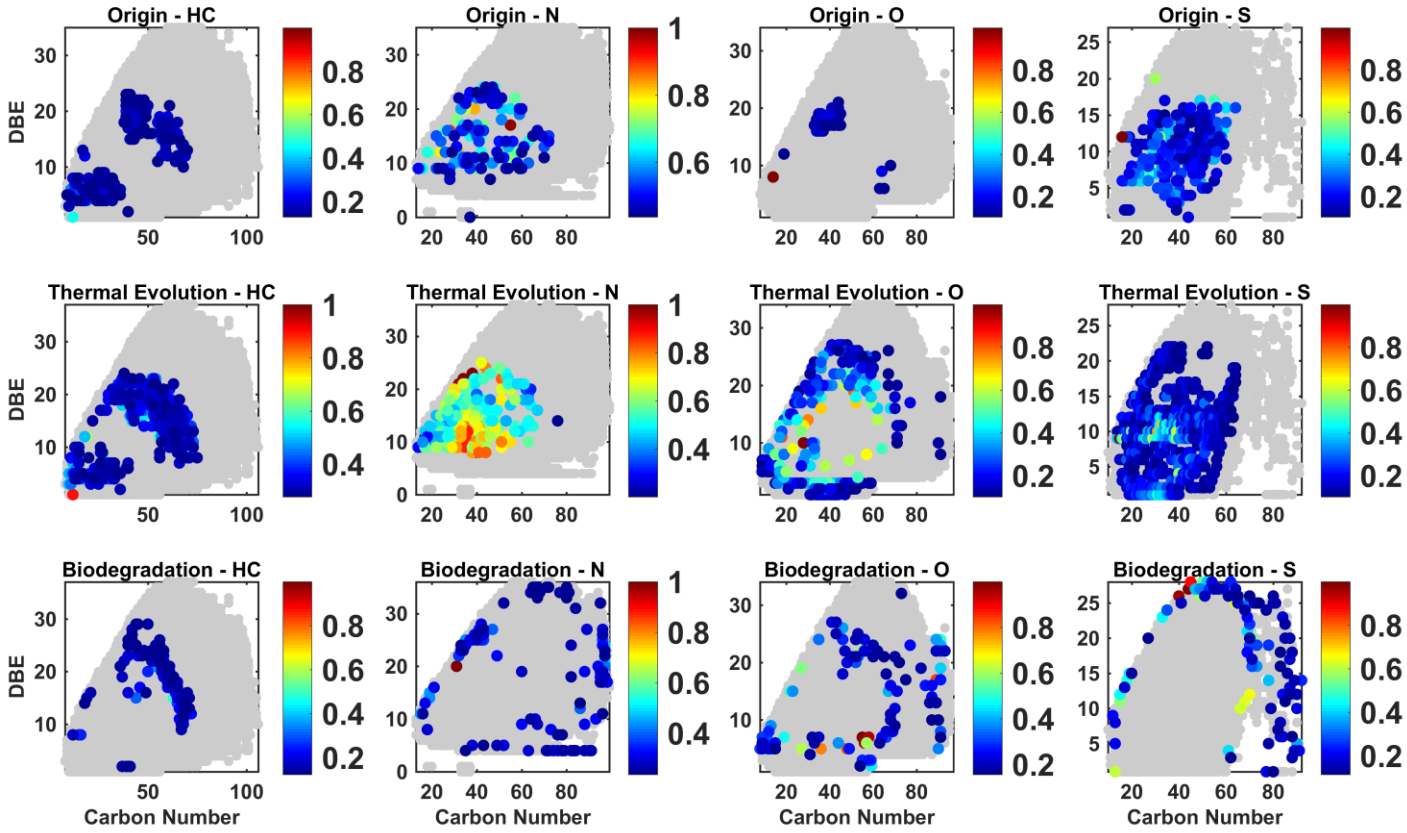

Figure 1. Carbon number versus DBE of more important variables from the heteroatom classes in APPI (+) FT-ICR MS.

Acknowledgements

The authors thank CAPES and Petrobras S/A for financial support.

References

Barker, M., Rayens, W., 2003. Partial least squares for discrimination. Journal of Chemometrics 17, 166–173.

Cornford, C., 2005. Petroleum Geology. The Petroleum System. Encyclopedia of Geology 268–294.

Head, I.M., Jones, D.M., Larter, S.R., 2003. Biological activity in the deep subsurface and the origin of heavy oil. Nature 2003 426:6964 426, 344–352.

Pereira, I., de Aguiar, D.V.A., Vasconselos, G., Vaz, B.G., 2019. Fourier transform mass spectrometry applied to petroleomics. Fundamentals and Applications of Fourier Transform Mass Spectrometry 509–528.

Ren, Z., Cui, J., Qi, K., Yang, G., Chen, Z., Yang, P., Wang, K., 2020. Control effects of temperature and thermal evolution history of deep and ultra-deep layers on hydrocarbon phase state and hydrocarbon generation history. Natural Gas Industry B 7, 453–461.

Rocha, Y. dos S., Pereira, R.C.L., Mendonça Filho, J.G., 2018. Geochemical characterization of lacustrine and marine oils from off-shore Brazilian sedimentary basins using negative-ion electrospray Fourier transform ion cyclotron resonance mass spectrometry (ESI FTICR-MS). Organic Geochemistry 124, 29–45.

Roque, J. V., Cardoso, W., Peternelli, L.A., Teófilo, R.F., 2019. Comprehensive new approaches for variable selection using ordered predictors selection. Analytica Chimica Acta 1075, 57–70.

USO DE MAPAS AUTO-ORGANIZÁVEIS PARA SELEÇÃO DE INTERVALOS ESTRATIGRÁFICOS PARA GEOCRONOLOGIA Re-Os: EXEMPLO DE APLICAÇÃO NA FORMAÇÃO PENDÊNCIAS, BACIA POTIGUAR, NE DO BRASIL

Ravi Gabriel dos Santos Pinheiro Sampaio[a], Luiz Fernandes Dutra[a], Antomat Avelino de Macêdo Filho[a]

[a] **Instituto de Geociências – Universidade de São Paulo (USP)**

ravigsps@usp.br; luizdutra@usp.br, antomat@alumni.usp.br

Introdução

A Bacia Potiguar é uma região estratégica para a produção de hidrocarbonetos na Margem Equatorial Brasileira. Os três sistemas petrolíferos da bacia estão associados ao evento de rifteamento Eocretaceo (sin-rifte I~140-128Ma, sin-rifte II~128-119Ma) e subsequente desenvolvimento de margem passiva do Atlântico Sul/Equatorial no estágio drifte [1,2]. Neste contexto, sua unidade basal, a Formação Pendências, é um dos principais *plays* exploratórios, sendo subdivida em quatro sequências [3]: I e II – relacionadas as fases iniciais de rifteamento, com altas taxas de sedimentação caracterizado por depósitos gravitacionais seguida por ambientes lacustrinos; enquanto III e IV caracterizam-se por ambientes lacustres e fluvio-deltaícos, indicando a progressão da quiescência tectônica para maior atividade tectônica e clima úmido à árido no topo [2]. Embora bem caracterizada do ponto de vista geológico/estratigráfico, poucos estudos detalhados abordaram aspectos geocronológicos das sequências I e II. O método ^{187}Re-^{188}Os é uma ferramenta geocronológica valiosa para caracterização de rochas sedimentares [4], ainda que a escolha de amostras adequada, sem evidências de deposição em ambientes oxidantes e ausência de bioturbação, seja uma etapa desafiadora [5,6]. O presente trabalho busca identificar zonas enriquecidas em Carbono Orgânico Total (TOC%) por meio do uso de mapas auto-organizáveis (*self-organizing maps,* SOM) aplicados a grandes bancos de dados de poços petrolíferos. Tais intervalos estratigráficos podem ter alto potencial para a aplicação da geocronologia por Re-Os dada a alta concentração de matéria orgânica. Utilizada em maior escala, a técnica pode ser útil para seleção de áreas-alvo, diminuindo a quantidade de análises expeditas em escala bacinal.

Metodologia

Considerando a disponibilidade do extenso banco de dados na plataforma REATE (https://reate.cprm.gov.br/anp) e o foco na alocação do melhor potencial para análise^{187}Re-^{188}Os, os dados de geoquímica orgânica (TOC% e pirólise rock eval) foram analisados no SOM e interpretados em conjunto com *gamma-ray.* Escolheu-se o campo de Lorena na porção sul da Bacia Potiguar, com dados extraídos do registro estratigráfico de dois poços (n=112; 1-LOR-1-RN e 4-LOR-2-RN), levando em conta o interesse econômico e o conhecimento geológico disponível.

O SOM é uma importante técnica para visualização e exploração de dados hiperdimensionais baseado na quantização vetorial. O método é principalmente utilizado para agrupamento, reconhecimento de padrões, redução de ruído e classificação [7]. O resultado da análise é apresentado em mapas, conhecidos como mapa de Kohonen, no qual cada célula (ou nós) é a representação de grupos discretos dos dados de entradas e da similaridade entre esses grupos. Os dados de entradas são tratados como vetores n-dimensionais, onde n é o número de variáveis. A quantidade de nós e, consequentemente, o tamanho do mapa é dependente do número de amostras [8,9]. Definiu-se aqui o tamanho do mapa como 10 X 8 e topologia toroidal.

Resultados e Discussões

A aplicação do algoritmo resultou na categorização dos dados dos poços 1-LOR-1-RN e 4-LOR-2-RN em três clusters (cls) com base na técnica do k-médios considerando o índice de davies-bouldin de 3. O foco principal da análise foi a concentração de TOC%, e os valores obtidos para o cls1, cls3 e cls2 foram, respectivamente, 1,30-1,81% σ =0,523; 2,11-3,82% σ =1,095 e 4,35-6,03% σ =1,030. Em relação aos hidrocarbonetos livres e retidos (S1 e S2 - mgHC/grocha), a média dos três cls foi de S1=0,25-0,53 σ = 0,192; 0,70-1,39 σ =0,497; 0,19-0,43 σ =0,277 e S2=3,11-7,23 σ=

3,522; 9,03-20,36 σ =6,809; 28,55- 42,47, σ =32,2 classificando o cls1 e cls3 como bons à muito bons geradores e o cls2 como excelente gerador.

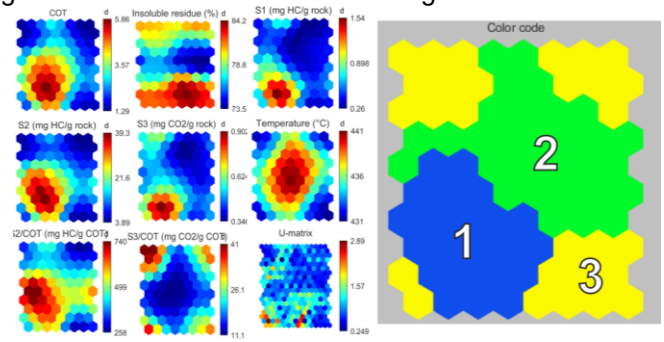

Figura 1. Mapas planos de componentes e respectivo agrupamento de clusters por k-médios.

Com base na análise estratigráfica dos poços, observou-se um aumento gradativo de fácies arenosas em direção ao topo da Formação Pendências, indicando a mudança do registro deposicional de trato de lago profundo para trato de lago raso, em 5ª ordem [10]. Esse padrão sugere estágios finais de quiescência tectônica e clima úmido, seguidos de um aumento na taxa de subsidência e aridez, como observado no arcabouço bacinal[3]. A base dos perfis estratigráficos relaciona-se às fácies lacustres de baixa energia e profundidades elevadas, correlacionáveis ao clímax da fase rifte[11] devido ausência de registros bioestratigráficos o posicionamento temporal é complexa.

A análise estratigráfica demonstrou que acima dos limites superiores do trato de lago profundo (1350m; 1390m) as amostragens concentram-se nos reservatórios areníticos e dessa maneira foram desconsideradas para avaliação da geocronologia dos folhelhos, entretanto reavaliação com enfoque na cronologia de geração e migração do óleo utilizando mesma técnica, certamente trará luz a cronologia de eventos na bacia.

Considerando o intervalo de interesse, com o *gamma ray*, as amostras do cls2 do poço 1-LOR-1-RN apresentam as condições ideais para a preservação do Re, devido à sua riqueza em matéria orgânica e menor granulometria. Nesse intervalo, duas amostras do *cls*2 se destacam (1458m; 3,18%TOC e 1548m; 4,44%TOC). No poço 4-LOR-2-RN, apenas os cls1 e cls3 estão presentes no intervalo de interesse, sendo que a amostra do *cls*3 (1368m; 4,6%TOC) é a mais promissora para a aplicação da técnica. Através de uma análise não supervisionada, o SOM é capaz de fornecer cls que são recomendáveis para a aplicação da geocronologia Re-Os.

Conclusões

A aplicação do SOM com dados de geoquímica orgânica para identificar intervalos estratigráficos adequados à geocronologia Re-Os no campo de Lorena apresenta grande potencial. Três cls foram identificados nos poços disponíveis, sendo os cls 3 e 2 os mais promissores para produção e geração. Recomenda-se a escolha desses intervalos amostrais aliados a perfis de *gamma ray*. O SOM permite uma escolha ágil de intervalos amostrais para a aplicação da técnica e, certamente mostra-se como uma poderosa ferramenta de análise em bancos de dados extensos, auxiliando na identificação e classificação de zonas com potencial de produção de hidrocarbonetos em escala bacinal.

Agradecimentos

Os autores agradecem à ANP, CNPq, FAPESP e USP pelo apoio financeiro e bolsas de estudo.

Referências

[1] - Matos, R. M. D, 2000. Tectonic Evolution of the Equatorial South Atlantic. In: Mohriak, W. U.; Talwani, M.(Ed). Atlantic Rifts and Continental Margins. p. 331-354.

[2] - Pessoa Neto, O.C., Soares, U.M., Da Silva, J.G.F., Roesner, E.H., Florencio, C.P., De Souza, C.A.V., 2007. Bacia Potiguar. Bol. Geociências Petrobras **15**, 357-369.

[3] - Soares, U. M., 2000. As relações entre tectonismo e sequências deposicionais no rifte potiguar - porção SW do Graben de Umbuzeiro, bacia potiguar emersa. **149 f**. Dissertação (Mestrado em Geodinâmica; Geofísica) - Universidade Federal do Rio Grande do Norte, Natal.

[4] -Yin, L., Zhao, P., Liu, J., & Jieqiang, L., 2023. Re-Os isotope system in organic-rich samples for dating and tracing: Methodology, principle, and application. Earth-Science Reviews, **238**, 104317.

[5] - Pietras, J. T., Dennett, A., Selby, D., & Birdwell, J. E., 2022. The role of organic matter diversity on the Re-Os systematics of organic-rich sedimentary units: Insights into the controls of isochron age determinations from the lacustrine Green River Formation. Chemical Geology, **604**, 120939.

[6]- Stein, H. J., & Hannah, J. L., 2014. Rhenium–Osmium Geochronology: Sulfides, Shales, Oils, and Mantle. In Springer eBooks (pp. 1–25). Springer Nature.

[7] - Fraser, S.J., and Dickson, B.L., 2007, A new method for data integration and integrated data interpretation: Self-organizing maps, in 5th Decennial International Conference onMineral Exploration, p. 907–910.

[8] - Carneiro, C. de C., Fraser, S.J., Crósta, A.P., Silva, A.M., and Barros, C.E. de M., 2012, Semiautomated geologic mapping using self-organizing maps and airborne geophysics
in the Brazilian Amazon: Geophysics, **v. 77**, p. K17–K24, doi:10.1190/geo2011-0302.1.

[9] - Cracknell, M.J., 2014, Machine learning for geological mapping: algorithms and applications:University of Tasmania, https://eprints.utas.edu.au/18571/.

[10] - Scholz, C. A., Moore Jr., T. C., Hutchinson, D. R., Golmshtok, A. Já., Klitgord, K. D., Kurotchkin, A. G., 1997. Comparative Sequence Stratigraphy of Low-Latitude versus High-Latitude Lacustrine Rift Basins: Seismic Data Examples from the East African and Baikal Rifts. Palaeogeography, Palaeoclimatology, Palaeoecology, Special Limo-Geological Congress issue.

[11] - Prosser, S.,1993. Rift-Related Linked Deposicional Systems and their Seismic Expression. Geological Society Special Publication, **v. 71**, p. 35-66.

ALI

WELCOMING AND DIVERSITY: EQUITY IN THE GEOSCIENCES SCENARIO

INICIATIVAS A FAVOR DA DIVERSIDADE NA PETROBRAS

CAROLINE MARCHON CAETANO[1*]

[1*]**PETROBRAS**

carolcaetano@petrobras.com.br

Introdução

O respeito aos direitos humanos é tema transversal na Petrobras. A empresa anualmente busca superar desafios que se apresentam num contexto mais amplo da sociedade, influenciado por fatores históricos e culturais, mas que não são justificativas para uma inação.

A publicação das Diretrizes de Direitos Humanos na Petrobras, a constituição da Comissão de Direitos Humanos e o estabelecimento de compromissos específicos de direitos humanos em nosso Plano Estratégico vêm ditando o modo de agir e galgando desafios maiores que beneficiam o clima organizacional, os relacionamentos interpessoais e os negócios.

Resultados e Discussões

Em janeiro de 2021, constituiu-se a Comissão de Direitos Humanos da Petrobras (Figura 1), que é responsável por gerir a implementação da agenda de direitos humanos estabelecida pelas Diretrizes de Direitos Humanos da Petrobras, de forma integrada, ampla e transversal no negócio na companhia.

Figura 1. Esquema da estrutura do comitê de Direitos Humanos. Fonte: Petrobras.

Cabe à comissão elaborar, implementar e monitorar o andamento do Plano de Ação de Direitos Humanos da Petrobras, garantindo o desdobramento de cada um dos compromissos relativos a direitos humanos previstos em nosso plano estratégico, bem como promover debates, disseminar conteúdos e assessorar as áreas no que tange ao tema.

No início de 2023 foi publicado o Posicionamento Petrobras de Diversidade e Combate ao Assédio e Discriminação. Nele, a empresa compromete-se em promover a diversidade e combater rigorosamente o assédio e a discriminação. Os primeiros passos para isso já foram dados com a redução do prazo para apurações e está sendo implantado um serviço de atendimento psicológico 24 horas para acolhimento e orientação.

Visando à integração e ao compartilhamento de práticas entre os grupos, realizou-se em 2021 o 1º Encontro Técnico de Grupos de Mulheres e de Diversidade da Petrobras, ação que teve continuidade em 2022 com o 2º, 3º e 4º encontros, acompanhando o crescimento do número de grupos. Nesses encontros, foram discutidos os planos de ação para o ano e boas práticas adotadas.

Uma delas se trata do Programa de Mentoria Feminina Corporativo, realizado em 2021. Em setembro de 2022, foi lançado, um novo ciclo. Nele, dobrou-se o número de mentoradas, de 15 para 30. Houve inscrição de 521 profissionais, o que demonstra o interesse das mulheres da companhia em participar do programa. Em iniciativa inédita, foram reservadas 20% das vagas para mulheres pretas e pardas e 10% para mulheres com deficiência. Importante informar que este programa inspirou vários outros em áreas específicas da companhia e, em 2022, 165 mentoradas passaram ou estão passando pelos vários programas de mentoria feminina da Petrobras.

A Petrobras se comprometeu em promover a diversidade, proporcionando um ambiente de trabalho inclusivo. Por isso, criaram-se comitês internos nas gerências executivas, tais com o DivEXP, Comitê da Diversidade da Exploração da Petrobras. O DivEXP conta com 5 pilares de atuação: o de gênero, LGBTQIA+, racial, etário e o de

PCD (Figura 2). Alguns desse pilares ainda estão se estruturando, mas o DivEXP está crescendo e atuando em diferentes frentes, como por exemplo, a elaboração do 1º Simpósio da Diversidade e Inclusão da Exploração da Petrobras – SimDivEXP (Figura 3).

Figura 2. Pilares do DivEXP. Fonte: DivEXP

Figura 3. 1º Simpósio da Diversidade e Inclusão da Exploração da Petrobras – SimDivEXP. Fonte: DivEXP

Conclusão

Reconhecemos que ainda são necessários inúmeros avanços rumo a uma sociedade mais justa, equitativa e igualitária. É dever da Petrobras liderar pelo exemplo e ser referência na promoção da diversidade, do respeito às pessoas, da justiça e dos direitos humanos.

Agradecimentos

Agradeço à Petrobras por todo o material disponibilizado. E ao Comitê de Diversidade da Exploração – DivEXP, pelos debates, pesquisas e ações em prol da Diversidade na empresa.

Referências

Gerência Executiva de Responsabilidade Social. 2022 Caderno de Direitos Humanos e Cidadania Corporativa.

Comitê da Diversidade da Exploração da Petrobras – DivEXP.

CENSUS OF GEOSCIENCES AND THE QUALITATIVE AND QUANTITATIVE ANALYSIS OF PROFESSIONAL INEQUALITIES

JÉSSICA DE SOUZA GABI BARCELLOS[1*]; TALITA GANTUS DE OLIVEIRA[2]; LAÍSA DE ASSIS BATISTA[3]; MARION FREITAS NEVES[4]; DARLLY ÉRIKA SILVA DOS REIS[4]; MÁRCIA ELISA BOSCATO GOMES[5]; ALICE FERNANDA DE OLIVEIRA COSTA[6]

[1]UNIVERSIDADE FEDERAL FLUMINENSE; [2]UNIVERSIDADE ESTADUAL DE CAMPINAS; [3]UNIVERSIDADE DE SÃO PAULO; [4]UNIVERSIDADE FEDERAL DO RIO DE JANEIRO; [5]UNIVERSIDADE FEDERAL DO RIO GRANDE DO SUL; [6]UNIVERSIDADE FEDERAL DE OURO PRETO

*jessicasgb@id.uff.br

Introduction

The Brazilian Association of Women in Geosciences (ABMGeo) together with the Network of Geoscientist Mothers (GeoMamas) is a space for women that seeks to raise demands based on their diverse bodies, minds, functions and attributions. It is an association that brings together women from different areas of geosciences (geography, geophysics, geology, oceanography, environmental sciences, earth sciences, natural sciences, marine sciences, exact sciences linked to geosciences). This insurgent movement has also been happening in other territories, with GeoLatinas, a group of Latin American women from different countries, being another example of these feminist and anti-racist organizational spaces in the geosciences. This construction has as its starting point the recognition of institutions in the reproduction of inequalities such as: racism, gender, economic, educational, mobility. Therefore, it is important for the promotion of structural changes.

Mapping these inequalities is the first step towards being able to welcome them and think about how to deal with these issues. In this sense, it becomes relevant to develop a unified, collectivized, and intuitive database that contains information from the geoscientific community to contribute to the development of academic research that helps in the elaboration of public and institutional policies. In view of these gaps, the Census of Geosciences project seeks to develop a database that includes the sexual, racial, gender, age, and socioeconomic diversity of geoscientists in each area of activity and training, as well as to map the violence suffered in the spaces of study and work.

Methodology

To achieve the proposed objective, a qualitative and quantitative research is developed from the collection of primary data, following the steps: (1) Definition of variables (parameters raised by the questionnaire); (2) data collection (carrying out the census survey); (3) statistical treatment of data; (4) analysis of results; (5) elaboration of the final report. Carrying out all the stages comprises the course of a year of project development, which started in September 2022. There were two data collection campaigns, divided into stages of three months each: the first between September and December 2022, and the second, in progress, between April and July 2023. Data is collected anonymously and voluntarily via an electronic form, being disseminated through the ABMGeo website, social networks, email lists and through the collaboration of participants who share the campaign.

Preliminary Results and Discussions

As the Census of Geosciences is in the 2nd phase of data collection, the results are still preliminary. To date, 1073 responses have been collected. Among the parameters raised are: age group; color/race; biological sex; gender identification; sexual orientation; state and country where you reside; disabled person (PCD); if you have already suffered violence or discrimination in an educational or work environment; exercise of parenting; area of expertise in geosciences etc. We present, below, the results referring to gender and ethnic-racial self-declaration (Figure 1 and Figure 2, respectively).

As can be seen from the data presented, the proportion of people who identify as female, 59.55%, is considerably higher than the proportion of people who identify as male, 38.77% (Figure 1). On the other hand, according to FAPESP (2023), in Exact Sciences, Geosciences and Engineering, male researchers predominate in research funding concessions, 69% of the total. Although data from the Census of Geosciences reveal a higher proportion of women in this area, contrary to what FAPESP (2023) shows, we understand

this result as a reflection of male disengagement in surveying the diversities in the professional environment.

The politicization of reproductive tasks elevates women to a social prestige that is embodied in feminized leaderships (Gago, 2020, p. 155) – for a sociocultural issue and related to instruments of transgenerational resistance. It is worth mentioning the proportion of 0.93% of people who do not identify with either the female or male gender, which corresponds to 10 people in the universe of data collected who respond to “another gender” (Figure 1). Although the data, quantitatively, are not as expressive as the other two categories (female and male), it is worth mentioning the invisibility of the non-binary, transgender and transsexual population in a cisheteronormative society. This population exists and manifests itself in the Census of Geosciences.

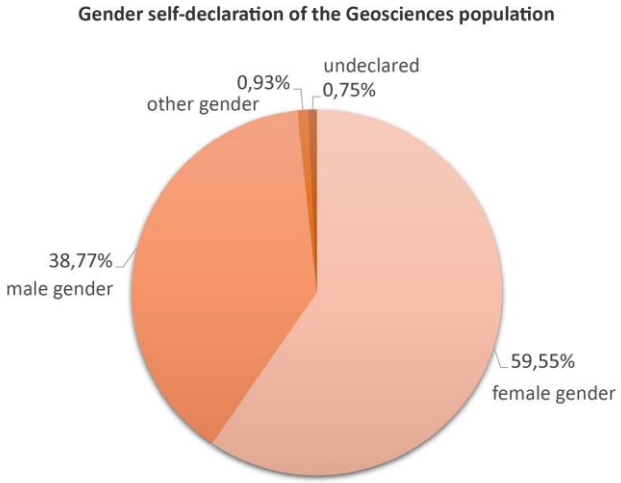

Figura 1. Graphic of self-declaration of gender identity from the universe of data collected by the Census of Geosciences.

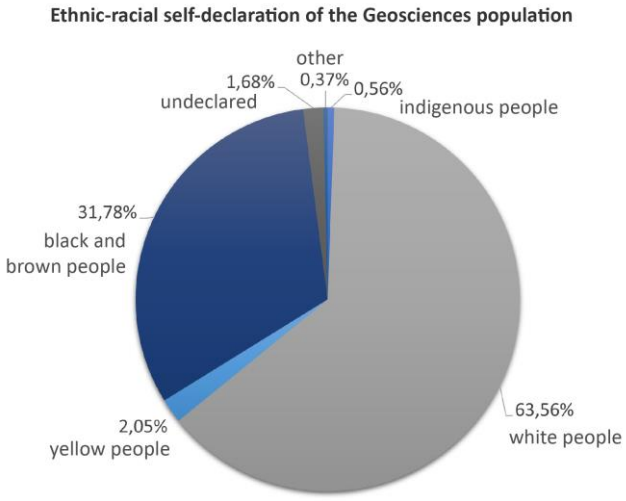

Figura 2. Graphic of ethnic-racial self-declaration of the universe of data collected by the Census of Geosciences.

With regard to ethnic-racial self-declaration data, although the Demographic Census of the Brazilian population, published by IBGE (2010) and updated by Ipea (2021), points out that the black population in Brazil represents 56.1% of the total, notes there is a racial under-representation in Geosciences, according to data collected by the ABMGeo Census, 31.78% (Figure 2). In relation to indigenous peoples, although there is a significant cosmogonic, cosmological and epistemic difference regarding the way in which the original peoples understand the production of colonial knowledge reproduced in universities – even more so in view of the ethnic diversities of these peoples –, the occupation of spaces academic formalities by this population is hampered by numerous issues that, in addition to being symbolic, are also material.

Racism is, in fact, a process in which “conditions of subalternity and privileges” are distributed among racialized groups in the political, economic and social spheres (Almeida, 2020, p. 34). Although some Brazilian universities already apply the indigenous entrance exam and already have affirmative action policies (social and racial admission quotas), the absence of student permanence policies, which affects not only indigenous people, but also the marginalized black population in this country, it is a major obstacle for Geosciences to become more plural and diverse, and in fact representative of the Brazilian population.

Conclusions

As the data collected by the Census of Geosciences are still in the survey phase, it is not possible to establish a definitive conclusion about the observation. It is therefore concluded that, up to the present moment, the census points to the extreme need to build an identification database, even if initial and partial, of Geosciences professionals. Finally, using data collected by the Census of Geosciences, it will be possible to build action plans to define goals, processes, and tools to combat inequalities and violence within the public and private institutions in which geoscience professionals work.

References

ALMEIDA, S. Racismo estrutural. 1a edição ed. São Paulo: Editora Jandaíra, 2020.

FAPESP. Fundação de Amparo à Pesquisa do Estado de São Paulo. Participação feminina nas solicitações de bolsas e auxílios da FAPESP. Revista Pesquisa Fapesp, Edição 325, 2023.

GAGO, V. A potência feminista ou o desejo de transformar tudo. 1a edição. Tradução ed. [s.l.] Editora Elefante, 2020.

IBGE. Instituto Brasileiro de Geografia e Estatística, 2010. Censo Demográfico Nacional. Disponível em: IBGE | Censo 2010.

IPEA. Instituto de Pesquisas Econômicas Aplicadas, 2021. Retrato das Desigualdades de Gênero e Raça.

Diversity and welcoming in working spaces: what do Brazilian geoscientists need?

Laísa de Assis Batista [a*], Darlly Érika dos Reis [b], Marion Freitas Neves[b], Luna Gripp Simões Alves [c], Talita Gantus de Oliveira[d], Ana Caroline Duarte Dutra[e], Fernanda Quaglio[f], Rosaline C. Figueiredo e Silva[g]

[a]University of São Paulo-USP, [b]Federal University of Rio de Janeiro-UFRJ, [c]Geological Survey of Brazil-CPRM; [d]State University of Campinas-UNICAMP, [e]Civil Defense of Petrópolis-RJ, [f]Federal University of São Paulo-UNIFESP, [g]Federal University of Minas Gerais-UFMG

*diretoriaabmgeo@gmail.com

Introduction

When it comes to the full development of a career, scientific or not, being part of a community and having a strong network play pivotal roles towards the construction of robust and successful projects. Beyond the building of such relationships between co-workers in a daily based environment, the professional engagement in institutional events such as congresses, symposiums, conferences and workshops are essential steps for being up to date and to make connections in different areas (e.g. Oester et al., 2017). In this context, undermining women participation in most of the above cited spaces can be linked to female under-representation in high-hierarchy positions of the Brazilian Sciences, as part of the so-called “scissors effect” (Areas et al., 2020).

Given the inherent dealing with a limited physical space within the Earth system, an additional feature of the career in Geosciences is the field work, essential for research, exploration and/or exploitation initiatives, no matter what the subject area is. This is another space of women (and transgender men) exclusion, once that topics such as menstruation, pregnancy, lactation and parenting are seeing as weaknesses or problems to the institutions (Pickering and Khosa, 2023; Carrilho, 2021), which are therefore ignored or poorly addressed on the planning of its policies and structures.

This work addresses the relationship between institutional recognition/welcoming and the (lack of) diversity in geoscientific spaces. Our subject is the response of 03 questions posed to the community of two Brazilian interdisciplinary scientific events: The IX Symposium of Quantification in Geosciences (SQGeo from the acronym in portuguese) and The III National Encounter on Natural Disasters (END from the acronym in portuguese). We also address the challenges faced by geoscientist mothers in the field work trips, based on two interviews published in the social media of the Association of Brazilian Women in Geosciences (ABMGeo) and its hub for mothers, the GeoMamas Network.

“Girls just wanna have fun…ding to their research!”, says the famous meme at the scientific-related media about women participation in STEM (accronym to science, technology, engineering and mathematics). In agreement, to ABMGeo and the GeoMamas Network, it starts with the right to be in all institutional spaces, to see and to be seen, and being fully accepted, whether you are a woman or not.

Materials and methods

A query on demands for in-person participation collected responses as part of the initiatives recommended by the GeoMamas Guide and the ABMGeo Guide for Diversity. The IX SQGeo occurred in Campinas/SP, between the 18th and 21st of September/2002. Marketing on welcoming initiatives and circling of the query occurred since June 23rd, mainly on social media (e.g. linktree and instagram). The III END occurred between Mach 6th to 8th, in Niterói/RJ, and the query was sent through e-mail to subscribed participants, one month before the event. At this stage, marketing on welcoming structures was also circled in social media.

We analyzed responses of 3 questions from these queries: (i) the self-declared gender of the participants (Figure 1); (ii) the self-declared race of the participants (Figure 2); (iii) what structures were desirable to make their participation a more agreeable experience (Figure 3). The inclusion policies adopted by each event granted the Atmosphere and Lithosphere insignia to END and SQGeo, respectively - a recognition from the GeoMamas Network of pro-breastfeeding and child-support structures at the events location (Figure 3), besides other pro-diversity and gender-equity initiatives.

Results and Discussion

- *The public engagement is a challenge even with high anticipation of the survey*: there were 46 responses out of a public of 142 persons in the IX SQGeo (~34%), and 60 responses out of a public of 195 persons for the III END (~30%).
- *There was a majority of cisgender white men*: the IX SQGeo responses show that 60% of the survey participants were cisgender men (Figure 1), and both events had between 64 (SQGeo) and 76% (END) of white participants responding to the query(Figure 2).

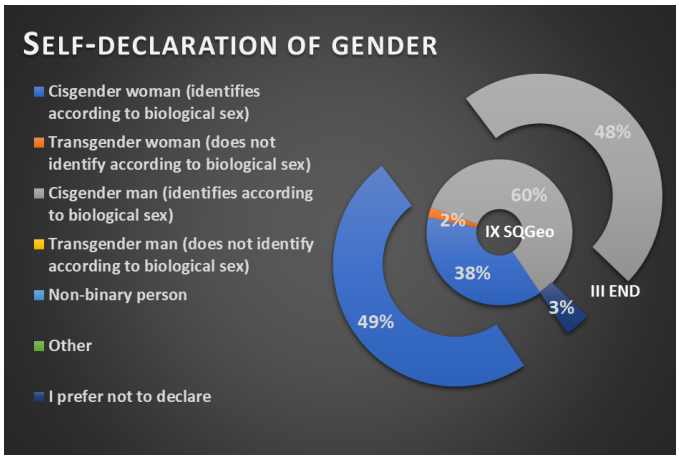

Figure 1. Self-declaration of gender data collected by the queries of IX SQGeo (inner chart) and III END (outer chart).

Figure 2. Race or ethnicity self-declaration data collected by the queries of IX SQGeo and III END.

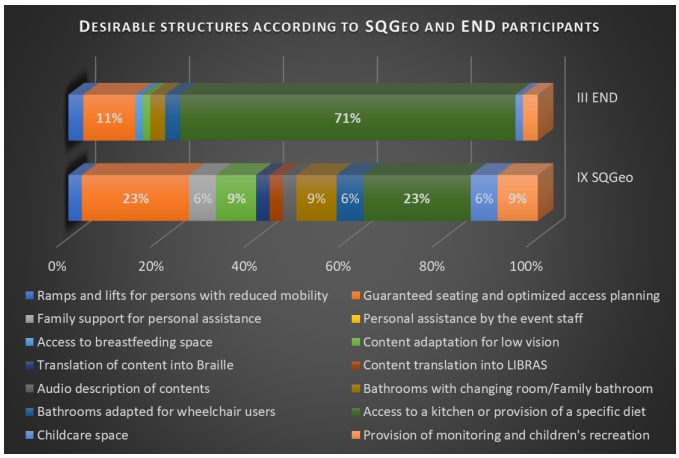

Figure 3. Desirable structures according to IX SQGeo and III END participants collected by the queries.

- *Women were more responsive to the survey:* although the near-equality of responses for gender distribution in the III END query (49% women and 47% men), data subscription shows that only 60 of the 195 participants were female. In this way, almost 50% of women replied to the query against only ~30% of men.
- *Capacitism, ageism and unhealthy catering:* desired structures suggest we´ve been ignoring multiple physical disabilities and the need for a balanced diet of the public in the events (Figure 3).
- *The unfulfilled absences:* almost total exclusion of indigenous, transgender and non-binary people shows the long way we have to perform towards intersectional equity (Figures 1 and 2).

Conclusions

Data shows that well-planned welcoming institutional spaces and affairs are necessary in order to improve the diversity at geoscientific events. Hostile policies that neglect specific needs such as the existence of equipped bathrooms or even the empathy of the involved community towards diversity are keeping off women, parents and children. Although the queries in these events tend to show demands more related to women and mother scientists, they made clear that people with physical disabilities, the LGBTQIAP+ community, people with food restrictions, the elderly community, neurodiverse people, and of course, poor people, tend to be neglected in scientific events. If diversity matters, as science shows, the right to be in these institutional spaces must be guaranteed. In the Geosciences, recognizing and normalizing the presence of parents, children, and diverse bodies and their needs is the first and further step to the construction of a plural community beyond the equity for gender.

Acknowledgements

The authors thank the organization committees of the IX SQGeo and of the III END, specially Franciele Zanandrea (END), Alice Cunha, Daniela Batista de Oliveira, Gabriela Bueno Fagundes de Freitas, and Maria José Mesquita (SQGeo), who helped to develop the queries and welcoming structures of both events.

References

Areas R., Abreu A.R.P., Santana A.E., Barbosa M.C., Nobre C. Gender and the scissors graph of Brazilian science: from equality to invisibility. 2020. OSF Preprints. https://doi.org/10.31219/osf.io/m6eb4.

Carrilho, A. (2021). Invisíveis, mas Necessárias: Mulheres Trabalhadoras da Mineração. Ed. Appris.

Oester, S., Cigliano, J. A., Hind-Ozan, E. J., & Parsons, E. C. M. 2017. Why conferences matter—an illustration from the International Marine Conservation Congress. *Frontiers in Marine Science*, *4*, 257. https://doi.org/10.3389/fmars.2017.00257.

Pickering, R. Khosa, R. 2023 Accessibility and inclusivity at EGU. Conferences, EGU GA. https://blogs.egu.eu/geolog/2023/05/12/the-geological-period-that-no-one-talks-about-menstruation-in-the-field/.